3

PNL-4172
UC-11

Liquefied Gaseous Fuels Safety and Environmental Control Assessment Program: Third Status Report

March 1982

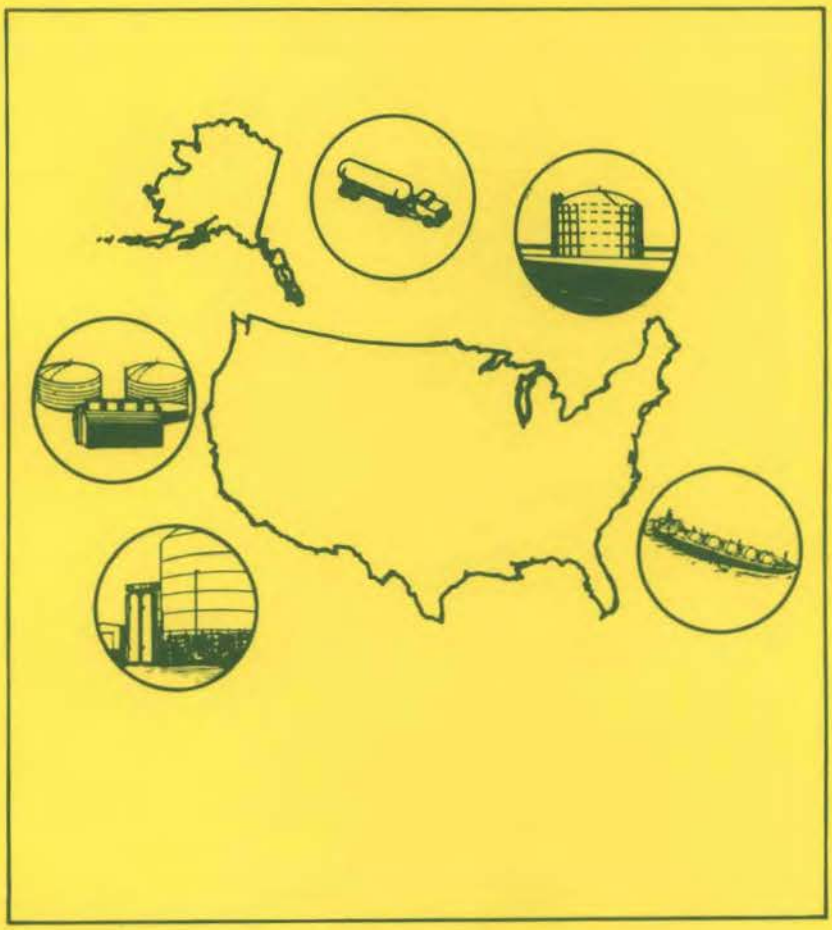

Prepared for the U.S. Department of Energy
under Contract DE-AC06-76RLO 1830

Pacific Northwest Laboratory
Operated for the U.S. Department of Energy
by Battelle Memorial Institute

Battelle

PNL-4172

DISCLAIMER

PACIFIC NORTHWEST LABORATORY
operated by
BATTELLE
for the
UNITED STATES DEPARTMENT OF ENERGY
under Contract DE-AC06-76RLO 1830

Printed in the United States of America
Available from
National Technical Information Service
United States Department of Commerce
5285 Port Royal Road
Springfield, Virginia 22151

NTIS Price Codes
Microfiche A01

Printed Copy

Pages	Price Codes
001-025	A02
026-050	A03
051-075	A04
076-100	A05
101-125	A06
126-150	A07
151-175	A08
176-200	A09
201-225	A010
226-250	A011
251-275	A012
276-300	A013

Liquefied Gaseous Fuels Safety and Environmental Control Assessment Program: Third Status Report

March 1982

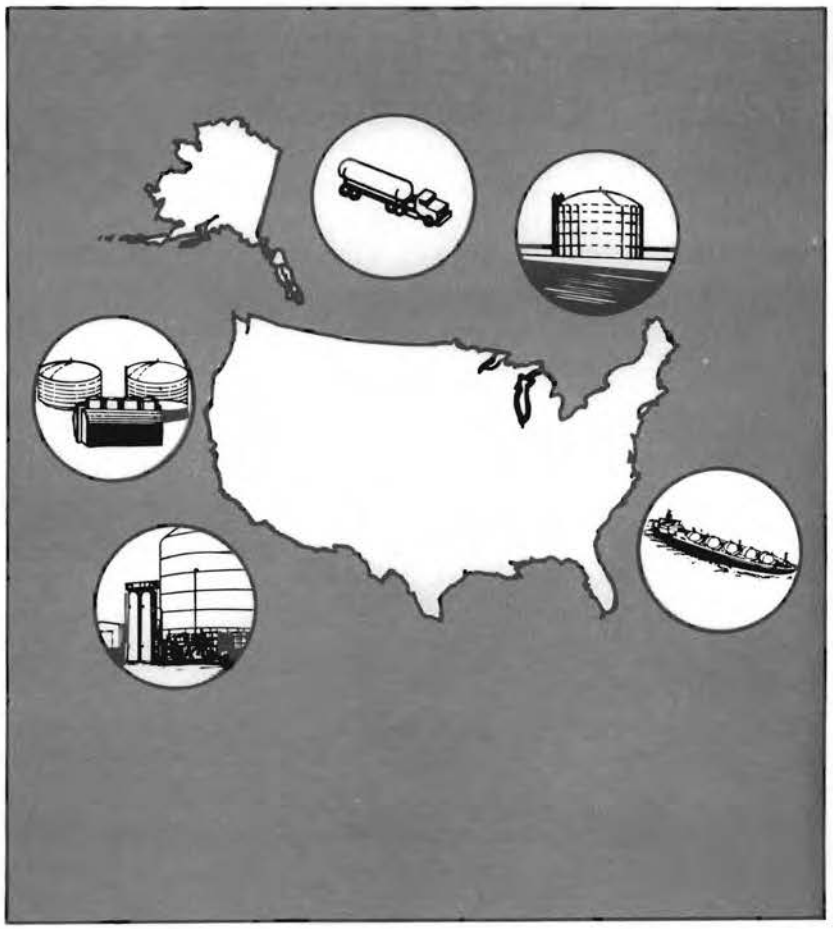

Prepared for the U.S. Department of Energy,
Office of Environmental Protection,
Safety and Emergency Preparedness,
under Contract DE-AC06-76RLO 1830

Pacific Northwest Laboratory
Richland, Washington 99352

ACKNOWLEDGEMENT

The Liquefied Gaseous Fuels Safety and Environmental Control Assessment Program is conducted by the Environmental and Safety Engineering Division (ESED), Office of the Assistant Secretary for Environmental Protection, Safety and Emergency Preparedness, U.S. Department of Energy. The Program is coordinated among the following agencies and organizations:

U.S. Department of Transportation
- Coast Guard
- Federal Railroad Administration
- Office of Pipeline Safety Regulations

National Aeronautics and Space Administration

National Science Foundation

The Fertilizer Institute

The Gas Research Institute

This document was compiled by Pacific Northwest Laboratory (PNL), operated by Battelle Memorial Institute, who is assisting the ESED program development, planning and implementation. Technical direction and guidance provided by Dr. John M. Cece and Dr. Henry F. Walter of ESED, greatly assisted this effort.

STATUS REPORT CONTRIBUTORS

This Status Report contains contributions from all contractors currently participating in the DOE Liquefied Gaseous Fuels (LGF) Safety and Environmental Control Assessment Program and is presented in two principal sections. Section I is an Executive Summary of work done by all program participants. Section II is a presentation of fourteen individual reports (A through N) on specific LGF Program activities. The emphasis of Section II is on research conducted by Lawrence Livermore National Laboratory (Reports A through M). Report N, an annotated bibliography of literature related to LNG safety and environmental control, was prepared by Pacific Northwest Laboratory (PNL) as part of its LGF Safety Studies Project. Other organizations who contributed to this Status Report are Aerojet Energy Conversion Company; Applied Technology Corporation; Arthur D. Little, Incorporated; C_V International, Incorporated; Institute of Gas Technology; and Massachusetts Institute of Technology.

Many individuals assisted the preparation and publication of this report. The following listing acknowledges the contributions of principal authors and others involved in this effort.

STATUS REPORT PREPARATION AND PUBLICATION EFFORT BY PNL

Task Management and Executive Summary

J. G. DeSteese

Task Coordination and Report Compilation

C. A. Counts

Technical and Editorial Review

N. M. Burleigh
J. M. Cece (DOE/ESED)
C. A. Counts
J. G. DeSteese
H. F. Walter (DOE/ESED)

Report Preparation

N. M. Burleigh
T. E. Hoopingarner
K. E. Rodriquez

TECHNICAL CONTRIBUTORS

Aerojet Energy Conversion Corporation

M. I. Rudnicki - Study of Gelled LNG

Applied Technology Corporation

J. R. Welker - LPG Spill and Safety Studies

Arthur D. Little, Incorporated

E. M. Drake - Novel Concepts for Preventing LNG Releases

C_v International, Incorporated

R. Tatge - Coaxial Cryogenic Pipeline

Institute of Gas Technology

P. J. Anderson, C. Landahl - LNG Storage Tank Studies

Lawrence Livermore National Laboratory

G. M. Bianchini - Report J

R. E. Blocker - Report J

R. T. Cederwell - Reports A, G, M

S. T. Chan - Reports C, E

D. L. Ermak - Reports A, C, E

H. C. Goldwire, Jr. - Reports A, B, D

P. M. Gresho - Report E

D. L. Hipple - Report J

W. J. Hogan - Reports A, J

R. P. Koopman - Reports A, B, D

J. W. McClure - Reports A, B

D. R. McIntyre - Report K

T. G. McRae - Reports A, B

D. L. Morgan - Reports A, C

L. K. Morris - Reports B, C

M. Ochoa - Report J

W. L. O'Neal - Report J

H. C. Rodean - Report A

J. H. Shinn - Reports A, F, G, K, L, M

P. A. Urtiew - Report H

W. Wakeman, Jr. - Report J

C. K. Westbrook - Report I

Massachusetts Institute of Technology

H. R. Chang, J. A. Fay, R. Ranck - Scale Effects in Liquefied Fuel Gas Hazard Analysis

H. R. Chang, R. C. Reid - Simultaneous Boiling and Spreading of LPG on Water

Pacific Northwest Laboratory

H. J. Bomelburg - Report N, LPG Research Assessment

D. L. Brenchley - Ammonia Safety and Environmental Control Assessment

W. L. Cliff - Special Studies

C. A. Counts - Report N, LPG Research Assessment

W. E. Davis - Report N

J. G. DeSteese - Report N, Project Summary, LPG Research Assessment, Special Studies

P. J. Pelto - Report N, LNG Release Prevention and Control

TABLE OF CONTENTS

SECTION I

EXECUTIVE SUMMARY

SECTION I

EXECUTIVE SUMMARY

The production and use of liquefied gaseous fuel (LGF) and energy materials provide direct and indirect benefits that improve the quality of life for individuals in our society. For a material such as liquefied natural gas (LNG), these benefits are accompanied by certain risks because of its hazardous nature when accidentally released or improperly handled. While much has already been done to minimize these risks, there is a consensus among representatives of the public, industry and government calling for more safety-related research and development (R&D) on LNG and other hazardous materials.

The U.S. Department of Energy, Office of the Assistant Secretary for Environmental Protection, Safety and Emergency Preparedness (DOE/EP) has a responsibility for identifying, characterizing and mitigating environmental, safety and health issues associated with the commercial use of specific energy materials. The Environmental and Safety Engineering Division (ESED), in the DOE/EP Office of Operational Safety, is responsible for assessing some of these materials, including liquefied gaseous fuels. To fulfill this responsibility, the ESED is conducting an R&D program that includes safety and environmental control assessments of LNG, liquefied petroleum gas (LPG), ammonia and hydrogen. The overall objective is to gather, analyze and disseminate technical information that will aid future decisions made by industry, regulatory agencies and the general public on facility siting, system operations and accident prevention and mitigation. This effort is known as the DOE Liquefied Gaseous Fuels Safety and Environmental Control Assessment Program[(a)] and is supported by a number of contributors including national laboratories, universities, technical institutions and industrial research contractors. As indicated in the Acknowledgment, the LGF Assessment Program is coordinated with related R&D sponsored by other agencies and organizations.

(a) In this report referred to as "the LGF Assessment Program" or "the DOE Program."

The ESED requested Pacific Northwest Laboratory (PNL) to assemble this status report on progress and accomplishments of the LGF Assessment Program during Fiscal Year (FY)-1980 and FY-1981. This report complements three previous documents in this series[(a)] that describe the DOE approach to safety and environmental research and the status of effort in the DOE Program from its initiation in FY-1977 to the first quarter of FY-1980.

I.1 SCOPE AND PURPOSE OF THE LGF ASSESSMENT PROGRAM

The need for a comprehensive, integrated R&D program to resolve LGF issues was identified by the ESED as a result of discussions with many experts from government, industry and academia. The development of a program specifically addressing LNG issues began in FY-1977 building on information developed in a cooperative program with the U.S. Coast Guard and the American Gas Association. Further input came from an Energy Research and Development Administration (ERDA)-sponsored LNG safety and control workshop (December 1976) which was attended by over 40 persons selected to represent a cross-section of cognizant experts from industry, government and academia. In the meantime, responsibility for this Program passed from ERDA to the DOE. Because many of the safety and environmental issues identified for LNG apply to the handling of other liquefied gaseous fuels, the scope was expanded to include safety and environmental concerns associated with LPG, ammonia and hydrogen.

The purpose of the LGF Assessment Program is, therefore, to develop additional safety and environmental control information on LNG and other significant liquefied gaseous fuels and energy materials. The emphasis of this effort is on information needed by industry, regulatory bodies and the general public for making decisions relating to the handling, transportation, storage and use of these materials.

(a) An Approach to Liquefied Natural Gas (LNG) Safety and Environmental Control Research. DOE/EV-0002, February 1978.

Liquefied Gaseous Fuels Safety and Environmental Control Assessment Program: A Status Report. DOE/EV-0036, May 1979.

Liquefied Gaseous Fuels Safety and Environmental Control Assessment Program: Second Status Report. DOE/EV-0085, October 1980.

I.2 PROGRAM OBJECTIVES

An outline of the LGF Assessment Program Plan describing the major research elements needed to achieve program objectives can be found in Section 2 of the first LGF Program Status Report (DOE/EV-0036). Three distinct objectives are identified to meet the goals of the integrated program:

1. Verify Predictive Capability
   Develop and validate analytical modeling capability to provide firm and technical foundation for the promulgation of regulations and to adequately support the development of prevention and control strategies, techniques and procedures. Wherever possible, theory and predictive capability will be based on laboratory experiments.
2. Verify Prevention Methods
   Investigate and validate methods to prevent the release to the environment of liquefied gaseous fuels. The focus is on materials, techniques, and strategies which are intended to prevent a release. These are, by nature, essentially "passive" systems.
3. Verify Control Methods
   Investigate and validate methods to control the release to the environment of liquefied gaseous fuels should a release occur. The focus is on materials, techniques, and strategies which are intended to reduce the impact of a release. By nature these will tend to be "active" systems.

I.3 SUMMARY OF REPORTS

This report continues the format of the two previous Status Reports in containing a collection of reports supplied by contributors to the LGF Assessment Program. The emphasis of this status report is on LNG research conducted principally by Lawrence Livermore National Laboratory (LLNL). Section II contains 13 reports (A through M) on LLNL efforts

grouped into the following categories:

- Details and Results of 40-m^3 LNG Spill Experiments
- LNG Dispersion Modeling and Analysis
- LNG Combustion Modeling and Analysis
- Facility Planning and Site Assessments for 500-m^3 Spill Tests at Frenchman Flat, Nevada

The LNG Bibliography included in Section II as Report N was prepared as part of the Literature Surveillance Task in the LGF Safety Studies Project conducted by PNL. The balance of this Executive Summary Section contains a review of the LLNL reports collected in Section II and summaries of other contractor activities contributing to the DOE Program.

I.3.1 Review of Reports A Through D

Four reports are included in Section II describing details and results of 40-m^3 LNG spill experiments conducted jointly by LLNL and the Naval Weapons Center (NWC) at China Lake, California.

Report A - Description and Analysis of Burro Series 40-m^3 LNG Spill Experiments

This report describes a series of nine field experiments in the range of 24 to 39 m^3 undertaken in 1980 to determine vapor transport and dispersion following LNG spills on water. An extensive array of instrumentation was deployed both upwind and downwind of the spill pond. Wind and gas concentration data were collected and analyzed to define the wind field and gas cloud as a function of time. Wind field, heat flux and humidity data were analyzed to describe fluid dynamic and thermodynamic processes associated with gas cloud dispersion.(a)

Several significant conclusions result from this effort. Turbulent processes in the lower atmospheric boundary layer were found to dominate the transport and dispersion of gas in all experiments except Burro 8. Burro 8, conducted under low wind speed conditions, showed that gravity

---

(a) The data acquisition system, 40-m^3 spill test plan and the China Lake LNG Spill Facility are described in detail by Reports O, Q and R respectively, in the Second DOE Program Status Report (DOE/EV-0085).

flow of the cold vapor displaced the ambient wind field causing the wind speed within the cloud to drop essentially to zero. Similar results are expected to occur in larger spills under a variety of conditions.

Large scale differential boiloff was observed resulting in the progressive enrichment of ethane and propane in the cloud. This is seen as an additional hazard because it increases the cloud's detonability. Energetic rapid phase transition (RPT) explosions occurred under different circumstances during the Burro 6 and Burro 9 tests. This raises the prospect that RPTs may increase the hazard potential of some accidents, and the resultant shockwave may be energetic enough to ignite the more easily detonable regions of the vapor cloud. Gas concentration measurements indicate that fluctuations about 5% in volumetric concentration are common. This implies the flammable extent of a gas cloud will be larger than is indicated by the mean lower flammability limit contour. Burro 8 data demonstrated that larger tests are necessary to determine the relationship between spill size and atmospheric dispersion characteristics.

Report B - Burro Series Gas Concentration Contours

Report B contains 110 gas concentration contour plots that correspond to the dispersion of LNG vapor during the Burro 8 and 9 spill experiments. LNG vapor-concentration data were used to generate two-dimensional contour plots as a function of time in both horizontal and vertical formats for several areas within the sensor array. The contours are of total hydrocarbon concentration and data from the instruments with faster response time were averaged so that all data have approximately the same time constant. The contours therefore describe the 10-s average LNG vapor-concentration distribution on a surface at a given time. This report provides details of the data analysis methodology.

Burro 8 was performed under stable atmospheric conditions in average wind speed of 1.8 m/s and showed most strongly the effects unique to dense cloud dispersion. Burro 9 was also important because the facility achieved its highest spill rate, the wind field allowed the cloud to stay within the array for the duration of the experiment, and nearly all sensors were

operational. The average wind speed was 5.7 m/s and the gas cloud behaved in a manner typical of a moderate or high wind speed test. However, RPT explosions occurred throughout this test throwing mud and water on the sensors in the 57-m arc rendering data from these sensors unreliable.

Report C - Comparison of Dense Gas Dispersion Model Simulations with Burro Series LNG Spill Test Results

The predictions from three vapor dispersion models for cold dense gas releases are compared with the results of several Burro Series LNG spill experiments. The simplest model (GD), a modified Gaussian plume model, predicted a vapor cloud that was too high and too narrow by about a factor of two in all cases. The second model (SLAB), a layer-averaged conservation equation model, generally predicted the maximum distance to the lower flammability limit (LFL) and cloud width quite well. However, SLAB predicted higher concentrations than those observed near the source and a different vertical concentration profile from that indicated by test results. The third model (FEM3) is a three-dimensional conservation equation model that was generally capable of predicting concentration distributions in time and space.

Report C contains brief descriptions of each model to clarify their physical bases and differences. Model predictions are compared with four of the experiments: Burro 3, 7, 8 and 9. The comparison of test results is based on 10-s average concentration data as described also in Report B. Burro 3 is unique in that it is the only case in which all three models underestimate the maximum distance to the LFL (X_{LFL}). Test results of Burro 7 show that the GD model underestimates and the SLAB model overestimates X_{LFL} by about 50 m and 60 m respectively. Burro 9 was terminated after 79 s because of RPT occurrence; however, sufficient data were collected to allow model comparisons. Burro 8 results, judged to be the most interesting of all the experiments, are compared with the predictions of each model in detail.

Of three models compared, the FEM3 is the least limited by various approximations and restricting assumptions, and provided the best overall description of the vapor cloud dispersion observed in these four Burro

experiments. Predictions of the vapor concentration distribution in time and space over the 5 to 15% flammable range were generally quite good. Estimates of the X_{LFL} are also quite good, or at least conservative. A particular achievement of FEM3 was the prediction of a bifurcated cloud structure observed in one experiment conducted with low ambient wind speed. However, the three-dimensional model was found to have numerical difficulties when it attempted to simulate spills under very low turbulence conditions.

The comparisons described in Report C illustrate the respective strengths and weaknesses of the three models and identify model components that require improvement.

Report D - Coyote Series 40-m^3 Liquefied Natural Gas (LNG) Dispersion RPT and Vapor Burn Tests

This report provides a brief description of the LNG spill tests known as the Coyote Series conducted during the period July to November 1981 as a joint effort between LLNL and NWC personnel. This series investigated RPT explosions and vapor cloud combustion and dispersion.

A total of 13 RPT spills were observed in five tests, with effort focused on RPT activity resulting from LNG interactions with water. Depending on operating and weather conditions, RPT testing was also done concurrently with vapor fire tests.

The major emphasis of this test series was the vapor burn tests. Report D shows the position of sensor stations and summarizes the test conditions of the series. In addition, a detailed listing is provided describing the instruments used and types of test conducted. The data produced by the Coyote Series are currently being analyzed and will be reported later in 1982.

I.3.2 Review of Reports E Through I

Four reports are included in Section II describing progress in the development of predictive models and data relating to atmospheric dispersion and combustion phenomena associated with LNG releases.

Report E - A Three-Dimensional, Conservation Equation Model for Simulating LNG Vapor Dispersion in the Atmosphere

Report E elaborates on the FEM3 numerical model simulating vapor dispersion following LNG releases that was compared with Burro Series test data in Report C. This report provides more details of the model's basis, structure and capabilities. The model is based on a finite element solution of the three-dimensional conservation equations for the simulation of spreading and dispersion of natural gas released onto water and over arbitrary topography. Simplicity is emphasized, represented by the choice of the simplest element, the 8-node isoparametric "brick" employing trilinear approximating functions for velocity, temperature and concentration and piecewise constant approximation for pressure. The forward Euler method is used as the simplest time integration method. Pressure is treated implicitly, being an inherently implicit variable in an incompressible fluid. The report presents the governing equations and a description of the time integration methods. The modeling of eddy diffusion and ground heat transfer coefficients is also described. Several of the cost-effective techniques used, including subcycling, mass lumping and reduced Gauss-Legendre quadrature, are discussed.

Report F - Theoretical and Empirical Basis for Experimental Simulation of Maritime Atmospheric Dispersion at Desert Sites

The problem of experimental simulations of maritime meteorological conditions is discussed in terms of selecting or modifying a desert atmospheric environment so that particular criteria of dynamic similarity are met and atmospheric dispersion test results may be generally applied. This study is an important consideration in determining whether tests undertaken in small lakes located at remote desert spill test sites in California and Nevada may adequately simulate LNG spills in a maritime environment. This report summarizes the similarity conditions, conventional generalizations and heat and humidity boundary layer effects that must be represented in a maritime meteorological simulation. A comparison is presented between conditions measured at desert sites and data taken in 1978 by the Naval Research Laboratory in the vicinity of Point Conception on the California coast.

This report concludes that the fundamental variables governing atmospheric dispersion scale similarly over ocean and inland sites. A shallow lake in the desert produces a significant atmospheric modification with humidity and temperature gradients approaching those observed over ocean sites. A shallow lake must extend about 1 km upwind to produce a 10-m deep boundary layer. The depth of the boundary layer can be selected by choosing the temperature gradient, wind speed and mean air temperature appropriately. The temperature gradient can be selected to simulate oceanic conditions by choosing both the season and time of day. A shallow lake in the desert is aerodynamically smoother than a rough sea, but the scaling will be correct if experiments are conducted at higher wind speed. Atmospheric turbulence in the inertial subrange will scale on the basis of aerodynamic roughness, atmospheric stability and the depth of the mixing zone. The unique degree of control for any value of atmospheric stability permitted by a desert lake simulation is seen as an advantage over conditions obtainable at any single oceanic site. However, further experimental studies are needed for generalizing conditions of dynamic similarity in the boundary layer over the normal observed range of atmospheric variability.

Report G - Observed Turbulence Intensities in Desert Boundary Layer

This report complements Report F by providing additional interpretation of meteorological data recorded at desert sites in Nevada and California. At Frenchman Flat, Nevada, experimental observations were taken on a 62-m meteorological tower instrumented with vertical propeller anerometers, wind vanes, cup anerometers, and aspirated thermistors. Data representative of a 5.5-m height above ground are discussed. Much lower turbulence intensities were observed under stable conditions than are commonly reported. The distinguishing features of this site are an extremely small surface roughness and a homogeneous upwind fetch for 3 km due to the flat playa. A vertical turbulence intensity of 4.1 was observed at Frenchman Flat, which is high compared to the value of 2.4 observed over rougher surfaces at China Lake, California.

Conclusions are that semi-empirical predictive formulas which fit data over rough surfaces and predict higher turbulent intensities for neutral and stable cases are not applicable to a smooth desert. Much better agreement is obtained if the hypothesis of Prandtl-type closure condition is assumed that would define the characteristic scale.

Report H - Flame Propagation in Gaseous Fuels Mixtures in Semiconfined Geometries

This report reviews previous work on flame propagation in gaseous fuels, discusses the phenomena involved and describes recent experiments performed at LLNL on combustion in semiconfined geometries. Most previous work on vaporized LNG/air mixtures has been performed in confined geometries to study ignition, flame acceleration transition to detonation and properties of fully developed detonations or in unconfined geometries to determine the minimum energy needed to initiate spherical detonations. Semiconfinement is the condition that most represents actual accidental spills. It is, however, an area of research that has been essentially neglected.

LLNL has begun small-scale laboratory experiments in an open semiconfined test chamber to investigate flame acceleration phenomena. Report H describes the experimental configuration of the first phase investigation, including the placement of obstacles in the chamber and presents results of using ionization probes as time-of-arrival detectors for the flame front. A comparison of the ionization probe data with Schlieren records leads to the important observation that the actual velocity of the flame front may be less significant than the rate at which the total mass of original mixture is transformed into combustion products.

The introduction of obstacles into the flow led to higher flame velocities. Several modifications made progressively during the test series caused unanticipated increases in flame acceleration. Schlieren photographs revealed the real cause of sudden accelerations, e.g., the flame getting through the slot under obstacles and starting the burn-up process from the bottom up.

The general lack of similar studies by other investigators makes it difficult to compare or correlate these results. A table is presented showing final flame velocities and over pressures measured in different geometries and scales comparing results of these experiments with those of other investigators.

In semiconfined geometries, flame velocities are expected to be lower than those in a confined tube. However, inertial confinement provided by a large cloud may cause a substantial overpressure which otherwise would not be expected. This research demonstrated the effects of obstacles on flame propagation in a semiconfined test chamber and provided a perspective for planning future experiments. The ultimate aim of this work is to gain confidence in identifying factors that affect flame acceleration processes so that they can be introduced into computational models providing a predictive capability for larger, more complicated cases.

Report I - Chemical Kinetics of Hydrocarbon Oxidation in Gaseous Detonations

Report I presents research on the chemical kinetics of hydrocarbon oxidation that extends LLNL investigations described in previous Status Reports.[a] In this report a theoretical model including a detailed chemical kinetic reaction mechanism is used to examine detonation properties for mixtures of fuel-air, fuel-oxygen and fuel-oxygen diluted with varying amounts of nitrogen. The five fuels considered are methane, ethane, ethylene, acetylene and methanol. Computed induction lengths are compared with available data on critical energy and critical tube diameter for detonation initiation as well as detonation limits in planar, cylindrical and spherical configurations. The reaction mechanisms used in these calculations have been developed and validated in previous publications. There is some disagreement regarding the critical initiation energies for fuel-air mixtures suggesting that initiation energy

(a) Report E in First LGF Assessment Program Status Report (DOE/EV-0036). Report F in Second LGF Assessment Program Status Report (DOE/EV-0085).

determined using linear tubes and explosive charges cannot be directly compared.

For the fuels considered in this report, reaction mechanisms are reliable enough that computation of the induction time is no longer a limiting factor in understanding detonation processes. The model used in this report is intentionally simplified to emphasize the kinetic factors involved. Modifications which have been developed and used by other authors should be included in a complete detonation model. However, calculations using the present model are simple and inexpensive using available computer codes and provide much useful information. The agreement between completed results and experimental data suggests that the approach can provide accurate and reliable information on detonation parameters over most conditions of interest.

I.3.3 Review of Reports J Through M

The final category of LLNL reports describe preparation and exploratory investigations relating to the 500-m^3 LGF Spill Test Facility planned at Frenchman Flat, Nevada.

Report J - 500-m^3 Spill Test Facility for Liquefied Gaseous Fuels

Report J is the first of four that discuss the conceptual design and preliminary evaluations to justify the use of Frenchman Flat at the Nevada Test Site for studying the effects of large LGF spills. The facility is designed to safely and reliably handle spill tests as large as 500 m^3. Fuels of current interest include LNG, LPG, ammonia and hydrogen. This report details experimental requirements, including spill size, rate, and related characteristics, atmospheric conditions, spill test candidates, and test parameters, including abort procedures and cool-down times. Site selection criteria are discussed, including environmental effects, hazards, administrative constraints, atmospheric conditions, and topography.

The facility design concept consists of two 150-psi LGF storage tanks installed in Phase 1 of the project as part of a 200-m^3 spill test facility. Two 250-psi LGF storage tanks would be installed later,

bringing the spill test capability up to 500 m^3. The tanks would be connected by a 24-in. diameter insulated underground spill pipe to a 1000-ft diameter spill pond. A 100-ft long extension to the spill pipe is planned to provide an opportunity for conducting spills on dry soil. Various nozzles and splash plates would be installed on the end of the pipe to vary spill velocity and direction on or below the water. An array of experimental measuring sensors would be placed up and downwind of the spill point and the facility controlled and monitored from a safe distance by remotely located control and recording systems.

Design concerns are detailed in terms of three principal questions concerning 1) the achievement of desired spill rate, 2) the efficacy of the delivery system, and 3) the protection of the tankage. The LGF storage system is described in detail, including the storage tanks, fill and transfer system, and the sub-cooling system. Similar details are given for the LGF spill system, including determination of pipe size, spill pipe system design, pipe material, insulation, expansion joints, spill nozzle system, pig system, dump tank system, and liquid nitrogen precooling system.

Hazards control measures described include hazards analysis, gas detection, fire detection, fire and explosion control, emergency shutdown systems, safe operating and testing procedures, and a quality assurance program. Control and monitoring systems include spill size control, spill rate control and general monitoring to measure temperature, pressure, gas concentration and liquid level. Planned civil engineering discussed includes the need for roads, spill basins, tank farm pad, waterlines, dispersion lake and electrical systems.

Report K - Ecological Background Relevant to Proposed Liquefied Gaseous Fuels Test Site Development at Frenchman Flat, Nevada

This report surveys ecological studies of the Nevada Test Site to determine what is known about ecosystems adjacent to Frenchman Flat. This background information is used to determine what ecological needs must be considered to avoid potential impacts of the planned LGF spill tests. Report K reviews the historical ecology of the Frenchman Flat area, discusses plant habitat, plant and animal nutritional dependencies, and animal species considerations.

Of the several species of plants and animals that should be protected, apparently none are found closer than 5 km from the playa. Two potential factors of concern are whether the proposed development and associated human activity will affect animal behavior, and whether the vegetation will propagate brush fires, or suffer undesirable changes as a result of fires. Recommendations are made for methods of estimating fuel biomass and other factors needed to estimate fire propagation, and procedures to document any changes in animal populations and plant productivity.

Report L - Environmental Issues of the Proposed LNG Spill Tests at Frenchman Flat

This effort was undertaken in response to a request by the LNG Working Group to review environmental issues relating to the proposed LNG spill tests at Frenchman Flat. The report answers 11 questions posed by the Manager of the Nevada Test Site. The questions relate to the phased development of a facility capable of supporting spill tests of 500 m^3 as described in Report J. Report L contains a brief overview of intended LNG operations, including descriptions of spill effects, combustion and explosion tests. The report addresses questions concerning whether planned experiments will cause the resuspension of radioactive particles, operational procedures for protecting endangered plants, and the quantity of dust and heat flux generated by test events. Other concerns considered are over-pressures, underpressures and ducting phenomena; the identity and quantity of released gases and down-wind concentrations with distance and the potential for explosive gas concentrations extending into surrounding structures. Finally, the effect of water on radioactive particles, the population and effects of animals in the area, potential for range fires and the maximum estimated damage to Nellis property and the Desert National Wildlife Range are considered.

Not all of the information required is available to answer these questions conclusively, however, many appear to be of little consequence. The advantage of the planned phased testing allows the effects of smaller spills to be observed before commitment is made to larger-scale tests.

This would provide time to review health and safety aspects of larger and potentially less certain effects of larger experiments. This report notes areas of ongoing additional work that should lead to the satisfactory assessment of outstanding issues.

Report M - Selecting Optimum Periods for Atmospheric Dispersion Tests over Water Surfaces at Frenchman Flat, Nevada Test Site

When LGF spill tests are conducted over water surfaces at Frenchman Flat, Nevada, it will be necessary to schedule tests so that meteorological conditions are optimized for experimental control and operational safety. An operating strategy based on meteorological data collected at Frenchman Flat is discussed in this report. Factors such as diurnal flow patterns, temperature structure, wind speed variation and variation in stability over water surfaces are considered. Report M also discusses seasonal factors, such as evaporation rates, wind and stability over a water surface, and temperature effects.

General conclusions are that for atmospheric dispersion testing over water surfaces at Frenchman Flat, the optimum daytime periods are between 11 a.m. and 6 p.m. from March through November, because of a consistent flow pattern and undirectional flow, as well as moderate, regularly increasing wind speeds. Using this time period as optimum, the atmospheric stability over water surfaces will be unstable in March-April, neutral in May, mildly stable through summer, and strongly stable in October-November. Two periods are identified, March-May and October-November to prevent freezing and to obtain favorable precipitation/evaporation ratios. These are also the periods of minimum thermal stress on equipment and personnel.

I.3.4 Review of Report N

Report N is the updated LNG Bibliography prepared by PNL as part of the Literature Surveillance Task in the LGF Safety Studies Project (see also subsection I.4.7).

I.4 SUMMARY OF WORK BY OTHER LGF ASSESSMENT PROGRAM CONTRACTORS

Although the principal emphasis of this Status Report is on work led by LLNL, other contractors contributing to the DOE Program have reportable achievements in FY-1980 and FY-1981. The following summaries review contributions to the LGF Assessment Program made by the Aerojet Energy Conversion Company (AEC), the Applied Technology Corporation (ATC), Arthur D. Little, Incorporated (ADL), C_V International, Incorporated (CVI), the Institute of Gas Technology (IGT) and the Massachusetts Institute of Technology (MIT). The final summary describes work in the LGF Safety Studies Project conducted by PNL.

I.4.1 Study of Gelled LNG (AEC)

The objective of work performed by the AEC was to investigate the feasibility of using gellation to reduce hazards associated with LNG storage, transportation and handling. Potential safety advantages of gelled liquefied natural gas (GELNG) were examined and the practicality of gelation on an industrial scale was studied.

The project involved gel characterization, optimization, safety tests, preliminary design of an industrial-scale gelation system and a preliminary economic assessment of the gelation process. LNG gels of varying concentration, using both water and methanol as gelants, were prepared and characterized. Selected gels were used in safety comparison tests and a preliminary design was made for an industrial-scale gelation system which would provide the basis for an economic assessment.

The preliminary economic assessment results showed the increased dollar cost of gelation for LNG tank truck applications to be small (~5%).

Vaporization rates determined from 0.4 gallon confined spills on sand, concrete, and water were found to be considerably lower for GELNG than for LNG. The GELNG could not be driven through a simulated crack with up to 20 psig driving pressure, whereas LNG was found to flow freely at all pressures. Plastic "yield strengths" were further improved using modified gelation techniques. A shear diagram was defined for future hydrodynamic calculations. Perforation leakage tests showed rapid cessation of GELNG flow at all driving pressures investigated while LNG flowed freely.

Confined water and land spill tests were conducted and vaporization and spread rate data obtained. Variation in spill orientation and energy clouded the results; however, the GELNG increased vaporization time significantly in water spill tests.

This effort was completed with the publication of the Final Technical Report.[a] Work in this area continued under sponsorship of the Gas Research Institute.

I.4.2 LPG Spill and Safety Studies (ATC)

Efforts conducted by the ATC included (1) research on vaporization, dispersion and radiant fluxes from LPG spills and (2) a study of LPG land transportation and storage safety.

Vaporization, Dispersion and Radiant Fluxes from LPG Spills

Both burning and non-burning spills of LPG (primarily propane) were studied. The non-burning spill studies included boiloff tests, dispersion tests, and liquid spray tests.

Boiling rates for propane spilled on soil, concrete, insulating concrete, asphalt, wood, sod, and foamed polymers were measured during both the transient and steady-state boiloff periods. Most of the transient tests were run in 5-ft^2 circular pits. Some of the tests were covered to exclude atmospheric effects. Simple one-dimensional heat transfer theory was used to determine the thermal conductivity of the substrate and the heat transfer coefficient between the substrate and the propane. Thermal conductivities were usually higher than the literature values for similar materials at ambient temperature. Heat transfer coefficients varied with substrate material, but were in the range expected to occur for propane. Mass transfer coefficients were determined for a range of variables and correlated as a function of the Reynolds number.

Vapor concentrations were measured downwind of propane pools 25 to 1600 ft^2 in area. The vapor concentrations along the plume centerline at ground level could be correlated satisfactorily with a Gaussian model. The

---

(a) Rudnicki, M.I. et al. 1981 Study of Gelled LNG, Final Technical Report. DOE/TIC-11452, prepared by the Aerojet Energy Conversion Company for the U.S. Department of Energy, Washington, D.C.

vaporization rates for the dispersion tests were near steady-state values because the pits had been cooled for at least a half hour before the vapor concentrations were determined. Pool temperatures were usually in the range of -70°F or less.

In a few tests, pressurized propane was discharged into the open air in an attempt to determine what fraction would vaporize or atomize and what fraction would collect as a pool. Even at rates up to 180 lb/min, no pooled propane could be collected.

Emitted and incident radiant heat fluxes were measured for fires with base areas from 25 ft^2 to 1600 ft^2. Simplified radiant flux models were found to be adequate to represent the results. The maximum effective radiant flux emitted by the propane fires was about 50,000 Btu/hr-ft^2. Fluxes for smaller fires can be expressed by

$$q_s = 50{,}000 \left(1 - e^{-1.126\ D}\right)$$

where q_s is the effective surface flux (Btu/hr-ft^2) and D is the flame diameter (ft). Flame heights could be predicted using the Thomas equation. A simple model based on an assumed cylindrical shape for the flame and the surface fluxes given by the equation above predicted the incident radiant fluxes surrounding the fire with good accuracy.

A final report on this study is being prepared for publication. No further work is planned in this task.

LPG Land Transportation and Storage Safety

Effort in this task was completed in 1981 with the publication of the Final Report.[a]

This report contains an analytical examination of fatal accidents involving LPG releases during transportation and/or transportation-related storage. Principal emphasis was on accidents during the nine-year period 1971-1979.

(a) Martinsen, W. E. and W. D. Cavin. 1981. LPG Land Transportation and Storage Safety. DOE/EV/06020-T5, prepared by the Applied Technology Corporation for the U.S. Department of Energy, Washington, D.C.

Fatalities to members of the general public (i.e., those at the scene of the accident through coincidence or curiosity) were of special interest.

Transportation accidents involving railroad tank cars, trucks, and pipelines were examined as were accidents at storage facilities. The main source of the necessary historical accident data were accident reports submitted to the Department of Transportation by LPG carriers, National Transportation Safety Board accident reports, articles in the National Fire Protection Association journals, other literature, and personal interviews with firemen, company personnel, and others with knowledge of certain accidents.

The data indicate that, on the average, releases of LPG during transportation and intermediate storage cause approximately six fatalities per year to members of the general public. The individual risk is about 1 death per 37,000,000 persons; about the same as the risk of a person on the ground being killed by an airplane crash, and much less than the risk of death by lightning, tornadoes, or dam failures.

I.4.3 Novel Concepts for Preventing LNG Releases (ADL)

ADL is investigating three novel concepts to establish their potential applicability as LNG release prevention systems.

Sealed Safety Monitor (SSM) for LNG Trucks

The objective of this study is to evaluate the SSM concept designed to monitor and record various parameters of LNG truck operations and, possibly, to anticipate and compensate for certain aspects of driver behavior in potential accident situations. The SSM would consist of a series of transducer, monitoring and recording devices coupled by a microprocessor control and packaged in a crash-resistant container. The results of this study are expected to include a preliminary SSM design and assessments of its cost effectiveness and implementation feasibility.

Work completed includes the identification of credible accident scenarios and critical monitoring functions. Fault tree and multi-linear event sequence analyses were applied to these accident scenarios to identify key monitoring parameters. A technical literature review and engineering analyses were conducted to refine the parameter selection and the selection of appropriate sensors was

undertaken. Analysis of accident mechanisms was focused on the following scenarios: 1) rollover while negotiating a gradual curve, 2) the "sudden lane change" maneuver, 3) brake lock, 4) brake system failure, and 5) steering tire failure. The first three scenarios were selected for the closest examination because they involve driver-vehicle interactions that may be anticipated and mitigated using the SSM.

Engineering analyses were performed for the steady-state cornering maneuver and brake lock. While the sudden lane change involves dynamic analysis beyond the scope of this study, the anticipation of rollover was amenable to analysis. A physical model was used as a means for predicting imminent rollover as a function of rear spring displacement. It was found that, although brake lock can be anticipated with wheel deceleration measurements on the vehicle, warning could not be provided fast enough to allow a driver response. Because active control systems appear to be more effective for preventing brake lock accidents, this scenario was not pursued further. The measurement of wheel rotation was, however, found to be an effective means of computing a variety of performance and investigative parameters. It is therefore considered an important parameter to be monitored. The results of analyses performed to date provide a basis for the proposed SSM design.

This study is about 65% complete.

Flexible Membrane Inside LNG Cargo Tanks

The objective of this concept is to investigate the feasibility of installing a bladder or curtain-type membrane in an LNG cargo tank to prevent or control spillage of LNG following a breach of the cargo containment structure. This study consists of three tasks: 1) examination of mechanical and structural feasibility, 2) selection of materials and 3) a cost effectiveness assessment.

Work completed to date includes review of major structural features of membrane and spherical cargo containment tank systems and a feasibility determination of installing and supporting curtain-type membrane systems within these tanks. It appears that a sufficient number of potential attachment points are available in the Technigaz and Gaz Transport design configurations to allow suspension of a curtain structure without interfering significantly with the motions or stress levels of the primary container due to thermal and product loads. For the spherical Moss cargo tank systems, attachment of a

curtain barrier at locations in the upper half of the sphere should present no significant stress or deformation problems.

Curtains or internal bladder systems will effectively separate the volume of the cargo tank to some degree. Such systems may interfere with the efficiency or thoroughness of inerting techniques currently in use. Alleviation of this problem may require additional or reconfigured piping within the tank.

The composite materials identified as potential containment membranes include a fiberglass cloth/aluminum foil composite presently in use as a secondary barrier in liquefied gas tanker applications; a fiberglass cloth/mylar composite used for flashing in architectural applications; a fluorocarbon coated fiberglass cloth material used in weather dome structures and a coated aramid fiber fabric. A test program has been developed to evaluate the important properties of each of these materials in a cryogenic environment. These tests will include the determination of tensile strength, notched tensile strength behavior (tear resistance), flexure cycling, and resistance to penetration.

Work in this project is approximately 35% complete.

LNG Flare System for Offloading a Disabled Vessel

The objective of the third ADL study is to evaluate the feasibility of a flare system for the rapid and safe incineration of the cargo in a disabled LNG tanker. This study is organized into six tasks: 1) design criteria and performance specifications, 2) selection of the preferred system configuration, 3) investigation of LNG transfer methods and procedures, 4) design of the flare system flotation, 5) preliminary design of the combustion system and 6) calculation of the radiant heat flux distribution. This project is about 95% complete.

In the work completed to date, design criteria and performance specifications have been established, alternative flare configurations were evaluated and the optimal system configuration was selected. Design criteria included a burn capacity of 5.7×10^8 scf in 24 hours and a target cost less than $4 million. Four approaches for flaring the LNG cargo were considered: 1) a free burning pool in a satellite array, 2) a large flare mounted on the LNG tanker, 3) an inerting system, and 4) a remote flare array. The remote

flare array was chosen as most feasible system. The design includes an array of small burners mounted on a catamaran. Based on an analysis of the costs and equipment associated with LNG vaporization, it was concluded that the LNG cargo should be transferred to the burners as a cryogenic liquid. A transfer line currently manufactured by Coflexip of Paris, France, was selected as the basis for design and costing.

A burner currently available from the National Air Oil Company was selected as part of the flare array design evaluation. The most promising design consists of an assembly of 1,350 burners spaced 1.5 ft apart on pipe strings. The dimensions of the burner array would be approximately 300 ft long and 55 ft wide. Preliminary estimates were made of the radiative heat flux received at the stern of the LNG tanker from an array of catamaran-mounted flares. It appears that the required standoff distance of the flare vehicle will be greater than 400 ft.

The overall conclusion of this effort is that LNG flaring appears to be feasible. There are no components of the conceptional flare system which are significantly beyond the state-of-the-art. The most critical elements in the design are the floating cryogenic LNG transfer lines and the sensitivity of the LNG tanker to radiation from the flare array.

I.4.4 Coaxial Cryogenic Pipeline (CVI)

CVI is conducting a cryogenic demonstration of a novel coaxial pipeline design. In concept, a coaxial system for transporting cryogenic fluids, such as LNG, appears to have safety advantages over single-wall pipe. The CVI coaxial system has a number of essential elements including: 1) the inner and outer concentric pipe spool pieces; 2) the spider that holds the relative position of two pipes, provides thermal coupling and allows vapor flow between them; and 3) the external insulation jacket. Both inner and outer pipe elements are maintained at a minimal differential temperature. This allows the pipe to be fabricated as fixed coaxial element in which thermally developed stresses are held at low allowable values. Liquid is transferred through the inner pipe, and vapor is circulated in the annular area. The annular space between the pipe elements provides containment for liquid released as a result of leakage or failure of the inner piping element.

The concept includes an isolation valve arrangement that can be separately- or slave-operated as the system design dictates. The emergency valve assembly allows for water hammer suppression in the event of a rapid valve closure during LNG transfer. As the isolation valves close, a synchronized third or emergency bypass valve opens transferring the liquid continuously from the inner pipe through the annulus between the piping back to storage. This allows the pumps to wind down without creating a significant pressure surge in the piping system.

The coaxial pipeline demonstration project is being conducted in four phases. Phase 1 has been completed and included the identification of state-of-the-art test hardware and special transition components. Thermal and structural analyses of the hardware and test loop configuration were performed using the ANSYS finite element program. These analyses identified the parameters necessary to demonstrate the performance of the hardware in the cryogenic temperature regime and also provided guidelines in the design of the final test loop configuration and LN_2 flow control systems. Phase 2, also completed, included the procurement of material and standard components, preparation and approval of shop fabrication drawings and hardware fabrication, and the selection and placement of the instrumentation. All of the preliminary activities in Phase 3 are complete and conduct of the cryogenic test cycles is imminent. Phase 4 will include a review of the test data and the preparation of a final program report that includes the conclusions and recommendations relating to the further development of this concept.

I.4.5 LNG Storage Tank Studies (IGT)

Two projects are being conducted by IGT with the goal of improving release prevention systems in LNG storage tanks.

Tank Dynamics

The first of these projects involves the improvement of practical release measures by developing design and operating procedures beyond current practice. The objective is to obtain quantitative data necessary to model the physics of tank vapor space pressure responses to boiloff compressor operation and atmospheric pressure changes. It is expected that this information may aid the specification of LNG storage tank operations and equipment to limit the

possibility of vapor venting or rollover. Data will be obtained from LNG storage tanks during periods when liquid is neither being added nor withdrawn from storage and during periods of LNG production. Tank vapor-pressure will be obtained using commercially available pressure transducers that are capable of directly measuring absolute pressure. Analysis and model development will be conducted to describe the physics of tank responses. This model will enable review and evaluation of tank operating parameters. The model prepared in this project will be compared with the observed behavior of an existing instrumented LNG storage tank over a period of two months.

Tank Sealants

The objective of the second IGT project is to assess the feasibility of using sealant additives to prevent LNG from leaking through defects in metal tanks. Sealant additives could be used in metal tankage at storage and transportation facilities, including self-supporting and membrane marine cargo tanks. This study will include: 1) the selection of candidate materials (e.g., polystyrene, polyacrylamide, and silica); 2) an evaluation and ranking of specific sealant additives; 3) an evaluation of equipment and methods for producing dispersions at cryogenic temperatures and 4) a determination of sealing efficiency and compatibility and stability of additives in the liquid phase. The exposure of sealant candidates to liquefied methane will be undertaken to demonstrate their behavior in the presence of hydrocarbons characteristic of LNG. Field performance projections and applications economics will be developed in this work.

I.4.6 LGF Safety Research at MIT

The DOE Program has supported two areas of research conducted at MIT.

Scale Effects in Liquefied Fuel Gas Hazard Analysis

This research was directed towards constructing a general method of correlating physical variables observed in experiments on the atmospheric dispersion of dense gases. The principal variables of interest are the maximum ground-level concentration of the released gas within the cloud, the width, length and height of the cloud, and drift speed. Cloud drift distance and time since formation would be the principal independent variables. The approach tried

was a combination of dimensional analysis and use of a simple entrainment model to suggest potentially useful methods for correlating the data.

In the analysis the atmospheric motion was characterized by three-dimensional variables: friction velocity (U_*), roughness height (Z_o), and the Monin-Obukhov length scale (L), which measures atmospheric stability at ground level. The initial state of the negatively buoyant cloud (assuming it to have been formed rapidly) is characterized by its buoyance (B) and volume (V). The simplest hypothesis that can be made regarding the dispersion of the cloud is that its behavior at times sufficiently long for the cloud to have been diluted to a small fraction of its initial concentration is independent of the details of its formation and can depend only upon the parameters U_*, Z_o, L, B and V. Furthermore, in describing the motion of the cloud relative to its mass center, if the effect of wind shear can be neglected compared with the effects of gravity, then Z_o (and probably L) would be eliminated as parameters. For an observer drifting with the cloud, the observable variables would be a function of the dimensionless time $U_*^2 t/B^{1/2}$, where t is the (dimensional) time. The corresponding dimensionless concentration is $B^{1/2}\chi/U_*^2 V$, where χ is the concentration of the released gas. These hypotheses thus form the basis for correlating cloud gas concentration with time.

To develop a correlation of the observables as a function of drift distance from the origin of the cloud, it was necessary to resort to a dynamic model of the cloud spread and entrainment. Because of wind shear (which depends upon Z_o and L), the local drift speed will depend upon cloud height and hence upon the cloud evolution. The dimensionless parameters which measure the effect of wind shear are $U_* Z_o/B^{1/2}$ $U_* L/B^{1/2}$.

This work correlated data obtained in field experiments and wind tunnel tests using dense gas or liquid gas vapors. As a part of this review, a catalog of test observations was compiled for both wind tunnel and field tests. Despite some scatter in the data, considerable progress has been made in the correlation of maximum concentration in the cloud as a function of time and distance from the spill origin.

Effort in this project was completed with the publication of the Final Technical Report.[a]

Simultaneous Boiling and Spreading of Liquefied Petroleum Gas on Water

The second MIT research project involved an experimental and theoretical investigation to study the boiling and spreading of liquid nitrogen, liquid methane, and LPG on water in a one-dimensional configuration. Primary emphasis was placed on the LPG studies.

Experimental work involved the design and construction of a spill/spread/boil apparatus which permitted the measurement of spreading and local boiloff rates. With the equations of continuity and momentum transfer, a mathematical model was developed to describe the boiling-spreading phenomena of cryogens spilled on water. The model accounted for a decrease in the density of the cryogenic liquid due to bubble formation.

The boiling and spreading rates of LPG were found to be the same as those of pure propane. An LPG spill was characterized first by very rapid and violent boiling and then highly irregular ice formation on the water surface. The measured local boiloff rates of LPG agreed reasonably well with theoretical predictions from a moving boundary heat transfer model. The spreading velocity of an LPG spill was found to be constant and determined by the size of the distributor opening. The maximum spreading distance was found to be unaffected by the spilling rate. These observations can be explained by assuming that the ice formation on the water surface controls the spreading of LPG spills. While the mathematical model did not predict the spreading front adequately, it predicted the maximum spreading distance reasonably well.

Publication of the Final Technical Report[b] in December 1981 marked the completion of this effort.

(a) Fay, J.A. and D. Ranck. 1981. Scale Effects in Liquefied Fuel Vapor Dispersion. DOE/EP-0032, prepared by the Massachusetts Institute of Technology for the U.S. Department of Energy, Washington, D.C.

(b) Chang, H.R. and R. C. Reid. 1981 Simultaneous Boiling and Spreading of Liquefied Petroleum Gas on Water. DOE/EV-04548-1, prepared by the Massachusetts Institute of Technology for the U.S. Department of Energy, Washington, D.C.

I.4.7 LGF Safety Studies at Pacific Northwest Laboratory

The LGF Safety Studies project conducted by PNL combines two previously separate projects: the LNG Safety Studies Project and the LPG Assessment Project. The combined Project provides research on LNG release prevention and control, technical surveillance and program development information supporting the DOE Program. This project also provides assessments of safety and environmental control issues relating to the production, transportation, storage and use of LPG and ammonia. The LGF Safety Studies Project is structured around five major tasks:

- LNG Release Prevention and Control Studies
- LNG Technical Surveillance
- Ammonia Safety and Environmental Control Assessment
- Assessment of LPG Research and Development Needs
- Special Studies

Progress in these tasks is summarized below.(a)

LNG Release Prevention and Control Studies

The objective of the LNG Release Prevention and Control Task is to develop an adequate understanding of LNG release prevention and control systems and the factors which may defeat them. Work in the LNG Release Prevention and Control Task focused on 6 subtasks: 1) facility scoping studies, 2) import terminal analysis, 3) peakshaving plant analysis, 4) storage tank analysis, 5) fire prevention and control assessment, and 6) human factors analysis.

A draft final report outlining results of a scoping assessment of LNG release prevention and control system was completed for DOE review. The report characterizes the basic types of LNG facilities and their release prevention and control systems, identifies possible weak links in research needs and provides an analytical framework for more detailed analyses.

Building upon this scoping assessment, PNL initiated more detailed assessments of release prevention and control systems in LNG import terminal

---

(a) Complete reports on most of these tasks are planned for inclusion in the next DOE Program Status Report.

and peakshaving facilities. Draft final reports summarizing the import terminal and peakshaving facility analyses were completed. A comparative safety analysis of LNG storage tanks was also completed. Representative above-ground metal and concrete tanks were defined and their response to release-initiating events compared. Release-initiating events considered include overfill, overpressure, underpressure, foundation failure, crack propagation, earthquake/tornado, impact and adjacent fires. The assessment of LNG fire and vapor control devices continued. Import terminal and peakshaving analyses provided a basis for examining the reliability and effectiveness of current fire and vapor control strategies.

Human factor engineering (HFE) practices in the LNG industry were reviewed using extensive bibliographic research followed by several site visits to peakshaving plants. Possible human error contributions to previous LNG accidents and incidents were analyzed in an attempt to assess the potential contributions of HFE to LNG safety. Conclusions of this study phase are that factors such as operator training, operating and maintenance procedures, alarms and warnings, and controls and displays are generally worthy of further examination.

LNG Technical Surveillance

The LNG Technical Surveillance Task was initiated to assist the ESED in establishing and maintaining technical surveillance of research and development activities relating to LNG safety and environmental control. Literature surveillance and the development of an LNG library continued. Four quarterly supplements to the LNG annotated bibliography (included in this Status Report as part of Report N) and additions to the LNG safety and control literature and research updates were completed and distributed to the sponsor and other contractors. A survey of information contained in European LNG literature continued under a subcontract performed by Battelle-Institut e.V. in Frankfurt, West Germany.

Ammonia Safety and Environmental Control Assessment

The objective of this task was to contribute program planning information by identifying potential problem areas related to ammonia safety and environmental control. This effort was initiated in FY-1979 and completed in FY-1981. The final assessment report was published and includes 1) a characterization of the ammonia industry, 2) a review of current

knowledge of ammonia release and dispersion phenomena and impacts, 3) the identification of safety and environmental problems, and 4) recommendations for R&D to mitigate these problems.[a]

Assessment of LPG Research and Development Needs

The objective of this assessment is to evaluate safety and environmental control issues relating to the production, transportation, storage and use of LPG. This task has involved the efforts of three subcontractors: Battelle Columbus Laboratories, the Institute of Gas Technology, and the Applied Technology Corporation. Battelle Columbus Laboratories provided system descriptions of LPG transportation by pipeline, rail and truck and an assessment of the state-of-the-art of release prevention and control in the LPG industry. The Institute of Gas Technology contributed descriptions of production, import/export and peakshaving plants, and barge and ship transportation systems. Both of these subcontractors and PNL identified and evaluated R&D needs and recommended R&D program elements that address LPG safety and environmental concerns. The Applied Technology Corporation provided an additional review of the draft final report.

This work has resulted in the collection of information on LPG characteristics, hazards and risks, release phenomenology and the state-of-the-art of release prevention and control. Based on the knowledge gained in developing this information, specific R&D projects are recommended that address knowledge gaps in LPG release phenomenology and needed improvements in release prevention and control.

Special Studies

The special studies task provides information that contributes to the planning and development of the DOE Program. In FY-1981 a special study was undertaken to assess the use of water as a simulant for modeling LGF boiling liquid expanding vapor explosion (BLEVE) conditions. In this study, information was developed on dimensionless parameters associated with BLEVEs and RPTs. The initial analysis of this work indicates that water at the right vapor density and temperature difference, i.e., difference in

(a) Brenchley, D.L., et al. 1981. Assessment of Research and Development (R&D) Needs in Ammonia Safety and Environmental Control. PNL-4006, Pacific Northwest Laboratory, Richland, Washington.

the initial liquid temperature and saturation temperature, may be used effectively as a simulant for modeling vapor growth in LGF thermal non-equilibrium vapor generating processes.

Other information requested by the sponsor was provided as needed to assist the development and technical surveillance of the DOE Program.

I.5 STATUS REPORT PURPOSE AND ORGANIZATION

The purpose of this report is to provide a detailed status review of current research addressing issues and needs identified in the DOE's coordinated Assessment Program on the safety and environmental control of liquefied gaseous fuels. Information developed in this Program should assist decisions regarding future facilities, the upgrading of existing facilities, and new hazard control techniques.

The balance of this report consists of a compilation of individual reports describing work that supports the objectives of the DOE Program. These reports are contained as Reports A through N in Section II of this report. To remain topical and preserve the perspectives of individual authors, these reports are presented without appreciable editing or format standardization. Collectively, they provide an update on the status of the principal activities in the LGF Assessment Program, and complement reports published in the previous Status Reports of this series.

SECTION II

THE REPORTS

REPORT A

Description and Analysis of Burro Series 40-m^3 LNG Spill Experiments

R. P. Koopman
R. T. Cederwall
D. L. Ermak
H. C. Goldwire, Jr.
W. J. Hogan
J. W. McClure
T. G. McRae
D. L. Morgan
H. C. Rodean
J. H. Shinn

Prepared for the
Environmental and Safety Engineering Division
U.S. Department of Energy
under Contract W-7405-ENG-48

Lawrence Livermore Laboratory
Livermore, California 94550

REPORT A
TABLE OF CONTENTS

SUMMARY

The U.S. Department of Energy sponsored a series of nine field experiments (Burro series) conducted jointly in 1980 by the Naval Weapons Center, China Lake, California, and the Lawrence Livermore National Laboratory to determine the transport and dispersion of vapor from spills of liquefied natural gas (LNG) on water. The spill volume ranged from 24 to 39 m^3, the spill rate from 11.3 to 18.4 m^3/min, the wind speed from 1.8 to 9.1 m/s, and the atmospheric stability from unstable to slightly stable. An extensive array of instrumentation was deployed both upwind and downwind of the spill pond. Wind speed and direction, gas concentration, temperature, humidity, and heat flux from the ground were measured at different distances from the spill point and at different elevations relative to ground level. The wind and gas-concentration data were processed and analyzed to define the wind field and gas cloud as a function of time. Wind-field, heat-flux, and humidity data were analyzed to further define the fluid dynamic and thermodynamic processes associated with the dispersion of the gas cloud. Data pertaining to differential boiling of LNG and observed rapid phase transition explosions were also analyzed.

The principal conclusions are summarized as follows: The turbulent processes in the lower atmospheric boundary layer dominated the transport and dispersion of gas for all experiments except Burro 8. Burro 8 was conducted under very low wind-speed conditions, and the gravity flow of the cold gas displaced the ambient wind field upward by about 1.5 m, causing the wind speed within the cloud to drop essentially to zero. We believe that what was observed to occur only during Burro 8, under very low wind conditions, is likely to occur on larger spills under a variety of conditions. The ability of large masses of cold dense gas to displace the normal atmospheric flow has profound implications for hazard prediction from large accidental spills. Larger spills are badly needed to determine if this phenomenon is likely to be important in case of an accident.

Large-scale differential boiloff of LNG was observed with resultant enrichment of ethane and propane in the cloud at late times. This ethane-enriched region propagates downwind and represents an additional hazard since it is more easily detonated than the methane-rich majority of the cloud.

Energetic rapid phase transition (RPT) explosions were not expected but did occur under at least two different circumstances during the Burro 6 and 9 tests. The explosions were quite violent and caused some damage to the facility. Two disturbing possibilities associated with the occurrence of RPTs arise: First, RPTs could be energetic enough to turn a small accident into a large one, and, second, the RPT-produced shock wave might be energetic enough to ignite the ethane-rich and more easily detonatable region of the vapor cloud. More large experiments at higher spill velocities will be required to determine how severe this hazard might be.

High-frequency (3–5 Hz) gas-concentration measurements indicate that fluctuations about 5% volumetric concentration are common with 10-s-average concentrations above 1%. This implies that the flammable extent of a gas cloud will be larger than is indicated by the mean lower flammability limit contour generated from either the experimental data or computer model calculations.

The goal of the program is to be able to predict the hazards associated with accidents involving LNG or other liquefied gaseous fuels. To that end data are being used for detailed comparisons with computer models, but it is clear that we do not have enough information on hand to draw general conclusions about the effects of varying atmospheric and spill conditions. The Burro 8 data have demonstrated to us that larger tests are necessary if the relationship between size and atmospheric dispersion is to be understood. Additional field experiments to investigate RPTs and vapor fires are currently underway, as is further analysis of the data and comparison with theory and models.

INTRODUCTION

The Burro series of LNG (liquefied natural gas) spill experiments was performed at the Naval Weapons Center (NWC), China Lake, California, between June 6 and September 17, 1980. These experiments were conducted jointly by personnel from NWC and the Lawrence Livermore National Laboratory (LLNL) as part of U.S. Department of Energy (DOE) research into LNG safety. In the first experiment, Burro 1, approximately 35 m^3 of liquefied nitrogen was spilled onto water to develop a fog-correction algorithm for the infrared gas sensor. In the eight remaining experiments, Burros 2 through 9, 24 to 39 m^3 of LNG was spilled onto water to measure the dispersion of the LNG vapor cloud in the atmosphere under various conditions. Only Burros 2 through 9 are considered in this report, with emphasis on Burros 3, 7, 8, and 9.

A more-detailed description of the Burro series is presented in Ref. 1, together with an extensive compilation of data. The "Experimental Description" section of this report is based largely on selected portions of Ref. 1 and contains brief descriptions of the test facility, instrumentation, data base, and spill experiments. The remainder of the report presents observations and analyses of the data obtained in these experiments. Topics discussed include the interaction of the wind field and gas cloud, LNG vapor dispersion, ground heat transfer, humidity enhancement, differential boiling of LNG, and the rapid phase transitions (RPTs) observed during Burros 6 and 9.

EXPERIMENTAL DESCRIPTION

FACILITY AND INSTRUMENTATION ARRAY

Since 1973, C. D. Lind of the NWC has been investigating the fire and explosion hazards of liquefied fuels. The original 5.7-m^3 spill facility was expanded in 1980 and is now capable of handling up to 40 m^3 of liquefied fuels.

Figure 1 is a site plan showing the layout of the facility. Liquefied fuel is forced out of the 40-m^3 tank through a 20-cm-diam vertical dip tube of stainless steel when the tank is pressurized with gaseous nitrogen (GN_2). A 25-cm-diam insulated spill line of stainless steel runs from the 40-m^3 tank to a junction north of the 5.7-m^3 tank. A 25-cm-diam line continues from this point to the center of the water test basin, where it expands to a diameter of 30 cm at the end, while a 15-cm-diam insulated spill line of stainless steel extends from the junction to the edge of a 15- × 15- × 0.15-m dry pond. A spill plate, attached to the end of the spill pipe (see Fig. 26) and generally located just below the water surface is used to divert the downward flow of LNG horizontally out onto the pond surface.

The water test basin has an average diameter of 58 m, with an average water level about 1.5 m below the surrounding ground level. The average depth of the water is approximately 1 m. The slopes of all but the south bank have been reduced to about 20% to provide less-turbulent wind flow over the water test basin. The terrain immediately downwind of the water test basin rises to a height of about 7 m above the water level at a downwind distance of about 80 m and remains relatively level thereafter.

After the tank is loaded and immediately before the spill, a sample is taken for later analysis to determine the composition of the LNG. At this point all personnel are cleared from the spill site, and subsequent steps are performed remotely. The remote vent valve is closed, the three stages of pressure regulation are set, and the spill tank is pressurized. The cool-down valve is opened, cooling the spill line; then the spill valve is opened and the test is conducted. A "heel" of approximately 1.2 m^3 is usually left in the tank after the test.

A large array of gas-sensing and wind-measuring instruments was deployed upwind and downwind of the spill site to measure properties of both the dispersing gas and the atmosphere into which it was dispersing. A schematic diagram of the array, superimposed on the topography around the spill facility, is shown in Fig. 2. The array centerline was oriented along a bearing of 45° true (N

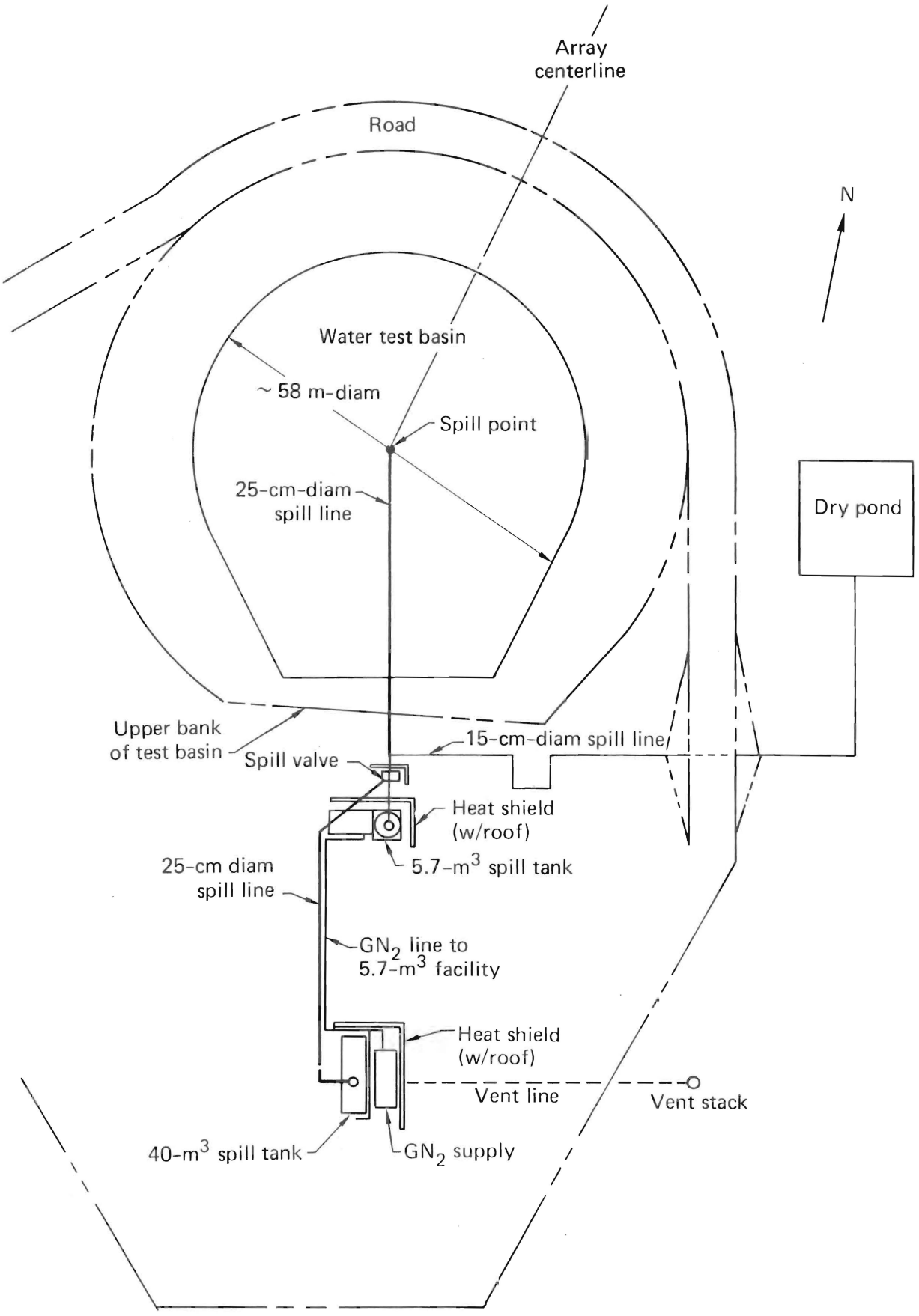

FIG. 1. Site plan of Naval Weapons Center (NWC) spill facility at China Lake.

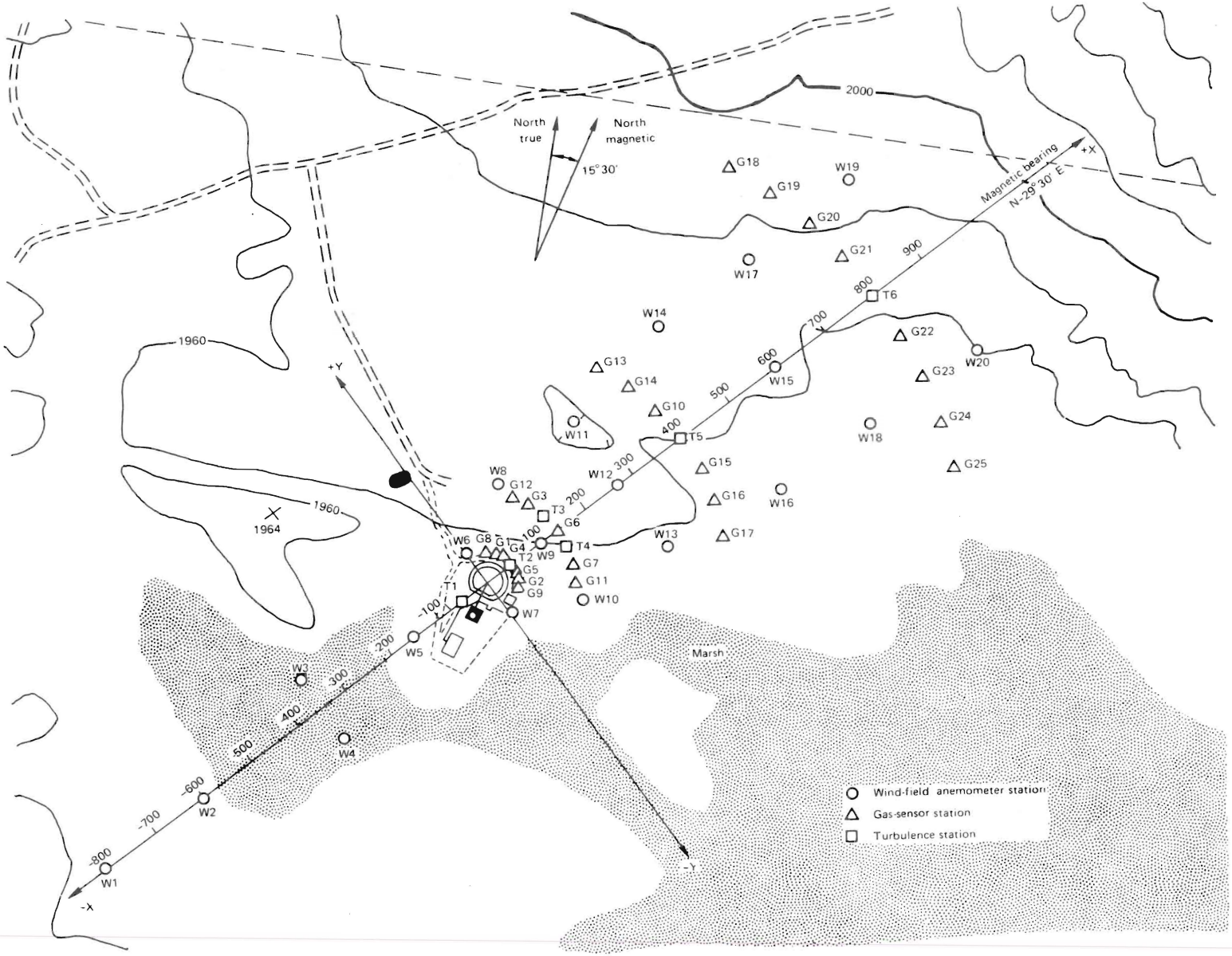

FIG. 2. Instrumentation array for 1980 LNG dispersion tests at the NWC, China Lake.

29° 30′ E magnetic), which coincides with the prevailing southwesterly wind direction (blowing from 225°) for the summer season. The acceptance angle for the array was about 50° (winds from 200 to 250°), and the spacing between gas stations varied from 13 m in the 57-m row to 80 m in the 800-m row.

The large array was composed of three smaller arrays: one array of 2-m-high cup-and-vane anemometers to map the wind field, one three-level array of gas sensors (at 1, 3, and 8 m) to track the cloud, and one three-level array of propeller bivane anemometers (at 1.36, 3, and 8 m) and fast gas sensors (at 1, 3, and 8 m) to track the cloud and to measure turbulence effects. A typical wind-field station is shown in Fig. 3, and a typical turbulence station is shown in Fig. 4.

The 20 wind-field stations were regularly spaced from 800 m upwind to 900 m downwind. The 25 gas stations and 5 turbulence stations were arranged in arcs at 57, 140, 400, and 800 m downwind from the spill point. An additional turbulence station just upwind of the spill pond had bivanes, a humidity sensor, and thermocouples, but no gas sensors.

The gas stations were similar to the turbulence stations, except that they had no anemometers. They also took data at a slower rate (1 sample/s, compared to 3 to 5 samples/s for the turbulence stations). Seven of the gas stations on or near the array centerline had humidity and heat-flux sensors, as well as the normally present gas and temperature sensors. The remaining 18 gas stations had three levels of gas sensors and thermocouples.

All of the stations were battery-powered and microprocessor-controlled, with some onboard memory. They communicated with the data-recording trailer by radiotelemetry, turning on instruments on command and sending back data when polled.

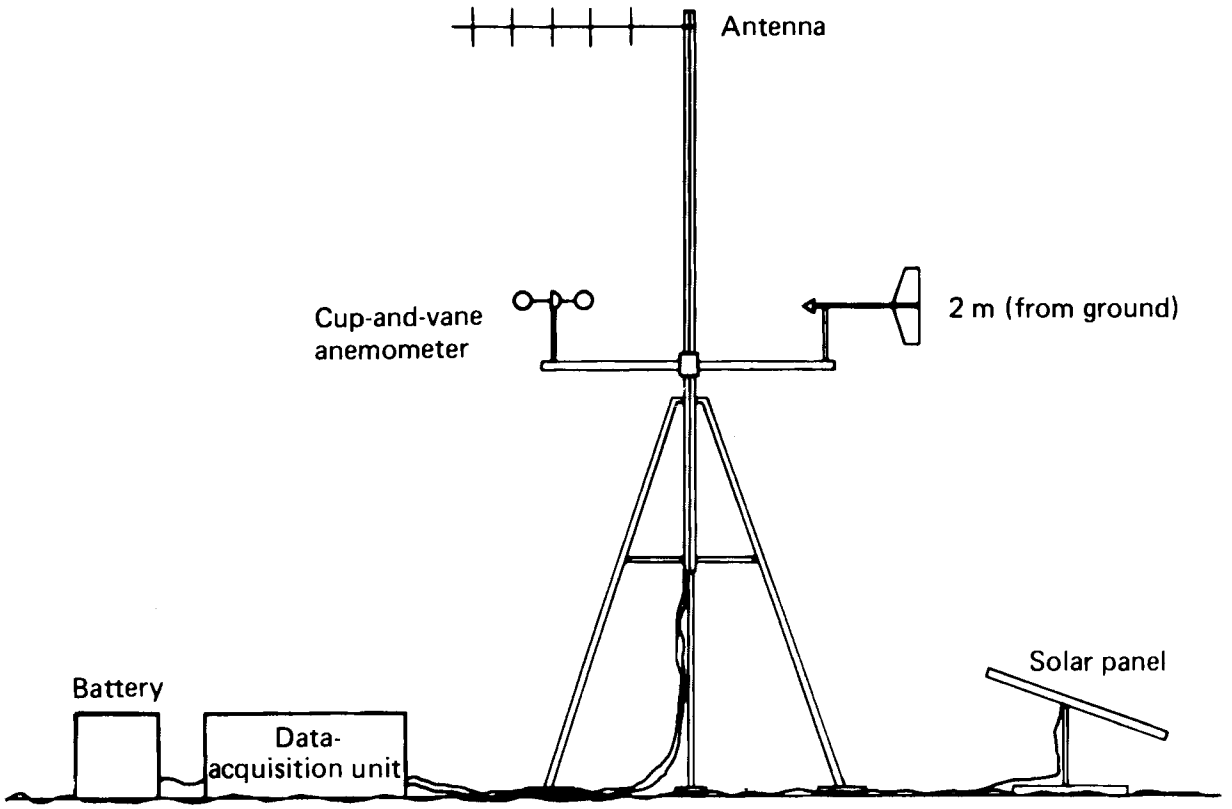

FIG. 3. Typical wind-field anemometer station.

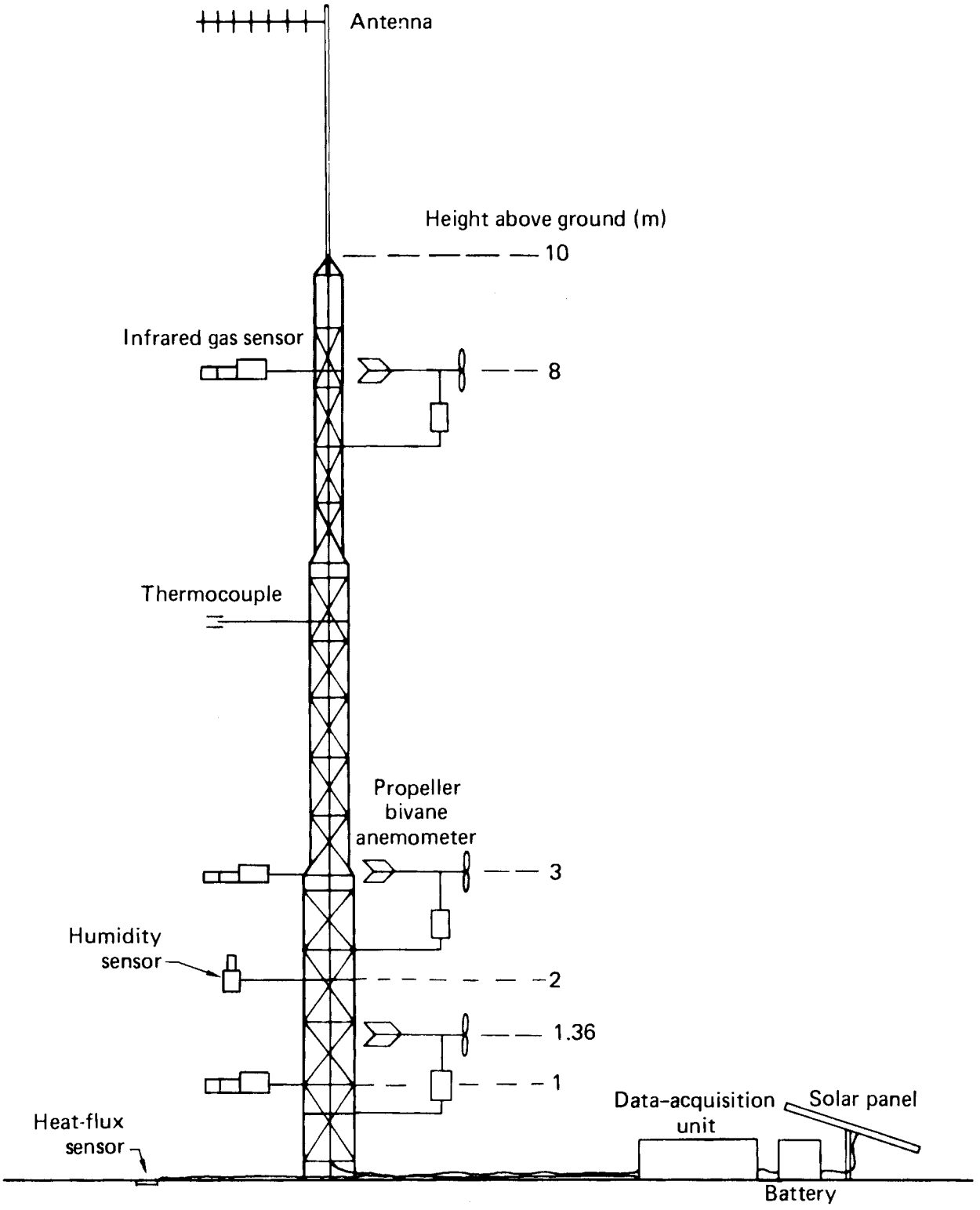

FIG. 4. Typical turbulence station.

INSTRUMENTATION

The instrumentation used in the Burro experiments is described in detail in Ref. 1. The following is a summary of the instruments used to acquire data.

Gas-Concentration Sensors

Three levels of gas-concentration sensors were installed at the 25 gas stations and 5 turbulence stations, for a total of 90 sensors. Thirty-three were infrared sensors developed by LLNL, 45 were IST (International Sensor Technology) solid-state sensors, and 12 were MSA (Mine Safety Appliance) catalytic sensors. A prototype version of a JPL (Jet Propulsion Laboratory) infrared sensor was fielded on Burros 7, 8, and 9, yielding data that agreed well with the LLNL infrared sensor operating next to it. In the following, gas concentration is given in terms of volumetric percent.

LLNL Infrared Sensors. We developed the LLNL infrared sensors because gas sensors suitable for use in LNG spills did not exist. What was needed was a fast, differential, infrared absorption sensor that was portable, would work in the dense fog associated with LNG spills, and would detect separately methane, ethane, and propane. The LLNL sensor[2] is fast and was developed to work in the fog (atmospheric water vapor condensed by the cold LNG vapors) and to detect separately methane and ethane-plus-propane. The JPL sensor[3] is also fast, but was developed to work in fog-free regions and to detect separately methane, ethane, and propane.

The 33 LLNL infrared sensors were deployed on six towers in the first two arcs or rows in the array and on the five downwind turbulence towers. Because these infrared sensors were expensive, IST and MSA sensors were purchased to complete the array.

In the LLNL sensors, infrared radiation from a source passes through an optical path open to the atmosphere. If hydrocarbons and/or water droplets are present, absorption (or scattering) occurs and the amounts of absorption specific to methane, ethane-plus-propane, and fog are detected at a pyroelectric detector. Absorption specific to these species is defined by four narrow band-pass filters between 3.0 and 3.9 μm. In the absence of fog, the two middle bands are used to determine the methane and ethane-plus-propane concentrations and the other two bands are used as reference channels to compensate for changes in system throughput resulting from dust on the lenses or temperature-induced baseline shifts. In the presence of fog, the two outer bands are also used to correct for spectral scattering due to fog particles. The calibration algorithms are based on experimental data for the hydrocarbons and on Mie scattering calculations and experimental data for fog obtained during the Burro 1 liquid-nitrogen spill. The single-gas calibration uncertainties were $\pm 5.5\%$ and $\pm 2.5\%$ of the gas-sensor reading, or $\pm 0.9\%$ and $\pm 0.3\%$ gas concentration for methane and ethane, respectively. If the reference channels were not used for compensation, methane uncertainties did not change markedly, but ethane uncertainties increased to $\pm 6.0\%$ of the sensor reading. In calibrations with methane–ethane mixtures, the ethane uncertainties were only slightly larger, but the methane results were consistently about 10% too high, probably because of the form of the calibration algorithm. The sensor responds to propane with about 40% more sensitivity than it does to ethane, so 1% propane appears as 1.4% ethane in the ethane-plus-propane channel. Several calibration checks in the field have shown that the calibrations are quite stable in that they did not change over four months of operation in the desert environment. The overall accuracy of the system can be estimated by combining the gas-concentration results with a self-consistency examination of the data from Burro 1, which had fog but no hydrocarbon gas. For the great majority of the Burro 1 data, the results showed quite variable fog concentrations but essentially no apparent hydrocarbons. The dense fog caused some sharp spikes to occur in the methane and ethane-plus-propane channels. However, the apparent average methane and ethane-plus-propane concentrations during the time dense fog was present were only 0.1 and 0.9%, respectively. Thus, the overall uncertainty in either the methane or ethane-plus-propane results is about $\pm 1\%$ gas concentration in the presence of dense fog.

IST Solid-State Sensors. The IST sensors were designed to detect hydrocarbon gas concentrations as high as 25%. They proved to be sensitive to humidity in the presence of methane, and they showed variable sensitivity to the higher hydrocarbons, ethane and propane. Corrections were developed for these effects and applied to the data.

Some sensors exhibited calibration and gain changes during the course of the experiments; consequently, all sensors were recalibrated after completion of the effort at China Lake. The result of these corrections to the IST sensor data is a fairly high residual uncertainty in their accuracy. Our current estimate is that the uncertainty is 20 to 30% of the indicated value for concentrations less than 5%, and, for higher concentrations, as high as 50% for some of the poorer sensors. When corrected IST data were compared with data from an LLNL infrared sensor at the same location during Burros 8 and 9, they showed agreement to within about 10% of reading.

MSA Catalytic Sensors. MSA sensors are well-understood, standard commercial units that operate on the catalytic principle and work well as long as the gas concentration remains below the stoichiometric mixture (10% for methane). The sensor response is very linear, and the uncertainty is about 10% of reading.

Humidity Sensors

Eight humidity sensors were mounted at stations throughout the array, including one at upwind turbulence station T-1. These sensors were developed at LLNL specifically for use in cold fog. The sensitive element is the commercially available Humicap (Vaisala). The Humicap cannot tolerate contact with liquid water so it is protected by a porous sintered frit that is heated to 40°C to evaporate the water droplets. Calibration data indicate a linear response over the 10 to 60% relative humidity range at 40°C and a nonlinear response below 10%. The average sensor accuracy is ±0.5% relative humidity. Side-by-side comparisons of the instruments show agreement to better than ±2%, while long-term drift is estimated to be less than ±3% relative humidity.

Wind-Field Anemometers

The wind-field measurements were made by commercially available two-axis cup-and-vane anemometers (Met-One) located at 20 stations, 2 m above the ground, both upwind and downwind of the spill point. They have a starting threshold of 0.2 m/s and a response-distance constant of 1.5 m. Data taken by these instruments were averaged for 10 s before being transmitted to the data- recording trailer. The wind-field anemometers were calibrated with respect to three standards from the same batch. The standards were then sent to the National Bureau of Standards (NBS) for calibration in a wind tunnel, and the results of this calibration were used for final calibration of the field instruments. The uncertainty in speed for these instruments is ±1%, or 0.07 m/s, whichever is greater.

Turbulence Anemometers

The six turbulence stations used standard, commercially available bivane anemometers (R. M. Young Co). Three of these anemometers were mounted on each tower at heights of 1.36, 3, and 8 m so that the vertical wind profile, as well as the various parameters related to atmospheric turbulence, could be determined. These anemometers have a starting threshold of 0.1 to 0.2 m/s and a response-distance constant of 1.0 m. Factory-supplied calibration curves were used, and data were taken at the rate of 3 to 5 Hz.

Heat-Flux Sensors

The heat-flux sensors were standard, commercially available heat-flux plates (Hy-Cal Engineering). They consisted of two banks of thermopiles separated by material of known thermal conductivity, forming a thin rectangular wafer that was buried just below the soil surface. These devices, along with the humidity sensors, were installed at seven downwind gas stations close to the array centerline.

Thermocouples

Standard Chromel-Alumel (type K) thermocouples were colocated with each gas sensor to provide temperature measurements of the gas cloud. The 10-mil thermocouples had a response time of about 0.5 s in a 5-m/s wind, corresponding roughly with the infrared gas sensors on the gas stations, which averaged data for 1 s. Data from the upwind NWC meteorological tower were used to determine the atmospheric temperature gradient in the lower 15 m.

Cameras

Photography was an important diagnostic tool, and cameras were in operation in all experiments except Burro 7. Remotely controlled 16-mm motion picture cameras were used in three locations. The crosswind camera was on top of the control bunker, about 220 m from the spill point. The upwind camera was about 70 m upwind of the spill

point (close to T-1) and about 1.5 m above ground level. The overhead camera was about 120 m north (downwind) of the spill point and about 45 m above ground level. The cameras were supplied by NWC personnel and operated from the bunker.

Infrared Imagers

The EG&G Remote Measurements group provided infrared imaging of several spills (Burros 2, 4, 6, and 9), using a helicopter-mounted Inframetrics dual-band infrared imager. The instrument had two channels—one sensitive to radiation with wavelengths between 4 and 6.5 μm and one sensitive to radiation with wavelengths between 7 and 14 μm. A strong methane infrared absorption band between 7 and 8.5 μm should allow the methane cloud to be imaged in the long-wavelength channel, using the ground as a thermal radiation source.

The overflights were successful in imaging the gas cloud as it dispersed downwind. Traces of the cloud were seen, in the 7- to 14-μm channel, as far downwind as 1500 m, where the gas concentration would have been substantially less than 1%. Unfortunately, the cold gas also cooled the ground, changing the source characteristics. Consequently, the observed image was a combination of methane absorption and the cold-ground effect.

Instrument modifications have been proposed to eliminate this effect. If the instrument were modified so that both channels were 7- to 14-μm channels and one channel were filtered so that it saw no methane absorption but only the cold-ground effect, the differences between the two channels would be approximately that part of the signal due to methane absorption only.

An attempt was made to measure the size of the LNG pool on the Burro 9 experiment by reducing the imager sensitivity to see through the dense fog and image the LNG pool against the water.

DATA RECORDING AND STORAGE

The data from each LNG spill were transferred from magnetic tape to the MASS storage system[4] at the LLNL Computation Center for archival preservation of the data. Most data manipulation, plotting, and contour generation were done with data-base files, created by the data-base management system FRAMIS,[5] using an LLNL-developed data analysis system called MATHSY.[6] This interactive, array-processing, mathematics and graphics system has been a powerful tool for analyzing, handling, and displaying the large quantities of data from the Burro experiments.

TEST SUMMARY

Table 1 is a summary of the test and meteorological conditions for the eight LNG spills in the Burro series. The array centerline stayed fixed at 225° for the duration of the series. Using wind-field data from the twenty 2-m-high anemometer stations, the mean and standard deviations for wind direction and wind speed were calculated over a 6-min period that began at the start of the spill. The descriptive atmospheric-stability category is based on the Richardson number. The numerical values for atmospheric-stability indices and other meteorological parameters were determined as described below.

The temperature and temperature-difference values were measured on an upwind NWC meteorological tower close to turbulence tower T-1. Temperature was measured at a height of 2 m, and temperature difference was measured between the 2-m sensor and sensors at heights of 1, 5, 10, and 15 m. T star (T_*) was calculated by linear regression, using the formula

$$T_* = \frac{\partial T}{\partial(\ln z)} \quad , \tag{1}$$

where z is the height above ground level.

The T_* values did not vary significantly during any experiment. The diabatically adjusted friction velocity, u star (u_*), was derived from turbulence-tower and wind-field data, using the relationship

$$u(z) = \frac{u_*}{k}\left(\ln\frac{z}{z_0} - \psi\right) \quad , \tag{2}$$

whose terms are defined at the bottom of Table 1.

For neutral-stability tests, the scaling parameters approach asymptotic values ($\psi \to 0$ and $\phi \to 1$ as $R \to 0$); therefore,

TABLE 1. Burro experiment summary and meteorological parameters (see Symbols below).

Parameter	Experiment							
	Burro 2	Burro 3	Burro 4	Burro 5	Burro 6	Burro 7	Burro 8	Burro 9
Date	6/18/80	7/2/80	7/9/80	7/16/80	8/5/80	8/27/80	9/3/80	9/17/80
Q (m^3)	34.3	34.0	35.3	35.8	27.5	39.4	28.4	24.2
dQ/dt (m^3/min)	11.9	12.2	12.1	11.3	12.8	13.6	16.0	18.4
u (m/s)	5.4 ± 1.8	5.4 ± 1.2	9.0 ± 1.2	7.4 ± 1.1	9.1 ± 1.1	8.4 ± 1.2	1.8 ± 0.3	5.7 ± 0.7
θ (deg)	221 ± 14	224 ± 13	217 ± 7	218 ± 11	220 ± 7	208 ± 5	235 ± 6	232 ± 4
Wind-speed tendency	Decreasing	Fairly constant	Fairly constant	Fairly constant	Fairly constant	Nearly constant	Decreasing	Slowly decreasing
Atmospheric stability	Unstable	Unstable	Slightly unstable	Slightly unstable	Slightly unstable	Neutral to slightly unstable	Slightly unstable	Neutral
T_2 (°C)	37.6	33.8	35.3	40.5	39.2	33.7	33.1	35.4
T* (°C)	-0.57	-0.65	-0.65	-0.60	-0.57	-0.23	+0.145	-0.100
u* (m/s)	0.248	0.249	0.403	0.333	0.406	0.372	0.074	0.252
α	1.40	1.46	1.17	1.23	1.14	1.06	0.623	1.05
H (W/m^2)	-122	-154	-159	-131	-132	-41	+2.2	-10
K_m (m^2/s)	0.278	0.291	0.377	0.327	0.371	0.316	0.037	0.212
R_2	-0.178	-0.221	-0.054	-0.079	-0.044	-0.018	+0.121	-0.014
L (m)	-11.2	-9.06	-37.1	-25.5	-45.5	-114	+16.5	-140

Symbols:

Q = spill volume

dQ/dt = spill rate

u = mean and standard deviation of wind speed at 2-m height

θ = mean and standard deviation of wind direction

T_2 = temperature at 2-m height

T* = dt/dlnz

u* = friction velocity, diabatically adjusted

α = turbulent Prandtl number, K_h/K_m

K_h = heat diffusivity at 2-m height

K_m = momentum diffusivity at 2-m height, diabatically adjusted

H = sensible heat flux, negative upward

R_2 = Richardson number at 2-m height

L = Monin–Obukhov length scale.

$$u_* = \frac{k}{\phi}\frac{\partial u}{\partial(\ln z)} \qquad (3)$$

$$R = \frac{\frac{g}{T}\left(\frac{\partial T}{\partial z} + \frac{g}{C_p}\right)}{\left(\frac{\partial u}{\partial z}\right)^2} \qquad (4)$$

where k = 0.4 (Von Karman's constant) and u = wind speed (space-averaged). One can then iteratively solve the wind-profile equation for the roughness length. At China Lake, the roughness length was approximately constant at a value of $z_0 = 2.05 \times 10^{-4}$ m.

where g = 9.8 m/s^2 and C_p = 1005 W s kg^{-1} °C^{-1}. If R is assumed to be equal to z/L, where L is the Monin–Obukhov length, the turbulent Prandtl number, α, and the parameters ϕ and ψ can be expressed as

$$\alpha = 1/\phi \quad ,$$
$$\phi = (1 - 16R)^{-1/4} \qquad \text{for } R \leq 0 \quad , \qquad (5)$$
$$\psi = 1.1(-R)^{1/2} \quad ,$$

and

$$\alpha = 1/\phi \quad ,$$
$$\phi = 1 + 5R \quad , \qquad \text{for } R > 0 \quad , \qquad (6)$$
$$\psi = -5R \quad ,$$

according to the theory of Dyer and Businger,[7,8] as modified from Lettau[9] with our approximations.

The sensible heat flux, H, defined to be negative upward, is calculated from

$$H = \rho C_p k \alpha^2 u_* \left(T_* + \frac{gz}{C_p} \right), \qquad (7)$$

where $\rho = 1.13 \times 10^{-3}$ g/cm^3 ($\pm 1\%$ for 30 to 40°C).

The diabatically adjusted momentum diffusivity, K, and the Monin–Obukhov length are calculated from the formulas

$$K = u_* kz/\phi \quad , \qquad (8)$$

and

$$L = \frac{\frac{u_*^3}{k}}{\frac{g}{T}\left(\frac{H}{\rho C_p}\right)} \qquad (9)$$

VAPOR DISPERSION

GENERAL ANALYSIS

Pool Size

The airborne infrared imager was used to measure pool size during the Burro 9 experiment. Its sensitivity was reduced in an attempt to see through the fog and image the LNG pool against the warm pond. The observed image was about 10 m in diameter; however, this should not be considered representative of other experiments since RPTs blew away the spill plate early in the test, drastically changing the nature of the LNG pool on the water surface.

Gas-Concentration Contours

The LNG vapor-concentration data were used to generate two-dimensional contour plots at 10-s intervals during the experiments. A 10-s average was chosen somewhat arbitrarily; the intent was to use an averaging time that was long enough to average out short-wavelength (much less than cloud width) fluctuations, but short enough to preserve cloud meander. Contour plots are generated for several surfaces: horizontal surfaces at heights of 1 and 3 m above the ground, and vertical crosswind cylindrical surfaces at each row of the sensor array. The contours are of total hydrocarbon concentration, with the data from the LLNL infrared methane and ethane-plus-propane channels being combined to correspond to the IST and MSA total hydrocarbon measurements. Data from the faster response-time instruments are also averaged, using a 10-s running average, so that all the data have approximately the same time constant. Therefore, the contours describe the 10-s-average LNG vapor–concentration distribution on a surface at a given time.

The horizontal contours are calculated over a region that extends downwind from the spill point ($x = 0$) to the final row of sensors at 800 m (see Fig. 2). To close the contours in the source region, the concentration at $x = 0$ is arbitrarily defined by a hyperbolic concentration distribution that is held constant during the spill and is decreased linearly to zero after the spill valve is closed.

In both the horizontal and vertical contour-plot concentrations, a "dummy" station is added to both ends of each sensor row at a distance equal to the station spacing for that row. When the LNG vapor cloud is well within the array and the concentration at the end of the row is essentially zero (<1%), the concentration at the corresponding "dummy" sensor is set equal to zero. If part of the cloud extends beyond the edge of the array, the "dummy" sensors are ignored and the contours are truncated at the edge of the array.

The gas concentration at each station location is set equal to zero at a height of 12 m. The concentration at the ground is extrapolated from the measured values at heights of 1 and 3 m. When the 3-m concentration is less than the 1-m value, the ground-level concentration is determined by using a quadratic extrapolation that passes through the 1- and 3-m concentration values and has a zero concentration gradient at the ground. For those cases where the 3-m concentration is greater than the 1-m value, the ground-level concentration is linearly extrapolated from these two values. Concentrations at points within the calculational region are determined by a linear interpolation in three dimensions.

Interpolating over the long distances between sensors in the 140-, 400-, and 800-m arcs produces some uncertainty in the calculation of gas-concentration values between these arcs. A linear interpolation scheme was used because of its inherent simplicity and ease of interpretation. If different interpolation schemes are used, different results are obtained between arcs. In particular, the distance to the lower flammability limit (LFL), i.e., the 5% contour for methane, is generally between the 140- and 400-m arcs for these tests. If we use Burro 3 as an example, the linear interpolation scheme produces an LFL distance of 255 m maximum. If the concentration is assumed to decrease with downwind distance as x^{-n}, then LFL distances of 252, 207, and 188 m are obtained for n = 1.0, 1.5, and 2.0, respectively. Thus it appears that linear interpolation gives a maximum LFL distance. Analysis of contours from all of the experiments indicates that the uncertainty in the LFL distance is approximately −40 to +20 m.

Since the distances between sensors on a tower and stations in an arc are much less than the distances between arcs, the uncertainty in contour location is much less for the vertical contours than it is for the horizontal contours. We estimate the uncertainty in the position of the vertical contours to be less than 1 m.

Cloud-Centerline Calculations

The wind field is one of the major factors influencing the transport and dispersion of the LNG vapor cloud. During each of the Burro experiments, the wind speed and direction varied significantly with time and position, and had a noticeable effect on the movement of the LNG vapor cloud. To more quantitatively describe the cloud meander caused by wind-field variations, an estimate was made of the LNG vapor-cloud centerline as a function of time.

The cloud-centerline calculation is performed with the ATMAS atmospheric transport code.[10] Using wind-velocity data obtained from the 20 wind-field stations and applying a 1/r interpolation–extrapolation scheme, the code estimates the wind velocity over the entire region of interest. Every 10 s the wind field is updated with new 10-s-averaged wind-velocity data. The cloud centerline is generated by creating, every 2.5 s, a marker particle (conceptionally, using ATMAS) at the spill point and then allowing it to be transported by the wind field. ATMAS calculates the marker-particle trajectories, using the atmospheric advection–diffusion equation with the diffusion terms set equal to zero. The positions of the marker particles constitute the cloud centerline.

A wind field whose velocity is uniform in time and space gives rise to a straight centerline, with the marker particles equally separated along the centerline. This was not the case for the Burro experiments, as can be seen from the wind-velocity variability statistics given in Table 1. As previously noted, there was significant variation in both wind speed and direction during the experiments.

In general, the agreement between the wind-field-calculated cloud centerline and the orientation of the horizontal gas-concentration contours is quite good. This is especially true when the centerline is near the center of the array, as was the case with Burro 9, as shown in Fig. 5. Although there were a few exceptions to this good agreement, they usually resulted from the presence of inoperative gas sensors, which tended to distort the concentration contours. The agreement was also somewhat poorer near the edges of the array, as in the Burro 7 experiment (see Fig. 6), primarily because of the lack of wind-velocity data in the regions near the edges of the array and because of the 1/r interpolation–extrapolation scheme used on ATMAS being somewhat biased in these regions.

Mass-Flux Calculations

The calculation of the mass flux of gas through an arc of gas-sensor stations can be used to determine indirectly the vapor generation rate on the spill pond. This is important since vapor generation was not measured directly. If the mass flux is integrated over time, it can be compared with the total quantity of LNG spilled to determine

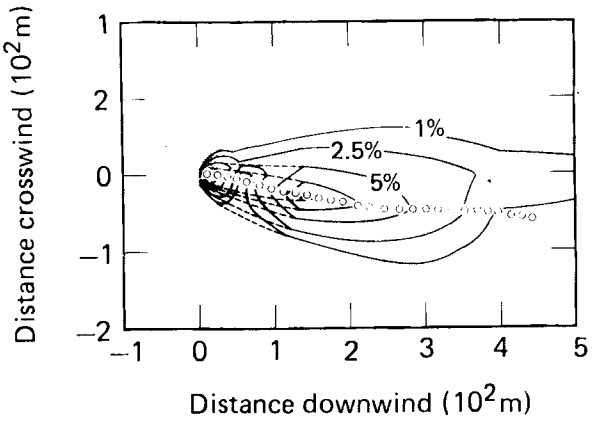

FIG. 5. Horizontal gas-concentration contours and central wind-field flowline for the Burro 9 experiment. Contours shown are 1, 2.5, 5, 7.5, and 10% by volume.

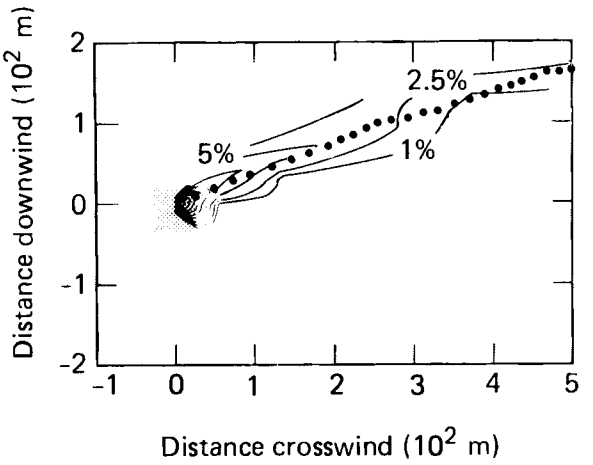

FIG. 6. Horizontal gas-concentration contours and central wind-field flowline for the Burro 7 experiment. Contours shown are 1, 2.5, 5, 7.5, 10, 12.5, and 15% by volume.

the mass balance and how well the array was able to measure the dispersing gas cloud. Such an evaluation is necessary to determine whether the number of sensors and their locations provided adequate coverage and to determine what coverage will be necessary on future experiments. Mass flux was calculated for the 140-m arc for Burros 8 and 9. Because of the low wind conditions for Burro 8, the cloud spread exceeded the width of the array, but most of the cloud was measured. On Burro 9, the entire cloud remained within the array as it traveled downwind; consequently, it provides a good test of mass balance.

The spatially integrated mass flux F(t) through the cylindrical surface of radius r, centered on the spill point at time t, is given by

$$F(t) = \frac{pM}{R} \int_z \int_\theta \frac{c(z,\theta,t)u(z,\theta,t)}{T(z,\theta,t)} \, r d\theta dz \quad , \tag{10}$$

where p is ambient atmospheric pressure, M is molecular weight, R is the gas constant, c is gas concentration, u is wind component normal to arc, T is temperature, θ is direction, and z is height. The cumulative mass is obtained by integrating Eq. (10) over time. Equation (10) is integrated numerically, with accuracy being dependent on the number of points used to approximate the integrand in space and time.

Gas-concentration values were interpolated by appropriate linear and quadratic relations described in the previous section. Wind-speed interpolation was logarithmic with height, and temperature interpolation was logarithmic with height from 0.1 to 1 m and linear above that.

Results of the mass-flux calculations for Burro 9 are presented in Fig. 7a. Integrating the interpolated data gives an integrated mass flux, shown by the dotted line. The arrival and departure of the cloud are quite obvious. The decrease in flux between 45 and 70 s is attributed to RPTs disrupting the vapor source. After integrating the flux from 0 to 200 s, a total mass of 7,439 kg is calculated to have passed through the 140-m arc. This represents 72.3% of the 10,285 kg spilled, and is a reasonably good accounting of the mass released. Errors in the gas-sensor calibrations would contribute to this discrepancy, as would the generally sparse nature of the gas-sampling (particularly in the vertical) array. The major source of uncertainty is probably due to the mud and water thrown on the sensors by the large RPTs. The readings appear to have been lowered enough on at least one of the stations to account for most of the 28% of the gas missing from the analysis. Taking this into account, the degree of agreement is quite satisfactory and indicates a good overall accounting of the gas-cloud and sensor calibrations.

Burro 8 was not affected by RPTs. Results of the mass-flux calculations are presented in Fig. 7b. The mass flux shows the arrival and rather gradual

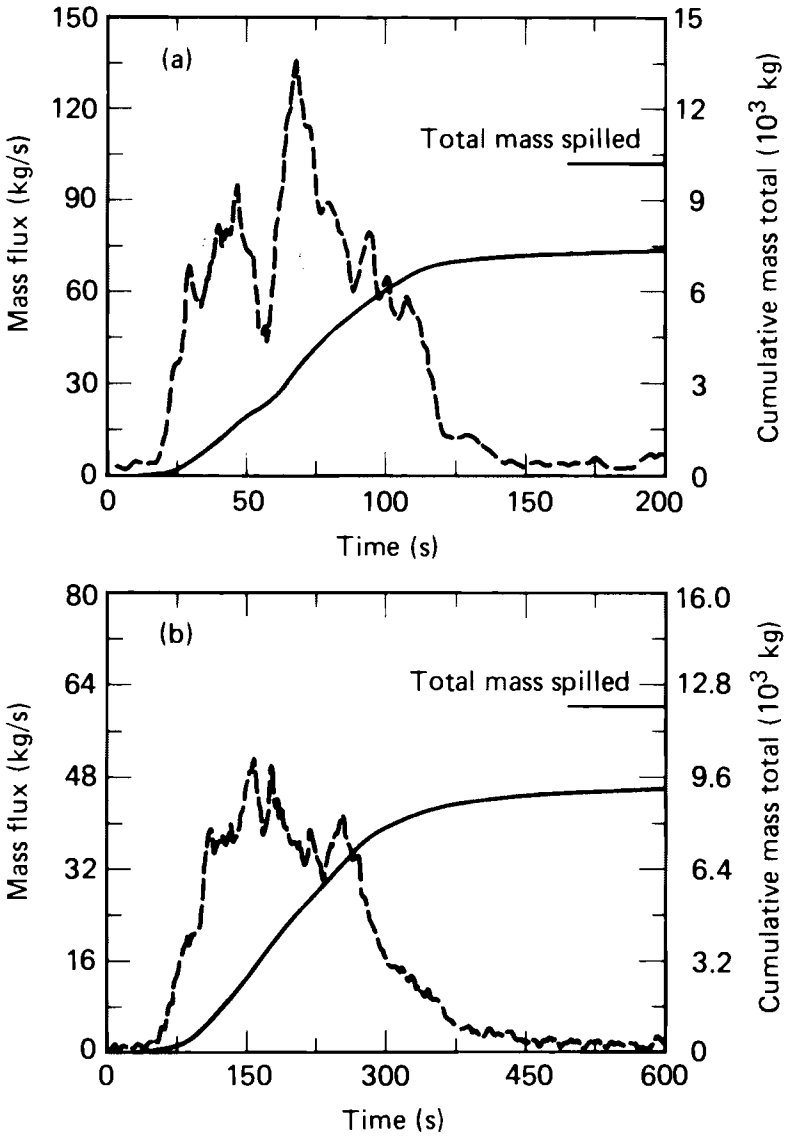

FIG. 7. Mass flux and integrated total mass for (a) Burro 9 and (b) Burro 8 (140-m arc).

departure of the cloud. Integrating from 0 to 600 s gives a total measured mass of 9,193 kg through the 140-m arc, or 76.2% of the total spilled (12,070 kg). Overhead photography indicated that the cloud spread was greater than the width of the array, an observation supported by significant measured gas concentrations at both edges of the array. If one were to assume that the ends of the arc were each extended by one tower—each 30 m beyond the present outboard towers—and that the concentration dropped linearly to zero at these assumed towers, the total mass would be 11,520 kg, or 95.4% of the total spilled. Thus we conclude that most of the cloud was contained within the 140-m arc and that concentrations beyond the edge towers probably dropped off quite rapidly.

GAS-CLOUD CHARACTERISTICS

As defined by the data in Table 1, the Burro experiments may be grouped in four categories according to the conditions for the experiments: (1) Burros 2 and 3 for low spill rates, moderate wind speeds, and unstable atmospheric conditions; (2) Burros 4–7 for low spill rates, high wind speeds, and unstable atmospheric conditions; (3) Burro 8 for high spill rate, very low wind speed, and slightly stable conditions; and (4) Burro 9 for high spill rate, moderate wind speed, and neutral atmospheric stability.

The gas-cloud centerline was best aligned with the array centerline for Burros 3, 5, 8, and 9. The array of operational gas sensors (see Fig. 2) was

most complete for Burros 7–9, but RPTs adversely affected the sensors in the 57-m arc during Burros 6 and 9.

After considering the above, Burros 3, 7, 8, and 9 were selected for discussion of gas-cloud characteristics for this report, one from each experimental category.

Burro 3

The Burro 3 cloud remained within the array, except at the 57-m arc, where it extended beyond both sides of the array between 150 and 200 s. The downwind location of the lower flammable limit (LFL), corresponding to 5% volumetric gas concentration at the 1-m level, is plotted for Burro 3 as a function of time in Fig. 8, together with similar plots for the other selected experiments. The downwind tip of the region enclosed by the 5% contour (LFL contour) extended to a maximum downwind distance of 270 m, with a width of about 80 m between 60 and 120 s (see Fig. 9). At about 150 s, the distance to the LFL decreased to about 100 m and the cloud bifurcated, producing high concentrations at the higher stations in the 57-m arc. Cloud bifurcation occurred during several experiments, and it appears to have been caused mainly by aerodynamic interaction between the gas cloud and the wind. The bifurcation disappeared at 190 s and the LFL moved downwind again at 220 s, after shutdown but before the cloud dissipated. The downwind extent of the cloud for any value of gas concentration was always less at the 3-m level than it was at the 1-m level, and the gas concentration decreased with height at all instrument arcs. The downwind location of the upper flammable limit (UFL), corresponding to 15% volumetric gas concentration, was almost always upwind of the 57-m arc, except during cloud bifurcation at 50 s and again at 150–180 s, when it extended to about 70 m downwind.

Burro 7

The Burro 7 cloud always extended beyond one edge of the array, but the cloud centerline appeared to move on and off the array several times during the spill. Burro 7 is an excellent example of cloud meander. The downwind location of the LFL for Burro 7, at the 1-m level, is plotted as a function of time in Fig. 8. The LFL location oscillated between about 100 and 200 m. Most of this variation was caused by the meandering of the cloud relative to the edge of the array (see Figs. 10a, and 10b), but some may have been caused by bifurcation of the 5% contour. The vertical gas-concentration contours for the 57-, 140-, and 400-m arcs showed less and less of the cloud within the array with increasing downwind distance. Because of this trend and the cloud meander, the location of the LFL is uncertain. Gas concentration decreased with height at all instrument arcs. The downwind location of the UFL was slightly downwind of the 57-m row (perhaps 20 m) during much of the spill, but the true location is uncertain because these high concentrations occurred at the end of the 57-m arc.

Burro 8

The Burro 8 cloud was centered, but extended beyond both sides of the array. However, mass-balance calculations indicate that most of the gas was accounted for within the array. The downwind location of the LFL for Burro 8, at the 1-m level, is plotted as a function of time in Fig. 8. Only in this case did the LFL appear to stabilize at a given location, approximately 320 m.

The Burro 8 cloud is especially interesting because the very low wind speed permitted the gravity flow of the cold, dense gas to be almost independent of the surrounding atmospheric boundary layer. Photography showed that the cloud extended about 40 m upwind of the spill point, as well as beyond both sides of the array. The cloud was wider and lower in height than that of any of the other Burro experiments. Figure 11a shows the 1-m gas-concentration contours at 200 s; this example is representative of these contours from about 100 to 260 s. As shown, the cloud was bifurcated much of the time, probably because of the interaction between the lateral gravity flow and the longitudinal atmospheric flow. The cloud, therefore, tended to divide into two lobes that appeared to be affected by the terrain. The flow of the upper one in Fig. 11a is uphill (Fig. 2), and the lower one is along the edge of the dry lake bed. Consequently, there is probably more gas in the lower (left) lobe than in the upper (right) lobe, as shown in Fig. 11b. The cloud height measured at the 57-m arc was much less than that for the other experiments. For example, the sensors at the 3-m elevation in the 57-m arc did not detect any gas until between 100 and 120 s, even though many of the sensors at 1 m detected gas at 20 s. This can be seen in Fig. 12, where (a) shows the low flat cloud that existed for the first 100 s and (b) shows the results of the introduction of some turbulence at 120 s.

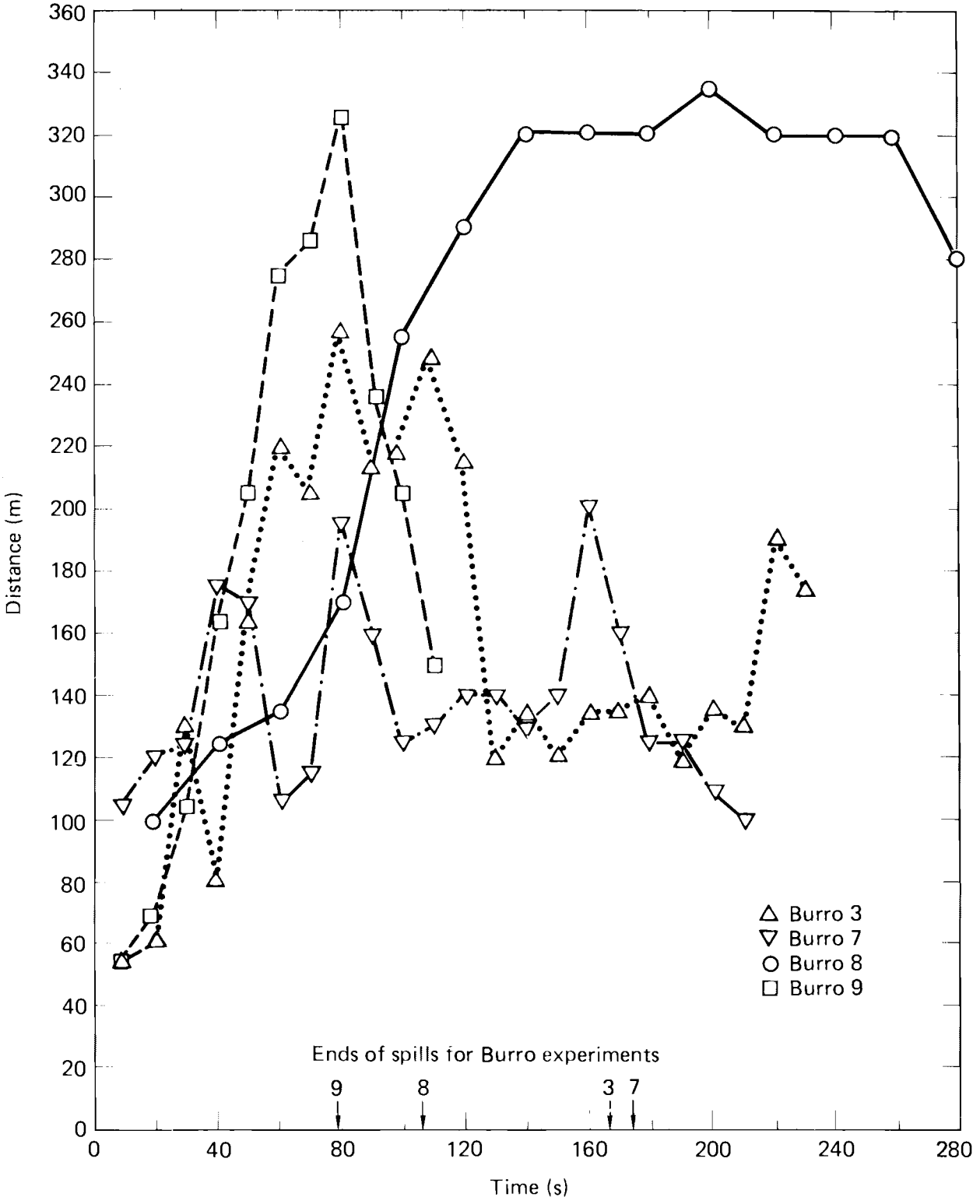

FIG. 8. Radial downwind distance to lower flammable limit (LFL) from gas-concentration contours at 1-m elevation for Burros 3, 7, 8, and 9.

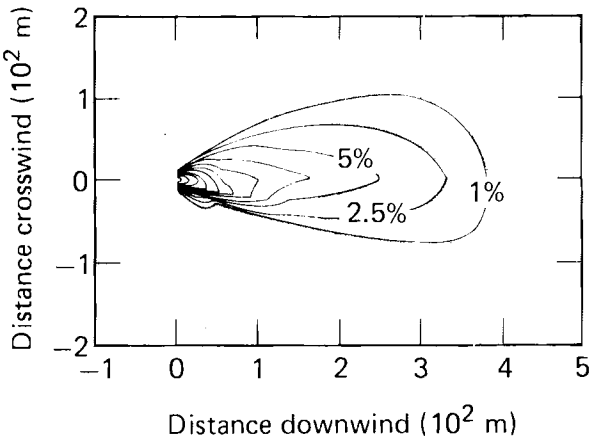

FIG. 9. Horizontal concentration contours for Burro 3, showing cloud shape during maximum downwind extent of the LFL. Gas-concentration contours are 1, 2.5, 5, 7.5, 10, 12.5, and 15% by volume.

The LFL at the 1-m level extended about the same distance downwind in both lobes (about 320 m, see Figs. 8 and 11a). However, the maximum concentration in the downhill lobe (left in Fig. 11b) may have been missed since ~5% concentrations were detected at the left edge of the 400-m row between 400 and 500 s, which may have been due to the meander of this part of the cloud back across the sensors.

Burro 9

The cloud was within the array for the entire test, and most of the gas sensors were operational on Burro 9. Unfortunately, RPT explosions adversely affected the data from the 57-m arc and slightly affected data from the 140-m arc. The downwind location of the LFL for Burro 9, at the 1-m level, is plotted as a function of time in Fig. 8. The LFL location did not stabilize during the short

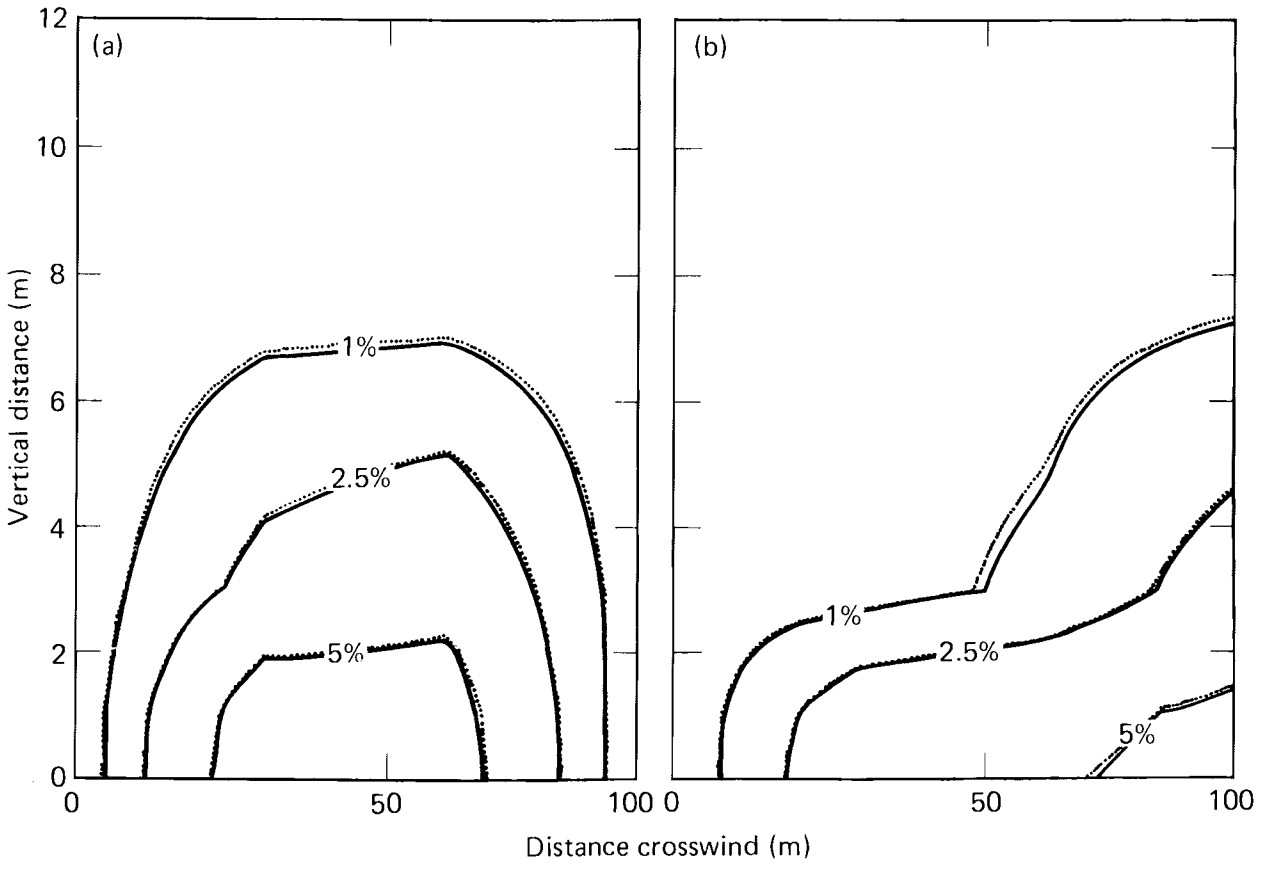

FIG. 10. Vertical concentration contours, 140-m arc, showing Burro 7 cloud meander (a) within array at 160 s and (b) over edge of array at 170 s.

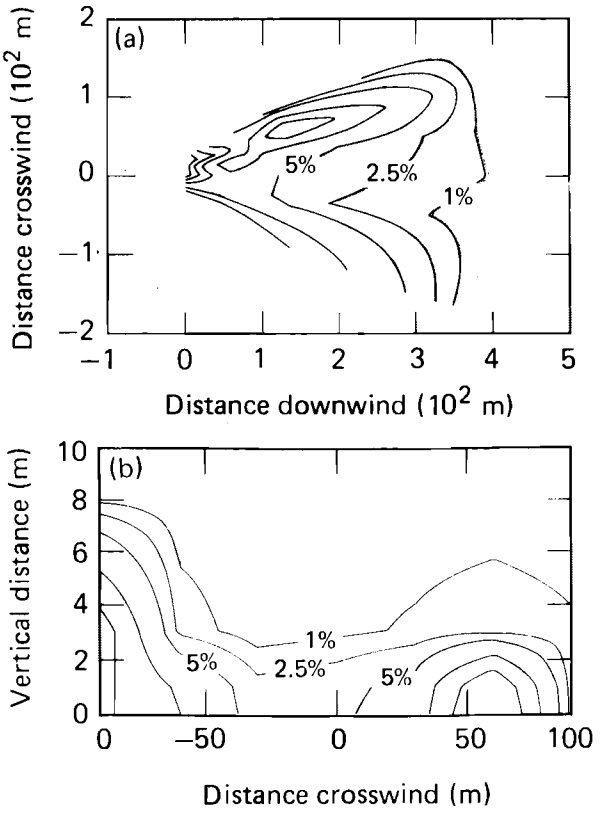

FIG. 11. Gas-concentration contours, showing Burro 8 bifurcated cloud (a) horizontally at 1-m elevation and (b) vertically at 140-m arc at 200 s. Contours are plotted as though the reader were looking back toward the spill pond and are shown for 1, 2.5, 5, 10, 15, and 25% by volume in each case.

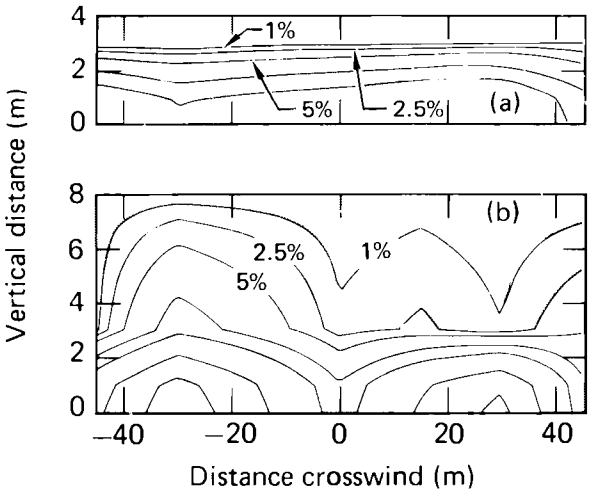

FIG. 12. Vertical concentration contours, showing Burro 8 cloud transition from (a) low, flat cloud at 100 s to (b) higher, irregular cloud 20 s later.

spill (only 79 s); the 1-m contour plot in Fig. 13 shows a maximum extent of 325 m, with a width of about 75 m at 80 s. The constriction in the contours

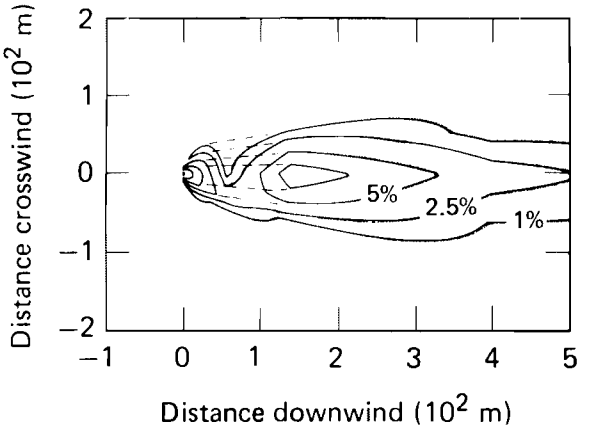

FIG. 13. Horizontal concentration contours for Burro 9 at 80 s, showing maximum downwind extent of the LFL (lower flammability limit). The dotted lines represent an attempt to correct for the effect of the RPT explosions on the sensors. Gas-concentration contours are shown for 1, 2.5, 5, 7.5, and 10% by volume.

at the 57-m row is a consequence of the effects of the RPT explosions on those gas sensors; the dotted lines represent our estimate of the actual contours. The high-concentration core of the gas cloud "lifted off" the surface between 140 and 400 m, as shown in Figs. 14a and 14b. This is believed to be a result of atmospheric boundary layer shear stress, not buoyancy.[11] It is not possible to make a statement about the UFL location because of the effects of the RPT explosions on the gas sensors in the 57-m row.

GAS-CONCENTRATION STATISTICS

As noted above, data were taken at a rate of 3 to 5 Hz at the turbulence stations and were smoothed before being used with data from other stations to generate the gas-concentration contours that represent 10-s-average concentrations. The methane channels of the LLNL infrared sensors were relatively noise-free down to 10-s mean concentrations of a few tenths of a percent. To better understand the significance of fluctuations about the 10-s-average values, the unsmoothed 3- to 5-Hz data from the turbulence-station gas sensors were processed to obtain peak concentration values and standard deviations from the mean for Burros 7, 8, and 9.

A total of 555 ten-second samples were obtained for mean concentrations of 0.1% and greater: 50 for Burro 7, 414 for Burro 8, and 91 for Burro 9. The peak-to-mean methane concentration ratios

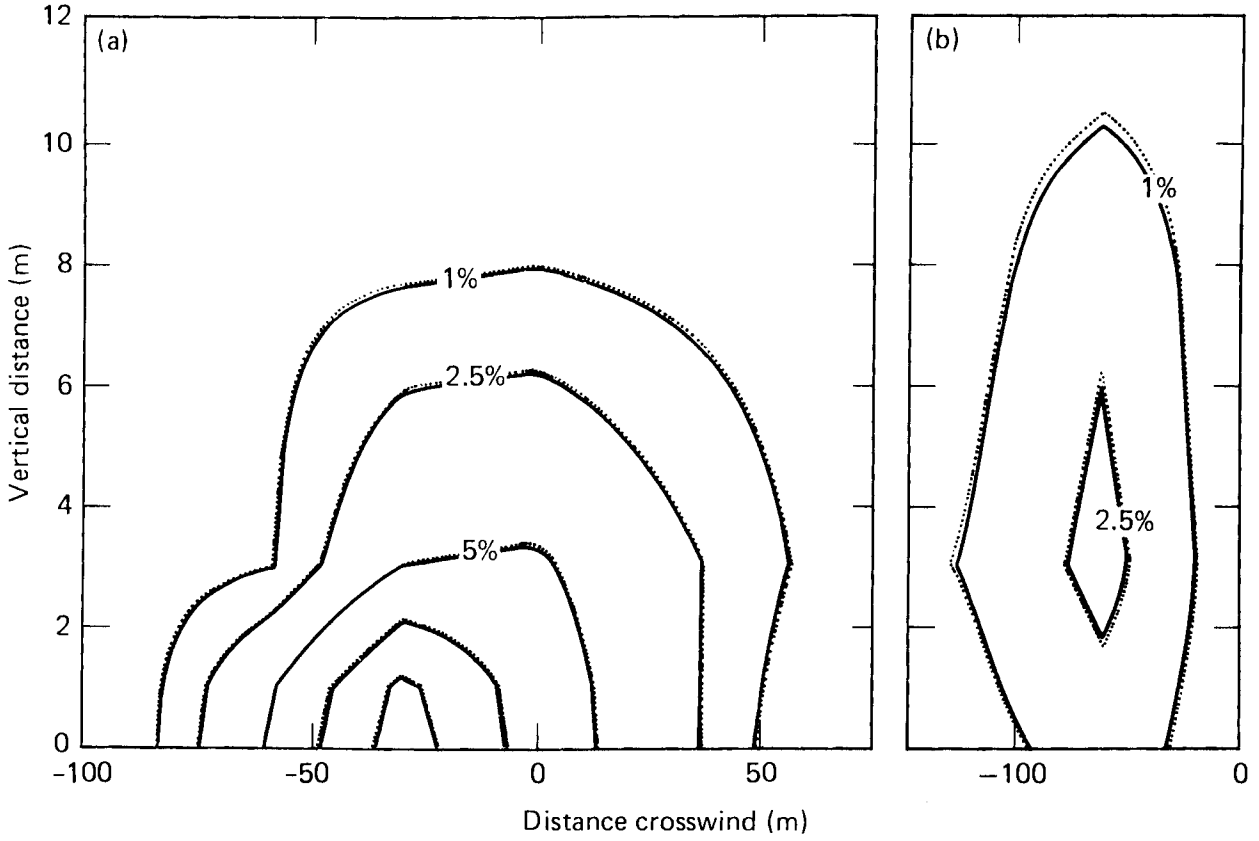

FIG. 14. **Vertical concentration contours for Burro 9, showing cloud liftoff, with highest concentration (a) on surface at 140-m arc and (b) above surface at 400-m arc. Contours are shown for 1, 2.5, 5, 7.5, and 10% by volume.**

for these 555 samples are plotted vs methane concentration in Fig. 15. Note the general trend for increasing peak-to-mean concentration ratio with decreasing mean concentration. Almost all peak-to-mean ratios greater than two to three are associated with one or more zero values of gas concentration in the 10-s sample. Note that, at mean concentrations of 0.5% and greater, peak-to-mean ratios higher than three are not very likely. Attention is called to two limit lines of peak-to-mean ratio vs mean concentration: one for 15% peak volumetric concentration (the upper flammability limit), the other for 5% volumetric concentration (the LFL for methane). Points on or between these lines are associated with gas concentrations in the flammable range. Thus, we see that flammable peak concentrations are not uncommon for mean concentrations above 1%.

Concentration fluctuations about the LFL are of special interest. A total of one-hundred 10-s samples were obtained for mean concentrations ranging from 2.5 to 10%: 25 for Burro 7, 58 for Burro 8, and 17 for Burro 9. The ratios of the peak-minus-mean to the standard deviations from the mean were calculated for these 100 points. Assuming a lognormal distribution for these fluctuations and their ratio,[11] the following geometric mean values were determined for the ratio of the peak-minus-mean to the standard deviation from the mean: 2.54 for Burro 7, 1.78 for Burro 8, and 2.18 for Burro 9. These values of approximately two are consistent with the lower range of values for peak-to-mean vs logarithmic standard deviation presented in Ref. 11.

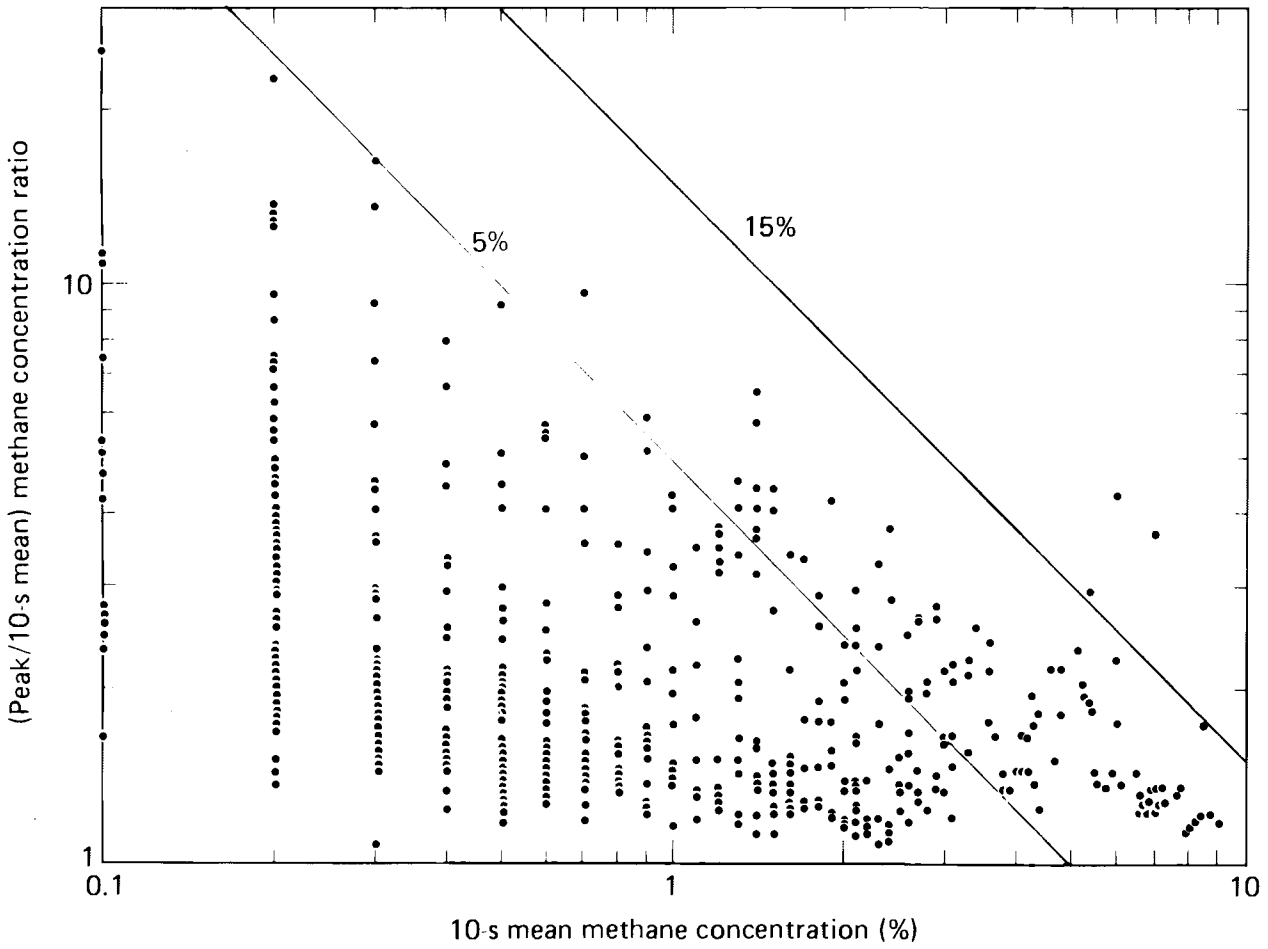

FIG. 15. Peak-to-mean concentration ratio vs mean concentration for Burros 7, 8, and 9. Points between the diagonal lines are within the flammable limits.

GAS-CLOUD DYNAMICS AND THERMODYNAMICS

MOMENTUM DISPLACEMENT BY COLD GAS

As stated previously and shown in Fig. 2, six turbulence stations with bivane anemometers were located at the 1.36-, 3-, and 8-m levels. In addition, there were 20 cup-and-vane anemometers to measure the horizontal wind at a height of 2 m. Data from these stations, especially from stations immediately upwind and downwind of the spill pond, were examined to determine if the cloud of cold gas affected the wind field.

In most experiments, the horizontal wind field was not obviously affected by the presence of the cold gas cloud. However on Burro 8, with the lowest wind speeds (see Table 1), the mean flow was observed to diverge around the cold cloud, as shown in Fig. 16, and was reduced significantly within the cloud, as shown in Fig. 17. The mean wind speed, u (based on a 60-s averaging window), at 1.36, 3, and 8 m during Burro 8 is plotted in Fig. 17a for station T-1 (upwind) and in Fig. 17b for station T-2 (downwind). It is clear that the introduction of the cold gas cloud significantly perturbed the wind field near the ground. Similar mean wind-speed plots for Burro 7 and Burro 9 did not show such an effect.

To quantify the effect of the cold gas on the flow field, we used profiles of mean wind speed at stations T-1 and T-2 to estimate displacement

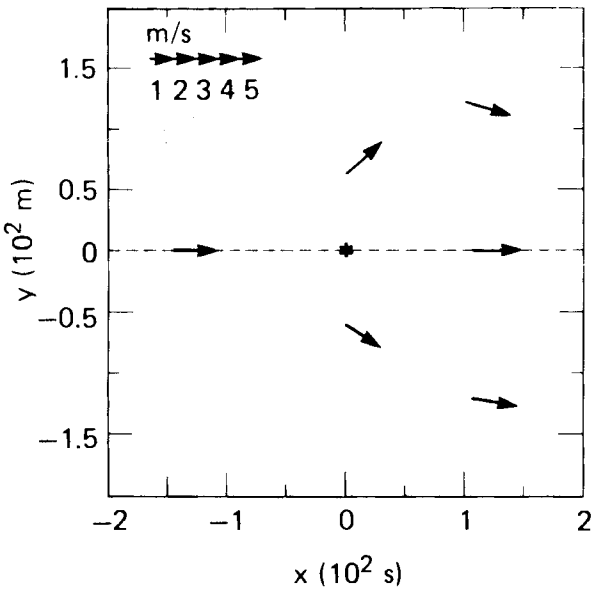

FIG. 16. Measured horizontal wind vectors at 2-m height during the Burro 8 experiment.

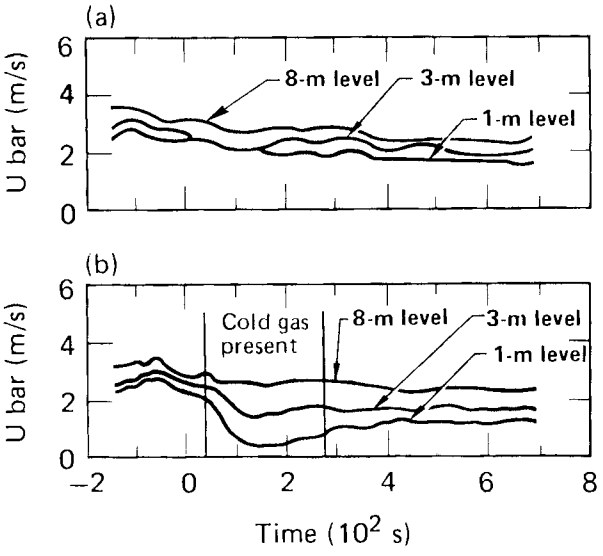

FIG. 17. Mean wind speed during Burro 8, (a) at station T-1 upwind of the spill pond and (b) at station T-2 downwind of the spill pond and within the gas cloud.

thickness—a measure of how boundary layer flow tends to be displaced upward by the introduction of cold gas. The displacement thickness δ is obtained by vertically integrating the momentum profiles, F,

$$\delta(t) = \int_z F(t)\, dz \approx \sum_{i=1}^{n} F_i \Delta z_i \quad . \quad (11)$$

The momentum defect profile, as defined here, is a relative measure of the momentum loss downwind of a thermal discontinuity, expressed for stations T-1 and T-2 as

$$F_i(t) = \left[\frac{u_i(t)}{u_8(t)}\right]_{T-1} - \left[\frac{u_i(t)}{u_8(t)}\right]_{T-2}, \quad (12)$$

where i refers to a given measurement height (1.36, 3, or 8 m) such that F goes to zero at 8 m.

The definition given in Eq. (12) differs somewhat from the classical form (as given by Schlichting,[12] for example). Equation (12) is normalized to the local 8-m wind speed rather than to the "free-stream" speed, and downwind speed profiles are subtracted from the upwind profiles to account for temporal changes (nonsteady winds).

Results for Burros 8 and 9 are shown in Fig. 18. Upward displacement of the flow as a result of cold-gas intrusion is clearly evident on Burro 8 and not apparent for the higher wind conditions of Burro 9. Thus it appears that entrainment of ambient air into the cold cloud was greatly reduced on the Burro 8 test, allowing the cloud to remain relatively decoupled from the ambient air and to displace the momentum field upward. This was supported by the observation that the residence time of the cloud at the gas stations was longer than expected for simple transport at the wind speed, an effect that was also observed only on the Burro 8 test.

SURFACE HEAT FLUX

Measurements of heat transfer from the ground were made during passage of the cold gas cloud, using heat-flux sensors in the ground. These sensors responded markedly to passage of the cold-gas cloud, as shown in Fig. 19. Typically, soil heat fluxes were over 200 W/m^2 when cold-gas temperatures were 15°C below ambient air at the 1-m height.

Most of the heating of the dispersing cold-gas cloud comes from adiabatic mixing of the cold gas with warm air, as well as the condensation and

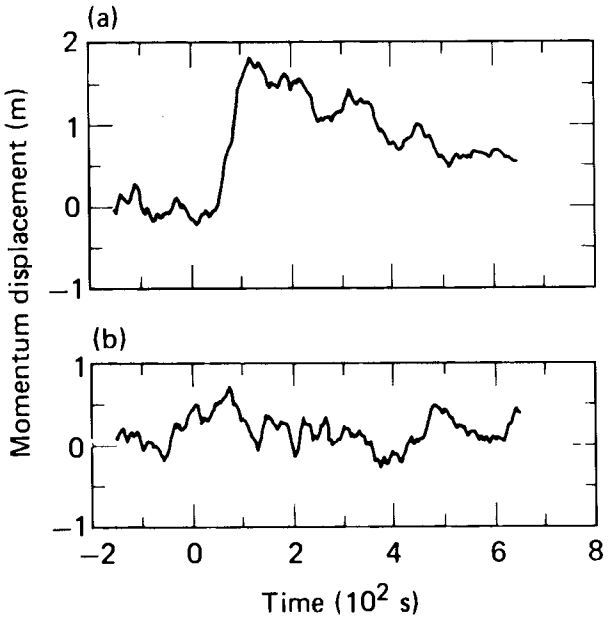

FIG. 18. Comparative momentum displacements of (a) the low-wind-speed Burro 8 and (b) higher-wind-speed Burro 9 experiments.

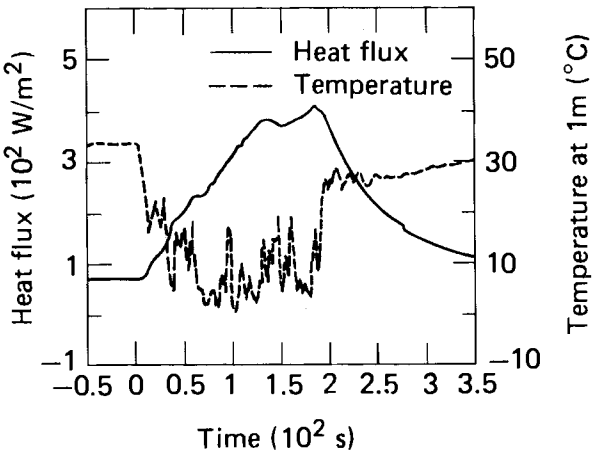

FIG. 19. Typical ground heat flux and gas temperature at 1-m height at the 57-m arc during the Burro 7 experiment.

freezing of water vapor in the air. Previous experiments have shown that this does not account for all of the cloud heating observed experimentally and that some significant amount may come from the ground.

Although a detailed energy balance analysis has not yet been performed, we investigated a simple heat-transfer model:

$$GF = V_H(\rho C_p)_{mix}\Delta T_1 \qquad (13)$$

where GF is the ground flux of heat to the gas mixture, ΔT_1 is the temperature decrease of the gas mixture at the one-metre height, and V_H is a representative energy-transfer velocity (regardless of the real mechanisms of transfer). Since both GF and ΔT_1 change with time, this equation is representative of heat gained by the cloud only if ΔT is characteristic of the temperature difference from soil to gas, and if GF is the only significant component of heat transfer.

We found over several tests (Burro 5, 7, 8, and 9), and at both 57 and 140 m downwind, that the heat-transfer velocity V_H was apparently independent of wind speed even when wind speed varied significantly. Furthermore, investigations of more-complicated models, including buoyancy terms and a drag coefficient, were not justified by the data. As a simple approximation, the Burro test data show that V_H is nearly constant, i.e., $V_H \simeq 0.0125$ m/s with a standard deviation of 36% between values from successive measurements.

This approximation, however crude, allows a simple boundary condition to be specified in dispersion models that include heat transfer from the ground to the cold gas. Validation or improvement of this simple heat-transfer model will occur when more-detailed energy-balance data become available.

HUMIDITY ENHANCEMENT

We investigated absolute humidity enhancement over several tests (Burros 2, 3, 5, 6, 7, 8, and 9) and at downwind distances of 57 and 140 m. Typical time traces of the humidity and gas concentration at the same station are shown in Fig. 20. We found that, to a good approximation, the relative increase in absolute humidity $(\rho_w - \rho_{w0})/\rho_{w0}$ is correlated to gas concentration C, in volumetric fraction, such that

$$\frac{1}{\rho_{w0}}\frac{d\rho_w}{dc} \simeq 14.8$$

with a standard deviation of 37% between values for successive measurements. This implies that in the Burro series of tests a 1% gas concentration was associated with a 15% increase in absolute humidity. The ambient, absolute humidity values

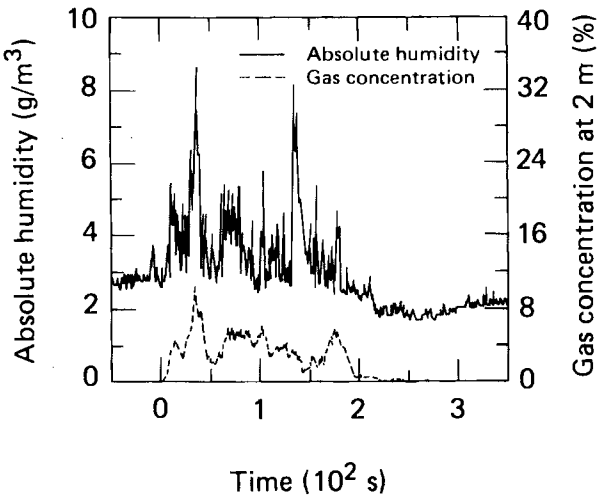

FIG. 20. Typical absolute humidity and gas concentration at 2-m height at the 57-m arc during the Burro 7 experiment.

(ρ_{w0}) averaged about 2.2 g/m^3 in the dry desert environment of the Burro tests. The humidity enhancement was negatively correlated to gas temperature also, but the variation between tests was very large. On some of the tests air temperature remained cold long after the humidity enhancement vanished because of the lag before ground temperatures returned to normal.

The measurement of humidity enhancement provides another element necessary to determine the overall energy balance of the dispersing cloud. Thus the thermodynamic effects of evaporation, condensation, and subsequent reevaporation of the additional water on the energy balance can be calculated. The relationship between humidity enhancement and the nature of the LNG spill and the extent of the cloud drift over water has not yet been determined. However, observations indicate that, under certain circumstances, humidity enhancement must be considered as a source of heat input to the cloud.

DIFFERENTIAL BOILING AND RAPID PHASE TRANSITIONS

Strong RPT explosions were observed during the Burro 6 and 9 experiments; one possible cause of these explosions is differential boiling of the LNG components. In this section, we examine the evidence for differential boiling of LNG and then review the physics of RPT explosions with respect to what was observed during the Burro series.

DIFFERENTIAL BOILING

The primary constituent of LNG is methane (95%), with smaller fractions of ethane, propane, and other heavier hydrocarbons. Although the ethane and propane concentrations are small in the liquid (4% and 1%, respectively), they are, in some respects, more hazardous than the methane since they have been shown to lower the initiation energy required to detonate mixtures of methane and air. LNG mixtures rich in ethane also exhibit a greater propensity toward RPT explosions than do those that are 95% methane, a point discussed in the following section. The initially small fraction of heavier hydrocarbons increases substantially late in the spill because of the differential boiloff of each species according to the differences in boiling-point temperatures. The normal boiling-point temperatures for methane, ethane, and propane are −161, −88, and −42°C, respectively.

Since the bulk of LNG is methane, the temperature of the liquid pool will be −161°C initially, as can be seen in the temperature-composition phase diagram for the methane–ethane system[13] shown in Fig. 21. The bulk temperature of the liquid does not increase appreciably until most of the methane has boiled off, leaving liquid rich in ethane (and propane). Consequently, high concentrations of the heavier hydrocarbons would be expected in the vapor only late in the spill.

In practically every test of the Burro series there was a noticeable increase in the ethane-plus-propane concentration at the end of the spill. This is illustrated by gas-concentration data from the methane and ethane-plus-propane channels shown in Fig. 22. Although this trend in the concentration data is in qualitative agreement with the expected enrichment resulting from differential boiloff, some technique for verifying the absolute values of these results is required. Verification was obtained by integrating the flux of ethane-plus-propane over the duration of the test and comparing this result to the assayed composition in the spill tank.

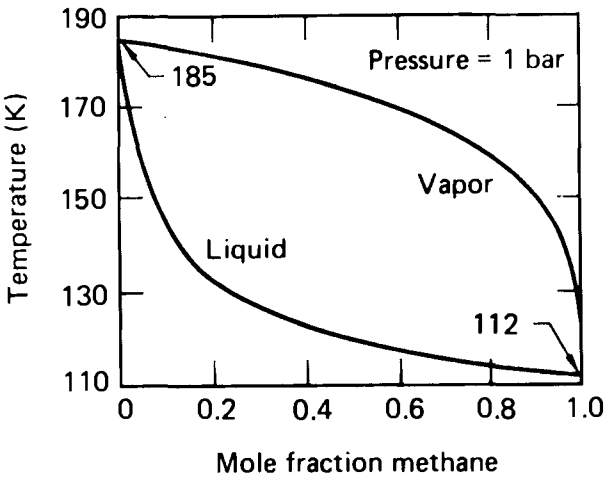

FIG. 21. Temperature-composition diagram for the methane–ethane system.[13]

To do this properly, the infrared sensor being analyzed must have observed gas concentrations typical of the general cloud composition for the duration of the spill. Unfortunately, the gas-concentration data of the 57-m row were obtained under heavy fog conditions early in the spill and had to be omitted from the analysis because of the sensitivity of the ethane-plus-propane data to the fog attenuation. Imposition of these constraints on the infrared concentration data produced two sets of data appropriate for ethane-plus-propane integration analysis. These two data sets are shown in Fig. 23 in terms of three parameters: R_0, the enrichment ratio determined from the pre-spill composition in the spill tank; R_c, the calculated vapor-cloud assay; and the instantaneous enrichment ratio R(t), defined as

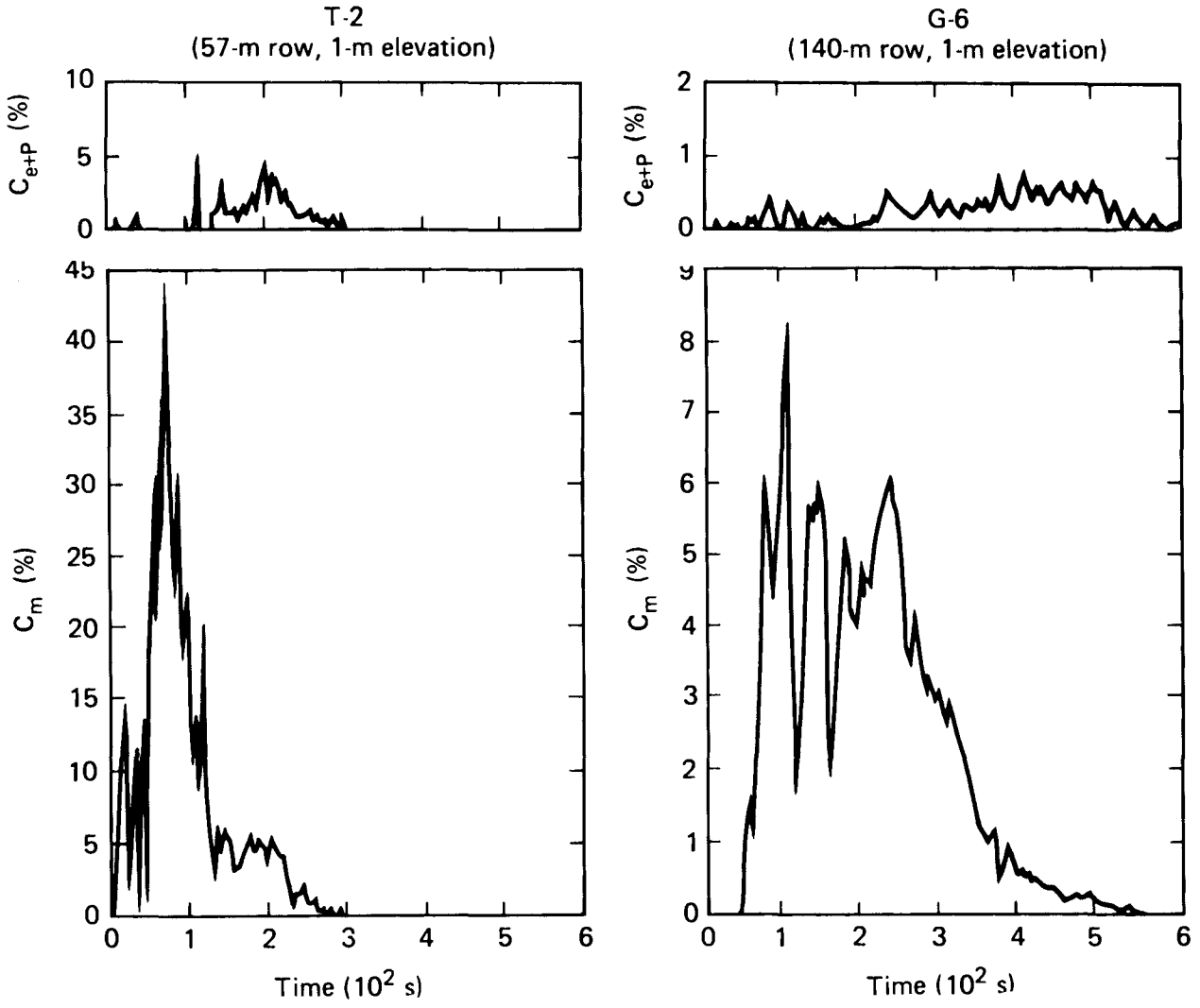

FIG. 22. Gas-concentration data for the ethane-plus-propane and methane channels from infrared sensors in the 57- and 140-m rows for the Burro 8 experiment.

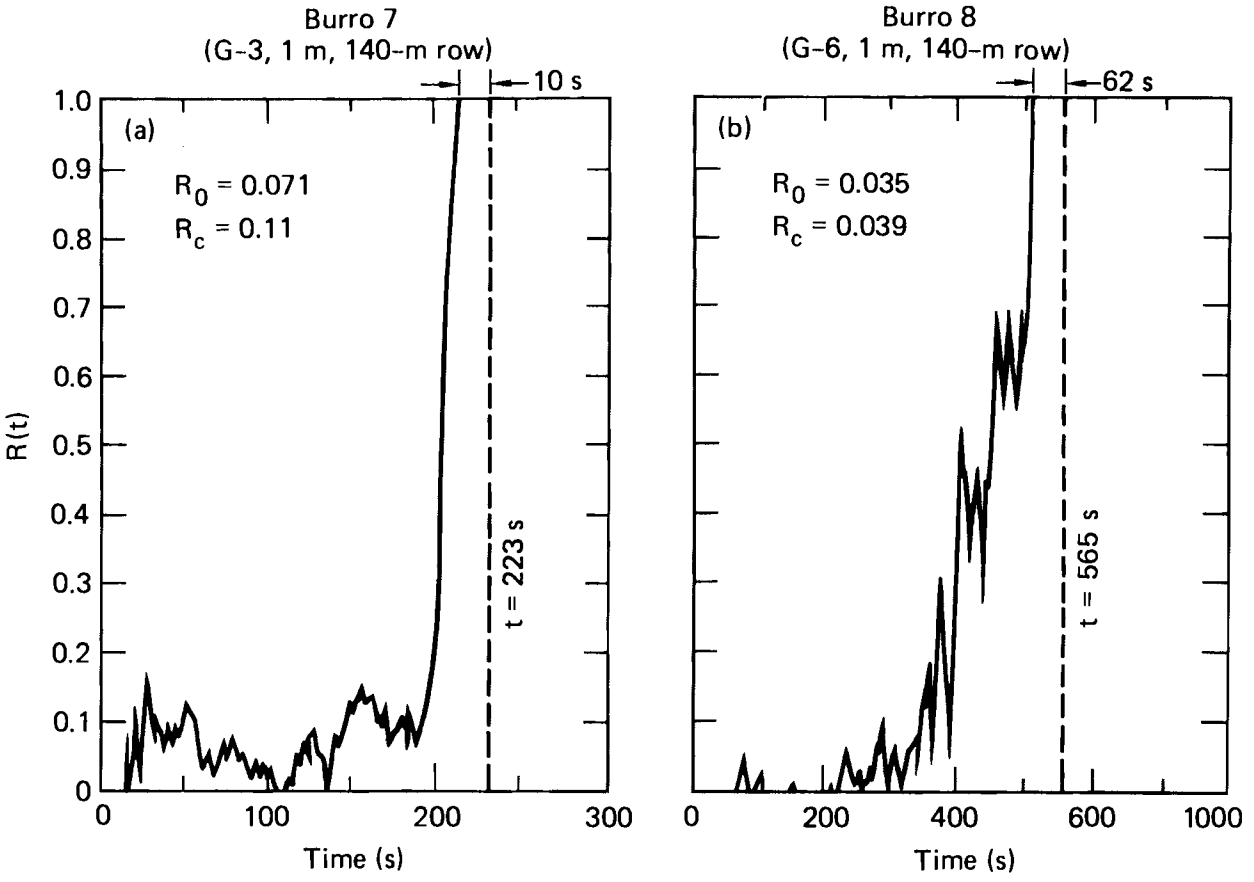

FIG. 23. Enrichment ratio vs time for two Burro series tests.

$$R(t) = \frac{u(t)C_{e+p}(t)}{u(t)\left(C_{e+p}(t) + C_m(t)\right)} \qquad (14)$$

where u(t) is the wind velocity at the sensor at time t, $C_{e+p}(t)$ is the instantaneous ethane-plus-propane concentration, and $C_m(t)$ is the instantaneous methane concentration. The integral over the duration of the test of the numerator of Eq. (14) divided by the integral of the denominator of Eq. (14) is defined as R_c, i.e.,

$$R_c = \frac{\int u(t)C_{e+p}(t)dt}{\int u(t)\left(C_{e+p}(t) + C_m(t)\right)dt} \; . \qquad (15)$$

R_0 and R_c should be equal. The results given in Fig. 23 show this to be nearly true for both Burro 7 and Burro 8.

The calculated cloud assay values (R_c) were determined by integrating Eq. (15) from t = 0 to the times indicated by the dashed lines on Fig. 23. These termination times correspond to the times beyond which the ethane-plus-propane concentration is less than 0.05%, a value well below the noise level of the instrument. Consequently, the period of duration for 100% ethane-plus-propane (10 s for Burro 7 and 62 s for Burro 8) is a maximum value in both cases. The calculated assay value for Burro 7 (R_c = 0.11) is very sensitive to the choice of integration termination time. For example, if integration is terminated at t = 213 s instead of t = 223 s, then R_c = 0.086—a value much closer to the tank assay value of 0.071. The calculated assay value for Burro 8 shows little variation with the choice of termination time (R_c = 0.039 for termination of t = 503 s, instead of t = 565 s). Although an accurate estimate of the extent of the enriched vapor cloud is difficult from the data in Fig. 23 because of the low concentration levels involved (less than 1%), it is evident that the effects of differential boiling on the pond were observed as far as 140 m downwind during the Burro series tests.

Gas-concentration measurements of methane, ethane, and propane were also obtained during the LLNL AVOCET series of tests in 1978.[14] Several grab-sample gas-concentration measurements were made as close as 8 m to the spill point during these 4- to 5-m^3 spills. The sample time was 1.8 s per sample, and 8 samples were generally obtained at each station during the course of each test. The

results from station 1 (8 m) of the AVOCET 2 test are shown in Fig. 24 in terms of the enrichment ratio. The integrated enrichment value in Fig. 24 (R_1 = 0.075) was determined without considering the wind speed and assuming a linear variation in gas concentration between sample times. As a result, the value is not as accurate as those determined from the Burro series data and does not agree with the tank assay, R_0 = 0.047, as well as the Burro series results do. Nevertheless, there is a striking similarity between the 5-m^3 spill data obtained at 8 m (Fig. 24) and the 40-m^3 data obtained at 57 and 140 m (Fig. 23).

The measured methane and ethane-plus-propane concentrations at the center of the 57- and 140-m rows for the Burro 8 test, shown in Fig. 22, show enrichment by the heavier hydrocarbons of the later portions of the vapor at both stations, with peak ethane-plus-propane concentrations of 4% at T-2, decreasing to 1/2% at G-6. The downwind spreading, in terms of detectable concentrations at downwind distances of the heavier hydrocarbons, appears to be comparable to the spreading of methane vapors. This indicates that the dynamics of the dispersion of methane and ethane-plus-propane vapors are similar. The concentrations at T-2 late in the spill (t = 200 s) show that both the methane and ethane-plus-propane vapors are above the LFL and that the heavier hydrocarbons make up about 40% of the cloud at this point. In fact, the stoichiometric mixture for a 40% ethane/60% methane ratio is 3.0% ethane, 4.5% methane, and 92.5% air. Further, experiments have demonstrated[15] that a stoichiometric mixture of LNG vapors in air enriched with 40% ethane can be detonated by explosive charges as small as 0.2 kg when the charges are immersed in the gas mixture. Calculations by Westbrook and Haselman[16] of a shock wave propagating through a homogenous stoichiometric ethane, methane, and air mixture show excellent agreement with the data of Bull et al.[15] for ethane-enriched LNG vapors. Thus, it would appear that enriched LNG vapor mixtures, such as those late in the Burro 8 spill (Fig. 22), could be detonated by shock waves from explosions of sufficient magnitude. It is not known whether such a detonation in the ethane-rich region of the cloud would continue to propagate when it reached the methane-rich gas–air mixtures. It is also important to note that spill- or accident-produced clouds are not uniform in composition or

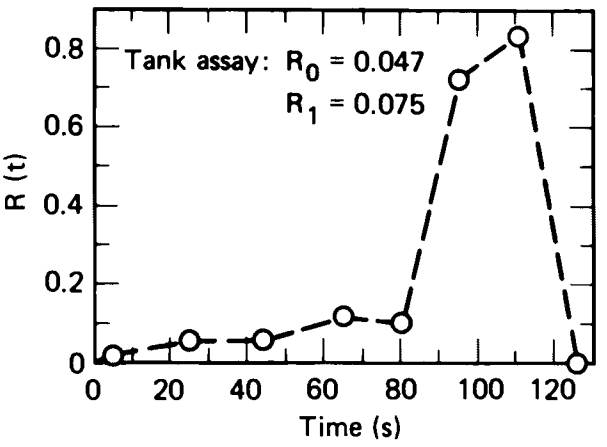

FIG. 24. Enrichment ratio from AVOCET 2 (grab samples, station 1).

well mixed, although very large clouds could have large homogeneous regions. The concentration fluctuations could also affect the propagation of the shock wave.

In considering the potential sources of initiation for such an accidental detonation in the ethane-enriched region, a disturbing new possibility arises. As will be discussed in the next section, four RPT explosions occurred on the Burro 9 test with overpressures, at 30 m, in excess of 0.18 psi (the largest being 0.72 psi). The pressure pulses observed had the characteristics of classical airblast shock waves. No data were collected during these experiments to allow determination of the characteristics of the pressure pulse near the explosion source. However, if we assume the worst case and extrapolate as though the explosion were from a TNT source, we find that the shock strengths from these four explosions would be sufficient for initiation of a detonation in a stoichiometric mixture in which the fuel is 40% ethane and 60% methane. Thus, sufficiently strong shocks may exist at the source of the RPT explosion. Furthermore, there appears to be a class of large RPT explosions, associated with differential boiloff of the LNG, that occur, preferentially, late in the spill at about the same time that the enriched region of the cloud is produced. We expect, of course, significant close-in differences between the RPT explosions and those from TNT. However, in our present analysis, we cannot discount the possibility that the shock wave produced by an RPT could ignite the ethane-rich portion of an

LNG vapor cloud. Close-in pressure and vapor-composition measurements will be necessary to resolve this issue.

RAPID PHASE TRANSITION EXPLOSIONS

The explosions from RPTs have interested the LNG industry since 1970, when two severe explosions were observed by the Bureau of Mines during a series of LNG spills on water.[17] Since then an extensive research effort has been launched to understand this phenomenon.[18–21] The currently accepted theories involve the superheating of LNG, followed either by homegeneous nucleation or by some other form of triggering mechanism to initiate vaporization. Superheating of the cryogen allows it to temporarily store the heat energy absorbed from the water and then to release this energy on the same time scale as a typical chemical explosive. It has been shown empirically[22] that, for a spontaneous RPT explosion to occur, the water temperature (T_w) and cryogen superheat limit temperature (T_{sl}) must be roughly equivalent, i.e., $T_w/T_{sl} \sim 1$. The superheat limit temperatures for methane, ethane, and propane are −104, −4, and 53°C, respectively. Consequently, the spilling of methane on ambient water (~25°C) should not, according to the aforementioned criteria, result in RPT explosions because $T_w/T_{sl} = 1.8$. On the other hand, the ratio is 1.1 for ethane and 0.9 for propane. Since LNG is primarily methane (~95%), one would not expect RPTs when spilling LNG on water. The RPT explosions that have occurred in the past during such spills have been attributed either to the enrichment of the LNG by heavier hydrocarbons (primarily ethane and propane) or to the collapse of the film boiling-vapor layer by the mutual impact of the two fluids.

There has been some effort at the Massachusetts Institute of Technology (MIT)[23,24] to determine the effects of the enrichment of LNG with the heavier hydrocarbons and the variations of impact velocity on the intensity of RPT explosions. The results of the enrichment experiments[23] showed that simple spills of LNG (nonimpacted) would not produce RPT explosions unless the ethane or propane concentrations were 50% or greater. The MIT impact tests,[24] involving an LNG mixture of 90% methane, 6% ethane, and 4% propane at impact velocities of 15 to 21.5 m/s/, did not result in any RPT explosions, although the criteria used to determine whether an explosion occurred were rather arbitrary.

Most of the MIT impact tests involved the pure cryogens, nitrogen, methane, ethane, and propane. The results of the tests were originally presented in terms of peak overpressure vs impact velocity.[24] Although the magnitudes of the overpressures were large (10 to 200 psig), the transducer was located only 10 cm from the impact point. A typical overpressure trace for water at 294 K impacting ethane at a velocity of 21.5 m/s was made up of numerous sharp pulses (<1/2 ms) with a total duration of approximately 5 ms. The TNT equivalent for the peak overpressure pulse of these data (assuming a free-air point-source explosion) is about 0.2 mg. The ears of the experimenter were used to differentiate between an explosion and rapid boiling. A more-quantitative assessment of the water–cryogen interaction could have been based on the integral of overpressure with time (pressure impulse) because this quantity would be conserved if the pressure disturbances were to form a shock wave.

The results of the MIT impact tests using pure cryogens[24] are summarized in Fig. 25, where the peak overpressures have been plotted against impact pressure instead of impact velocity. The impact pressure is equal to $1/2\ \rho u^2$, where ρ is the water density and u is the impact velocity. As can be seen in the figure, the peak overpressure appears to be directly proportional to the impact pressure, with no apparent threshold. With the exception of ethane, all the cryogens appear to have an approximately common relation for peak overpressure vs impact pressure, with water temperature as a key parameter. The maximum peak overpressure recorded during these experiments was 200 psig and was observed for 306 K water impacted on ethane at a velocity of 15 m/s (0.611 atm). The only difference between this data point (T_w = 306 K) and the 92-psig peak overpressure observed with the same liquids and impact velocities is a water-temperature difference of 12°C. In general, the implications of the MIT impact experiments are that the higher the water temperature, the more intense the RPT explosion, especially in the case of ethane.

RPT explosions have been observed several times during the LLNL LNG spill tests at the NWC. Two explosions occurred at the beginning of the

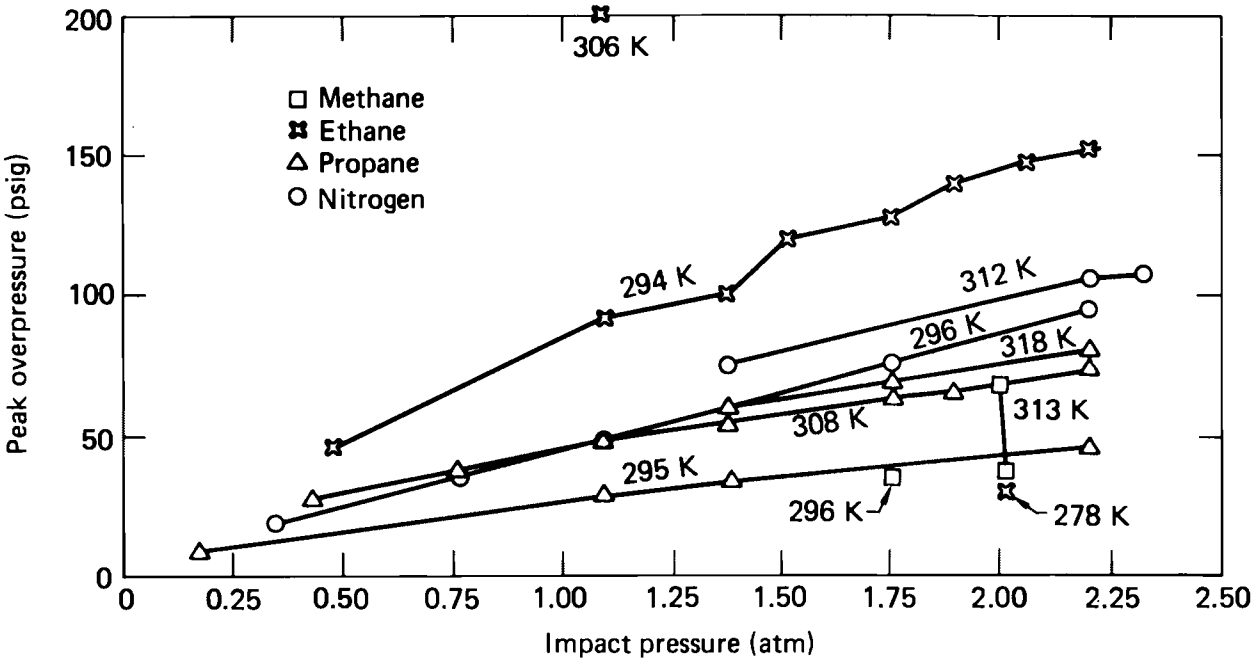

FIG. 25. Results of water-on-cryogen impact tests at Massachusetts Institute of Technology[24] at various water temperatures.

AVOCET 3 and 4 spills in 1978. These LNG spills were of small total volume (4.5 m^3) and at lower spill rates (~3.5 m^3/min) than the Burro series spills in 1980. The impact velocities of the AVOCET spills were on the order of 1.5 m/s, and the storage-tank-mixture assays never indicated more than 9% higher hydrocarbons.

The AVOCET RPT explosions were attributed to the presence of a highly enriched "heel" left in the spill pipe after the pre-spill cooldown period. The spill pipe was cooled by periodically allowing a small amount of LNG through the spill valve before a spill. Some cooldown fluid would have remained in the spill pipe since it was slightly lower at the tank than at the pond center. The enrichment was a result of the much lower boiling point of the methane, causing it to quickly boil off, leaving mostly ethane and propane in the pipe. This enriched "heel" was then forced out the spill-pipe exit ahead of the tank LNG when the spill valve was opened.

Numerous RPT explosions occurred with varying severity and frequency during two of the Burro series spills in 1980. A summary of all available data pertinent to RPT explosions for the Burro series spills is given in Table 2. Several large explosions occurred during the Burro 6 and 9 spills. Examination of Table 2 shows that many variables are involved: pressurization technique, spill rate, spill-plate location, LNG composition, and the time of occurrence of the RPT explosions. Unfortunately, these variables were not controlled; as a result, one cannot deduce the precise cause of the RPT explosions. Clearly the heavy hydrocarbon concentrations, as measured in the tank shortly before each spill, are much lower than the 60% minimum required to produce simple spill RPT explosions according to Porteous.[23] Also, the estimated impact velocity associated with the maximum spill rate obtained (Burro 9) was less than 5 m/s (assuming liquid phase only)—well below the range of impact velocities for which the RPTs were observed at MIT.[24]

There were several large RPT explosions very late (~130 s) in the Burro 6 spill. These explosions occurred in rapid succession and out on the pond, away from the spill point. In this case, we believe that the explosions were the result of the enrichment of the LNG, caused by the differential boiloff of the methane on the pond. It is not yet apparent why this happened during Burro 6 and not during Burros 2 through 5 since the spill rates and tank compositions for the five spills were similar. The only obvious difference was that Burro 6 involved partial self-pressurization and may have had less dissolved nitrogen present. However, the nitrogen

TABLE 2. Burro-series RPT explosion summary.

Experiment	RPT	Time of experiment	Ambient temperature (°C)	Self-pressurization	Average spill rate (m^3/min)	Spill-plate location	LNG composition (%)				
							CH_4	C_2H_6	C_3H_8	C_4H_{10}	C_4H_8
2			36.8	No	11.9	About 5 cm below water	96.11	3.0	0.75	0.06	0.08
3			34.0	No	12.2	About 5 cm below water					
4			35.4	No	12.1	Below water	94.19	4.28	1.24	0.13	0.16
5			41.2	No	11.3	Water level	94.82	3.65	1.24	0.12	0.17
6	Several large	Late in spill	39.5	Yes	12.8	?	96.39	3.01	0.48	0.05	0.06
7			33.8	Yes	13.6	Above water	92.87	5.80	1.16	0.08	0.09
8			33.2	Yes	16.0	Above water	96.99	2.84	0.57	0.04	0.06
9	Numerous very large	Throughout entire spill	35.4	Yes	18.4	About 5 cm below water	93.62	5.2	0.94	0.10	0.14

should have come out of solution very early in the spill and not affected the pool characteristics at the times of the RPT explosions.

The spill plate that was attached to the spill-pipe exit also complicated analysis of the Burro series RPT explosions. Although the spill plate was submerged in the early tests (Burros 2 and 3), allowing the LNG to come into initial contact with the water, the spill rate was lower, resulting in a lower impact pressure. As the spill rate increased (Burros 6 through 8), little (if any) water was available for the initial direct impact of the LNG until Burro 9. This was caused by the evaporation and resultant lowering of the pond water level, which customarily occurs each summer. Before the Burro 9 spill, the spill plate was lowered about 5 cm below the surface of the water, allowing LNG spilled at the maximum spill rate to interact more readily with the water. Unfortunately, there were other differences between the Burro 9 spill and the previous ones: an unusual cooldown and the loss of the spill plate during the spill.

The typical Burro series cooldown procedure was as follows. Several hours before the estimated spill time, the test director would begin to cool down the portion of the spill pipe up to the spill valve (see Fig. 26). This was accomplished by closing the tank vent valve and allowing the tank to partially self-pressurize by evaporation, forcing the LNG up the dip tube, where it spilled over into the 53-m-long section of pipe leading to the spill valve. The pipe vent valve allowed vaporized gases in this pipe section to escape so that the entire volume (2.2 m^3) could be filled with LNG. Lind estimates that the methane concentration in this section of the spill pipe could be no less than 85% as a result of the preferential methane evaporation. This self-pressurization scheme produced pressures of about 5 psi in the tank 15 min before the test. The pressure was then boosted slowly to 30 psi, using compressed nitrogen. During the cooldown procedure the bypass valve was partially opened, and some LNG was allowed to trickle out the remaining 41 m of the spill pipe in an attempt to

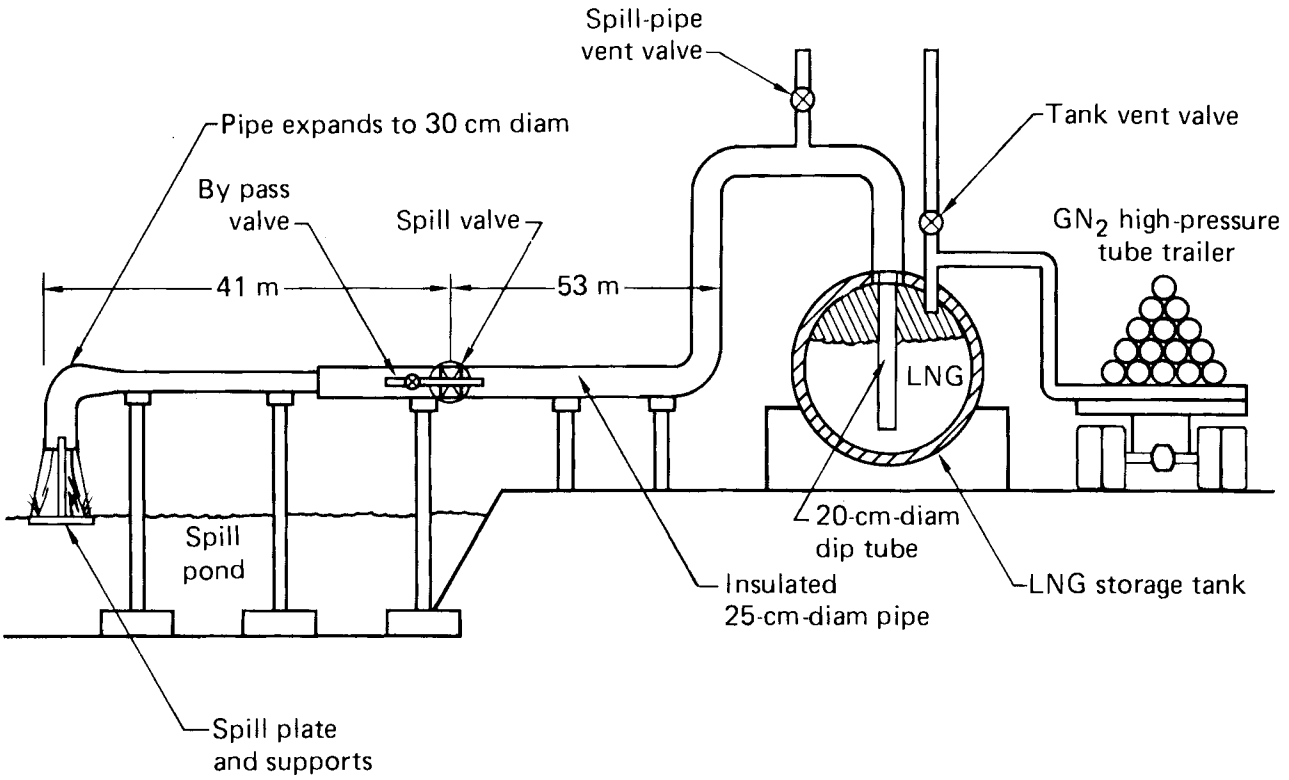

FIG. 26. The 40-m^3 LNG spill facility at the NWC.

cool this pipe section. The LNG in this last section of the spill pipe was surely further enriched with the heavier hydrocarbons; however, an accurate estimate of the degree of enrichment is difficult.

During Burro 9 cooldown the bypass valve malfunctioned, allowing a larger than normal flow of LNG out the spill pipe before the spill. Consequently, an abnormally large amount of enriched LNG may have been in the spill pipe when the spill valve was opened. Perhaps the pressure wave generated when the spill valve first opened forced the enriched LNG in the last 41-m-long section of the spill pipe out the exhaust ahead of the main body of LNG and produced the first few RPT explosions. This scenario is substantiated somewhat by the timing of the RPT explosions and by the flow-rate data obtained just upstream of the spill valve. Using the flowrate data and assuming single-phase (liquid) flow for the duration of the spill, a simple calculation shows that at least 10 s would be required for the LNG on the upstream side of the spill valve to reach the pond surface. As shown in Table 3, there were three RPT explosions before this. The second largest explosion occurred at 21.4 s when the LNG initially in the 53-m-long section of the spill pipe was being exhausted, and the storage-tank LNG was spilling out when the largest RPT explosion occurred at 35.1 s. This would seem to indicate that LNG containing only 6 to 7% heavier hydrocarbons and impacting at velocities of less than 7 m/s (assuming single-phase flow) can produce significant RPT explosions. One must also consider that the spill plate was knocked loose some time before the largest explosion (35.1 s), greatly changing the LNG–water interaction dynamics. The exact time of this occurrence and its effect on the RPT explosions is not known.

Lind recorded 20 significant RPT explosions during the Burro 9 spill.[25] The largest 11 and their times of occurrence are given in Table 3. Films indicate that large airblast overpressures are not necessarily associated with large water plumes, indicating that some of the explosions occurred deep (about 1 m) underwater. Damage to the facility also indicates that large explosions must have occurred essentially at the pond bottom. About 50 MJ of

TABLE 3. Occurrence times and magnitudes of major Burro 9 RPT explosions.

Time[a] (s)	Static pressure[b] (psi)	TNT equivalent[c] (g)
6.5	0.12	65
7.1	0.15	115
9.2	0.27	530
21.4	0.57	3400
35.1	0.72	6300
43.2	0.10	41
46.0	0.12	65
54.1	0.12	65
54.9	0.13	80
66.9	0.19	215
72.7	0.12	65

[a] t = 0 is start of spill-valve opening.

[b] Measured at distance of 30 m.

[c] Equivalent free-air point-source explosion of TNT.

energy (total) was released in the 20 explosions, which corresponds to 11 kg of TNT. The polymorphic detonation theory developed at Washington State University[26,27] allows one to estimate the minimum amount of superheated cryogen needed to produce a detonation of known magnitude. The theory employs the volume change of the phase transformation as the energy required to sustain a detonation wave, and the superheat phenomenon as the energy-storage mechanism. The initial work by Rabie[26] was extended by Hixson[27] to describe detonation properties based on more-realistic equations of state, however the equations are involved and, as yet, have only been used to calculate the bounds of the detonation properties for methane and propane. If the fluid is heated to the superheat temperature limit at 1 atm, the energy available for detonation is about 83 J/g for methane and 112 J/g for propane. The minimum volumes of methane, ethane, and propane necessary to produce the energy release of the Burro 9 RPT explosions are 1.46, 0.93, and 0.79 m^3, respectively. This is certainly a lower limit since the attenuation of the blast waves from the underwater explosions was not accounted for. The actual volumes spilled were 22.66, 1.26 and 0.23 m^3, respectively. The required volume of ethane was calculated, using an estimated available detonation energy of 100 J/g. Clearly, only a small fraction of the methane would have to be superheated, whereas practically the entire spilled volumes of ethane and propane would have to be heated to the superheat limit at the same moment to produce the measured explosive energy release. Thus, it is clear that significant amounts of methane must have contributed to these RPTs. This is further evidence that a standard mixture of LNG (~95% methane) spilled onto the water at low velocity is capable of undergoing significant RPT explosions.

At this time, we can only make general conclusions about the RPT explosions during the Burro series. The late explosions of Burro 6 were most likely caused by enrichment of the LNG pool as a result of the differential boiloff of the methane. However, it is very difficult to draw any conclusions about the Burro 9 RPT explosions because of the lack of quantitative information on the pertinent parameters. The pressure measurements—fielded by Lind after the initial RPT occurrence on Burro 6—produced very useful data during the Burro 9 RPTs, but not enough data were obtained to understand the mechanism or to predict what might happen during an accident. In the Coyote series (Summer 1981) being conducted at China Lake, a sequence of spills will be dedicated to the investigation of LNG RPT explosions. The facility will be adequately instrumented for this purpose, and the test matrix is designed to vary the LNG impact pressure and spill-plate depth in a controlled and systematic manner.

CONCLUSIONS

Of the eight Burro series LNG spill experiments performed at China Lake in 1980, four proved to be identifiably different from each other and amenable to analysis. The Burro 3 test was performed in an unstable atmosphere, with a modest wind speed and a low spill rate. Burro 7 had a low spill rate, high wind speed, and slightly unstable atmosphere. The Burro 8 test was particularly interesting in that it had a high spill rate, very low wind speed, and slightly stable conditions. Burro 9 had the highest spill rate of all, moderate wind speed, neutral atmospheric stability, and numerous RPTs. Most of our analysis has been centered on these four tests.

An extensive array of instrumentation was deployed both upwind and downwind of the spill pond. Wind speed and direction, humidity, and temperature were measured both upwind and downwind. Four radial arcs containing 30 gas-sensor stations were deployed downwind to 800 m from the spill pond and measured gas concentration and temperature at three elevations, as well as humidity and heat flux from the ground.

The gas-concentration and wind-field data were processed and analyzed to define the gas cloud as a function of time, using contour plots and the wind field as a function of time using wind-field flow lines. The gas-cloud orientation and the wind-field flow lines were generally consistent in that the maximum gas concentrations generally lay along the wind-field centerline. The notable exception to this was Burro 8 in which the gas flow was dominated by gravity, producing a highly bifurcated cloud that tended to follow low regions of the terrain. The bifurcated cloud caused maximum gas concentrations to occur on either side of the wind-field centerline. Other exceptions occurred when the cloud extended beyond one side of the array and the extrapolated wind field was not reliable or when several gas sensors were not operational, causing distortions in the gas contours.

Additional consistency checks were made in an attempt to demonstrate the validity of the data. The mass flux of gas through an arc of gas sensors (140-m arc) was calculated and integrated over the duration of the test for both Burro 8 and 9. The cloud stayed within the array for Burro 9 and, if RPT effects are taken into account, the gas sensors accounted for essentially all of the LNG spilled. The gas cloud from Burro 8 was visibly wider than the instrument array, but the mass-balance calculation indicates that 76% of the gas was detected. The mass flux of ethane-plus-propane was also calculated and integrated over the spill duration. The results compared favorably with the tank assays at the time of the tests.

The normal turbulent flow in the lower atmospheric boundary layer totally dominated the transport and dispersion of gas on all of the tests except Burro 8. On this test, the wind speed was low and the gas flow was dominated by gravity. This produced an exceptionally wide low cloud that actually displaced the ambient wind field upward by about 1.5 m, causing the wind speed within the cloud to drop essentially to zero. We believe that what was observed to occur during Burro 8, under very low wind conditions, is likely to occur on larger spills under a variety of conditions. The ability of large masses of cold dense gas to displace the normal atmospheric flow has profound implications for hazard prediction from large accidental spills. Larger spills are badly needed to determine if this phenomena is likely to be important in case of an accident.

Time histories of the downwind distance to the LFL were obtained from the gas-concentration contours for Burros 7 through 9. The downwind LFL location appeared to stabilize only in the case of Burro 8, where it was 330 m at a height of 1 m. However, the occurrence of 5% gas concentrations at a height of 3 m at the outermost stations in the 400-m arc, late in the test, indicate that the furthest extent of the LFL may have been missed.

Large-scale differential boiloff of the various constituents of the LNG was again observed on this series of tests. Substantial ethane and propane enrichment of the cloud occurred late in the spills and propagated downwind. Flammable mixtures with enrichments of the fuel ranging from 40 to 100% ethane and propane were observed to travel downwind substantially beyond the 57-m arc, reaching the 140-m arc in some cases. This ethane-enriched region represents an additional hazard since it is more easily detonated than the methane-rich majority of the cloud.

Data and theory available before the Burro series indicated that RPT explosions were not likely to occur. Although numerous explosions were observed on both Burros 6 and 9, they occurred under very different circumstances. Differential boiling

of the LNG and the consequent enrichment in higher hydrocarbons of the LNG appear to be involved in the Burro 6 explosions, but the Burro 9 explosions appear to be due substantially to the direct interaction of LNG with water. The explosions were energetic enough to have caused some damage to the facility, with a maximum overpressure (static) of 0.72 psi being recorded at 30 m. Two disturbing possibilities associated with the occurrence of RPTs arise: First, RPTs could be energetic enough to turn a small accident into a large one, and, second, the RPT-produced shock wave might be energetic enough to ignite the ethane-rich and more easily detonable region of the vapor cloud. More large experiments at higher spill velocities will be required to determine how severe these hazards might be.

The high-frequency data (3 to 5 Hz) indicate significant fluctuations about the 10-s-average values used as the basis for discussions of gas-transport and contour plots. Fluctuations above 5% gas concentration are commonly associated with 10-s mean concentrations above 1%. This implies that the flammable extent of a gas cloud will be larger than is indicated by the mean lower flammability limit contour generated from either the experimental data or computer model calculations.

The heat flux from the ground into the cold cloud was found to be independent of wind speed. Although several more-complicated models were tried, the data correlate best with a simple linear dependence on temperature difference between the ground and the cloud.

Humidity measurements made both upwind and downwind in the array indicated that the water content of the gas cloud was substantially higher than the ambient air. The correlation showed that a 1% gas concentration was associated with a 15% increase in absolute humidity. The mechanism by which this additional water is entrained by the cloud during the spill process is not yet known. However, both humidity and heat flux contribute to the overall energy balance of the dispersing gas cloud and can affect the nature of the dispersion.

The data discussed in this report are part of the ongoing DOE program of safety research into liquefied gaseous fuels. The goal of the program is to be able to predict the hazards associated with accidents involving LNG or other liquefied gaseous fuels. To that end, the data are being used for detailed comparisons with computer models, but it is clear that we do not have enough information on hand to draw general conclusions about the effects of varying atmospheric and spill conditions. The Burro 8 data have demonstrated to us that larger tests are necessary if the relationship between spill size and atmospheric dispersion is to be understood. Additional field experiments to investigate RPTs and vapor fires are currently underway, as is further analysis of the data and comparison with theory and models.

ACKNOWLEDGMENTS

This paper is based on the results of work by many others who contributed to the success of the experiment and the data analysis. While we cannot mention them all, we would like to single out a few for special thanks. First and foremost are Lyle Kamppinen, Rod Kiefer, John Baker, Troy Williams, and Miles Spann of the LLNL Electrical Engineering Department and the crew of electronics technicians from both LLNL and the EG&G Special Measurements Department, without whose dedication, innovation, and technical excellence this work would not have been possible.

We would also like to acknowledge the contribution of Bill Wakeman, Greg Bianchi, Rex Blocker, and the other mechanical engineers and technicians who helped with the field work. Our special thanks go to Louise Morris who generated the gas-concentration contours, to Don Baltz and other members of the EG&G Scientific Services Department who did much of the data-acquisition-system programming, to Bill Ginsberg and other members of the EG&G Remote Measurements Department who did helicopter-based infrared imaging of the tests, and to Jeff Simmonds and his group from the Jet Propulsion Laboratory who built and fielded the FBDR infrared gas sensor.

This work is also the direct result of capable and supportive program leadership. We would like to acknowledge John Cece, our DOE contract monitor, Bill Hogan, our LLNL LGF Program Leader, and Doug Lind, the leader of the NWC team for their help in making these experiments a success.

REFERENCES

1. R.P. Koopman, L. M. Kamppinen, W. J. Hogan, and C. D. Lind, *Burro Series Data Report: LLNL/NWC 1980 LNG Spill Tests*, Lawrence Livermore National Laboratory, Livermore, Calif., UCID-19075 (1981).
2. G. E. Bingham, R. D. Kiefer, C. H. Gillespie, T. G. McRae, H. C. Goldwire, and R. P. Koopman, *A Portable, Fast-Response Multiwavelength Infrared Sensor for Methane and Ethane in the Presence of Heavy Fog*, Lawrence Livermore National Laboratory, Livermore, Calif., UCRL-84850 (1980).
3. J. M. Conley, J. J. Simmonds, R. A. Britten, and M. Sinna, "A Four Band Differential Radiometer for Monitoring LNG Vapors," *Liquefied Gaseous Fuels Safety and Environmental Control Assessment Program: Second Status Report*, U.S. Department of Energy, DOE/EV-0085, Report L (1980).
4. P. Dubois, J. Fletcher, and M. Richards, *Livermore Time-Sharing System: Chapter 4, Files*, Computer Information Center, Lawrence Livermore National Laboratory, Livermore, Calif., CIC LTSS-4, Ed. 2, Rev. 1 (1976).
5. S. E. Jones and D. R. Ries, *A Relational Data Base Management System for Scientific Data*, Lawrence Livermore National Laboratory, Livermore, Calif., UCRL-80769 (1978).
6. G. Peterson and A. B. Budgor, "The Computer Language MATHSY and Applications to Solid State Physics," *Comm. ACM* **23**, 466 (1980).
7. C. A. Paulsen, "The Mathematical Representation of Wind Speed and Temperature Profiles in the Unstable Atmospheric Surface Layer," *J. App. Meteor.* **9**, 857 (1970).
8. A. J. Dyer, "A Review of Flux-Profile Relationships," *Boundary-Layer Meteor.* **7**, 363 (1974).
9. H. H. Lettau, "Wind and Temperature Profile Prediction for Diabatic Surface Layers Including Strong Inversion Cases," *Boundary-Layer Meteor.* **17**, 443, (1979).
10. D. L. Ermak, R. A. Nyholm, and R. Lange, *ATMAS: A Three-Dimensional Atmospheric Transport Model to Treat Multiple Area Sources*, Lawrence Livermore National Laboratory, Livermore, Calif., UCRL-52603 (1978).
11. G. T. Csanady, *Turbulent Diffusion in the Environment* (D. Reidel Publishing Company, Dortecht, Holland, 1973), p. 145 and 225.
12. H. Schlichting, *Boundary Layer Theory* (McGraw-Hill Book Company, New York, 1960), 4th ed., p. 27.
13. J. A. Valencia-Chavez and R. C. Reid, "The Effect of Composition on the Boiling Rates of Liquefied Natural Gas for Confined Spills on Water," *Int. J. Heat Mass Transfer* **22**, 831-838 (1979).
14. R. P. Koopman, B. R. Bowman, and D. L. Ermak, "Data and Calculations of Dispersion on 5 m^3 LNG Spill Tests," *Liquefied Gaseous Fuels Safety and Environmental Control Assessment Program: Second Status Report*, U.S. Department of Energy, DOE/EV-0085, Report P (1980).
15. D. C. Bull, J. E. Ellsworth, and G. Hooper, *Initiation of Spherical Detonation in Hydrocarbon/Air Mixtures*, presented at the Sixth International Colloquium on Gasdynamics of Explosions and Reactive Systems, Stockholm, Sweden (1977).
16. C. K. Westbrook and L. C. Haselman, "Chemical Kinetics in LNG Detonations," *Liquefied Gaseous Fuels Safety and Environmental Control Assessment Program: Second Status Report*, U.S. Department of Energy, DOE/EV-0085, Report F (1980).
17. D. S. Burgess, J. Biordi, and J. Murphy, *Hazards of Spillage of LNG Into Water*, U.S. Bureau of Mines, PMSRC Report 4177 (1972).
18. D. L. Katz and C. M. Sliepcevich, "LNG/Water Explosions: Cause and Effect," *Hydro. Proc.* **50**(11), 240 (1971).
19. E. Nakanishi and R. C. Reid, "Liquid Natural Gas-Water Reactions," *Chem. Eng. Prog.* **67**(12), 36 (1971).
20. T. Enger and D. E. Hartman, *Mechanics of the LNG-Water Interactions*, presented at the American Gas Association Distribution Conference, Atlanta, Georgia (1972).
21. J. R. Holt and A. H. Muenker, *Flameless Vapor Explosions in LNG/Hydrocarbon Spills*, Exxon Research and Engineering Company, Linden, New Jersey, GRU.2 GPR.72 (1972).

22. W. M. Porteous and R. C. Reid, "Light Hydrocarbon Vapor Explosions," *Chem. Eng. Prog.* **12**(5), 83 (1976).
23. W. M. Porteous, *Super Heating and Cryogenic Vapor Explosions,* Ph.D. thesis, Massachusetts Institute of Technology, Cambridge, Massachusetts (1975).
24. B. M. Jazayeri, *Impact Cryogenic Vapor Explosions,* M.S. thesis, Massachusetts Institute of Technology, Cambridge, Massachusetts (1975).
25. C. W. Lind, Naval Weapons Center, China Lake, California, private communication (1980).
26. R. L. Rabie, G. R. Fowles, and W. Fickett, "The Polymorphic Detonation," *Phys. Fluids* **22**, 422 (1979).
27. R. S. Hixson, *Vapor Phase Detonations in Light Hydrocarbons,* Ph.D. thesis, Washington State University, Pullman, Washington (1980).

REPORT B

Burro Series Gas Concentration Contours

T. G. McRae
H. C. Goldwire, Jr
R. P. Koopman
J. W. McClure
L. K. Morris

Prepared for the
Environmental and Safety Engineering
Division
U.S. Department of Energy
under Contract W-7405-ENG-48

Lawrence Livermore Laboratory
Livermore, California 94550

REPORT B

TABLE OF CONTENTS

SUMMARY

Gas concentration contours generated from the data taken during the Burro series experiments 8 and 9 are presented. The contours are presented as a function of time in both a horizontal and a vertical format for several areas within the array.

INTRODUCTION

The U.S. Department of Energy sponsored a series of nine field experiments (the Burro series), conducted jointly in 1980 by the Naval Weapons Center, China Lake, California, and the Lawrence Livermore National Laboratory, which were performed to determine the transport and dispersion of vapor from spills of liquefied natural gas (LNG) on water. Those tests, and the analysis of the data obtained from them, are discussed in other reports.[1,2] The data central to much of that discussion are the gas concentration data and the contours generated from that data. Selected contours were presented as part of the analysis report,[1] which is presented as Report A in this document. It is the purpose of this report to simply present the complete time-series sets of contours for some of the more important tests.

STUDY DESIGN

The LNG vapor-concentration data were used to generate two-dimensional contour plots at 10-s time intervals during the experiments. A 10-s average was chosen somewhat arbitrarily; the intent was to use an averaging time that was long enough to average out short-wavelength (much less than cloud width) fluctuations, but short enough to preserve cloud meander. Contour plots are generated for several surfaces: horizontal surfaces at heights of 1 and 3 m above the ground, and vertical crosswind cylindrical surfaces at each row of

the sensor array. The contours are of total hydrocarbon concentration, with data from the faster response-time instruments averaged, using a 19-s running average, so that all the data have approximately the same time constant. Therefore, the contours describe the 10-s average LNG vapor-concentration distribution on a surface at a given time.

The horizontal contours are calculated over a region that extends downwind from the spill point ($x = 0$) to the final row of sensors at 800 m. To close the contours in the source region, the concentration at $x = 0$ is arbitrarily defined by a hyperbolic concentration distribution that is held constant during the spill and is decreased linearly to zero after the spill valve is closed.

In both the horizontal and vertical contour-plot concentrations, a "dummy" station is added to both ends of each sensor row at a distance equal to the station spacing for that row. When the LNG vapor cloud is well within the array and the concentration at the end of the row is essentially zero (<1%), the concentration at the corresponding "dummy" sensor is set equal to zero. If part of the cloud extends beyond the edge of the array, the "dummy" sensors are ignored and the contours are truncated at the edge of the array.

The gas concentration at each station location is set equal to zero at a height of 12 m. The concentration at the ground is extrapolated from the measured values at heights of 1 and 3 m. When the 3-m concentration is less than the 1-m value, the ground-level concentration is determined by using a quadratic extrapolation that passes through the 1- and 3-m concentration values and has a zero concentration gradient at the ground. For those cases where the 3-m concentration is greater than the 1-m value, the ground-level concentration is linearly extrapolated from these two values. Concentrations at points within the calculational region are determined by a linear interpolation in three dimensions.

Interpolating over the long distances between sensors in the 140-, 400-, and 800-m arcs produces some uncertainty in the calculation of gas-concentration values between these arcs. A linear interpolation scheme was used

because of its inherent simplicity and ease of interpretation. If different interpolation schemes are used, different results will be obtained between arcs. In particular, the distance to the lower flammability limit (LFL), i.e., the 5% contour for methane, is generally between the 140- and 400-m arcs for these tests. Comparing logarithmic interpolation with linear interpolation for concentration versus downwind distance data from several of the tests, shows that logarithmic interpolation results in an LFL distance which can be as much as 80 m shorter than linear interpolation. Analysis of contours from all of the experiments, using a variety of interpolation schemes, indicates that, in general, the uncertainty in the LFL distance is -40 to +20 m.

Since the distance between sensors on a tower and stations in an arc are much less than the distances between arcs, the uncertainty in contour location is much less for the vertical contours than it is for the horizontal contours. We estimate the uncertainty in the position of the vertical contours to be less than 1 m.

STUDY RESULTS

The Burro 8 and Burro 9 tests are the two most important tests in the experimental series. Burro 8 was performed under stable atmospheric conditions in an average wind speed of 1.8 m/s and showed most strongly the effects unique to dense gas dispersion. The horizontal gas concentration contours at 1 m above ground level for the Burro 8 test are shown in Figures 1 to 20, at 20-second intervals, starting at 20 seconds and continuing for 400 seconds. The outermost contour shown is 1% followed by 2.5%, 5%, 10%, 15%, 25%, and 35%, etc. Contours above 15% are shown in 10% increments up to the maximum measured concentration. Each contour consists of a dotted and solid line. The dotted contour is for a concentration 0.05% less its adjacent solid contour to indicate the direction and magnitude of the concentration gradient. On the Burro 8 tests, the furthest extent of the LFL was recorded at the 3-m height between 380 seconds and 440 seconds. Horizontal contours at

3 m are shown for this time interval in Figures 21 to 24. Vertical concentration contours have also been constructed from the gas sensor data at each of the four arcs of stations. Shown in Figures 25 to 44 are the vertical gas concentration contours from the 57-m arc, starting with 1% at the top followed by 2.5%, 5%, 15%, 25%, and 35%, plotted as a function of height above ground level. The contours are shown for 20 to 400 seconds, in 20-second increments, and are as would be seen when facing the pond from the down wind side. A similar set of vertical concentration contours for the 140-m arc of stations is shown in Figures 45 to 62 for 60 to 400 seconds in 20-second increments. Vertical contours for the 400-m arc are shown in Figures 63 to 77 starting at 220 seconds and continuing to 500 seconds, in 20-second increments. Gas concentrations above the LFL reach this arc at 380 seconds as can be seen in Figure 71. Concentration contours for the 800-m arc are not shown because these concentrations were always less than the LFL. These concentrations were used in generating the horizontal concentration contours, however.

The Burro 9 test was also important in that the facility achieved its highest spill rate, the wind field was such that the cloud stayed within the array over the duration of the experiment, and nearly all of our sensors were operational. The average wind speed was 5.7 m/s and the gas cloud behaved in a manner typical for the moderate or high wind speed tests. Horizontal gas concentration contours at 1 m above ground level are shown for Burro 9 in Figures 79 to 91. The outermost contour is 1% followed by 2.5%, 5%, 7.5%, 10%, etc., in 2.5% increments. The horizontal contours at 3 m are not shown since the furthest extent of the LFL occurs at a height of 1 m in this test. Rapid phase transition (RPT) explosions occured throughout this test throwing mud and water on the sensors in the 57-m arc. This data is not very reliable; consequently the vertical contours in the 57-m arc are not shown and the perturbation in the horizontal contours at 57-m should be ignored. Vertical contours for the 140-m arc are shown in Figures 92 to 101 for the period from 30 seconds to 170 seconds, in 10-second increments. Similarily, vertical contours for the 400-m arc are shown in Figures 102 to 110, starting at 90 seconds and continuing until 170 seconds in 10-second increments. Concentrations in the 800-m arc never exceed 2.5% and are not shown, although they were used to generate the horizontal contours.

REFERENCES

1. R.P. Koopman, R.T. Cederwall, D.L. Ermak, H.C. Goldwire Jr., J.W. McClure, T.G. McRae, D.L. Morgan, H.C. Rodean, and J.H. Shinn, Description and Analysis of Burro Series 40-m^3 LNG Spill Experiments. UCRL-53186 Lawrence Livermore National Laboratory, Livermore, California, 1981.

2. R.P. Koopman, L.M. Kamppinen, W.J. Hogan, and C.D. Lind, Burro Series Data Report: LLNL/NWC 1980 LNG Spill Tests. UCID-19075 Lawrence Livermore National Laboratory, Livermore, California, 1981.

CONCENTRATION CONTOURS FOR BURRO 8 AND BURRO 9

Concentration contours shown in Figures 1 through 110 generally correspond to the following increments:

Burro 8 - 1%, 2.5%, 5%, 10%, 25% and 35%

Burro 9 - 1%, 2.5%, 5%, 7.5% and 10%

Many of the figures have more or less than the number of contours indicated above. Where fewer contours are shown they represent the above increments taken in ascending order up to the maximum concentrations measured. Figures with more than the above concentration increments contain contours in 10% increments above the maximum in the above ranges.

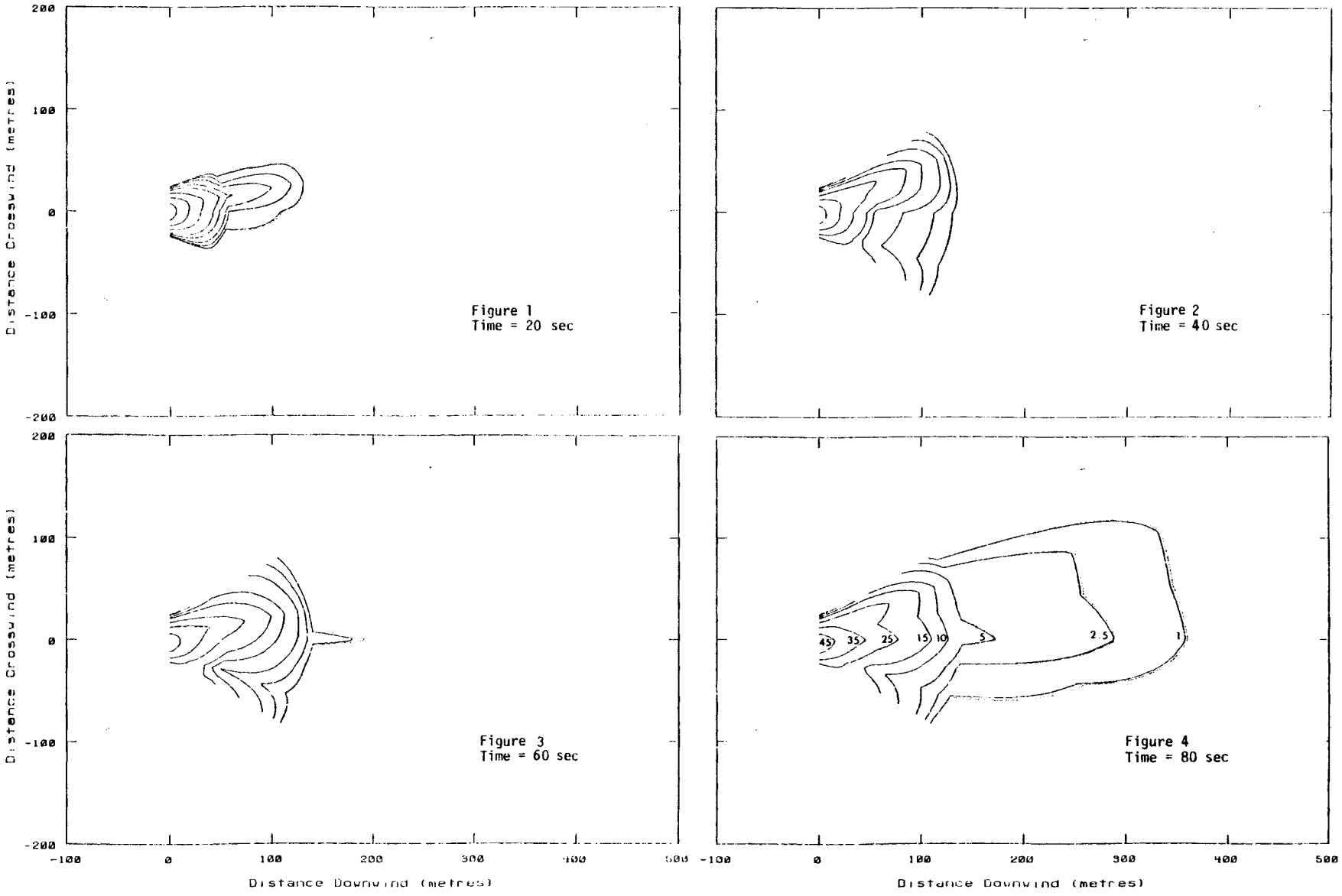

FIGURES 1-4. Burro 8 Horizontal Concentration Contours at 1 m Above Ground Level. Contours at 1%, 2.5%, 5%, 10%, 15%, 25% and 35% Gas Concentrations.

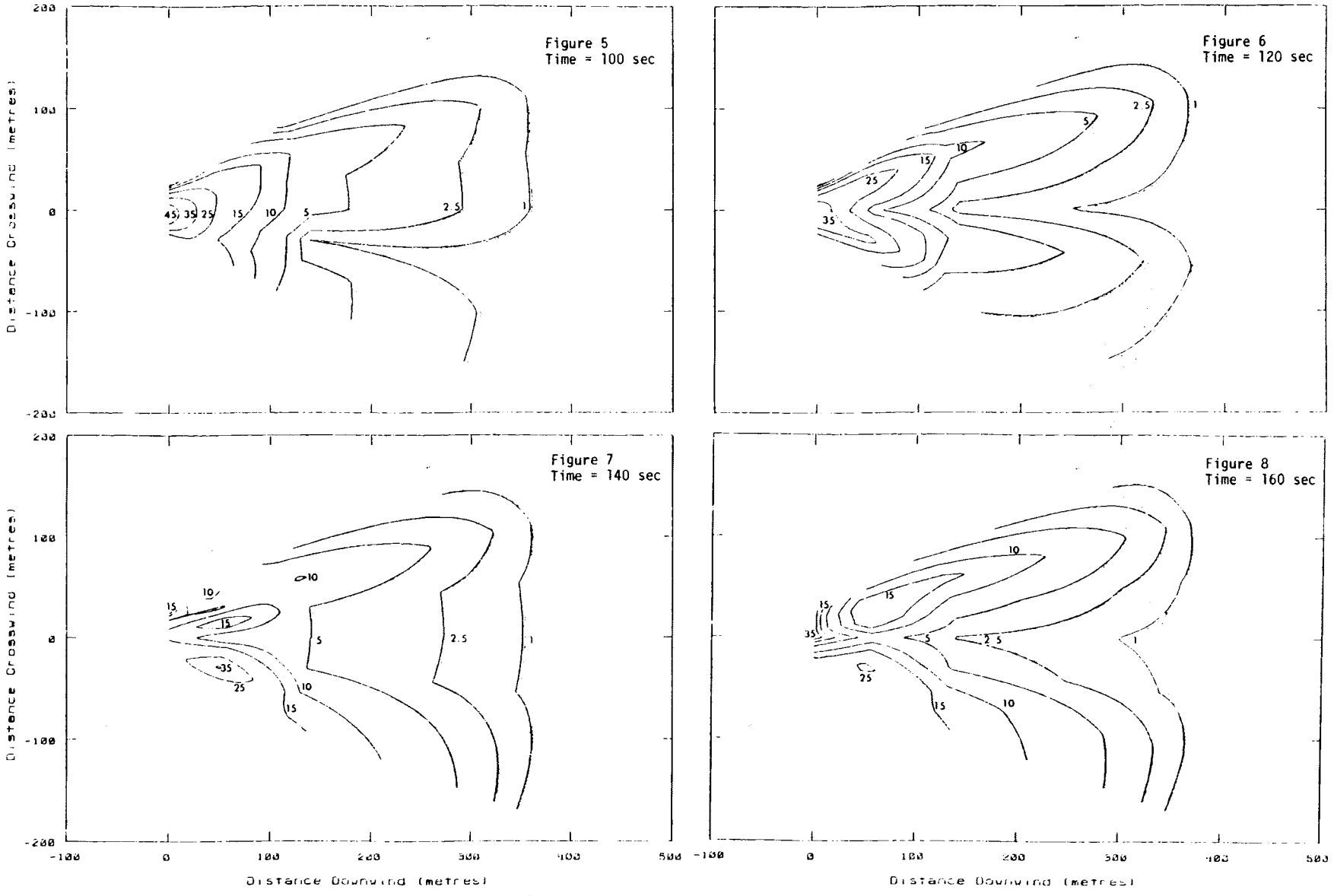

FIGURES 5-8. Burro 8 Horizontal Concentration Contours at 1 m Above Ground Level. Contours at 1%, 2.5%, 5%, 10%, 15%, 25% and 35% Gas Concentrations.

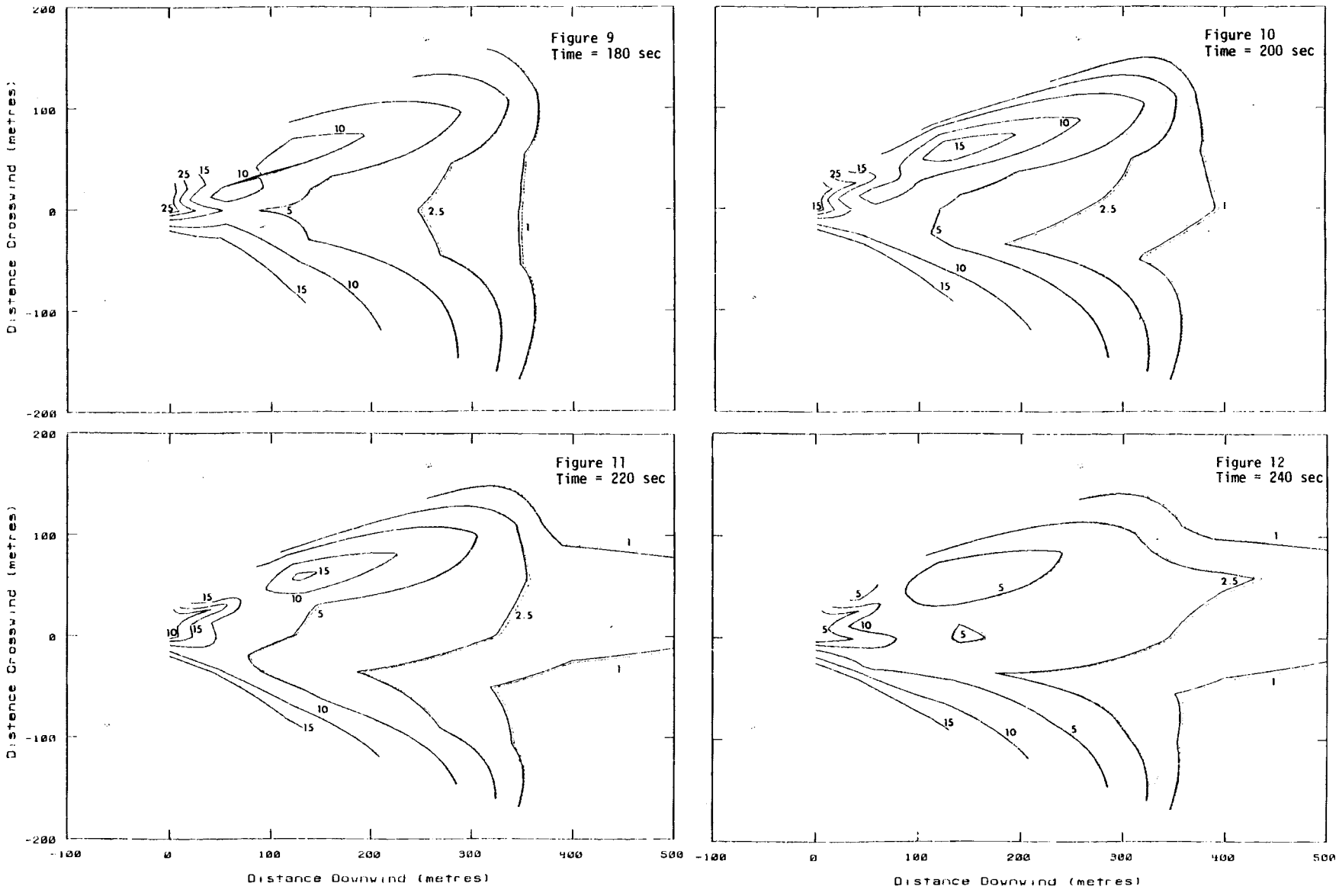

FIGURES 9-12. Burro 8 Horizontal Concentration Contours at 1 m Above Ground Level. Contours at 1%, 2.5%, 5%, 10%, 15%, 25% and 35% Gas Concentrations.

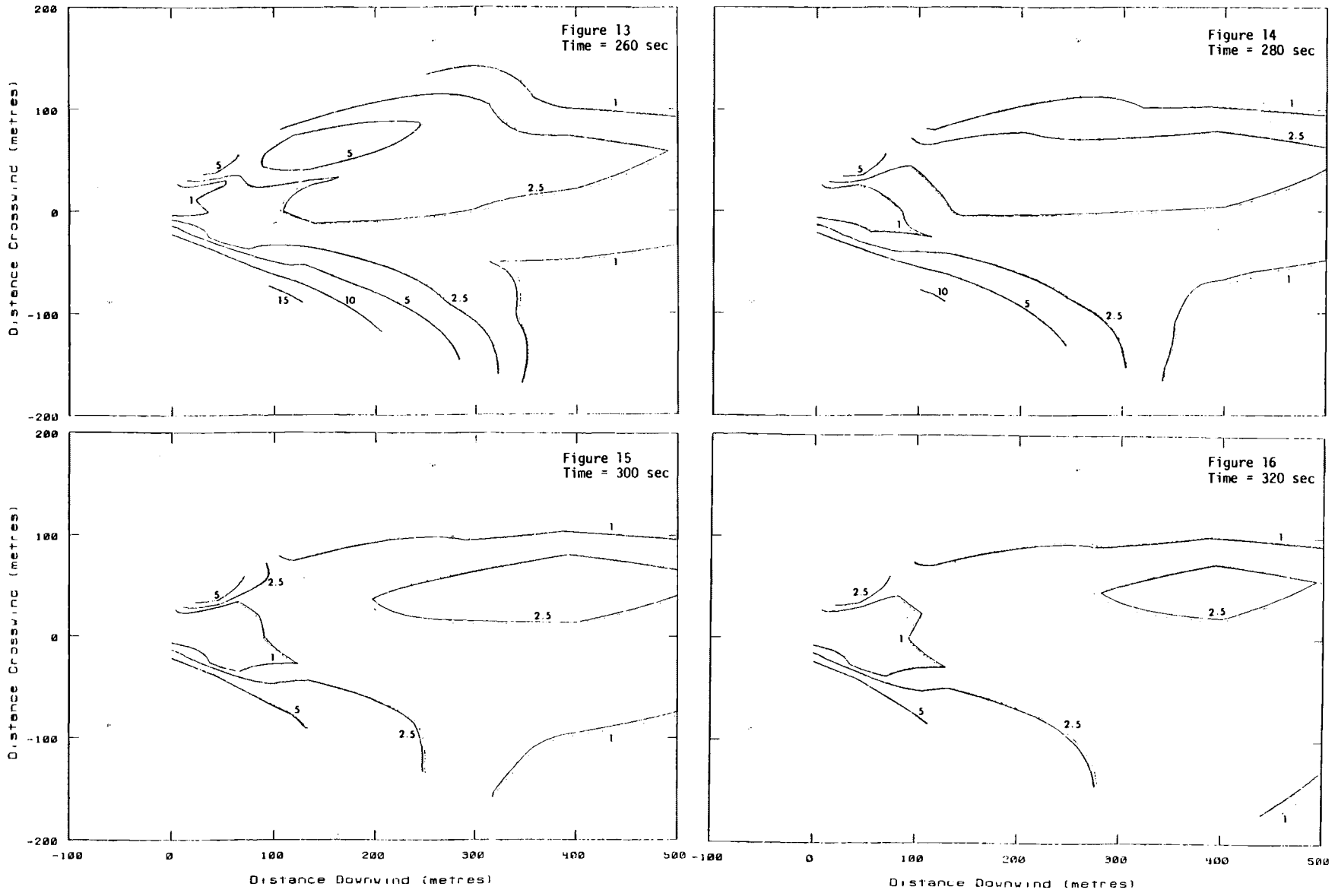

FIGURES 13-16. Burro 8 Horizontal Concentration Contours at 1 m Above Ground Level. Contours at 1%, 2.5%, 5%, 10%, 15%, 25% and 35% Gas Concentrations.

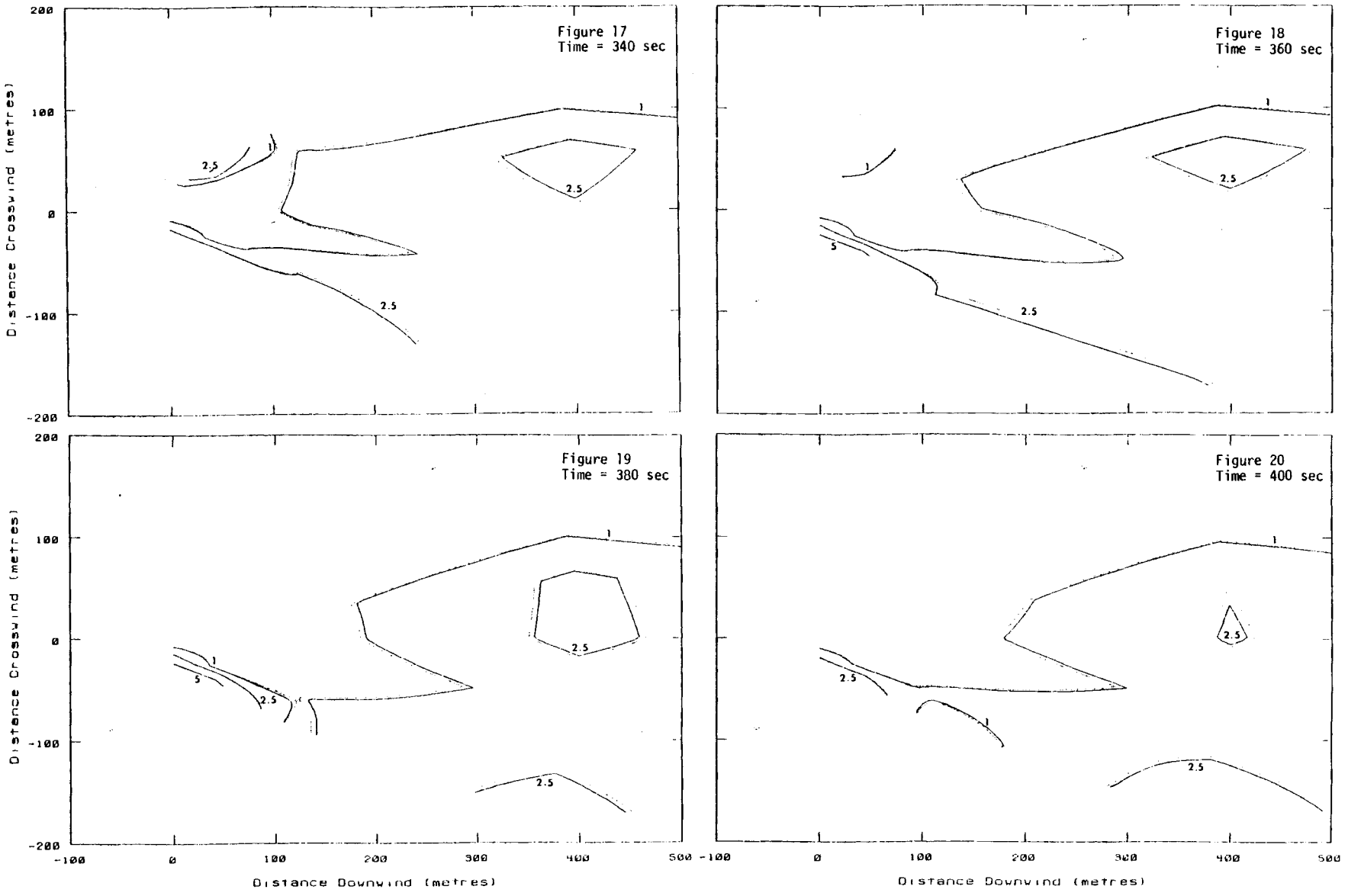

FIGURES 17-20. Burro 8 Horizontal Concentration Contours at 1 m Above Ground Level. Contours at 1%, 2.5%, 5%, 10%, 15%, 25% and 35% Gas Concentrations.

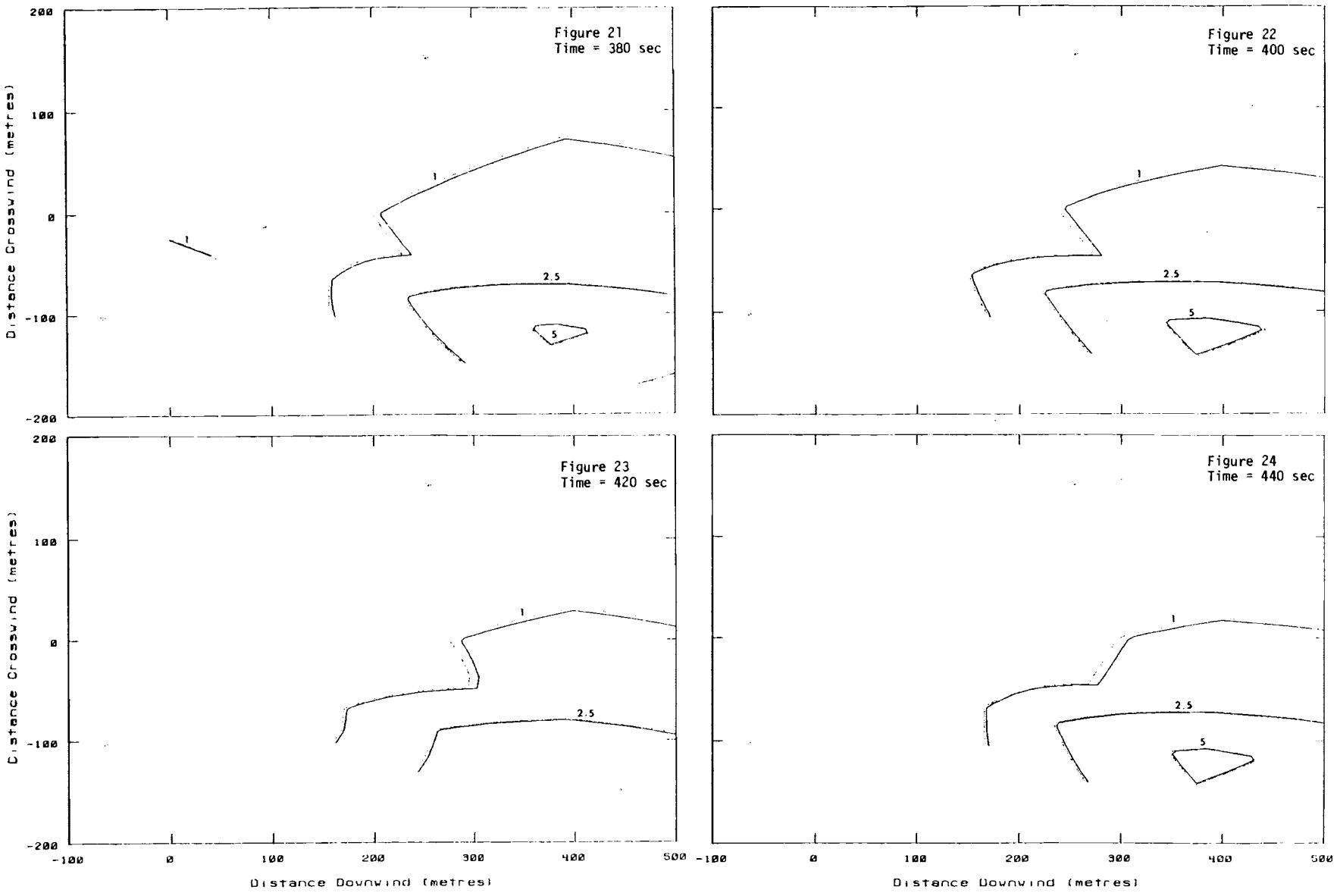

FIGURES 21-24. Burro 8 Horizontal Concentration Contours at 3 m Above Ground Level. Contours at 1%, 2.5%, 5%, 10%, 15%, 25% and 35% Gas Concentrations.

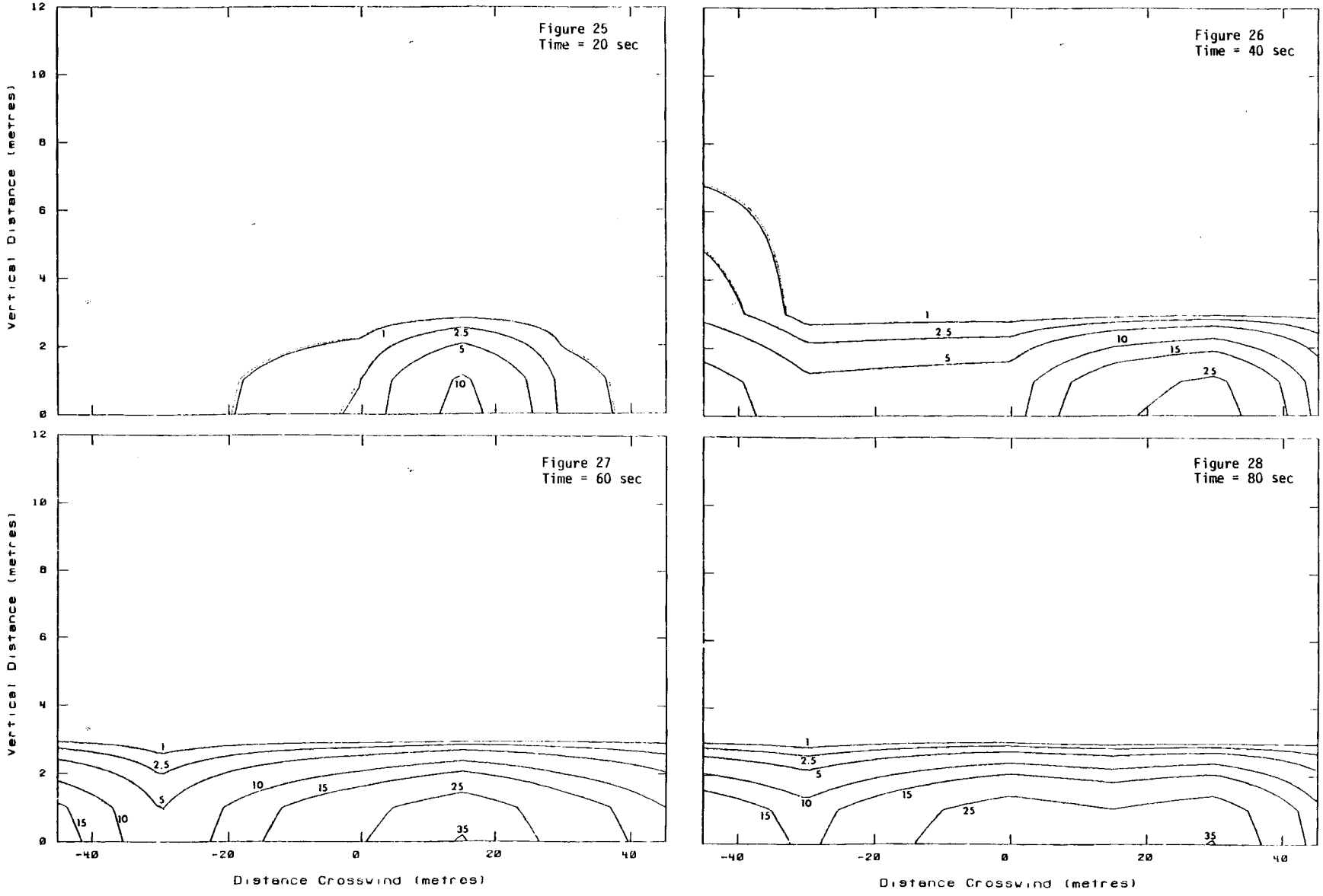

FIGURES 25-28. Burro 8 Vertical Concentration Contours at Row 1 Instrument Array. Contours at 1%, 2.5%, 5%, 10%, 15%, 25% and 35% Gas Concentrations.

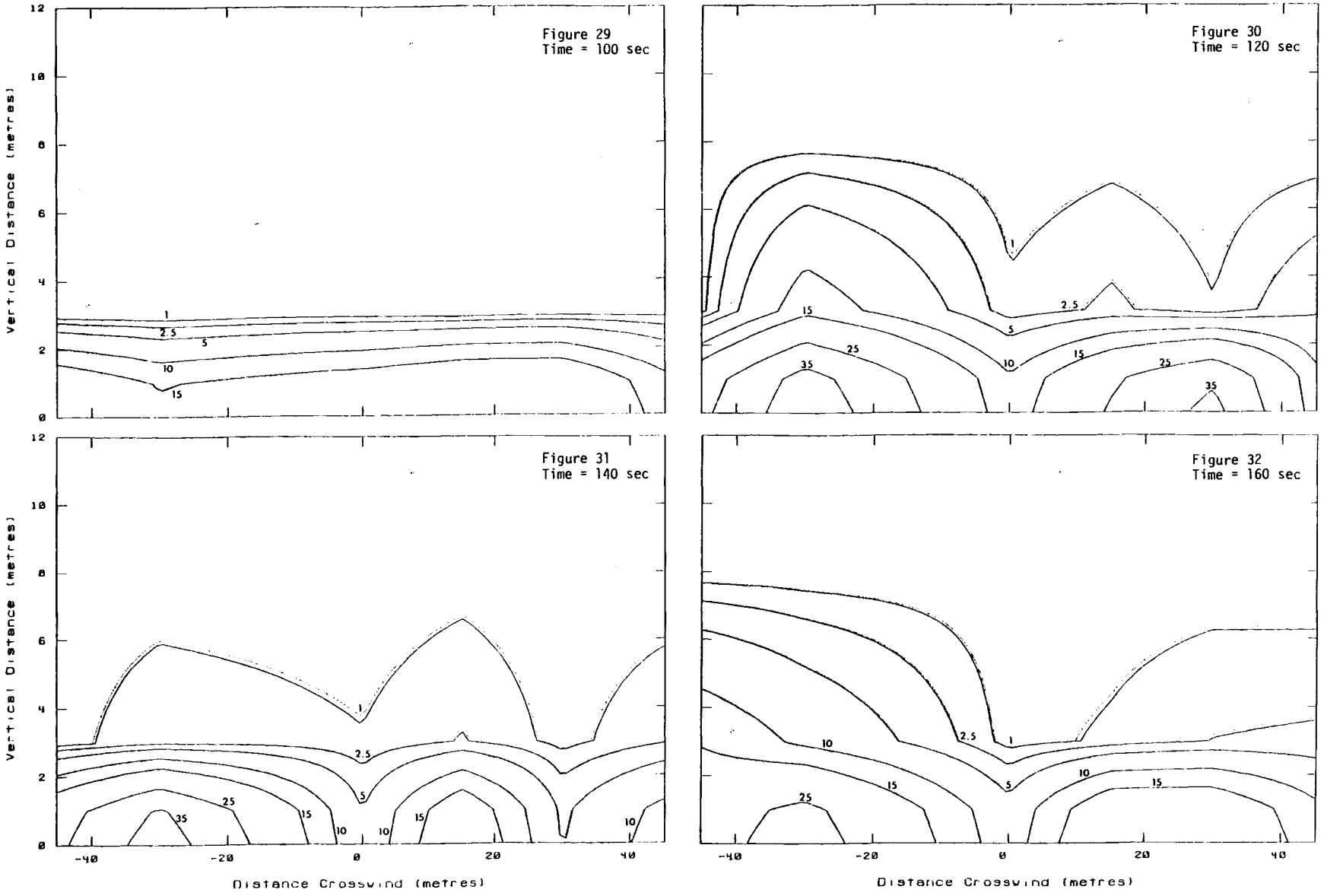

FIGURES 29-32. Burro 8 Vertical Concentration Contours at Row 1 Instrument Array. Contours at 1%, 2.5%, 5%, 10%, 15%, 25% and 35% Gas Concentrations.

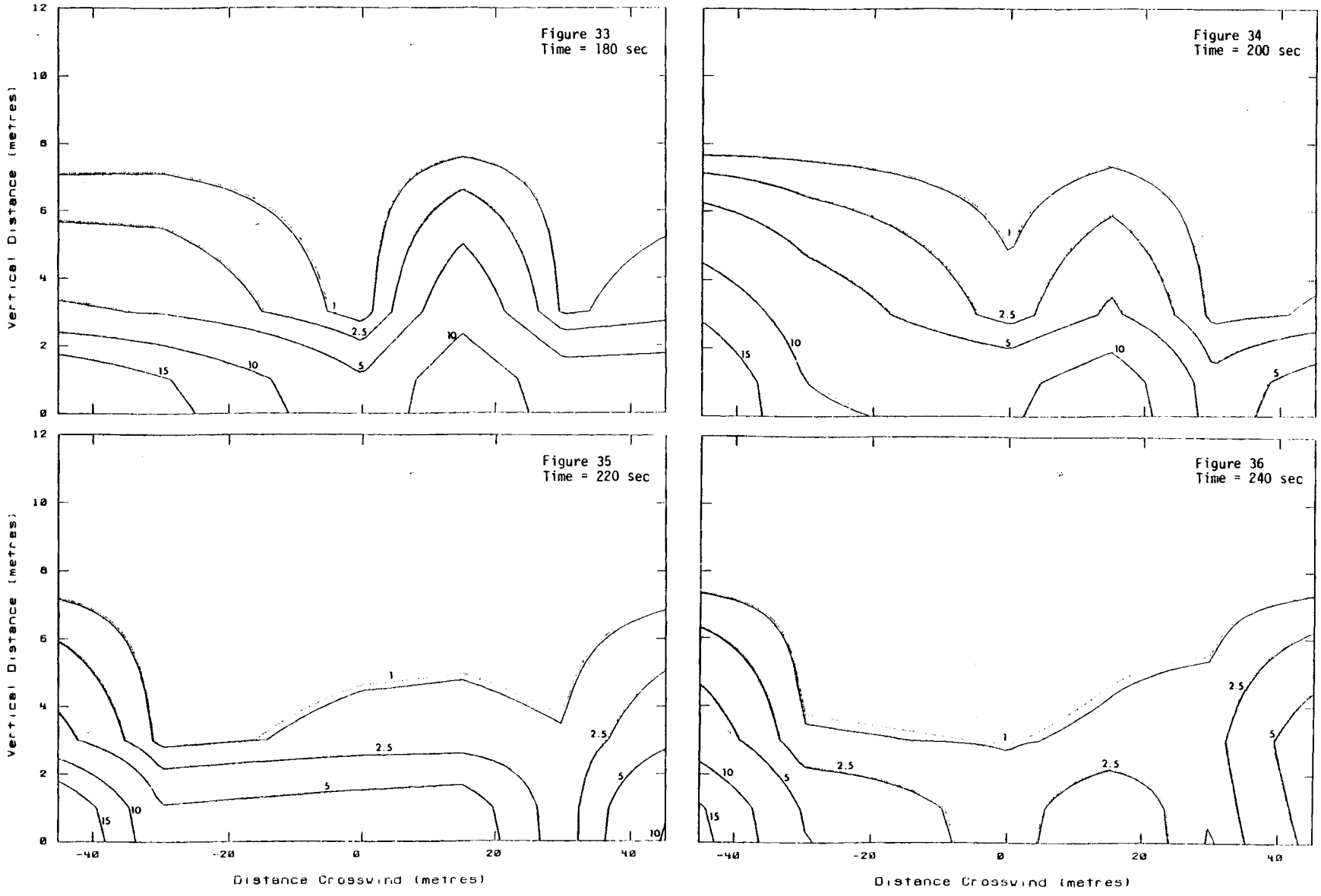

FIGURES 33-36. Burro 8 Vertical Concentration Contours at Row 1 Instrument Array. Contours at 1%, 2.5%, 5%, 10%, 15%, 25% and 35% Gas Concentrations.

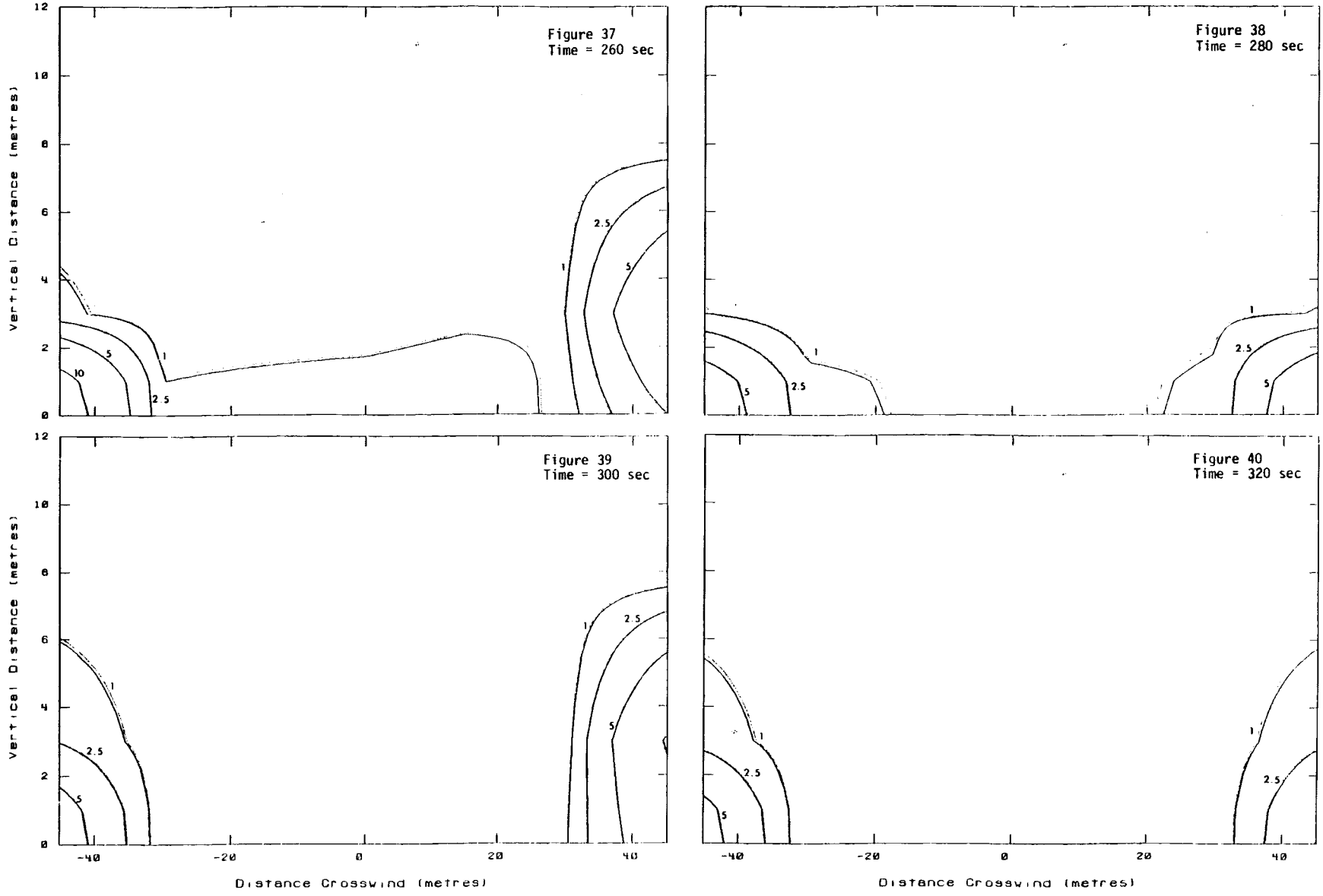

FIGURES 37-40. Burro 8 Vertical Concentration Contours at Row 1 Instrument Array. Contours at 1%, 2.5%, 5%, 10%, 15%, 25% and 35% Gas Concentrations.

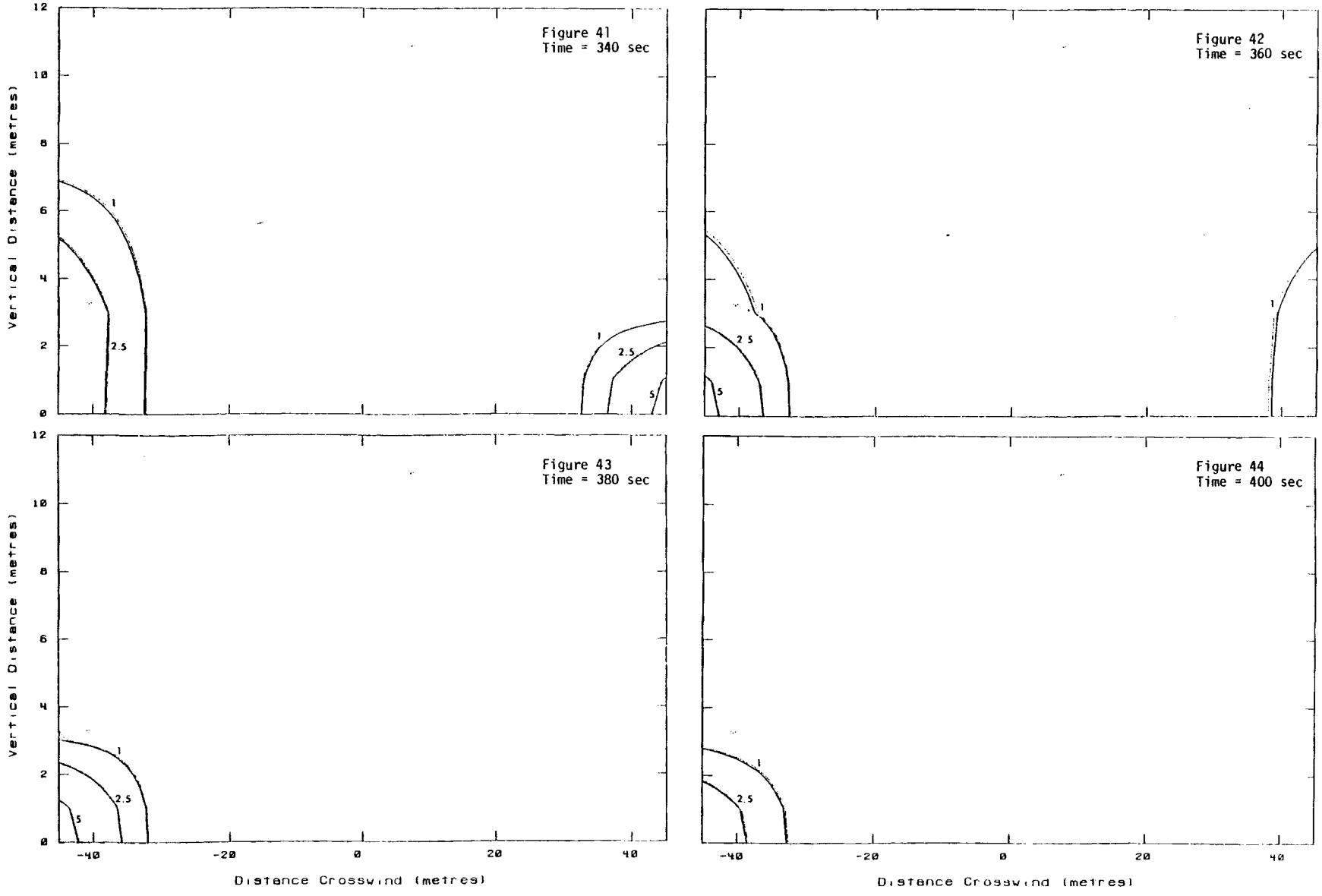

FIGURES 41-44. Burro 8 Vertical Concentration Contours at Row 1 Instrument Array. Contours at 1%, 2.5%, 5%, 10%, 15%, 25% and 35% Gas Concentrations.

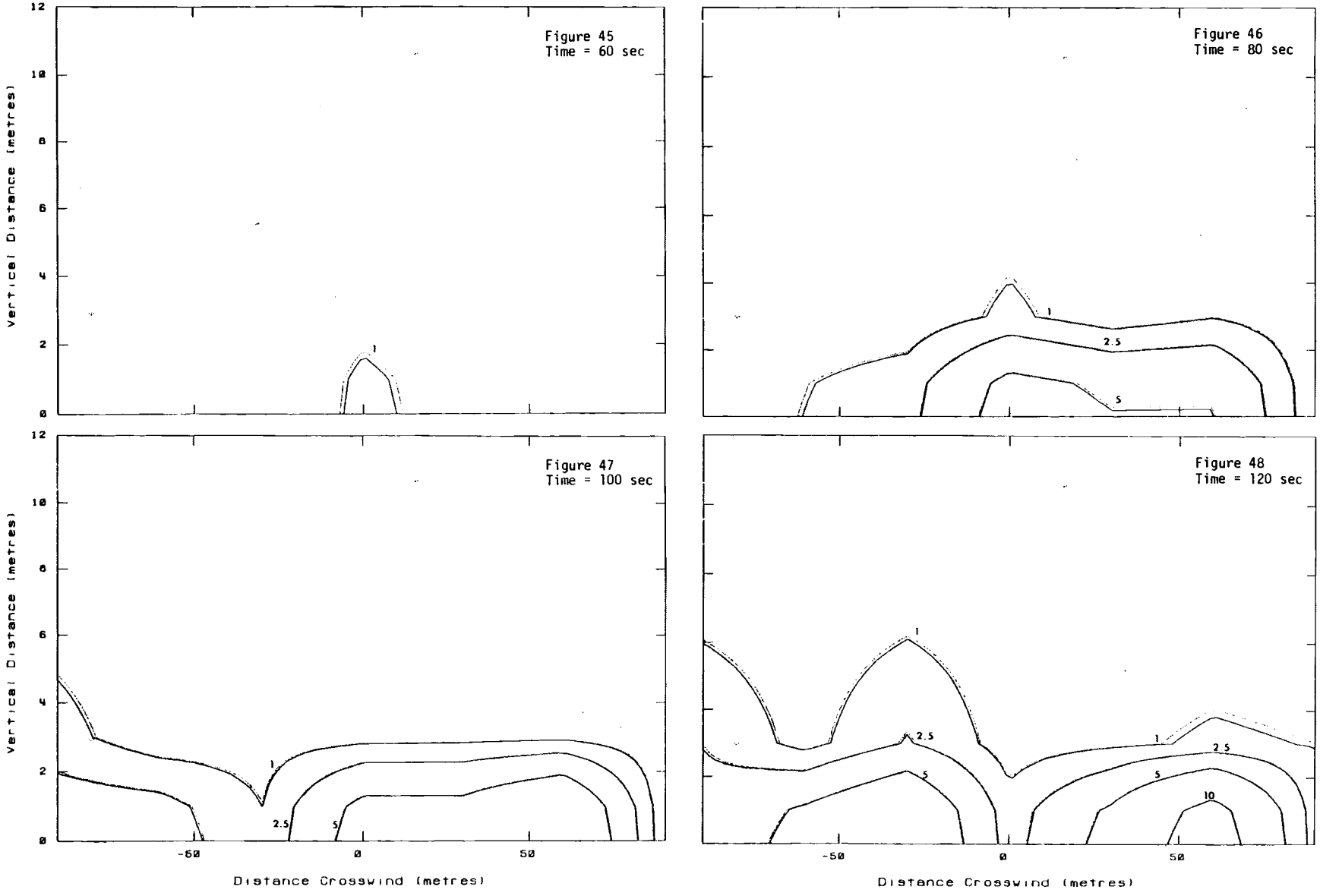

FIGURES 45-48. Burro 8 Vertical Concentration Contours at Row 2 Instrument Array. Contours at 1%, 2.5%, 5%, 10%, 15%, 25% and 35% Gas Concentrations.

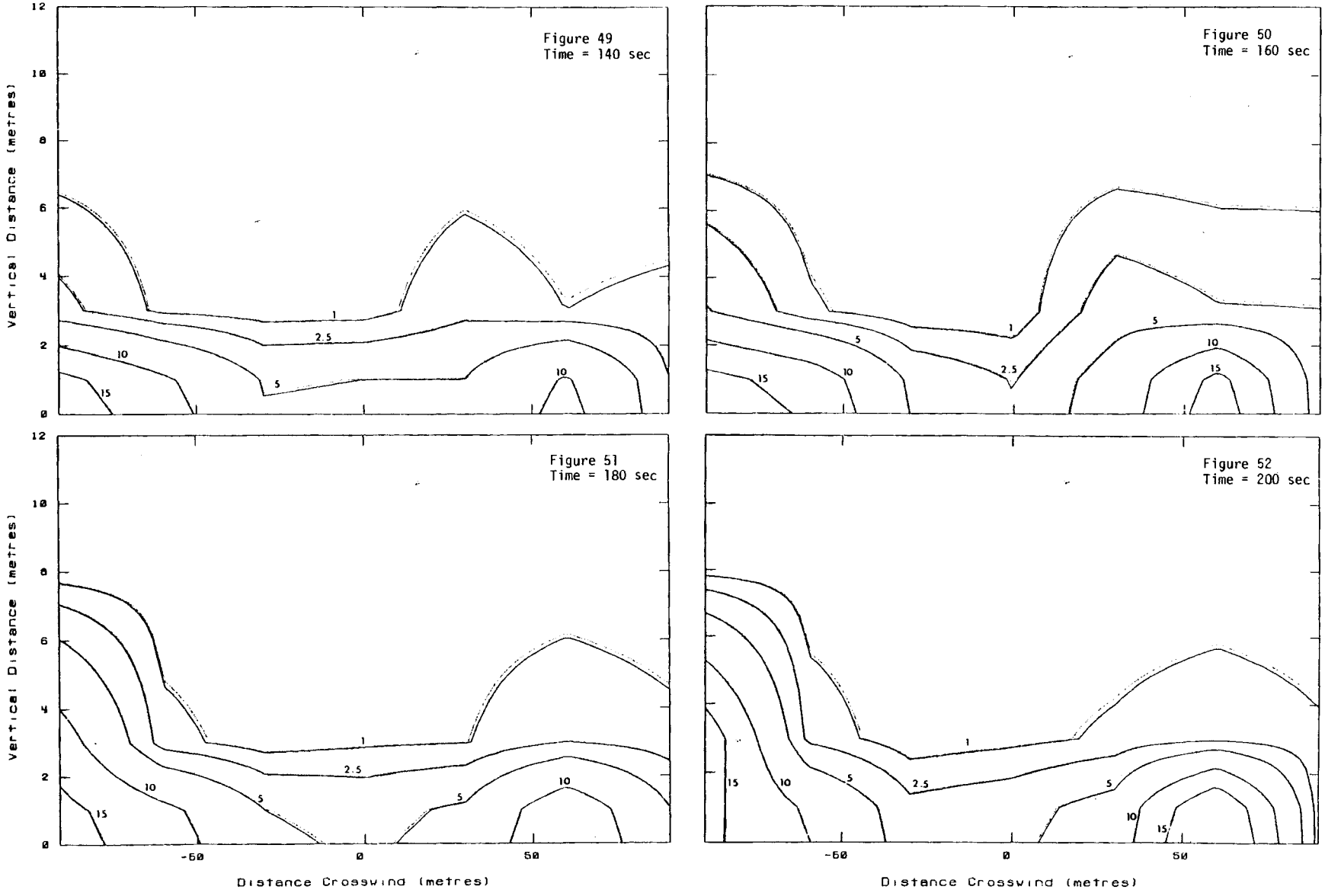

FIGURES 49-52. Burro 8 Vertical Concentration Contours at Row 2 Instrument Array. Contours at 1%, 2.5%, 5%, 10%, 15%, 25% and 35% Gas Concentrations.

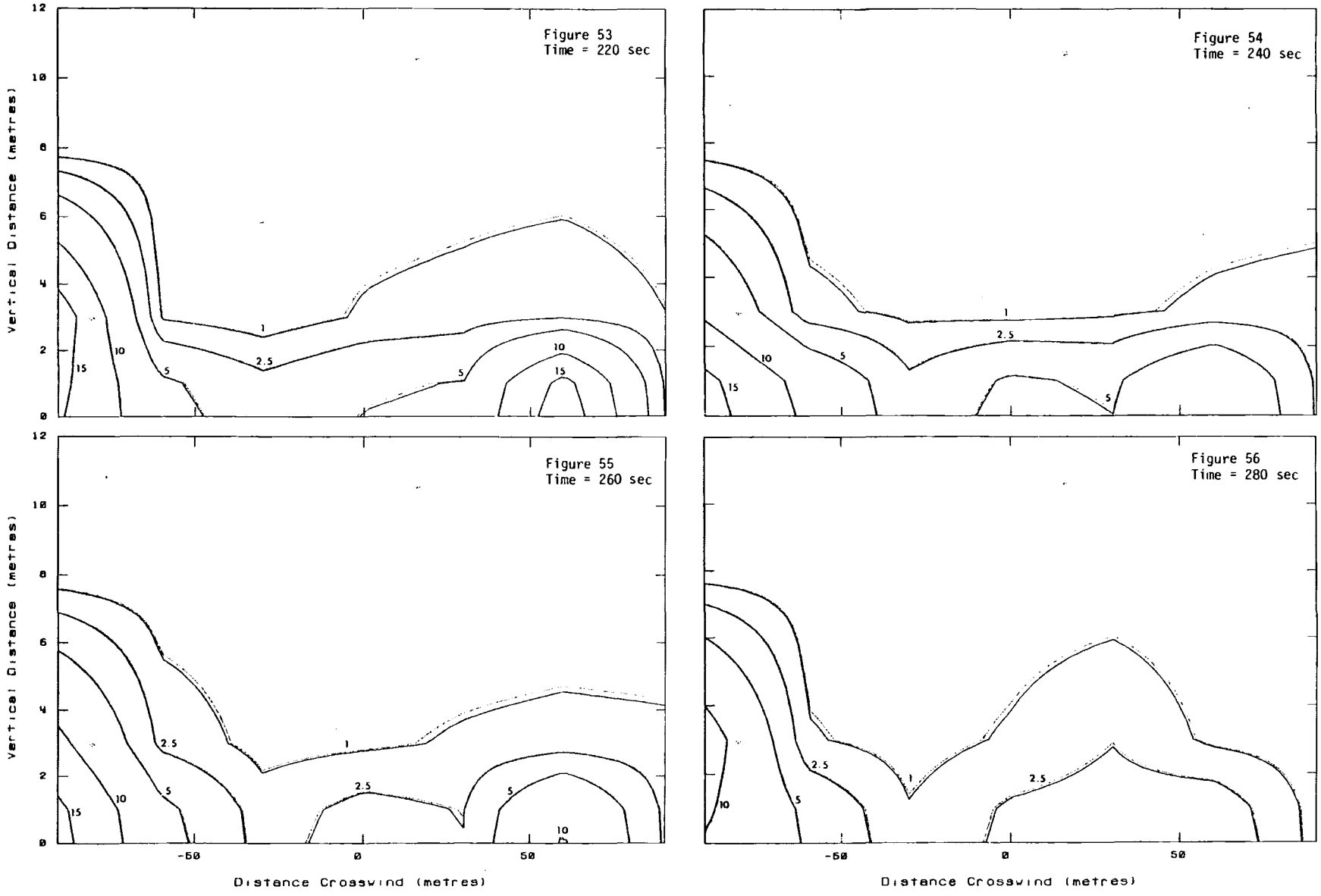

FIGURES 53-56. Burro 8 Vertical Concentration Contours at Row 2 Instrument Array. Contours at 1%, 2.5%, 5%, 10%, 15%, 25% and 35% Gas Concentrations.

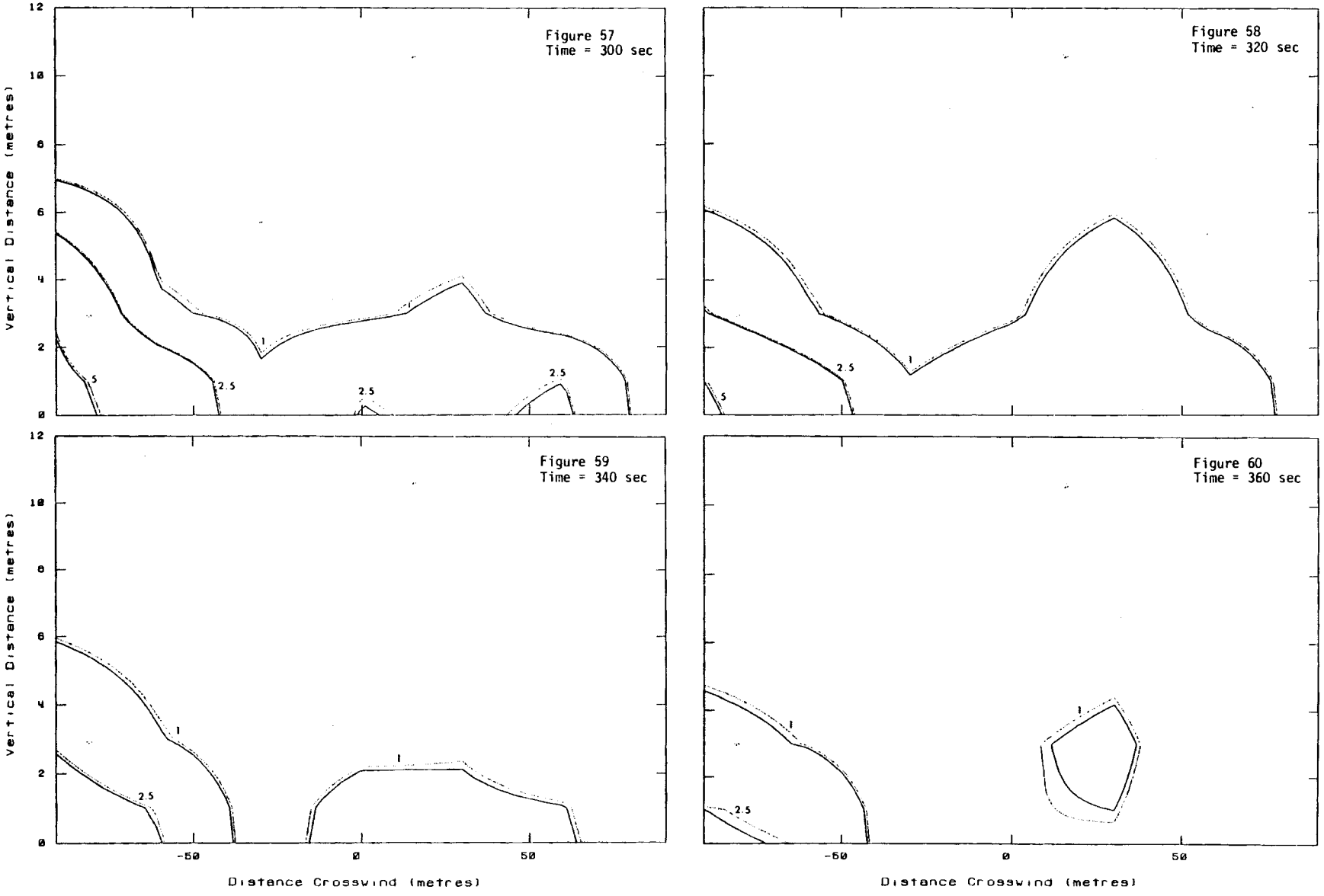

FIGURES 57-60. Burro 8 Vertical Concentration Contours at Row 2 Instrument Array. Contours at 1%, 2.5%, 5%, 10%, 15%, 25% and 35% Gas Concentrations.

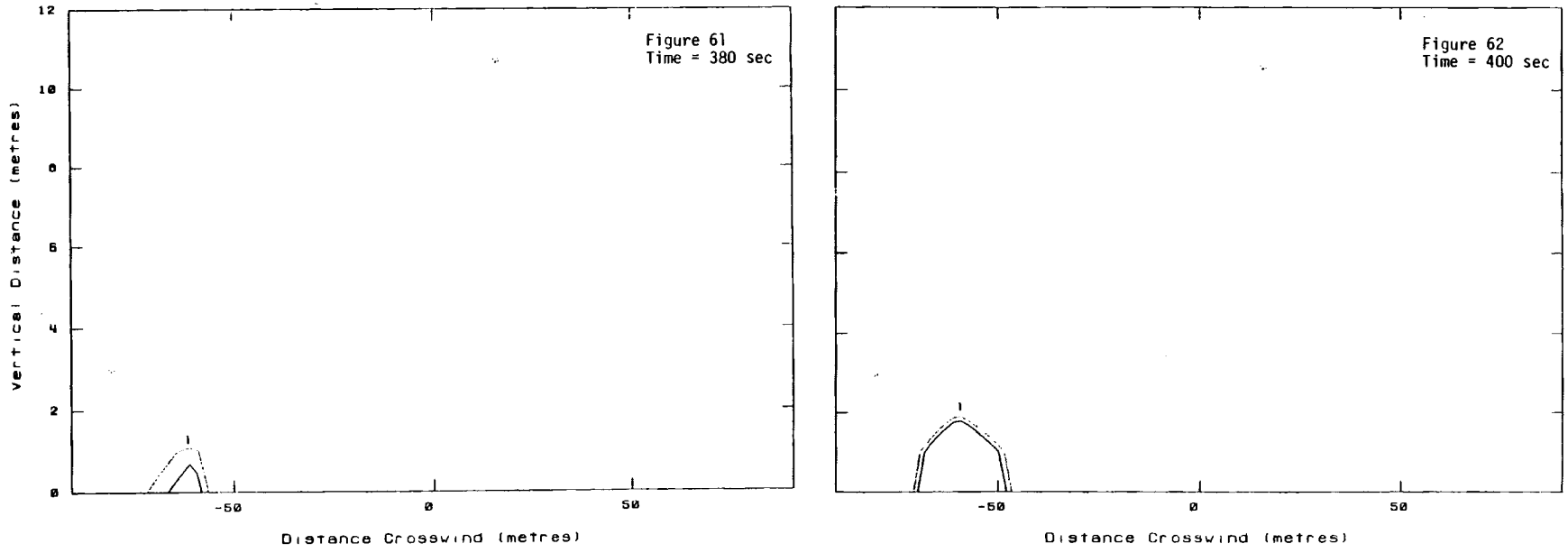

FIGURES 61 and 62. Burro 8 Vertical Concentration Contours at Row 2 Instrument Array. Contours at 1%, 2.5%, 5%, 10%, 15% and 35% Gas Concentrations.

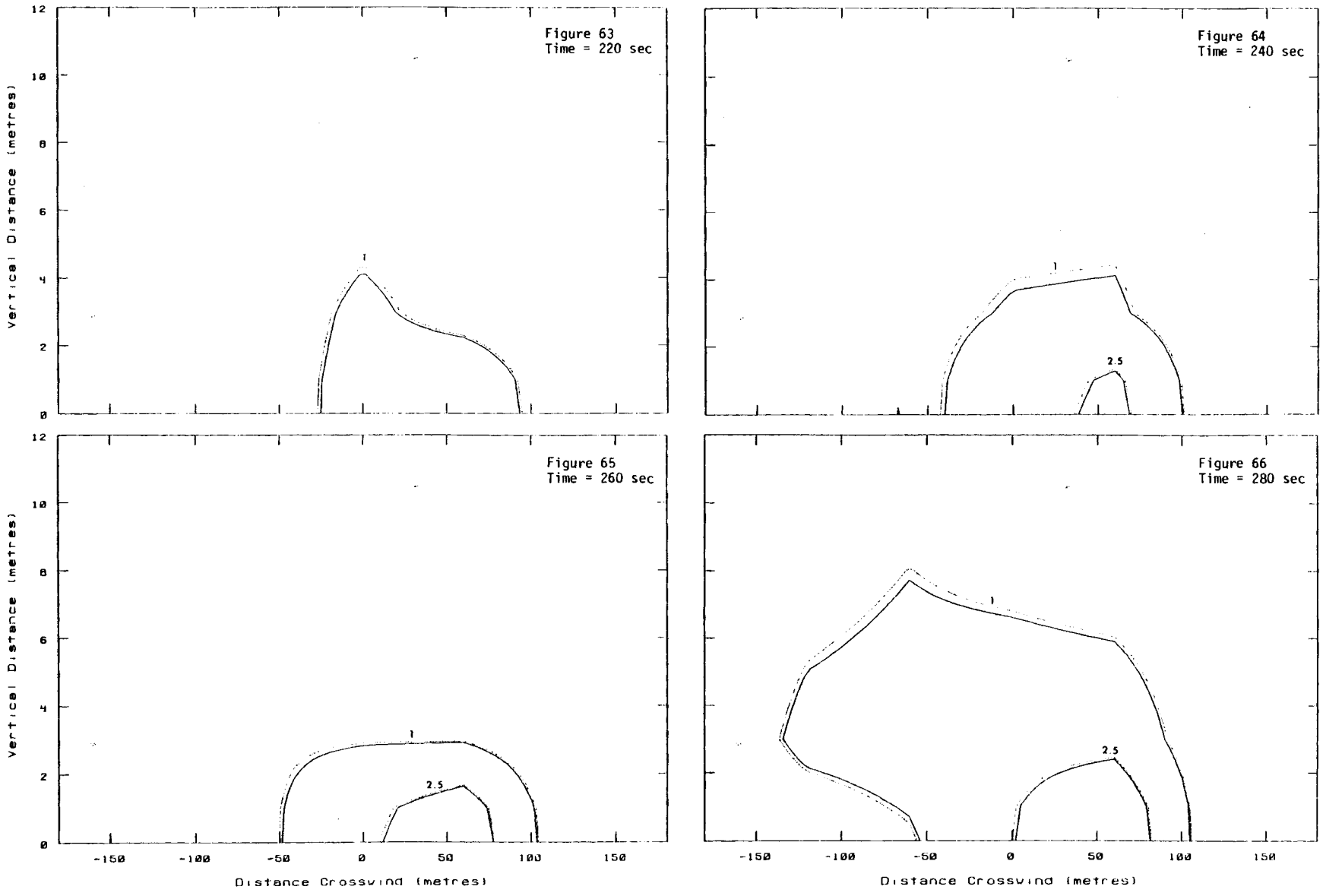

FIGURES 63-66. Burro 8 Vertical Concentration Contours at Row 3 Instrument Array. Contours at 1%, 2.5%, 5%, 10%, 15%, 25% and 35% Gas Concentrations.

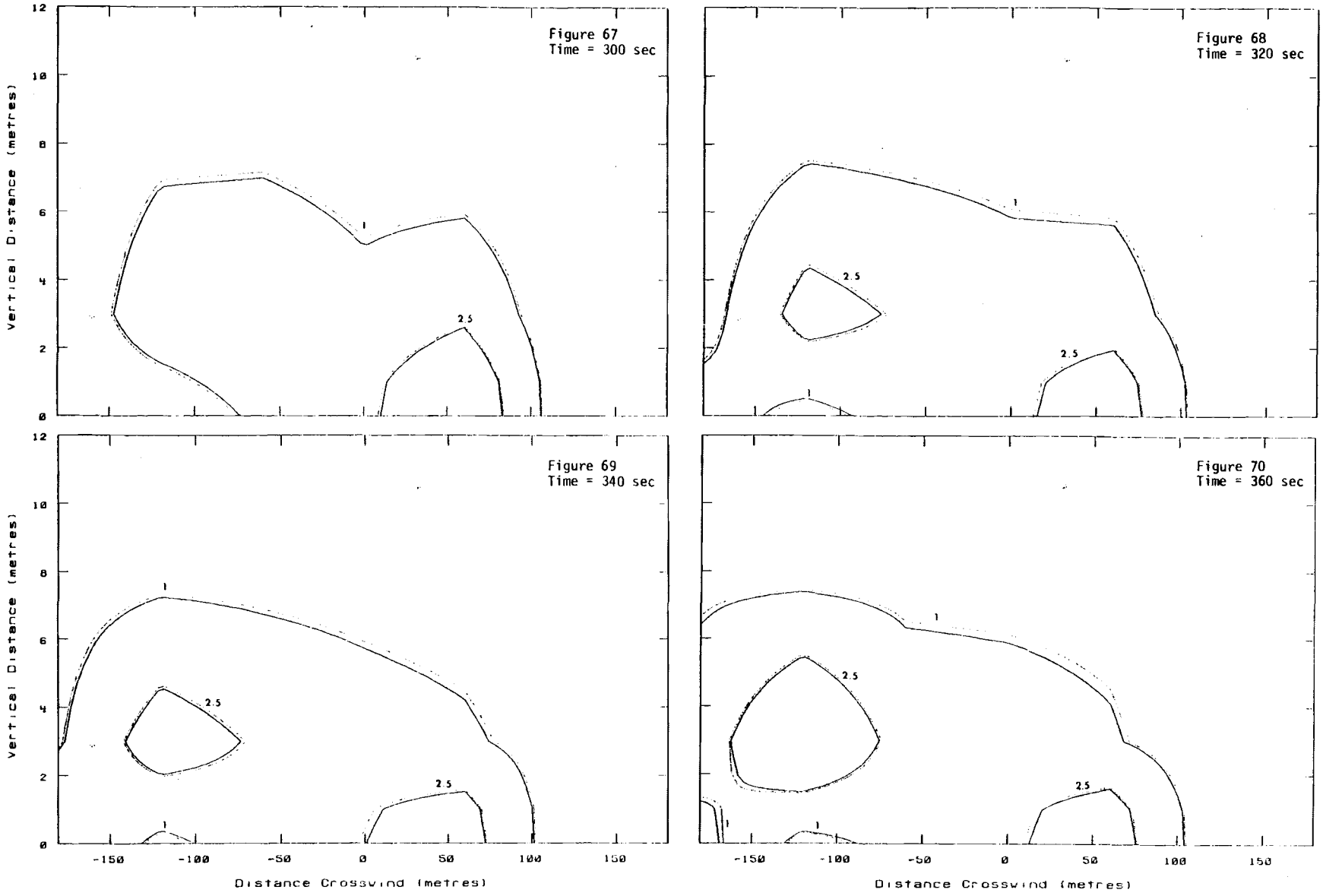

FIGURES 67-70. Burro 8 Vertical Concentration Contours at Row 3 Instrument Array. Contours at 1%, 2.5%, 5%, 10%, 15%, 25% and 35% Gas Concentrations.

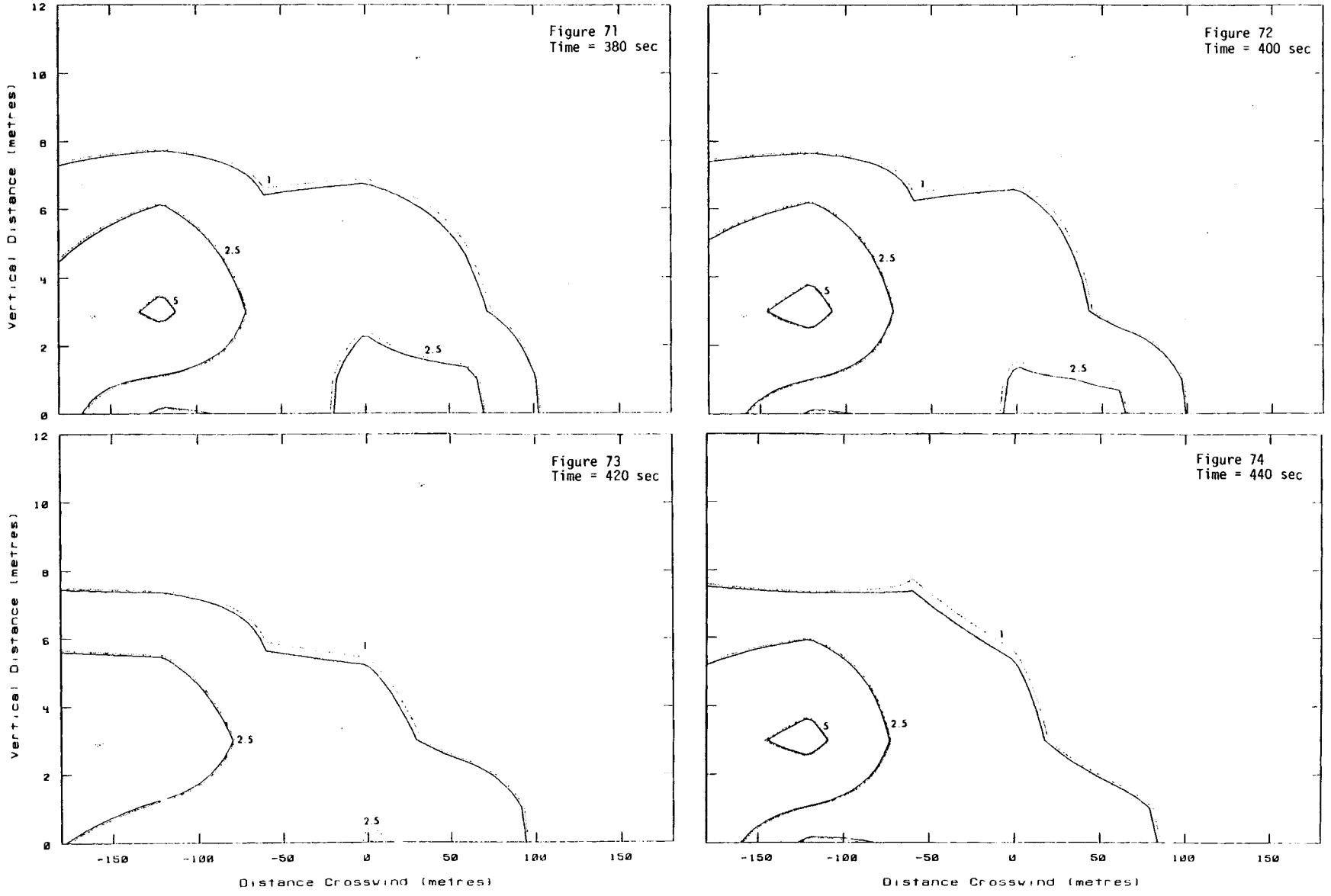

FIGURES 71-74. Burro 8 Vertical Concentration Contours at Row 3 Instrument Array. Contours at 1%, 2.5%, 5%, 10%, 15%, 25% and 35% Gas Concentrations.

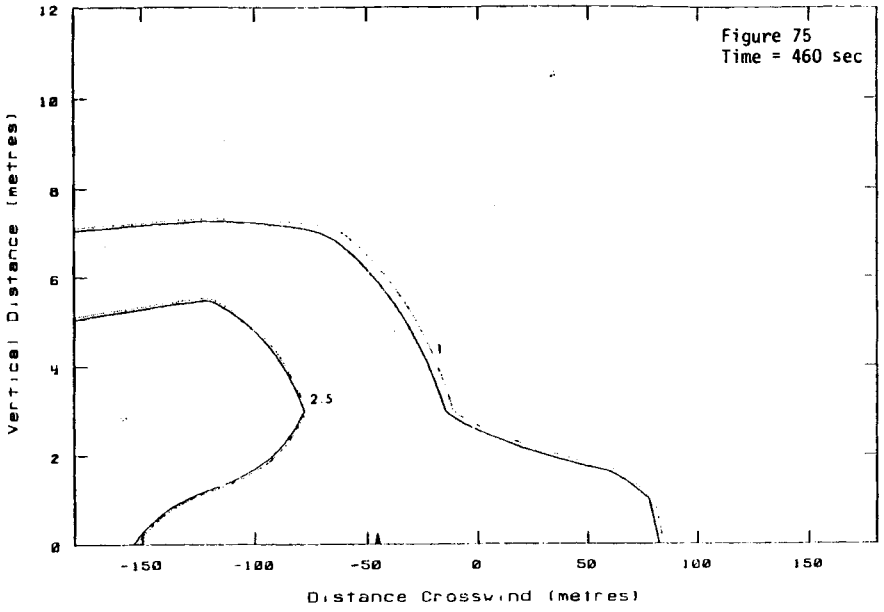

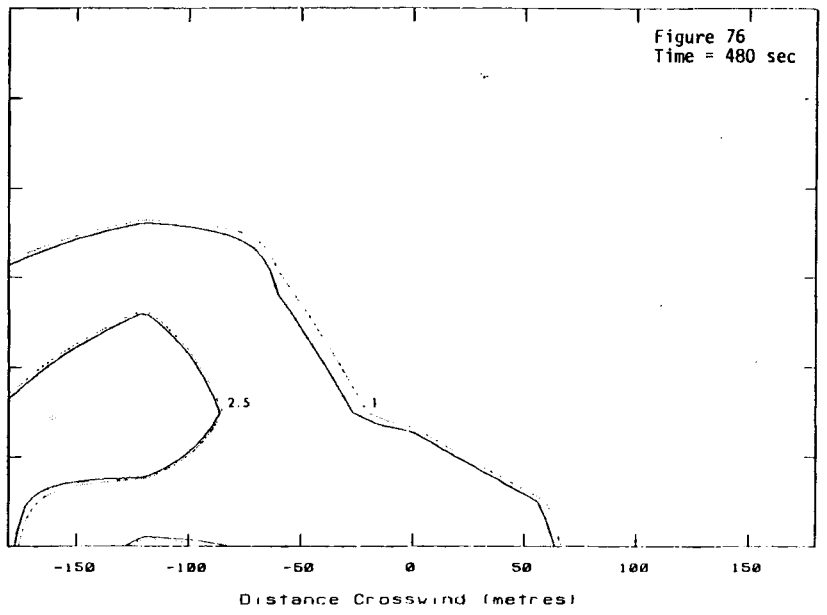

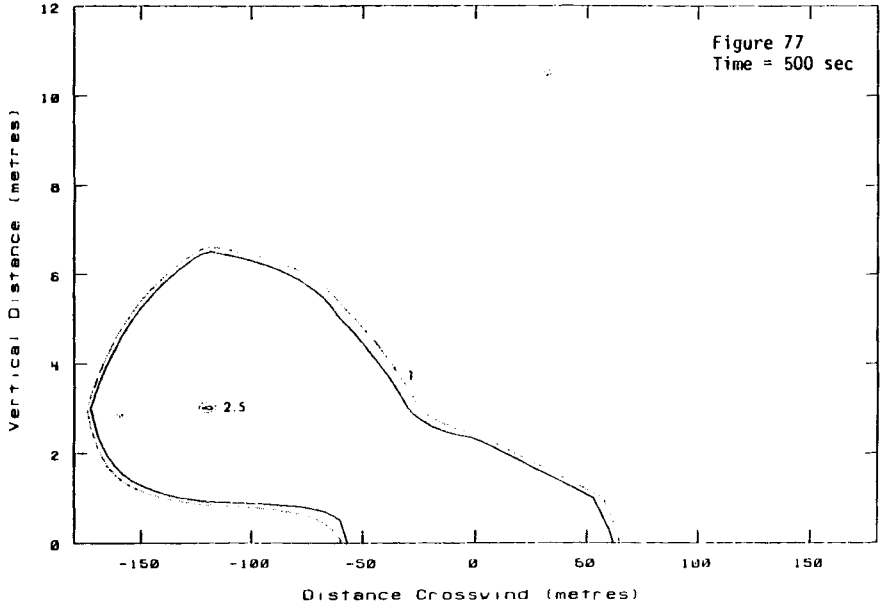

FIGURES 75-77. Burro 8 Vertical Concentration Contours at Row 3 Instrument Array. Contours at 1%, 2.5%, 5%, 10%, 15%, 25% and 35% Gas Concentrations.

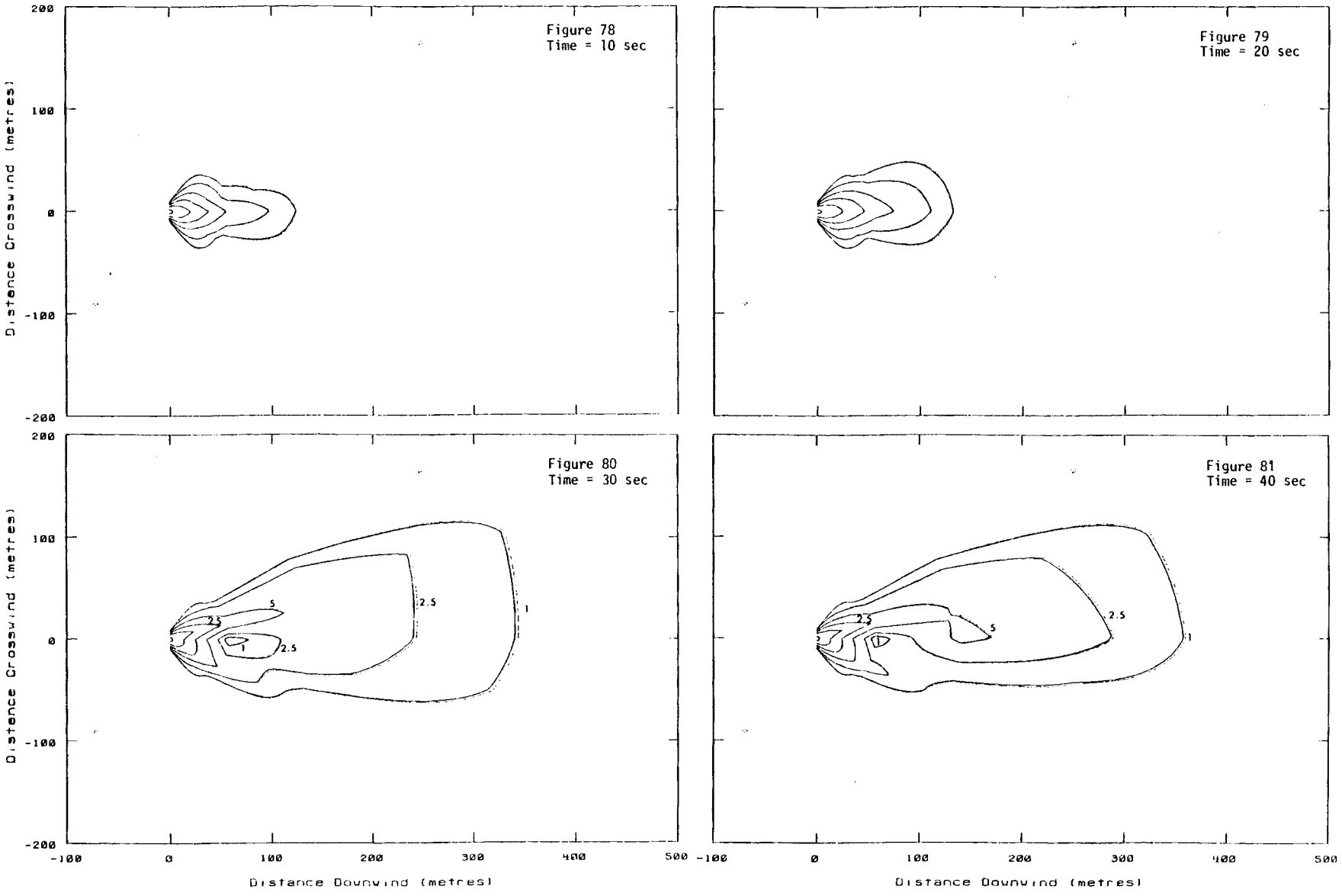

FIGURES 78-81. Burro 9 Horizontal Concentration Contours at 1 m Above Ground Level. Contours at 1%, 2.5%, 5%, 7.5%, and 10% Gas Concentrations.

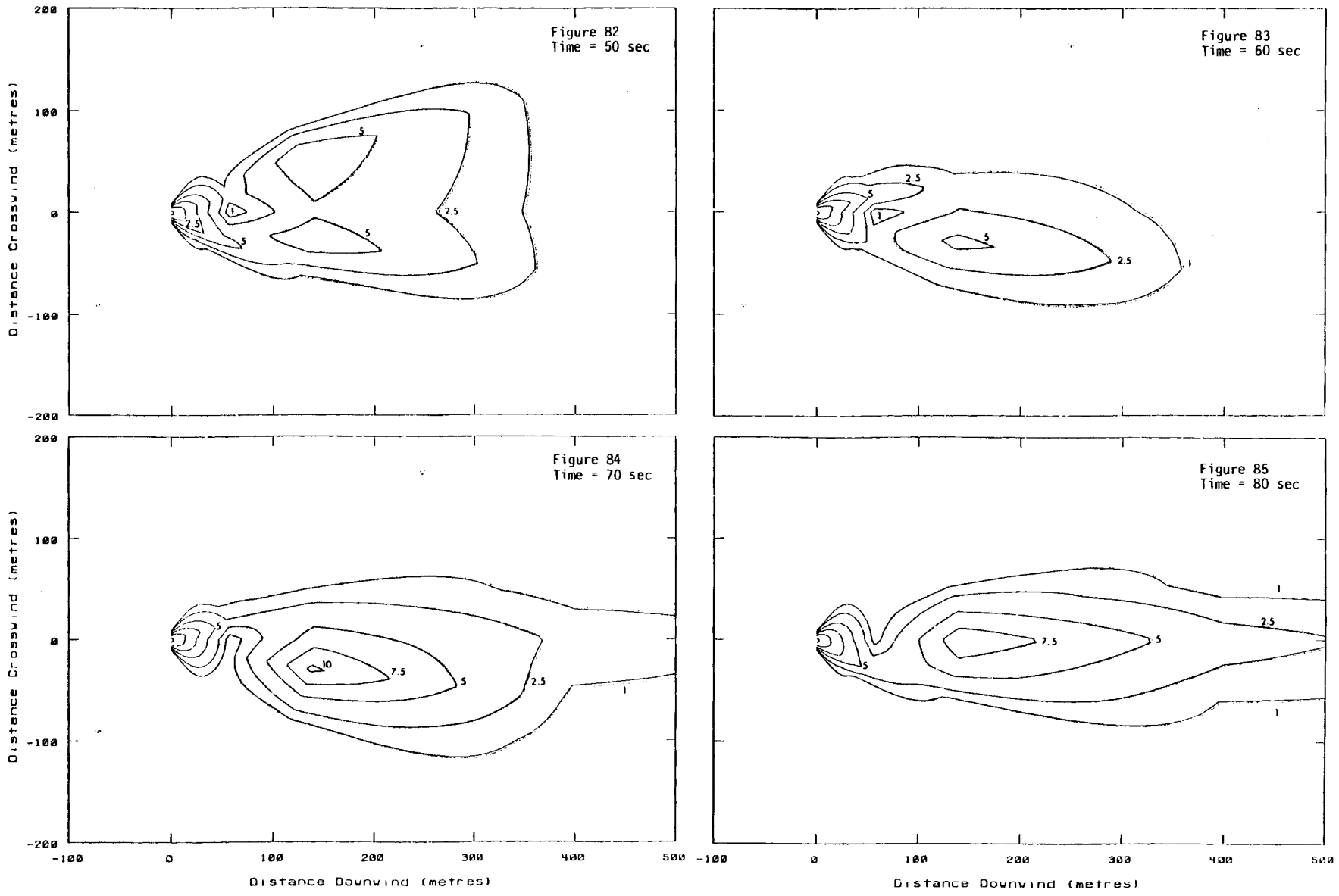

FIGURES 82-85. Burro 9 Horizontal Concentration Contours at 1 m Above Ground Level. Contours at 1%, 2.5%, 5%, 7.5%, and 10% Gas Concentrations.

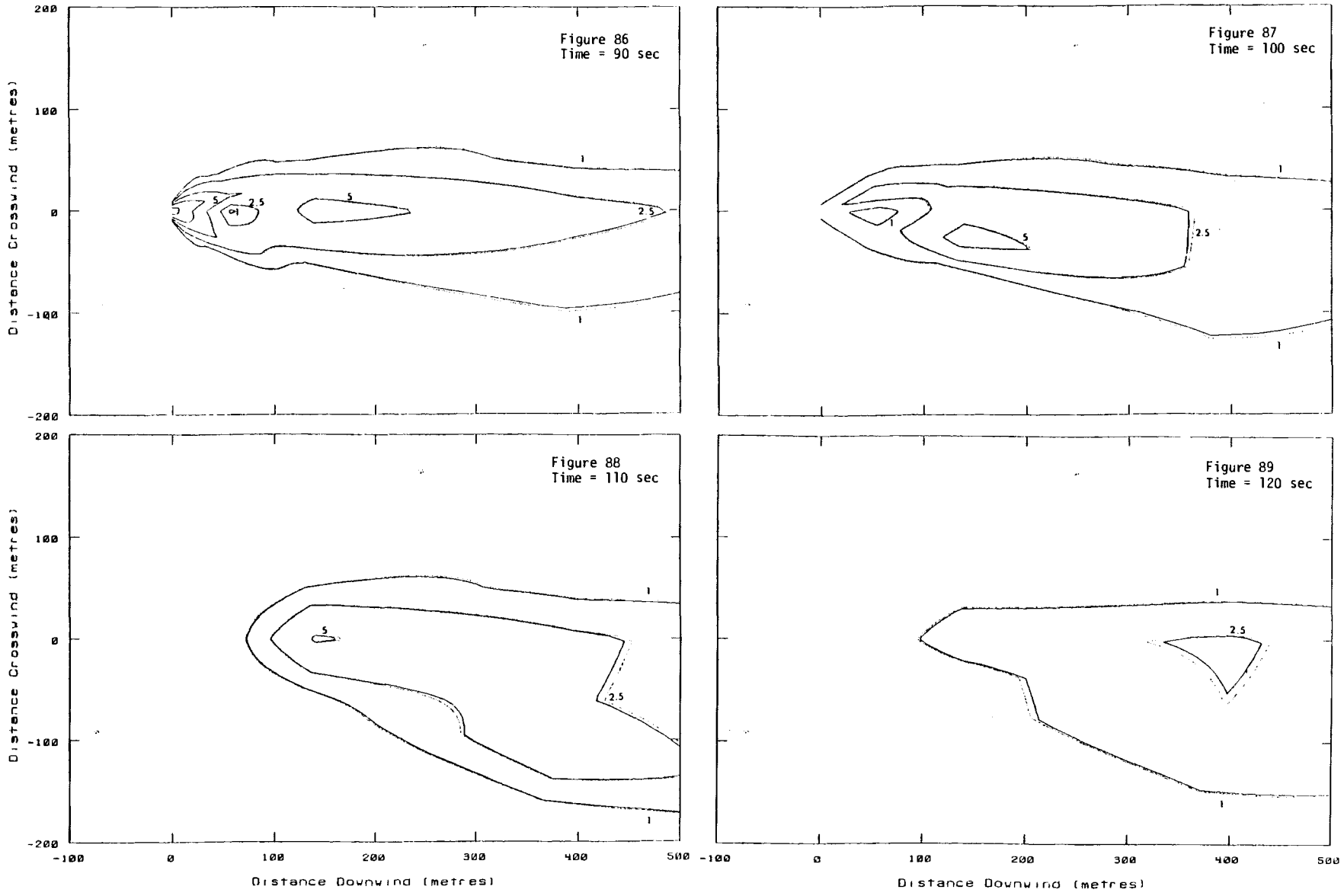

FIGURES 86-89. Burro 9 Horizontal Concentration Contours at 1 m Above Ground Level. Contours at 1%, 2.5%, 5%, 7.5%, and 10% Gas Concentrations.

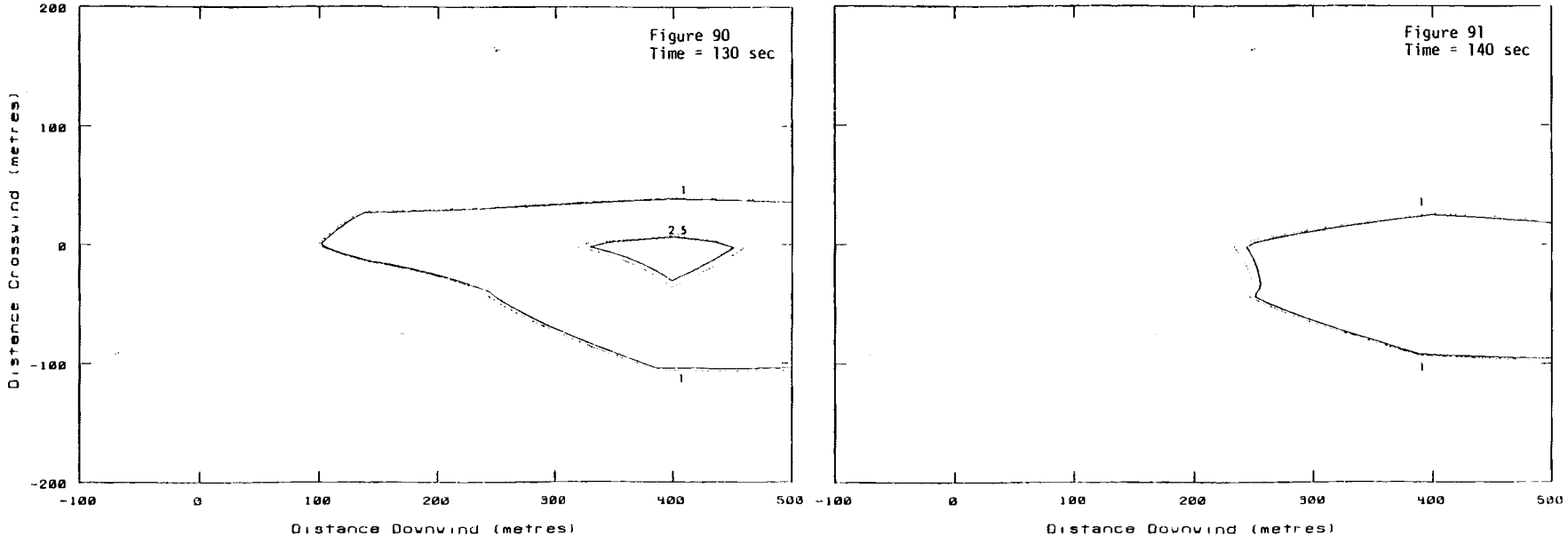

FIGURES 90 and 91. Burro 9 Horizontal Concentration Contours at 1 m Above Ground Level. Contours at 1%, 2.5%, 5%, 7.5%, and 10% Gas Concentrations

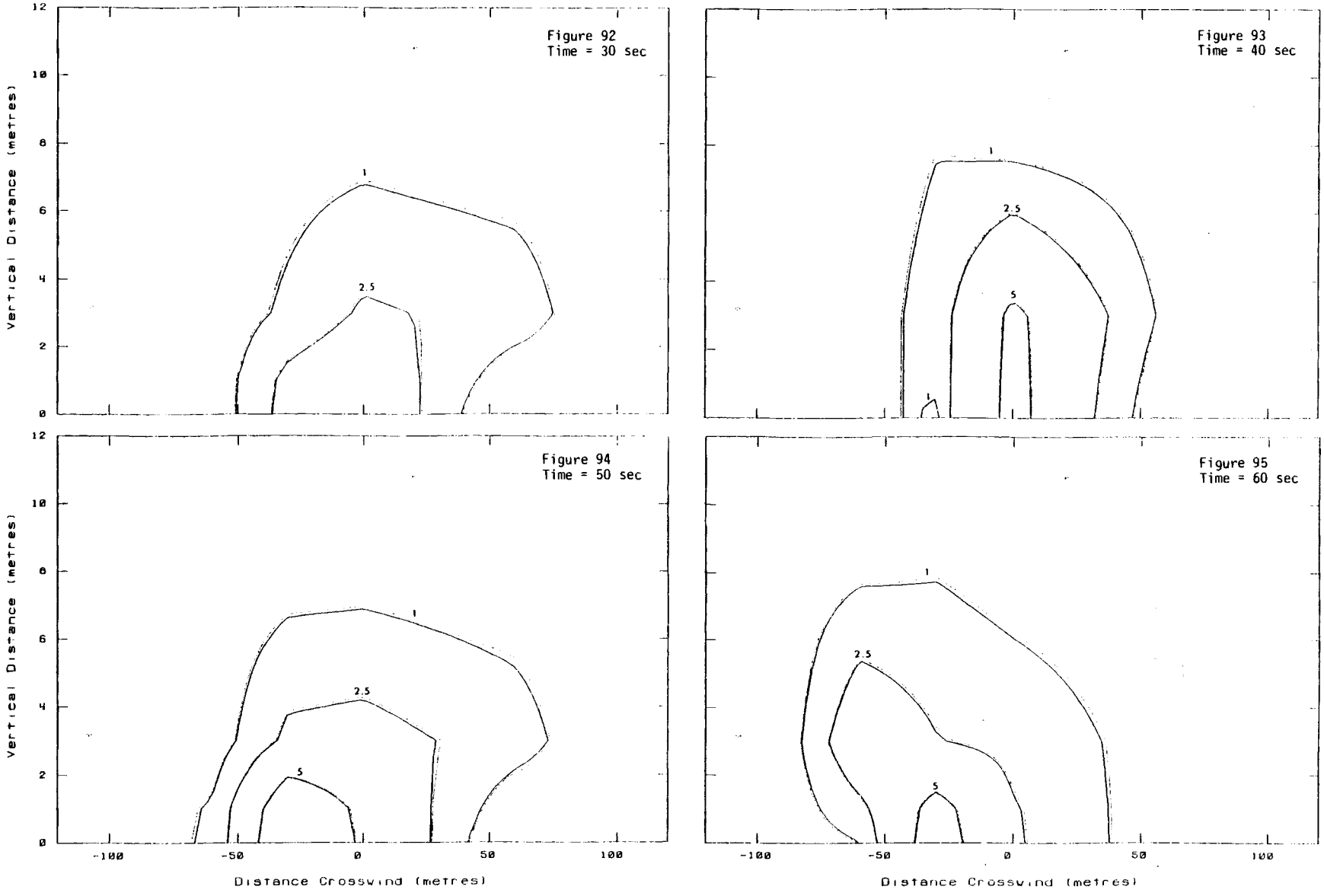

FIGURES 92-95. Burro 9 Vertical Concentration Contours at Row 2 Instrument Array. Contours at 1%, 2.5%, 5%, 7.5%, 10% Gas Concentrations.

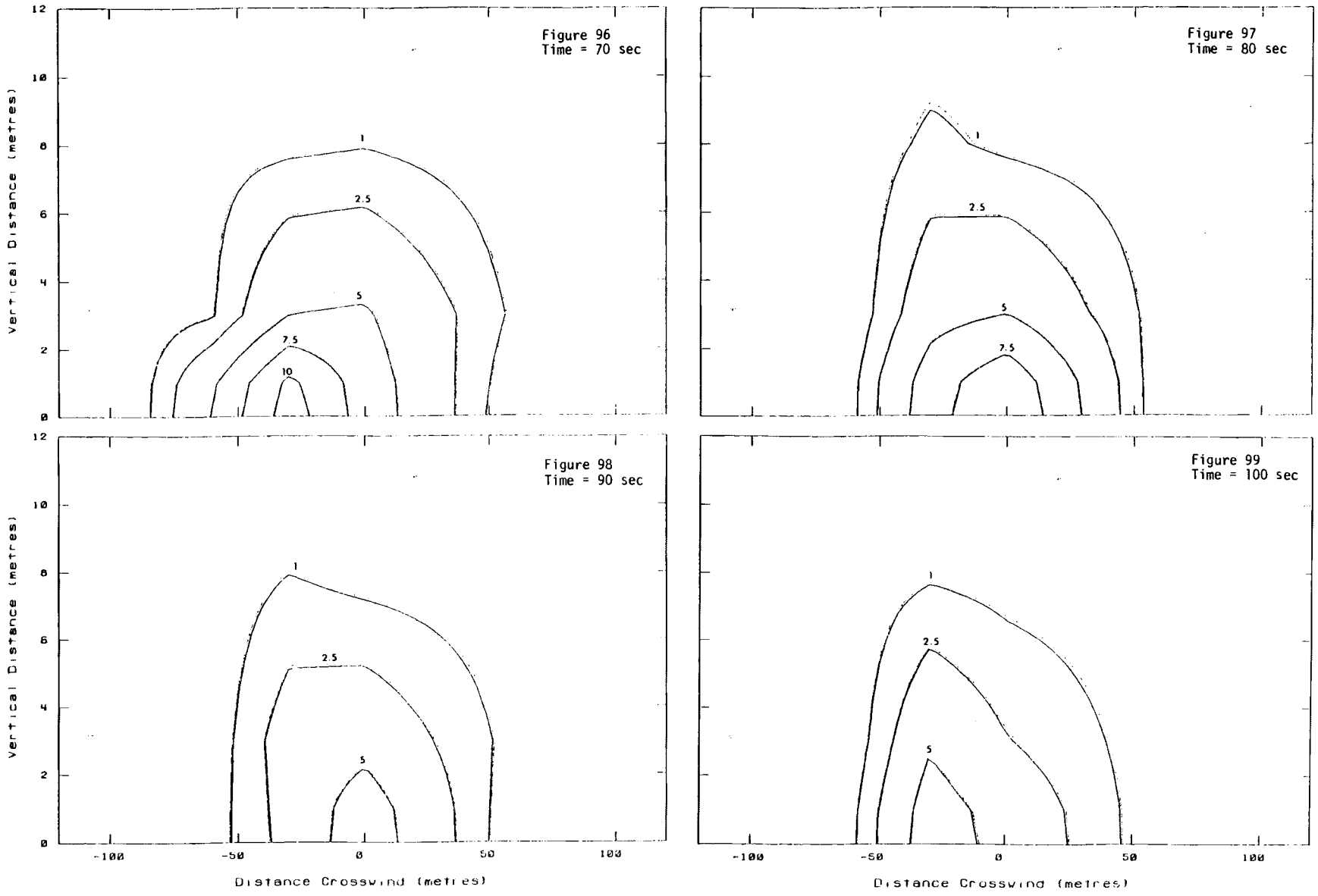

FIGURES 96-99. Burro 9 Vertical Concentration Contours at Row 2 Instrument Array. Contours at 1%, 2.5%, 5%, 7.5%, 10% Gas Concentrations.

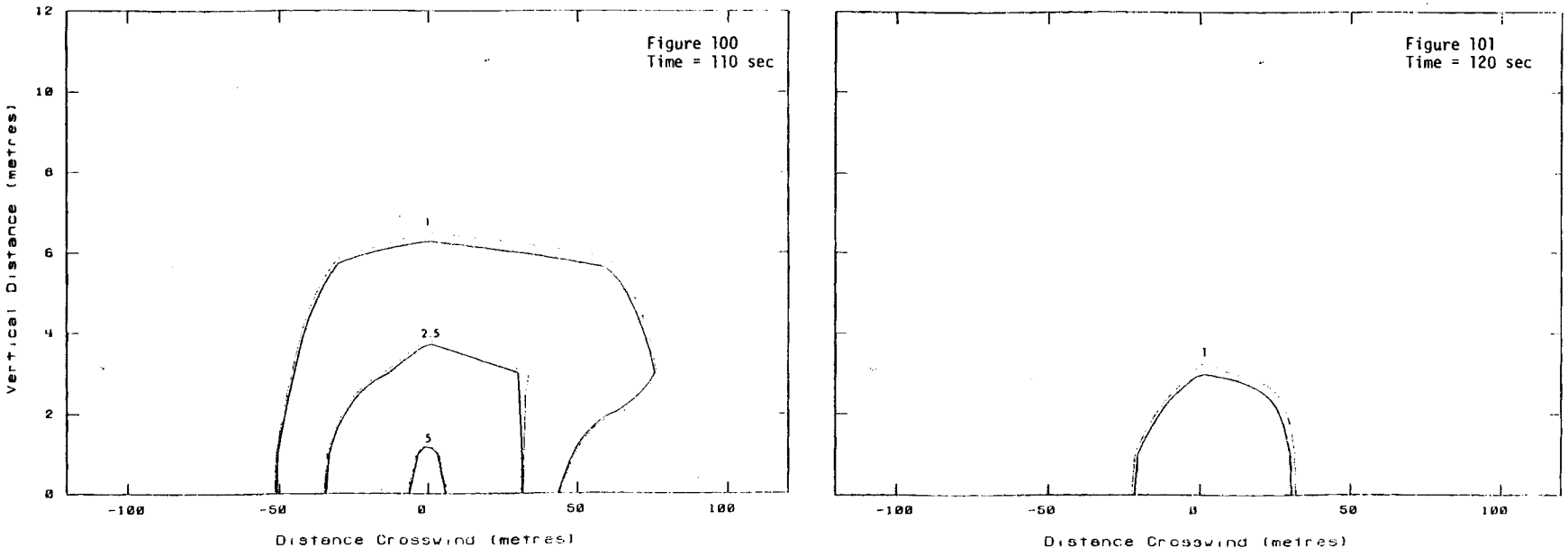

FIGURES 100 and 101. Burro 9 Vertical Concentration Contours at Row 2 Instrument Array. Contours at 1%, 2.5%, 5%, 7.5%, 10% Gas Concentrations.

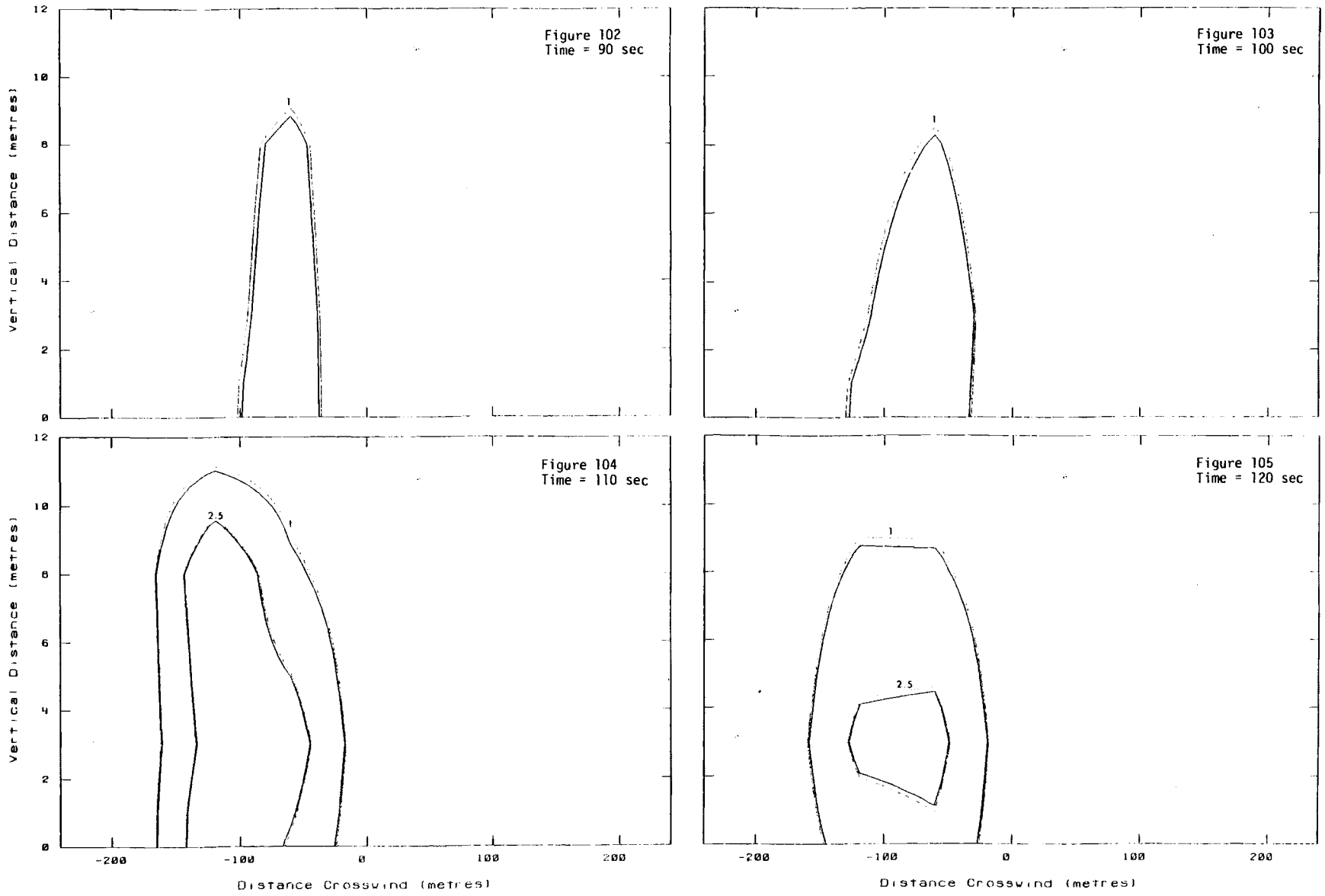

FIGURES 102-105. Burro 9 Vertical Concentration Contours at Row 3 Instrument Array. Contours at 1%, 2.5%, 5%, 7.5%, and 10% Gas Concentrations.

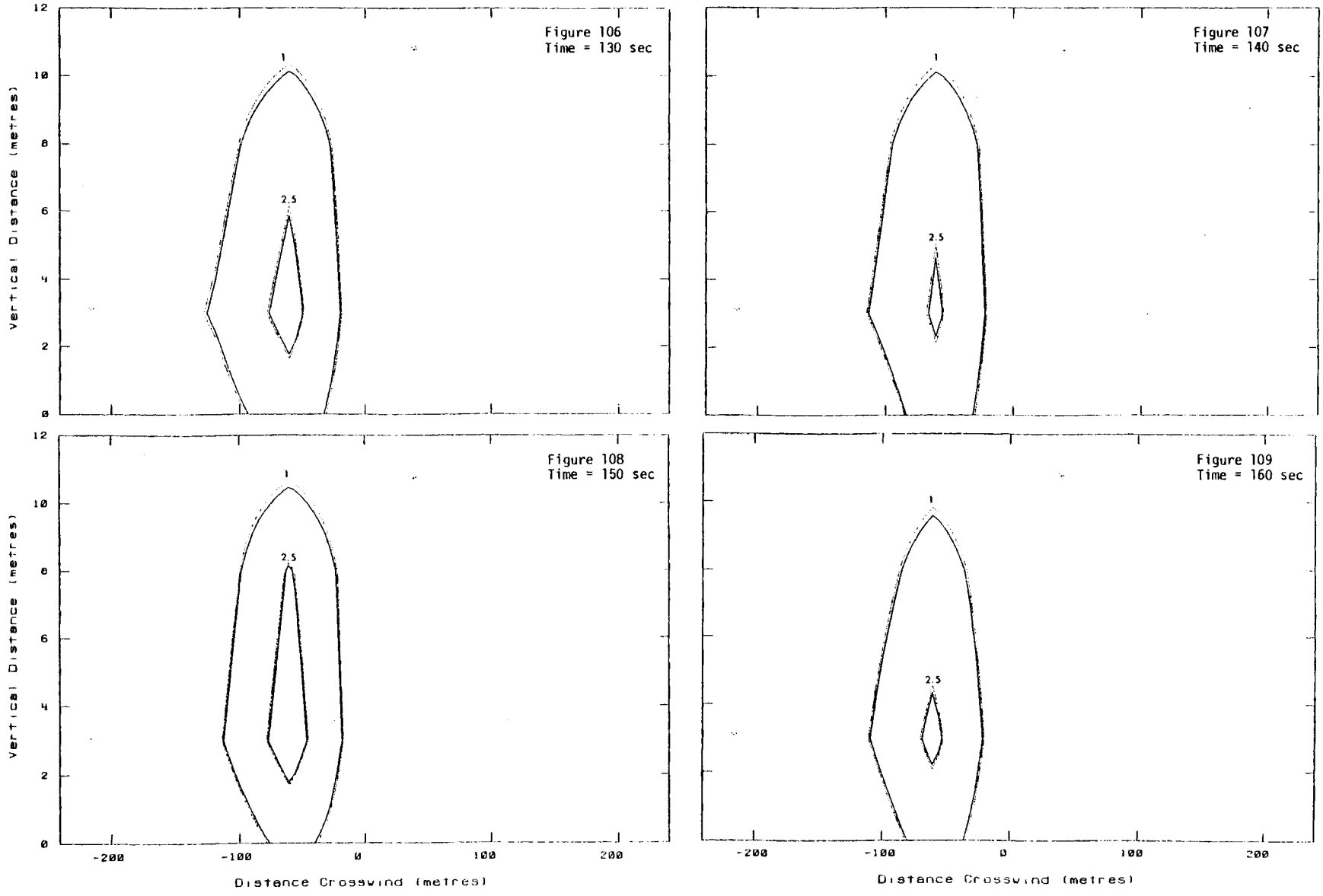

FIGURES 106-109. Burro 9 Vertical Concentration Contours at Row 3 Instrument Array. Contours at 1%, 2.5%, 5%, 7.5%, and 10% Gas Concentrations.

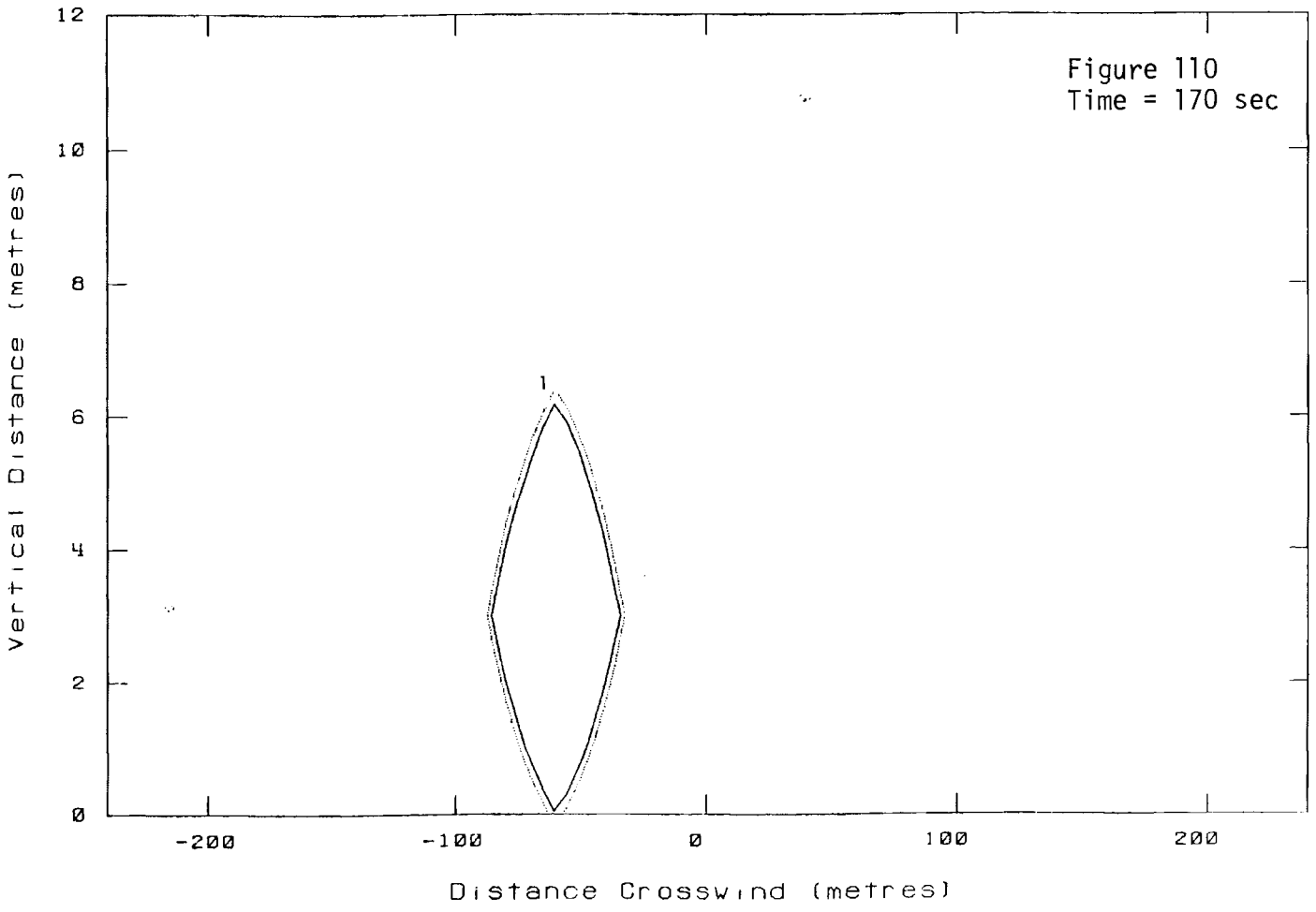

FIGURE 110. Burro 9 Vertical Concentration Contours at Row 3 Instrument Array. Contours at 1%, 2.5%, %5, 7.5%, and 10% Gas Concentrations.

REPORT C

A Comparison of Dense Gas Dispersion Model Simulations with Burro Series LNG Spill Tests Results

D. L. Ermak
S. T. Chan
D. L. Morgan
L. K. Morris

Prepared for the
Environmental and Safety Engineering
Division
U.S. Department of Energy
under Contract W-7405-ENG-48

Lawrence Livermore Laboratory
Livermore, California 94550

REPORT C

TABLE OF CONTENTS

SUMMARY

The predictions from three vapor dispersion models for cold dense gas releases are compared with the results from several 40-m^3 LNG spill experiments conducted at China Lake, California, in 1980. The models vary considerably in the degree to which they approximate important physical phenomena and include restricting assumptions. The simplest model (GD), a modified Gaussian plume model, predicted a vapor cloud that was too high and too narrow by about a factor of two in all cases. The second model (SLAB), a layer-averaged conservation equation model with one independent spatial variable (downwind distance), generally predicted the maximum distance to the lower flammability limit (LFL) and cloud width quite well. However, the observed vertical concentration profile was often more gradual than the nearly uniform profile assumed in the layer-averaged model, and concentrations near the source were generally higher than observed. The final model (FEM3) is a fully three-dimensional conservation equation model that generally predicted the concentration distribution in time and space rather well. A particular achievement of this model was the prediction of a bifurcated cloud structure observed in one experiment conducted with a low ambient wind speed. The three-dimensional model does have numerical difficulties, however, when attempting to simulate spills under very low turbulence (diffusion) conditions.

INTRODUCTION

Lawrence Livermore National Laboratory (LLNL) is conducting safety research under the sponsorship of the U.S. Department of Energy (DOE) to develop and experimentally verify models to predict the possible consequences of liquefied natural gas (LNG) spills. As part of the DOE program, LLNL and the Naval Weapons Center jointly conducted a series of LNG vapor dispersion experiments in the summer of 1980 at China Lake, California [1,2]. This paper presents a comparison of the predictions from three vapor dispersion models for cold dense gas releases with the results from several of these experiments.

During the last decade, a number of denser-than-air dispersion models were proposed in the literature [3-9]. Most of these models are based on the classical atmospheric advection-diffusion equation for a neutrally buoyant trace emission with ad hoc modifications to account for density effects. After making the typical approximations, a one-dimensional, Gaussian-plume type model is obtained which conserves the mass of the emitted species but neglects momentum and energy effects. One of the models, SIGMET [9], is based on the complete set of conservation equations for species, mass, momentum, and energy, and is three-dimensional. While this type of model includes a more complete description of the dispersion process, it also is numerically more complex and costly to run on a computer.

In a review on the predictability of LNG vapor dispersion, Havens [10] compares the results from several of these models. He considers a single scenario, namely, that of an instantaneous release of 25,000 m^3 of LNG on water under neutral atmospheric stability conditions, and looks at the model predictions of the maximum downwind distance to the lower flammability limit

(LFL). The agreement between models is fairly poor, with the predictions varying by over an order of magnitude.

Recently, a few additional models have appeared in the literature. Chan et al. [11, 12] have developed a three-dimensional fluid dynamics model which uses the finite element method to solve the basic conservation equations. Also, a few one-dimensional models [13-16], which attempt to improve the parameterizations for the more important physical processes and include momentum and energy conservation in some average manner, have been developed.

In order to determine the range of conditions for which these models are applicable, detailed data from well-instrumented, large-scale field experiments is needed. A major goal of the DOE program is to help provide this data and the Burro Series of experiments are a significant step in that direction. The concentration data obtained in these experiments has been used to generate contour plots which show the time evolution of the LNG vapor concentration in three-dimensional space [1]. We have made similar contour plots of the results from three dispersion models and present them here in a comparison with the experimental results.

The three dispersion models used in this study are briefly described in the following section and are seen to span the range in complexity from the simple Gaussian-plume type model to the three-dimensional, conservation equation type model. We compare the ability of each model to predict the observed vapor dispersion over the flammable range of fuel-air mixtures, and identify those parts of the models which appear to need improvement. Emphasis is given to those situations where the observed vapor dispersion is most markedly different from that of a neutrally buoyant trace emission.

DISPERSION MODELS

The three models used in this study are the Germeles-Drake modified Gaussian plume model [7]; a modified version of Zeman's one-dimensional, slab-averaged, conservation equation model [15]; and the fully three-dimensional, conservation equation model of Chan et al. [12]. These models will be referred to as GD, SLAB, and FEM3 respectively and are described in significant detail in the references given above. Here we will only briefly describe each model to clarify the physical basis for each and the differences between them. In particular, the entrainment and turbulence submodels are described, due to the dominant role which they play in controlling cloud dispersion.

The Burro tests are closely approximated as spills of constant rate and finite duration. For this type of spill, all of these models treat the source of natural gas (NG) vapor in essentially the same way. The liquid pool of LNG is assumed to be in a steady state with a constant evaporation rate equal to the average spill rate in mass per unit time. The shape of the source area is somewhat different in each model; however, the area is always the same and is given by $A = \dot{V}/W$ where $\dot{V}$ is the volumetric spill rate of LNG and W is the liquid regression rate of evaporation, assumed to be 4.2×10^{-4} m/sec. The GD model prediction of the dispersing vapor cloud is not time dependent for this type of spill. The model assumes the spill duration is long enough for the vapor cloud to reach steady state. The other two models are time dependent in this regard and treat the finite duration of the spill explicitly.

The vapor dispersion aspects of each model are described separately below.

GD MODEL

The GD model is derived from the steady state, Gaussian plume, point source solution to the atmospheric advection-diffusion equation,

$$\frac{\partial c}{\partial t} + U \frac{\partial c}{\partial x} = K_y \frac{\partial^2 c}{\partial y^2} + K_z \frac{\partial^2 c}{\partial z^2} \quad , \tag{1}$$

for the concentration c of the emitted species. Here U is the wind speed (assumed to be constant and in the x direction) and K_y and K_z are the horizontal and vertical turbulent diffusivities, respectively. Turbulent diffusion in the x direction is neglected, as it is assumed to be negligible in comparison to the advection of the wind. The turbulent diffusivities are taken to be functions of time since release or, equivalently in this model, functions of the downwind distance x. The GD equation for the concentration of NG vapor is obtained by integrating the point source solution over a finite line source of length L transverse to the wind and located a distance x_v upwind of the true source. The result is:

$$c(x,y,z) = \frac{\dot{V}_v}{[2\pi]^{\frac{1}{2}}\, UL\sigma_z} \cdot \exp\left[\frac{-z^2}{2\,\sigma_z^2}\right] \cdot \left\{ \operatorname{erf}\left[\frac{(L/2)-y}{2^{\frac{1}{2}}\sigma_y}\right] + \operatorname{erf}\left[\frac{(L/2)+y}{2^{\frac{1}{2}}\sigma_y}\right] \right\} \tag{2}$$

where the constant $\dot{V}_v$ is the volumetric source rate of NG vapor at ambient conditions and is approximately 630 times the liquid volume spill rate $\dot{V}$.

The dispersion coefficients σ_y and σ_z are functions of both the downwind distance from the true source x and a virtual source distance x_v, and are related to the turbulence diffusivities (K_y and K_z) by the expression:

$$\sigma^2(x+x_v) = \frac{2}{U} \int_0^{x+x_v} K(x')dx' \quad . \tag{3}$$

In the GD model, the Pasquill-Gifford dispersion coefficients [17] for continuous ground level sources are used for σ_y and σ_z. These dispersion coefficients are empirically based on atmospheric dispersion experiments of trace emissions. There are six sets of dispersion curves corresponding to six general weather conditions ranging from the most unstable class A to the most stable class F.

The source length L and the virtual source distance x_v are determined by a gravity spread calculation on a cylindrically shaped volume of NG vapor equal to the volume evaporated in the time it takes for the wind to traverse the liquid pool. Initially, the cylindrical cloud is assumed to be pure NG vapor at the boiling temperature and to have a radius equal to the liquid pool radius. The initial height of the cylindrical cloud is $H_i = 2R_i W_v/U$ where W_v is the vapor source velocity which is approximately 250 times the liquid regression rate W. While the properties of the cylindrical cloud are assumed to be homogeneous, the height, radius, temperature, and density change with time due to three processes: gravity spread of the denser-than-air cloud, air entrainment into the cloud, and surface heating of the cloud.

Gravity spread is assumed to increase the cylindrical cloud radius at the rate:

$$\dot{R} = \left[2g \frac{(\rho-\rho_a)}{\rho_a} H \right]^{1/2} , \qquad (4)$$

where g is the acceleration of gravity, ρ is the cloud density, and ρ_a is the ambient air density. Air entrainment is assumed to occur only at the top of the cylindrical cloud. It increases the mass and temperature of the cloud and provides an additional source of heat due to the possible

condensation and freezing of water vapor by the cold LNG vapor. Together with surface heating, the mass and energy rate equations for the cylindrical cloud are:

$$\dot{M} = \pi \rho_a R^2 w_e \tag{5}$$

$$\dot{E} = \rho_a \pi R^2 C_{pa} T_a w_e + \varepsilon_v + \varepsilon_w \tag{6}$$

where w_e is the entrainment rate, $M = \pi \rho R^2 H$, $E = MC_p T$, C_p and T are the cloud specific heat and temperature, C_{pa} and T_a are the ambient air specific heat and temperature, ε_v is the heat of condensation and freezing of water vapor in the cloud, and ε_w is the surface heat flux. Equations (4-6), along with the time independent ideal gas law (see Eq. (20)), are solved as functions of time.

When the radial velocity of the cylindrical cloud, $\dot{R}$, decreases to the point where it is equal to the wind velocity, U, the gravity spread calculation is stopped. The conditions in the cylindrical cloud at this time determine the value for the finite source length L and the virtual source distance x_v in Eq. (2). The source length L is set equal to the diameter of the cylindrical cloud, and the virtual source distance x_v is determined by setting the concentration at the source center, c(0,0,0), equal to the concentration in the cylindrical cloud. With L and x_v determined, the concentration of the NG vapor cloud as given by Eq. (2) is fully defined.

SLAB MODEL

The SLAB model treats the dispersion of LNG vapor as a well-defined cloud of height h and half-width B. Inside the cloud, the properties are assumed to be nearly uniform in the crosswind plane so that they vary only with time and in the downwind direction. This assumption allows the cloud to be described in terms of slab or layer-averaged properties, such as

$$\bar{\rho}(x) = \frac{1}{Bh} \int_0^B dy \int_0^h dz\ \rho(x,y,z) \tag{7}$$

for the cloud density. It also justifies the use of the approximation that the average of the product is equal to the product of the averages (i.e., $\overline{\rho U} = \bar{\rho} \cdot \bar{U}$) in deriving the conservation equations. Cloud dispersion is assumed to occur due to the entrainment of air at the top and sides of the cloud and due to gravity spread, which is treated using the hydrostatic approximation. At the cloud-ground interface, heat and momentum exchange are also allowed to occur.

The above assumptions and approximations are used to derive the layer-averaged conservation equations for mass, NG vapor, momentum, and energy. These equations, along with a rate equation for the cloud half-width, are

$$\frac{\partial(\rho Bh)}{\partial t} + \frac{\partial(U\rho Bh)}{\partial x} = \rho_a v_e h + \rho_a w_e B + \rho_s W_s B_s \ , \tag{8}$$

$$\frac{\partial \omega}{\partial t} + U \frac{\partial \omega}{\partial x} = - \frac{\rho_a v_e \omega}{\rho B} - \frac{\rho_a w_e \omega}{\rho h} + \frac{\rho_s W_s B_s (1-\omega)}{\rho Bh} \ , \tag{9}$$

$$\frac{\partial U}{\partial t} + U\frac{\partial U}{\partial x} = -\frac{g}{2\rho Bh}\frac{\partial\left[(\rho-\rho_a)\,Bh^2\right]}{\partial x} + \frac{\rho_a}{\rho}\left[\frac{v_e}{B}+\frac{w_e}{h}\right](U_a-U) - \frac{p_s W_s B_s U}{\rho Bh} - \frac{\tau_x}{\rho h} \quad , \qquad (10)$$

$$\frac{\partial V_g}{\partial t} + U\frac{\partial V_g}{\partial x} = \frac{gh}{\rho B}(\rho-\rho_a) - \frac{\rho_a}{\rho}\left(\frac{v_e}{B}+\frac{w_e}{h}\right)V_g - \frac{\rho_s W_s B_s V_g}{\rho Bh} - \frac{2\tau_y}{\rho h} \quad , \qquad (11)$$

$$\frac{\partial T}{\partial t} + U\frac{\partial T}{\partial x} = \frac{\rho_a C_{pa}}{\rho C_p}\left(\frac{v_e}{B}+\frac{w_e}{h}\right)(T_a-T) + \frac{\rho_s C_{pn} W_s B_s (T_s-T)}{\rho C_p Bh} + \frac{j}{\rho h C_p} \quad , \qquad (12)$$

$$\frac{\partial B}{\partial t} + U\frac{\partial B}{\partial x} = V_g + v_e \quad . \qquad (13)$$

The above equations, together with the ideal gas approximation for the equation of state and specific heat (see Eqs. (20) and (21)) form the SLAB model. The main cloud variables are the cloud height h and half-width B, the layer-averaged density ρ, mass fraction ω, velocity in the direction of the wind U, temperature T, and the crosswind cloud velocity at the side edges V_g. The bar over a quantity to designate a layer-average has been dropped since it is understood that all quantities are averaged in this manner. The remaining parameters are the acceleration of gravity g, the NG source velocity W_s and source half-width B_s, the specific heat C_p, the molecular weight M, the vertical and horizontal entrainment rates w_e, v_e, and the surface momentum and heat fluxes τ, j. The subscripts "s", "a", and "n" designate an NG source-related property, an ambient air property, and an NG vapor property respectively.

The vertical entrainment rate is taken to be a density-weighted combination of an ambient air entrainment rate and a stably stratified dense layer entrainment rate [18] and is:

$$w_e = \frac{\pi^{\frac{1}{2}} k U_{a*}(\rho_s - \rho)}{\phi_a(\rho_s - \rho_a)} + \frac{2.5\rho_a U_*^3}{g\,(\rho_s - \rho_a)\,h} \quad , \tag{14}$$

$$\text{where } \phi_a = \begin{cases} (1\text{-}16\ Ri)^{-1/4} & , \ Ri \leq 0 \quad , \\ 1\text{+}5\ Ri & , \ Ri > 0 \quad , \end{cases}$$

and Ri is the ambient Richardson number, k is von Karman's constant, $U_* = c_f U$, and c_f is a friction constant (found to be approximately 0.038 at China Lake). A comparison of the two terms shows the second term to be much less than the first except when $\rho \sim \rho_s$ or $h \sim 0$. The second term is generally quite small so that the effect of increased density in this model is to reduce the rate of air entrainment into the cloud.

The horizontal entrainment rate is

$$v_e = (1.8)^2 (h/B) w_e \quad . \tag{15}$$

The rationale for the ratio factor (h/B) is based on the assumption that in the source region or whenever the cloud is low and flat (i.e., $h \ll B$), horizontal entrainment will do little to dilute the cloud. As the cloud disperses and becomes more dilute, gravity spread decreases and entrainment becomes the dominant dispersal mechanism. At sufficiently far downwind distances, h and B become proportional to w_e and v_e, respectively, and then $v_e \doteq 1.8\ w_e$. This result reflects the empirical observation that the

horizontal and vertical standard deviations for both the wind speed and the spread of a trace emission in the atmosphere are approximately proportional by this factor.

The six coupled, nonlinear partial differential equations (PDE) of the SLAB model are solved using the PDECOL [19] computer software package. PDECOL uses finite element collocation methods based on piecewise polynomials for the spatial discretization techniques and standard implicit methods for the time integration. To improve numerical stability, a diffusion term with a coefficient of about 1 m^2/s was added to each PDE. The main effect of this term on the model predictions is to smooth the leading and trailing edges of the cloud.

FEM3 MODEL

In the FEM3 model, the dispersion of NG vapor is predicted by solving the three-dimensional conservation equations for the mean (time-averaged) quantities in a turbulent flow field. A generalized anelastic approximation, adapted from Ogura and Philips [20], is used to accommodate large density changes in both time and space while precluding sound waves. The result is the following form for the conservation equations of mass, momentum, energy, and species:

$$\nabla \cdot (\rho \underline{u}) = 0 \quad , \tag{16}$$

$$\frac{\partial(\rho \underline{u})}{\partial t} + \rho \underline{u} \cdot \nabla \underline{u} = -\nabla p + \nabla \cdot (\rho \underline{\underline{K}}^m \cdot \nabla \underline{u}) + (\rho - \rho_h)\underline{g} \quad , \tag{17}$$

$$\frac{\partial \theta}{\partial t} + \underline{u} \cdot \nabla\theta = \nabla \cdot (\underline{\underline{K}}^{\theta} \cdot \nabla\theta) + \frac{C_{pn}-C_{pa}}{C_p} (\underline{\underline{K}}^{\omega} \cdot \nabla\omega) \cdot \nabla\theta + S \quad , \tag{18}$$

$$\frac{\partial \omega}{\partial t} + \underline{u} \cdot \nabla\omega = \nabla \cdot (\underline{\underline{K}}^{\omega} \cdot \nabla\omega) \quad . \tag{19}$$

These equations, along with the ideal gas law approximation for the density and the specific heat,

$$\rho = \frac{M_n M_a P}{RT \left[M_n + (M_a - M_n)\omega \right]} = \frac{MP}{RT} \quad , \tag{20}$$

$$C_p = C_{pn}(1-\omega) + C_{pa}\omega \quad , \tag{21}$$

are the main governing equations. Here $\underline{u} = (u,v,w)$ is the velocity, ρ is the density of the mixture, p is the pressure deviation from an adiabatic atmosphere at rest with corresponding density ρ_h, $\underline{g}$ is the acceleration of gravity, θ is the potential temperature deviation from an adiabatic atmosphere, S is the temperature source term (e.g., latent heat), ω is the mass fraction of NG vapor, and $\underline{\underline{K}}^{m}$, $\underline{\underline{K}}^{\theta}$, and $\underline{\underline{K}}^{\omega}$ are the diagonal eddy diffusion tensors for the momentum, energy, and NG vapor, respectively. In the equation of state, P is the absolute pressure, R is the universal gas constant, T is the absolute temperature ($T/(\theta+\theta_o) = (P/P_o)^{R/MC_p}$), and M is the suitably averaged molecular weight of the mixture. As before, subscripts "n" and "a" denote NG and air, respectively.

The main step in developing the generalized anelastic approximation is to replace the continuity equation, $\nabla \cdot (\rho \underline{u}) = -\partial\rho/\partial t$, by Eq. (16). The variation of density with time is then determined implicitly by the time variation of temperature, pressure, and composition via the ideal gas law, Eq. (20). The anelastic approximation is very similar to the incompressibility approximation, $\nabla \cdot \underline{u} = 0$, for constant density flows. In both cases, compressibility effects are assumed to be negligible since the Mach number is always very small (generally ≤ 0.05 for LNG simulations) and therefore, acoustic waves are assumed to be unimportant and can be filtered a priori.

Turbulent diffusion in this model is treated by using a K-theory approach in which the turbulence level is modified by the cold, dense cloud in high concentration regions, yet approaches ambient levels as the cloud becomes more dilute. The three diffusivity tensors are assumed to be diagonal and equal with different elements for the vertical and horizontal directions. The vertical diffusion coefficient K_v is expressed as the sum of two terms,

$$K_v = K_a(1-\omega) + K_\rho \omega \quad , \tag{22}$$

where K_a is the ambient vertical diffusivity and K_ρ is a dense-layer diffusivity. The horizontal diffusivity K_H is simply taken to be 6.5 times as large as the vertical diffusivity.

The ambient atmospheric conditions are characterized by the diffusivity

$$K_a = \frac{k\, U_{a*} z}{\phi_a} \quad \text{where } \phi_a = \begin{cases} (1-16Ri)^{-1/4}, & Ri \leq 0 \quad , \\ 1+5Ri \quad , & Ri > 0 \quad , \end{cases} \tag{23a}$$

and the wind velocity profile

$$U_a = \frac{U_{a*}}{k} \left(\ln z/z_o - \psi_a\right) \quad \text{where } \psi_a = \begin{cases} 1.1(-Ri)^{1/2}, & Ri \leq 0 \\ -5\ Ri, & Ri > 0 \end{cases} , \tag{23b}$$

Here k is von Karman's constant, U_{a*} is the ambient friction velocity, Ri is the ambient Richardson number, and it is assumed that Ri = z/L where L is the Monin-Obukhov length. The ambient wind velocity profile is approximated in the finite element code by a quadratic and by using a specified shear stress boundary condition at z = 0 to avoid the need for an excessively fine grid to resolve the logarithmic function near the ground. The ambient diffusivity is also modified near the ground by replacing z in Eq. (23a) by $z + z_j e^{-z/z_j}$ where z_j is a constant whose value is determined by requiring the ambient vertical momentum flux, $\rho_a K_a(\partial U_a/\partial z)$, at the ground to be $\rho_a U_{a*}^2$. In the Burro simulations the quadratic wind profile fit was made using the average velocity data at the 1, 3, and 8 m heights, and the value of z_j was calculated to be about 1.4 m.

Two submodels for K_ρ are used in this study. One is a Richardson number diffusivity for a stably stratified density layer that is similar to the dense-layer entrainment rate used in the SLAB model and is given by

$$K_\rho = K_{\rho r} = \frac{1.25\ \rho U_*^3}{g(\rho - \rho_a)} , \tag{24}$$

which tends to reduce the turbulence level from the ambient value in high NG concentration regions. The other model is a mixing length model given by

$$K_\rho = K_{\rho m} = \frac{\rho_a}{\rho} \frac{K_a}{\frac{\partial U_a}{\partial z}} \left[\sum_{i,j}^{3} \left(\frac{\partial U_i}{\partial x_j} \right)^2 \right]^{1/2} , \tag{25}$$

where the turbulence level is proportional to the overall shear. Both submodels were used in each simulation; however, the results were essentially identical (except in one experiment, Burro 8) so only results obtained with the latter submodel will be presented.

The main governing equations, Eqs. (16-21), along with those for the submodels, are solved numerically with appropriate initial and boundary conditions. Equations (16-19) are spatially descretized by the finite element method in conjunction with the Galerkin method of weighted residuals. The time integration scheme is basically the explicit forward Euler method except for pressure which must be computed implicitly.

MODEL COMPARISONS

The three models differ considerably in their approach to simulating the atmospheric dispersion of a cold, dense-gas release. Perhaps the most obvious differences are related to the degree to which each model incorporates the basic conservation laws and three-dimensional effects. The GD model is based on the single conservation of species equation and neglects momentum and energy effects after the initial gravity spread calculation to determine the vapor cloud dimensions at the source. On the other hand, the SLAB model includes the conservation equations of mass, momentum, and energy, in addition to the species equation, but only in an average way. Variations in the crosswind plane are neglected, and all properties of the vapor cloud are expressed as crosswind averages which vary in the downwind direction only. The FEM3 model includes the most complete description of the conservation laws by treating them explicitly in three dimensions.

A unique feature of the SLAB model is that it calculates only crosswind-averaged properties, and characterizes the cloud shape by the height h and half-width B. The parameters B and h do not correspond to any particular concentration level. Rather, they can be considered to describe a surface which encloses the bulk of the cloud, for example 90%. Consequently, the crosswind concentration distribution is not specified, although it was assumed to be nearly uniform, and it is difficult to compare the predicted cloud shape from this model with the contour plots obtained from the experiments. To overcome this difficulty, we have assumed the following distribution for the vapor cloud concentration:

$$c(x,y,z) = c(x) \cdot \left\{ 1 - [2y/3B(x)]^2 \right\} \cdot \left\{ 1 - [2z/3h(x)]^2 \right\} \quad , \tag{26}$$

where $c(x)$ is the layer-averaged concentration expressed as the volume fraction and $c(x,y,z)$ is zero for $z > 3h/2$ and $|y| > 3B/2$. The use of Eq. (26) allows for the calculation of concentration contour plots which are based on the average concentration and the cloud height and width. While the choice of a quadratic distribution is arbitrary, it is somewhat consistent with the assumption of near uniformity. It should be noted that the maximum distance to the LFL (or any other concentration level) is not affected by the use of Eq. (26) since it is applied after the average properties are calculated.

There are other important differences and these are related to the manner in which each model treats the effects of gravity and turbulence. As noted above, the GD model treats gravity spreading of the denser-than-air cloud only in the calculation of the vapor cloud height and width at the source. Gravity

effects are totally neglected after tnis initial calculation. The downwind dispersion of the vapor cloud is assumed to be due to atmospheric turbulence and is governed by empirical coefficients for a neutrally buoyant trace emission. In contrast to this, the SLAB and FEM3 models treat the effects of gravity continuously throughout the calculation. This is done in the FEM3 model by solving the three momentum conservation equations at each point, while the SLAB model solves two layer-averaged momentum equations and uses the hydrostatic approximation.

These two latter models differ considerably in their approach to turbulence. The SLAB model uses the somewhat artificial concept of entrainment across the cloud-air interface and essentially neglects turbulence within the vapor cloud. Air is entrained into the cloud at the surface and then is assumed to mix rapidly in the cloud. Thus, there are two separate regions: the cloud and the ambient atmosphere. Mixing between the two is assumed to occur at the interface and is governed by an entrainment velocity which depends on the local properties of both the cloud and the surrounding atmosphere. The FEM3 model assumes that turbulence can be described as a diffusion process and uses a continuous diffusion coefficient which depends on the local properties of the LNG vapor-air mixture. While the entrainment and diffusion concepts are peculiar to the SLAB and FEM3 models respectively, the choice of a particular entrainment or diffusion submodel is not an essential aspect of the models. Several submodels have been proposed in the literature and could be used without changing the whole model.

BURRO LNG SPILL TESTS

The Burro series of experiments included eight LNG dispersion tests with spill volumes of up to 40 m^3 and spill rates of up to 20 m^3/min. The experiments were initialized by spilling the LNG onto the surface of a 1 m deep water pond. The LNG exits from a 25 cm diameter pipe about a meter above the surface of the pond, flowing straight down. Approximately 2 cm below the water surface, the LNG stream encounters a steel plate which directs it radially outward along the surface of the water. The spill pond is only about 58 m in diameter; consequently, while the spill is onto water, most of the dispersion occurs over land.

Ground level immediately surrounding the pond is about 1.5 m above the water level. Downwind of the pond, the terrain rises at the rate of about 7° to a height of 7 m above the water level at a distance of 80 m and remains relatively flat thereafter. Looking downwind from the spill point, the terrain slopes slightly ($\lesssim$ 1°), rising to the left and dropping to the right. There is a gully just beyond the right side of the instrumentation array that drops to an elevation of about 4-6 m below the centerline of the array. The effect of terrain on the dispersion of the LNG vapor is difficult to quantify, although it is quite apparent in Burro 8 and is discussed further in the following sections.

Model predictions are compared with four of the experiments: Burro 3, 7, 8, and 9. A summary of the test conditions for each of these experiments is given in Table 1. At China Lake, the roughness length z_0 and the velocity friction coefficient c_f, defined as the ratio of the friction velocity U_* to the wind velocity at 2 m height, were found to be nearly constant and had

TABLE 1. SUMMARY OF BURRO TEST CONDITIONS

	Burro 3	Burro 7	Burro 8	Burro 9
$V(m^3)$	34.0	39.4	28.4	24.2
$V(m^3/min)$	12.2	13.6	16.0	18.4
$U_2(m/s)$	5.4	8.4	1.8	5.7
$T_2(°C)$	34.	34.	33.	35.
$T_*(°C)$	-0.65	-0.23	+0.145	-0.10
Stability	C	D	E	D
$K_2(m^2/s)$	0.29	0.32	0.037	0.21

Definitions

V = LNG volume spilled

V = mean LNG spill rate

U_2 = mean wind speed at 2 m height

T_2 = mean temperature at 2 m height

T_* = $\partial T/\partial(\ln z)$

Stability = estimated Pasquill-Gifford stability class

K_2 = momentum diffusivity at 2 m height

average values of $z_o = 2.05 \times 10^{-4}$ m and $c_f = 0.038$. The estimated Pasquill-Gifford atmospheric stability class, used in the GD model calculations, is based on the methods proposed in Turner [21] and by Golder [22]. The method for calculating the momentum diffusivity, along with a more detailed description of the ambient atmospheric conditions, is given in [2].

Instrumentation for measuring the concentration of the NG vapor cloud as it dispersed downwind were located in four arcs at 57 m, 140 m, 400 m, and 800 m downwind of the spill point. There were about seven stations in each arc and the NG vapor concentration was measured at three heights (1 m, 3 m, and 8 m) at each station. In these tests, the 5% volume fraction level, corresponding approximately to the lower flammability limit (LFL), was generally within or just slightly beyond the 400-m arc.

Measurements of the heat transfer from the ground were also made during the passage of the cold NG vapor cloud. A simple heat transfer model

$$\Delta H = V_H \rho C_p \Delta T_1 \quad , \tag{27}$$

was investigated where ΔH is the ground heat flux to the cloud, ΔT_1 is the temperature decrease from ambient at 1 m height, and V_H is an effective heat transfer velocity. Several models for V_H, including ones using velocity and buoyancy terms, were used to fit the data. However, the best fit was obtained by using the constant value of $V_H = 0.0125$ m/s and this value is used in the model calculations.

COMPARISON OF BURRO RESULTS WITH MODEL PREDICTIONS

In comparing the model calculations with experimental results, consideration must be given to the time duration over which the data is to be averaged since the models only calculate time-averaged or ensemble-averaged quantities. Here we compare the model results to concentration data from the Burro experiments that have been averaged using a 10-s moving average. This time interval was chosen somewhat arbitrarily; the intent was to use an averaging time that is long enough to smooth out short-wavelength (much less than cloud width) fluctuations, but short enough to preserve cloud meander. Even with this averaging, the experimental concentration contours tended to fluctuate with time. Since the main interest in this work is related tc safety, we generally emphasize the maximum extent of the concentration contours and, in particular, the maximum extent of the flammable region. Regarding fluctuations about the 10-s average, peak concentrations of 5% (LFL) or greater were commonly observed when the 10-s average concentration was less than 5%, but were almost never observed when the 10-s average concentration was less than 1% [2].

The 10-s average concentration data was linearly interpolated in space to generate concentration contour plots at 10-s intervals. Obviously, there is an uncertainty in the location of the experimental contours which depends on the distance between measurements. Within a row of instruments, the interpolation uncertainties are believed to be less than a meter in the vertical and only a few meters or less in the horizontal since the instruments

are fairly close. The interpolation uncertainties between rows of instruments are considerably greater since the distance between rows is larger. The maximum extent of the 5% contour (X_{LFL}) was generally located between the 140- and 400-m rows where the interpolation uncertainty in X_{LFL} is estimated to be approximately -40 to +20 m. These estimates were obtained from investigations involving a number of tests [2].

BURRO 3

In this comparison, Burro 3 is unique in that it is the only case in which all three models underestimate the maximum distance to the LFL (X_{LFL}) as determined by the contour plots of the experimental data. This is shown in Table 2 where X_{LFL} is given for all four experiments and for each model simulation. The SLAB and FEM3 models underestimate X_{LFL} by 40 and 65 m respectively, and the GD model underestimates it by 130 m. In addition, the predicted cloud behavior of the SLAB and FEM3 models over the duration of the test was considerably different than observed in the experiment.

The duration of the Burro 3 spill was 167 s, which is long enough that one might expect the resultant vapor cloud to set up a quasi-steady state (as predicted by the SLAB and FEM3 models) at least within the 5% concentration level. However, the contour plots of the field data show a different behavior. As expected, X_{LFL} initially increases as the cloud develops. Between 60 and 120 s from the time the spill began, X_{LFL} oscillates between 215 and 255 m. After 120 s and for the next 100 s, X_{LFL} decreases to a value of 120-140 m. Also during this latter period, the vapor cloud is bifurcated for about 45 s. The reason for this change in cloud shape is

TABLE 2. MAXIMUM DOWNWIND EXTENT OF THE LFL (In meters)

	Expt.*	GD	GD+	SLAB	FEM3
Burro 3	255	126	190	215	190
Burro 7	200	150	212	264	210
Burro 9	325	235	344	315	330
Burro 8	420	661	1150	418	630

*The estimated uncertainty in the experimental value is -40 to +20 m.

thought to be related to a local reduction in the wind speed in the vicinity of the spill pond, but is not completely understood.

Nor can it be fully explained why the maximum X_{LFL} value during the first half of the spill is so much greater than the model predictions. Several possible explanations as to why the models underestimated X_{LFL} in only this experiment have been investigated. For example, changes in the LNG spill rate were checked but found to be too small to account for the large value of X_{LFL}. The effect of inoperative stations on the contour plots was also investigated; however, if there were any effect, it would tend to reduce X_{LFL} because of missing peak concentrations. The largest discovered uncertainty in the experimental value of X_{LFL} is due to interpolating the concentration between the 140- and 400-m rows. If this is considered, the SLAB model prediction of X_{LFL} is within the lower limit of the experimental value and the FEM3 result is just below it.

As seen in Table 2, the GD estimate of X_{LFL} is significantly lower than either of the other two models. One might suggest that it is more appropriate to use a higher stability class in the GD simulations since the model predictions are being compared to 10-s average concentrations and the Pasquill-Gifford dispersion coefficients were designed for 10-min or longer averages. For this reason, a second GD run was made for each experiment with the stability increased by one class. The results are shown in Table 2 under the GD+ heading. An increase in stability is seen to improve the X_{LFL} estimates for the high wind speed, less stable cases (Burro 3, 7, and 9); however, it leads to an overestimate of X_{LFL} by more than a factor of two in the low wind speed, stable case of Burro 8.

The downwind distance to the LFL is only one measure of the models' ability to simulate the experiments. A better evaluation can be made by

comparing the location and shape of the LFL contour, and, in general, by comparing a range of contours which show the overall concentration distribution. Such a contour plot is shown in Fig. 1(a) where crosswind concentration contours 57 m downwind are plotted at a time of 100 s. The uncertainty in the location of these contours is much less than the uncertainty in X_{LFL} since the distance between instruments is much less. Also shown in Fig. 1 are the model predictions, which include only half the distribution since they assume the cloud is symmetric about the cloud centerline. The scale in each of the plots is identical, and the experimental contours have been translated along the crosswind axis so that they are roughly centered within the plot.

As can be seen in Fig. 1, the contours from the FEM3 calculation are in very good agreement with those generated from the experimental data. The SLAB model appears to predict the overall height and width of the cloud fairly well, especially if one considers the 5% contour as representative of the overall cloud dimensions. However, the 1% contour is significantly lower than in the experiment, and the 15% contour is both higher and wider. This suggests that the quadratic function used in Eq. (26) for the concentration distribution is not the most appropriate, especially in the vertical direction.

The GD model is seen to predict a cloud which is too high and too narrow. The GD 5% contour is about twice as high and nearly half as wide as in the experiment. Also shown in Fig. 1(c) is a GD simulation in which the stability class is increased by one from that given in Table 1. While this change in stability improved the prediction of X_{LFL} (see Table 2), it did little to improve the shape of the cloud. It is still too high and too narrow. This characteristic of the GD model was found to hold for each of the Burro experiments used in this study.

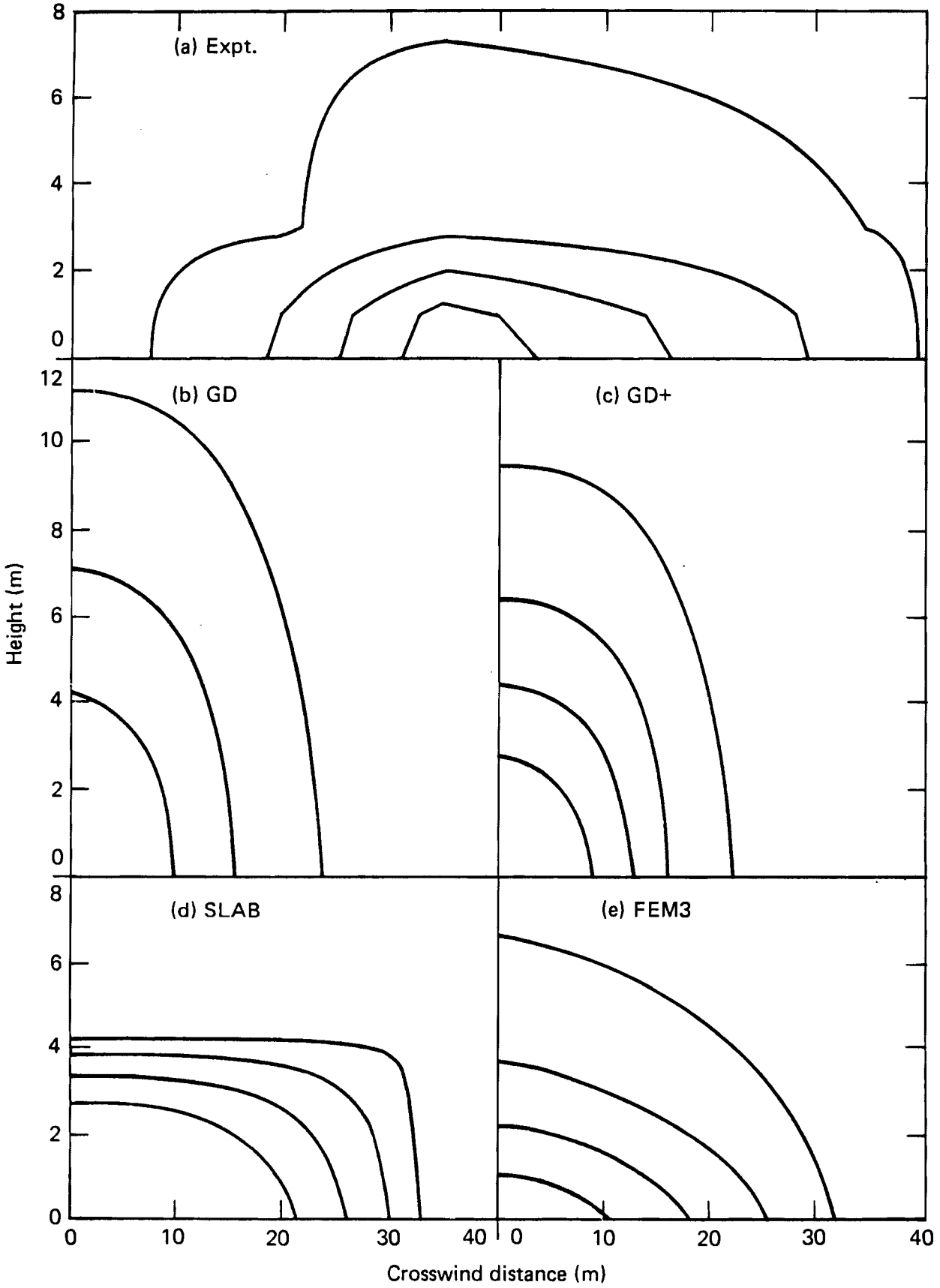

Figure 1. Burro 3 crosswind contour plots of cloud concentration 57 m downwind at t = 100 s. The experimental contour plot shows the full cloud width while the model results show only the half-width. The contour lines designate the 1, 5, 10, and 15% levels and the vertical to horizontal distance scale is 1 to 4.

BURRO 7

The Burro 7 spill rate and duration were quite similar to that of Burro 3, but the wind speed was about 60% higher and the atmospheric stability was estimated to be one class higher. The wind direction took the cloud along the edge of the instrumentation array as it moved downwind and the cloud centerline extended beyond the edge of the array during much of the spill. The cloud meandered over the array three times, and each time a maximum X_{LFL} value of 190-200 m was calculated. As can be seen in Table 2, the FEM3 estimate of X_{LFL} was in good agreement with this value. The SLAB model overestimates X_{LFL} by about 60 m, while the GD model underestimates it by about 50 m. These last two estimates are not too far outside the uncertainty limits of the experimental value due to the interpolation between the 140- and 400-m rows.

In Fig. 2 a contour plot of the cloud concentration observed in the experiment at the first row of instruments and t = 140 s is compared to similar plots from the SLAB and FEM3 models. The model results do not compare very well with experiment in this row. The experimental cloud is bifurcated, which the models do not predict, and is wider than the simulated clouds. For example, the 1% contour in the experimental contour plot is 72 m wide, while it is about 45 and 55 m wide in the SLAB and FEM3 plots respectively. The models also predict significantly higher concentrations. The maximum concentration observed in this row in the experiment was about 12%, while it was over 25% in the SLAB result and about 17% for the FEM3 result.

The models do significantly better in the second row 140 m downwind, as can be seen in Fig. 3. In particular, the FEM3 model does very well. The 1%

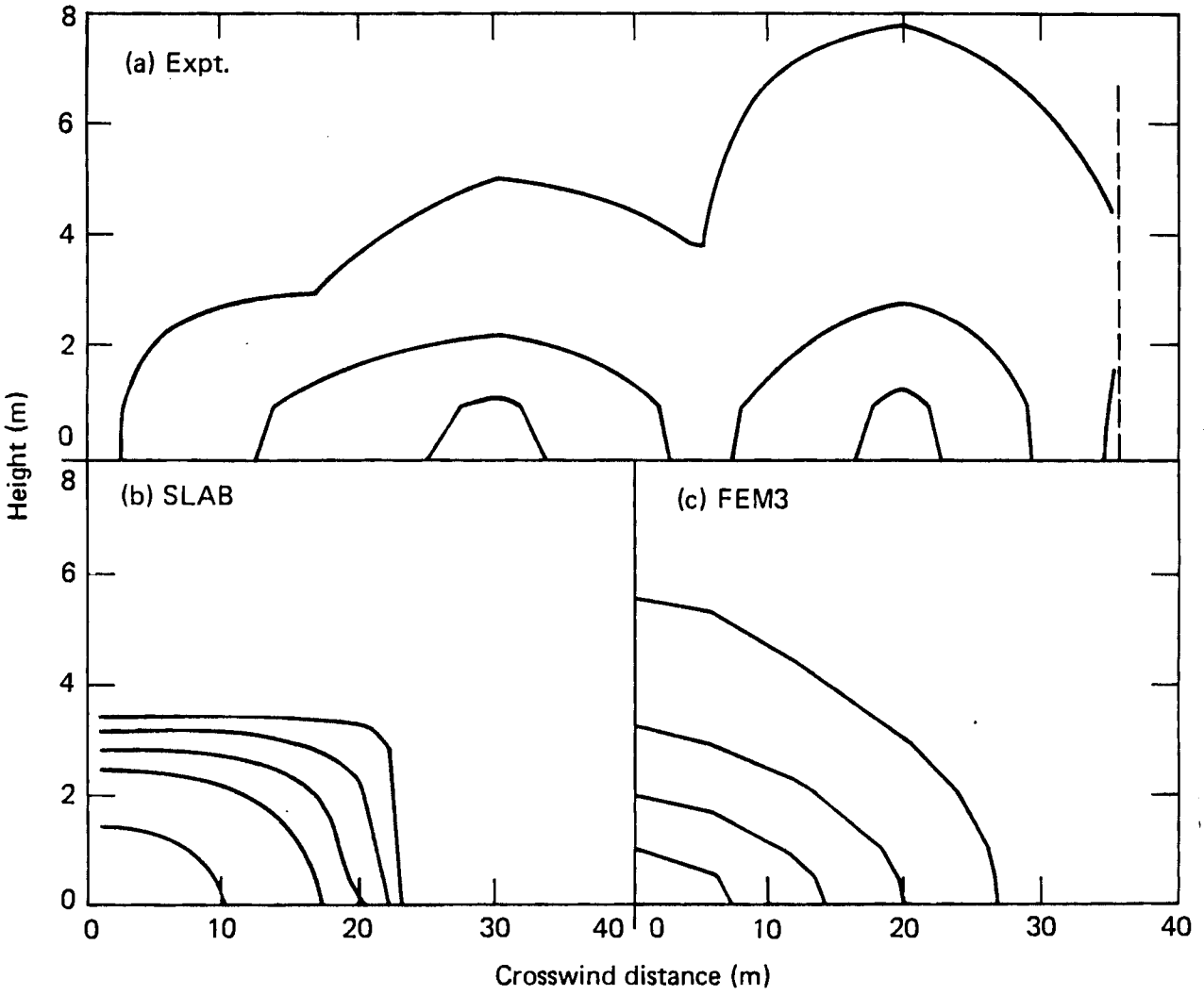

Figure 2. Burro 7 crosswind contour plots of cloud concentration 57 m downwind at t = 140 s. The dashed line in plot (a) indicates the outer edge of the instrument array. The contour lines designate the 1, 5, 10, 15, and 25% levels and the vertical to horizontal distance scale is 1 to 4.

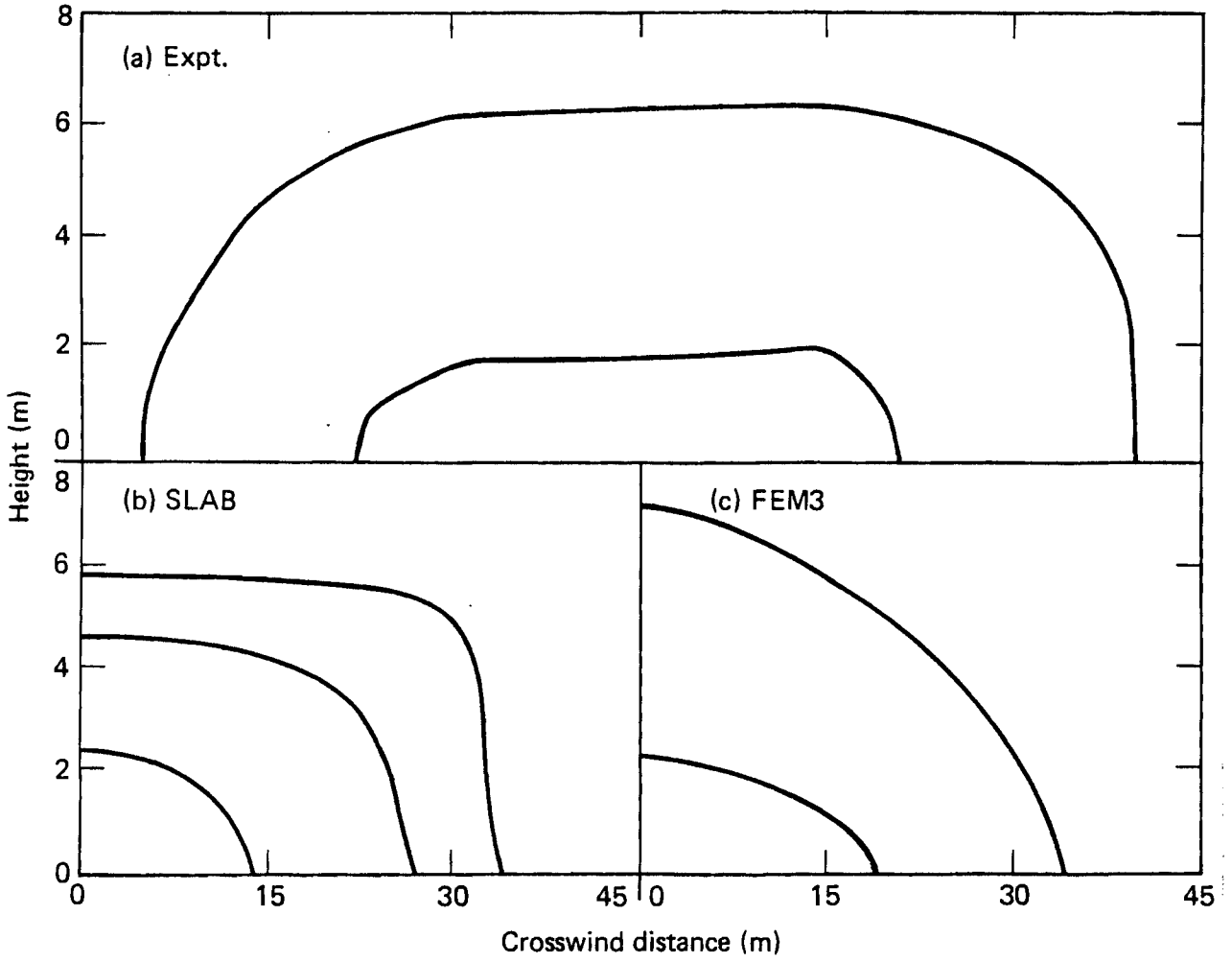

Figure 3. Burro 7 crosswind contour plots of cloud concentration 140 m downwind at t = 160 s. The contour lines designated the 1, 5, and 10% levels and the vertical to horizontal distance scale is 1 to 4.

contour is 80 m wide and 6.5 m high in the experimental plot and 68 m wide and 7.2 m high in the FEM3 result. Similarly, the 5% contour is about 40 m wide and 2.2 m high in both plots. The SLAB model prediction of the cloud height and width as given by the 1% contour is in fair agreement with experiment at this downwind distance also. It still predicts too high a maximum concentration, as would be expected since it overestimates X_{LFL}. Perhaps a more important difference between the SLAB and experimental plots is the vertical concentration profile. In the SLAB result, the 5% contour is more than twice as high as in the experimental plot, while the 1% contour is somewhat lower than that in the experiment. This discrepancy between the SLAB and experimental vertical profiles was observed in all the higher wind speed cases (Burro 3, 7, and 9).

BURRO 9

Burro 9 had the highest spill rate of all the Burro experiments and was conducted under a fairly high wind speed, as were Burro 3 and 7. A series of rapid-phase-transition (RPT) explosions occurred during this experiment, and as a consequence, the spill was terminated after only 79 s. The RPTs threw enough water and mud on the first row of instruments to render the infrared gas sensors inoperable for most of the test. Figure 4(a) shows a horizontal contour plot of the cloud concentration at a height of 1 m just after the spill was terminated. The maximum X_{LFL} value of 325 m was obtained in the experimental contour plots at this time; however, this value may be larger than the actual value by about 25 to 40 m as a result of interpolation

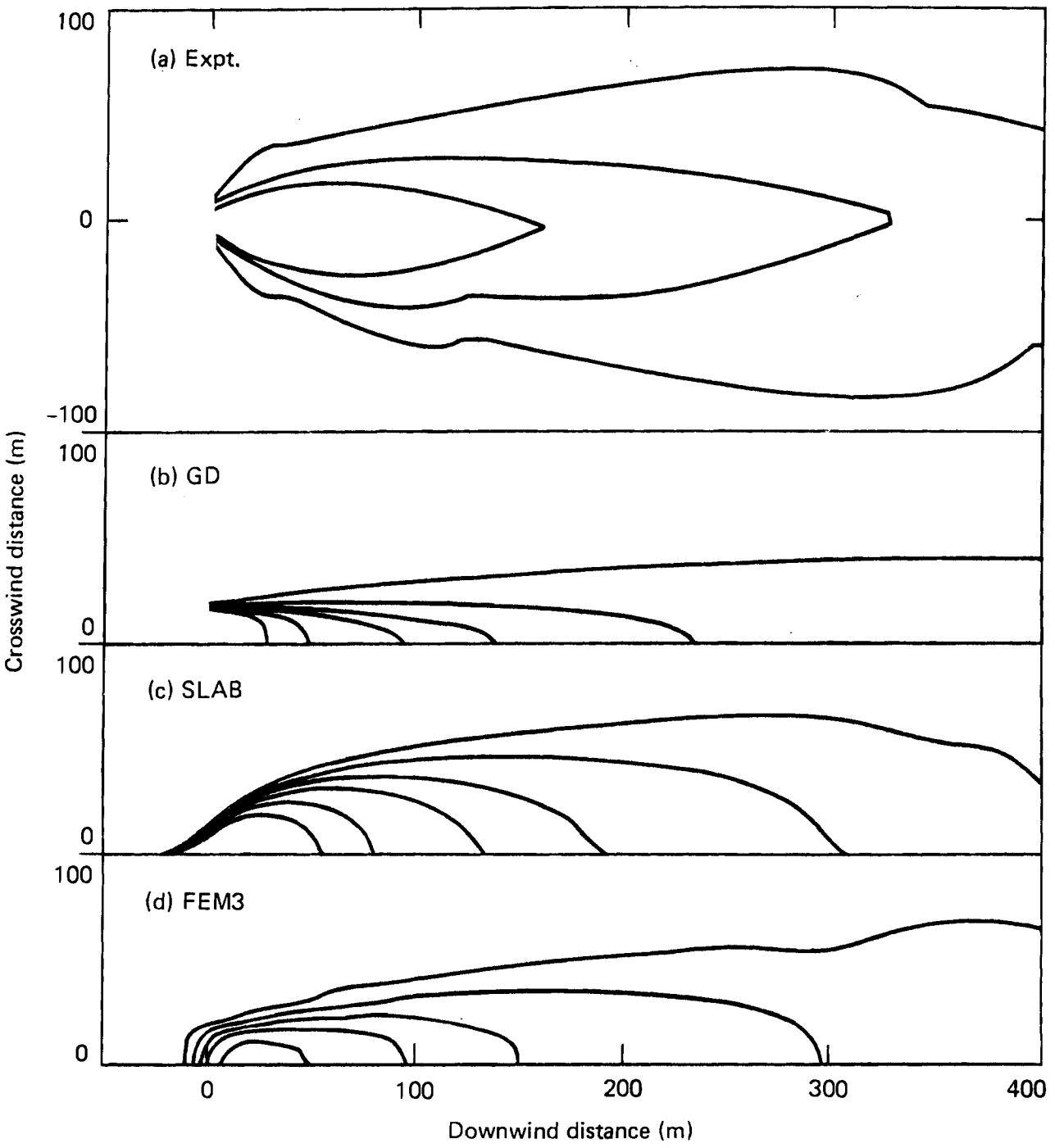

Figure 4. Burro 9 horizontal contour plots of cloud concentration 1 m above ground at t = 80 s. The experimental contour plot shows the full cloud width while the model results show only the half-width. Data from the first row of instruments was excluded from the experimental plot since these measurements were degraded by the RPT explosions. The contour lines designate the 1, 5, 10, 15, 25, and 35% contours and the crosswind to downwind distance scale is 1 to 1.

uncertainties. The value of X_{LFL} jumped up to 325 m just as the leading edge of the cloud reached the 400-m row and then rapidly fell to a value below 250 m after the spill valve was closed. In the two 10-s intervals before this, X_{LFL} was 275 and 285 m, respectively.

Also shown in Fig. 4 are the corresponding contour plots from each of the three models. At the time of this plot, the SLAB and FEM3 results for X_{LFL} have not reached their maximum value. The maximum downwind distance of the 5% contour continued to move downwind for an additional 10 to 20 s after the spill was terminated. The maximum value for both models is in good agreement with the experimental value as shown in Table 2. The GD result shown in Fig. 4(b) is a steady-state result since this model is not time dependent. The X_{LFL} value for the GD model is significantly less than the corresponding value for the other two models and the experimental result. The GD cloud width is also seen to be too narrow, just as it was in the Burro 3 and 7 results. For example, the 5% contour has a maximum width of 30 m in the GD plot while it has a 70 m width in the experimental plot. A comparison of the higher concentration levels is not possible since the RPTs significantly hampered the operation of the first row of instruments.

A view of the crosswind cloud structure is shown in Fig. 5 where the experimental results are compared to the SLAB and FEM3 results at a downwind distance of 140 m. The FEM3 model result agrees very well with the experimental plot, especially with regard to the vertical profile. The 1, 5, and 10% contours have maximum heights of 1.3, 3.3, and 8.0 m in the experimental plot and 1.3, 3.4, and 9.5 m in the FEM3 plot. As was the case with the previous examples, the SLAB model predicts too high a height for the higher contours (5 and 10%) and too low a height for the lower contours (1%).

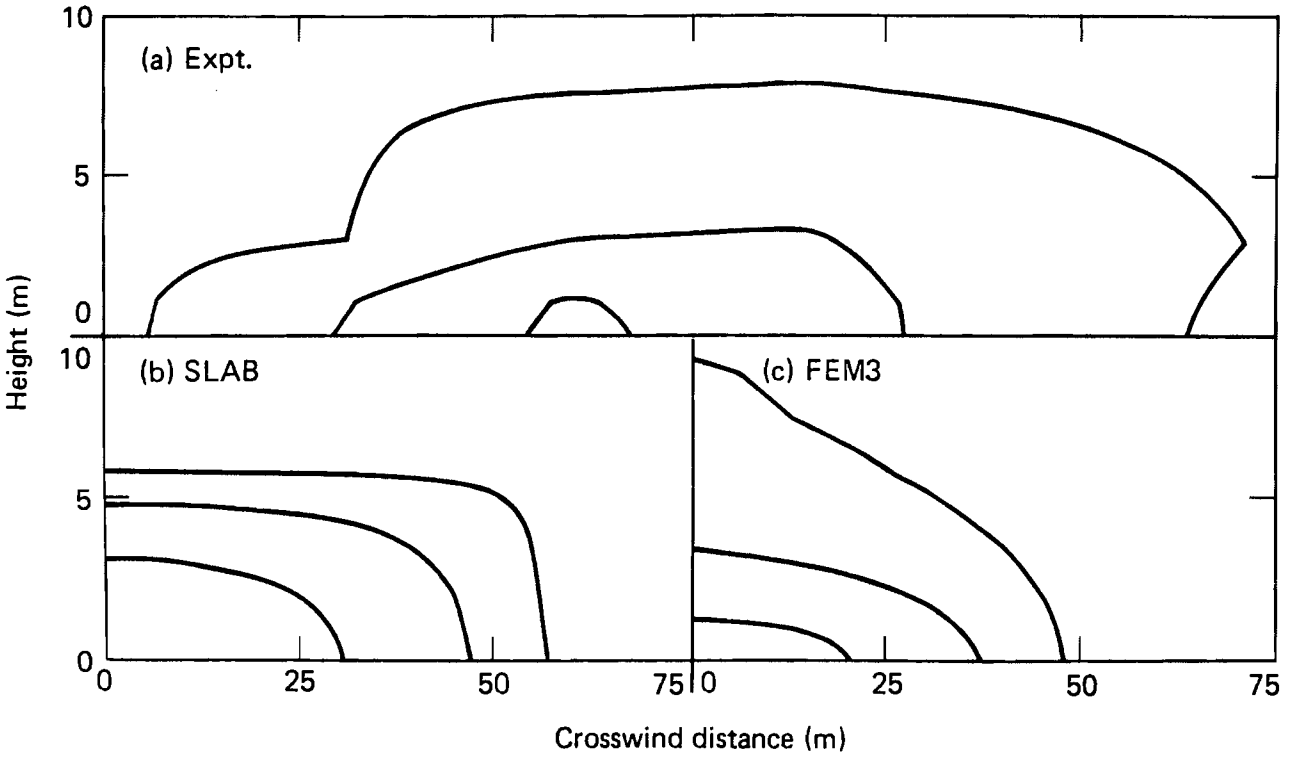

Figure 5. Burro 9 crosswind contour plots of cloud concentration 140 m downwind at t = 70 s. The contour lines designate the 1, 5, and 10% levels and the vertical to horizontal distance scale is 1 to 4.

The GD model (result not shown in figure) produces a cloud which is much higher than observed in the experiment. For example, the 5% contour has a maximum height of 8.5 m and the 1% contour has a height of 15.6 m.

Any interpolation error in the experimental result for the height of the contours in Fig. 5(a) is undoubtedly quite small since these heights are very close to the heights of the instruments. If a concentration profile of $c = c_o \cdot \exp\left[-(z/z_o)^n\right]$ is fitted to the experimental data, the power of the exponent for the best fit is found to be n = 1.0. This suggests that the vertical profile, at least in this case, is closer to an exponential than it is to a quadratic (used in the SLAB model) or a Gaussian (used in the GD model).

The maximum recorded concentration was always at the lowest (1-m) station in the first two rows. However, at the 400-m row, the maximum concentration measurement was observed to occur most of the time at the 3-m height, as shown in Fig. 6(a) (note, the inner contour is the 2.5% level). Neither the SLAB nor the FEM3 models predict this result (see Fig. 6) although they do predict the general height, width, and concentration level of the cloud fairly well. The SLAB model is not capable of predicting an elevated peak concentration since the vertical profile is specified to be quadratic with the peak at ground level. However, this is not the case with the FEM3 model. Several possible reasons for this discrepancy seem plausible, including insufficient heat sources to make the cloud buoyant and an inaccurate approximation to the ambient velocity profile near the ground.

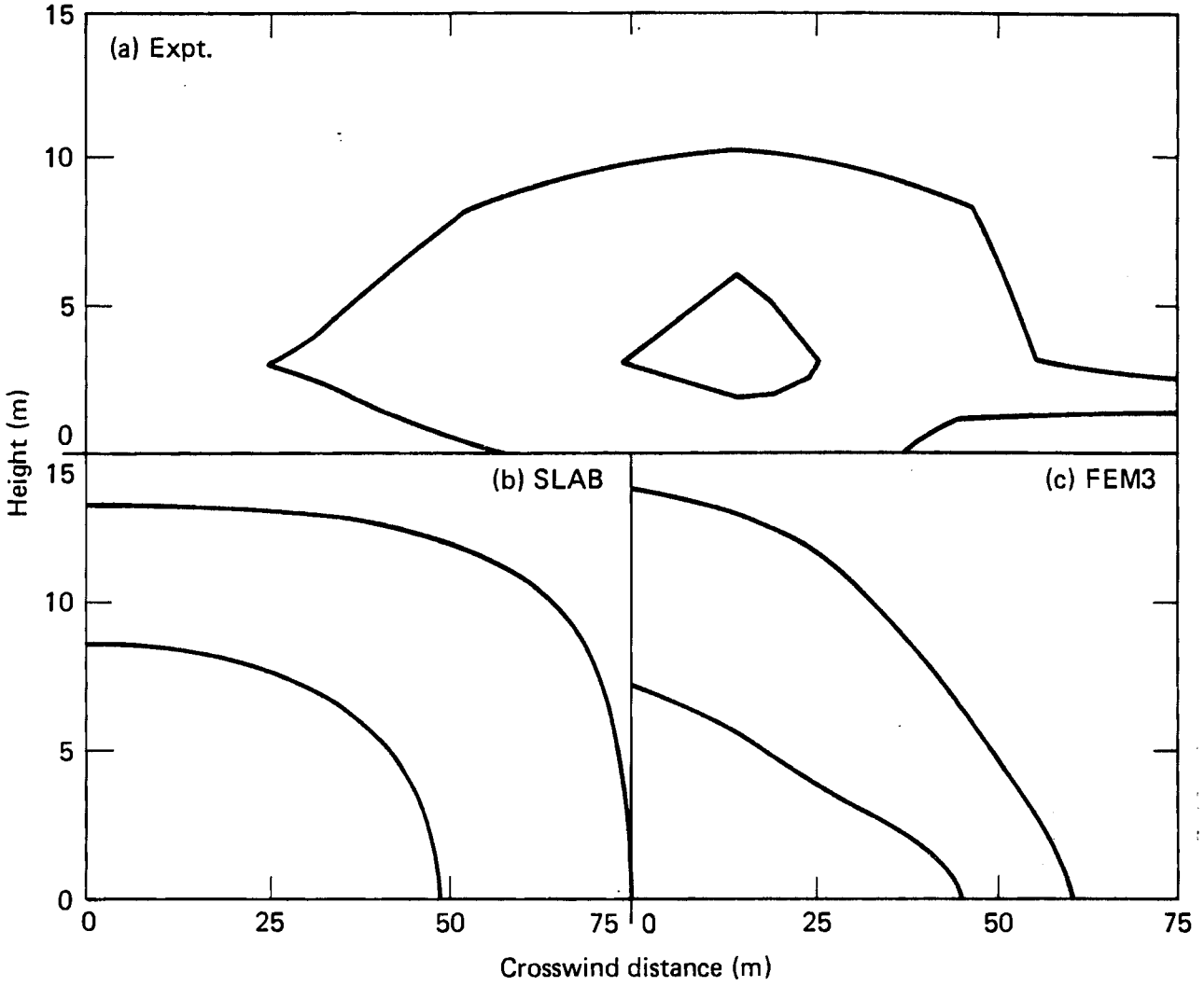

Figure 6. Burro 9 crosswind contour plots of cloud concentration 400 m downwind at t = 120 s. The contour lines designate the 1 and 2.5% levels and the vertical to horizontal distance scale is 1 to 4.

BURRO 8

Burro 8 was perhaps the most interesting of all the experiments. It was conducted under low wind speed and stable atmospheric conditions. The resulting vapor cloud was much wider than any of the others and it had a very distinct bifurcated structure. This can be seen in Fig. 7(a) which shows a horizontal contour plot of the cloud concentration 1 m above ground at t = 160 s. Although not shown in Fig. 7(a), the vapor cloud was observed to still exist upwind of the spill point at this time even though the spill was terminated more that 50 s earlier.

The FEM3 model ran into some difficulties in attempting to simulate the low horizontal diffusivity predicted by its turbulence submodel. Spurious oscillations due to insufficient spatial resolution in the horizontal plane began to occur about 140 s into the simulation. (Adequate spatial resolution would have required about an order of magnitude increase in mesh points.) To overcome this problem, the horizontal diffusivity was increased, and the simulation was rerun using a constant horizontal diffusivity of 2 m^2/s. The second simulation generally agreed quite well with the first run during the initial 140 s of the simulation, and is used here for times later than 140 s.

Also shown in Fig. 7 are the corresponding results from the three models. The bifurcated structure, so apparent in the experimental results, is not observed in these model plots, although a bifurcated structure did occur in the FEM3 result at higher elevations and will be shown later. While the structure is different, the value of X_{LFL} at this time is just under 300 m for both lobes of the experimental result, and for both the SLAB and FEM3 model results.

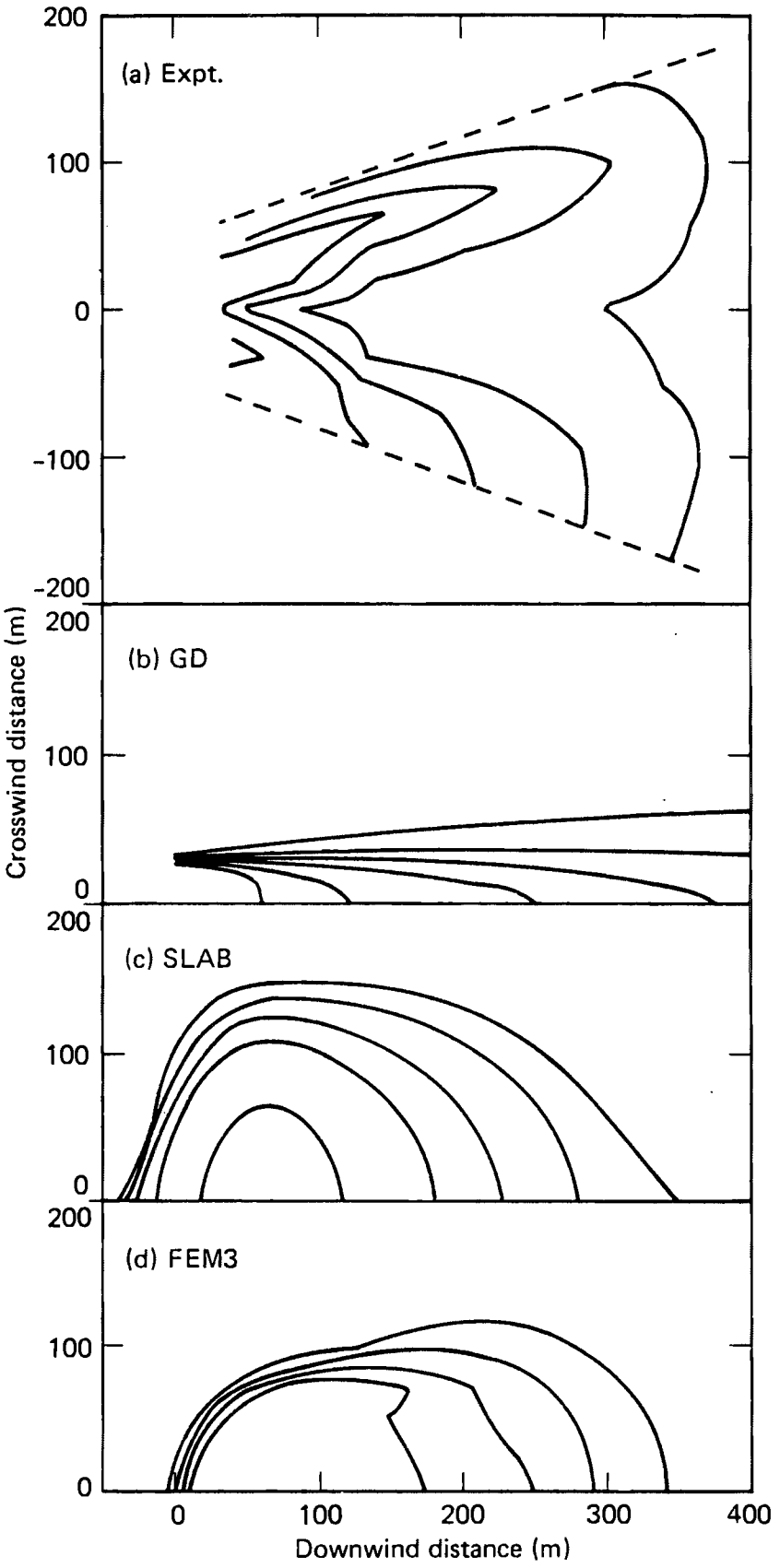

Figure 7. Burro 8 horizontal contour plots of cloud concentration 1 m above ground at t = 160 s. The dashed lines in plot (a) indicate the outer extent of the instrumentation array. The contour lines designate the 1, 5, 10, 15, 25, and 35% levels and the crosswind to downwind distance scale is 1 to 1.

The downwind distance to the LFL continued to grow for a considerable length of time after the spill was terminated at t = 106 s. The value of X_{LFL} in the experimental plots reached a maximum of 325 m and remained in the vicinity of 300 m for well up to t = 280 s. However, the actual maximum value of X_{LFL} in the lower lobe of Fig. 7(a) may have been missed since this lobe extends well beyond the edge of the array over a dry lake bed whose elevation is about 6 m below that of the instrument array centerline. In addition, a "puff" of vapor with a greater than 5% gas concentration entered the array from this side between 380 and 440 s and passed through the 400-m row of instruments at the 3-m level. Consequently, the maximum X_{LFL} value shown in Table 2 for this experiment is 420 m. The maximum X_{LFL} values for the GD, SLAB, and FEM3 models were 660, 418, and 630 m respectively. As noted earlier, the GD result using a higher stability class (GD+) was 1150 m, a significant overestimation. The net effect of terrain on the vapor dispersion in this experiment is difficult to quantify, although it undoubtedly did play a significant role. The presence of topographical features has been shown to reduce the distance to the LFL in wind tunnel experiments [23], so the experimental value of X_{LFL} might have been greater if the terrain were flat. Another factor which complicates comparison of the models with experiment is changes in the ambient wind speed. In this experiment, the ambient wind speed decreased in a fairly steady fashion by about 30% over the duration of the test.

The vapor cloud lingered over the source region for a considerable length of time after the LNG spill was terminated. While there were no concentration measurements within the spill pond area, we can look at when the leading and trailing edges of the cloud passed a particular row of instruments and

the time difference to the LNG spill time. This was done for the 140 m row and the results are shown in Table 3, where the arrival and departure times of the 1% and 5% concentration levels are given. The difference between these two times is seen to be 90 to 260 s longer than the spill time of 106 s, depending on the concentration level and the lobe of the bifurcated cloud being considered. The SLAB and FEM3 results are also shown in Table 3. The SLAB results are in very good agreement with those for lobe 2. The good agreement at the 1% concentration level was probably helped considerably by the diffusion terms. These terms were added to the SLAB model to increase numerical stability, and their main effect is to broaden the leading and trailing edges. The FEM3 results for the 5% concentration level are also in good agreement with the lobe 2 results, but the trailing edge of the 1% contour does not linger behind the cloud as long as in the experiment.

The GD model does not predict time-dependent phenomena such as the movement of the leading and trailing edges of the cloud. Looking at the steady-state prediction, the major deficiency in the GD simulation is, again, the shape of the predicted vapor cloud. As can be seen in Fig. 7(b), the GD vapor cloud is very narrow in comparison to the experiment. In contrast to this, the SLAB and FEM3 vapor clouds, shown in Fig. 7(c) and (d), are much wider and quite similar to the experiment. In comparing the SLAB and FEM3 model results with each other, the vapor cloud is seen to be significantly wider in the SLAB plot than in the FEM3 plot, especially over the first 200 m downwind where gravity spread is the major factor controlling cloud width. The actual width of the cloud in this region cannot be determined accurately since the vapor cloud extended well beyond the edges of the first two rows of instruments.

TABLE 3. CLOUD ARRIVAL AND DEPARTURE TIMES AT THE 140-m ROW

	Experiment			
	Lobe 1*	Lobe 2	SLAB	FEM3
Arrival time				
1% concentration	55	55	55	60
5% concentration	75	75	65	65
Departure time				
1% concentration	420	360	350	265
5% concentration	320	270	275	255
Arrival minus departure time**				
1% concentration	365	305	295	205
5 % concentration	245	195	210	190

* Lobe 1 is the lobe over the lower terrain

** For comparison, the spill time was 106 s.

The crosswind cloud shape and structure can be seen quite well, however, in Fig. 8(a) which shows a crosswind contour plot of the cloud concentration 140 m downwind at t = 200 s. The left lobe in Fig. 8(a) appears to be somewhat larger than the right one. This is probably due to gravity and topography effects since the terrain is about 6 m lower on this side of the array than it is in the middle, as noted earlier. Figures 8(b) and 8(c) show the corresponding SLAB and FEM3 results. The SLAB cloud is very low and much wider than the the FEM3 result. If one extrapolates the two lobes of the experimental plot beyond the edges of the array, it appears as though the larger left lobe is about as wide as the SLAB half-width and the smaller right lobe is about as wide as the FEM3 half-width.

The bifurcated structure of the FEM3 result is shown quite clearly in Fig. 8(c). Qualitatively, it compares fairly well with the experimental result, especially in the extended lobe region. In the region of the cloud centerline, however, the model predicts concentrations which are too high. Consequently, the bifurcated structure is not apparent at low elevations, such as in the horizontal contour plot of Fig. 7(d) at 1 m height. Besides accounting for terrain effects, improvements in the turbulence submodel and more accurate treatment of the velocity profile near the ground are undoubtedly needed for more quantitative agreement with experiment.

The bifurcated structure of the concentration distribution is shown in the FEM3 simulations to be due to a crosswind eddy which develops as a result of gravity spreading of the denser-than-air LNG vapor cloud. One might suspect that the crosswind gravity spread velocities in the Burro 8 test were significantly larger than those in the other experiments; however, this does not appear to be the case. Figure 9 compares FEM3 calculations of typical

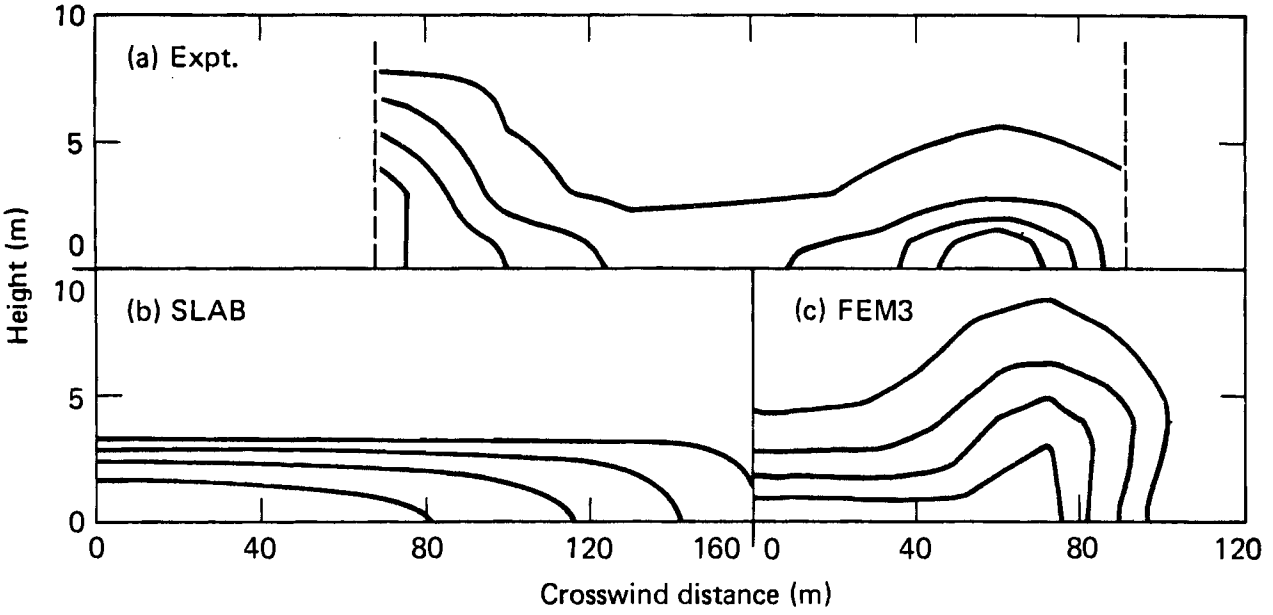

Figure 8 Burro 8 crosswind contour plots of cloud concentration 140 m downwind at t = 200 s. The dashed lines in plot (a) indicate the outer extent of the instrumentaion array. The contour lines designate the 1, 5, 10, and 15% levels and the vertical to horizontal distance scale is 1 to 6.

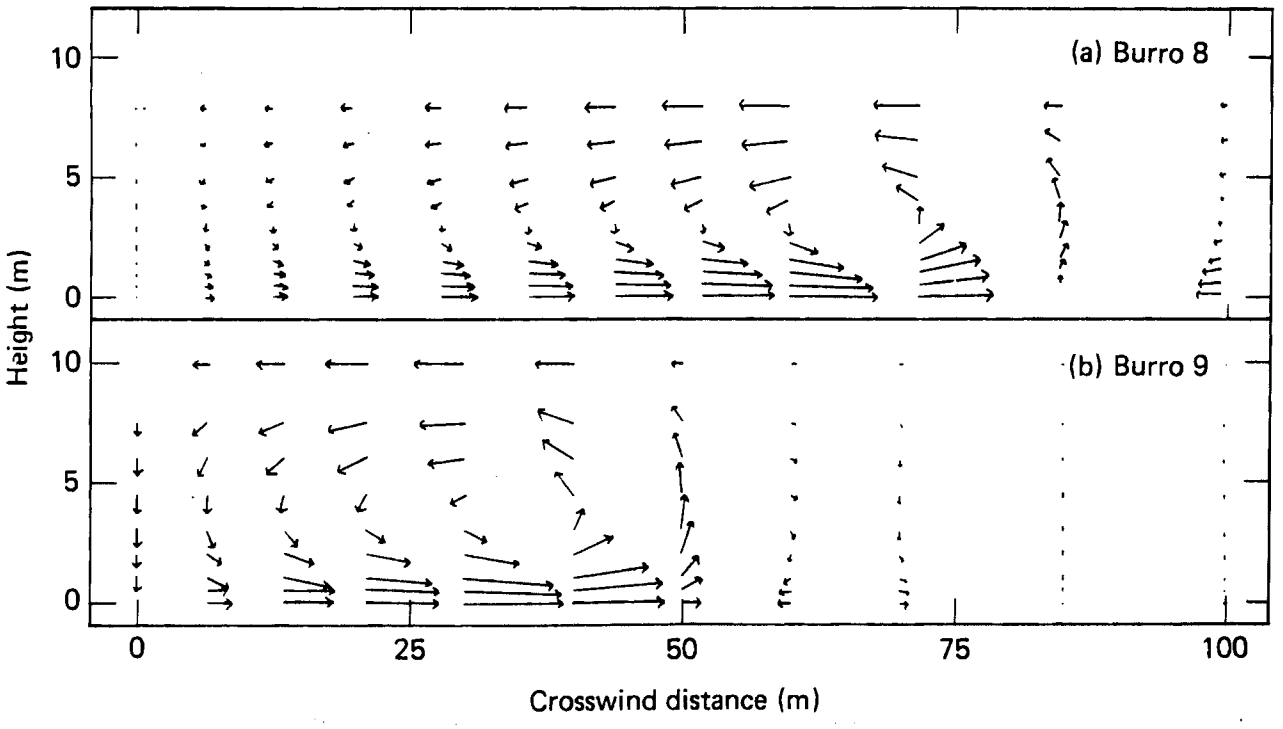

Figure 9 Typical crosswind velocity plots 140 m downwind for (a) Burro 8 and (b) Burro 9 as calculated by the FEM3 model. The maximum crosswind velocity in both cases is about 0.9 m/s. The vertical to horizontal distance scale is 1 to 2.

crosswind velocity plots for both (a) Burro 8 and (b) Burro 9 at a downwind distance of 140 m. While the eddy is much wider in the Burro 8 case, the velocities are quite similar. In both simulations, maximum crosswind velocities ranged from about 0.5 to 0.9 m/s during the time the vapor cloud passed this downwind distance. The major difference between the two velocity fields is the magnitude of the downwind components. In Burro 8, the downwind velocity is only about twice as large as the maximum crosswind gravity spread velocity, while in Burro 9 (and also Burro 3 and 7), the downwind velocity is at least six times as large as the maximum crosswind gravity spread velocity. Consequently, the bifurcated concentration structure observed in Burro 8 is not due to a larger gravity spread velocity in this experiment. Rather, it is mainly the result of a higher ratio between the gravity spread velocity and the downwind velocity.

DISCUSSION AND CONCLUSIONS

The range of applicability of any particular model generally depends on the degree to which important physical phenomena are approximated. Of the three models used in this study, the FEM3 model is the least limited by various approximations and restricting assumptions, and it did indeed provide the best overall description of LNG vapor cloud dispersion as observed in the four experiments addressed here. Predictions of the vapor concentration distribution in time and space over the range from 5% to 15% (the LNG flammability limits) were generally quite good. Estimates of the maximum distance to the LFL were also quite good or at least conservative (overestimated X_{LFL}).

A major accomplishment of the FEM3 model was the prediction of the bifurcated structure of the very wide vapor cloud in Burro 8. This behavior was observed in only this one experiment, which occurred under low wind speed and stable atmospheric conditions. Neither of the other two models could have reproduced this behavior since the crosswind concentration distribution was prescribed in these models and not subject to change by the conditions in the cloud. The FEM3 simulation not only predicts this behavior, but also provides the necessary information to understand how it is generated by the crosswind gravity spread vortex flow. Additional model simulations would provide more insight into the atmospheric and spill conditions under which this phenomenon would be expected to occur. For more quantitative agreement with experiment, improvements are needed in the turbulence submodel, the approximations for the velocity profile near the ground, and the treatment of terrain. The numerical difficulties associated with low turbulence levels must also be addressed.

The SLAB model also provided a fairly good description of the observed concentration distribution and good estimates of the maximum distance to the LFL. The excellent prediction of X_{LFL} in Burro 8 is very encouraging, however, we are cautious that this agreement might be somewhat fortuitous. If the China Lake terrain significantly reduced X_{LFL} from what it would be under flat terrain conditions, then the SLAB estimate will prove to be too short. Obviously, additional experiments under low wind speed conditions and over flat terrain are needed to verify the models in this range of atmospheric conditions.

Assuming a crosswind concentration profile for the SLAB model greatly facilitated comparison with the experimental contour plots. The quadratic vertical profile with peak concentration and zero gradient at the ground was most applicable to the Burro 8 experiment where the vapor cloud was nearly a uniform layer close to the ground. However, in the higher wind speed experiments, the concentration gradient was much steeper near the ground, and an exponential profile might be more appropriate under these conditions. If a profile is assumed, it would be preferable to incorporate this assumption into the derivation of the basic conservation equations rather than just apply it after the species equation is solved, as was done here. In this regard, a profile whose shape could vary with changes in the cloud properties (such as going from negative to positive buoyancy) would also be desirable; however, this might be exceeding the limits of the model. It would probably be more profitable to try to improve the main submodels such as the entrainment and surface heat flux and friction submodels.

The GD model estimates of the vapor cloud concentration distribution were significantly poorer than those of the other two models. In all four

simulations, the predicted cloud was roughly twice as high and twice as narrow as in the experiments. The main reason for this is that the GD model includes gravity effects only in the initial calculation of the vapor source height and width, but does not include gravity effects on the subsequent downwind dispersion of the vapor cloud.

This discrepancy in cloud shape between the GD model results and the experiments illustrates the importance of gravity spread on the crosswind concentration distribution, even when the wind speed is high and turbulence within the cloud is dominated by the ambient atmospheric conditions. In the three high wind speed simulations (Burro 3, 7, and 9), the initial GD gravity spread calculation did not even increase the width of the vapor source, since the ambient wind speed was greater than the calculated gravity spread velocity. Consequently, these GD simulations were equivalent to Gaussian plume calculations for a trace release of a neutrally buoyant emission. Neglecting the effects of gravity on the denser-than-air cloud results in a predicted vapor cloud which is much too high and too narrow, even under strong wind speed conditions.

In the model simulations, the maximum distance to the LFL is quite sensitive to the turbulence level. For example, in the GD model, turbulence level is controlled by specifying the stability class. Increasing the stability class in effect lowers the turbulence level. When the stability was increased by just one class, the value of X_{LFL} increased by 40 to 75%, depending on the initial stability category and the LNG spill rate. Similar results were found using the FEM3 model. In these calculations (not previously shown), the LNG vapor source rate was similar to that in the Burro experiments and a constant diffusivity with a wind speed of 4 m/s was used.

When the vertical diffusivity was decreased from .5 to .2 m^2/s, with a similar decrease in the horizontal diffusivity, the steady state value of X_{LFL} increased by a factor of two, showing considerable sensitivity to the turbulence level.

It is interesting to note that the turbulence level, as calculated by the FEM3 turbulence submodel equation, returned to a value quite close to the ambient level within only a few tens of metres from the LNG vapor source, even for Burro 8. This suggests that the turbulence level over a significant portion of the vapor cloud may be fairly close to the ambient level, even though gravity effects on cloud width and height are still important at these downwind locations. However, this has not been confirmed by comparison with experimental data.

With regard to the vapor source, the effective LNG evaporation rate and, in turn, the radius of the liquid pool and vapor source have remained fairly uncertain in field-scale LNG spill tests on water where the liquid pool radius is not confined. Recent analysis of IR data taken during Burro 9 suggests that the liquid LNG pool was only 5 m in radius. This implies an effective evaporation rate which is 10 times as great as the value assumed in this study and, therefore, vapor source radii which are 1/3 as large as those used in these model simulations. It should be noted that there is considerable uncertainty surrounding this observation, especially in light of the numerous RPT explosions which occurred during this experiment. The effect of such an increase in the evaporation rate on the model predictions has not been thoroughly analyzed. While the source radius would decrease by a factor of 1/3 as noted above, the overall evaporation rate (mass/time) would remain the same and be equal to the LNG spill rate (assuming the liquid pool rapidly

reaches a quasi-steady state). Clearly, the effect on cloud concentration will be greatest in the high concentration regions surrounding the vapor source and will decrease with distance from the liquid pool.

This comparison of three dense-gas dispersion models of varying levels of sophistication with the results from the Burro series of LNG dispersion experiments has provided considerable insight into the strengths and weaknesses of the three different types of models and has identified important model components that require improvement. The comparison of cloud structure between the three-dimensional, conservation equation model, FEM3, and the experiments, was generally quite good. In particular, the FEM3 prediction of a bifurcated cloud structure in Burro 8 was very encouraging. The one-dimensional, averaged conservation equation model, SLAB, also compared fairly well with experiment, especially in the prediction of the maximum distance to the LFL. In contrast to the other two models, the modified Gaussian plume model, GD, compared rather poorly with the observed cloud structure.

The experiments used in this study were performed over a limited range of spill scenarios. Consequently, additional comparisons with well-instrumented, large-scale experiments are needed in order to evaluate each model's ability to accurately simulate very large spills over a broad range of atmospheric conditions. In this regard, recent Shell LNG and propane spill experiments conducted at Maplin Sands, England, [24] and additional LNG experiments currently underway at China Lake, California, will be most helpful.

ACKNOWLEDGMENTS

The authors are indebted to all of those who participated in the Burro Series of LNG spill experiments. We would especially like to thank R.P. Koopman, R.T. Cederwall, and H.C. Rodean for their many helpful discussions regarding the data obtained in these experiments. We also wish to thank E.J. Kansa for his advice in applying boundary conditions in the SLAB and FEM3 models and D.J. Bergmann for running the GD computer simulations. This work was performed under the auspices of the U.S. Department of Energy by the Lawrence Livermore National Laboratory under Contract No. W-7405-Eng-48.

REFERENCES

1. R.P. Koopman, Burro Series Data Report: LLNL/NWC 1980 LNG Spill Tests, Lawrence Livermore National Laboratory Report UCID-19075, June 1981.

2. R.T. Cederwall, D.L. Ermak, H.C. Goldwire, Jr., R.P. Koopman, J.W. McClure, T.G. McRae, D.L. Morgan, H.C. Rodean, and J.H. Shinn, Description and Analysis of Burro Series 40-m^3 LNG Spill Experiments, Lawrence Livermore National Laboratory Report UCRL-86704, October 1981.

3. D.S. Burgess, J. Biordi, and J. Murphy, Hazards of Spillage of LNG into Water, U.S. Bureau of Mines, NTIS AD 754498, 1972.

4. G.F. Feldbauer, J.J. Heigl, W. McQueen, R.H. Whipp, and W.G. May, Spills of LNG on Water - Vaporization and Downwind Drift of Combustible Mixtures, Esso Research and Engineering Company Report No. EE61E-72, November 1972.

5. P.P.K. Raj and A.S. Kalelkar, Assessment Models in Support of the Hazards Assessment Handbook (CG-446-3), NTIS AD 776617, January 1974.

6. A.P. van Ulden, On the Spreading of a Heavy Gas Released Near the Ground, Proceedings 1st International Symposium on Loss Prevention and Safety Promotion in the Process Industries, Delft, Netherlands, 1974, pp 221-226.

7. A.E. Germeles and E.M. Drake, Gravity Spreading and Atmospheric Dispersion of LNG Vapor Clouds, 4th International Symposium on Transport of Hazardous Cargoes by Sea and Inland Waterways, Jacksonville, Florida, October 1975.

8. J.A. Fay and D.H. Lewis, Jr., The Inflammability and Dispersion of LNG Vapor Clouds, 4th International Symposium on Transport of Hazardous Cargoes by Sea and Inland Waterways, Jacksonville, Florida, October 1975.

9. W.G. England, L.H. Teuscher, L.E. Hauser, and B. Freeman, Atmospheric Dispersion of Liquefied Natural Gas Vapor Clouds Using SIGMET, a Three-Dimensional, Time-Dependent, Hydrodynamic Computer Model, Heat Transfer, and Fluid Mechanics Institute, Washington State University, June 1978.

10. J.A. Havens, An Assessment of Predictability of LNG Vapor Dispersion from Catastrophic Spills onto Water, Journal of Hazardous Materials, 3 (1980) 267.

11. S.T. Chan, P.M. Gresho, R.L. Lee, and C.D. Upson, Simulation of Three-Dimensional, Time-Dependent, Incompressible Flows by a Finite Element Metnod, Proceedings of the AIAA 5th Computational Fluid Dynamics Conference, Palo Alto, California, June 1981.

12. S.T. Chan, P.M. Gresho, and D.L. Ermak, A Three-Dimensional, Conservation Equation Model for Simulating LNG Vapor Dispersion in the Atmosphere, Lawrence Livermore National Laboratory Report UCID-19210, September 1981.

13. R.A. Cox and R.J. Carpenter, Further Development of a Dense Vapor Cloud Dispersion Model for Hazard Analysis, Symposium "Schwere Gase", Battelle-Institute, Frankfurt am Main, September 1979.

14. K.J. Eidsvik, A Model for Heavy Gas Dispersion in the Atmosphere, Atmospheric Environment, 14 (1980) 769.

15. O. Zeman, The Dynamics and Modeling of Heavier-Than-Air Cold Gas Releases, Journal of Atmospheric Science, (in press).

16. G.W. Colenbrander, A Mathematical Model for the Transient Behavior of Dense Vapor Clouds, 3rd International Symposium on Loss Prevention and Safety Promotion in the Process Industries, Basle, Switzerland, September 1980.

17. F.A. Gifford, Jr., Use of Routine Meteorological Observations for Estimating Atmospheric Dispersions, Nuclear Safety, 2 (1961) 47.

18. H. Kato and O.M. Phillips, On the Penetration of a Turbulent Layer into Stratified Fluid, Journal of Fluid Mecnanics, 37 (1969) 643.

19. N.K. Madsen and R.F. Sincovec, ALGORITHM 540 PDECOL, General Collocation Software for Partial Differential Equations, ACM Transactions on Mathematical Software, 5 (1979) 326.

20. Y. Ogura and N. Phillips, Scale Analysis of Deep and Shallow Convection in the Atmosphere, Journal of Atmospheric Science, 19 (1962) 173.

21. D.B. Turner, Workbook of Atmospheric Dispersion Estimates, U.S. Department of Health, Education, and Welfare, PB-191 482, 1970.

22. D. Golder, Relations Among Stability Parameters in the Surface Layer, Boundary-Layer Meteorology, 3 (1972) 47.

23. D.E. Neff and R.N. Meroney, Dispersion of Vapor form LNG Spills-Simulation in a Meteorological Wind Tunnel of Spills at China Lake Naval Weapons Center, California, Colorado State University Report CER78-79DEN-RNM41, 1979.

24. D.R. Blackmore, J. Eyre, J.B. Homer, and J.A. Martin, Refrigerated Gas Safety Research, American Gas Association Transmission Conference, Atlanta, Georgia, May 1981.

REPORT D

Coyote Series 40-m^3 Liquefied Natural Gas (LNG) RPT and Vapor Burn Tests

H. C. Goldwire, Jr.
R. P. Koopman

Prepared for the
Environmental and Safety Engineering
Division
U.S. Department of Energy
under Contract W-7405-ENG-48

Lawrence Livermore Laboratory
Livermore, California 94550

REPORT D

TABLE OF CONTENTS

SUMMARY

In July 1981 a Lawrence Livermore National Laboratory (LLNL) experimental team returned to the Naval Weapons Center (NWC) at China Lake, California, to continue the 40-m^3 LNG spill tests started last year (1[a], 2,3[b]). This year, as last, the experiments were a joint effort between LLNL and NWC personnel. Last year the emphasis of the experiments was directed exclusively toward gas dispersion. This year investigations were extended into the rapid phase transformation (RPT) explosions observed on several of the dispersion tests last year. Combustion and dispersion measurements during vapor cloud fires were also made.

DESCRIPTION OF TESTS

The RPT tests were a joint effort and initiated this test series since they required only one operational data collection station. A schematic drawing of the RPT instrumentation is shown in Figure 1. A total of 13 RPT spills in five tests were conducted at various times from July to November 1981. A summary of these tests is given in Table 1. The second test was a preliminary vapor burn to check the survivability of the instruments in a vapor fire and to assess vapor fire hazards with a small spill before doing the large spills. RPT testing was also done concurrently with the vapor fires, the choice depending upon operational and weather circumstances. The goal of the RPT tests is to understand the physics behind RPT explosions so that their severity in an accident situation can be predicted. Last year we observed explosions under two different situations. The first occurred late in the spill and out on the LNG pool away from the spill pipe, and the second occurred immediately after the spill began and at the point where the LNG impacted the water. The first type appears to be associated with differential boiloff of the LNG on the pond while the second type appears to depend on the LNG

---

a. Included as Report Q in U.S. Department of Energy (DOE). 1980. Liquefied Gaseous Fuels Safety and Environmental Control Assessment: Second Status Report. DOE/EV-0085 Vol. 2. Washington, D.C.

b. See Report A of this Status Report.

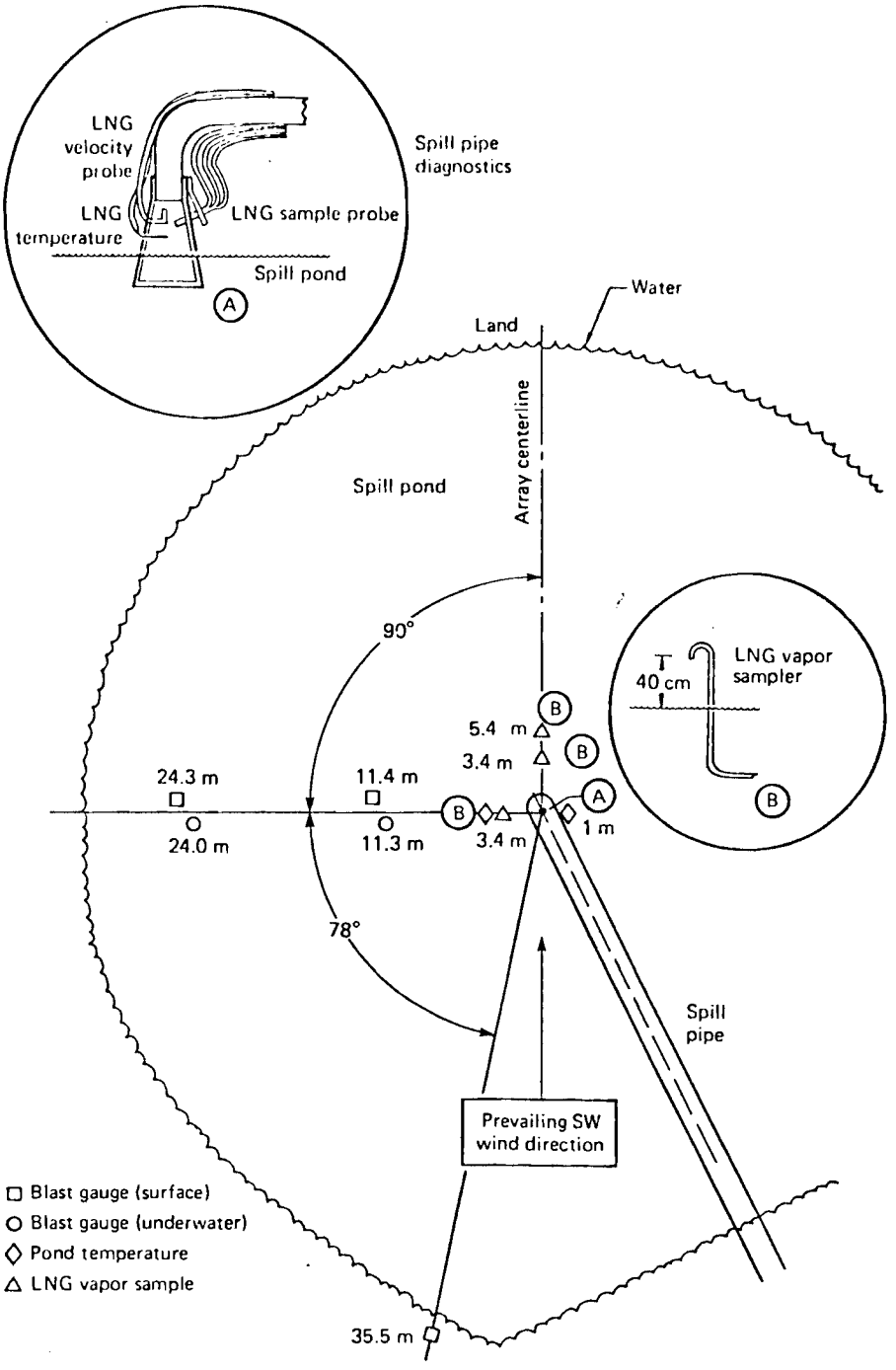

Figure 1. RPT diagnostics on the spill pond.

TABLE 1 COYOTE SERIES TEST SUMMARY

Coyote Test	Date	Test Type	Material Spilled	Composition % CH4 % C2H6 % C3H8	Spill Rate (m^3/min)	Spill Volume (m^3)	Spill Plate Depth(in.)	Wind Speed (m/s)	Pond Temp (°C)	RPTs	IR Imaging
1	7/30	RPT	LNG	81.7 14.5 3.8	6	14	12	6.4	30	small early large late	none
2	8/20	vapor burn	LNG	70 23.4 6.6	16	8	1	5.9	27.6	small early	none
3	9/2	vapor burn	LNG	79.4 16.4 4.2	13.5	14.6	1	5.8	22.8	none	side
4	9/25	RPT	LNG	78.8 17.3 3.9	6.8 12.1 18.5	3.8 6.0 5.2	10.0	6.6	21	small early none large early	none
5	10/7	vapor burn	LNG	74.9 20.5 4.6	17.1	28	2.5	10	17.2	large late	side
6	10/27	vapor* burn	LNG	81.8 14.6 3.6	16.6	22.8	2	4.8	15.0	none	downwind side overhead
7	11/12	vapor* burn	LCH_4	99.5 0.5 0	14.0	26	13	6.0	13.6	none	downwind side overhead
8	11/13	RPT	LCH_4	99.7 0.3 0	7.5 14.2 19.4	3.7 5.4 9.7	13	8.6	13	none none none	overhead
9	11/16	RPT	LN_2	--	7.2 9.9 13.3	3.6 3.3 8.2	14	4.1	15	none none none	none
10	11/24	RPT	LNG	70.2 17.2 12.6	13.8 19.3 18.8	4.6 4.5 5.0	14 removed	7.8	11	none none large early	none

*Jet ignitor used

interaction with the water.

In this series, efforts were focused on the second type situation. LLNL personnel attempted to measure the species concentration, temperature of the LNG and the water, and the velocity of the LNG as it exits the spill pipe. This approach should yield data to allow a comparison with Reid's (4) laboratory scale experiments in which the shock overpressure was observed to depend on impact pressure, water temperature, and type of cryogen. In addition, NWC personnel installed blast gauges, both above and below the water, to measure the overpressure from the explosions as well as close-in cameras to film and locate the events.

Species concentration at several places over the LNG pool during the RPT tests and the vapor burn tests was also measured. This will be important for studying RPT explosions which occur late in the spill and on the spill pond away from the impact point. These type explosions did not occur often during the RPT series since the RPT spills are of short duration and involve only small amounts of LNG. The RPT explosion diagnostics were present for all tests, including vapor burn tests.

The major thrust of this year's effort was toward the vapor burn tests. A sketch of the array of instrument stations used for these experiments is shown in Figure 2. The gas concentration contours superimposed are from the 1980 Burro 9 experiment. A typical instrument station is shown in Figure 3. These experiments involved a series of five spills up to 40-m^3 under a restricted range of atmospheric conditions with ignition near the upwind edge of the cloud. One test involved nearly pure methane. Table 1 summarizes conditions for these tests. The experiments will provide information on the combustion characteristics of a well-mixed gas cloud in the open atmosphere. The effect of wind and atmospheric turbulence on flame propagation also will be investigated. In addition to the standard dispersion diagnostics of gas species concentration, temperature, wind speed and direction, heat flux, and turbulence, a new instrument designed to measure local flame velocity and several calorimeters to measure flame heating were fielded

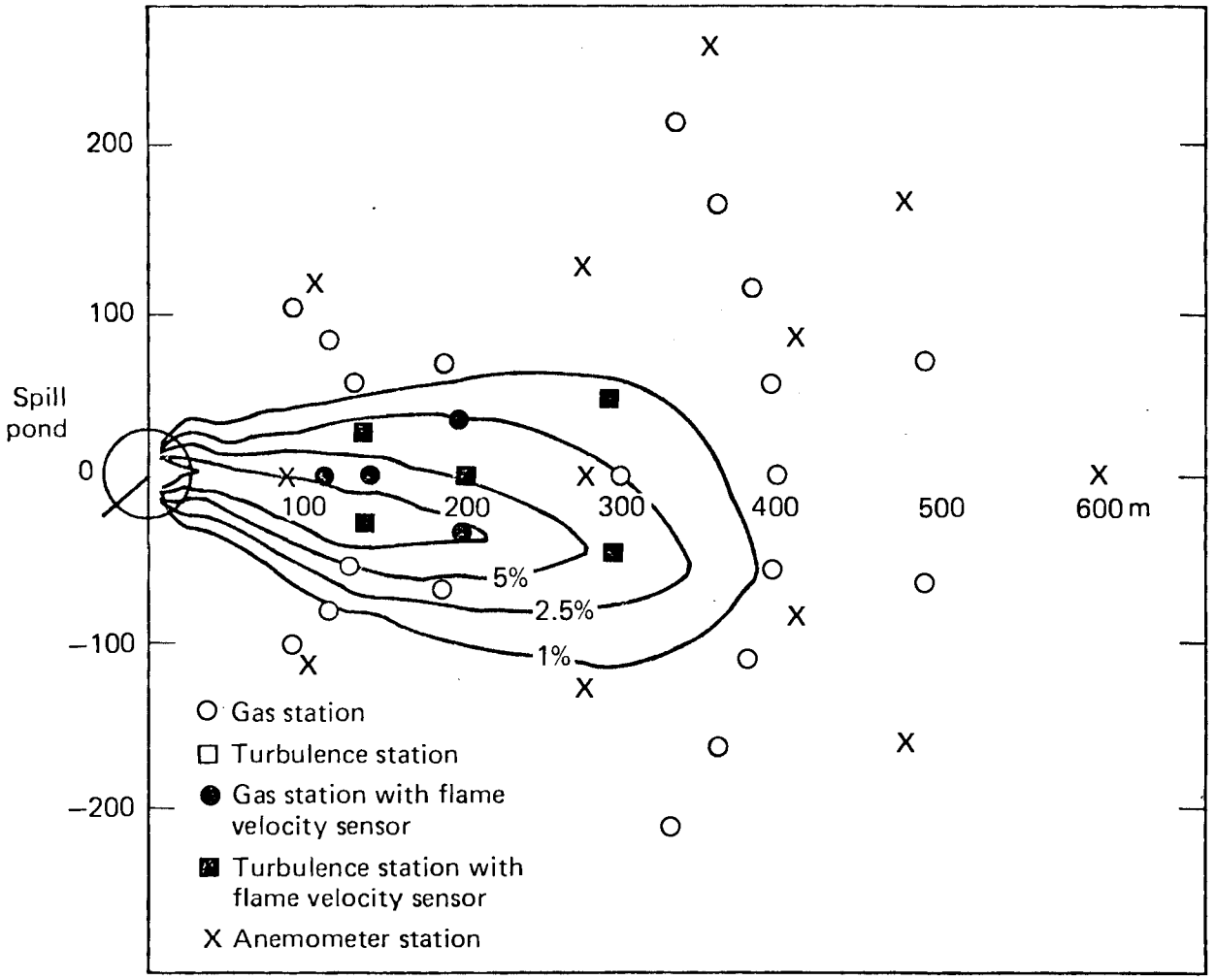

Figure 2. The vapor fire instrument array for the Coyote Series, LNG spill experiments, 1981.

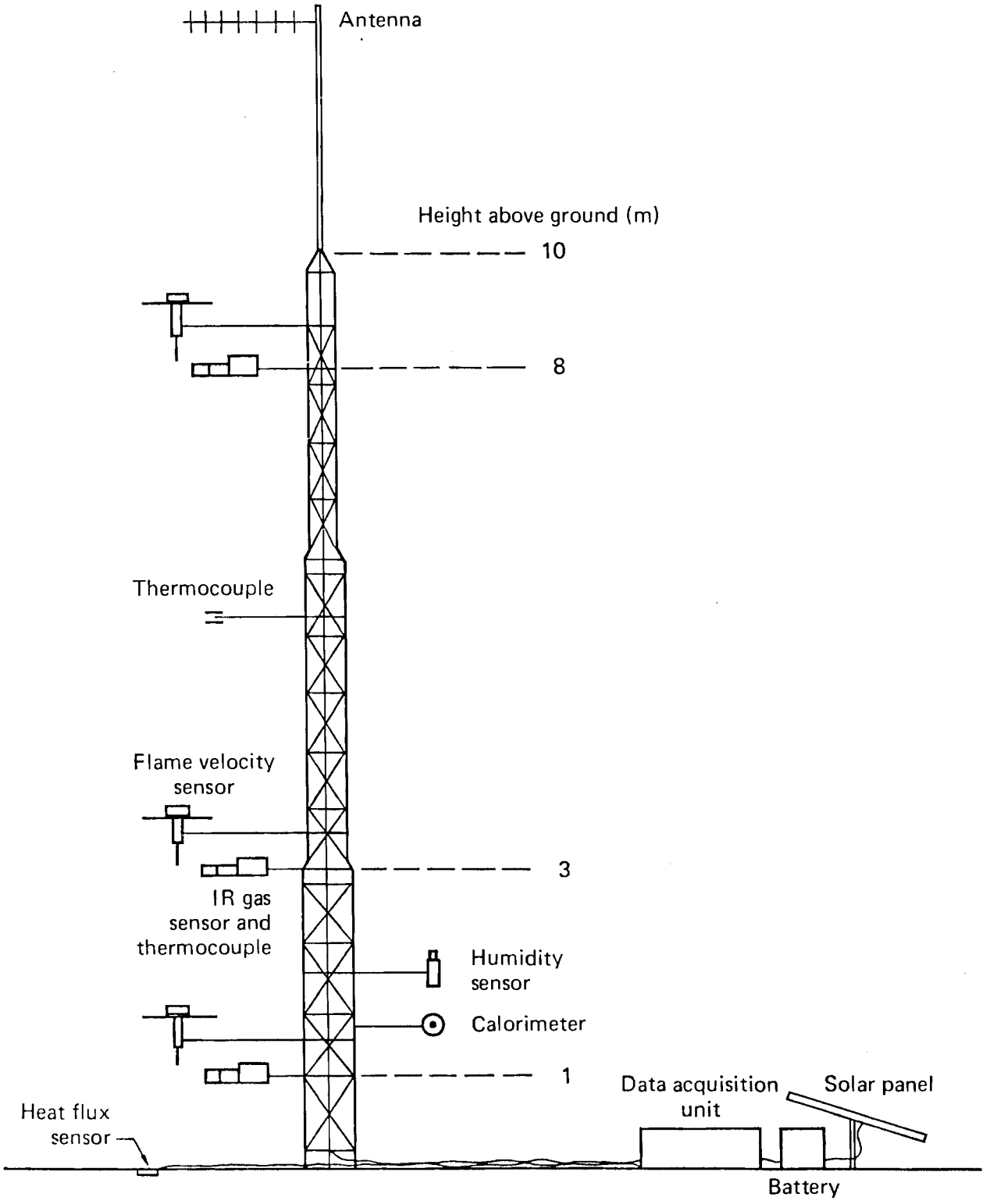

Figure 3. A typical gas sensor station with flame velocity sensors.

by LLNL. Also, EG&G flew their IR imager on two tests to view the flame front from above so that global flame velocities can be determined. NWC personnel were responsible for photography and for making radiometric measurements outside of the flame. Both NWC and LLNL personnel conducted IR imaging from ground level.

Following is a summary of the test series with details on instruments used and types of tests conducted.

1. RPT Series -

Instruments: Gas Sensor station 1 only.
Three IR sensors for vapor composition on the pond (LLNL).
Anarad sensor for LNG composition (LLNL).
LNG temperature (LLNL).
Pond temperature (LLNL).
LNG velocity (LLNL).
Blast gauges (NWC).
Photography (NWC).

Tests: Splash plate was lowered to 12-14" below water surface for all tests to protect facility pipe supports from damage and provide sufficient water for LNG-water interaction to occur.

a) A series of 3-10 m^3 spills with nominal LNG composition (~20% heavy hydrocarbons) and nominal spill rates of 5, 10, and 20 m^3/min. Spills were terminated upon occurrence of large RPTs.

b) Test sequence described in a) with nearly pure liquid methane (0% heavy hydrocarbons) and also liquid nitrogen.

c) Conducted one test with splash plate totally removed.

2. Preliminary Vapor Burn -

Instruments: Two stations, at 57 m and 110 m.
Tests: One - 5 m^3 -- Nominal wind conditions.

3. Vapor Burns -

Instruments: New array configuration (see Figure 2).
Gas concentration, heat flux, temperature, wind field, and humidity as in 1980 (LLNL).
Flame resistant anemometers (LLNL).
External radiometers (NWC).
Calorimeters (LLNL).
Real-time gas concentration at igniters (LLNL).
Flame velocity sensors (27) (LLNL).
IR Imaging from above (EG&G) and from side (NWC and LLNL).
Continue RPT diagnostics (see 1).

Tests:

a) 15 m^3 @ 14 m^3/min, nominal afternoon (unstable atmosphere) southwesterly wind conditions (~6 m/s). Ignition at ~100 m downwind of spill point 35 seconds after spill valve closed.

b) 28 m^3 @ 17 m^3/min, highly unstable, high wind speed (~10 m/s). Ignition at ~100 m 25 seconds after valve closure.

c) 23 m^3 @ 17 m^3/min, neutral, moderate wind speed (~5 m/s), evening conditions. Ignition at ~100 m 28 seconds after.

d) 26 m^3 @ 14 m^3/min, moderate wind speed (~6 m/s). Ignition at ~100 m, 29 seconds after spill valve closed. Test of strong position source.

REFERENCES

1. R.P. Koopman, Experimental Plan for 40-m^3 Liquified Natural Gas (LNG) Dispersion Tests, Lawrence Livermore National Laboratory Report UCID-18585 (1981).

2. R.P. Koopman, L.M. Kamppinen, W.J. Hogan, and C.D. Lind, Burro Series Data Report, LLNL/NWC 1980 LNG Spill Tests, Lawrence Livermore National Laboratory Report UCID-19075 (1981).

3. R.P. Koopman, R.T. Cederwall, D.L. Ermak, H.C. Goldwire, J.W. McClure, T.G. McRae, D.L. Morgan, H.C. Rodean, and J.H. Shinn, Description and Analysis of Burro Series 40 m^3 LNG Spill Experiments, Lawrence Livermore National Laboratory Report UCRL-53186 (1981).

4. B. Jazayeri, Impact Cryogenic Vapor Explosions, M.S. Thesis. Massachusetts Institute of Technology, Cambridge, Massachusetts (1975).

REPORT E

A Three-Dimensional, Conservation Equation Model for Simulating LNG Vapor Dispersion in the Atmosphere

S. T. Chan
P. M. Gresho
D. L. Ermak

Prepared for the
Environmental and Safety Engineering
Division
U.S. Department of Energy
under Contract W-7405-ENG-48

Lawrence Livermore Laboratory
Livermore, California 94550

REPORT E

TABLE OF CONTENTS

SUMMARY

A numerical model for simulating the vapor spread and dispersion associated with LNG releases in the atmosphere is described herein. The model is based on solving the set of three-dimensional, time-dependent, conservation equations governing incompressible flows. Spatial discretization is performed via a modified Galerkin finite element method (GFEM), and time integration is carried out via the forward Euler method (pressure is computed implicitly, however). Several cost-effective techniques (including subcycling, mass lumping, and reduced Gauss-Legendre quadrature) which have been implemented are discussed. Numerical results obtained using this model are presented and compared in separate reports.

INTRODUCTION

Accurate and verified numerical models for the prediction of the gravitational spread and atmospheric dispersion of natural gas (NG) released into the atmosphere following a potential accident involving LNG facilities are required in order to assess the associated hazards. LLNL is involved in experimental, numerical, and model verification studies for the Department of Energy. In this report, we summarize our current status involving one of the models: the time-dependent, finite element solution of the three-dimensional conservation equations for the simulation of the spreading and dispersion of NG when released onto water and/or over arbitrary topography.

In order to obtain a working code in minimum time, we have thus far emphasized simplicity. This led to: (1) the choice of the simplest element - the 8-node isoparametric "brick" employing piecewise trilinear approximating functions for velocity, temperature, and concentration, and piecewise-constant approximation for the pressure, and (2) the use of the simplest time integration method - explicit (forward) Euler. The pressure, being an inherently implicit variable in an incompressible fluid, is, of course, treated implicitly.

In what may be called "Phase 1" of our code, we followed most of the rules of the Galerkin method and generated a code with only two ad hoc modifications ("cheats" on the Galerkin method) which we summarize here: (1) the mass matrices, which couple the time derivatives in the honest FEM, were replaced by diagonal (lumped mass) matrices somewhat like (but often better than) the typical finite difference approach, (2) the nonlinear advection terms (e.g. $\underline{u}\cdot\nabla T$) were a priori modified to permit simpler and faster computation (in essence, the conventional triply-subscripted coefficients were replaced by simpler doubly-subscripted ones by

employing the element centroid values for the advecting velocities). Even with these simplifications, however, the resulting code was rather expensive and real time simulations appeared to be out of reach; for example, a simulation of heavy gas dispersion required about three hours of computer time on the CRAY-1 (1/3 CPU, 2/3 I/O!) to simulate several minutes of real time.

In order to generate a faster, more vectorized code, we modified the "Phase 1" version to "Phase 2" by two further cost-effective simplifications, which we will summarize and discuss in some detail here. The principal additional simplification is the use of one-point Gauss-Legendre quadrature (rather than 2x2x2 or higher) to evaluate the element level integrals associated with the FEM. This approximation, which tends to result in a discretized model which is perhaps better described as a blend of finite elements and finite differences, leads to significant cost reduction in two areas: (1) the element "matrices" are computed as needed ("on the fly") rather than being stored on disk (this storage accounted for most of the I/O cost in the Phase 1 code) and (2) the entire algorithm is more amenable to efficient vectorization. The second major simplification is associated with the time integration aspect of the simulation and is referred to as "subcycling." Briefly, this trick permits us to reduce the frequency of the expensive (again, mostly I/O) pressure update calculation by using a combination of four items: (1) the major time steps are based on temporal accuracy and are dynamically computed via local truncation error estimates, (2) the minor (smaller) time steps, based on stability estimates, are used to compute advection and diffusion with a simple extrapolation approximation employed for the pressure gradient, (3) a mass adjustment scheme is employed at each major time step to re-enforce the satisfaction of the continuity equation, and (4) the corresponding (compatible) pressure field is computed. As a result of the above simplifications, we have improved the computational speed by an order of magnitude, yet with comparable accuracy as compared with the "phase 1" code.

In the remainder of this report, we present the governing conservation equations, briefly describe the finite element spatial discretization process and the time integration scheme, elaborate on the two new cost-effective techniques referred to above, discuss in some detail the submodels currently used for turbulence and ground heat transfer, and finally indicate some practical applications which have been made with the current model.

GOVERNING EQUATIONS

In this section, we summarize and briefly discuss the set of governing equations, together with their associated initial and boundary conditions, being solved to model the LNG vapor spread and dispersion phenomena. In order to accommodate large density changes in both space and time and yet to preclude sound waves, we have generalized the "anelastic" approximation (Ogura and Phillips, 1962) and obtained a set of equations which are slightly different from those usually derived for incompressible flows (the standard Boussinesq approximations appear to be inadequate for our purposes, see for example, Daley and Pracht, 1968 and Lee et al., 1981). The equations describing our current model, written for the mean (time-averaged) quantities in a turbulent flow field are:

$$\frac{\partial(\rho \underline{u})}{\partial t} + \rho \underline{u} \cdot \nabla \underline{u} = -\nabla p + \nabla \cdot (\rho \underline{\underline{K}}^{m} \cdot \nabla \underline{u}) + (\rho - \rho_h)\, \underline{g} \qquad (1a)$$

$$\nabla\cdot(\rho\underline{u}) = 0 \tag{1b}$$

$$\frac{\partial\theta}{\partial t} + \underline{u}\cdot\nabla\theta = \nabla\cdot(\underline{\underline{K}}^{\theta}\cdot\nabla\theta) + \frac{C_{P_N}-C_{P_A}}{C_P}(\underline{\underline{K}}^{\omega}\cdot\nabla\omega)\cdot\nabla\theta + S \tag{2}$$

$$\frac{\partial\omega}{\partial t} + \underline{u}\cdot\nabla\omega = \nabla\cdot(\underline{\underline{K}}^{\omega}\cdot\nabla\omega) \tag{3}$$

and

$$\rho = \frac{PM}{RT} = \frac{P}{RT\left(\frac{\omega}{M_N} + \frac{1-\omega}{M_A}\right)} \tag{4}$$

where $\underline{u} = (u,v,w)$ is the velocity, ρ is the density of the mixture, p is the pressure deviation from an adiabatic atmosphere at rest, with corresponding density defined as ρ_h, $\underline{g}$ is the acceleration due to gravity, θ is the potential temperature deviation from an adiabatic atmosphere, S is the source term for temperature (e.g., latent heat), ω is the mass fraction of NG vapor, and $\underline{\underline{K}}^{m}$, $\underline{\underline{K}}^{\theta}$, and $\underline{\underline{K}}^{\omega}$ are the diagonal eddy diffusion tensors (which are parameterized using K-theory) for the momentum, energy, and NG vapor, respectively, and C_{P_N}, C_{P_A}, and $C_p = \omega C_{P_N} + (1-\omega)C_{P_A}$ are the specific heats for NG vapor, air, and the mixture, respectively. In the equation of state, P is the absolute pressure, R is the universal gas constant, T is the absolute temperature $(T/(\theta+\theta_o) = (P/P_o)^{R/MC_P})$, and M_N, M_A are the molecular weights of NG and air, respectively. The above set of equations, together with appropriate initial and boundary conditions, are solved to yield velocity, pressure, potential temperature, mass fraction of NG vapor, and density of the mixture as functions of time and space.

The appropriate initial conditions for the above equations are a "solenoidal" velocity field $(\nabla\cdot\rho_o\underline{u}_o = 0)$ and some distribution of temperature and mass fraction appropriate for the case being simulated. For instance, an instantaneous spill can be simulated by specifying a subregion of the computational domain initially as being occupied by the spilled NG vapor, with temperature and mass fraction set to the relevant values and the remaining region initialized as unperturbed. On the other hand, if continuous or finite-duration LNG spills are to be simulated, it is more realistic to model such cases via appropriate boundary conditions, and thus the deviation temperature and mass fraction of NG vapor in the computational domain can be initialized as zero.

For boundary conditions, either the velocity itself (such as velocity at the inlet boundary or that over a source injection area) or the corresponding "tractions" (used to permit flow through) can be specified; for NG vapor, the most common boundary condition is that of no diffusive flux but, for the area over which NG vapor is being injected, a general mass transfer boundary condition is more appropriate.

SPATIAL DISCRETIZATION AND REDUCED GAUSS-LEGENDRE QUADRATURE

Equations (1) through (3) are discretized spatially by the finite element method in conjunction with the Galerkin method of weighted residuals. The primary unknowns, U, V, W, (U = ρu, V = ρv, W = ρw), p, θ, and ω (φ is computed subsequently by Eq. (4)), are approximated as

$$U = \sum_{j=1}^{n} \phi_j(\underline{x})\, U_j(t) \tag{5a}$$

with similar expressions for V, W, θ, ω, and

$$p = \sum_{j=1}^{m} \psi_j(\underline{x})\, p_j(t) \tag{5b}$$

where, in the discretized domain, there are n nodes for velocity, temperature, and concentration, and m nodes for pressure. The approximation functions, $\{\phi_i(\underline{x})\}$, are piecewise continuous polynomials which are one degree higher than those for the pressure approximation, $\{\psi_i(\underline{x})\}$. Currently, we are using the 8-node isoparametric "brick" element with trilinear velocity and piecewise constant pressure. After substituting Eq. (5) into Eqs. (1) through (3), premultiplying each of the equations by appropriate weighting functions, and integrating the diffusion and pressure gradient terms by parts, we obtain a coupled system of nonlinear, first-order ordinary differential equations. This system of equations, written in a compact matrix form, is:

$$M\dot{U} + [K + N(U)]u + CP = F \tag{6a}$$

$$C^T U = 0 \tag{6b}$$

$$M_s\dot{\theta} + [K_\theta + N_s(u)]\theta = F_\theta \tag{7}$$

$$M_s\dot{\omega} + [K_\omega + N_s(u)]\omega = F_\omega \tag{8}$$

where now U and u are global vectors of length 3n containing all nodal values of ρu and u, respectively, P is a global vector of length m containing pressure values, M, K, and N (all of size 3n x 3n) are the mass matrix, the diffusion matrix, and the advection matrix, respectively, C is the 3n x m pressure gradient matrix and its transpose, C^T, is the m x 3n divergence matrix, F is a global vector of length 3n incorporating natural (traction) boundary conditions and the buoyancy force. The matrices in Eqs. (7) and (8) for temperature and the concentration of NG vapor are defined similarly except their "size" is n instead of 3n.

As mentioned earlier, we have resorted to the approximation referred to as 1-point quadrature, in which all element integrals are approximated by their value at the element centroid multiplied by the element volume. The reasons for resorting to such a simplification are: (1) the I/O cost of storing (more accurate) element level information on disc and retrieving it at every time step is very high (especially on the CRAY, where CPU performance is quite high relative to I/O) and

(2) the cost of recomputing all integrals at every time step using a more accurate Gauss rule is also too high - by about an order of magnitude.

We note first that the idea is not new; it has already been successfully employed in explicit FEM solid mechanics codes, (see for example, Hallquist, 1980; Key et al., 1978) and it is this fact which encouraged us to try it. This trick, however, is not totally free of problems, as we discuss below.

Element Volume. Since it has been claimed (see Zienkiewicz, 1977) that convergence of the FEM requires, among other things, an exact calculation of element volume, we have not (yet) cheated in this area. We use a 2x2x2 Gauss rule to compute element volumes and store the resulting vector in core.

Gradient and Divergence. Although we are well aware that 1-point quadrature cannot integrate the C matrix correctly on the general distorted element (Leone et al., 1979) and thus we probably do not retain the element level mass balances associated with the correct integration, preliminary results seem to indicate that the resulting errors are quite acceptable. We will continue to explore this point and report further findings in a subsequent publication.

Advection. We first describe the resulting approximation to $\underline{u}\cdot\nabla T$ on a regular mesh: the average (centroid) velocity in an element is multiplied by the average temperature gradient in the element and the result is averaged over all elements (typically 8) sharing the node in question. For distorted elements, the interpretation appears to be similar except that a volume-weighted final average is employed (using, as mentioned earlier, exact element volumes). This approximation appears to be reasonable and well-behaved.

Diffusion. The biggest problem thus far encountered with 1-point quadrature is the approximation to the Laplacian operator (K, K_θ, K_ω in Eqs. 6a, 7, and 8). This problem can be described very simply — the diffusion matrix is singular with respect to certain solution patterns — but is subject to various interpretations. In the Lagrangian codes of solid mechanics, the problem is described in terms of so-called hourglass patterns (see, for example, Kosloff and Frazier, 1978) and is interpreted in terms of zero energy deformations or mode shapes. In fluid mechanics (in an Eulerian reference frame), it seems more appropriate to associate the problem with the common "2Δx" waves; these waves (null vectors of the singular matrix) are not diffused by the 1-point quadrature diffusion matrix. While there is only one such wave in 2-D (associated with alternating nodal values of +1 and -1), there are four in 3-D and the associated nodal values (on a single element) are shown in Fig. 1. The first of these is the three-dimensional wave and the other three are two-dimensional, one in each plane.

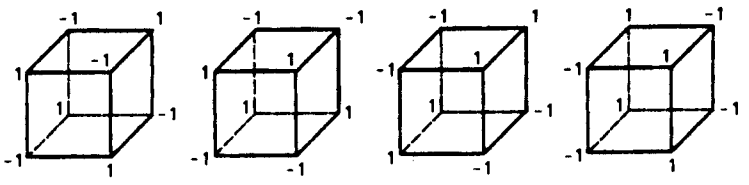

Figure 1. "2Δx" wave patterns on a single element.

The "patch job" for this deficiency, which is also borrowed from the solid mechanics community, is to augment the singular matrix with an "hourglass correction matrix", a procedure which appears to be both simple and effective. Rather than using the more rigorous (and expensive) corrections suggested by Kosloff, we employ the simpler procedure developed by Hallquist (1980); viz, the hourglass matrix is defined, element-wise, by an outer product of the associated null vector with itself. This matrix is then multiplied by an "appropriate" scalar ("tuning"; see below) and added to the singular 1-point diffusion matrix. Figure 2 shows the stencils (for a cube of side length ℓ) associated with several discrete approximations to ∇^2 as well as the three-dimensional hourglass matrix, K_{HGl}. (Note: All the matrices except K_{HGl} have been multiplied by $48\ell^2$.) Noteworthy here is that K_{1p} and even K_{2p} (2-point quadrature - exact for a brick) look rather "suspicious" in that the coefficients closest to the central node are either positive or zero, in marked contrast to the well-known finite difference stencil.

A better perspective may be gained by studying the behavior of these schemes on an appropriate prototypical test case, pure transient diffusion. If the "heat equation,"

$$\partial T/\partial t = \alpha \nabla^2 T \quad , \tag{9}$$

is solved on the 3-D infinite span with an initial condition given by

$$T(0) = e^{ik(x+y+z)} \, , \tag{10}$$

where k is the wave number, the "sine-wave" diffuses according to the exact solution,

$$T(x,y,z,t) = T(0)e^{-3\alpha k^2 t} \quad . \tag{11}$$

Through a Fourier analysis, the effective diffusivity ($\bar{\alpha}$) associated with each scheme can be obtained. Figure 3 shows the ratio of the effective diffusivity to the desired diffusivity, $\bar{\alpha}/\alpha$, of the discrete forms mentioned above, as a function of wave number, with $k\ell$ varying from 0 to π (the associated wavelength varies from infinity to the limit of the grid, $2\Delta x$). The suspicion associated with the stencils corresponding to K_{1p} and K_{2p} is indeed verified - as is the singularity of K_{1p} to the $2\Delta x$ wave. As expected, K_{FD} performs much better. The much-improved behavior of the augmented 1-point matrix is shown by the dashed line.

It is noteworthy that the poor performance of K_{2p} is caused solely by the process of mass lumping. If the consistent mass matrix were employed, the (honest) FEM result would actually display overdamping rather than underdamping.

TIME INTEGRATION OF THE FEM EQUATIONS

Time Stepping Procedure

The forward Euler method of time integration, applied to Eqn. (6a) gives

$$U_{n+1} = U_n + \Delta t M^{-1}[F_n - Ku_n - N(U_n)u_n - CP_n] \tag{12}$$

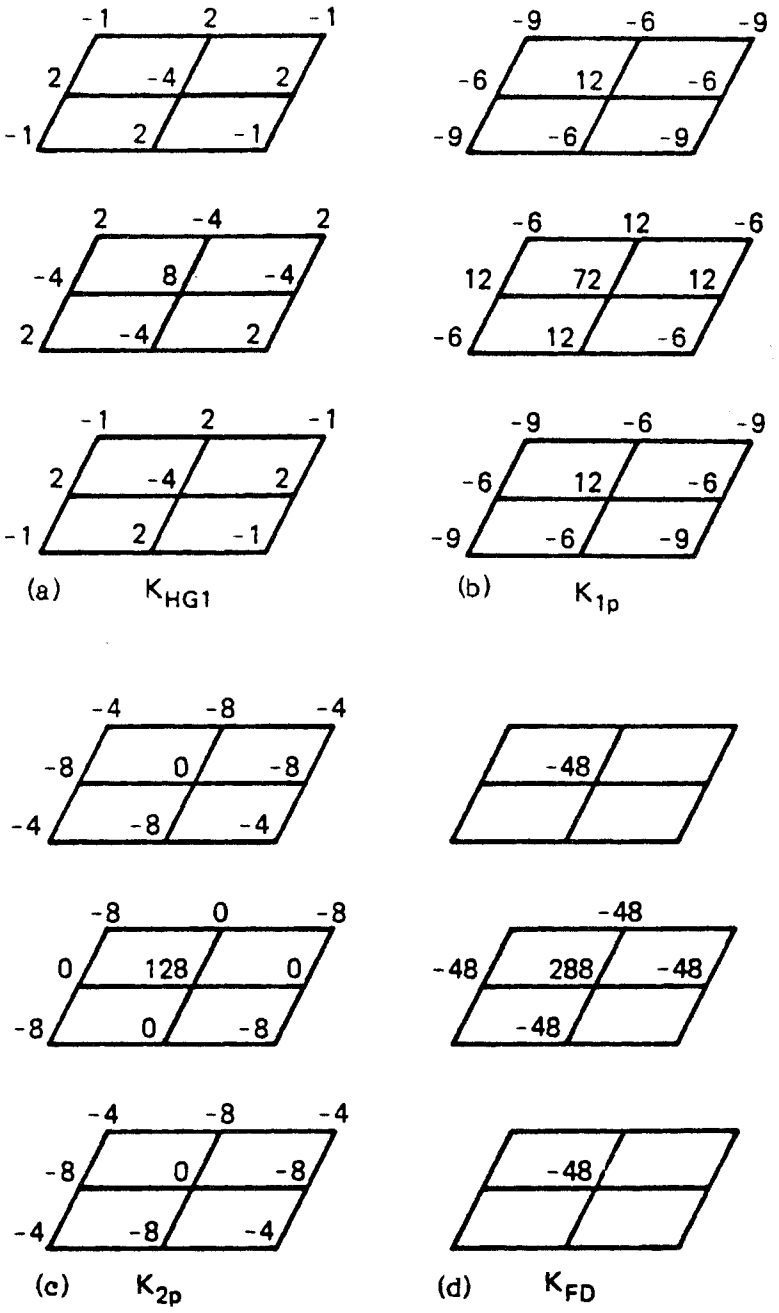

Figure 2. The 3-D "hourglass" matrix stencil (a) and various stencils (for a cube) associated with discrete approximations to the Laplacian operator: (b) one-point quadrature stencil; (c) 2x2x2 quadrature stencil; (d) finite difference stencil.

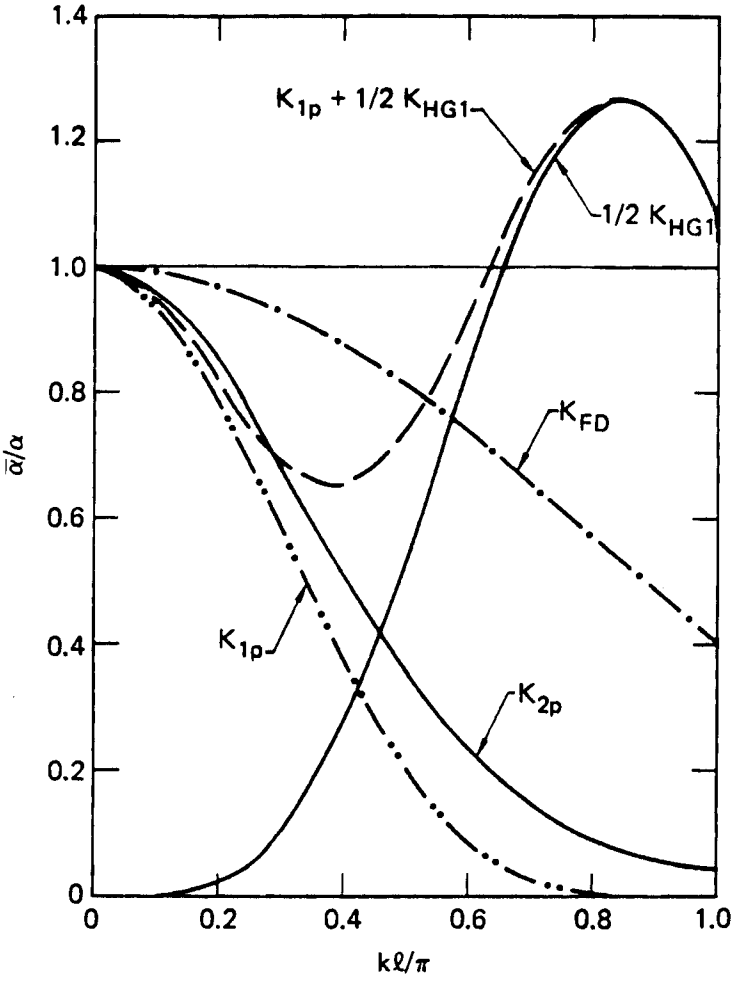

Figure 3. The ratio of effective diffusivity to the desired diffusivity vs non-dimensional wave numbers associated with various discrete approximations to the transient heat equation.

where U_n is the vector of nodal mass fluxes (u_n are nodal velocities) at time t_n and Δt is the step-size. Before this equation can be used to advance the velocity, however, the pressure at time t_n must be computed. This is done by combining Eq. (6a) with a time-differentiated version of Eq. (6b) ($C^T\dot{U}=0$ since $C^TU=0$ for all time) to generate the consistent discretized Poisson equation for the pressure, evaluated at time t_n,

$$(C^TM^{-1}C)P_n = C^TM^{-1}[F_n-Ku_n-N(U_n)u_n] \tag{13}$$

The sequence of steps for advancing the velocity and pressure from t_n to t_{n+1} is thus (given that U_n is available and that it satisfies $C^TU_n = 0$):

(1) Form the acceleration vector (sans the pressure gradient)

$$A_n = M^{-1}[F_n-Ku_n-N(U_n)u_n] \tag{14}$$

(2) Solve the linear algebraic system (discrete Poisson equation) for the compatible pressure via

$$(C^TM^{-1}C)\,P_n = C^TA_n \tag{15}$$

(3) Update the mass flux, accounting for the pressure gradient,

$$U_{n+1} = U_n + \Delta t(A_n - M^{-1}CP_n) \tag{16}$$

(4) Finally, in an "uncoupled step," update the temperature and concentration, again using the forward Euler method,

$$\theta_{n+1} = \theta_n + \Delta t\, M_s^{-1}[F_{\theta_n} - K_\theta \theta_n - N_s(u_n)\theta_n], \tag{17}$$

$$\omega_{n+1} = \omega_n + \Delta t\, M_s^{-1}[F_{\omega_n} - K_\omega \omega_n - N_s(u_n)\omega_n]. \tag{18}$$

This is the basic scheme used in our Phase 1 code and is a straightforward and legitimate method for solving the ODE's of Eqns. (6) through (8). Several additional comments are appropriate before discussing the less legitimate (subcycling) shortcuts employed in Phase 2:

(1) The presence of M^{-1} in the above equations explains why we employ the lumped mass approximation (M^{-1} is then a vector rather than a full matrix). While this approximation is known to reduce the accuracy (especially in regard to phase speed errors, (see Gresho et al, 1980), it is simple and probably cost-effective for very large problems.

(2) The pressure "Laplacian" matrix, $C^TM^{-1}C$, is symmetric and invariant with time. Hence we have chosen to solve (15) via direct methods, using an efficient profile (or skyline) solver recently developed by Taylor et al (1980). This matrix is formed and factored in the pre-processor code and stored on disk for later retrieval by the main code. During the time integration, each pressure update is obtained by reading the disk file and performing one forward reduction and a back substitution.

(3) The explicit Euler method, while simple and fast, has one serious disadvantage (as do essentially all explicit schemes): it is only conditionably stable. The integration may become unstable if any one of several stability limits is exceeded: (1) the diffusive limit, (2) a linear advective-diffusive stability limit, and (3) certain types of nonlinear advection stability limits (Hirt, 1968). While we are not able to predict these Δt limits a priori for the nonlinear FEM system on an arbitrary mesh, we have generally been reasonably successful by satisfying the following step-size restrictions, which come from analyzing the constant coefficient advection-diffusion equation via second-order centered finite differences on a grid with fixed Δx, Δy, and Δz:

(a) Diffusive limit:

$$\Delta t \leq \frac{1/2\kappa}{1/\Delta x^2 + 1/\Delta y^2 + 1/\Delta z^2} \tag{19}$$

(b) Linear advective-diffusive limit:

$$\Delta t \leq \frac{2\kappa}{u^2 + v^2 + w^2} \quad , \tag{20}$$

where κ is the diffusivity (μ/ρ for the Navier-Stokes equations). While the diffusive limit is well-known (e.g. Roache, 1976), there has been some confusion regarding the advective-diffusive limit (see, Hindmarsh and Gresho, 1982).

(4) The above linear advective-diffusive limit, unfortunately, is often quite stringent for most practical applications, because of the rather high Reynolds numbers. This stability limit, however, can be relaxed by adding the so-called tensor diffusivity as discussed below.

By performing a Taylor series analysis (in time) of the forward Euler time integration of the advection-diffusion equation

$$\frac{\partial T}{\partial t} + \underline{u}\cdot\nabla T = \nabla\cdot(\kappa\nabla T), \tag{21}$$

it can be shown (Dukowicz and Ramshaw, 1979) that this time integration method, in effect, introduces a (negative) tensor diffusivity (or viscosity) given in 2D by

$$\underline{\underline{\kappa}}_N = \frac{\Delta t}{2} \begin{bmatrix} u^2 & uv \\ uv & v^2 \end{bmatrix} \tag{22}$$

into the equation, such that the effective equation being modeled looks more like

$$\frac{\partial T}{\partial t} + \underline{u}\cdot\nabla T = \nabla\cdot[(\kappa\underline{\underline{I}} - \underline{\underline{\kappa}}_N)\cdot\nabla T] + O(\Delta t), \tag{23}$$

where $\underline{\underline{I}}$ is the identity matrix. Thus, if Δt is too large, the effective diffusivity is negative and the numerical scheme becomes unstable. This effect can also be

interpreted as an effective reduction in κ or an effective increase in P_e (Peclet number, $U_o \ell/\kappa$). The trick then, is to solve Eq. (21) only after adding the necessary "compensating diffusion" or tensor viscosity, to balance that implicitly introduced by the Euler integration scheme, a la Eq. (23); i.e., explicitly κ is replaced by $\kappa \underline{\underline{I}} + \underline{\underline{\kappa}}_N$ in the discretized equations.

While we have not yet completed the stability analysis of (21) using the FEM stencil (with or without balancing diffusion), we have been successful using results from 1D, in which (the 1D version of) Eqs. (19) and (20) are replaced by

$$\Delta t \leq (\kappa/u^2)\left[\sqrt{(u\Delta x/\kappa)^2 + 1} - 1\right]. \tag{24}$$

Whereas Eq. (20) causes the Courant number ($u\Delta t/\Delta x$) to approach zero like $u\Delta t/\Delta x = 2\kappa/u\Delta x$ as the "grid Reynolds number", $u\Delta x/\kappa$ increases, the result from Eq. (24) is $u\Delta t/\Delta x \to 1$ as $u\Delta x/\kappa \to \infty$; i.e. the more reasonable Courant limit is recovered.

Subcycling

The principal shortcoming of our Phase 1 code, which caused it to be uncomfortably expensive, is related to the following two points: (1) the stability-limited step-size is often much smaller than would be needed to accurately integrate the ODE's, and (2) the pressure updates, while not so expensive in CPU cost (typically $\sim$ 10% of the total cost of a time step), are inordinately expensive in I/O cost - reading the large disc file (1-2 million words) containing the factored Laplacian matrix requires several seconds.

Based on the premise that the pressure and the associated continuity constraint equations have little or no effect on the stability of the explicit scheme, we have devised a subcycling strategy which permits less frequent updates of the pressure and a concomitant savings in computer time. The major ingredients of subcycling have already been described; here we summarize the entire process with reference to the schematic in Fig. 4.

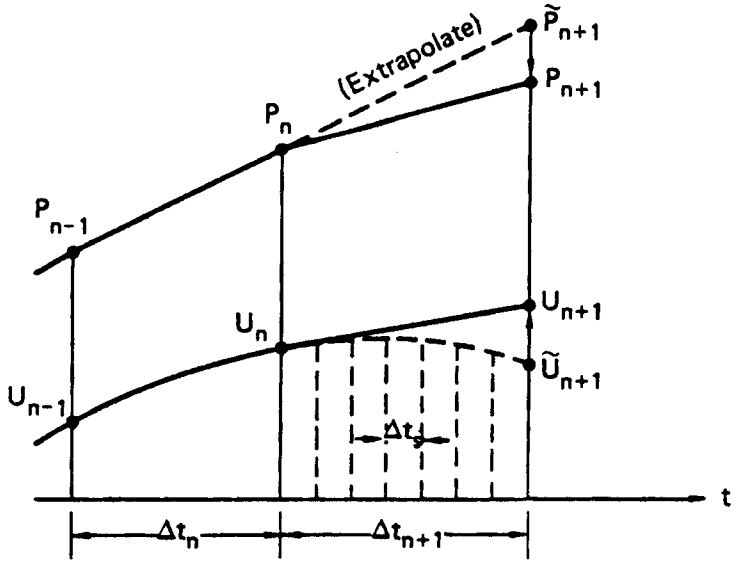

Figure 4. Schematic of the subcycling process.

We assume that the minor time step (Δt_s) has been pre-selected based on the more stringent of either the diffusive limit or the Courant limit and will be used throughout the time integration. This is the subcycle step-size; the rest of the scheme is as follows:

(1) Assume that U, $\dot{U}$, and P are known at t_n and t_{n-1}. Estimate the local time truncation error vector, d_n, for U via

$$d_n \equiv U_n - U(t_n) \simeq -\frac{(\Delta t_n)^2}{2}\ddot{U}_n \simeq -\frac{\Delta t_n}{2}(\dot{U}_n - \dot{U}_{n-1}) \quad , \tag{25}$$

where $U(t_n)$ represents the (unknown) exact solution on the assumption that U_{n-1} is exact, and $\dot{U}_n = (U_n - U_{n-1})/\Delta t_n$. A similar error estimate is then made for T and ω, and a combined, relative RMS norm, e, is computed. The next (major) time step size is then obtained from

$$\Delta t_{n+1} = \Delta t_n (\epsilon/e)^{1/2} \quad , \tag{26}$$

where we have used the fact (from (25)) that the local error varies like $(\Delta t)^2$ and ϵ is an (input) error tolerance parameter related to the desired local accuracy. A typical value for ϵ is .001 which implies that a local error of about 0.1% is acceptable.

(2) Assuming that $\Delta t_{n+1} >> \Delta t_s$ (otherwise we do not subcycle), an estimate of the pressure at t_{n+1} ($\tilde{P}_{n+1}$) is obtained via linear extrapolation. This extrapolated pressure is used (along with P_n via linear interpolation) to estimate the pressure gradient (CP) during the subcycle steps; i.e., while an approximate pressure gradient is employed, the continuity equations are completely ignored during subcycling. After the appropriate number ($\Delta t_{n+1}/\Delta t_s$) of minor steps is completed, during each of which the advection and diffusion terms in the momentum, energy, and species equations are updated (in part, to maintain stability), the mass adjustment process is invoked; i.e.,

(3) Given $\tilde{U}_{n+1}$ and $\tilde{P}_{n+1}$ as estimates to U_{n+1} and P_{n+1}, the mass flux is "adjusted" according to

$$U_{n+1} = \tilde{U}_{n+1} - M^{-1} C \lambda_{n+1} \quad , \tag{27}$$

where λ_{n+1} is a vector of Lagrange multipliers, obtained by first solving the linear system

$$(C^T M^{-1} C)\lambda_{n+1} = C^T \tilde{U}_{n+1} \quad . \tag{28}$$

It can be shown (Sani et al., 1978) that this procedure is a minimal least squares adjustment, from $\tilde{U}_{n+1}$ to U_{n+1}, subject to the constraint that $C^T U_{n+1} = 0$; i.e. U_{n+1} is mass consistent whereas $\tilde{U}_{n+1}$ is not.

(4) Finally, the compatible pressure field is obtained by solving an equivalent linear system for P_{n+1}, a la Eqn. (15) with n replaced by n+1; i.e., the mass consistent velocity field (which satisfies Eq. (6b)) is employed to compute P_{n+1}.

It is clear that two re-solutions using the same factored matrix are required at each major timestep. Hence, subcycling can only be cost-effective when the subcycle ratio, $\Delta t_{n+1}/\Delta t_s$, is significantly greater than 2 (based on our current limited experience, this ratio can vary from $\sim$3 to 10 or more, depending on the "dynamics"); it can be especially effective if the solution is approaching a steady state.

MODELING OF EDDY DIFFUSION AND GROUND HEAT TRANSFER COEFFICIENTS

Flows which are driven by gravity currents often exhibit regions of highly turbulent motion. For NG flows, the density front typically consists of an elevated head in which there is intense mixing of NG with the ambient air. Detailed features of turbulence under such circumstances can probably be best handled by models which employ higher order closure formulations. However, the practicality of these more complex turbulence models is yet to be established for three-dimensional calculations. In view of this, we developed our first model based on a simple eddy exchange coefficient (K-theory) concept. Such models have been used rather successfully for certain planetary boundary layer (PBL) flows (e.g., Mahrer and Pielke, 1977; Kemper et al., 1979).

There are, however, a few distinct differences between the modeling of turbulence for NG and PBL flows which should be considered: (i) the heights of interest for NG spill scenarios are usually much lower ($\sim$ 100 m or less) than are normally required for the PBL; (ii) NG vapor clouds at temperatures near that of LNG are much denser ($\sim$ 1.5 times) than the ambient air and can develop strong gravity currents; and (iii) NG flows exhibit large temperature differences (typically on the order of tens of degrees) at the surface where the cold gas is in contact with a much warmer surface. Consequently, the turbulence field within high NG concentration regions of the cloud is expected to be largely self-induced by the flow of the NG cloud and possibly quite different than in the surrounding atmosphere.

In the present version of the model, an ad hoc approach is used in which the turbulence level is modified by the cold, dense cloud in high concentration regions, yet approaches ambient levels as the cloud becomes more dilute. The three diagonal eddy diffusion tensors, $\underline{K}^m$, $\underline{K}^\theta$, and $\underline{K}^\omega$, are assumed to be equal. Using this approach, the diffusion tensor has three non-zero coefficients (K_H, K_H, K_v). The vertical diffusion coefficient K_v is expressed as a weighted sum of two terms

$$K_v = K_a (1-\omega) + K_\rho \omega \tag{29}$$

where K_a is the ambient vertical diffusivity, K_ρ is a dense-layer diffusivity, and the horizontal diffusivity K_H is assumed to be proportional to K_v. While the ratio K_H/K_v is expected to depend on the local stability, a constant value of 6.5 is currently being used. This ratio, along with the ambient diffusivity described below, produces a cloud from a trace emission whose width is about twice as large as the height.

The model for the ambient diffusivity is based on the theory of Dyer and Hicks, 1970 and Businger, et al., 1971 (for a review, see Dyer, 1974) in which the ambient wind velocity profile is expressed as

$$U_a = \frac{U_{a*}}{k}(\ln z/z_o - \psi_a), \quad \text{where } \psi_a \doteq \begin{cases} 1.1\ (-Ri)^{1/2}, & Ri \leq 0 \\ -5\ Ri, & Ri > 0 \end{cases}, \tag{30a}$$

the ambient diffusivity is given by

$$K_a = \frac{kU_{a*}z}{\phi_a}, \quad \text{where } \phi_a \doteq \begin{cases} (1-16\ Ri)^{-1/4}, & Ri \leq 0 \\ 1+5\ Ri, & Ri > 0 \end{cases}, \tag{30b}$$

and ϕ_a is also related to the velocity gradient by

$$\frac{\partial U_a}{\partial z} = \frac{U_{a*}\phi_a}{kz} \quad . \tag{30c}$$

Here k is von Karman's constant, U_{a*} is the ambient friction velocity, Ri is the ambient Richardson number, and it is assumed that Ri = z/L, where L is the Monin-Obukhov length. To avoid the necessity of an excessively fine grid to resolve the logarithmic function near the ground, the ambient wind velocity, Eq. (30a) is approximated in the numerical model by a quadratic profile and by using slip boundary conditions at z = 0. The ambient diffusivity is also modified near the ground by replacing "z" in Eq. (30b) by "$z + z_j e^{-z/z_j}$" where z_j is a constant whose value is determined by requiring the vertical momentum flux at the ground to be $\rho_a U_{a*}^2$, i.e.,

$$\rho_a K_a \frac{\partial U_a}{\partial z}\bigg|_{z=0} = \rho_a U_{a*}^2 \tag{31}$$

as given by Eq. (30b and c).

Two models are currently available for K_ρ. One is a Richardson number diffusivity for a stably stratified density layer. Taking the Richardson number to be

$$R_i \doteq \frac{g(\gamma-1)(\rho-\rho_a)k^2 z}{\rho U_*^2} \tag{32a}$$

where γ is the ratio of specific heats, then the diffusivity is

$$K_\rho = K_{\rho r} \doteq \frac{kU_* z}{5\ Ri} = \frac{1.25\ \rho U_*^3}{g(\rho-\rho_a)} \quad . \tag{32b}$$

A comparison of the $K_{\rho r}$ and K_a terms in Eq. (29) for typical LNG values, shows the $K_{\rho r}$ term to be generally much less than the K_a term. Consequently, the effect of $K_{\rho r}$ on K_v is to reduce the turbulence level in high density regions. The other model is a mixing length model given by

$$K_\rho = K_{\rho m} = \frac{\rho_a}{\rho}\frac{K_a}{\frac{\partial U_a}{\partial z}}\left[\sum_{i,j}^{3}\left(\frac{\partial U_i}{\partial x_j}\right)^2\right]^{1/2} \tag{33}$$

where the mixing length (Haltiner, 1980) is a density ratio weighted ambient mixing length, $\ell^2_a = K_a/(\partial U_a/\partial z)$. In this model the turbulence level is proportional to the overall shear and is somewhat dampened in high density regions by the weighting factor ρ_a/ρ.

Finally, to account for the heat flux from the ground surface into the NG cloud, a bulk coefficient model given by

$$\Delta H = V_H \rho C_p (T-T_r) \tag{34}$$

is used. Here ΔH is the heat flux, T_r is the prescribed reference temperature, and V_H is an effective "heat transfer velocity" which is expressed as either an empirical constant or in the form $V_H = C_f U_r$, where U_r is a reference velocity and C_f is a surface friction coefficient which is usually a function of surface roughness (for example, see Zeman, 1979). In the recent LNG spill tests at China Lake, California, V_H appeared to be independent of wind speed and had an average value of $V_H = .0125$ m/s (Shinn, 1980).

NUMERICAL RESULTS

The model described above has been utilized in a number of practical applications, including LNG vapor dispersion simulations. Some preliminary results (using the simplest K-theory model - constant K) are contained in two earlier reports (Gresho et al., 1981; Chan et al., 1981). A comparison of results for several LNG vapor dispersion cases as predicted by the present model with field data and those obtained by other models are presented and discussed in Ermak et al. (1982).

ACKNOWLEDGDMENTS

This work was performed under the auspices of the U.S. Department of Energy by the Lawrence Livermore National Laboratory under contract No. W-7405-Eng-48. The authors are grateful to the following LLNL colleagues: Dr. Robert L. Lee for many helpful discussions on the current model, Craig D. Upson for providing assistance in computer programming, and Dr. John O. Hallquist for discussion on hourglass modes. We would also like to thank Dr. Michael J. P. Cullen of the British Meteorological Office for many useful discussions on $2\Delta X$ waves and related problems.

REFERENCES

Businger, J. A., J. C. Wyngaard, Y. Izumi, and E. F. Bradley, 1971: Flux Profile Relationships in the Atmospheric Surface Layer, J. Atmos. Sci., 28, 181-189.

Chan, S. T., P. M. Gresho, R. L. Lee, C. D. Upson, 1981: Simulation of Three-Dimensional, Time-Dependent, Incompressible Flows by a Finite Element Method, Proceedings of the AIAA 5th Computational Fluid Dynamics Conference, pp. 354-363.

Daley, B. and W. Pracht, 1968: Numerical Study of Density - Current Surges, Phys. of Fluids, 11, 1, 15-30.

Dyer, A. J., 1974: A Review of Flux-Profile Relationships, Boundary-Layer Meteorol., 7, 363-372.

Dyer, A. J. and B. B. Hicks, 1970: Flux-Gradient Relationships in the Constant Flux Layer, Quart. J. Roy. Meteorol. Soc., 96, 715-721.

Dukowicz, J., J. Ramshaw, 1979: Tensor Viscosity Method for Convection in Numerical Fluid Dynamics, J. Comp. Physics, 32, 71-79.

Ermak, D. L., S. T. Chan, D. L. Morgan, and L. K. Morris, 1982: "A Comparison of Dense-Gas Dispersion Model Simulations with Burro Series LNG Spill Test Results," submitted to J. Hazard. Materials.

Gresho, P. M., R. L. Lee and C. D. Upson, 1980: FEM Solution of the Navier-Stokes Equations for Vortex Shedding Behind a Cylinder: Experiments with the Four-Node Element, Finite Elements in Water Resources, Proceedings of Third Inter. Conf., Univ. of Miss., USA.

Gresho, P. M., S. T. Chan, R. L. Lee, and C. D. Upson, "Solution of the Time-Dependent, Three-Dimensional Incompressible Navier-Stokes Equations via FEM," presented at the International Conference on Numerical Methods for Laminar and Turbulent Flow, Venice, Italy, July 1981.

Hallquist, J. O., 1980: User's Manual for DYNA2D - An Explicit Two-Dimensional Hydrodynamic Finite Element Code with Interactive Rezoning, UCID-18756.

Haltiner, G. J. and R. T. Williams, 1980: Numerical Prediction and Dynamic Meteorology, John Wiley & Sons, p. 272.

Hindmarsh, A., and P. Gresho, 1982: The Stability of Explicit Euler Time-Intergration for Certain Finite Difference Approximations of the Multi-Dimensional Advection-Diffusion Equations, submitted to Int. J. Num. Meth. Fluids.

Hirt, C. W., 1968: Heuristic Stability Theory for Finite-Difference Equations, J. Comp. Phys., 2, 339-355.

Kemper, J. E., P. E. Long and W. A. Shafer, 1979: Forecast Guidance Products from the Techniques Development Laboratory's Boundary Layer Model, Preprints Fourth Conference on Numerical Weather Predictions, Silver Spring, MD, AMS, 270-277.

Key, S. W., Z. E. Beisinger, and R. D. Krieg, 1978: HONDO-II: A Finite Element Computer Program for the Large Deformation, Dynamic Response of Axisymmetric Solids, Sandia Report SAND 78-0422.

Kosloff, D. and G. A. Frazier, 1978: Treatment of Hourglass Patterns in Low Order Finite Element Codes, Int. J. Num. & Ana. Meth. Geomech., Vol. 2, 57-72.

Lee, R. L., P. M. Gresho, S. T. Chan, and C. D. Upson, 1981: A Three-Dimensional, Finite Element Model for Simulating Heavier-Than-Air Gaseous Releases Over Variable Terrain, presented at the NATO/CCMS 12th International Technical Meeting on Air Pollution Modeling and Its Applications, Menlo Park, California.

Leone, J. M., P. M. Gresho, S. T. Chan, and R. L. Lee, 1979: A Note on the Accuracy of Gauss-Legendre Quadrature in the Finite Element Method, Int. J. Num. Meth. Eng., Vol. 14, 769-773.

Mahrer, Y. and R. A. Pielke, 1977: A Numerical Study of Airflow over Terrain, Beitr. Phy. Atm., 50, 98-113.

Ogura, Y., and N. Phillips, 1962: Scale Analysis of Deep and Shallow Convection in the Atmosphere, J. Atm. Sci., 19, 173-179.

Roache, P., 1976: Computational Fluid Dynamics, 2nd Ed., Hermosa Press, Albuquerque, New Mexico.

Sani, R. L., P. M. Gresho, D. R. Tuerpe, and R. L. Lee, 1978: The Imposition of Incompressibility constraints via Variational Adjustment of Velocity Fields, presented at the International Conference on Numerical Methods in Laminar and Turbulent Flow, Swansea, United Kingdom.

Shinn, J. H., 1981: private communcations, Lawrence Livermore National Laboratory, California.

Taylor, R. L., E. L. Wilson, and S. J. Sackett, 1980: Direct Solution of Equations by Frontal and Variable Band, Active Column Methods," Proc. U.S. European Workshop on Nonlinear Finite Element Analysis in Structural Mechanics, Bochum, W. Germany, July, 521-552.

Zeman, O., 1979: Parameterization of the Dynamics of Stable Boundary Layers and Nocturnal Jets, J. Atmos. Sci., 36, 792-804.

Zienkiewicz, O. C., 1977: The Finite Element Method, 3rd Edition, McGraw-Hill Book Co. (U.K.) Ltd.

STC:clm:0039F

REPORT F

The Theoretical and Empirical Basis for Experimental Simulation of Maritime Atmospheric Dispersion at Desert Sites

J. H. Shinn

Prepared for the
Environmental and Safety Engineering
Division
U.S. Department of Energy
under Contract W-7405-ENG-48

Lawrence Livermore Laboratory
Livermore, California 94550

REPORT F

TABLE OF CONTENTS

SUMMARY

The problem of experimental simulations of maritime meteorological conditions is discussed in terms of selecting or modifying the desert atmospheric environment so that particular criteria of dynamic similarity are met and the atmospheric dispersion test results may be generally applied. Fundamental scaling variables are defined and it is shown how a shallow lake in the desert is a significant modification to the desert environment. Humidity and temperature gradients are presented and upwind fetch (horizontal extent) requirements are derived. Aerodynamic roughness of the shallow lake and rough seas are compared which results in a scale-up factor for wind speed. Temperature gradients, wind speed, mean air temperature, and atmospheric stability can be selected to permit a unique degree of control for experimental simulations, giving an advantage over what would be obtained at any single oceanic site. Atmospheric turbulence, which predicts the lateral and vertical spread of diffusing plumes, is compared between oceanic and inland sites. Finally, the implications of normal atmospheric variability to experimental design, and the measurement requirements for atmospheric stability, aerodynamic roughness, and mixing zone depth are described.

INTRODUCTION

This study determines the meteorological basis for carrying out field studies of atmospheric dispersion, whereby maritime conditions may be experimentally simulated at remote desert sites. In particular we are concerned about performing controlled underwater releases of liquified natural gas (LNG) in small lakes located at remote desert sites in California and Nevada. These sites may for our purposes be classified as Mojave Desert basins and are chosen so that the emission of combustible gases may be practically and safely investigated.

Following the underwater release of LNG there will be a sequence of pool spread, boiloff and cold-gas spread. These processes are not well understood and

must be studied under controlled conditions so that the atmospheric dispersion of natural gas, principally methane, can be predicted with acceptable certainty. An application of these predictions would be, for example, in the hazards analysis associated with ship transport and loading at LNG terminals; in such analysis it is necessary to locate the probable range where, following an accidental release, the methane-air mixture may be diluted to the concentration known as the flammability limit.

The problem of experimental simulation of maritime meteorological conditions becomes one of selecting or modifying the desert atmospheric environment so that the test results may later be generally applied. To show how this is done, we will discuss the criteria required for proper simulation and will present appropriate meteorological data from Mojave Desert sites.

SIMILARITY CONDITIONS

The principles of atmospheric dispersion are transferred from one site to the next by proper utilization of the conditions of dynamic similarity. In practice this means that one defines a number of reduced variables to express such quantities as gas concentrations, travel distances, and scales of turbulent diffusion.

Similarity conditions for dispersion in the atmospheric surface boundary layer will depend on the following elementary variables: mean wind speed ($\bar{u}$), the RMS components of turbulence (σ_u, σ_v, σ_w), the Monin-Obukhov scaling length (L), the characteristic shear expressed by the friction velocity (u_*), the characteristic mean temperature gradient (T_*), and the depth of the mixing zone expressed as the height of the mixing layer (z_i). These variables are the minimum needed for a rigorous expression of similarity, which enables a generalization of a working hypothesis from one site to another.

Working definitions of the above are as follows. Mean speed,

$$\bar{u} = \frac{1}{t_o} \int_o^{t_o} u(t)dt \qquad (1)$$

for u(t) a time series over period t_o. When the wind components are measured by a vane-axial anemometer (anemometer bivane) measuring vector speed (V),

elevation (E), and azimuth (A) we must convert to a natural coordinate system to obtain u, v, w, the longitudinal, lateral, and vertical wind components respectively. Then, at any instant:

$$u = V \cos E \cos (A - \bar{A}) \tag{2}$$

$$v = -V \cos E \sin (A - \bar{A})$$

$$w = V \sin E$$

And, the RMS components are given by,

$$\sigma_u^2 = \cos^2 \bar{E} \, (\text{Var } V) + \bar{V}^2 \sin^2 \bar{E} \, (\text{Var } E) \tag{3}$$

$$\sigma_v^2 = \bar{V}^2 \cos^2 \bar{E} \, (\text{Var } A)$$

$$\sigma_w^2 = \sin^2 \bar{E} \, (\text{Var } V) + \bar{V}^2 \cos^2 \bar{E} \, (\text{Var } E)$$

In a time series which is sufficiently long to encompass all frequencies of turbulent energy, $\bar{E} = 0$, and Equation (3) reduces to the more commonly used approximate form:

$$\sigma_u = (\text{Var } V)^{1/2} \tag{4}$$

$$\sigma_v = \bar{V} \, (\text{Var } A)^{1/2}$$

$$\sigma_w = \bar{V} \, (\text{Var } E)^{1/2}$$

The friction velocity (u_*) is the product of shear ($d\bar{u}/dz$) and a mixing length, or it can be thought of as proportional to the local wind speed by a drag coefficient. Since the mixing length is proportional to height in the surface boundary layer, in practice, between any two levels on a tower (z_1, z_2):

$$u_* = (\bar{U}_2 - \bar{U}_1)\ k/\ln(z_2/z_1) \tag{5}$$

where k is von Karman's constant.

Likewise, the characteristic temperature gradient (T_*) is analoguous:

$$T_* = (\bar{T}_2 - \bar{T}_1)\ /\ln(z_2/z_1) \tag{6}$$

The mean shear over the layer is therefore:

$$\frac{d\bar{u}}{dz} = \frac{u_*}{k(z_2 z_1)^{1/2}} \tag{7}$$

and the mean temperature gradient over the layer is:

$$\frac{d\bar{T}}{dz} = \frac{T_*}{(z_2 z_1)^{1/2}} \tag{8}$$

The Monin-Obukhov length scale of atmospheric stability is defined as the ratio of mechanical turbulent energy production rate to the bouyant energy production rate:

$$L = (u_*^3/k)/(-gH/\rho C_p \bar{T}) \tag{9}$$

where terms are defined as before, g is the gravitational acceleration, H is the sensible heat flux, ρ is the density of the gas mixture, and C_p is the heat capacity of the gas mixture at ambient pressure. The most practical definition of H is given by:

$$H \simeq -\rho C_p k u_* T_* \tag{10}$$

where $T_* >> (gz/C_p)$ and u_* is large. So that under these conditions,

$$L \simeq u_*^2 \, \bar{T}/gk^2T_* \tag{11}$$

The height of the mixing layer z_i must be determined by taking detailed temperature soundings of atmospheric boundary layer from the surface up to heights of 1000-2000 m, searching for the lowest level where:

$$\frac{dT}{dz} + \frac{g}{C_p} > 0 \tag{12}$$

or, alternatively the lowest level where the surface air, raised adiabatically, will reach ambient temperature.

In many situations, an alternative to measurement of L is preferred, and there are some dispersion models which classify atmospheric stability very roughly (i.e., A, B, C, D, E, F). Such models are non-rigorous since atmospheric stability is a continuous function of the variables expressed by Equation (9) and stability is a function of height, even without the presence of a cold gas. Dynamic similarity from one experiment to another or one site to another can only be certain when the dimensionless stability variable, z/L, is used. A reasonable substitution for z/L, however, is the Richardson number (Ri) defined as follows:

$$Ri = \frac{g}{\bar{T}} \left[\frac{dT}{dz} + \frac{g}{Cp} \right] \Bigg/ \left[\frac{d\bar{u}}{dz} \right]^2 \tag{13}$$

which can very practically be calculated using the Equations (5)-(8). It has been shown empirically that when the atmosphere is unstable or neutral,

$$z/L = Ri, \qquad Ri < 0 \tag{14}$$

and that for a limited range of stable conditions:

$$z/L \simeq Ri/(1 - 5Ri), \; 0 < Ri < .15 \tag{15}$$

The use of the Richardson number as a stability index is preferred for the practical reasons that in cases when heat flux H becomes small, L increases uncertainly, and when the approximate solution for H in Equation (10) no longer holds, H becomes difficult to measure. On the other hand for stable cases when Ri gets large, the condition in Equation (15) is not met and no unique relationship exists between these stability indices. In fact, for very stable cases, the entire concept of boundary layer similarity breaks down. The only practical alternative is to measure both z/L and Ri for their obvious advantages.

Assuming that the conditions of dynamic similarity are quantified according to the above procedure, investigation of the fine structure of turbulence becomes another tool for LNG dispersion-hypothesis development. Let us define the steady-state diffusion equation for methane vapor concentration (q) in the flux divergence form as follows:

$$\bar{u}\,\frac{\partial q}{\partial x} = \frac{\partial}{\partial y}\left[\overline{v'q'}\right] + \frac{\partial}{\partial z}\left[\overline{w'q'}\right] \qquad (16)$$

where the quantities with overbars represent time-averaged covariances between instantaneous velocity deviations and the fluctuations in the scaler concentrations (q'):

$$v' = v - \bar{v} \qquad \overline{v'v'} = \sigma_v^2 \qquad (17)$$

$$w' = w - \bar{w} \qquad \overline{w'w'} = \sigma_w^2$$

$$q' = q - \bar{q} \qquad \overline{q'q'} = \sigma_q^2$$

These definitions from first principles of statistical-mechanical turbulence theory do not constrain us to conventional flux-gradient formulations, which may be improper for cold vapor dispersion.

CONVENTIONAL GENERALIZATIONS

The measured distributions of dispersing gas concentration are conventionally expressed by the standard deviations of the gas concentration distribution

(σ_y, σ_z) along the lateral and vertical directions (respectively) in a plane normal to the centerline of the plume. Individual realizations of concentration in the dispersing plume do not have Gaussian properties although a composite or long-time average plume may empirically approximate the Gaussian form. It is realized, therefore, that prediction of concentrations is a probabilistic rather than deterministic undertaking, and a recent consensus of meteorologists conducting boundary layer dispersion studies is that under "ideal" conditions the certainty of predicting time-averaged concentrations is no better than a factor of two[1]. "Ideal" conditions are those where the variables expressed by Equations (1) - (13) are all measured with good accuracy. Less than ideal conditions will prevail in real accidents at sea or in the coastal zone.

This subject of generalization to predict σ_y and σ_z from measured variables, such as σ_v, σ_w, $\bar{u}$, and L has been reviewed elsewhere. A considerable expertise relevant to this problem was developed by the Nuclear Regulatory Commission for use at coastal nuclear reactor sites.[2] It was also the topic of a 1977 Workshop of the American Meteorological Society[3], and is a major research objective of the Environmental Protection Agency as summarized by Irwin in 1979[4]. It is deduced from their conclusions that any simulation experiment should measure σ_v and σ_w in order to avoid additional uncertainty due to possible local sources of variability.

In the definitions given by Equations (1) through (15), we identified the criteria of wind speed, turbulence, and stability which we will present empirically in more detail later. Another consideration, however, is the distribution of the state variables of major thermodynamic importance in the experimental simulations, i.e., the vertical distribution of temperature and humidity in the modified boundary layer over shallow lakes in the desert, since these play a role in heat exchange between the cold gas and air.

HEAT AND HUMIDITY BOUNDARY LAYERS

A peculiar property of air flow over water surfaces is the apparent humidity and temperature discontinuity between the air and the water surface. That is, measurements of vapor pressure and temperature taken close to the surface (for example, at 10 cm) show that their values are approximately the same as the air above (for example, at 500 cm) rather than that of the water surface. The

vertical gradients of vapor pressure and temperature above the sea surface over the height interval 0.1 to 10 m are typically one-tenth as steep as would be predicted by the vapor pressure or temperature difference between the water and air.[5] This proportionality is expressed as follows:

$$\frac{dT}{dz} = \Gamma \frac{(T_a - T_o)}{z} \tag{18}$$

$$\frac{de}{dz} = \Gamma \frac{(e_a - e_o)}{z}$$

where e is the vapor pressure, the subscripts (a and o) refer to the air at some conveniently large height and to the water surface (respectively), the "profile coefficient" is Γ as defined by Roll[5], and the other variables are as previously defined. From data given by Roll, we derive the profile coefficient depending on wind speed:

$$\Gamma = 0.17 - 0.22/\bar{u}_6 \tag{19}$$

where $\bar{u}_6$ is the wind speed (m/s^{-1}) at the 6 m height. Equation (19) is valid for speeds greater than 1.5 m/s^{-1} and where the air-water temperature difference is not large.

As a first approximation we have obtained records from Class A evaporation pans collected over three-year periods at both Jackass Flat and at Frenchman Flat, Nevada Test Site. (Occasional measurements at a shallow lake on Frenchman Flat confirms that the approximation is reasonable). The data on water temperature, mid-day (maximum) air temperature, wind speed, and relative humidity have enabled us to calculate mid-day temperature and vapor pressure vertical profiles expected over an extensive shallow lake in these desert sites using Equations (18) and (19). We have chosen average data from two months, November and May, to compare with data taken in 1978 by the Naval Research Laboratory in the vicinity of Point Conception.[6] Figure 1 shows that the mid-day vapor pressure profiles in November would differ in magnitude but have like gradients (slopes). The air above the shallow lake would be drier than over the ocean, but not remarkably drier. In May, on the other hand, the mid-day vapor pressure profiles show that the air would be more moist near the surface of the shallow lake in the desert, but the gradient would be

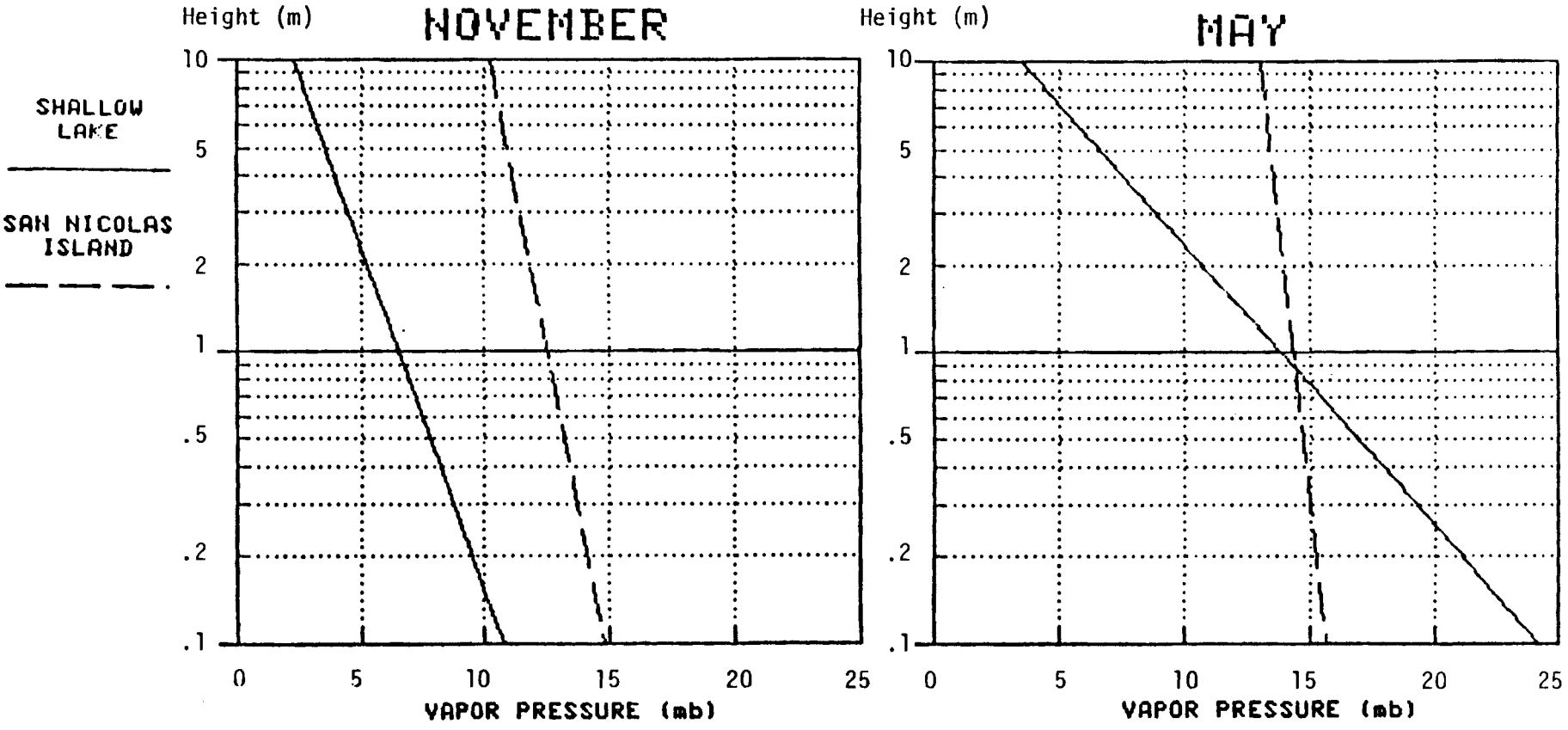

Fig. 1. Humidity profiles at mid-day over a shallow lake in the desert compared with over the ocean near Point Conception.

considerably steeper. The reason for the differences in humidity profiles is that the water temperature in the shallow lake goes through greater seasonal amplitudes than in the ocean.

The temperature differences are also reflected in the air temperature profiles. For a shallow lake in the desert, the temperature gradients again reflect the influence of the water surface temperature; for example, in November, the mid-day gradients are not unlike those over the ocean at Point Conception even though the magnitudes differ (see Figure 2). In the summer, however, the shallow lake surface is cooler than air over the desert and the temperature gradients have the opposite sign. For example, in May, the mid-day shallow lake temperature profiles are quite different compared to the normal at Santa Barbara[7,8] and the cooler than normal at San Nicolas Island[6] on Figure 2.

Let us investigate the temperature gradient by using the definition of T_* expressed in Equations (8) and (6). First, using the water temperature and maximum air temperature for the shallow lake (evaporation pans) in the desert and for the ocean near Point Conception (Santa Barbara)[7,8], we compute T_* for mid-day (averaged over each month) with the aid of Equations (18) and (19). We see that over the shallow lake the mid-day temperature gradient goes through a large seasonal amplitude as compared with the oceanic site on Figure 3. The shallow lake in the desert is apparently a good simulator of the Point Conception temperature gradient for six months of the year.

By means of tower measurements of air temperature at Frenchman Flat, we computed T_* at mid-day (1400h) using Equation (6). These T_* values over the dry desert are also shown on Figure 3. It is obvious that a shallow lake is a significant modification to the desert in the sense that the temperature gradient is significantly different in the air above the lake compared to above the desert, even to the extent of having opposite directions of heat flow.

As the air flows from the desert to the shallow lake, it could undergo transition from one thermal regime to another, as well as a change in surface roughness regimes. These impose a requirement on the horizontal extent of the shallow lake for proper simulation of maritime conditions.

HORIZONTAL EXTENT OF A SHALLOW LAKE REQUIRED FOR UPWIND FETCH

Aerodynamic drag may be expressed as a characteristic surface-roughness length, z_0. In practice, it is extracted from measurements expressed in Equation (5),

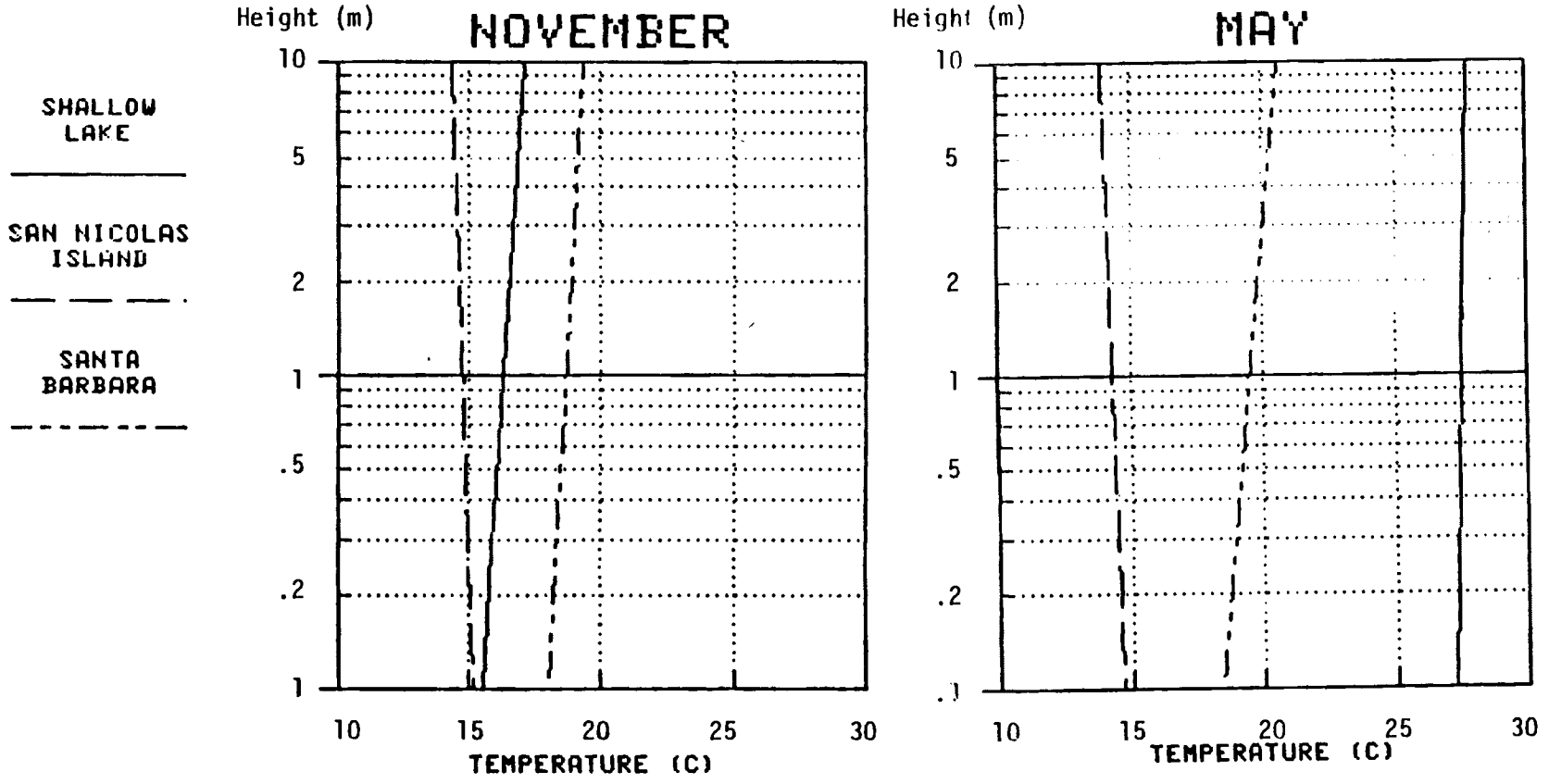

Fig. 2. Temperature profiles at mid-day over a shallow lake in the desert compared with over the ocean near Point Conception.

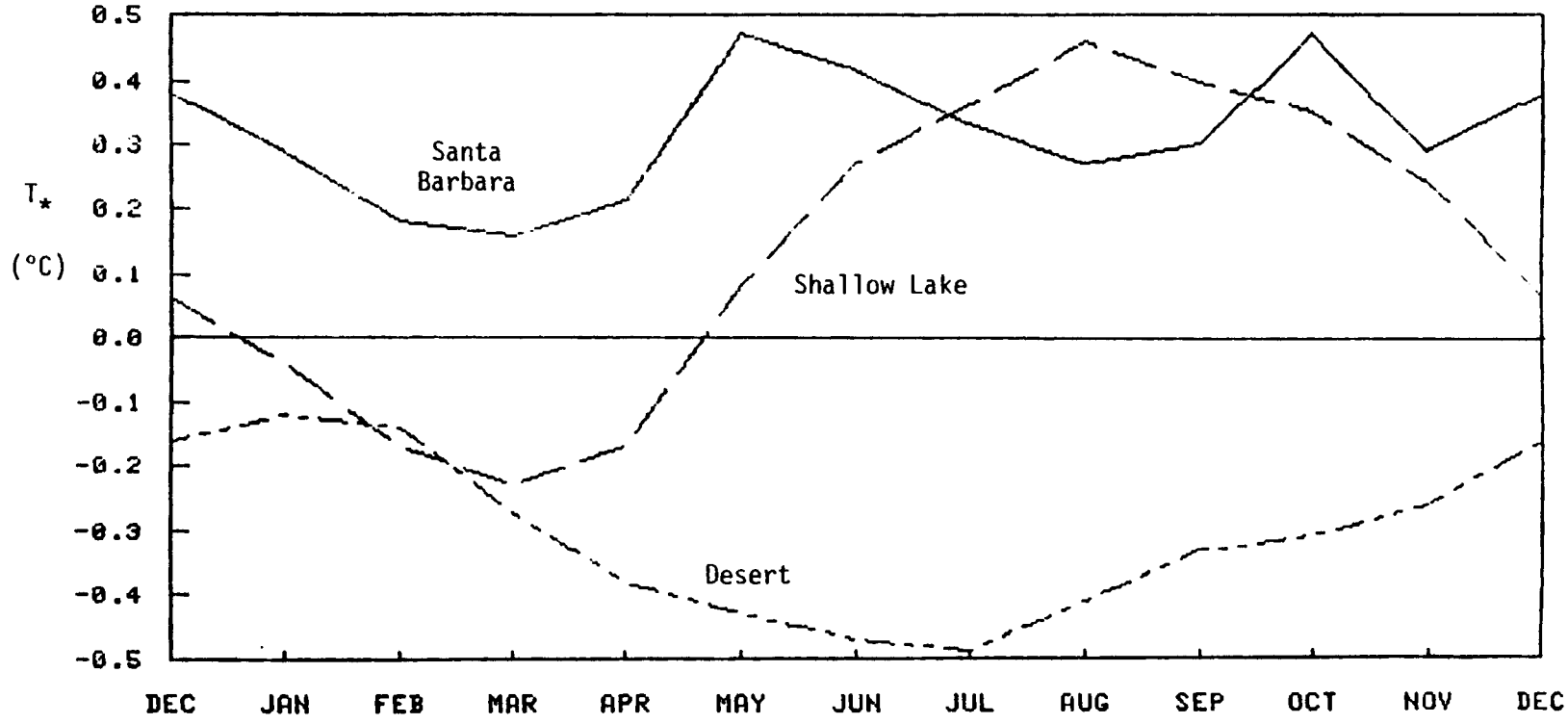

Fig. 3. Air temperature gradient parameter T_* for mid-day at a shallow lake in a desert, a dry desert, and an oceanic site.

carried out during neutral stability conditions ($z/L = 0$), and solving the surface boundary layer wind profile equation:

$$\bar{u} = (u_*/k) \ln(z/z_0) \tag{20}$$

The depth (δ) of a boundary layer resulting from a step change in temperature is conveniently expressed by Elliott's simple formula[9]:

$$\delta/z_0 = 0.35(X/z_0)^{0.8} \tag{21}$$

where X is the fetch or upwind distance to the discontinuity. This equation is overly simplified in that it does not take into account the effects of wind speed or T_*. The formula of Andreas et al., is an improvement[10]:

$$\frac{\delta}{z_0} = \beta \left[\frac{z_0}{-L}\right]^{0.8} \left[\frac{X}{z_0}\right]^{0.4} \tag{22}$$

The coefficient, β, and the empirical form of Equation (22) are not valid for $(z_0/-L) < 10^{-4}$, since it is obviously wrong for $z_0/L = 0$, and in fact was verified only for rough seas (large z_0) where T_* was very large. For lower values of z_0/L, Equation (21) must be used. By substituting the definitions from Equations (11) and (20) into Equation (22) and investigating cases at the same site, we obtain:

$$\delta = \text{Constant} \left[T_*/\bar{u}^2 \bar{T}\right]^{0.8} \tag{23}$$

It now becomes evident that by choosing the temperature gradient, wind speed, and mean air temperature appropriately, any desired depth of the boundary layer may be obtained.

The surface roughness of a shallow lake will be different from that of the sea if the water is insufficiently deep to allow wave formation. Let us compare values of the bulk drag coefficient at the 10-meter height defined as follows:

$$C_D = (u_*/u_{10})^2 \tag{24}$$

The values of C_D over rough water are consistently 1.2×10^{-3} and have a variability about this mean of about 20%.[11,12] Although there is a suspicion that C_D depends upon wind speed, any relationship is usually lost within the scatter of the data.[12,13] SethuRaman arbitrarily separates out three flow regimes the sea[13]: aerodynamically smooth ($10^3 C_D = 0.67$), aerodynamically rough ($10^3 C_D = 2.26$) and those moderately rough or transition values in between. The drag coefficient over a shallow lake of limited horizontal extent will always be in the aerodynamically smooth or transition regime. Our measurements over a 15 cm deep lake in the desert at Frenchman Flat, Nevada showed that even with $\bar{u} > 5$m/s, $10^3 C_D = 0.9$, which is close to the aerodynamically smooth category. This wide range of C_D values between smooth and rough has a great influence on z_o.

We may take the lowest value of z_o as a representative case, which is consistent with our observation that a shallow lake in the desert is nearly aerodynamically smooth. The measured value of C_D at Frenchman Flat ($10^3 C_D = 0.9$) yields from Equations (20) and (24):

$$z_o = 1.7 \times 10^{-5} \text{ m (shallow lake)} \tag{25}$$

We must estimate the depth of the boundary layer from Equation (22), since Equation (23) is not validated in this case ($-z_o/L < 10^{-4}$ for $-L > .17$ m). Using the value of z_o measured on the shallow lake at Frenchman Flat, Equations (25) and (22), we find that for boundary layer depth $\delta = 10$ m the required fetch $X = 1030$ m. Thus a 10 m deep boundary layer will require a water surface extending about 1 km upwind. Tests can be conducted at low to moderate wind speeds and large T_* magnitude to assure that the depth is sufficient.

STABILITY CONDITIONS

The stability of the atmosphere plays a role in the gas dispersion, for example, in the lateral and vertical plume dimensions respectively:

$$\sigma_y = \frac{\sigma_v}{u_*} f\left(X, \frac{z}{L}, z_i\right) \tag{26}$$

$$\sigma_z = \frac{\sigma_w}{u_*} g\left(X, \frac{z}{L}, z_i\right)$$

where the functions f and g are specified from empirical conventions.[3,4] Here σ_v, σ_w are lateral and vertical turbulence from Equation (4), z/L is the stability index from Equations (14) and (15), and z_i is the depth of the mixing layer which is equal to the inversion height (Equation (12)) over water surfaces, especially during night and early morning hours. Under neutral conditions, z_i can be estimated by 0.25 u_*/f, where f is the coriolis parameter.[14] From the definition of L in Equations (9) and (11), we note that z/L is proportional to T_*/u_*^2.

Thus the ability to simulate maritime stability conditions at a shallow lake in the desert depends on proper choice of T_*, $\bar{u}$, and z_o. (These boundary layer parameters are discussed in the previous section.) The mid-day values of T_* over the shallow lake in the desert are similar to those at Point Conception for about 6 months of the year. The value of the drag coefficient experienced by C_D in Equation (10) is lower over a shallow lake which is aerodynamically smoother than over a rough sea. Using SethuRaman's results where 10^3 C_D = .67 in the smooth case and 10^3 C_D = 2.26 in the rough case, and Equation (24), we find that values of u_* will be equal for differing wind speeds at ten meter height as follows:

$$(\bar{u}_{10})_{smooth} = 1.84\ (\bar{u}_{10})_{rough} \tag{27}$$

In this way, proper scaling may be obtained at higher speeds. Windspeeds are quite predictable in the Mojave Desert basins, being dominated by southwesterly winds which are strong from before noon to after sunset.

Further selection for appropriate stability values rests in choosing experimental T_* and $\bar{u}$ during specific times of the day. The values of T_* previously discussed and plotted in Figure 3 were the average monthly mid-day values. Our experiments over a shallow lake (15 cm depth) at Frenchman Flat show that from mid-day to evening some selection for T_* may be made (see Figures 4 and 5). In the summertime, T_* values are a minimum at mid-day and increase positively until after sunset. Figure 4 shows a typical hot summer afternoon and evening (September 12, 1979) with solar radiation decreasing. Winds are normally very persistent in direction and steady in speed (3-4 m/sec) during this period. Thus the stable (positive) values of z/L could be selected in a predictable fashion

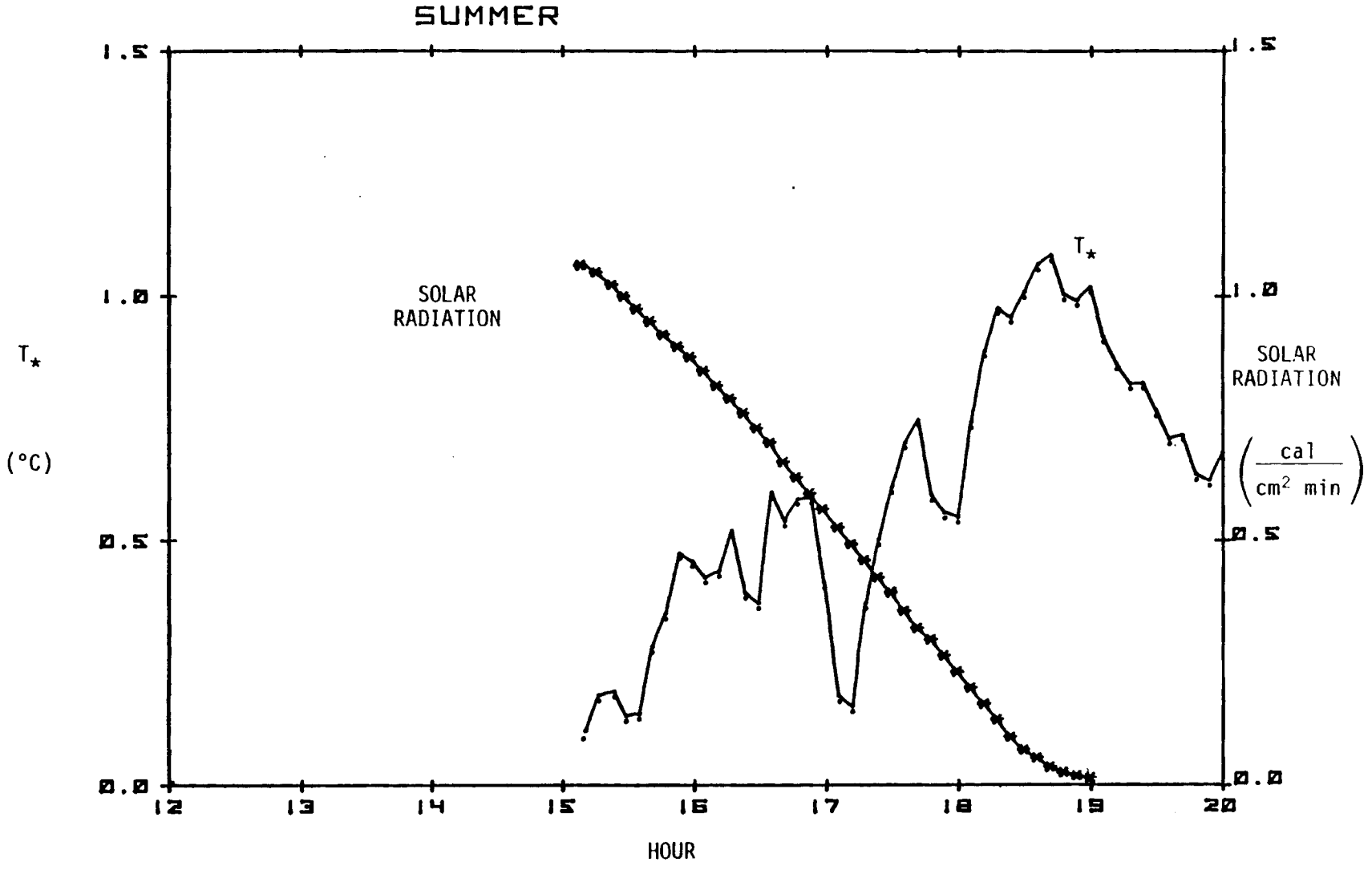

Fig. 4. Solar radiation and $T_\star$ values during the afternoon and evening of Sept. 12, 1979 at a shallow lake on Frenchman Flat, Nevada.

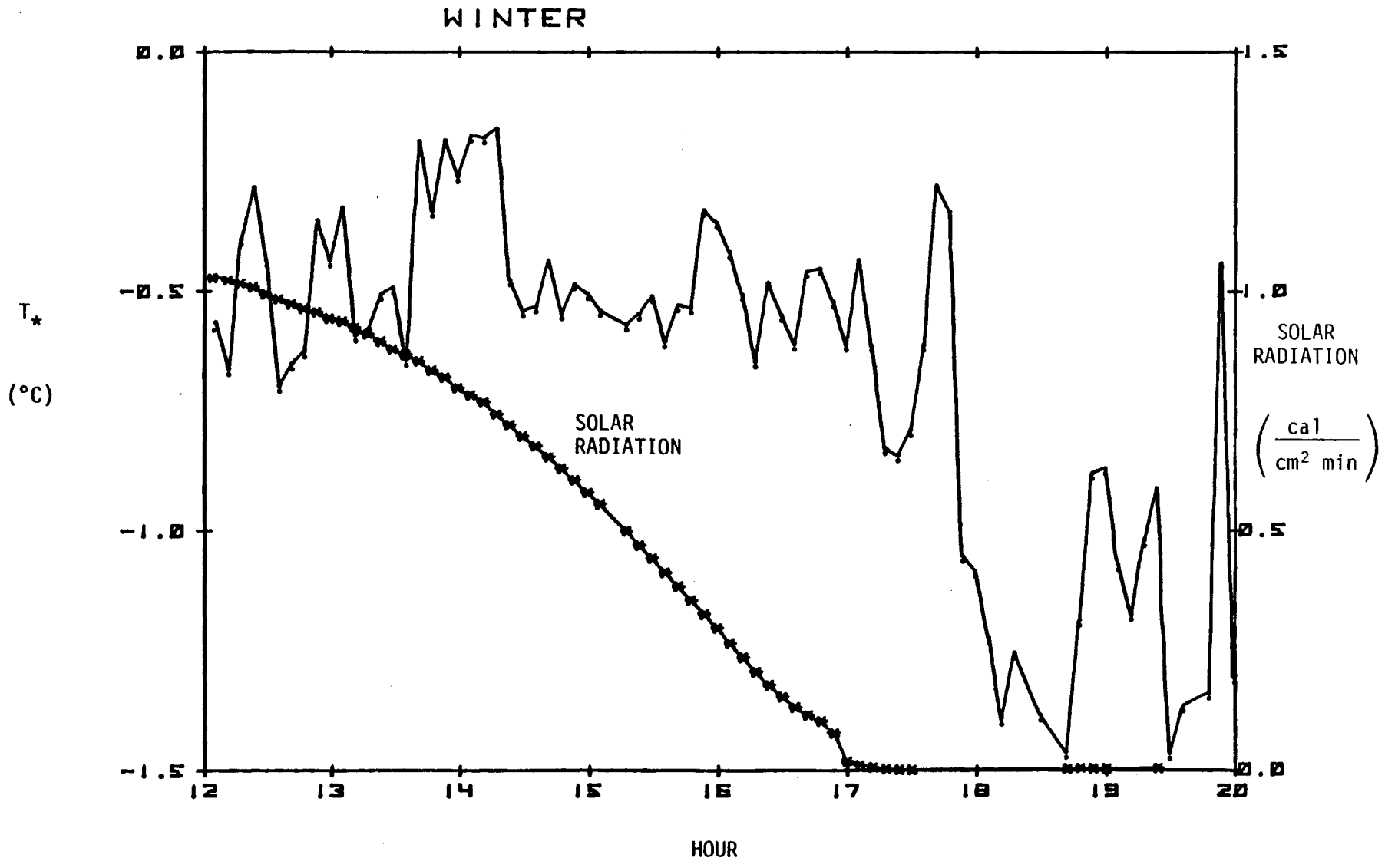

Fig. 5. Solar radiation and T_* values during the afternoon and evening of Feb. 3, 1979 at a shallow lake on Frenchman Flat, Nevada.

in summertime. Figure 5 shows a typical cold winter afternoon and evening (February 3, 1979) at the shallow lake where solar radiation is decreasing but T_* remains large and negative until after sunset. (This large instability occurs because the water is so much warmer than the air). During the winter afternoons the winds are also persistent and steady, but at a lower speed (2-3 m/sec) than summer; thus very unstable cases can be selected for experimentation.

It appears that the wide range of T_* values and the predictable winds in the desert permit a unique degree of control for any value of stability and in fact perhaps give an advantage in this regard over what would be obtained at any single oceanic site.

TURBULENCE

According to similarity theory, the spectrum of velocity component fluctuations can be normalized,

$$f\,S_v(f) = \sigma_v^2\, G\left(\frac{fz}{\bar{u}}, \frac{z}{L}\right) \tag{28}$$

$$f\,S_w(f) = \sigma_w^2\, F\left(\frac{fz}{\bar{u}}, \frac{z}{L}\right)$$

where f is the frequency, $fz/\bar{u}$ is a non-dimensional frequency, S(f) is a spectral density distribution determined by the functions G and F for the lateral (v) and vertical (w) components respectively, and z/L is the stability index. Upon integration of Equation 28 over all frequencies, one obtains the total variances σ_v^2, σ_w^2, which are also the turbulent kinetic energy components (Equation (17)) that predict the lateral and vertical spread of a diffusing gas plume (σ_y, σ_z) from Equation 26.

Whether or not the maritime conditions of turbulence can be simulated over dry land depends upon the universal nature of the functions G and F and of their integrals. A survey of many studies over both terrestrial and oceanic sites shows that the high frequency end of the spectral density distribution follows the well-known theory of Kolmogorov [15],

$$S(f) \sim f^{-5/3} \tag{29}$$

in both the lateral and vertical components, which is a region defined as the "inertial subrange" were approximately $fz/\bar{u} > 0.3$. Comparisons show that spectral density data in the inertial-subrange region scale to u_* regardless of whether the site is terrestrial or oceanic. At lower frequencies, there are local influences on the shape of the functions, apparently related to wind meandering, and in general, data are not strictly comparable from site to site.

Integrating over all frequencies in Equation (28) leads to the relations

$$\sigma_v/u_* = G'\left(\frac{z}{L}\right) \tag{30}$$

$$\sigma_w/u_* = F'\left(\frac{z}{L}\right) \tag{31}$$

Lumley and Panofsky noted that the vertical turbulence (Equation (31)) is empirically verified to be a "universal" function of z/L, but the horizontal component (Equation (30)) is not.[15] Panofsky et al. compared land measurements (northwest Minnesota and eastern Colorado) with water measurements (Lake Huron, Carribbean, and East China Sea) and suggest the following parameterization for the unstable (negative L) case.[16]

$$\sigma_v/u_* = \left[12 + 0.5(z_i/-L)\right]^{1/3} \tag{32}$$

$$\sigma_w/u_* = 1.3\left[1 + 3(z/-L)\right]^{1/3} \tag{33}$$

It is generally agreed that for the neutral stability conditions (z/L = 0), the relations Equations (32) and (33) revert to constants

$$\sigma_v/u_* = A \tag{34}$$

$$\sigma_w/u_* = B \tag{35}$$

We can compare many investigator's results under these conditions; see Table 1. We find that in neutral stability, the lateral and vertical turbulence over both oceanic and terrestrial sites will scale to u_* in the same manner.

Table 1. Neutral Stability Values for Lateral and Vertical Turbulence, Comparing Maritime with Terrestrial Studies.

Lateral (σ_v/u_*) A.	Vertical (σ_w/u_*) B.	Location	Investigator
-	1.32(.09)*	Ocean off Barbados and San Diego	Pond et al.[17]
2.0(.8)*	1.4(.5)*	Ocean off Long Island	SethuRaman et al.[18]
1.3-2.6	0.7-1.3	Survey of several inland tower studies	Lumley and Panofsky[15]
2.0-3.3	0.5-0.8	Frenchman Flat, Nevada	Shinn and Cederwall[19]
2.3	1.3	Oceanic and inland sites, Equations (32) and (33)	Panofsky et al.[16]

*Standard deviations in parentheses.

An examination of Equation (32) will show that σ_v/u_* depends of z_i/L where z_i is the depth of the mixing zone, as contrasted to Equation (33). This is because σ_v does not depend on height (as does σ_w which is directly influenced by proximity to the boundary), but instead should scale to the characteristic convective velocity of the boundary layer which depends directly on the product of $u_*(z_i/L)^{1/3}$, according to Panofsky et al.[16]

The mixing zone is thus another fundamental scaling variable of atmospheric dispersion. There are not enough data to compare oceanic and terrestrial sites, and the mixing depth cannot yet be predicted or parameterized to other fundamental variables at this stage of knowledge. It must therefore be measured along with other fundamental variables during experiments so that results can be compared between sites.

Our measurements of σ_v/u_* and σ_w/u_* over a range of stability (z/L) values at Frenchman Flat, Nevada Test Site, are shown in Figures 6 and 7.[19] For comparison purposes, equations from Panofsky et al. are also shown.[16] In general, the data from Frenchman Flat show that the empirical scaling equations are not completely accurate. The scatter observed of the turbulence data reflects true atmospheric variability rather than instrumental errors. Therefore an ensemble of experimental studies is required so that the conditions of similarity can be generalized within the normal range of atmospheric variability.

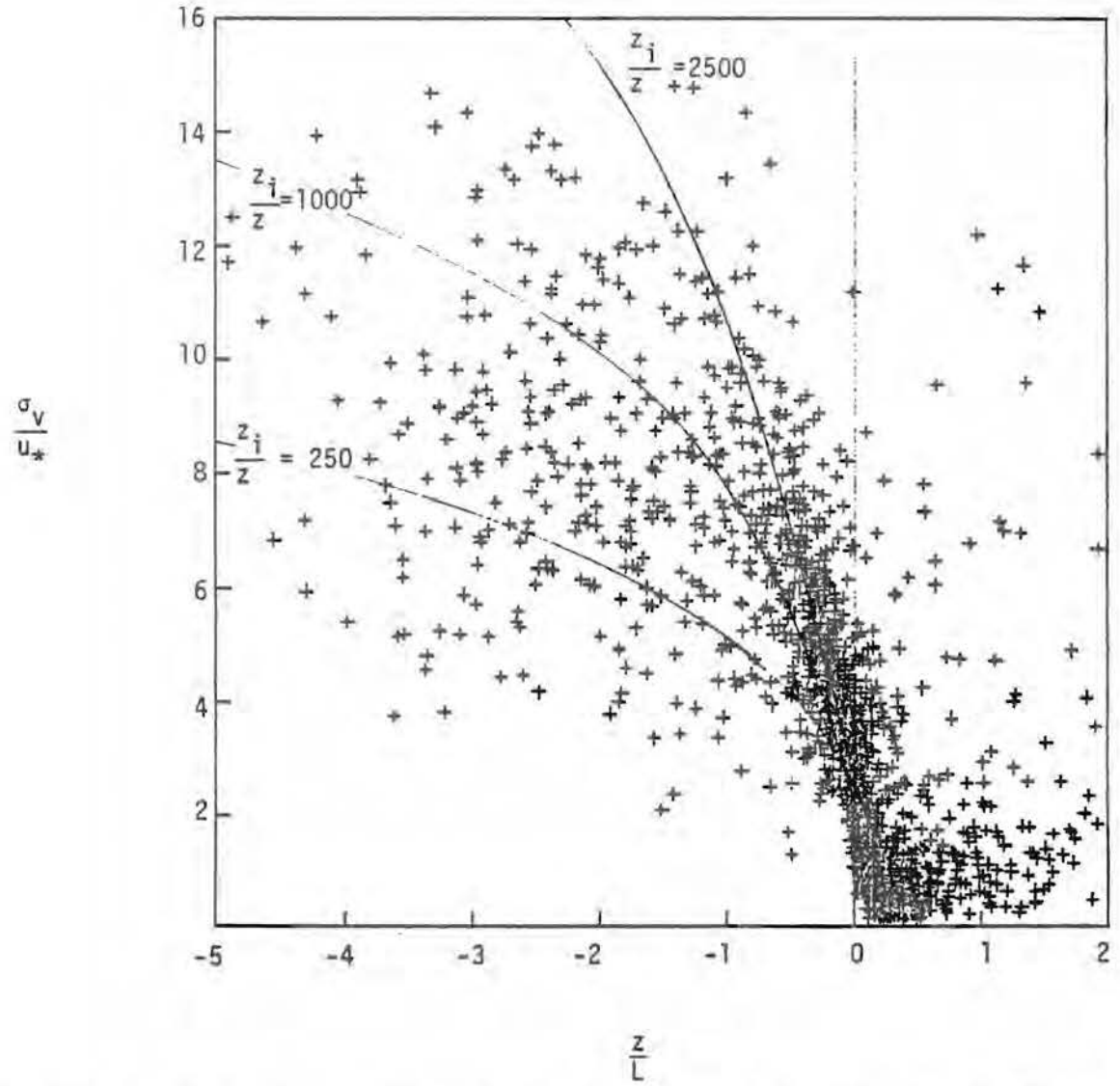

Fig. 6. Lateral turbulence intensity as a function of stability index z/L at the 5.5 m height, Frenchman Flat. Curves shown are the Panofsky et al. (1977) function: $\sigma_v/u_* = (12 + 0.5\ z_i/-L)^{1/3}$ where z_i is the mixing zone height.

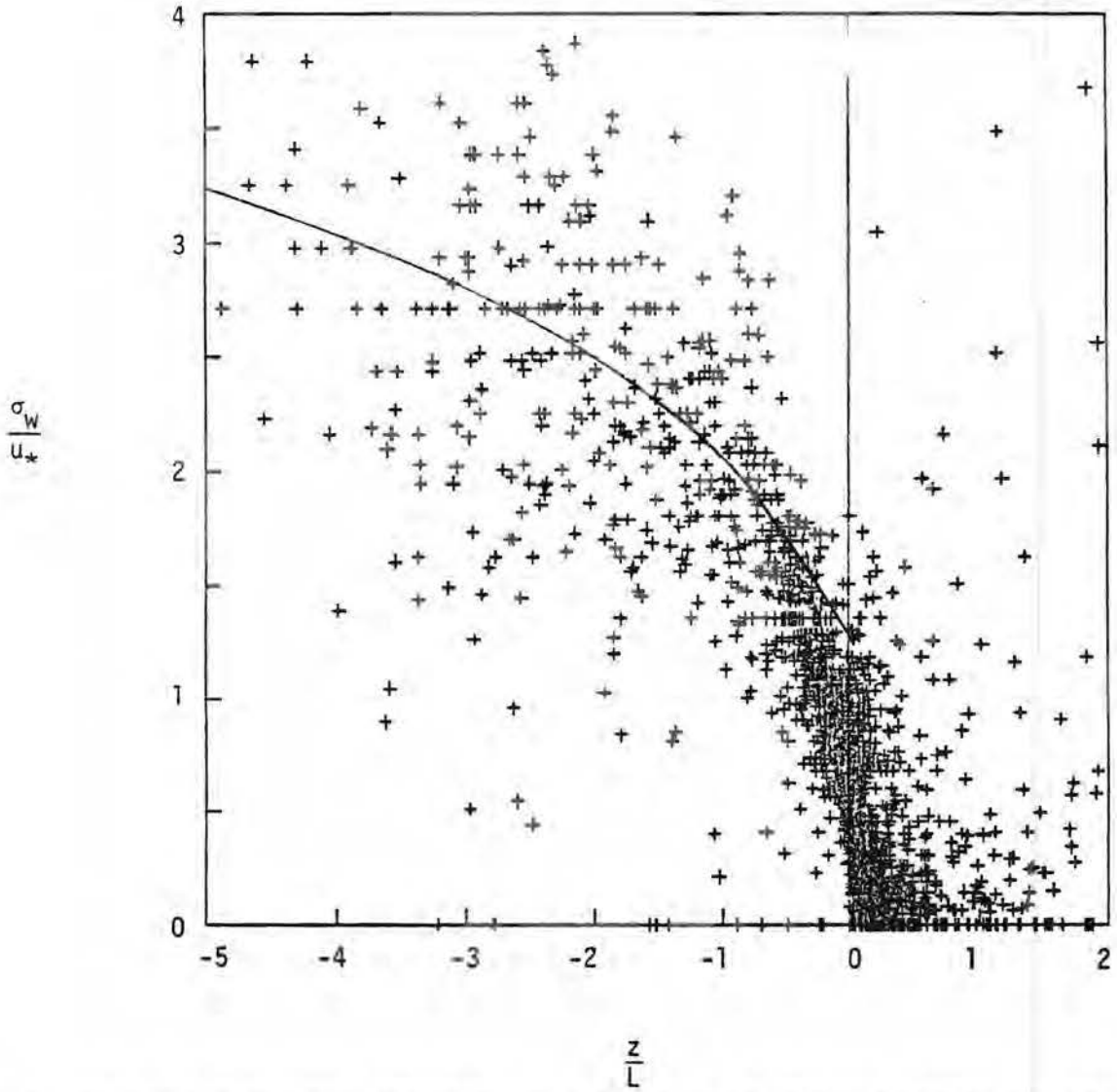

Fig. 7. Vertical turbulence intensity as a function of stability index z/L at the 5.5 m height, Frenchman Flat. Curve shown is the Panofsky et al.(1977) function: $\sigma_w/u_* = 1.3(1 + 3z/-L)^{1/3}$.

CONCLUDING COMMENTS

The fundamental variables of atmospheric dispersion have been shown to scale similarly over ocean and inland sites. A shallow lake in the desert is a significant atmospheric modification to the extent that humidity and temperature gradients for extended times will approach those observed over ocean sites. The shallow lake must extend about 1 km upwind to produce a 10 m deep boundary layer. The depth of the boundary layer can be selected by choosing the temperature gradient, wind speed, and mean air temperature appropriately. The temperature gradient can be selected to simulate oceanic conditions by choosing both the season of the year and the time of the day appropriately, as shown by our measurements over a shallow lake at Frenchman Flat. The shallow lake in the desert is aerodynamically smoother than a rough sea, but the scaling will be correct if experiments are conducted at higher wind speeds (for example, a factor of 1.84 at Frenchman Flat). In fact, simulations in a desert permit a unique degree of control for any value of atmospheric stability, and give an advantage in this regard over what would be obtained at any single oceanic site.

Atmospheric turbulence in the inertial subrange will scale to aerodynamic roughness, atmospheric stability, and the depth of the mixing zone in either oceanic or inland sites. But an ensemble of experimental studies is required so that the conditions of dynamic similarity in the boundary layer can be generalized within the normal, observed range of atmospheric variability.

ACKNOWLEDGMENTS

Some experimental data used in this report was provided by the Nevada Test Site Baselines Study. Richard Cederwall developed computer codes, Donald Homan provided data base management, Gale Holladay was the Electronics Engineer in charge of field acquisition, and Cleo Fry was coordinator of field activities. The author is grateful for their support and assistance.

Work performed under the auspices of the U.S. Department of Energy by the Lawrence Livermore Laboratory under contract number W-7405-ENG-48.

REFERENCES

1. Committee on Atmospheric Turbulence and Diffusion (S.R. Hanna, Chairman), "Accuracy of Dispersion Model", Bulletin American Meteorological Society 59(8):1025-26 (1978).

2. Raynor, G.S., P. Michael, and S. SethuRaman, Recommendations for Meteorological Measurement Programs and Atmospheric Prediction Methods for Use at Coastal Nuclear Reactor Sites, U.S. Nuclear Regulatory Commission Report NUREG/CR-0936 (1979).

3. Hanna, S.R., G.A. Briggs, J.A. Deardorff, B.A. Egan, F.A. Gifford, and F. Pasquill, "AMS Workshop on Stability Classification Schemes and Sigma Curves--Summary of Recommendations", Bulletin American Meteorological Society 58(12):1305-1309 (1977).

4. Irwin, J.S., "Estimating Plume Dispersion--A Recommended Generalized Scheme", Fourth Symposium on Turbulence, Diffusion, and Air Pollution, (Preprint Volume) American Meteorological Society, Reno, Nevada, January, 1979, 62-69 (1979).

5. Roll, H.V., Physics of the Marine Atmosphere, International Geophysical Series Volume 7, Academic Press, New York, 426 p (1965).

6. Blanc, T.V., Micrometeorological Data for 1978 Cooperative Experiment for West Coast Oceanography and Meteorology at San Nicolas Island, California, Vol. 1:May 9-15 data and Vol. 2:May 16-22 data, NRL Memo Report 3871, U.S. Naval Research Laboratory (1978). See also Blanc, T.V., Micrometeorological Data Report for the November 1978 Electro-Optics Meteorology Experiment at San Nicolas Island, California, NRL Memo Report 4056, U.S. Naval Research Laboratory (1979).

7. U.S. Dept. of Commerce, Surface Water Temperature and Salinity, Coast and Geodetic Survey Publication 31-3 (1962).

8. U.S. National Oceanic and Atmospheric Administration, Climatological Data: California 82 (Normal Max Temperature Data, 1941-1970) (1978).

9. Elliott, W.P., "The Growth of the Atmospheric Internal Boundary Layer", Transactions American Geophysical Union 39:1048-1054 (1958).

10. Andreas, E.L., C.A. Paulson, R.M. Williams, R.W. Lindsay, and J.A. Businger, "The Turbulent Heat Flux from Arctic Leads", Boundary Layer Meteorology 17: 57-91 (1979).

11. Emmanuel, C.B., "Drag and Bulk Aerodynamic Coefficients over Shallow Water", Boundary Layer Meteorology 8:465-474 (1975).

12. Badgley, F.I., C.A. Paulson, and M. Miyake, Profiles of Wind, Temperature, and Humidity over the Arabian Sea, International Indian Ocean Expedition Meteorological Monograph Number 6, University of Hawaii Press (1972).

13. SethuRaman, S., "Momentum Flux and Wave Spectra Measurements from an Air-Sea Interaction Buoy", Boundary Layer Meteorology 16:279-291 (1979).

14. Wyngaard, J.C., "On Surface-Layer Turbulence", Chapter 3, in Workshop on Micrometeorology, ed. D.A. Haugen, published by American Meteorological Society (1973).

15. Lumley, J.L. and H.A. Panofsky, The Structure of Atmospheric Turbulence, Interscience Division of John Wiley Publishers (1964).

16. Panofsky, H.A., H. Tennekes, D.H. Lenschow, and J.C. Wyngaard, "The Characteristics of Turbulent Velocity Components in the Surface Layer under Convective Conditions", Boundary Layer Meteorology 11:355-361 (1977).

17. Pond, S., G.T. Phelps, J.E. Paquin, G. McBean, and R.W. Steward, "Measurements of the Turbulent Fluxes of Momentum, Moisture, and Sensible Heat Over the Ocean", Journal of the Atmospheric Sciences 28(6):901-917 (1971).

18. SethuRaman, S., R.E. Meyers, and R.M. Brown, "A Comparison of a Eulerian and a Lagrangian Time Scale for Over-Water Atmospheric Flows during Stable Conditions", Boundary Layer Meteorology 14:557-565 (1978).

19. Shinn, J.H. and R.T. Cederwall, "A Study of Frequency Distributions of Atmospheric Dispersion Characteristics at Mojave Desert Sites", Lawrence Livermore Laboratory UCID Report in press. Presented at 61st AAAS Annual Meeting (Pacific Division) and American Meteorological Society, Session on Air Pollution, Davis, California, June 24, 1980, Lawrence Livermore Laboratory Abstract UCRL-84223 (1980).

REPORT G

Observed Turbulence Intensities in a Desert Boundary Layer

J. H. Shinn
R. T. Cederwall

Prepared for the
Environmental and Safety Engineering
Division
U.S. Department of Energy
under Contract W-7405-ENG-48

Lawrence Livermore Laboratory
Livermore, California 94550

REPORT G

TABLE OF CONTENTS

INTRODUCTION

A number of applied problems in atmospheric dispersion require the prediction of vertical and lateral turbulence intensities near the ground as a function of the local atmospheric stability. We have investigated σ_w/u_* over a wide range of stabilities at two desert sites in Nevada and California. The study was part of a meteorological baseline for field tests of atmospheric dispersion during liquified natural gas (LNG) spills. The data collected at Frenchman Flat (Nevada Test Site) during neutral and stable cases seem to be remarkably different from those of other published studies and lead us to hypothesize that, under certain conditions, different semi-empirical approaches would be required to predict turbulence intensities.

THEORY

The relationship between vertical turbulence intensity, σ_w/u_*, and Monin-Obukhov stability parameter, z/L, is generally agreed to approach the free-convection limit:

$$\sigma_w/u_* \approx A(-z/L)^{1/3} \quad -z/L >> 0 \quad . \tag{1}$$

For example, Panofsky et al. (1977) have surveyed a number of field studies and derived an empirical expression meeting both the condition of Eq. (1) and a consensus of neutral and stable results that show:

$$\sigma_w/u_* \approx 1.3 \quad z/L \geq 0 \quad . \tag{2}$$

Binkowski (1979) has developed a semi-empirical method for obtaining second moment closure to the turbulent energy equation yielding a predictive formulation for σ_w/u_* as a function of z/L, which has the same essential properties of (1) and (2). This result agreed with field data from Kansas and Minnesota. From this and other efforts to effect closure of the turbulent energy equations (Herbert and Panhans, 1979, Panhans and Herbert, 1979), it becomes evident that the success of the σ_w/u_* prediction rides on the success of relating the scaled momentum parameter ϕ_m to z/L, where

$$\phi_m = (kz/u_*)\ du/dz \quad . \tag{3}$$

On the other hand there is less likely a unique dependence of lateral turbulence intensity, σ_v/u_*, upon z/L. This may be due in part to the influence of the depth of the mixed layer (Panofsky et al., 1977) on σ_v/u_*.

EXPERIMENTAL OBSERVATIONS

At Frenchman Flat on the Nevada Test Site a 62 meter meteorological tower was instrumented with vertical propellor anemometers, sensitive wind vanes and cup anemometers, and aspirated thermistors. Each of these were scanned once a second with RMS and averages determined every three minutes by a microprocessor-based data acquisition system. The data of September-November 1979 were analyzed to determine u_* and L from profile measurements between 3 and 10 meter heights, while σ_w and σ_v data from each of two levels were averaged.

Data representative of the 5.5 height above ground showed features unlike other studies (Figure 1). We eliminated from the analysis periods when sensors would be near their thresholds ($u < 1.5$ m/s), and because of the wealth of data (n = 1925) chose to plot only the medians and upper and lower quartiles for each z/L value. We observed a steep gradient of σ_w/u_* near neutral stability rather than an approach to the expected constant of Eq. 2. We also observed much lower turbulence intensities under stable conditions than commonly reported. The distinguishing features of this site are an extremely small surface roughness ($z_o \approx 10^{-5}$ m) and a homogeneous upwind fetch for 3 km due to the flat playa. Since care was taken with the observations and analysis, we believe that what we have observed is a natural effect of the surface roughness and the lack of influence of mesoscale, organized flows during stable conditions. The characterisitic eddy structure may be expressed by the ratio σ_v/σ_w. We found that σ_v and σ_w were highly correlated ($r = 0.9$) regardless of z/L, giving confidence that the sensors were not anomalous since σ_v and σ_w are measured by separate devices.

A value $\sigma_v/\sigma_w = 4.1$ was observed at Frenchman Flat which was high compared to a value of 2.4 observed by us over rougher surfaces in a desert at China Lake, Naval Weapons Center, California. A value of 1.5 has been reported for rougher surfaces under neutral conditions (Binkowsky, 1979). We believe that the large value of σ_v/σ_w at Frenchman Flat indicates a reduced magnitude of σ_w relative to σ_v due to decreased roughness. Thus under certain conditions, better parameterization is required.

On the other hand, our data agree very well with Eq. 1 (A = 2.1) and also agree with the results of Binkowski for unstable conditions.

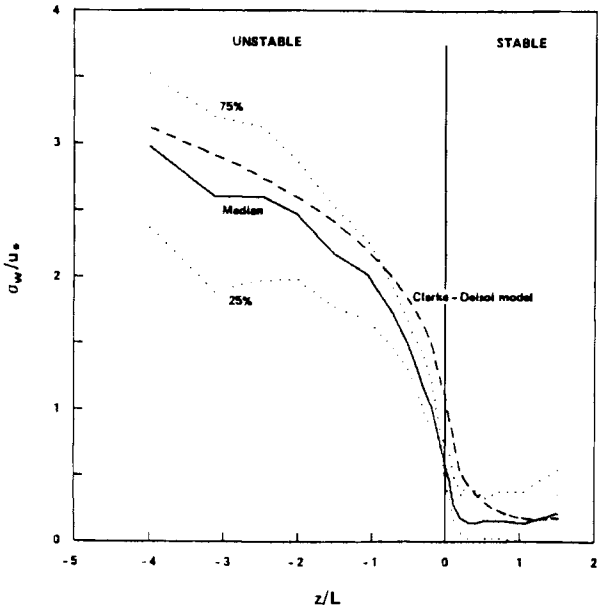

Figure 1. Vertical turbulence intensity versus atmospheric stability for 1925 samples at Frenchman Flat (Sept-Oct, 1979); solid line is median value, dotted lines are first and third quartiles, and dashed line is predicted value from Clarke-Delsol model.

DISCUSSION

We have found that semi-empirical predictive formulas which fit data over rougher surfaces and predict higher turbulent intensities for neutral and stable cases (Eq. 2) must be rejected for the smooth desert. However, based upon the hypothesis that a Prandtl-type closure condition would define the characteristic scale and consequently σ_w/u_*, we assume:

$$\sigma_w/u_* \sim u_* /kz(du/kz) \qquad (4)$$

where k is Karman's constant. From Eq. 3:

$$\sigma_w/u_* \sim 1/\phi_m \qquad (5)$$

Following Herbert and Panhans (1979), we choose the Clarke-Delsol parameterizations:

$$\phi_m = (1 - 15\ z/L)^{-11/40} \qquad z/L \leq 0 \qquad (6a)$$

$$\phi_m = (1 + 5\ z/L)/(1 + \alpha z/L + 5\alpha(z/L)^2) \qquad 0 \leq z/L \leq 1 \qquad (6b)$$

$$\phi_m = 6/(1 + 6\alpha z/L) \qquad z/L \geq 1 \qquad (6c)$$

where $\alpha = 0.0079$.

The results of predicting σ_w/u_* by (5) and (6) are shown in Figure 1. Much better agreement in the neutral and stable case is obtained.

ACKNOWLEDGMENTS

Work was performed under the auspices of the U.S. Department of Energy by the Lawrence Livermore National Laboratory under contract number W-7405-ENG-48.

REFERENCES

Binkowski, F. S., 1979: A simple semi-empirical theory for turbulence in the atmospheric surface layer. Atmospheric Environment, 13, 247-253.

Herbert, F. and Panhans, W-G., 1979: Theoretical studies of the parameterization of the non-neutral surface boundary layer. Part I: Governing physical concepts. Boundary-Layer Meteorology, 16, 155-167.

Panhans, W-G. and Herbert, F., 1979: Theoretical studies of the parameterization of the non-neutral surface boundary layer. Part II: An improved similarity model. Boundary-Layer Meteorology, 16, 169-179.

Panofsky, H. A., Tennekes, H., Lenschow, D. H., and Wyngaard, J. C., 1977: The characteristics of turbulent velocity components in the surface layer under convective conditions. Boundary-Layer Meteorology, 11, 355-361.

REPORT H

Flame Propagation in Gaseous Fuel Mixtures in Semiconfined Geometries

P. A. Urtiew

Prepared for the
Environmental and Safety Engineering
Division
U.S. Department of Energy
under Contract W-7405-ENG-48

Lawrence Livermore Laboratory
Livermore, California 94550

REPORT H

TABLE OF CONTENTS

SUMMARY

The possible hazardous consequences of large spills of liquefied natural gas (LNG) are not completely known at present, but research into the problem is advancing steadily. Here we review previous work on flame propagation in gaseous fuels contained in semiconfined geometries. We formulate our present understanding of the phenomena involved, describing some of the parameters that may have an effect on flame propagation, flame acceleration, and the transition from deflagration to detonation. We describe some of our recent experiments on combustion in semiconfined geometries. Our results suggest that turbulence-producing obstacles in the flow path are the primary cause of acceleration of the flame front. Other parameters remain to be investigated, however, before we can give a satisfactory explanation of flame acceleration.

INTRODUCTION

The ever increasing demand for various forms of energy will probably lead to importation and use of large quantities of liquefied natural gas (LNG). There is serious concern about the safety associated with LNG's transportation, loading, storage, etc. The magnitude of the danger from a large spill of LNG is not well known, even though this fuel has been in use for some time. So far, except for one devastating accident in Cleveland, Ohio, in 1944, no serious accidents with LNG have occurred in the U.S. However, with the amount of LNG that is being considered for use here in the near future, the probability of accidental spills becomes ever greater. Thus we need to know more about what to expect if a spill of a considerable amount of LNG should occur, and if the resulting combustible cloud of fuel-air mixture should find a suitable ignition source. Would this flame burn locally, form a pool fire, or a fireball? Would it propagate as a deflagration wave? Would the deflagration wave accelerate to form a rapid deflagration, a galloping detonation, or even make the transition to a full-fledged detonation wave?

Many investigations have been conducted with various ignition sources and fuels in different experimental arrangements to determine when and under what conditions a detonation process can be started and sustained. The opinion formed in these investigations is that, in an unconfined area without obstacles to cause turbulent eddies, a detonation process cannot be started in an LNG-air cloud by a "mild" ignition source. More specifically, Bull et al.[1] state that an ignition source containing less energy than is in a 3-kg charge of tetryl cannot start a detonation in a cloud of air mixed with natural gas containing 10% of ethane or propane in methane.

The investigations just mentioned relate to the detonation process, which is the most destructive outcome of all the possibilities. However, devastating levels of overpressure can also be produced by a rapid deflagration and even from an accelerating flame. Figure 1 shows what various overpressures can

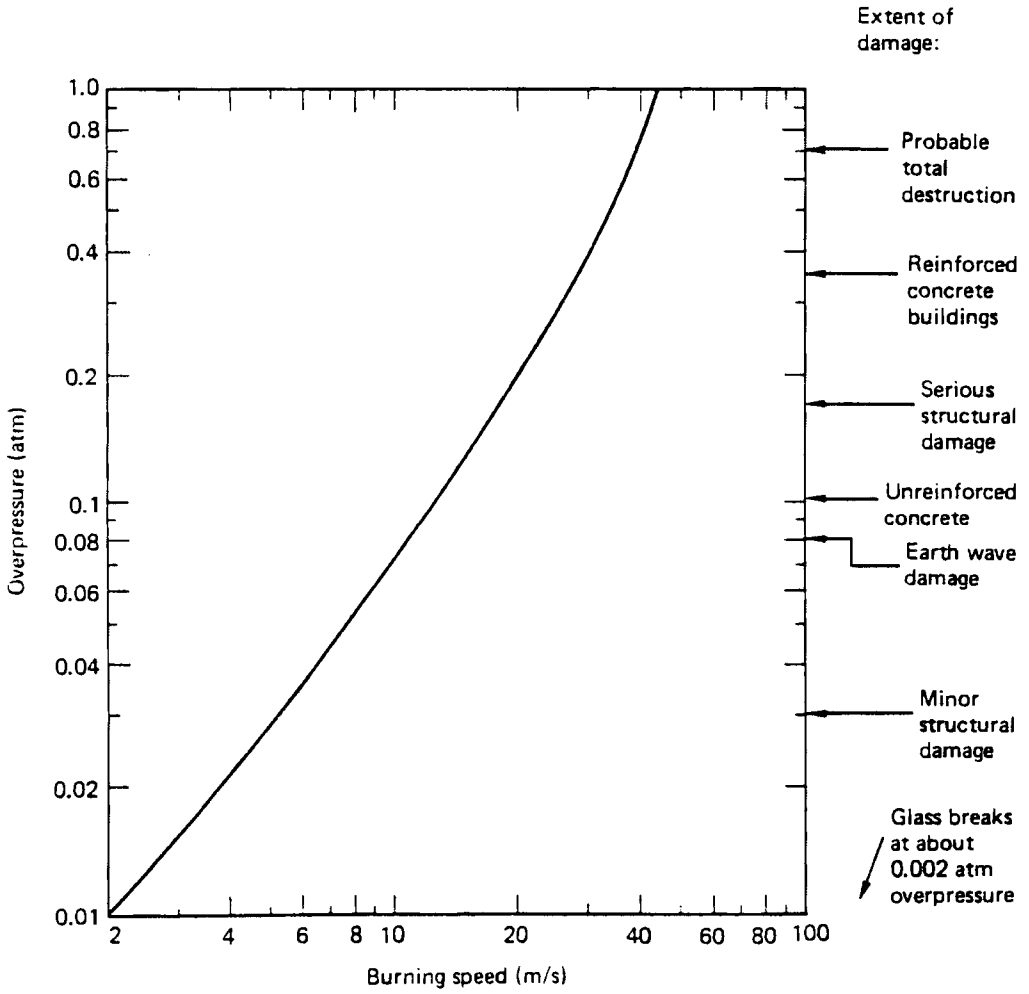

FIG. 1. Overpressure as a function of burning velocity. Right-hand scale relates structural damage to overpressure.

do to different types of structures, and what burning velocities are associated with the overpressures. These results are based on calculations made assuming a self-similar flow beyond a constant-flame-velocity model in a spherical geometry.[2,3] Here one can see that flames moving at 40 m/s relative to the medium ahead can cause overpressures of nearly 0.8 atm, sufficient to totally destroy a solid building. Recently, by applying acoustic source theory, Strehlow[4] has found that in a nonspherical cloud the overpressure generated by the flame is much smaller than that expected from a one-dimensional (spherical) theory. However, there still remains the question of whether or not the flame can accelerate, and if so, what can cause such an acceleration and what are the governing parameters.

The purpose of this report is to address various physical effects which may play a significant role, to describe current experimental efforts directed toward a better understanding of the problem in order to facilitate its resolution and modeling, and to set the stage for forthcoming investigative work both experimental and theoretical.

HISTORICAL BACKGROUND

Most of the work done on vaporized LNG-air mixtures has been either in confined geometries (tubes or vessels), for the purpose of studying ignition, flame acceleration, transition to detonation, and properties of the fully developed detonation, or in unconfined geometries, for the sole purpose of determining the minimum amount of energy needed to cause a direct initiation of a spherical detonation.

The confined geometries have been covered rather extensively by various groups, among which are the Ohio State group led by Bollinger,[5] the Berkeley group led by Oppenheim,[6] the group at Poitiers, France, under the supervision of Manson,[7] the group at Göttingen, Germany, under the direction of Wagner,[8] and the group in the USSR under Shchelkin.[9] All of these studies, as evident from some of the joint review papers in this area,[10-12] converged to more or less the same conclusion: that flame acceleration and transition to detonation in confined geometries, such as closed-end tubes, is caused by several processes which interact and self-magnify. Burning of the medium releases energy, which generates pressure waves propagating away from the flame front. The pressure waves interact with the confining walls, generating turbulence in

the flow and thereby disturbing and increasing the flame surface area. This in turn causes more energy release and thus more and stronger pressure waves, which again enhance flame acceleration. The process eventually becomes unstable and reaches a point at which transition to detonation becomes inevitable.

Such flame acceleration in confined geometries depends on a large number of parameters, including the diameter and geometry of the confining tube, its wall roughness and boundary conditions at the ends, the chemical properties and sound speed of the gaseous fuel mixture, and finally the strength and nature of the ignition source. All of these parameters affect the two main flame-acceleration mechanisms, which are the flame-shock interactions and the turbulence.

The second type of studies, performed in so-called unconfined geometries, are not so extensive. Most of them have been directed toward the establishment of the critical size of charge required to set off the detonation process in an unconfined explosive cloud. Among these studies one should particularly mention the work of Freiwald and Koch,[13] Kogarko et al.,[14] Bach et al.[15] and more recently that of Lee,[16] Bull et al.,[17] Lind and Whitson,[18] and Pfortner.[19] In all of these studies the conclusions are very similar: Deflagration-to-detonation transition (ddt) in spherical geometry is possible but highly improbable. It has been observed by Freiwald and Koch[13] and Kogarko et al.,[14] but only in very energetic systems such as $C_2H_2 + 2O_2 + 2N_2$ and $C_3H_8 + 5O_2$. In fuel-air mixtures, such a transition in an ideally spherical geometry is practically impossible. Here, too, the main mechanism for flame acceleration leading to ddt was found to be turbulence. Large-scale eddies and sufficiently intense fine-scale turbulence to promote mixing of hot combustion products with unburned fuel and air are considered to be the major causes for enhancement of combustion, resulting in higher energy release and flame acceleration. Thus flame acceleration causing higher flame speeds and associated overpressures can occur in a real system if a mechanism exists to create turbulence. The flame acceleration can then lead to further instability of the process, which could eventually lead to a transition to detonation. Flame accelerations and, in some cases, rapid deflagrations have been observed under experimental conditions[20,21] and deduced from evidence found in accident cases.[22]

Falling between these two extreme cases are studies in <u>semiconfined</u> geometries, an area of investigation that has been practically untouched. In

real life, accidental spills will most probably not occur in ideal confined or unconfined geometries but rather in some trenches, water channels, streets, harbors, etc., which more appropriately may be classified as semiconfined geometries. Some small, laboratory-scale studies have been done in order to simulate accidental burning in mine galleries or over pools of liquid fuels. Most of these studies have no direct application to our evaluation of hazards associated with spills of LNG. However, some of the results of these studies are worth mentioning because they may bear significantly on defining the mechanisms and conditions responsible for causing flame accelerations.

Kaptein and Hermance[23] have studied laminar flames in semiconfined channels filled with vapors of benzene, hexane, heptane, and methyl alcohol fuels. They found that a flame may reach higher velocities if it remains laminar in shape, and that flame velocities depend strongly on the extent of confinement and on the thickness of the mixing layer. They also found that the flow field ahead of the flame is perturbed and shows evidence of being preconditioned by pressure waves generated at the flame front.

Full-scale tests of Kawensky et al.[24] in an experimental mine can be considered as semiconfined in the sense that explosive gas was layered near the top of the mine. The results show significant increase in the flame speed as the thickness of the flammable layer is increased. Thicknesses of 18, 45, and 157 cm led to flame speeds of 53, 126, and 150 m/s respectively. These velocities are in the laboratory frame of reference and should not be confused with the velocity of the flame relative to the gas ahead of it.

Lind and Whitson[18] have measured flame speed in a hemispherical bag filled with methane-air and propane-air mixtures, obtaining velocities on the order of 5-9 m/s and 6-12 m/s respectively. However, their spilled LNG tests ignited at the far end of the cloud revealed velocities closer to 15-17 m/s.

Some time ago, Pfortner[25] at ICT (near Karlsruhe in Germany) performed some experiments with methane-air mixtures in a hemispheroidal bag 40 m in diameter and 8 m high at the center. At the time of this writing, his precise results were not yet available. More recently, however, the group from Poitiers, France,[26] reported on some small-scale soap bubble experiments with methane-air, ethylene-air, and propane-air mixtures. The results showed that the overpressures developed during a spherical burn depend very much on the complete history of the flame front. Stratified charges (made with two concentric soap bubbles) clearly demonstrated that forced accelerations of the flame due to sudden changes in composition may cause overpressures to build up

far beyond those predicted with the constant-velocity model for the largest flame speed encountered during the experiment. Thus, the main conclusion was that in systems with variable flame velocities, prediction of mechanical effects (e.g., overpressure) on the environment requires an accurate knowledge of the complete flame history. If predictions are made on the basis of the constant-flame-velocity model, the effects may be underestimated.

Under the direction of Prof. Strehlow, one of his graduate students, Huseman,[27] has set up a test chamber for studying methane-air flame acceleration. However, the system has not yet been put into full use and no systematic studies have yet been performed.

A more rigorous approach to the problem of flame propagation, acceleration, and transition to detonation in semiconfined and unconfined geometries is now being pursued by Lee and his group at McGill University in Canada.[28] Their starting geometries, strictly speaking, cannot be considered as semiconfined. However, their aim, at this point, is to study the effects of obstacles on flame acceleration, and a somewhat more confined geometry amplifies the effect so that it can be detected more easily. In the cylindrical geometry, depending on the size and spacing of the obstacles, they observed flame speeds of over 400 m/s,[29] and in the one-dimensional tube with circular obstacles they observed even higher values.[30] As a result of such high flame speeds, they also observed considerable overpressures.

Lee and his co-workers are also conducting a study in a truly semiconfined chamber investigating the influence of confinement on acceleration of the flame front with and without obstacles in the flow field.[31] Their efforts in this area are furthered by an appropriate theoretical venting model which seems to support their experimental findings.

PRESENT UNDERSTANDING OF THE PROBLEM

As evident from the previous section, the experiments performed so far have not resulted in definitive answers to the questions of what one may expect if and when an actual spill should occur, and which parameters play an important role during such a spill. It is conceivable that, in a large cloud, buoyancy forces may become important, roughness of the terrain or natural obstacles such as houses or trees may create preferred semiconfined flame paths, and large-scale eddies of atmospheric motion or wind may enhance

turbulent mixing. All of these effects could cause the flame to accelerate and develop into a disastrous fire with damaging heat and overpressures. It is therefore important to define various parameters of the flow and to investigate their effects that might prove to be significant for a large spill.

Since experiments with the very large spills that are possible are prohibitively difficult and expensive to perform under controlled conditions, we will have to rely on our modeling capability, which in turn must be based on small-scale laboratory experiments and somewhat larger but still manageable field tests.

Using previous findings, we can list some of the physical phenomena that affect the combustion process in a cloud of combustible gas, either contributing to the flame's acceleration or forcing it down to extinction:

- Buoyancy of lighter gases relative to heavier ones is an aid to combustion. During the burning process, the lighter reaction products surge upward and exchange with the heavier cold gas, promoting further mixing of fresh air with the unreacted fuel and thereby enhancing the combustion. Fire storms have been known for some time to result from such action in large fires.
- Gradients in, or nonuniform distribution of, temperature and/or composition may actually act to slow down and even inhibit the combustion process, although under certain conditions they may enhance it. This is particularly true when ignition occurs near the lower flammability limit (LFL) and proceeds toward the composition of stoichiometry. Higher initial temperatures expand the flammability limits and thus promote combustion into regions below the LFL at normal temperatures and pressures.
- Rough terrain can significantly alter the combustion process by disturbing the flow of the gas mixture and producing wrinkles and vortexes in the flame front, which enhance burning.
- Weather conditions are important. For example, rain will increase the evaporation rate of the spilled liquefied gas, and wind will generate large disturbances in the flow of the gas cloud.

All these phenomena may affect the combustion process individually, and they may also work together to multiply their individual effects--i.e., they may depend synergistically on each other and thereby cause further enhancement. They all affect the process in one common fashion: They distort the flame and thereby increase its burning surface area and burning rate. In more general terms, they disturb the flow in front of the flame and produce a condition known as turbulence.

Turbulence is a very broad term for nonuniformities created in the flow. It may be caused internally by a self-generating process such as shifting of local volumes of gas due to buoyancy effects, or it may be caused by external means such as physical obstacles (trees, houses, bridges, etc.) or by atmospheric motions such as winds of various intensity. All these effects produce turbulent eddies of different size and intensity. So, in order to associate turbulence with flame acceleration, one must first learn how to define the size and intensity of the turbulent eddies, and then determine their effect on the propagation of the flame.

CURRENT EXPERIMENTAL EFFORT

Led by the necessity to understand the phenomenon of flame acceleration before large spills of LNG are subjected to an accidental or planned ignition, we began our own small-scale laboratory experiments in an open semiconfined test chamber. The system, illustrated in Fig. 2, is 90 cm long, 30 cm high,

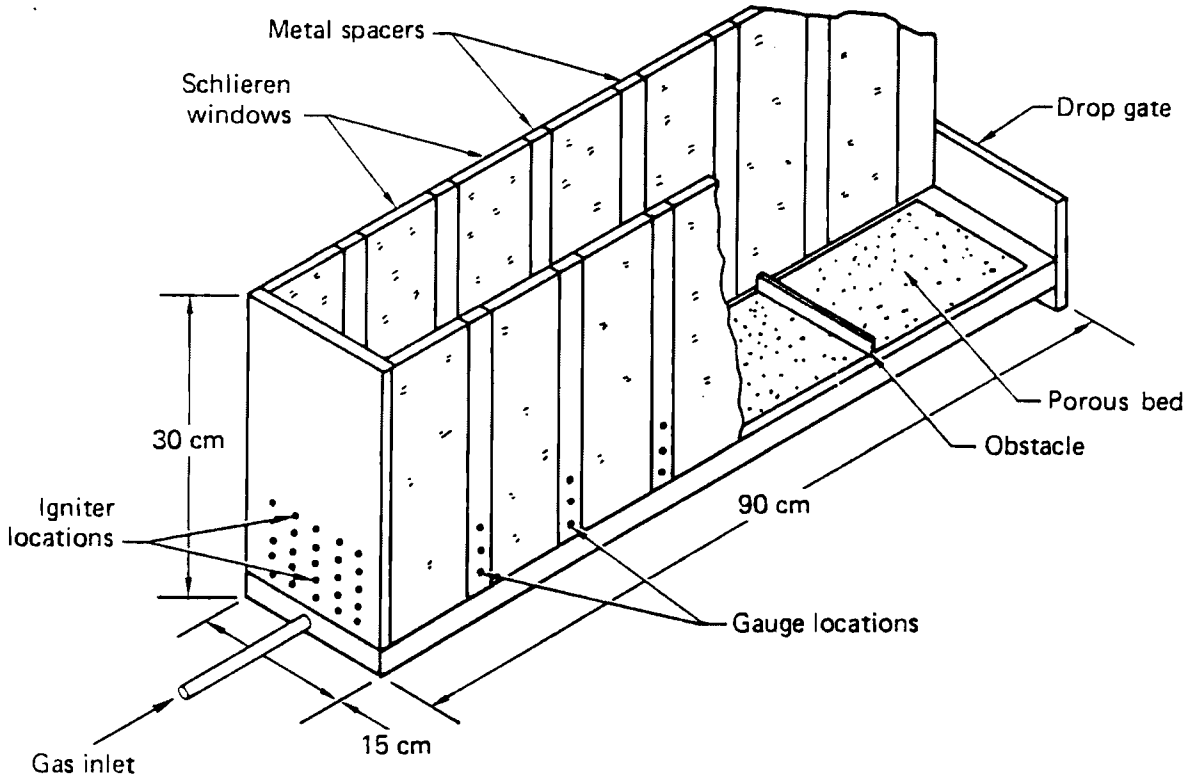

FIG. 2. Open test chamber used to carry out the semiconfined combustion experiments described in this report.

and 15 cm wide. It is open on top and at the far end to prevent pressure buildup due to confinement. The sidewalls are made of high-quality glass panels to allow optical observation with a 30.5-cm schlieren system. Metal ribs between individual glass panels serve as holders for ionization probes and pressure gauges. A bank of 25 spark plugs is installed in the back wall to provide the type of ignition desired. A single spark plug can be fired for a point-source ignition, five spark plugs for a line ignition, or even all 25 simultaneously for a plane ignition. The open far end is provided with an adjustable drop door, which is held in place so as to block only a certain part of the test chamber and then released just before firing.

The floor of the test chamber is porous, made of sintered brass, to allow filling from the bottom across the whole horizontal cross section. Under the porous floor there is a plenum chamber, which is filled from a cylinder containing premixed gas, through a safety-designed manifold system. The filling is monitored by an MSI-type concentration sensor initially calibrated for a particular mixture desired.

The orientation of the test chamber shown in Fig. 2 is for experiments with heavier-than-air propane gas. For the lighter-than-air methane gas the system will have to be turned and held upside down. All the tests in this series were carried out with premixed, CO-balanced, propane-air mixtures, i.e., 5.66 vol% propane in air. The height of the cloud is controlled by the height of the drop door at the end of the chamber, or by a removable sliding sheet placed at a particular height during the filling procedure and removed just before firing.

To study the effect of turbulence, we placed obstacles on the floor across the whole width of the chamber. They were 35 and 92 mm high, evenly spaced 9.5 cm apart behind each metal spacer to allow unobstructed view of the pocket burnout. If more details of the flow pattern over the individual obstacles are desired, the obstacles can be placed anywhere in the field of view as well.

Since our gas supply was from a cylinder of premixed gas, the whole operation had to be handled remotely from a control panel outside the test cell. For better visualization of what happens during the experiment, a TV monitor was installed with a videotape recorder. Thus, in addition to the more familiar diagnostic techniques mentioned above, we have an instant replay capability to check qualitatively the speed and shape of the flame front.

EXPERIMENT RESULTS

The results described here are based on the data taken during the first phase of our investigation, which was conducted in a laboratory given to us for a limited time only. Some changes became necessary during the course of this investigation, and for lack of time previous runs could not be verified under the new conditions. This resulted in some ambiguity in interpretation and difficulty in making firm conclusions.

One of the main objectives of this laboratory-scale investigation was to test the applicability of ionization probes as time-of-arrival detectors of the flame front. We planned to verify the ionization probe results against those of the optical schlieren system, which gives visual indications of how the flame propagates. Comparisons of the ionization probe data with the schlieren records are given in Figs. 3, 4, and 5 (see pages 20-22) for the case of no obstacles, small obstacles (35 mm), and large obstacles (92 mm). These figures are time-space diagrams, with time starting from the firing signal that goes to the spark ignition source. The space scale contains information about location of individual windows as well as location of the metal spacers holding the ionization probes.

The 12-inch (30-cm) schlieren system allowed us to photograph the event through only three windows at a time. To follow the combustion process through the entire flame bed, we had to make a composite from records of four different tests. This is evident from the four separate arrays of schlieren data denoting the flame path as it appears on the photograph. The breaks in time illustrate variations from one test to another.

The ionization probe data corresponding to the same four tests are illustrated by points connected with dashed lines.

The apparent discrepancy between electronic and optical visualization is due to the physical position of the respective measurements. While the ionization probes, being located at the wall, sense the flame only when it passes through at that location, the optical measurement is made at the very tip of the flame front, which may be a significant distance ahead of the flame's trailing edge near the wall. This phenomenon is particularly evident in the no-obstacle case, illustrated in Fig. 6. Here ionization probes were placed near the bottom of the test chamber, and the tip of the flame front, where the optical measurements are made, appears to be some 12 cm above that location. In tests with the obstacles, the ionization probes were placed at the wall but

just above the height of the obstacles. The flame passing over the obstacles must have spread over the entire width of the flame bed, and hence gave better correlation between the two flame-detection systems. Sets of schlieren photographs taken with small and large obstacles are shown in Figs. 7 and 8 respectively.

In determining the velocity of the flame front, the ionization probe data alone can sometimes be very misleading. In cases where the obstacles are raised some distance above the floor, the flame may jet under an obstacle into the next pocket and reach the next ionization probe before the main body of the flame, which propagates above the obstacles. This phenomenon is illustrated in Fig. 9, which represents the time-space diagram for shot 77. One frame of the photographic sequence--showing the flame jetting under the obstacle—is shown as an insert; the exact time of the frame is 120.4 ms after ignition. The analysis shows that the two flame fronts pass over obstacles at velocities of 6.4 and 8.6 m/s respectively. But the local flame velocity, if deduced from the ionization probe data, reaches a value as high as 117 m/s.

This discrepancy leads us to an important observation: It may not be the actual velocity of the flame front that is significant. but rather the rate at which the total mass of original gas mixture is transformed into products of combustion. After all, it is the total burnout time that determines the rate of maximum volume expansion due to combustion--not the local burning velocity. This overall reaction time leads to a maximum rate of energy release which in turn is the cause for generation of overpressure in the system.

The ionization-probe detection system is very useful, and perhaps in some cases even more important than the optical system, especially during large-scale tests, when the optical system becomes very impractical or simply unavailable. However, as evident from Fig. 9, one should not blindly accept the value of the local flame velocity as determined from two adjacent ionization probes, but rather one should take the whole array of these probes and get an average value of the flame propagation rate.

Another objective of this investigation was to measure the velocity of the flame front under various conditions and see whether we could detect any acceleration that might be caused by introducing obstacles into the flow or by changing some of the initial conditions.

To establish the baseline against which we could observe the effects of introducing barriers into the flow, we ran a few tests without obstacles. Figure 10 shows a time-space plot of all the ionization probe data taken for

the shots with no obstacles. On the time-space diagram the slope of the trace indicates the velocity of propagation. Thus, in this case the flame propagated through the chamber with a velocity on the order of 2-3 m/s. The trace of 10 m/s occurred when a plate covering the lower portion of the chamber was introduced at a height of 14 cm above the floor. The flame speed without upper confinement agrees well with Lee's prediction of laminar burn rate modified by the density ratio across the flame:

$$R_f = V + S_L$$

$$= \frac{\rho_0}{\rho_1} S_L + S_L$$

$$= \left(\frac{\rho_0}{\rho_1} + 1 \right) S_L = 8.5(0.43) \approx 3.2 \text{ m/s} \quad .$$

Here S_L is the laminar burning velocity of the mixture, ρ_0 and ρ_1 are the density before and after burning, respectively, V is the flow velocity of the gas put into motion by the flame, and R_f is the flame speed relative to a stationary observer.

Introduction of obstacles into the flow led to higher flame velocities. In this series of tests only two obstacle heights were used: 35 and 92 mm. Spacing is also expected to have some effect, but it was not varied here.

Figure 11 shows the ionization probe records taken with both small and large obstacles in the flow, plotted on the time-space diagram as before. From this figure it appears that the smaller obstacles have a larger effect on the flame velocity, accelerating it to 6 m/s as compared with only 4 m/s for the higher obstacles. This result, however, may not be conclusive: As we mentioned earlier, in this series of tests we did not vary the spacing between obstacles, and that may very well have an effect.

During this investigation, one modification of the system led to the next; to improve the filling procedure, a modification of the obstacle was introduced which inadvertently produced a dramatic increase in flame acceleration. All obstacles were raised some 4 mm above the floor to provide space for a plate which would cover the floor and prevent gas from entering the chamber before a certain time. The increase in flame acceleration was noticed immediately, and by varying location of the ignition source it became even more dramatic.

Figure 12 is a time-space plot containing the ionization probe data taken with the 92-mm obstacles. There are three distinct groups of traces, resulting in three flame speeds. The traces with the slowest flame speed of 4 m/s were shown earlier in Fig. 11; they were taken with no space under the obstacles. The next group of traces correspond to the case where only the first three obstacles were fixed to the floor while the rest of them were raised, leaving a slot of about 4 mm and providing a passage for gas and the flame. Here the slope of the traces is smaller, indicating that the flame propagates faster. This is because the gas from the previous cell is allowed to flow through the space under the obstacle, disturbing the gas in the next pocket and setting it up for a faster burnout. Some of the traces show a sudden acceleration of the flame toward the end of the chamber. The schlieren photographs reveal the real cause for this sudden acceleration--it is the flame getting through the slot under the obstacle, starting the burnout process from the bottom up.

This phenomenon is even more pronounced in the records corresponding to the third group of traces, causing the flame to reach velocities of 20 m/s or more. In this case all the obstacles were raised about 4 mm off the floor, and there was a clear passage for both gas and flame jets to shoot under the obstacle.

Schlieren photographs illustrating both cases are shown in Figs. 13 and 14. Of interest here is the manner in which the pocket burns out and when it does so in comparison with the flame front in the main stream above the obstacles. Figure 13 is a sequence of schlieren records illustrating the flame propagation over obstacles with no space under them. Figure 14 demonstrates the effect of space under the obstacles. Initially the main stream flame appears to be faster, and the flame in the pocket is influenced by the flow induced from above. However, in the next pocket, the pocket flame develops faster and competes with the main stream flame.

Figure 15 shows the case where the pocket flame develops faster and precedes the main stream flame, causing the overall process of burning to attain a high velocity. As illustrated earlier, in a true sense the flame itself does not attain a high velocity, but only the overall process as deduced from the ionization probe data.

As was also mentioned before, in the case of raised obstacles, location of the ignition source played an important role in causing the flame to accelerate, especially during the initial stages of flame propagation. With ignition near the floor of the chamber, the flame has a shorter path to the next

pocket under the obstacle than over it, which results--as one would expect--in an almost immediate flame jetting action and hence fast flames. Ignition at a higher level above the floor may cause the flame to go faster above the obstacle and therefore slow down the initial stage of the process. If such flame travel above the obstacle persists it may bring the opposite effect of burning down and back into the previous pocket, as illustrated in the last three frames of the sequence shown in Fig. 16. The effects of ignition on the overall burnout of the system are demonstrated by the ionization probe data plotted in Fig. 17.

Thus we have seen how the flame is affected by obstacles in the flow field, causing it to propagate faster. We have seen that space under the obstacles causes the flame to accelerate even further, and we have seen the mechanism for this acceleration. We have also seen the effect of confinement (Fig. 10) and the effect of changing the ignition point (Fig. 16). What we have not seen so far is the mechanism for continuous acceleration. Unless there is a change in the flow field, such as raised obstacles for example, the flame seems to have reached its final velocity somewhere at the very beginning, near the first obstacle. After this characteristic velocity has been attained there is no visible evidence of further acceleration. This, of course, may be a limitation of our experimental scale, not only in the distance traveled by the flame but also in the height and width of the gas volume.

COMPARISON WITH OTHER INVESTIGATIONS

As mentioned before, the semiconfined geometry has not been given proper attention in previous studies, although an accidental spill in real life will most probably occur in highly nonideal conditions. We have tried to simulate the nonideal condition by working with a chamber that is partially confined but at the same time geometrically uniform and fit for computational modeling.

Lack of similar studies by other investigators makes it difficult to compare notes and make correlations of our results. However, in spite of this deficiency in available data, we think that it is still worthwhile comparing our results with those of others who have dealt, in any geometry, with flame propagation and acceleration due to obstacles. We have done this in the form of a table associating the dimensions of experimental apparatus with the maximum flame velocities attained during the tests.

Table 1 contains data from the hemispherical bag tests by Lind and Whitson,[18] cylindrical chamber tests done at McGill University[28] and Gottingen,[29] one-dimensional tube tests done at McGill University[30] and Norway,[32] and our semiconfined laboratory-scale flame bed tests. This table illustrates not only the fact that every scale-up of test apparatus leads to a considerable gain in the highest value of the flame velocity, but also the

Table 1. Comparison of final flame velocities and overpressures measured in different geometries and scales.

Geometry	Small scale	Large scale
Spherical 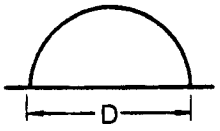	(See Ref. 26) Fuel: H_2, C_2H_4, C_3H_8 in air D = 20 cm V_{max} = 20 m/s	(See Ref. 18) Fuel: 4 to 5% C_3H_8 in air 10% CH_4 in air D = 10 to 20 m V_{max} = 5 to 12 m/s
Cylindrical 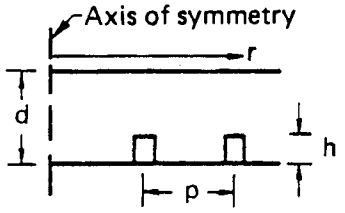	(See Ref. 28) r = 30 cm d = 1.27 to 6.37 cm h = 1.27 to 2.2 cm p = 1.27 to 5.43 cm V_{max} = 130 m/s ΔP_{max} =	(See Ref. 29) r = 120 cm d = 3.5 to 20 cm h = 1.25 to 4 cm p = 3.75 to 10 cm V_{max} = 415 m/s ΔP_{max} = 0.64 bar
Open tube 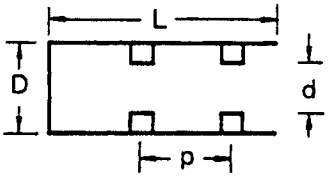	(See Ref. 30) L = 1.2 m D = 15.2 cm, 6.3 cm d = 4.45 cm, 10.75 cm p = 7.5 to 10 cm $1 - (d/D)^2 = 0.5$ V_{max} = 100 m/s, 550 m/s ΔP_{max} = 10.9 bars	(See Ref. 31) L = 10 m D = 2.5 m d = 1 to 2.1 m p = 0.5 to 2.5 m $1 - (d/D)^2 = 0.3$ to 0.84 V_{max} = 800 m/s ΔP_{max} = 5 bars
Open channel 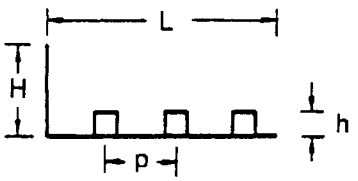	L = 90 cm H = 30 cm h = 3.5 to 9.2 cm p = 9.5 cm V_{max} = 10 m/s	

danger of underestimating the relationship of one type of conditions to the other. There is no doubt that in experiments conducted by Lee and his group,[28-31] confinement plays a significant role; but one should not overlook the effect of obstacles within that confinement.

In semiconfined geometries, one does not expect the flame to attain as high a velocity as in a confined tube. However, the inertial confinement of a large cloud may affect the outcome sufficiently to cause a substantial overpressure, which otherwise would not be expected.

CONCLUDING COMMENTS

We have briefly reviewed the general aspects of flame propagation through gaseous combustible media and the results of work done so far in confined, unconfined, and semiconfined geometries. Present understanding of the problem is formulated, and some of our experimental efforts in this area are described. The effect of obstacles on flame propagation in a semiconfined test chamber has been demonstrated. Our analysis of the photographic schlieren records depicting flame structure and its interaction with obstacles provides us with a clear visual picture of the process and a proper perspective for planning future experiments. The ultimate aim of the program is to gain confidence in identifying different factors affecting the flame acceleration process and to put them into computational models so that we can attain predictive capability for larger and more complicated cases. Small-scale experiments followed by intermediate-scale field tests will provide the necessary input for attaining this goal.

ACKNOWLEDGMENTS

The author wishes to thank all those who helped him formulate the scope of the program, design and construct the apparatus, and finally decipher the results. In particular, he would like to extend his gratitude to Steve Perry for invaluable technical assistance in running the experiments.

REFERENCES

1. D. C. Bull, J. E. Elsworth, and G. Hooper, "Susceptibility of Methane/Ethane Mixtures to Gaseous Detonation in Air," Combustion and Flame 34, 327-330 (1979).
2. A. L. Kuhl, M. M. Kamel, and A. K. Oppenheim, "Pressure Waves Generated by Steady Flames," 14th Symposium (International) on Combustion (The Combustion Institute, Pittsburgh, Pa., 1973), pp. 1201-1215.
3. R. A. Strehlow and W. E. Baker, The Characterization and Evaluation of Accidental Explosions, NASA CR 134779 AAE 75-3. Prepared for Aerospace Safety Research and Data Institute, Lewis Research Center, Cleveland, Ohio (1975).
4. R. A. Strehlow, "The Blast Wave from Deflagrative Explosions: An Acoustic Approach," paper presented at 13th Loss Prevention Symposium of AIChE, Philadelphia, Pa., June 1980.
5. L. E. Bollinger, "Formulation of Detonation Waves in Combustible Gaseous Mixtures," paper 4-15 presented at WSS/CI meeting, Stanford University, Stanford, Calif., April 1966.
6. A. K. Oppenheim, "On the Dynamics of the Development of Detonation in a Gaseous Medium," Archiwum Mechaniki Stosowanej 2(16), 403-424 (1964).
7. J. P. Saint-Cloud, Cl. Guerraud, C. Brochet, et N. Manson, "Quelques Particularités des Détonations Très Instables dans les Mélanges Gazeux" ("Some Particularities of Very Unstable Detonations in Gaseous Mixtures"), Astronautica Acta 17, 487-498 (1972). (In French.)
8. H. Gg. Wagner, "Reaction Zone and Stability of Gaseous Detonations," Ninth Symposium (International) on Combustion (Academic Press, New York, 1963), pp. 454-460.
9. K. I. Shchelkin, "Instability of Combustion and Detonation in Gases," Soviet Physics--Uspekhi 8(No. 50), 780-797 (1966).
10. A. K. Oppenheim, N. Manson, and H. Gg. Wagner, "Recent Progress in Detonation Research," AIAA Journal 1(No. 10), 2243-2252 (1963).
11. J. H. Lee, R. I. Soloukhin, and A. K. Oppenheim, "Current Views on Gaseous Detonation," Astronautica Acta 14, 565-584 (1969).
12. R. A. Strehlow, "Gas Phase Detonations: Recent Developments," Combustion and Flame 12(No. 2), 81-101 (1968).

13. H. Freiwald and H. W. Koch, "Spherical Detonations of Acetylene-Oxygen-Nitrogen Mixtures as a Function of Nature and Strength of Initiation," Ninth Symposium (International) on Combustion (Academic Press, New York, 1963), pp. 275-281.

14. S. M. Kogarko, V. V. Adushkin, and A. G. Lyamin, "Investigation of Spherical Detonation in Gaseous Mixture," Nauchno-Tekhnich. Probl. Gorenia i Vzryva, No. 2, 22-34 (1965). (In Russian.)

15. G. Bach, R. Knystautas, and J. H. Lee, "Initiation Criteria for Diverging Gaseous Detonations," 13th Symposium (International) on Combustion (The Combustion Institute, Pittsburgh, Pa., 1971), pp. 1097-1110.

16. J. H. Lee, "Initiation of Gaseous Detonation," Annual Reviews of Physical Chemistry 28, 75-104 (1977).

17. D. C. Bull, J. E. Elsworth, and G. Hooper, "Concentration Limits to Unconfined Detonation in Ethane/Air," Combustion and Flame 35(No. 1), 27-40 (1979).

18. C. D. Lind and J. C. Whitson, Explosion Hazards Associated with Spills of Large Quantities of Hazardous Materials. Phase II, U. S. Dept. of Transportation, USCG, ORD, Washington, D.C., CG-D-85-77 (1977).

19. H. Pfortner, "Zundverhalten von Erdgas/Luft-Gemischen in Freien Wolken" ("Ignition of Natural-Gas/Air Mixtures in Free Clouds"), GWF-Gas/Erdgas 120, 19-24 (1979).

20. S. M. Kogarko, "Generation of a Spherical Detonation in Gaseous Mixtures," paper presented at EUROMECH 82 Symposium in Warsaw, Poland, 1976.

21. W. B. Benedick, private communication (1979).

22. R. A. Strehlow, private communication (1980).

23. M. Kaptein and C. E. Hermance, "Horizontal Propagation of Laminar Flames Through Vertically Diffusing Mixtures Above a Ground Plane," 16th Symposium (International) on Combustion (The Combustion Institute, Pittsburgh, Pa., 1976), pp. 1295-1306.

24. E. M. Kawensky, D. W. Mitchell, and E. C. Seiler, "Flame and Pressure Development from Gas Explosions in the Experimental Coal Mine," paper presented at 12th International Conference of Directors of Safety in Mines Research, Dortmund, Germany, 1967.

25. H. Pförtner, private communication (1979).

26. B. Deshaies and J. C. Leyer, "Flow Field Induced by Unconfined Spherical Accelerating Flames," Combustion and Flame 40(No. 2), 141-153 (1981).

27. P. G. Huseman, Two and Three Dimensional Unconfined Flame Studies, M.S. thesis, University of Illinois (1979).

28. I. O. Moen, M. Donato, R. Knystautas, and J. H. Lee, Flame Acceleration Due to Turbulence Produced by Obstacles, McGill University, Montreal, Canada, preprint (1979).

29. I. O. Moen, M. Donato, R. Knystautas, J. H. Lee, and H. Gg. Wagner, "Turbulent Flame Propagation and Acceleration in the Presence of Obstacles," Proceedings of the Seventh International Colloquium on Gas Dynamics of Explosions and Reactive Systems, to be published as Progress in AIAA in 1980.

30. C. Chan, J. H. S. Lee, I. O. Moen, and P. Thibault, "Turbulent Flame Acceleration and Pressure Development in Tubes," McGill University, Montreal, Canada, private communication (1980).

31. C. Chan, I. O. Moen, and J. H. S. Lee, "Influence of Confinement on Flame Acceleration due to Repeated Obstacles," McGill University, Montreal, Canada, private communication (1981).

32. I. O. Moen, private communication on experiments in Norway (August 1980).

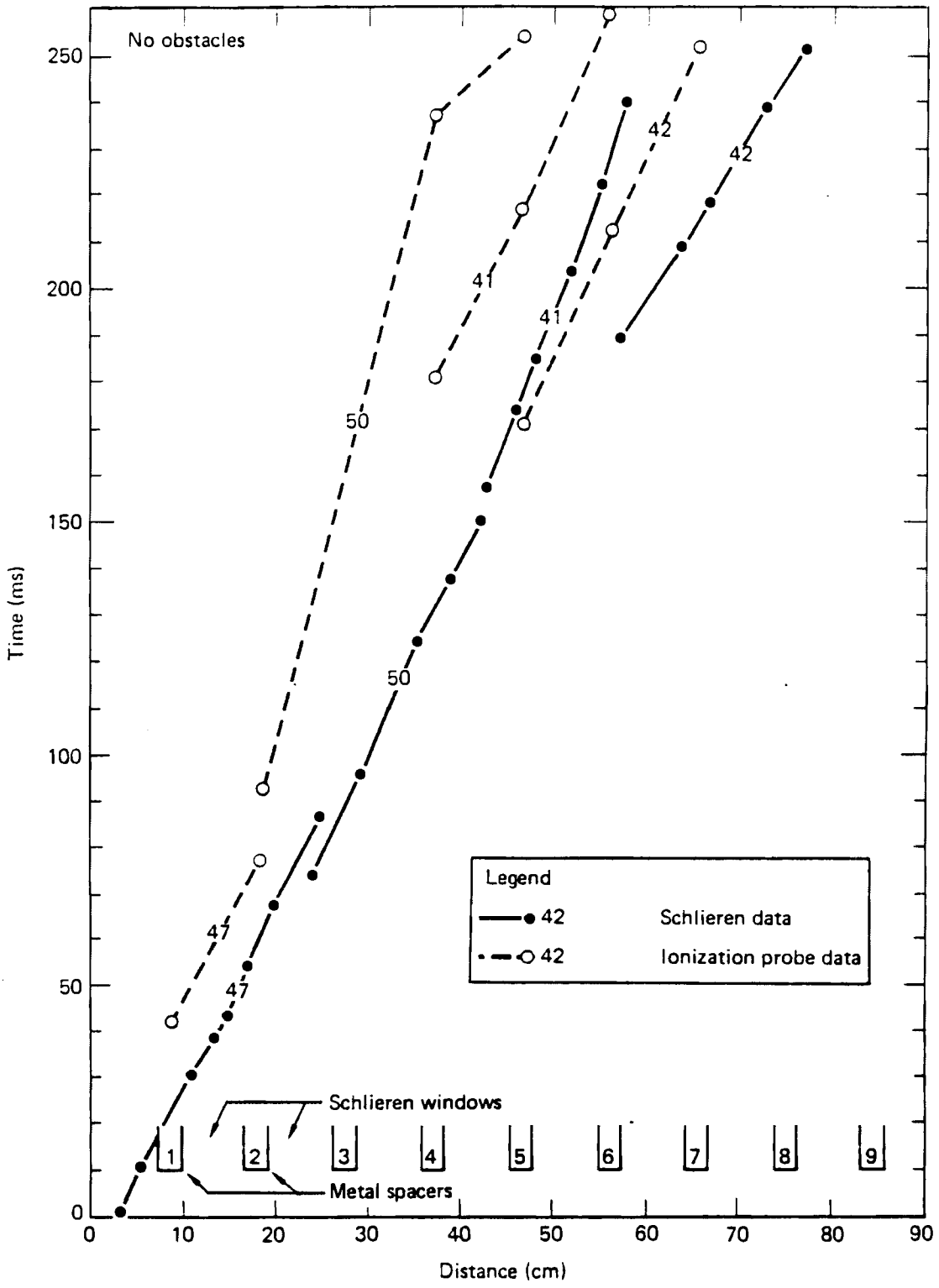

FIG. 3. Time-space plots of the burning process with no obstacles in the chamber, showing correlation between the ionization probe data and the schlieren records. Arabic numerals represent shot numbers.

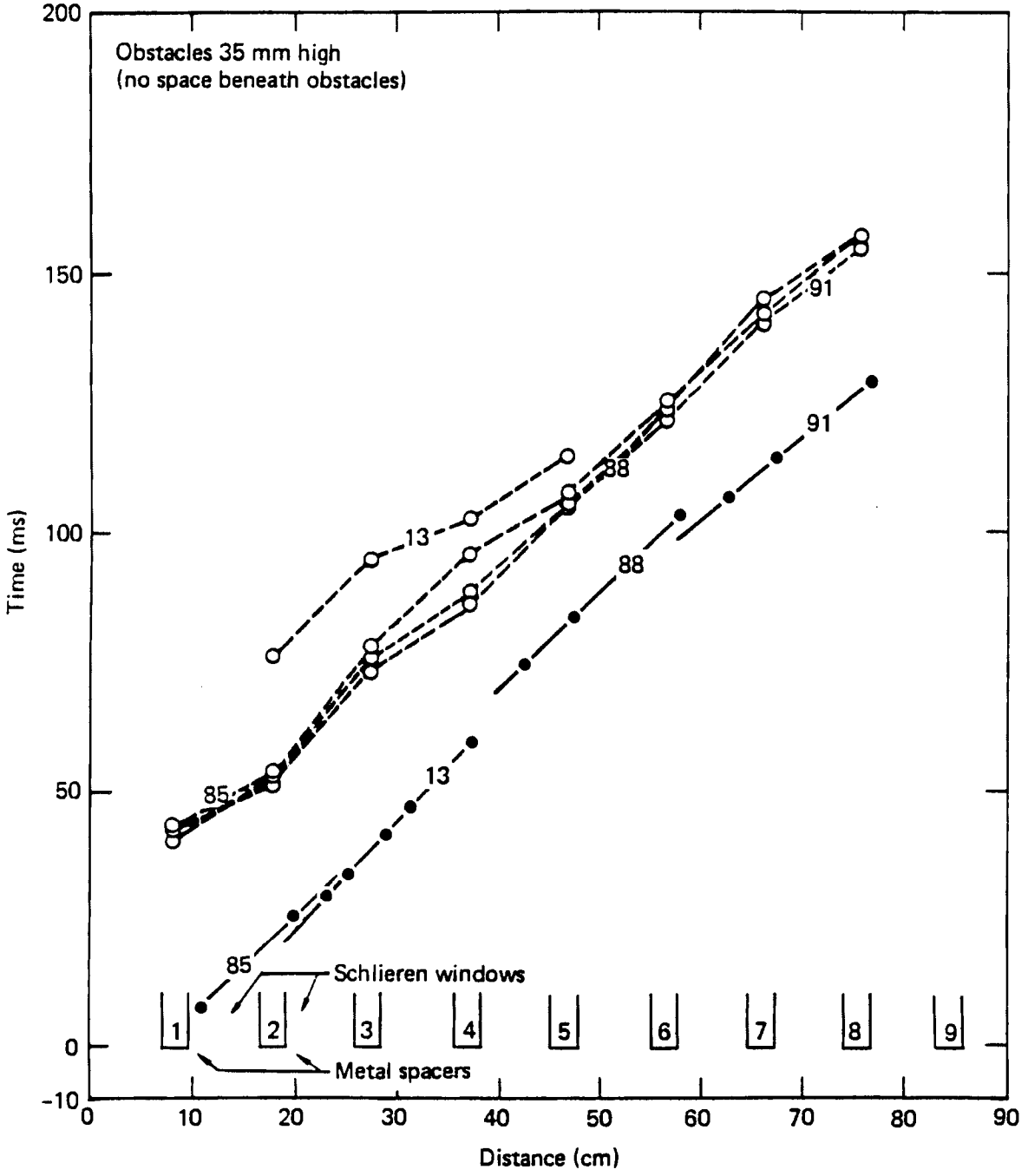

FIG. 4. Time-space plots of the burning process with 35-mm obstacles in the chamber, showing correlation between ionization probe data and schlieren records.

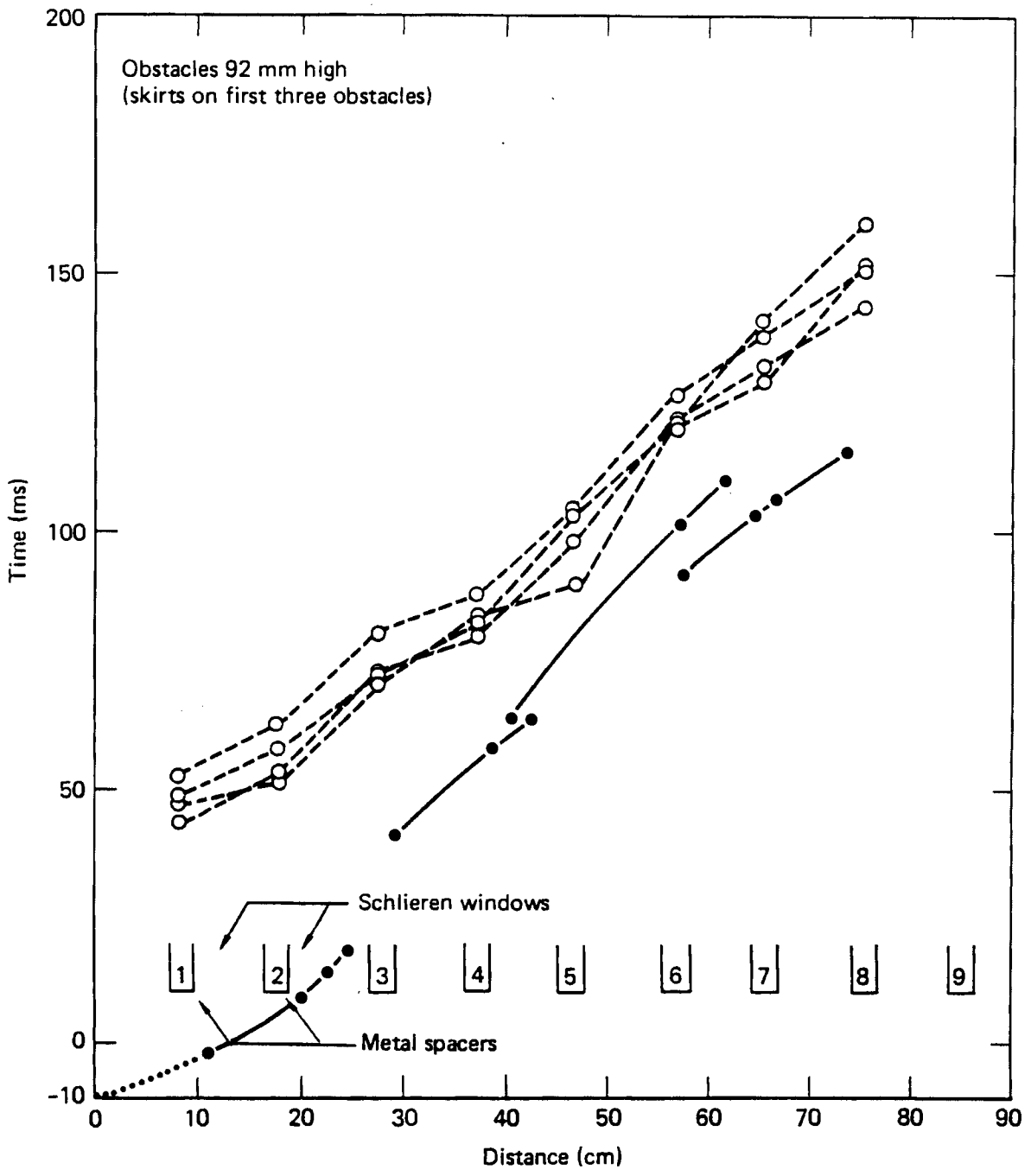

FIG. 5. Time-space plots of the burning process with 92-mm obstacles in the chamber, showing correlation between ionization probe data and schlieren records.

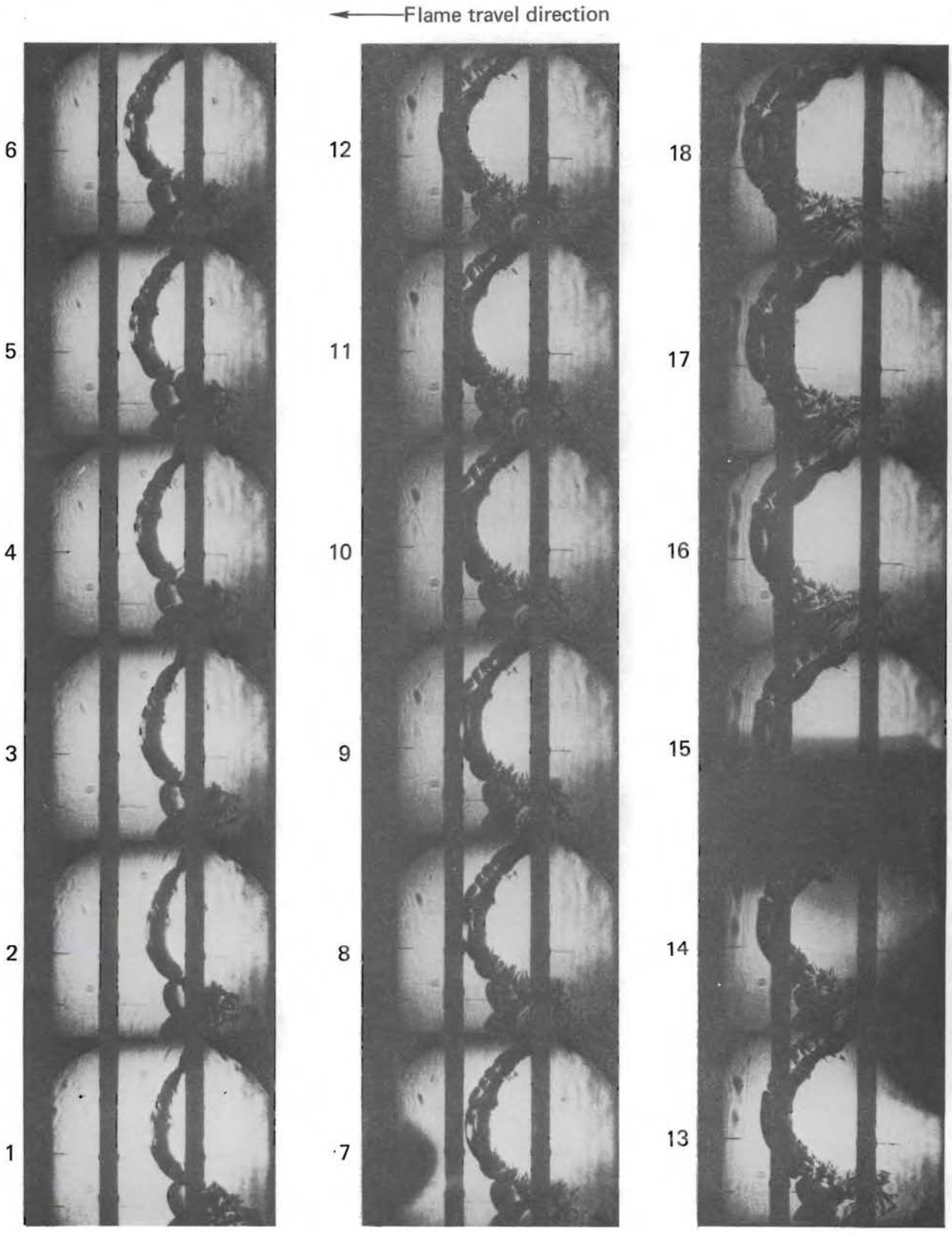

FIG. 6. Sequence of schlieren photographs made on shot 50 (time interval 2.17 ms). Sequence begins at lower left corner, flame travels from right to left. This sequence was used to correlate ionization probe data in Fig. 3.

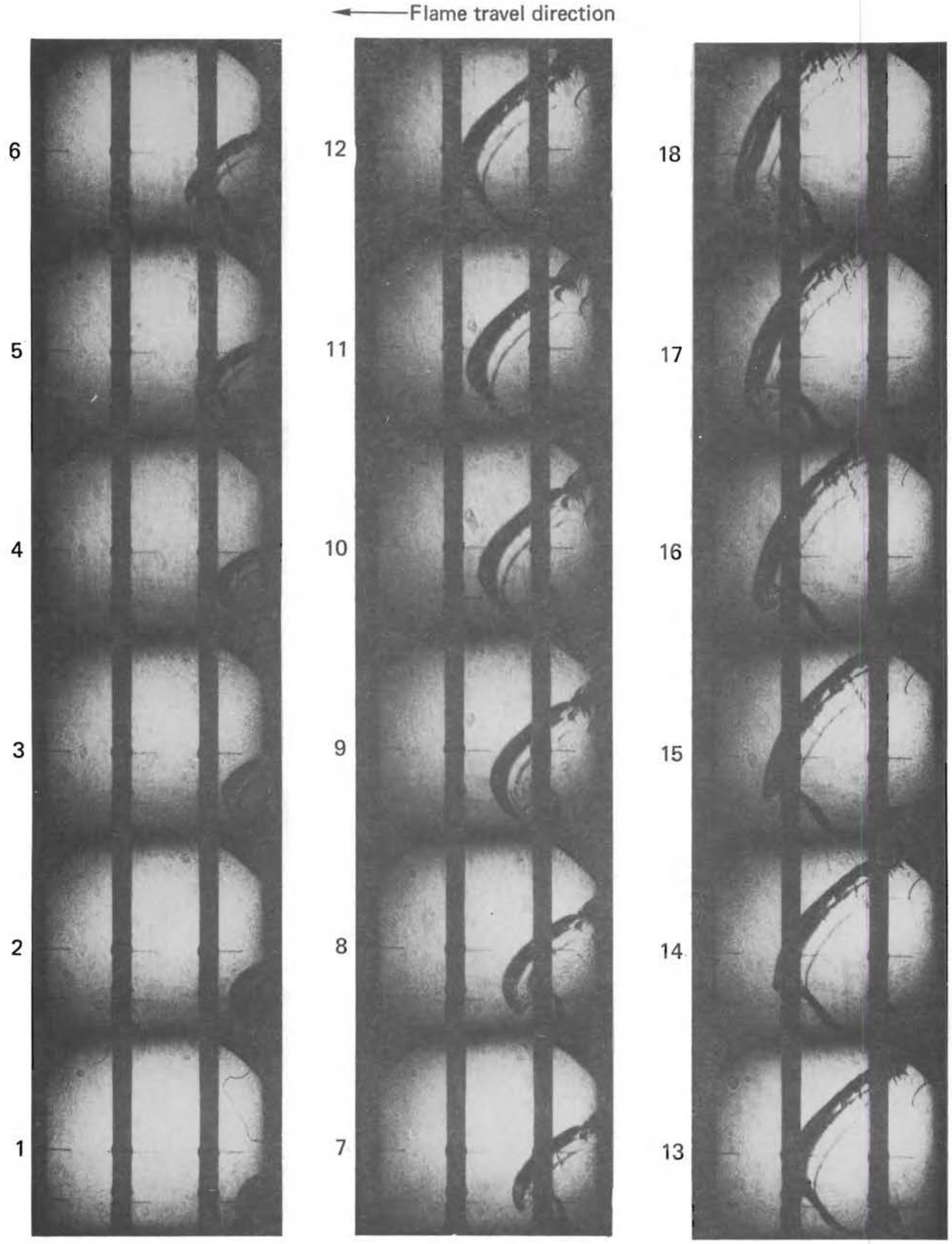

FIG. 7. Sequence of schlieren photographs made on shot 85 (time interval 2.17 ms). Sequence begins at lower left corner, flame travels from right to left. This sequence was used to correlate ionization probe data in Fig. 4.

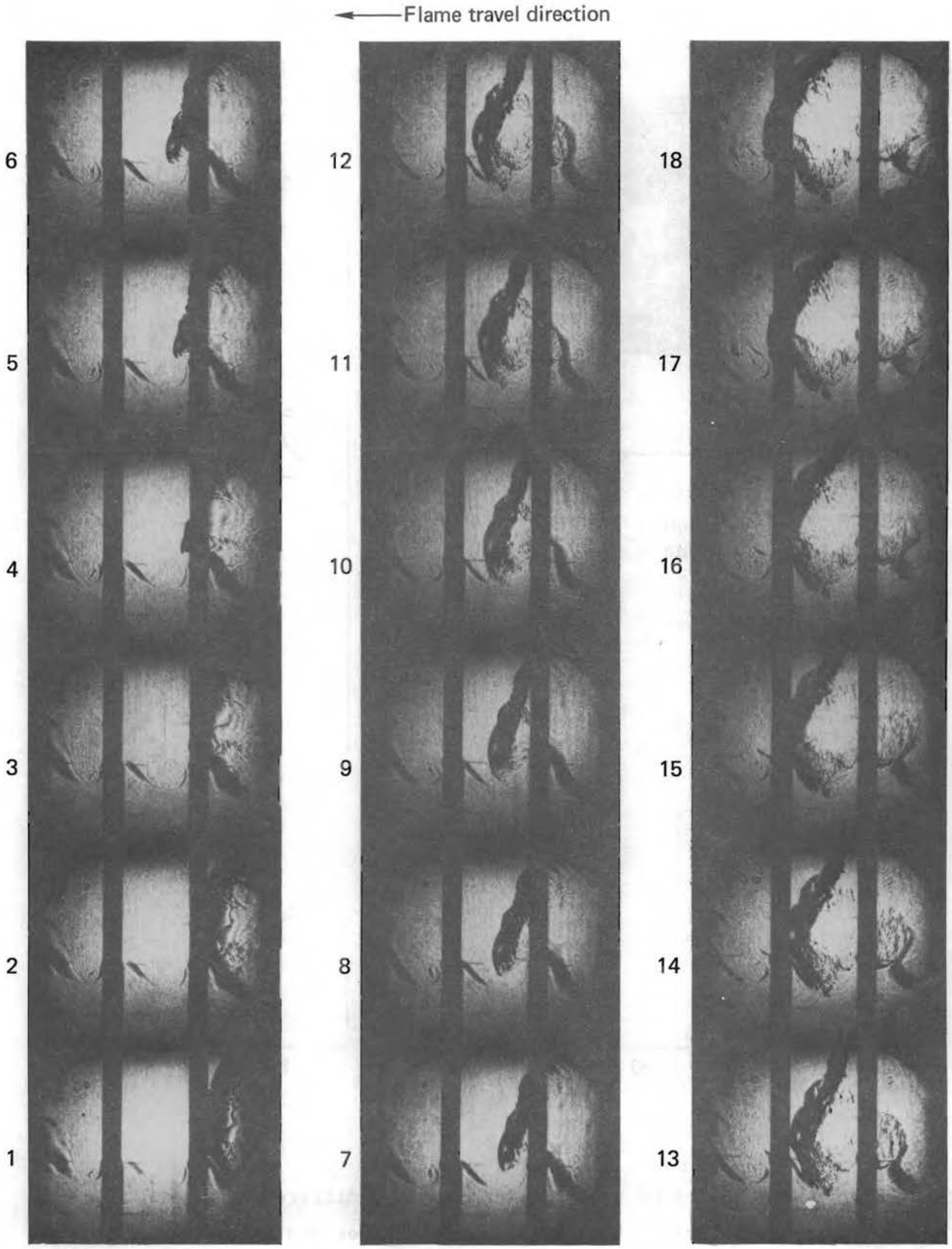

FIG. 8. Sequence of schlieren photographs made on shot 74 (time interval 1.09 ms). Sequence begins at lower left corner, flame travels from right to left. This sequence was used to correlate ionization probe data in Fig. 5.

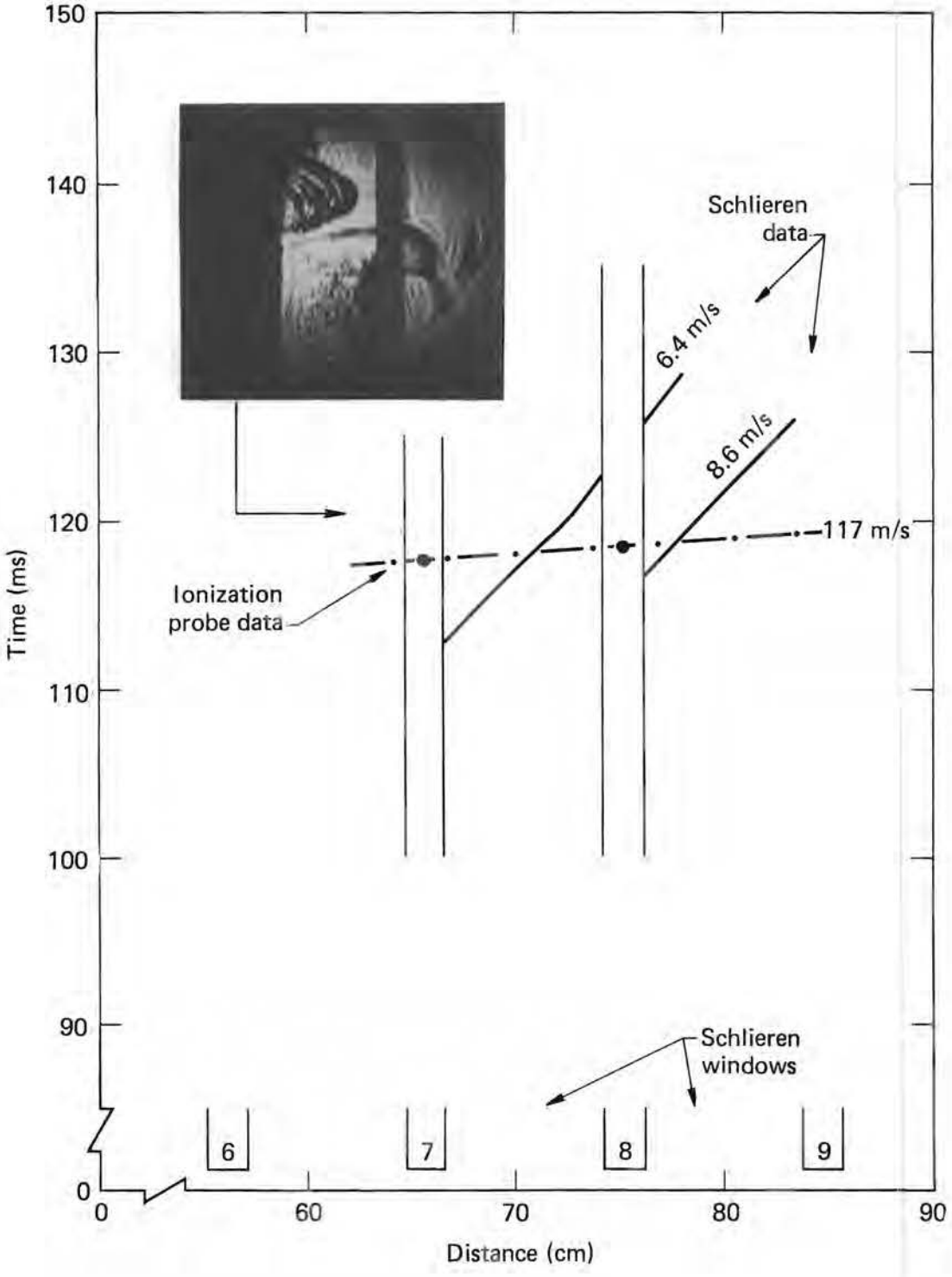

FIG. 9. Time-space plot of shot 77, illustrating difference between apparent flame velocity as indicated by the ionization probes and true flame velocity as deduced from the schlieren records. Inset photo shows convoluted flame front that produces the misleading ionization-probe data.

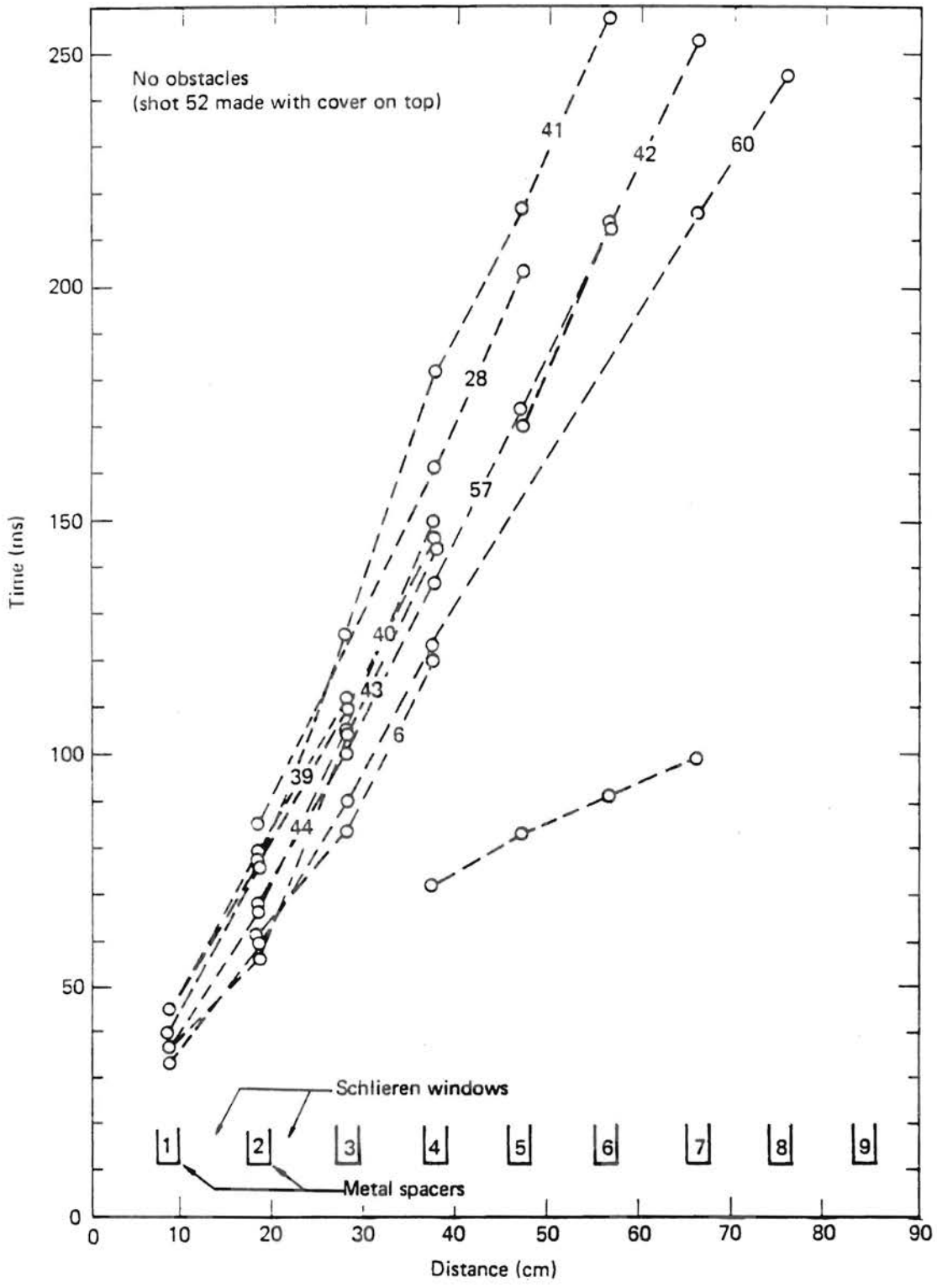

FIG. 10. Time-space plots of all ionization probe data taken with no obstacles in the chamber. Shot 52 was made with the cover left in the test chamber.

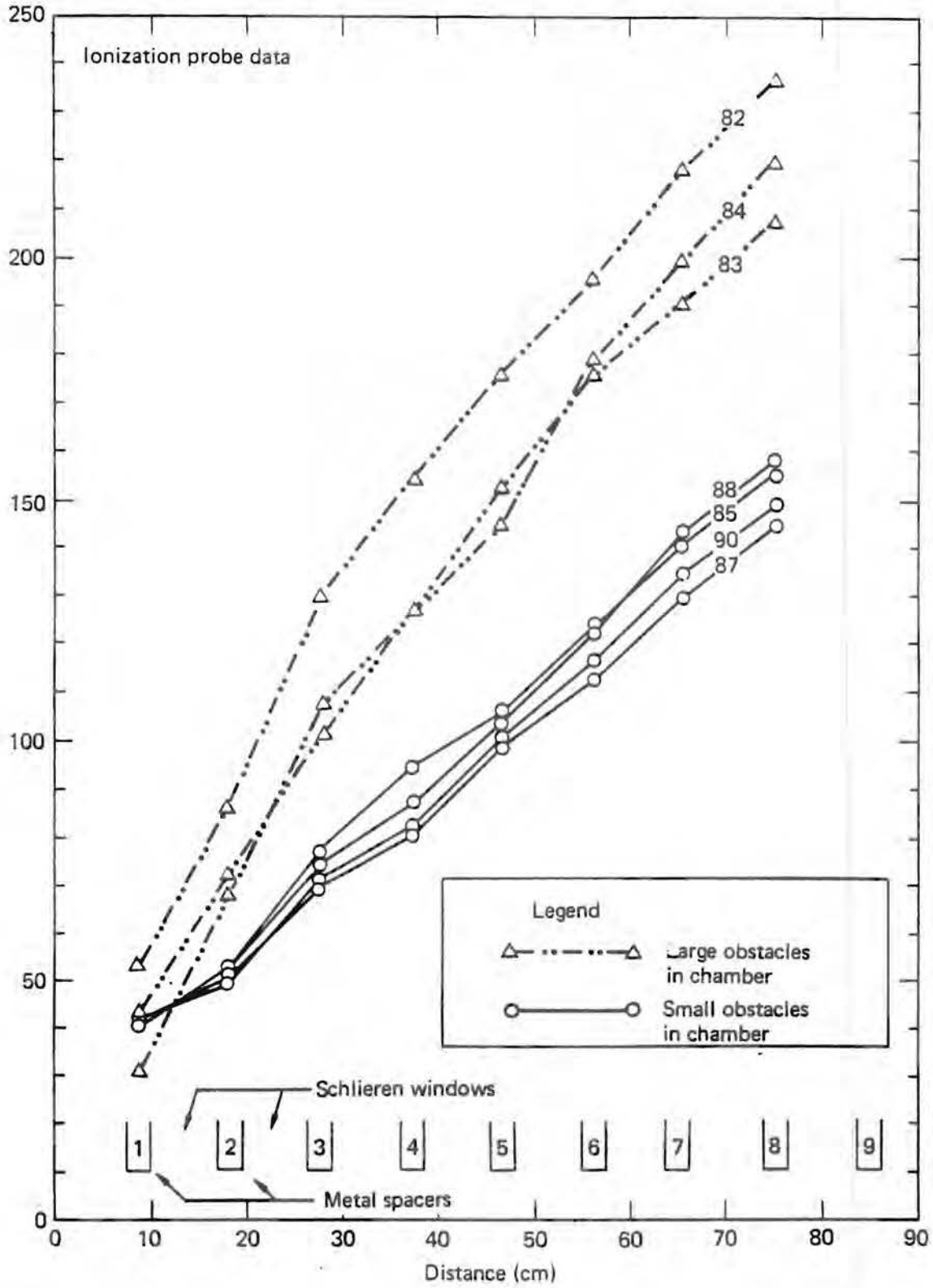

FIG. 11. Time-space plots of some ionization probe data taken with the 35-mm and 92-mm obstacles in the chamber.

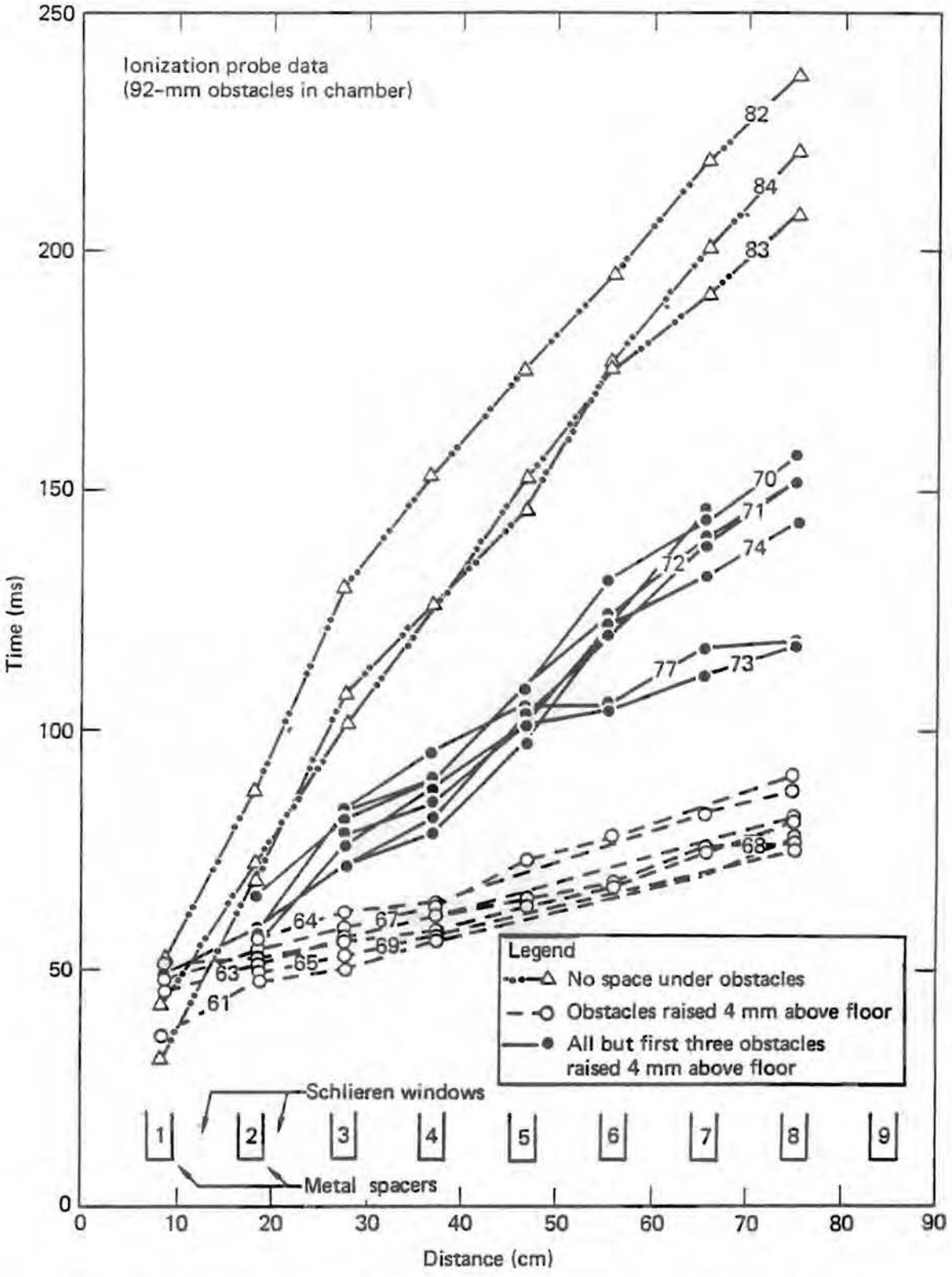

FIG. 12. Time-space plots of ionization probe data taken with the 92-mm obstacles in the chamber.

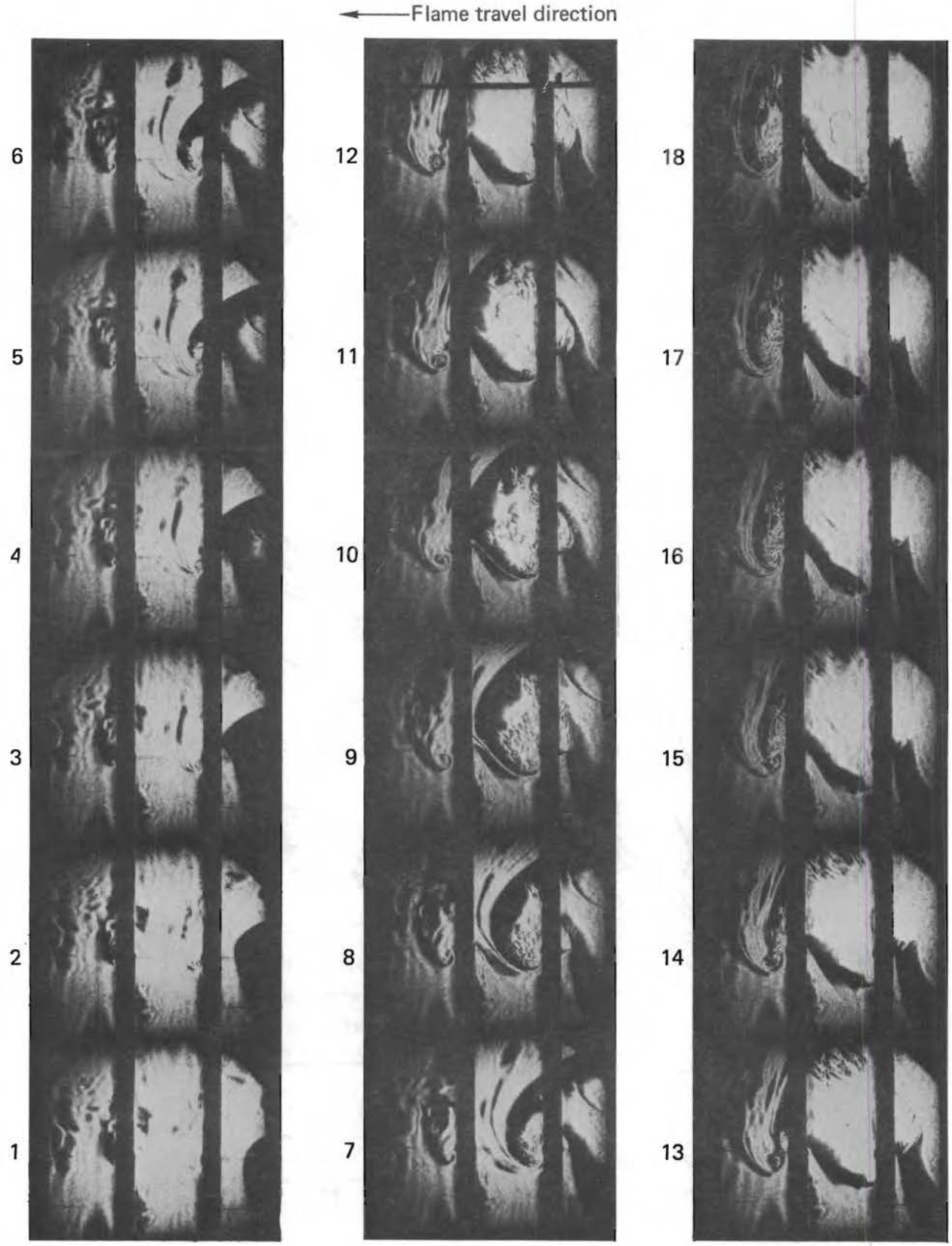

FIG. 13. Sequence of schlieren records from shot 84 (time interval 2.17 ms). Sequence begins at lower left corner, flame travels from right to left.

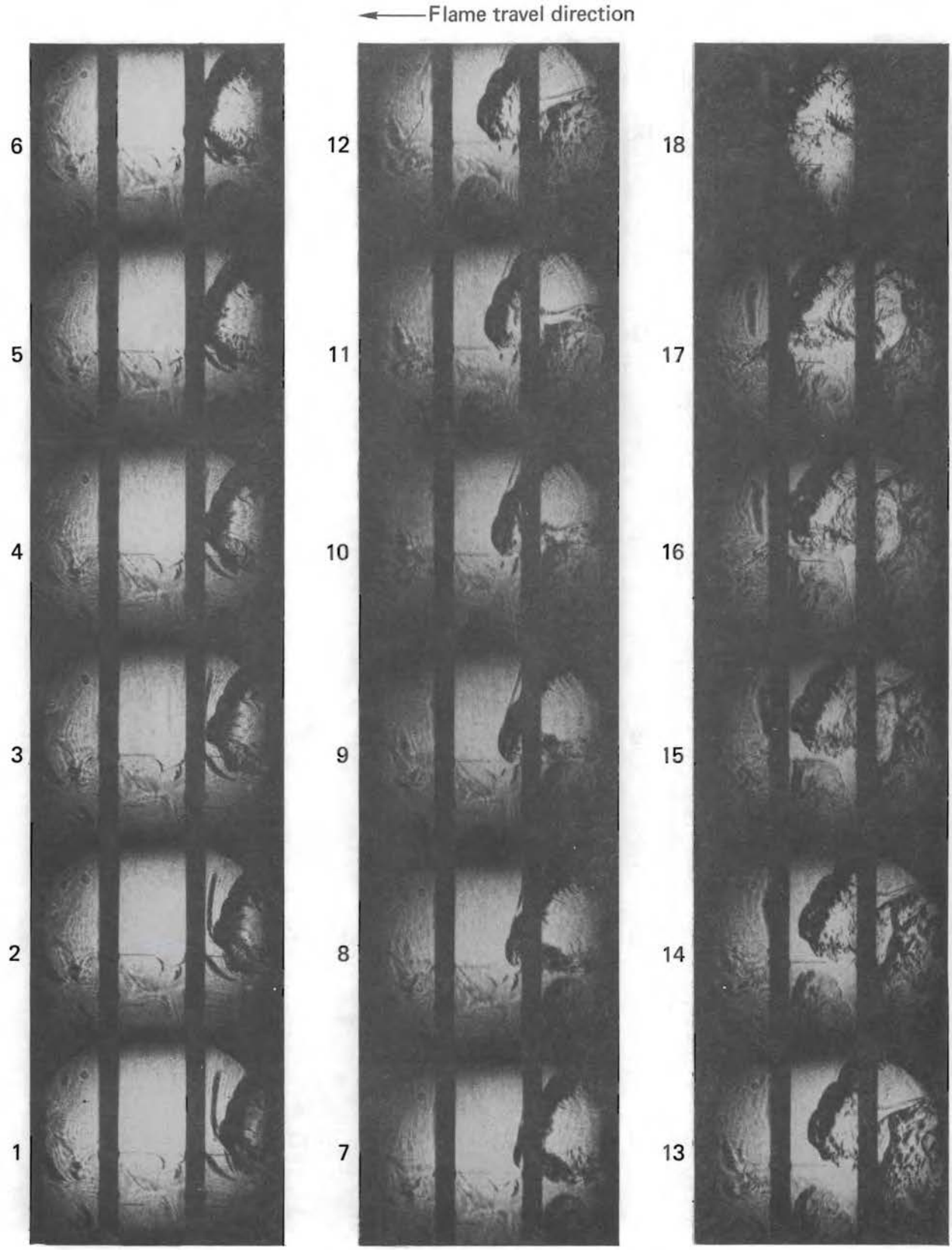

FIG. 14. Sequence of schlieren records from shot 78 (time interval 1.09 ms). Sequence begins at lower left corner, flame travels from right to left.

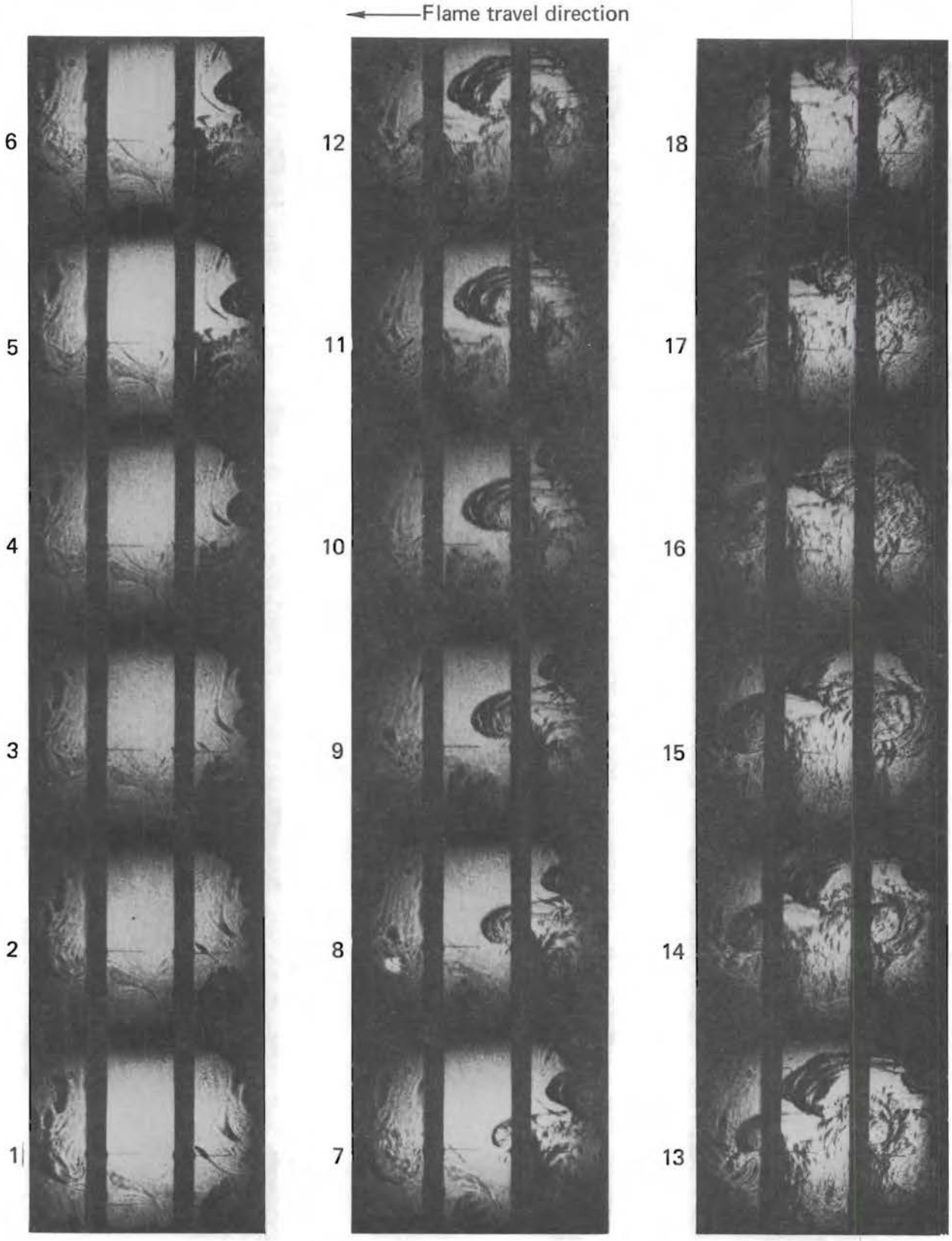

FIG. 15. Sequence of schlieren records from shot 80 (time interval 1.09 ms). Sequence begins at lower left corner, flame travels from right to left.

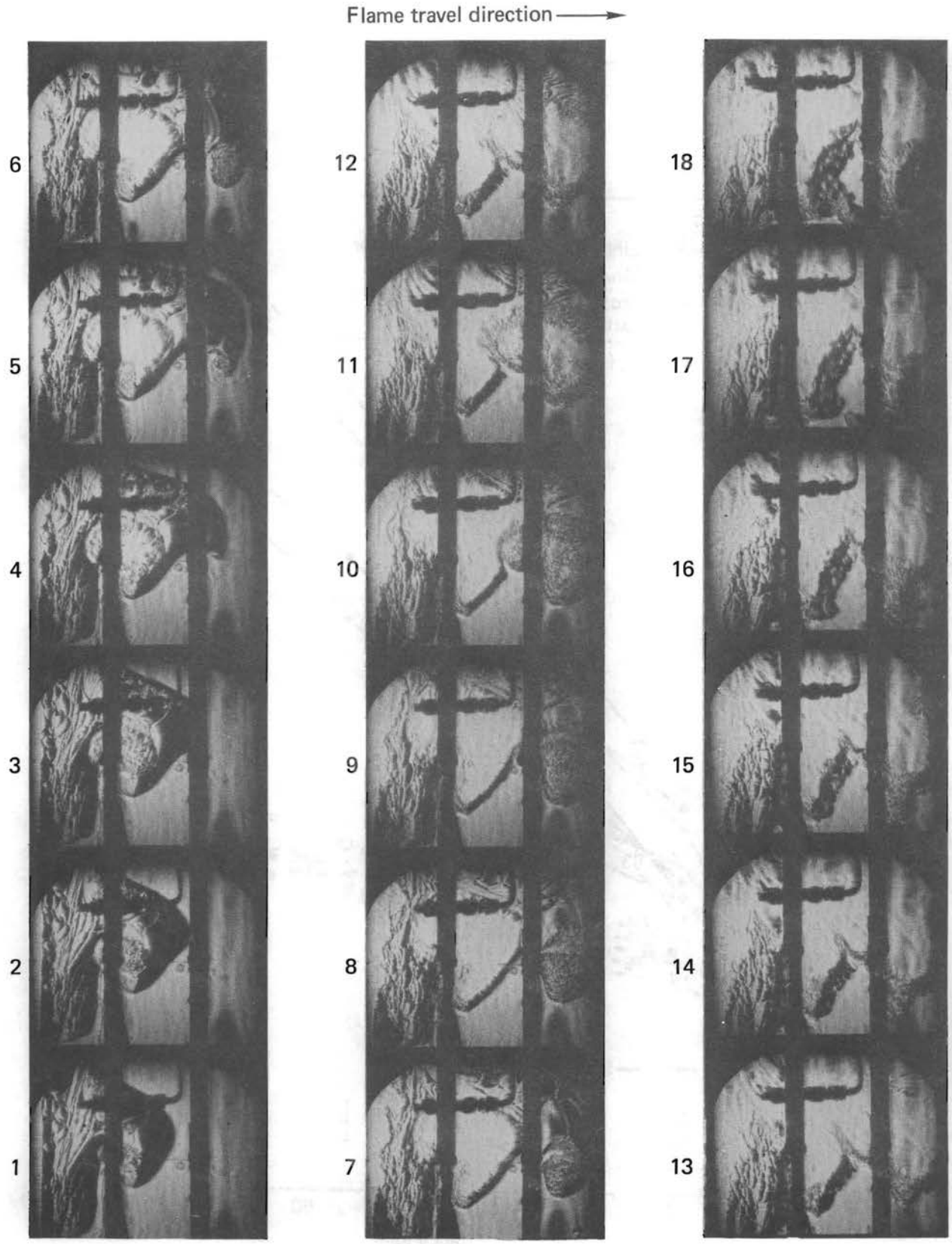

FIG. 16. Sequence of schlieren records from shot 9 (time interval 2.17 ms), depicting flame propagation back into the previous pocket through a space under the obstacle. Sequence begins at lower left corner, flame travels from left to right.

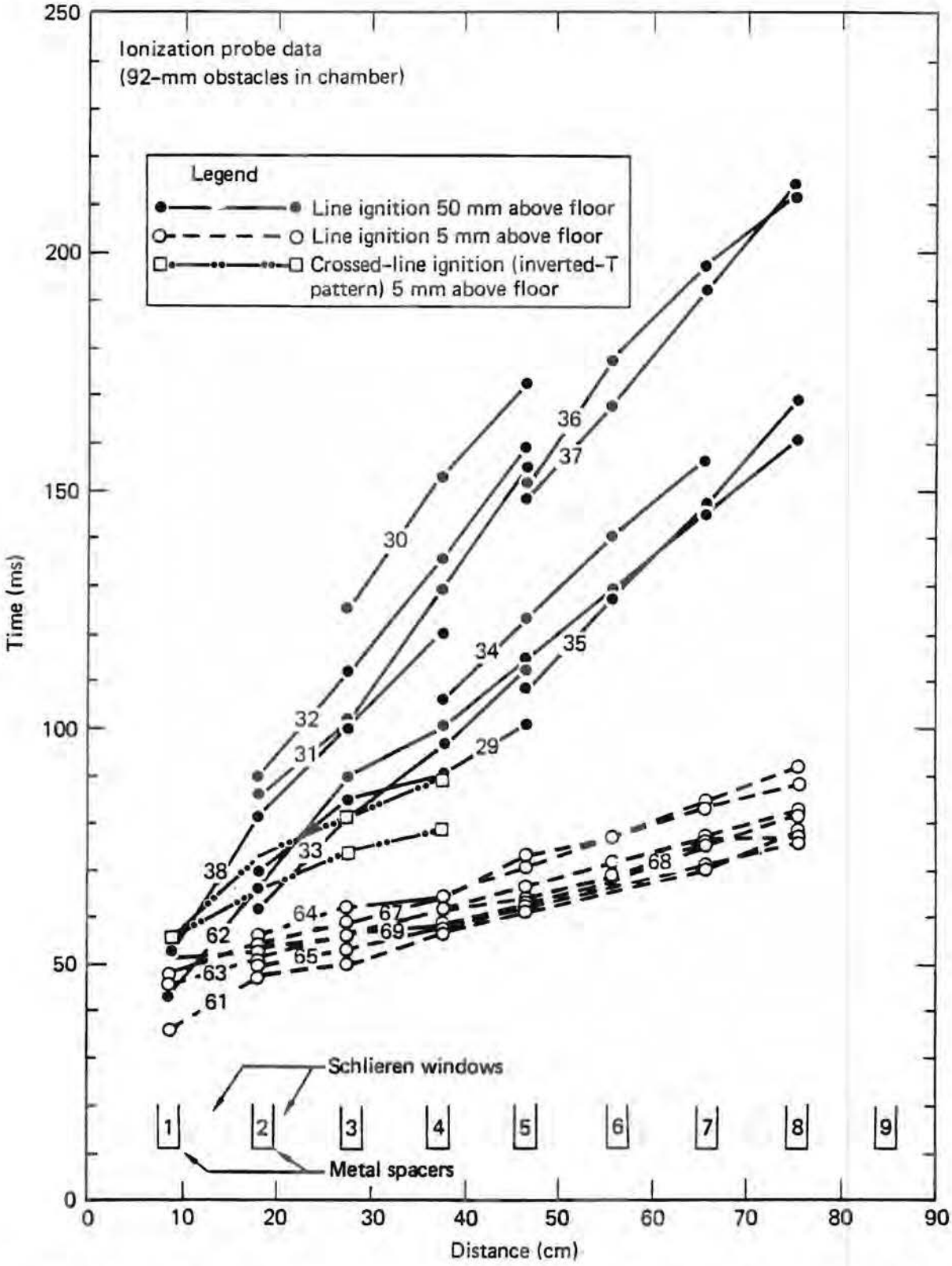

FIG. 17. Time-space plots of ionization probe data taken with 92-mm obstacles in the chamber and various modes of ignition.

REPORT I

Chemical Kinetics of Hydrocarbon Oxidation in Gaseous Detonations

C. K. Westbrook

Prepared for the
Environmental and Safety Engineering
Division
U.S. Department of Energy
under Contract W-7405-ENG-48

Lawrence Livermore Laboratory
Livermore, California 94550

REPORT I

TABLE OF CONTENTS

SUMMARY

A theoretical model including a detailed chemical kinetic reaction mechanism for hydrocarbon oxidation is used to examine detonation properties for mixtures of fuel/air, fuel/oxygen, and fuel/oxygen diluted with varying amounts of nitrogen. Fuels considered are methane, ethane, ethylene, acetylene, and methanol. Computed induction lengths are compared with available experimental data for critical energy and critical tube diameter for initation of detonation, as well as detonation limits in planar, cylindrical, and spherical configurations.

INTRODUCTION

Gaseous detonation waves have been studied experimentally for many years. Detonation limits, propagation rates, and other properties have been examined for many fuel-oxidizer mixtures. Theoretical descriptions of detonation behavior have appeared more recently, showing how hydrodynamic and chemical kinetic processes interact in detonation waves. The weakest part of most existing detonation models is their submodel for chemical kinetics. Since kinetic induction times play a prominent role in all of these models, the lack of reliable kinetics models has been a serious problem. Detailed reaction mechanisms for hydrogen oxidation have been used to examine detonations in H_2-air and H_2-O_2 [1-4] demonstrating the value of including a detailed reaction mechanism in the overall model. However, there is a need for similar kinetic models for the oxidation of hydrocarbon fuels in oxygen or in air [5-8]. Reviews of the current status of hydrocarbon oxidation mechanisms [9,10] suggest that such mechanisms have in fact advanced to the point where they can be used to examine chemical kinetic factors involved in the initiation and propagation of gaseous detonations.

In this paper a detailed chemical kinetic reaction mechanism is used to compute induction times for the oxidation of a number of hydrocarbon fuels. These calculations are combined with computed Chapman-Jouguet (CJ) conditions and used to examine some of the properties of gaseous detonations. Using a reliable kinetics model, one level of uncertainty in the theoretical analysis of detonation phenomena can be removed. Furthermore, such a model provides an improved basis for extrapolation of results from regimes in which experimental data are available to others where data are sparse or unreliable. This type of approach can also help to indicate which detonation properties such as cell size or ignition limits scale with experimental parameters and where such scaling laws are likely to break down.

CHEMICAL KINETICS

The reaction mechanism used in these calculations has been developed and validated in a series of papers [11-14]. The elementary reactions and their rate expressions are summarized in Table I. Individual references for the rates can be found in Reference [14]. Reverse reaction rates are computed from the forward rates and the appropriate thermodynamic data [15,16]. The mechanism has been shown to describe oxidation of methane [11,12], methanol [13], and ethylene [14] over wide ranges of experimental conditions. It has also been used to describe the shock tube oxidation of ethane [12,17], although a truly comprehensive mechanism for ethane oxidation has not yet been developed. The elementary reactions and reaction rates in Table I dealing with acetylene oxidation have been based on the shock tube study of Jachimowski [18], but a comprehensive mechanism for acetylene oxidation is also not yet available. As a result the reliability of the mechanism is not as great when ethane or acetylene are the fuels as when methane, ethylene, or methanol are used. However, since the parameter regimes in a detonation are similar to those in shock tubes, it can be expected that the mechanism should give quite reasonable results for the oxidation of acetylene and ethane in detonation waves.

The reaction mechanism does not include the formation and oxidation of species with three or more carbon atoms, such as C_3H_8, C_3H_6, C_4H_{10} or C_4H_8. Such species will be important primarily for very rich conditions when C_2H_4 and C_2H_6 fuels are involved, and for very rich C_2H_2, CH_4 and CH_3OH to a lesser extent. Reaction paths involving C_3 and C_4 species are not included because the rates of their formation and consumption reactions are not as well known in most cases as the others in Table I and their inclusion would contribute a substantial degree of

Table I
Fuel oxidation mechanism. Reaction rates in cm^3-mole-sec-kcal units, $k=AT^n\exp(-E_a/RT)$

	Reaction	Forward rate log A	n	E_a	Reverse rate log A	n	E_a
1	$H+O_2 \rightarrow O+OH$	14.27	0	16.79	13.17	0	0.68
2	$H_2+O \rightarrow H+OH$	10.26	1	8.90	9.92	1	6.95
3	$H_2O+O \rightarrow OH+OH$	13.53	0	18.35	12.50	0	1.10
4	$H_2O+H \rightarrow H_2+OH$	13.98	0	20.30	13.34	0	5.15
5	$H_2O_2+OH \rightarrow H_2O+HO_2$	13.00	0	1.80	13.45	0	32.79
6	$H_2O+M \rightarrow H+OH+M$	16.34	0	105.00	23.15	-2	0.00
7	$H+O_2+M \rightarrow HO_2+M$	15.22	0	-1.00	15.36	0	45.90
8	$HO_2+O \rightarrow OH+O_2$	13.70	0	1.00	13.81	0	56.61
9	$HO_2+H \rightarrow OH+OH$	14.40	0	1.90	13.08	0	40.10
10	$HO_2+H \rightarrow H_2+O_2$	13.40	0	0.70	13.74	0	57.80
11	$HO_2+OH \rightarrow H_2O+O_2$	13.70	0	1.00	14.80	0	73.86
12	$H_2O_2+O_2 \rightarrow HO_2+HO_2$	13.60	0	42.64	13.00	0	1.00
13	$H_2O_2+M \rightarrow OH+OH+M$	17.08	0	45.50	14.96	0	-5.07
14	$H_2O_2+H \rightarrow HO_2+H_2$	12.23	0	3.75	11.86	0	18.70
15	$O+H+M \rightarrow OH+M$	16.00	0	0.00	19.90	-1	103.72
16	$O_2+M \rightarrow O+O+M$	15.71	0	115.00	15.67	-0.28	0.00
17	$H_2+M \rightarrow H+H+M$	14.34	0	96.00	15.48	0	0.00
18	$CO+OH \rightarrow CO_2+H$	7.11	1.3	-0.77	9.15	1.3	21.58
19	$CO+HO_2 \rightarrow CO_2+OH$	14.18	0	23.65	15.23	0	85.50
20	$CO+O+M \rightarrow CO_2+M$	15.77	0	4.10	21.74	-1	131.78
21	$CO_2+O \rightarrow CO+O_2$	12.44	0	43.83	11.50	0	37.60
22	$HCO+OH \rightarrow CO+H_2O$	14.00	0	0.00	15.45	0	105.15
23	$HCO+M \rightarrow H+CO+M$	14.16	0	19.00	11.70	1	1.55
24	$HCO+H \rightarrow CO+H_2$	14.30	0	0.00	15.12	0	90.00
25	$HCO+O \rightarrow CO+OH$	14.00	0	0.00	14.46	0	87.90

Table I (continued)
Fuel oxidation mechanism. Reaction rates in cm^3-mole-sec-kcal units, $k=AT^n\exp(-E_a/RT)$

	Reaction		Forward rate log A	n	E_a	Reverse rate log A	n	E_a
26	$HCO+HO_2$	$\rightarrow CH_2O+O_2$	14.00	0	3.00	15.56	0	46.04
27	$HCO+O_2$	$\rightarrow CO+HO_2$	12.60	0	7.00	12.95	0	39.29
28	CH_2O+M	$\rightarrow HCO+H+M$	16.52	0	81.00	11.15	1	-11.77
29	CH_2O+OH	$\rightarrow HCO+H_2O$	12.88	0	0.17	12.41	0	29.99
30	CH_2O+H	$\rightarrow HCO+H_2$	14.52	0	10.50	13.42	0	25.17
31	CH_2O+O	$\rightarrow HCO+OH$	13.70	0	4.60	12.24	0	17.17
32	CH_2O+HO_2	$\rightarrow HCO+H_2O_2$	12.00	0	8.00	11.04	0	6.59
33	CH_4+M	$\rightarrow CH_3+H+M$	17.15	0	88.40	11.45	1	-19.52
34	CH_4+H	$\rightarrow CH_3+H_2$	14.10	0	11.90	12.68	0	11.43
35	CH_4+OH	$\rightarrow CH_3+H_2O$	3.54	3.08	2.00	2.76	3.08	16.68
36	CH_4+O	$\rightarrow CH_3+OH$	13.20	0	9.20	11.43	0	6.64
37	CH_4+HO_2	$\rightarrow CH_3+H_2O_2$	13.30	0	18.00	12.02	0	1.45
38	CH_3+HO_2	$\rightarrow CH_3O+OH$	13.51	0	0.00	10.00	0	0.00
39	CH_3+OH	$\rightarrow CH_2O+H_2$	12.60	0	0.00	14.08	0	71.73
40	CH_3+O	$\rightarrow CH_2O+H$	14.11	0	2.00	15.23	0	71.63
41	CH_3+O_2	$\rightarrow CH_3O+O$	13.68	0	29.00	14.48	0	0.73
42	CH_2O+CH_3	$\rightarrow CH_4+HCO$	10.00	0.5	6.00	10.32	0.5	21.14
43	CH_3+HCO	$\rightarrow CH_4+CO$	11.48	0.5	0.00	13.71	0.5	90.47
44	CH_3+HO_2	$\rightarrow CH_4+O_2$	12.00	0	0.40	13.88	0	58.59
45	CH_3O+M	$\rightarrow CH_2O+H+M$	13.70	0	21.00	9.00	1	-2.56
46	CH_3O+O_2	$\rightarrow CH_2O+HO_2$	12.00	0	6.00	11.11	0	32.17
47	C_2H_6	$\rightarrow CH_3+CH_3$	19.35	-1	88.31	12.95	0	0.00
48	$C_2H_6+CH_3$	$\rightarrow C_2H_5+CH_4$	-0.26	4	8.28	10.48	0	12.50
49	C_2H_6+H	$\rightarrow C_2H_5+H_2$	2.73	3.5	5.20	2.99	3.5	27.32
50	C_2H_6+OH	$\rightarrow C_2H_5+H_2O$	13.05	0	2.45	13.30	0	24.57

Table I (continued)
Fuel oxidation mechanism. Reaction rates in cm^3-mole-sec-kcal units, $k=AT^n\exp(-E_a/RT)$

	Reaction		Forward rate log A	n	E_a	Reverse rate log A	n	E_a
51	C_2H_6+O	$\rightarrow C_2H_5+OH$	13.40	0	6.36	12.66	0	11.23
52	C_2H_5+M	$\rightarrow C_2H_4+H+M$	15.30	0	30.00	10.62	0	-11.03
53	$C_2H_5+O_2$	$\rightarrow C_2H_4+HO_2$	12.00	0	5.00	11.12	0	13.70
54	$C_2H_4+C_2H_4$	$\rightarrow C_2H_5+C_2H_3$	14.70	0	64.70	14.17	0	-2.61
55	C_2H_4+M	$\rightarrow C_2H_2+H_2$	17.41	0	79.28	12.66	1	36.52
56	C_2H_4+M	$\rightarrow C_2H_3+H+M$	17.58	0	98.16	17.30	0	0.00
57	C_2H_4+O	$\rightarrow CH_3+HCO$	12.52	0	1.13	11.20	0	31.18
58	C_2H_4+O	$\rightarrow CH_2O+CH_2$	13.40	0	5.00	12.48	0	15.68
59	C_2H_4+H	$\rightarrow C_2H_3+H_2$	7.18	2	6.00	6.24	2	5.11
60	C_2H_4+OH	$\rightarrow C_2H_3+H_2O$	12.68	0	1.23	12.08	0	14.00
61	C_2H_4+OH	$\rightarrow CH_3+CH_2O$	12.30	0	0.96	11.78	0	16.48
62	C_2H_3+M	$\rightarrow C_2H_2+H+M$	14.90	0	31.50	11.09	1	-10.36
63	$C_2H_3+O_2$	$\rightarrow C_2H_2+HO_2$	12.00	0	10.00	12.00	0	17.87
64	C_2H_2+M	$\rightarrow C_2H+H+M$	14.00	0	114.00	9.04	1	0.77
65	$C_2H_2+O_2$	$\rightarrow HCO+HCO$	12.60	0	28.00	11.00	0	63.65
66	C_2H_2+H	$\rightarrow C_2H+H_2$	14.30	0	19.00	13.62	0	13.21
67	C_2H_2+OH	$\rightarrow C_2H+H_2O$	12.78	0	7.00	12.73	0	16.36
68	C_2H_2+OH	$\rightarrow CH_3+CO$	12.08	0	0.50	12.41	0	58.00
69	C_2H_2+O	$\rightarrow C_2H+OH$	15.51	-0.6	17.00	14.47	-0.6	0.91
70	C_2H_2+O	$\rightarrow CH_2+CO$	13.83	0	4.00	13.10	0	54.67
71	C_2H+O_2	$\rightarrow HCO+CO$	13.00	0	7.00	12.93	0	138.40
72	C_2H+O	$\rightarrow CO+CH$	13.70	0	0.00	13.50	0	59.43
73	CH_2+O_2	$\rightarrow HCO+OH$	14.00	0	3.70	13.61	0	76.58
74	CH_2+O	$\rightarrow CH+OH$	11.28	0.68	25.00	10.77	0.68	25.93
75	CH_2+H	$\rightarrow CH+H_2$	11.43	0.67	25.70	11.28	0.67	28.72

Table I (continued)
Fuel oxidation mechanism. Reaction rates in
cm^3-mole-sec-kcal units, $k=AT^{n}exp(-E_a/RT)$

	Reaction		Forward rate			Reverse rate		
			log A	n	E_a	log A	n	E_a
76	CH_2+OH	$\rightarrow CH+H_2O$	11.43	0.67	25.70	11.91	0.67	43.88
77	$CH+O_2$	$\rightarrow CO+OH$	11.13	0.67	25.70	11.71	0.67	185.60
78	$CH+O_2$	$\rightarrow HCO+O$	13.00	0	0.00	13.13	0	71.95
79	CH_3OH+M	$\rightarrow CH_3+OH+M$	18.48	0	80.00	13.16	1	-10.98
80	CH_3OH+OH	$\rightarrow CH_2OH+H_2O$	12.60	0	2.00	7.27	1.66	25.31
81	CH_3OH+O	$\rightarrow CH_2OH+OH$	12.23	0	2.29	5.90	1.66	8.35
82	CH_3OH+H	$\rightarrow CH_2OH+H_2$	13.48	0	7.00	7.51	1.66	15.16
83	CH_3OH+H	$\rightarrow CH_3+H_2O$	12.72	0	5.34	12.32	0	36.95
84	CH_3OH+CH_3	$\rightarrow CH_2OH+CH_4$	11.26	0	9.80	6.70	1.66	18.43
85	CH_3OH+HO_2	$\rightarrow CH_2OH+H_2O_2$	12.80	0	19.36	7.00	1.66	11.44
86	CH_2OH+M	$\rightarrow CH_2O+H+M$	13.40	0	29.00	16.69	-0.66	7.58
87	CH_2OH+O_2	$\rightarrow CH_2O+HO_2$	12.00	0	6.00	17.94	-1.66	28.32

uncertainty to the computed results. The principal effect of neglecting them will be an underestimate of induction times for very fuel-rich mixtures; for lean and stoichiometric mixtures the effect will be minimal.

In the past, models of detonations have used global rate expressions for the chemical induction times of the selected fuel-oxidizer mixtures, but such expressions are not always satisfactory, even when the global expressions have been based on shock tube data. Most shock tube experiments are carried out with high dilution by Ar, He or N_2, so that fuel and oxygen concentrations are quite low. The overall reaction orders and global expressions for induction time often change with the amount of dilution, so the induction times computed from global expressions can often be seriously in error when applied to undiluted fuel-oxygen or fuel-air mixtures. For relative induction times a global expression may be useful, but the calculation of absolute induction times requires a detailed reaction mechanism.

DETONATION MODEL

The general model used is the Zeldovich-von Neumann-Doring (ZND) model in which, locally, a detonation consists of a shock wave traveling at the CJ velocity, followed by a reaction zone. The shock wave compresses and heats the fuel-oxidizer mixture which then begins to react. In most mixtures, the overall fuel oxidation consists of a relatively long induction period during which the temperature and pressure of the gas mixture remain nearly constant, followed by a rapid release of chemical energy and temperature increase.

For each fuel-oxidizer mixture selected, a calculation is first made of the relevant CJ conditions [19], assuming that the initial pressure is atmospheric and the initial temperature is 300 K. From the resulting value of

the detonation velocity D_{CJ}, the temperature T_1, pressure P_1, and particle velocity u_1 of the post-shock, unreacted gases can be calculated from the shock conservation relations and are then used as initial conditions for the chemical kinetics model. It is well established that the shock velocity varies within a single detonation cell from an initial value of about 1.2 D_{CJ} to a minimum of about 0.8 D_{CJ}, so the CJ conditions used here represent average values, and the computed induction times will also be averages.

For the kinetics calculations, the reactive mixture is assumed to remain at a constant volume over its reaction time, and the induction time is defined in terms of its temperature history. Most of the mixtures examined underwent a large temperature increase of 1500-2000 K, and the induction time was defined as the time of maximum rate of temperature increase. In most cases this coincided approximately with the time at which the temperature had completed about half of its total increase. This is not, strictly speaking, a true induction period, often defined as the time required for a small (i.e., 1-5%) temperature or pressure increase, but here the release of macroscopic amounts of energy is of primary interest. In addition to the induction time τ, it is useful to define the induction length $\Delta \equiv \tau(D-u_1)$.

Atkinson et al.[1] pointed out that variations in CJ and particle velocity with equivalence ratio were significant, and that the induction length Δ should be used rather than the induction time τ in comparisons between computed and experimental results. Although the variations in D and u_1 in the hydrocarbon systems examined here are not as large as in H_2-air systems, it was found that the use of Δ in the presentation of the calculated results provided consistently better agreement with experimental data.

This model of the detonation is a simple one and neglects several potentially significant effects arising from hydrodynamic-kinetic interactions. Variations of density, temperature, and particle velocity in the post-shock unreacted mixture are not considered, changes which will usually tend to increase the induction period. Boni et al. [20], using a global kinetic model, found that such interactions produced a decoupling between the shock front and reaction zone which drastically increased the required energy for ignition of spherical unconfined methane-air mixtures. In cases where such interactions are important, the present model will be inadequate. The effects of cellular structure of the detonation are not considered, although Libouton et al. [21] showed in H_2-O_2 and CO-H_2-O_2 detonations that coupling between detailed kinetics and thermal perturbations arising from the cellular structure of the detonation can be important.

Five hydrocarbon fuels were examined, including methane, ethane, ethylene, acetylene and methanol. Four series of calculations were carried out, consisting of:

1. Fuel-air mixtures, with the fuel fraction (equivalence ratio) being varied.
2. Fuel-O_2 mixtures, again with the fuel fraction being varied.
3. Fuel-O_2-N_2 mixtures in which the ratio $\beta \equiv N_2/O_2$ is varied between zero (i.e. fuel-O_2 mixture) and 3.76 (i.e. fuel-air mixture). The ratio of fuel to O_2 is held fixed, with sufficient O_2 to oxidize the fuel completely to CO_2 and H_2O (CO_2 stoichiometry).
4. Fuel-O_2-N_2 mixtures in which β is varied between zero and 3.76, as above. However, here the ratio of fuel to O_2 is fixed at the level required to produce CO and H_2O (CO stoichiometry).

FUEL-AIR MIXTURES

Mixtures of fuel with air as oxidizer are considered first. The initial post-shock temperatures are summarized in Figure 1. For each fuel-air mixture there is a strong dependence of T_1 on equivalence ratio. Since the induction time is a sensitive function of this temperature, it is clear that the thermodynamic properties of the shock play a major part in the induction process. Atkinson et al. suggested that, even when detailed kinetic models were not available, thermodynamic data could be used to predict the equivalence ratio corresponding to maximum detonability for a given fuel; computed results in the present paper confirmed this suggestion.

Computed induction lengths for all five fuels are plotted in Figure 2. On the lean side of stoichiometric the curves are very steep as $\phi \to 0.5$. Borisov and Loban [22] determined lean limits for detonation in a 70 mm diameter tube for both ethane-air and ethylene-air of $\phi_L = 0.49$, Kogarko [23] found a lean limit for methane-air in a 305 mm tube of $\phi_L = 0.65$, and Bull [6] and Lewis and von Elbe [24] give a value of $\phi_L = 0.5$ for acetylene-air in a 14 mm tube. All of these experimental values for ϕ_L are entirely consistent with the computed results.

For rich mixtures the variations in induction length between the five fuels are considerably greater than for lean mixtures. In Figure 2 the curves for CH_4-air and C_2H_6-air rise most rapidly with increasing equivalence ratio. Experimental data for propagation of detonations in a 305 mm tube with methane-air [23] indicated a fuel-rich limit of $\phi_R \approx 1.7$, while Borisov and Loban [22], using a 70 mm tube, found $\phi_R \approx 2.3$ for ethane-air and $\phi_R \approx 2.5$ for ethylene-air. At these experimentally-determined rich limits, the ratio of the tube diameter d to the induction length Δ for CH_4, C_2H_6 and C_2H_4 is approximately 3, 1 and 7, respectively. If it

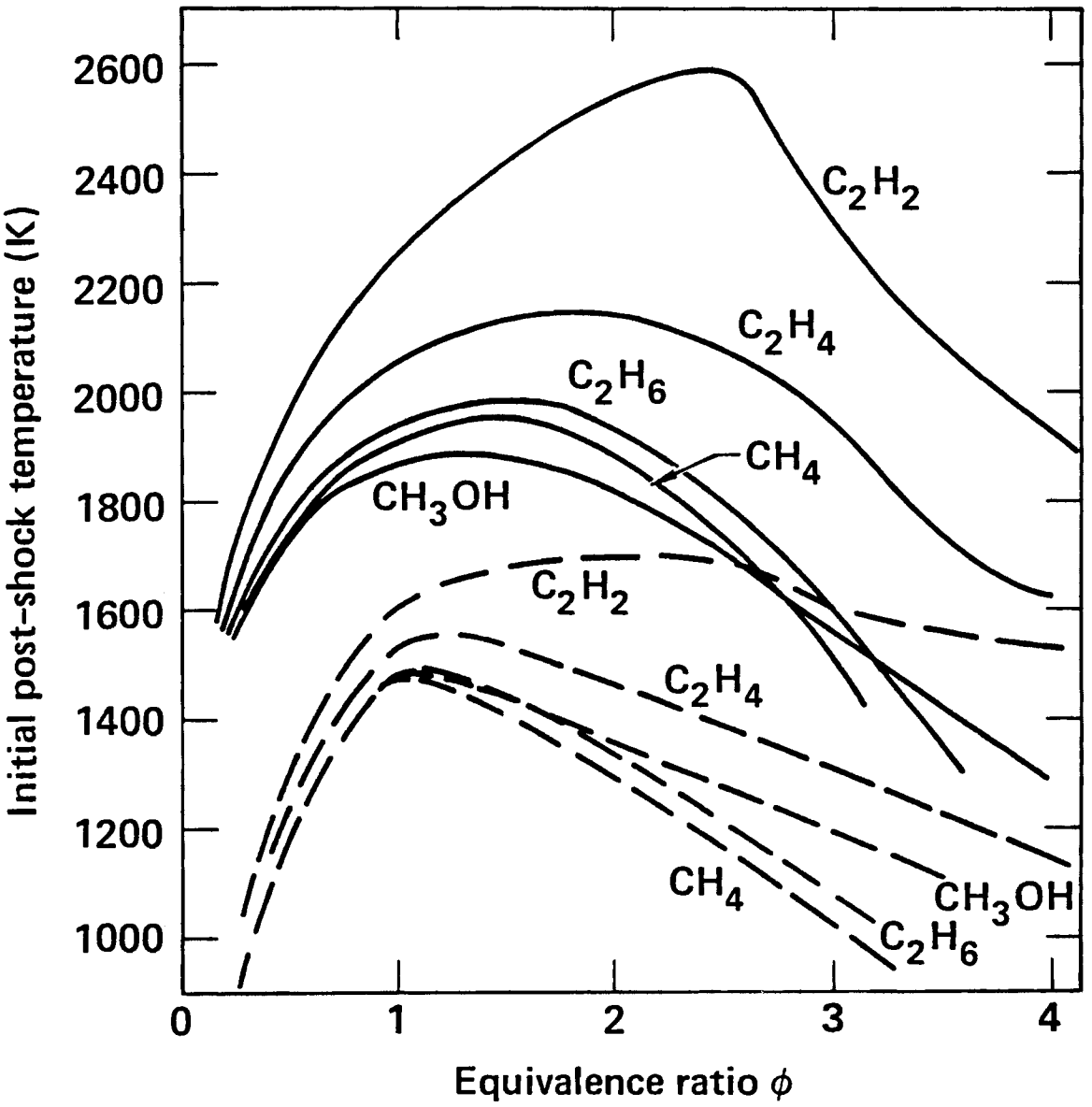

FIGURE 1. Post-shock unreacted temperatures for fuel-oxygen (solid curves) and fuel-air (dashed curves) mixtures.

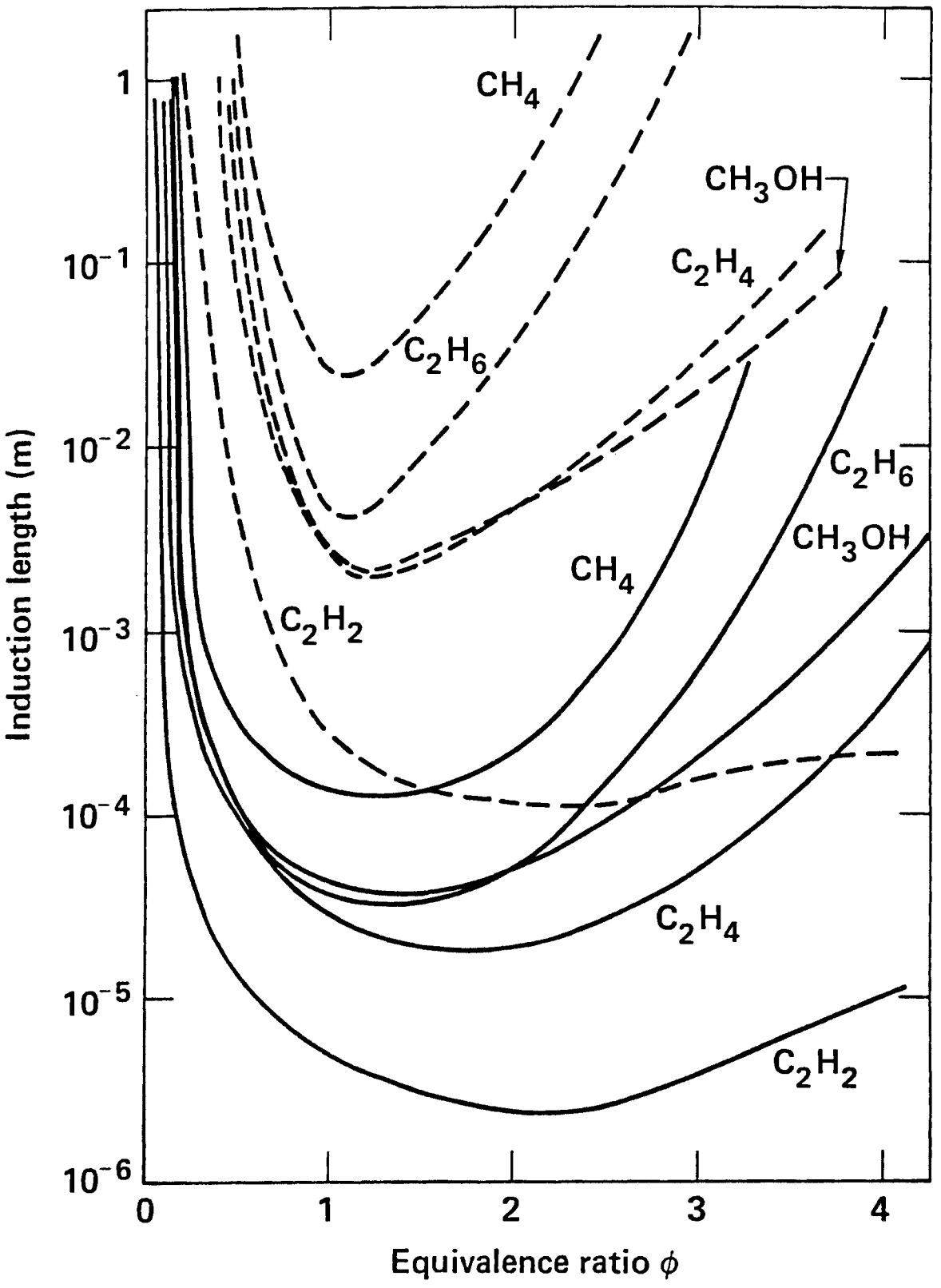

FIGURE 2. Induction length Δ for fuel-oxygen (solid curves) and fuel-air (dashed curves) mixtures.

is assumed that at the limit, single-spin detonation occurs with a transverse wave spacing $b \simeq 2d$, then the ratio b/Δ is approximately 6, 2 and 14 respectively. As computed results will show below, these ratios are considerably smaller than for the comparable fuel-O_2 mixtures.

No experimental data on detonation limits for methanol-air were found. From the curves in Figure 2 it appears that detonation limits in tubes for CH_3OH-air might be quite similar to those for C_2H_4-air. The curve for rich acetylene-air is qualitatively different from those for the other fuel-air mixtures. The induction length remains very small even for values of ϕ beyond the range shown in Figure 2. For example, at $\phi = 5$, Δ is still less than 0.25 mm. This is consistent with observations that acetylene-air is detonable for nearly all values of equivalence ratio greater than $\phi = 0.5$.

UNCONFINED SPHERICAL DETONATIONS

The critical energy E_c for initiation of detonation can be related to the chemical kinetic induction time by means of the Zeldovich criterion [25]

$$E_c = k_1 \Delta^{j+1}$$

where $j = 0, 1, 2$ for planar, cylindrical, and spherical geometry respectively. The constant k_1 depends on many factors which vary from one theoretical model to another [26,27]. On the basis of comparisons between computed and experimental data, it is possible to examine how much this constant of proportionality varies with equivalence ratio and fuel type.

For ethane Δ^3 from the model is plotted against equivalence ratio ϕ in Figure 3. The minimum, $\Delta^3 \simeq 6.4 \times 10^{-8}$ m^3, occurs slightly on the rich side, at $\phi \simeq 1.15$. For spherical detonations in ethane-air, computed values of Δ^3 can be compared with the experimental data for

critical energy of initiation determined by Bull et al. [8]. These data are summarized in Figure 3, where the constant of proportionality k_1 has been chosen equal to 2.5×10^5 kg-m^{-3}. The agreement between computed and experimental data is good, with the minima in Δ^3 and E_c both occuring for $\phi = 1.15$. In agreement with Bull et al., the current model does not predict absolute lean or rich limits to initiation of detonation, finding that the curve in Figure 3 becomes very steep but never truly vertical. Therefore absolute detonation limits must depend on factors other than chemical kinetics.

Computed results for Δ^3 in C_2H_4-air mixtures are summarized in Figure 4, with a minimum value of $\Delta^3 = 6.9 \times 10^{-9}$ m^3 at $\phi \approx 1.25$. Several sets of experimental data for critical initiation energy of spherical detonation are included in Figure 4, given by Bull [6]. Best agreement between computed values of Δ^3 and the experimental data was obtained with a proportionality constant of $k_1 = 7.3 \times 10^5$ kg-m^{-3}, larger than the constant determined for C_2H_6-air by a factor of 2.9.

There is some disagreement in the experimental literature regarding the critical initiation energies for fuel-air mixtures. For example, Bull et al. [5] reported a value for E_c of 1.5×10^5 joules for a stoichiometric C_2H_6-air mixture, while Matsui and Lee [28] found $E_c = 5.09 \times 10^6$ joules. Similar differences in E_c were reported by these authors for C_2H_4-air, CH_4-air and C_3H_8-air mixtures. Some care must be taken in relating these numbers. Matsui and Lee state that their mixtures are "stoichiometric", but from their quoted fuel percentages it is clear that they are instead considering fuel-rich mixtures at "CO stoichiometric". For ethane, this is actually $\phi = 1.4$. The same is true for ethylene-air where Matsui and Lee found E_c to be 1.2×10^5 joules in what is actually a rich

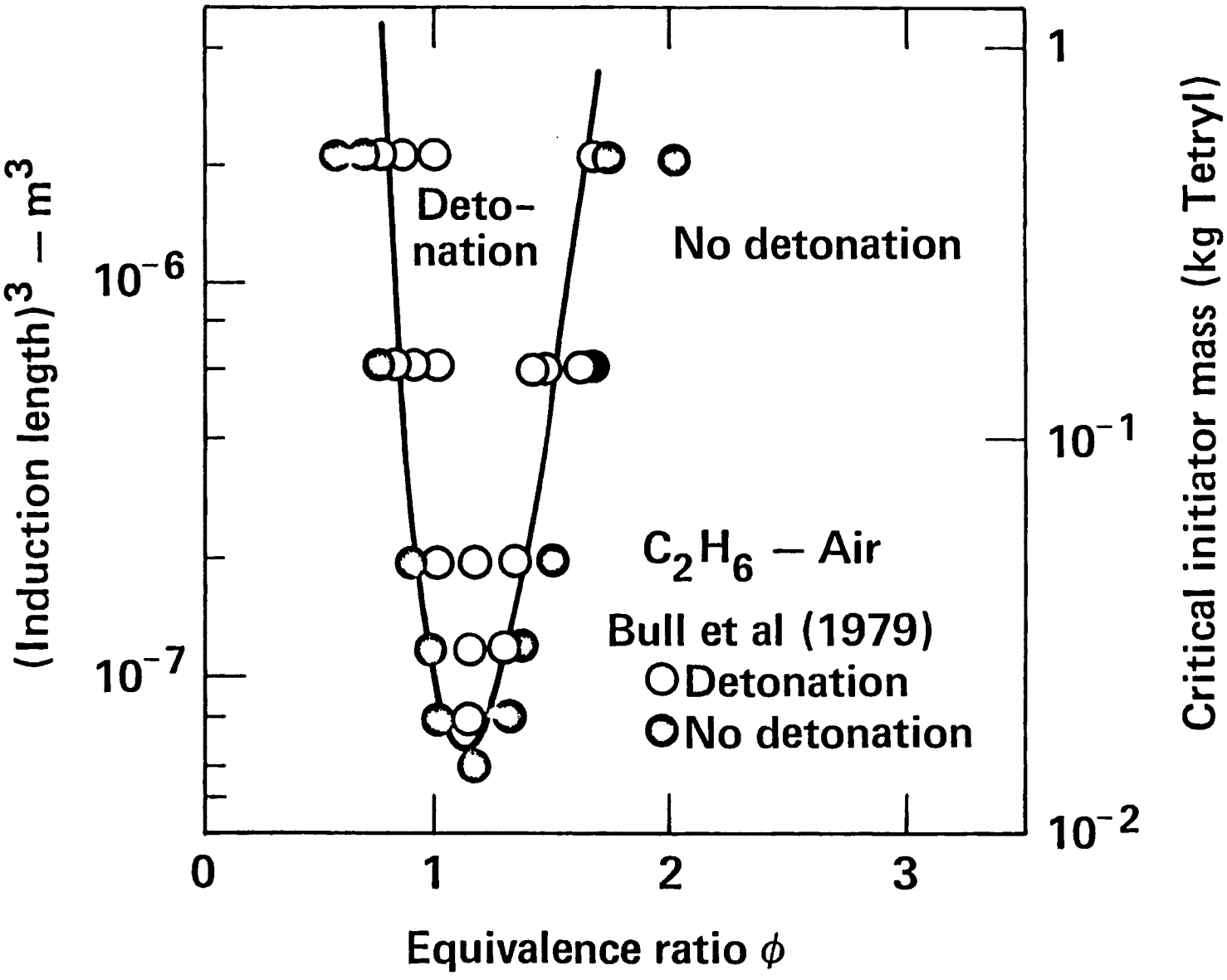

FIGURE 3. Cube of induction length for C_2H_6-air mixtures, with data from Bull et al. [8] on critical initiation energy.

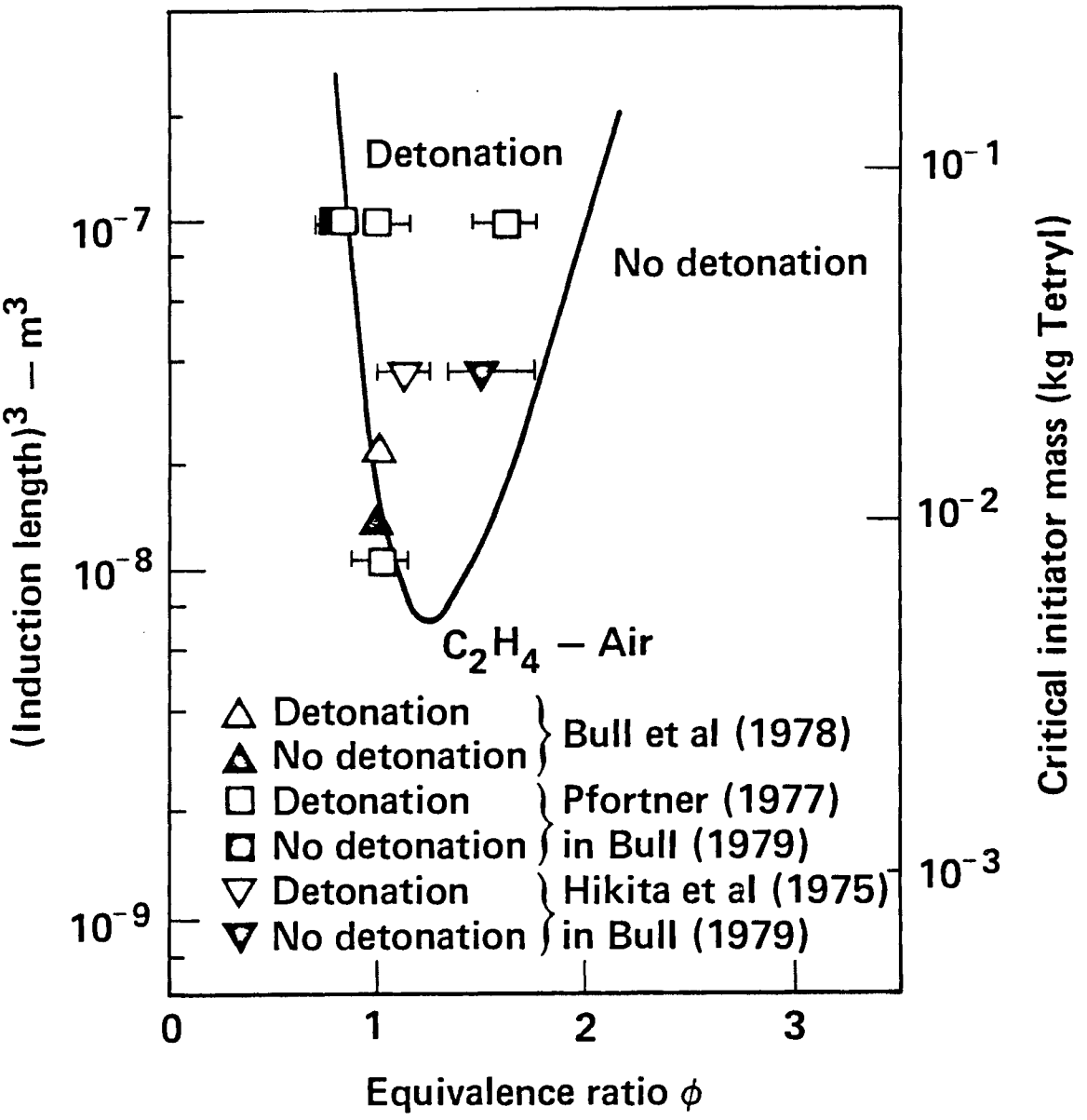

FIGURE 4. Cube of induction length for C_2H_4-air mixtures, with data from Bull [6] on critical initiation energy.

mixture (ϕ = 1.5), while Bull et al. find $E_c = 5.3 \times 10^4$ joules at ϕ=1. To compare these results at the same value of equivalence ratio, the data of Matsui and Lee can be converted to conventional stoichiometry by assuming that the variation of E_c with Δ^3 over the required range of equivalence ratio is given by the Zeldovich criterion, with values for Δ^3 taken from the model results. When this is done, the critical initiation energies for C_2H_4, C_2H_6 and CH_4 can be compared as shown in Table II. Converting the data of Matsui and Lee to the same equivalence ratio as that of Bull et al. leaves the Matsui and Lee value of E_c for C_2H_6-air higher by a factor of 10. Agreement is better for C_2H_4, and both papers estimate the same value for CH_4-air, although neither actually performed the CH_4-air experiments. The ratios of critical initiation energies for ethane-air to ethylene-air are also different, a ratio of 2.8 from Bull et al. and a ratio of 9.4 from Matsui and Lee. From the model, the ratio $\Delta^3(C_2H_6\text{-air})/\Delta^3(C_2H_4\text{-air})$ is computed to be 5.6.

All of the experimental results of Bull et al., including CH_4-O_2-N_2 data to be discussed below, are internally self-consistent with respect to values of E_c. For direct initiation in spherical geometry with C_2H_4, C_2H_6 and CH_4 as fuels, the coefficient k_1 from the Zeldovich criterion varies by less than a factor two from an average of 2.1×10^9 kJ/m^3. The results of Matsui and Lee are likewise internally self-consistent, including experimental data for E_c in fuel-air, as well as fuel-O_2 and fuel-O_2-N_2 mixtures to be discussed below, but with the much larger value $k_1 = 2 \times 10^{10}$ kJ/m^3. The disagreement in k_1 of a factor of 10 must be attributed to differences in the respective experimental configurations. Bull et al. used high explosive charges while Matsui and Lee initiated mixtures by

Table II

Critical initiation energy for spherical detonation

in stoichiometric fuel-air mixtures

	$E_c(CH_4)$ joules	$E_c(C_2H_4)$ joules	$E_c(C_2H_6)$ joules	$\frac{E_c(C_2H_6)}{E_c(C_2H_4)}$
Bull et al. (1978)	8.8×10^7	5.3×10^4	1.5×10^5	2.8
Matsui and Lee[a](1979)	8.8×10^7	1.7×10^5	1.6×10^6	9.4
Present model[b]	3.3×10^8	3.4×10^5	1.9×10^6	5.6

[a]Converted to ϕ=1 from "CO stoichiometric"
[b]Values determined later in this paper

means of a planar detonation from a linear tube. The computed results presented here suggest that initiation energies determined using the linear tube and explosive charges cannot be directly compared. Available experimental data on direct initiation by high explosive charges, summarized by Bull [6], and on initiation by a planar detonation from a linear tube show a considerable degree of internal consistency for values of E_c when a single initiation mechanism is used.

Computed results for Δ^3 vs ϕ for CH_4-air mixtures are given in Figure 5. Experimental data are not available for direct comparison, since detonations in CH_4-air are so difficult to initiate in spherical geometry, although Benedick [29] reports initiation of CH_4-air mixtures in a planar configuration. From the relative magnitudes of Δ^3 for CH_4, C_2H_6, and C_2H_4 mixtures in air, the model predicts that stoichiometric CH_4-air should require a much greater high explosive initiator mass than C_2H_4-air or C_2H_6-air. Using as a reference the value for C_2H_4-air (ϕ = 1.5) of Matsui and Lee of 1.2×10^5 joules, stoichiometric CH_4-air would require approximately 1.66×10^8 joules for spherical initiation, equivalent to 39 kg of Tetryl high explosive. If instead the value of 6×10^4 joules quoted for C_2H_4-air (ϕ=1.0) by Bull et al.[5] is used as a reference, the prediction for E_c in stoichiometric CH_4-air is 5.8×10^7 joules or 13.6 kg of Tetryl. These can be compared with the estimate of 22 kg by Bull et al. [5] based on extrapolations of data obtained in CH_4-O_2-N_2 mixtures. Matsui and Lee provide an estimate of 53 kg of Tetryl for rich (ϕ=1.33) CH_4-air; scaled by the ratio $\Delta^3(\phi=1)/\Delta^3(\phi=1.33)$ this yields a prediction for E_c in stoichiometric CH_4-air of 21 kg of Tetryl.

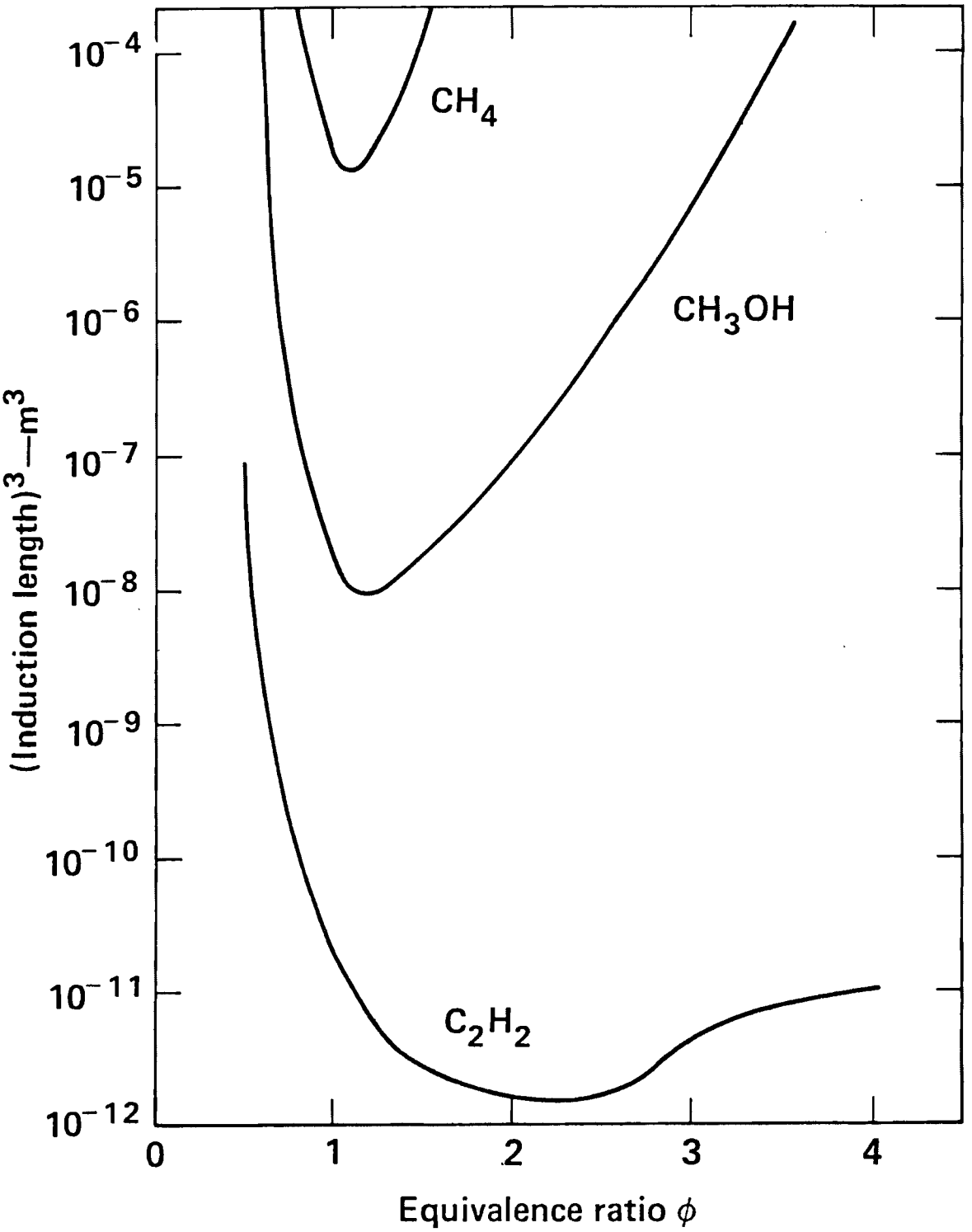

FIGURE 5. Cube of induction length for CH_4-air, CH_3OH-air and C_2H_2-air mixtures.

Results computed for Δ^3 in acetylene-air mixtures are also shown in Figure 5. The minimum value is about three orders of magnitude smaller than for ethylene-air, in agreement with results reported by Matsui and Lee. Modeling results by Bull [6], using global kinetics mechanisms, predicted that the minimum initiation energy for acetylene-air is lower than that for ethylene-air by only a factor of ten.

Finally, computed results for Δ^3 for CH_3OH-air mixtures are summarized in Figure 5. These values are quite similar to those for C_2H_4-air in magnitude and in dependence on equivalence ratio, suggesting that lean and rich limits for spherical detonation and minimum initiation energies in methanol-air would be close to those for ethylene-air.

FUEL-OXYGEN MIXTURES

The calculations described above were repeated for each fuel mixed with oxygen (O_2) rather than with air. In fuel-oxygen mixtures the heats of reaction, CJ velocities, and particle velocities are all considerably larger than in fuel-air mixtures. The post-shock unreacted temperatures for each mixture are shown in Figure 1. As noted for the fuel-air mixtures, these temperatures are strong functions of composition, and the minimum induction lengths for each fuel-oxygen mixture occur at about the same value of equivalence ratio as the peak value of T_1. Induction lengths calculated from these post-shock conditions and the kinetics model are summarized in Figure 2. Comparing these results with those for fuel-air mixtures shows that the fuel-O_2 induction lengths are smaller by a factor of about 100. The fuel-O_2 curves are wider and rise more slowly towards the rich limit than the fuel-air results.

For fuel-oxygen mixtures in 25.4 mm tubes [30,31], measured lean limits are ϕ_L = 0.075 (C_2H_2), 0.18 (CH_4), 0.13 (C_2H_4), and 0.13 (C_2H_6), while the rich limits are ϕ_R = 2.52 (CH_4), 4.5 (C_2H_4), and 3.03 (C_2H_6). Acetylene-oxygen mixtures will sustain detonations for C_2H_2 concentrations as large as 92% [24,30]. For all four of these fuel-oxygen mixtures, the curves in Figure 2 are so steep on the lean side that very nearly the same lean limit ϕ_L will be observed for any tube diameter larger than about ten millimeters, and computed lean limits are in good agreement with the experimental data. At the rich limits, the ratio b/Δ of transverse wave spacing to induction length for CH_4 is 65, for C_2H_4 it is 30, and for C_2H_6 it is 70. Pawel et al. [32] determined ϕ_R for CH_4-O_2 in several tubes ranging in diameter from 4 to 26 mm, and for these data, b/Δ varies from 45 to 80. Strehlow and Engel [33] measured transverse wave spacings in stoichiometric CH_4-O_2, C_2H_4-O_2 and C_2H_2-O_2 mixtures. For these cases b/Δ is computed to be about 20 for methane-O_2 and about 100 for the other two fuel-O_2 mixtures.

From the fuel-air results discussed earlier and these fuel-O_2 results, two distinct trends emerge for the ratio b/Δ. First, this ratio is considerably smaller in fuel-air than in fuel-O_2 mixtures, and second, b/Δ seems to decrease as the equivalence ratio approaches the rich limit. Both trends can best be understood in terms of the post-shock unreacted temperatures shown in Figure 1. Elementary reaction rates and overall induction times vary exponentially with temperature, so Δ increases much more rapidly with decreasing T_1 than do the other factors influencing the transverse wave spacing.

From the computed data, it would be expected that detonation limits in CH_3OH - O_2 would be similar to those for C_2H_6 - O_2 mixtures. It was

noted earlier that computed induction lengths for methanol-air and ethylene-air mixtures were very similar, while here methanol-O_2 and ethane-O_2 are very similar. Although all of the induction lengths are shorter for fuel-oxygen, the relative magnitudes for C_2H_2 - C_2H_4 - C_2H_6 - CH_4 remain nearly the same. Only for CH_3OH is there a relative change. The rate of methanol oxidation has a distinctly smaller dependence on temperature than that for the other fuels, reflected in the values obtained for the overall activation energy for fuel oxidation in shock tubes. For methanol, the overall activation energy is about 35 kcal/mole[34] while values for the other fuels are 40 kcal/mole or more [35]. Post-shock, unreacted gas temperatures are much higher for fuel-O_2 mixtures than for fuel-air mixtures, so all of the fuel-O_2 induction times are much smaller, but because of the differences in overall activation energies the effect on methanol mixtures is less pronounced.

UNCONFINED SPHERICAL DETONATIONS

Following the discussion earlier for fuel-air mixtures, it is possible to relate computed induction lengths for fuel-oxygen mixtures to experimental data on critical energies of initiation of detonation, E_c. Matsui and Lee measured E_c for a range of fuel-oxygen equivalence ratios, and Carlson [36] determined detonability limits at a fixed initiator energy level (400 joules) as well as minimum initiation energies for a number of fuel-O_2 mixtures. Both studies involved spherical detonations and included C_2H_2, C_2H_4, and C_2H_6 as fuels. Only Matsui and Lee included CH_4-O_2 mixtures.

Comparisons between computed values of Δ^3 and values for E_c measured by Matsui and Lee are shown in Figure 6, along with computed values for Δ^3 for CH_3OH-O_2 mixtures for which experimental data are not available. The

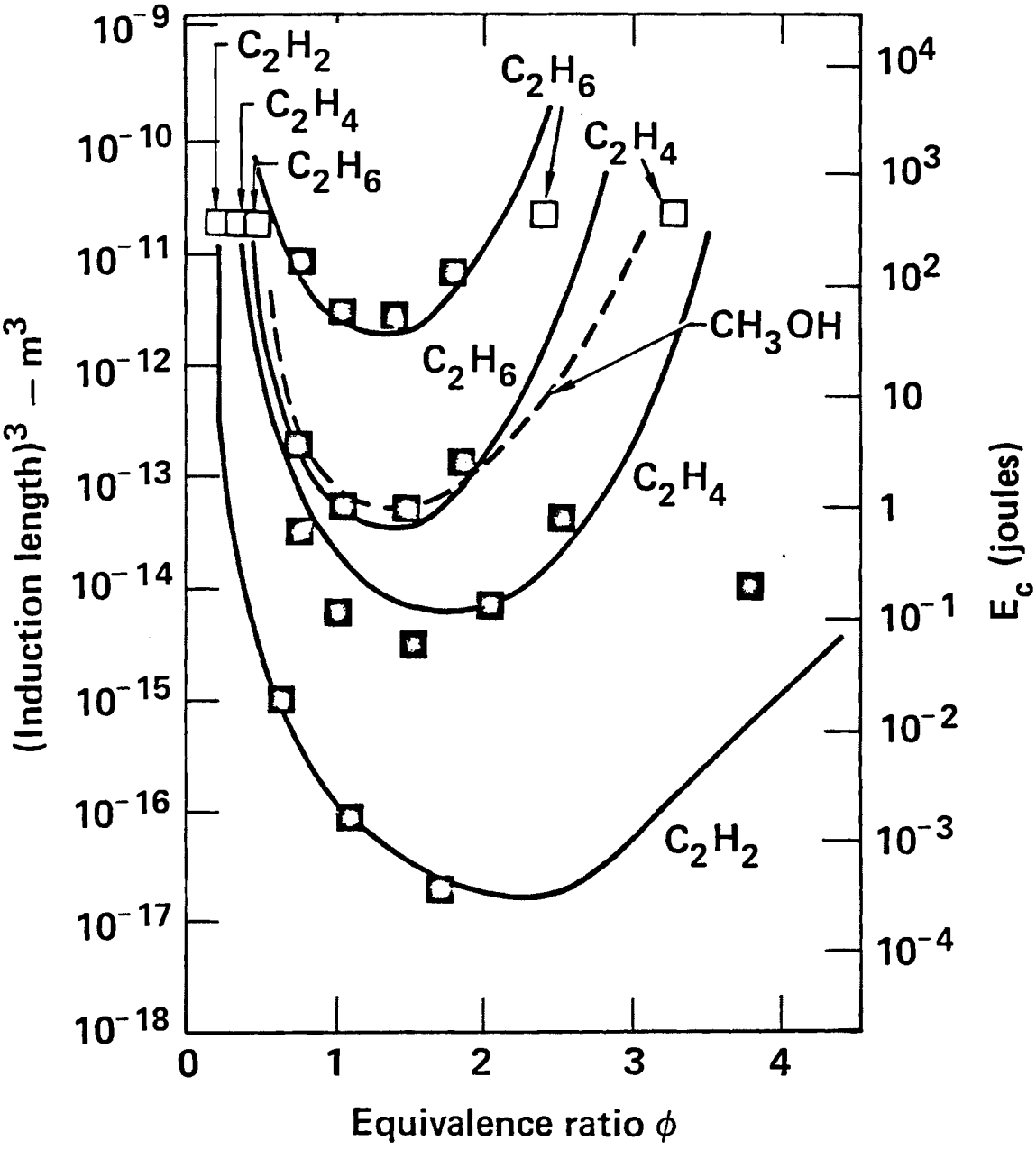

FIGURE 6. Cube of induction length for fuel-O_2 mixtures. Solid squares are critical initiation energies given by Matsui and Lee [28], and open squares are lean and rich limits for spherical detonation using 400 joules initiation energy [36].

experimentally observed spacing between values of E_c for the different fuels is well reproduced by the relative values for Δ^3. A single constant of proportionality can be used, such that $E_c = 2 \times 10^{10} \Delta^3$ kJ. Since the detonation velocities and heat release per unit mass for all of these fuel-O_2 mixtures are very nearly equal, this result should be expected on the basis of the detonation kernel theory of Lee and Ramamurthi [26] for initiation of detonation. This suggests that it should be possible, on the basis of computed induction time data, to predict E_c for other related fuel-O_2 mixtures with reasonable confidence.

Carlson's results are also indicated in Figure 6. Predicted values for Δ^3 agree well with the measured lean limits, while predicted rich limits are slightly too large. Although not included in Carlson's paper, methane would appear to be detonable over a range of $0.7 < \phi < 2$ with the 400 joule high explosive detonators. However, comparison of the energy scale in Figure 6 with the values for minimum initiation energy E_{min} given by Carlson indicates that for each fuel-O_2 mixture, Carlson observes a value for E_{min} higher by about a factor of ten than Matsui and Lee, as pointed out in the latter paper. Given this distinction, it appears from Figure 6 that CH_4-O_2 would have been almost, but not quite, detonable in Carlson's experiments. Furthermore, the rich limits for C_2H_4-O_2 and C_2H_6-O_2 then agree very well with the computed values for Δ^3.

Computed data for methanol-oxygen are given by the dashed curve in Figure 6. Although experimental data were not available, from the model it appears that values for critical initiation energies and limits for spherical detonation for CH_3OH-O_2 should be similar to those for C_2H_6-O_2.

FUEL-OXYGEN-NITROGEN MIXTURES

For many practical applications, detonation properties of fuel-air mixtures are of principal interest. However, since the study of detonations in such mixtures often involves large high explosive initiator charges and large quantities of the fuel-air medium, it has proved convenient to study detonations in fuel-O_2 mixtures diluted with smaller amounts of N_2 than are present in air. Results can then be extrapolated to predict detonation properties in fuel-air. In this paper only stoichiometric and "CO stoichiometric" fuel-O_2 mixtures diluted with N_2 are discussed, although complete ternary mixtures have been studied for some fuels [37,38]. For each fuel-O_2-N_2 mixture, induction times and induction lengths were computed. The results are summarized in Figure 7, where the solid curves represent stoichiometric mixtures and the dashed curves represent CO stoichiometric mixtures, each diluted with various amounts of N_2.

The critical tube diameter d_c required to initiate a spherical detonation has been found to be proportional to the induction length Δ [28,39,40] for these types of fuels. Experimental data for d_c for a variety of fuel-O_2-N_2 mixtures are included in Figure 7. Most of the data were reported by Matsui and Lee, but results for C_2H_4 (CO_2 stoichiometry) determined by Moen et al.[40] and for C_2H_2 (CO_2 stoichiometry) by Zeldovich et al. [25] are also included. All of these results were obtained with initial pressures of 760 torr with the exception of those of Zeldovich et al., which are carried out at 800 torr. The constant of proportionality between d_c and Δ has been chosen such that $d_c = 380\ \Delta$, assuming that a single relationship exists between Δ and d_c, with a proportionality that is independent of fuel type or the amount of N_2 dilution. The agreement between predicted and experimentally determined values of d_c confirms that

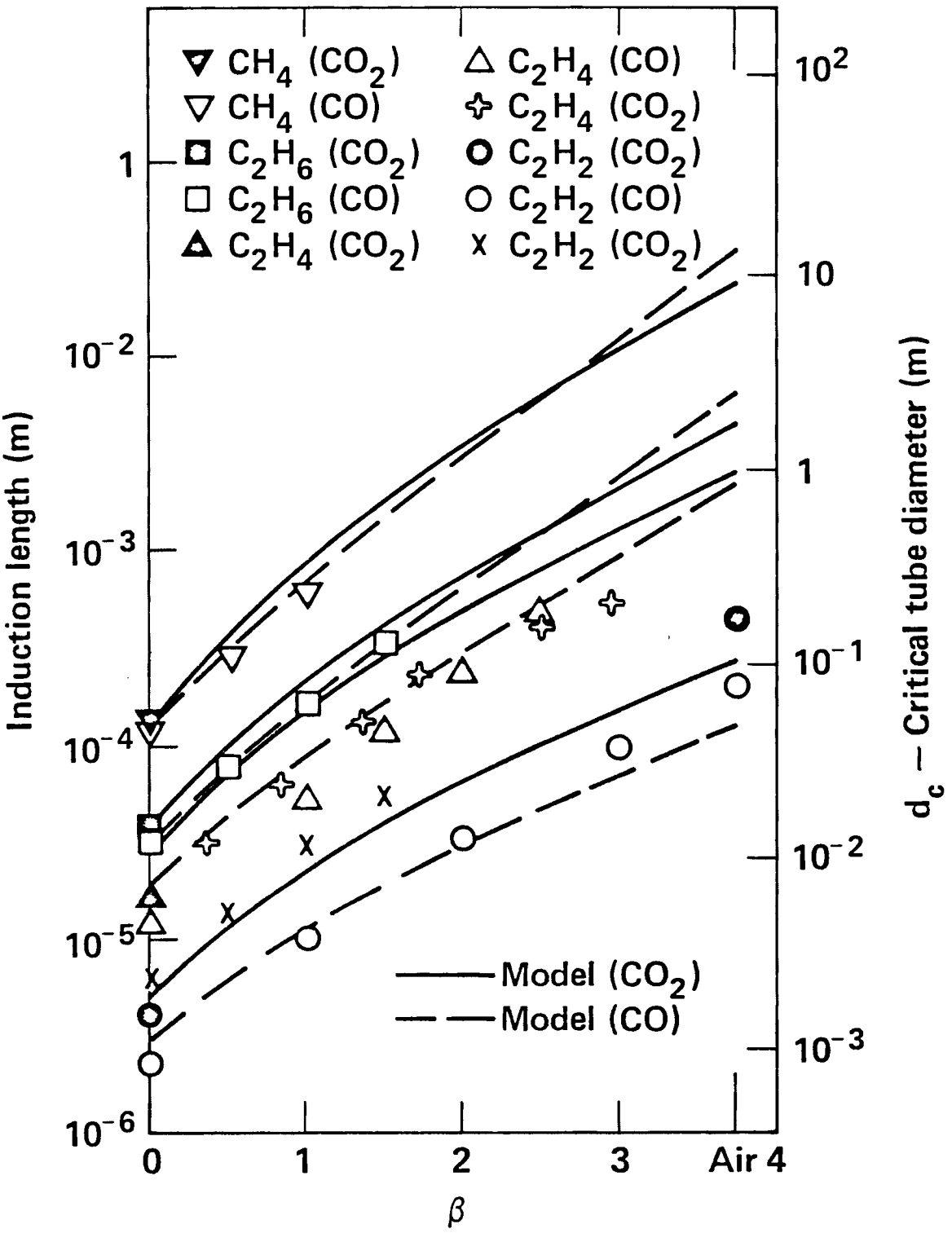

FIGURE 7. Induction length Δ for fuel-O_2-N_2 mixtures, for (in order from bottom to top) C_2H_2, C_2H_4, C_2H_6 and CH_4. Also shown as individual symbols are experimental data for critical tube diameter d_c for initiation of spherical detonation. Data from Moen et al. [40] are indicated by + symbols, from Zeldovich et al. [25] as x symbols, and all other data from Matsui and Lee [28].

this assumption is reasonably accurate. It also means that predictions for other similar fuels can be made with some confidence. When this is done for CH_3OH-O_2 and CH_3OH-air mixtures, the model predicts d_c = 1.70 cm and 97.7 cm respectively with CO_2 stoichiometry and d_c = 1.44 cm and 98.0 cm for CO stoichiometry, placing CH_3OH close to C_2H_4 in Figure 7.

It has been shown [41] that 13 transverse waves are needed in a circular tube of critical diameter d_c to initiate an unconfined hemispherical detonation, so that d_c = 13 b. When this is combined with the above expression d_c = 380 Δ, the result gives b/Δ = 29, an average between the values determined above of about 60 for fuel-O_2 mixtures and 10-20 for fuel-air mixtures.

Recently the problem of direct initiation of detonation in unconfined fuel-air mixtures by high explosive charges has been approached by the method of N_2 dilution of fuel-O_2 mixtures. Bull et al. [42] and Nicholls et al. [43] determined the minimum amount of solid high explosive required to initiate a self-sustained detonation in mixtures of CH_4-$2O_2$-$2\beta N_2$, in spherical and cylindrical geometry respectively. In a purely modeling study, Boni et al. [20] examined spherical detonations in CH_4-$2O_2$-$2\beta N_2$ mixtures, reporting computed results which agreed with Bull et al. [42] over the range of β which had been studied experimentally. However, Boni et al. found that for $\beta > 3$ (a range not studied experimentally by Bull et al.), E_c increased sharply due to a decoupling of the reaction zone from the shock front. As a result their model predicts $M_c \approx 10^4 - 10^6$ kg of Tetryl high explosive, in contrast with the estimate of 22 kg made by Bull et al.

Assuming that the Zeldovich criterion is applicable, the present model can estimate E_c by computing the variation of Δ^{j+1} with β and calibrating

this curve at one experimental point. Results of this process for spherical geometry with CH_4-$2O_2$-$2\beta N_2$ mixtures are shown in Figure 8. Over some ranges of β this plot is nearly straight, but there is considerable curvature over the entire range $0 < \beta < 3.76$. Also shown are experimental data points from Bull et al. [42], with $E_c = 1.0 \times 10^6 \Delta^3$ kg of Tetryl, equivalent to $E_c = 4.27 \times 10^9 \Delta^3$ kJ for high explosive initiation. Values for E_c at $\beta = 0$ (CH_4-$2O_2$) and at $\beta = 3.76$ (stoichiometric CH_4-air) can then be estimated on the basis of their relative chemical induction lengths. For $\beta = 0$ this gives $E_c = 2.4 \times 10^{-6}$ kg of Tetryl or 10.2 joules, whereas Bull et al. estimated a value of $E_c = 2.3 \times 10^{-5}$ kg. However, they assumed that the variation of log E_c was linear with β while Figure 8 indicates some curvature for $0 < \beta < 1$, leading to the lower value for E_c from the model. For stoichiometric CH_4-air the model predicts $E_c = 16.3$ kg of Tetryl, less than the 22 kg estimate of Bull et al. based on a straight line fit to the data in Figure 8.

Nicholls et al. [43] used the same approach in cylindrical geometry to estimate the detonability of stoichiometric methane-air. Comparison between experimental values for E_c and computed values for Δ^2 is shown in Figure 9, as well as the straight line used by Nicholls et al. to fit their own data. For the range covered by the experiments ($1 < \beta < 3$), the straight line fit and that defined by Δ^2 are nearly equivalent. The straight line fit gives $E_c(\beta=0) = 14$ joules/cm while the present model gives $E_c(\beta=0) = 18.8$ joules/cm. The principal difference arises as $\beta \to 3.76$. Nicholls et al. estimate $E_c(\beta=3.76) = 7.5 \times 10^6$ joules/cm, while the model gives $E_c(\beta=3.76) = 6.7 \times 10^5$ joules/cm, an order of magnitude lower.

The variation in computed values of Δ^3 with β for all of the fuels except CH_3OH is shown in Figure 10. Matsui and Lee define the relative

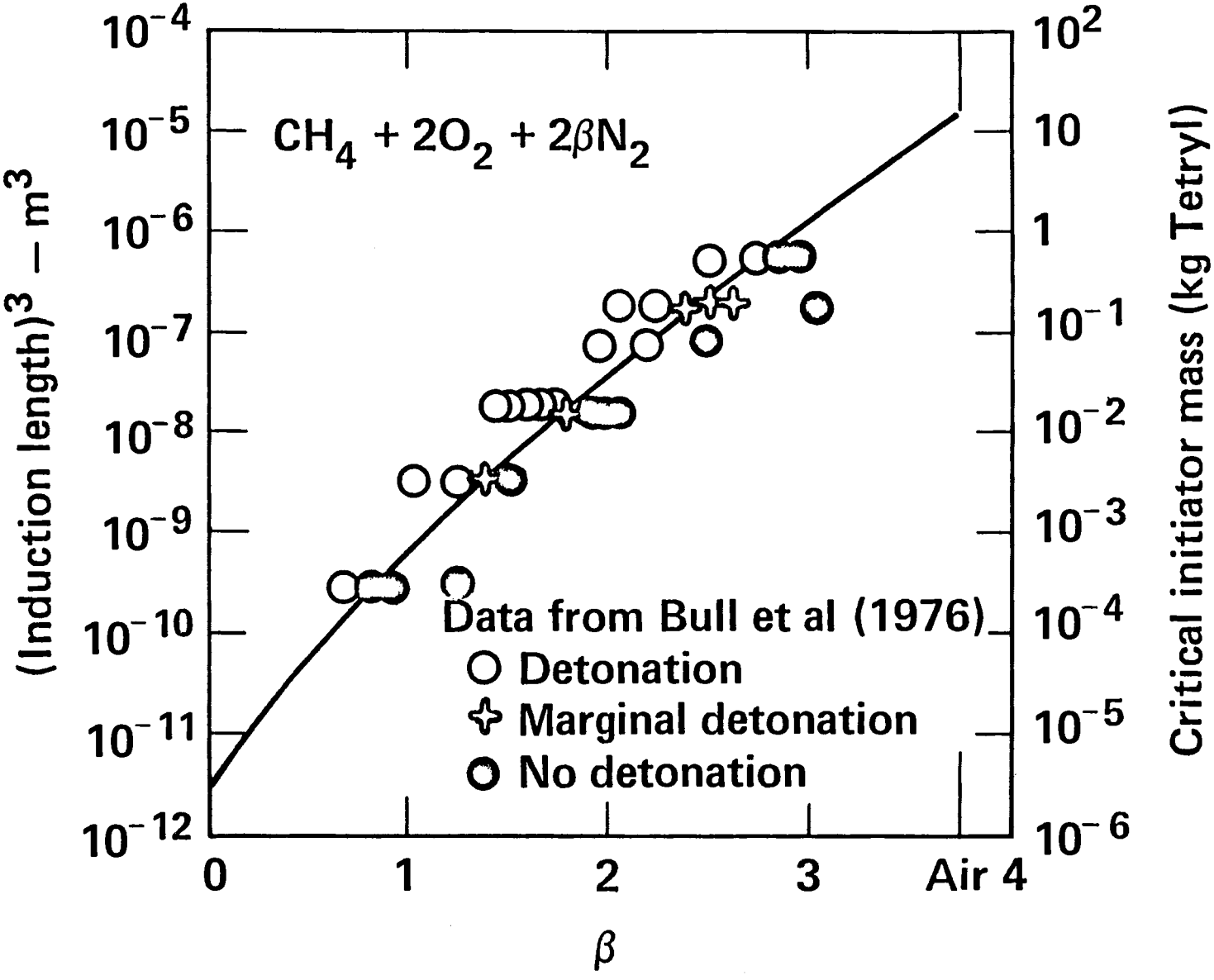

FIGURE 8. Cube of induction length for CH_4-$2O_2$-$2\beta N_2$ mixtures. Also shown are data from Bull et al. [42] for critical initiation energy.

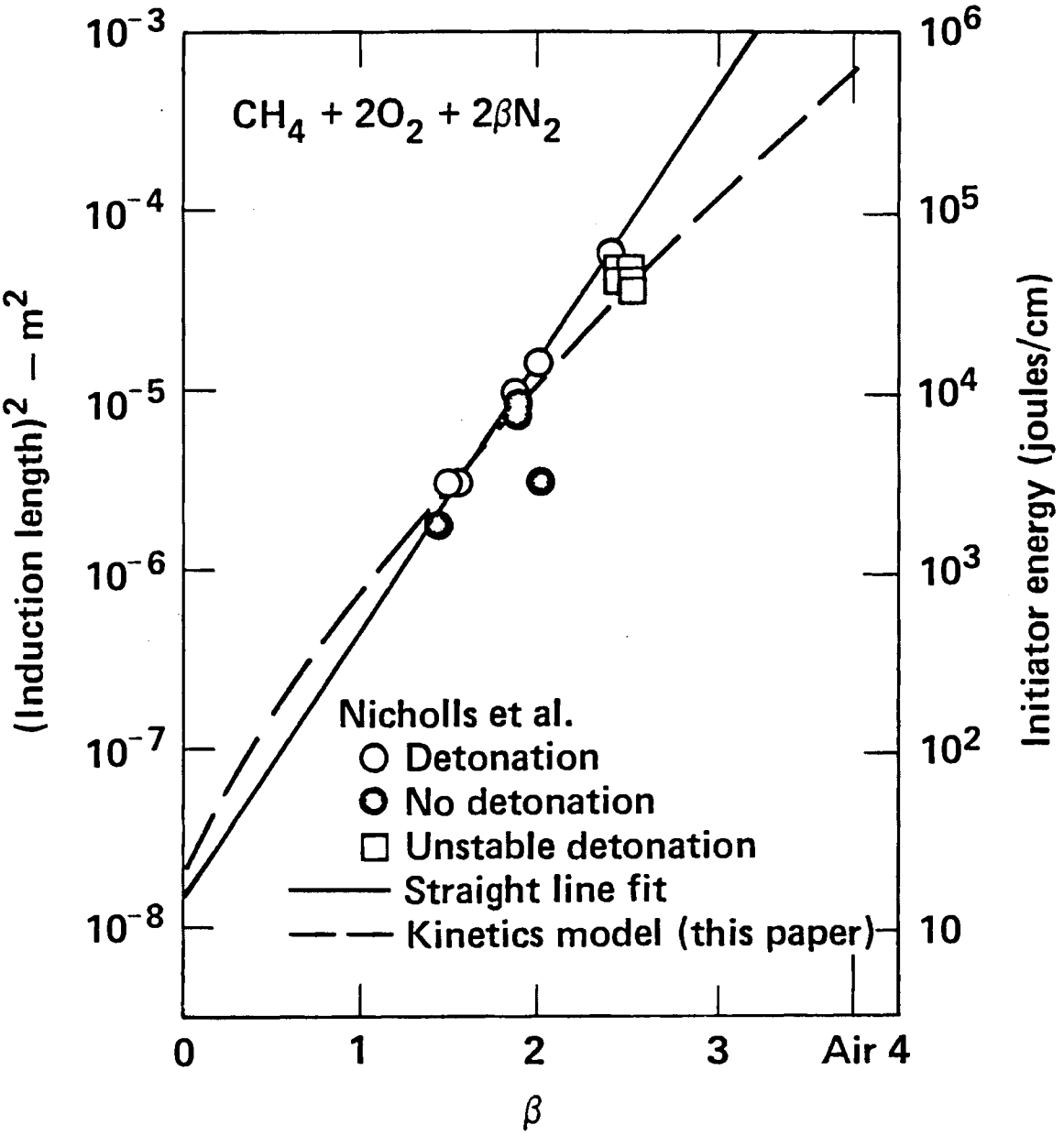

FIGURE 9. Square of induction length for CH_4-$2O_2$-$2\beta N_2$ mixtures. Also shown are data from Nicholls et al. [43] for critical initiation energy.

detonation hazard D_H as the ratio of E_c for a given mixture to E_c for $C_2H_2 + 1.5O_2$. Because D_H is a ratio, it should be much less dependent on the method of initiation than E_c itself. The present model can be used to estimate D_H for each fuel-oxidizer mixture by computing the ratio of Δ^3 to that for $C_2H_2 + 1.5O_2$. The second scale in Figure 10 summarizes these results, together with values determined by Matsui and Lee. The fuel-O_2 values agree well with experiment except for CH_4-O_2 for which the model predicts somewhat too large a value, and the agreement for fuel-air mixtures between computed values of D_H and those estimated by Matsui and Lee by extrapolation from lower values of β is quite reasonable.

The initiation of detonation in CH_4-air has been examined in another way, using stoichiometric mixtures of methane and ethane in air. The fuel composition ratio CH_4/C_2H_6 can then be used in the same way that the N_2/O_2 ratio β was used to extrapolate to stoichiometric CH_4-air. Experimental studies of this type in cylindrical geometry by VanderMolen and Nicholls [44] and in spherical geometry by Bull et al. [7] used this approach. In both studies it was concluded that large high explosive charges would be required for CH_4-air. However, considerable extrapolation was required, with the fuel consisting of no more than 90% CH_4 in the study of VanderMolen and Nicholls and no more than 80% CH_4 in that of Bull et al. Modeling studies [12,17] used the procedures described in the present paper to provide a realistic means of extrapolating to conditions not accessible experimentally, showing that the induction time is a very sensitive function of the methane/ethane ratio for mixtures containing more than 70% CH_4. Agreement between computed induction times and experimental detonation initiation data demonstrated that the present model can be applied reliably to mixtures of fuels as well as the single-component fuels considered here.

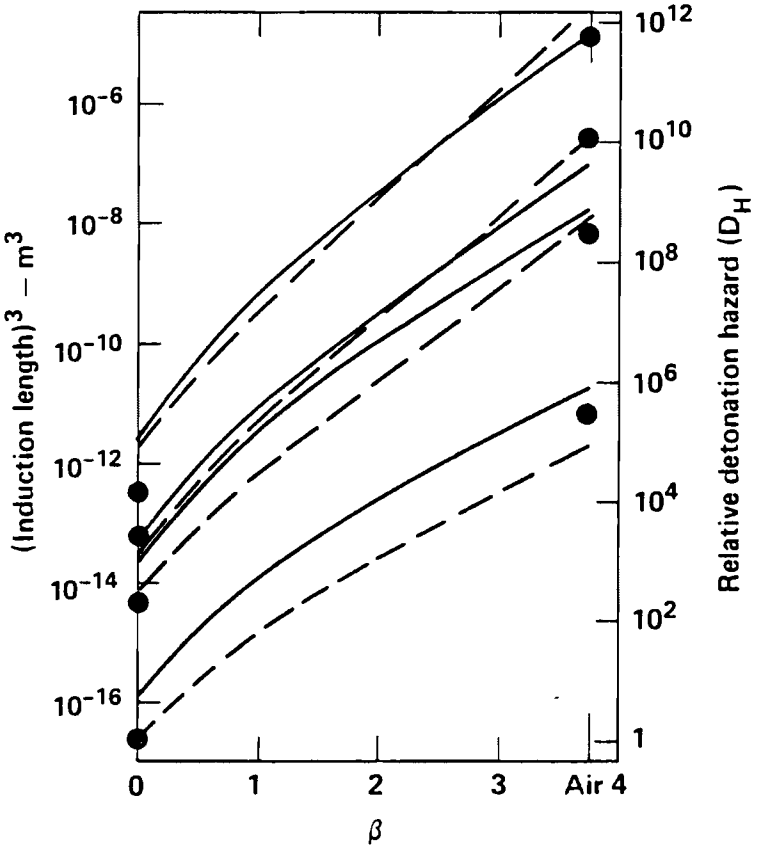

FIGURE 10. Cube of induction length for fuel-O_2-N_2 mixtures at CO (dashed curves) and CO_2 (solid curves) stoichiometric, for (in order from bottom to top) C_2H_2, C_2H_4, C_2H_6 and CH_4. Solid circles represent values of D_H from Matsui and Lee [28] for (in increasing order) C_2H_2, C_2H_4, C_2H_6 and CH_4 at β=0 and β=3.76.

CONCLUDING COMMENTS

The chemical induction time plays a key role in theoretical models for initiation and stability of detonations. Previous models have been limited by their dependence upon overall global correlations of shock tube results, obtained in most cases for very dilute fuel-oxidizer mixtures. Experimental data on the variation of induction time with fuel-oxygen equivalence ratio, amount of dilution, and pressure are rarely included in these global correlations. However, detailed kinetic reaction mechanisms for some hydrocarbon fuels are now available which possess the flexibility and generality required to predict induction times for fuel-O_2 and fuel-air mixtures of interest in detonation processes. For the fuels considered here (CH_4, C_2H_4, C_2H_6, C_2H_2, and CH_3OH) as well as for H_2 [1], the reaction mechanisms are reliable enough that computation of the induction time is no longer the limiting factor in our understanding of processes in detonations. The approach can be applied to non-hydrocarbon fuels such as ammonia, hydrazine, or nitromethane for which detailed mechanisms either have been or could be developed.

Atkinson et al. [1] discussed the effects of post-shock temperature on detonation limits in H_2-air mixtures by pointing out that below ~1350 K, the recombination Reaction 7, $H + O_2 + M = HO_2 + M$ becomes faster than the principal chain branching Reaction 1, $H + O_2 = O + OH$. The reduced chain branching rate becomes too low to sustain the rapid ignition processes required for detonation. When the fuel consists of hydrocarbon species, another factor becomes involved, the reactions of the hydrocarbon fuel and its intermediate product species with H atoms. At the post-shock temperatures considered here, the rates of Reaction 34, $CH_4 + H = CH_3 + H_2$, Reaction 49, $C_2H_6 + H = C_2H_5 + H_2$, and Reaction 82, $CH_3OH + H = CH_2OH + H_2$

are considerably faster than the rate of Reaction 1. As a result, these fuels act somewhat like inhibitors, reducing substantially the fraction of the H atoms which can react with O_2 to provide chain branching. For ethylene, the rate of Reaction 59, $C_2H_4 + H = C_2H_3 + H_2$ is about the same as that of Reaction 1, so C_2H_4 is a less effective inhibitor and is more detonable than CH_4, C_2H_6 and CH_3OH. The rate of Reaction 66, $C_2H_2 + H = C_2H + H_2$ is only about half that of Reaction 1 and competes least effectively for H atoms. In the oxidation of C_2H_4 and C_2H_2, relatively little fuel is consumed by reactions with H atoms. Instead, most fuel consumption is accomplished by reactions with OH radicals and O atoms [9,10,14] which are provided in large measure by Reaction 1. In contrast, rates of reactions between H atoms and methane, ethane, and methanol are high, and a substantial fraction of their consumption is through such reactions. It appears that a generalization can be made, that the detonability of hydrocarbon fuels can often be related to the degree to which the fuel molecule inhibits chain branching through Reaction 1.

The model used here is intentionally oversimplified in order to emphasize the purely kinetic factors involved. Modifications which have been developed and used by other authors should be included in a complete detonation model. Most significantly, the variations in the state of the reacting gas behind the initial shock should be considered, including particularly the effects of post-shock variations in pressure, temperature, and particle velocity caused by rarefactions, wave interactions, contact with confining walls, and other fluid mechanical factors. Eventually a complete model must include a time dependent multidimensional fluid mechanics model which can treat shock

properties correctly, coupled with a detailed kinetics model such as that discussed in this paper. However, in many cases the present model, using kinetic models alone, can provide a great deal of useful information. These calculations are simple and inexpensive to carry out, using any of a large number of available computer programs capable of integrating stiff kinetics equations, and the agreement between computed results and available experimental data suggests that the approach can provide accurate and reliable information on detonation parameters over most conditions of interest.

ACKNOWLEDGMENTS

It is a pleasure to thank a number of people for their help in this work, including in particular Dr. Paul Urtiew for many valuable discussions, Ms. Lila L. Chase who carried out many of the computer calculations, and Professor F. L. Dryer for help in constructing the kinetics model. Useful discussions with Dr. C. M. Tarver, Dr. I. O. Moen, Professor R. A. Strehlow, and Dr. R. E. Mitchell are also gratefully appreciated. This work was performed under the auspices of the U.S. Department of Energy by the Lawrence Livermore National Laboratory under contract number W-7405-ENG-48.

REFERENCES

1. Atkinson, R., Bull, D. C., and Shuff, P. J., Combust. Flame 39, 287 (1980).

2. Strehlow, R. A. and Rubins, P. M., AIAA J. 7, 1335 (1969).

3. Dove, J. E., and Tribbeck, T. D., Astr. Acta 15, 387 (1970).

4. Tsuge, S., Furukawa, H., Matsukawa, M., and Nakagawa, T., Astr. Acta 15, 377 (1970).

5. Bull, D. C., Elsworth, J. E., and Hooper, G., Acta Astr. 5, 997 (1978).

6. Bull, D. C., Trans. I. Chem. Eng. 57, 219 (1979).

7. Bull, D. C., Elsworth, J. E., and Hooper, G., Combust. Flame 34, 327 (1979).

8. Bull, D. C., Elsworth, J. E., and Hooper, G., Combust. Flame 35, 27 (1979).

9. Westbrook, C. K., and Dryer, F. L., Eighteenth Symposium (International) on Combustion, The Combustion Institute, Pittsburgh, p. 749 (1981).

10. Gardiner, W. C., Jr., and Olson, D. B., Ann. Rev. Phys. Chem. 31, 377 (1980).

11. Westbrook, C. K. Creighton, J., Lund, C., and Dryer, F. L., J. Phys. Chem. 81, 2542 (1977).

12. Westbrook, C. K., Comb. Sci. and Tech. 20, 5 (1979).

13. Westbrook, C. K., and Dryer, F. L., Comb. Sci. and Tech. 20, 125 (1979).

14. Westbrook, C. K., Schug, K. P., and Dryer, F. L., In preparation, (1981).

15. JANAF Thermochemical Tables, U. S. National Bureau of Standards NSRDS-NBS 37 and supplements. D. R. Stull and H. Prophet, eds (1971).

16. Bahn, G. S., NASA report CR-2178 (1973).

17. Westbrook, C. K., and Haselman, L. C., Progress in Aeronautics and Astronautics, vol. 75, p. 193 (1981).

18. Jachimowski, C. J., Combust. Flame 29, 55 (1977).

19. Cowperthwaite, M. and Zwisler, W. H., Stanford Research Institute Publication SRI-Z106, 1973.

20. Boni, A. A., Wilson, C. W., Chapman, M., and Cook, J. L., Acta Astronautica 5, 1153 (1978).

21. Libouton, J. C., Dormal, M., and van Tiggelen, P. J., Progress in Aeronautics and Astronautics, vol. 75, 1981.

22. Borisov, A. A., and Loban, S. A., Fiz. Goreniya Vzryva 13, 729 (1977).

23. Kogarko, S. M., Sov. Phys. Tech. Phys. 28, 1904 (1958).

24. Lewis, B., and von Elbe, G., Combustion, Flames and Explosions of Gases. Academic Press, New York (1961).

25. Zeldovich, Y. B., Kogarko, S. M., and Semenov, N. N., Soviet Phys. Tech. Phys. 1, 1689 (1956).

26. Lee, J. H., and Ramamurthi, K., Combust. Flame 27, 331 (1976).

27. Sichel, M., Acta Astr. 4, 409 (1977).

28. Matsui, H., and Lee, J. H., Seventeenth Symposium (International) on Combustion, The Combustion Institute, Pittsburgh, p. 1269 (1979).

29. Benedick, W. B., Combust. Flame 35, 89 (1979).

30. Faraday, A. G., PhD thesis, University of London, 1971.

31. Michels, H. J., Munday, G., and Ubbelohde, A. R., Proc. Roy. Soc. Lond. A, 319, 461 (1970).

32. Pawel, D., Vasatko, H., and Wagner, H. Gg., AFOSR 69-2095TR AD-692900 (1967).

33. Strehlow, R. A., and Engel, C. D., AIAA J. 7, 492 (1969).

34. Bowman, C. T., Combust. Flame 25, 343 (1975).

35. Burcat, A., Scheller, K., and Lifshitz, A., Combust. Flame 16, 29 (1971).

36. Carlson, G. A., Combust. Flame 21, 383 (1973).

37. Guhlmann, K., Pusch, W., and Wagner, H. Gg., Ber. Bunsenges. Phys. Chim. 70, 143 (1966).

38. Freiwald, H., and Koch, H. W., Ninth Symposium (International) on Combustion, Academic Press, New York, 1963.

39. Lee, J. H. S., Ann. Rev. Phys. Chem. 28, 75 (1977).

40. Moen, I. O., Donato, M., Knystautas, R., and Lee, J. H., Eighteenth Symposium (International) on Combustion, The Combustion Institute, Pittsburgh, in press (1981).

41. Mitrofanov, V.V. and Soloukhin, R.I., Soviet Phys. Dokl. 9, 1055 (1964).

42. Bull, D. C., Elsworth, J. E., Hooper, G., and Quinn, C. P., J. Phys. D. Appl. Phys. 9, 1991 (1976).

43. Nicholls, J. A., Sichel, M., Gabrijel, Z., Oza, R. D., and Vandermolen, R., Seventeenth Symposium (International) on Combustion, The Combustion Institute, Pittsburgh, p. 1223 (1979).

44. Vander Molen, R., and Nicholls, J. A., Comb. Sci. Tech. 21, 75 (1979).

REPORT J

500-m^3 Spill Test Facility for Liquefied Gaseous Fuels

W. C. O'Neal
G. M. Bianchini
R. E. Blocker
D. L. Hipple
W. J. Hogan
M. Ochoa, Jr.
W. Wakeman, Jr.

Prepared for the
Environmental and Safety Engineering
Division
U.S. Department of Energy
under Contract W-7405-ENG-48

Lawrence Livermore Laboratory
Livermore, California 94550

REPORT J

TABLE OF CONTENTS

SUMMARY

We describe a test facility planned for the Frenchman Flat area of the Nevada Test Site to study the effects of large spills of liquefied gaseous fuels. The facility is designed to safely and reliably handle test spills as large as 500 m^3. Fuels of interest at present are liquefied natural gas, liquefied petroleum gas, liquefied ammonia, and liquefied hydrogen.

INTRODUCTION

The Lawrence Livermore National Laboratory is participating in the Liquefied Gaseous Fuels Safety and Environmental Control Assessment Program, under the direction of the Office of Operational Safety of the Department of Energy (DOE). The goal of the DOE program is to provide safety information needed by industry, regulatory agencies, and the public for selecting sites for liquefied gaseous fuel (LGF) terminals and storage facilities and for design and operation of these facilities as well as transport facilities such as ships, railcars, and trucks. The Laboratory's responsibilities include developing computer models to predict the effects of large spills of LGFs, and designing, building, and operating a large LGF spill test facility where experiments can be done to verify the computer models.

To adequately verify the computer models, the LGF spill test facility must be capable of handling experiments of sufficient size and operational variability to test the models over a significant range of phenomena. Once verified, the models can be used to accurately predict the effects of accidental spills 50 to 300 times larger than the verifying experiments.

The new test facility will be able to spill 10 to 500 m^3 of liquefied natural gas (LNG) initially, and the same quantities of liquefied petroleum gas

(LPG), liquefied ammonia (LNH_3), or, with some modification, liquefied hydrogen (LH_2) later. The experiments to be done involve spilling, evaporation, dispersion, burning, and explosion of LGFs at various rates, volumes, atmospheric conditions, and experimental arrangements.

The scope of the project described here includes the conceptual design, detailed design, procurement, construction, and liquid-nitrogen proof-testing of a 500-m^3-capacity LGF spill test facility. The project will be carried out in two phases. Phase 1 is the design of the entire facility and the construction of a 200-m^3 spill test capability. A six-month LNG spill test series will be conducted at this initial facility. At the appropriate time, orders will be placed for the Phase 2 equipment (two 150-m^3 storage tanks, process piping and valves, and the dispersion lake system). After the test series, the Phase 2 addition will be installed, completing construction of the 500-m^3 facility.

The liquefied gaseous fuels to be used in the spill tests require special handling to remain in the liquid state. LPG and LNH_3 will remain liquid at room temperature if kept under 200 to 250 psi pressure, and they are usually stored and transported under these conditions; to remain liquid at atmospheric pressure, they must be refrigerated. LNG and LH_2 are normally stored at atmospheric pressure and cryogenic temperatures (LNG at -260°F and LH_2 at -423°F). All materials used for constructing the parts of the facility that contain liquefied gaseous fuels must be metallurgically, chemically, and structurally sound at the cryogenic temperatures involved.

In addition to the exacting requirements for materials at cryogenic temperatures, our designs and analyses give detailed consideration to heat transfer, fluid dynamics, thermodynamics, thermal stress, pressure stresses, and seismic loads and stresses. Requirements for storage, transfer between tanks, loading, unloading, subcooling, spilling, and recovery are complicated because of the four different products which are to be stored and spilled at different pressures, temperatures, and spill rates. Two-phase flow of the LGF, caused by unavoidable heat absorption, will limit the maximum attainable spill rate.

Safety of the facility is a prime design consideration because of the combustible and explosive properties of all these products and the toxicity of ammonia. The proximity of the spill test area to the storage tank area results in higher than normal environmental pressures and heat fluxes being imposed on the equipment during experimental or accidental fires and explosions. Design and analysis include these factors.

EXPERIMENTAL REQUIREMENTS

In determining the experimental requirements, studies were made of the existing computer models for LNG spill effects. U.S. Coast Guard studies of possible LNG accidental spill scenarios conclude that the largest credible rapid-spill size is 25,000 m^3, the contents of a single LNG ship tank.[1] On the basis of these studies, experimental requirements for the spill facility were determined (see Table 1).

TABLE 1. Experimental requirements for the 500-m^3 LGF spill facility.

Spill sizes	10 to 500 m^3.
Spill rates	Continuous spills at 10 to 200 m^3/min; instantaneous spills, as large as feasible.
Spill velocities	5 to 25 m/s (independent of rate).
Spill surfaces	Water and soil.
Dispersion surfaces	Shallow lake and dry soil.
Wind speeds	0 to 15 m/s.
Types of tests	Spilling, spreading evaporation, and dispersion. Rapid phase transformations. Vapor cloud fires. Vapor cloud explosions. Vapor cloud fireballs.
Types of LGF's	Initially LNG; in the future, LPG, LNH_3, and LH_2.
Test hours	Night or day.
Frequency of tests	Two or more tests per day.
Aborting procedure	Test fuel in spill pipe to be recovered.
Cooldown time	3 hours maximum.

SITE SELECTION

We conducted studies (see Ref. 2) to determine the experimental and administrative requirements for carrying out the LNG tests. The result was a list of desired characteristics, as shown in Table 2. We used this list to screen 69 federally owned sites as possible locations for the LNG spill test facility. All except five were eliminated because of environmental and safety concerns. The five that remained, judged to be about equal with respect to the environmental impact of carrying out the tests, were:

Frenchman Flat, Nevada
White Sands Missile Range, New Mexico
Hill Air Force Range, Utah
Wendover Air Force Range, Utah
China Lake Naval Weapons Center, California

TABLE 2. Criteria used in evaluating potential sites for the 500-m^3 LGF spill test facility.

1.	Minimal environmental effects.
2.	Low safety hazards.
3.	Minimal administrative constraints.
4.	Acceptable surface winds.
5.	Flat land.
6.	Wide range of atmospheric conditions.
7.	Large body of water.
8.	Available water supply.
9.	Low costs.
10.	Rainfall.
11.	Variable topography.

Four of these five were in turn eliminated because of other factors, such as cost and logistics, leaving Frenchman Flat as the most suitable (see Ref. 3). Frenchman Flat had many desirable features, including its sparse environment, large controlled area, flat topography, consistent SW winds, variable atmospheric conditions, and available water supply. Frenchman Flat is within the Nevada Test Site (NTS), a DOE test area about 80 miles north of Las Vegas, Nevada (see Fig. 1). To conduct the LNG spill tests there, a new environmental impact statement is not necessary, because the existing statements for Frenchman Flat and Nellis Air Force Range are adequate.

FACILITY DESIGN CONCEPT

The spill facility design concept (shown in Fig. 2) consists of two 150-psi LGF storage tanks installed in Phase 1 and two 250-psi LGF storage tanks to be installed later. The Phase 1 facility will store and spill up to 200 m^3 of LGF, and the Phase 2 facility will be sized for 500 m^3. The tanks will be connected to a 1600-ft-long, 24-in.-diam insulated underground spill pipe which leads to a 1000-ft-diam spill pond. The center of the pond will be 25 ft deep. For spill tests on water, the LGF will be forced out of the tanks and out the spill pipe by 150-psi nitrogen or helium gas stored in 2500-psi, 2300-ft^3 pressure vessels. To drive out the LGF remaining in the spill pipe after the storage tanks are emptied, a cryogenic pipeline pig will be forced through the spill pipe by injecting nitrogen or helium gas at 150 to 250 psi behind the pig.

To conduct spills on dry soil, the shallow periphery of one side of the spill pond will be drained and a 100-ft-long extension will be installed on the end of the spill pipe, extending it to the peripheral area. Various nozzles and splash plates will be installed on the end of the pipe to vary spill velocity and direction on or below the water. An array of experimental measurement sensors will be placed upwind and downwind from the spill point.

The facility will be controlled and monitored from a safe distance by remotely located control and recording systems. For day-to-day operations and facility checkout, a local control panel is provided.

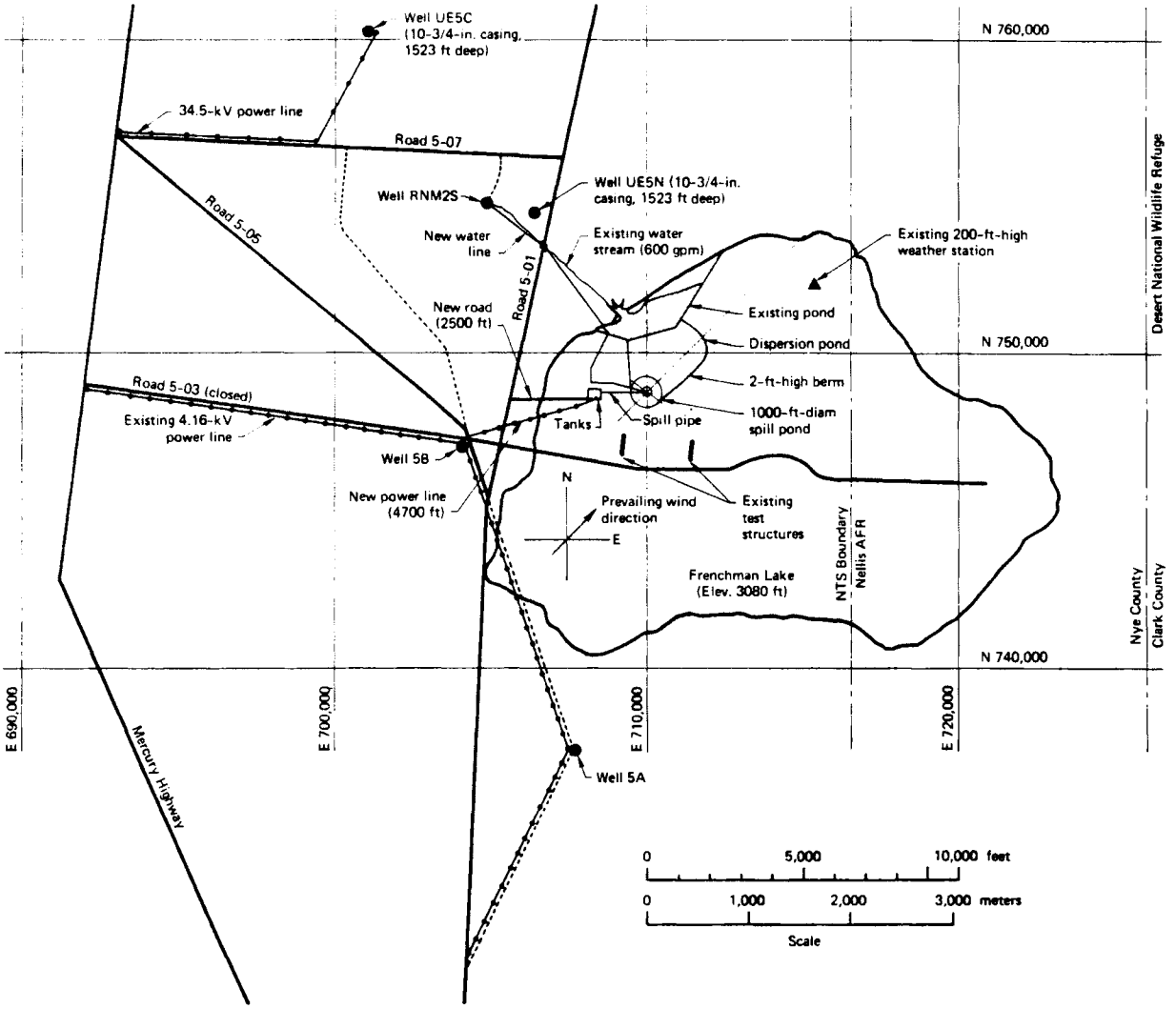

FIG. 1. Location of the LGF spill test facility in Frenchman Flat at the Nevada Test Site, showing existing features and new construction that will be involved.

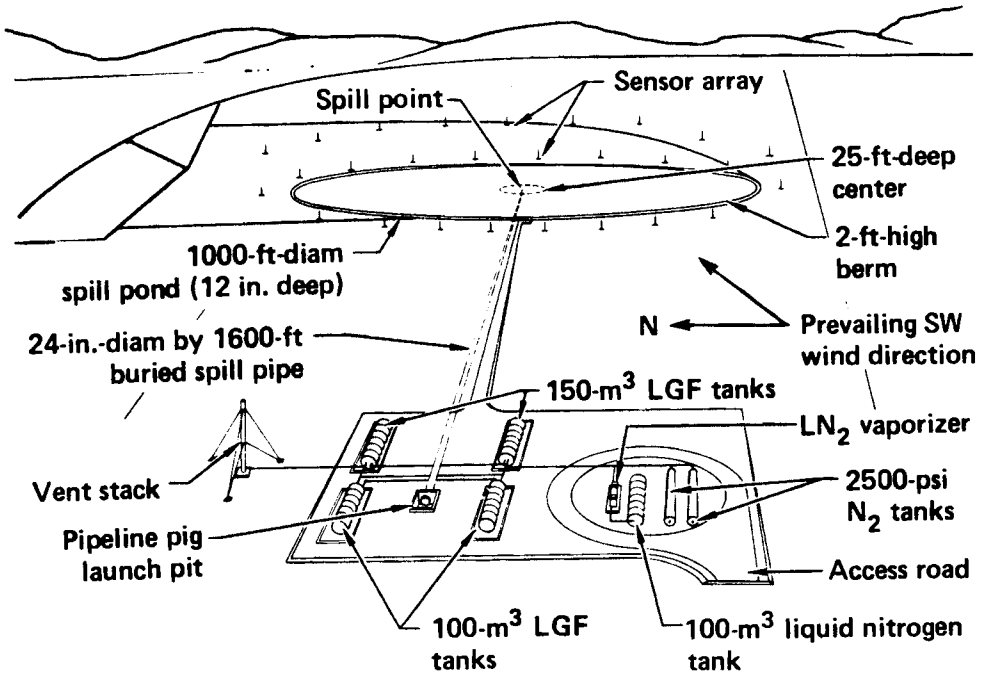

FIG. 2. Design concept of the LGF spill test facility.

DESIGN CONCERNS

The primary design concerns for the LGF spill test facility are threefold: (1) Can the facility achieve the desired 200-m^3/min spill rate of LNG? (2) Will the proposed pigging system force the LGF out of the spill pipe accurately and reliably? (3) Can the tankage area be better protected from experimental effects by the large (1500-ft) standoff distance or by burial or shielding? These questions will be thoroughly analyzed, taking into consideration personnel and equipment safety, experimental performance, and cost. An analysis of LNG spill effects by our scientists will give heat and blast effects as functions of distance from the spill point. By comparing these determinations with the known heat and blast resistance of the facility equipment, including appropriate safety factors, we will determine the standoff distance and shielding required to protect the facility from experimental and accidental effects.

LGF STORAGE SYSTEM

Liquefied gaseous fuel is delivered to the LGF storage system by tanker truck and stored there during periods of test operations. The storage system consists of LGF tanks, valves, vent piping, LGF subcooling system, transfer piping, and associated measuring equipment.

STORAGE TANKS

The Phase 1 tanks are two surplus 150-psi, 28,000-gal (105-m^3) tanks now located at the NRDS area of NTS. They were used there for storing LN_2, but were originally designed for storing liquid oxygen (LOX) for the Atlas Missile Program. For Atlas, they stored the LOX at atmospheric pressure, and were pressurized to 150 psi with oxygen for rapid transfer of the LOX into Atlas missiles. The inner tanks (of 304 stainless steel) are ASME code vessels, but the outer vacuum vessels (of carbon steel) are not. The annular space between the outer and inner vessels is filled with perlite (expanded volcanic ash) and evacuated, providing insulation that holds the boiloff rate to about 0.1% per day for LNG. These tanks can be used to store LNG, LN_2, LPG, and LNH_3 at up to 150 psi, but they cannot be used to store LH_2. The grade of 304 stainless steel and the welding procedures used in the tanks were not selected for LH_2, and the design expansion and contraction allowance is not large enough for LH_2 temperature (-423°F). The 150-m^3 tanks for Phase 2 will be designed for LNG, LPG, LH_2, LN_2, and LNH_3 up to 250 psi.

The two surplus LGF tanks for Phase 1 will be moved to Frenchman Flat, installed on foundations, and recertified. Some of the steps in recertification will be: inspection, leak-testing, drying out or replacing the perlite, pressure-testing, cold-shocking with LN_2, painting, and replacing the gaskets and seals. The tanks will be instrumented with vacuum and pressure gages, thermocouples, liquid-level sensors, and gas sensors.

FILL AND TRANSFER SYSTEM

This system of valves, couplings, and piping is used for unloading LGF or LN_2 into the storage tanks, transferring LGF from one tank to another, and unloading LGF from tanks back into trucks when necessary. Vent and pressure-relief valves release gas into the vent system. To transfer LGF between tanks or to load LGF into tank trucks, LGF tanks will be pressurized at 25 to 30 psi with N_2 gas which will drive the LGF out of the tanks. LGF can also be moved from one tank to another by using the subcooling recirculation pump described below. Vapor return lines will carry ullage vapors to vent lines.

SUBCOOLING SYSTEM

This system consists of a liquid-nitrogen-cooled coldbox with internal tubes for LGF. A pump will circulate LGF from its storage tank through the tubes and back into the tank, thus subcooling the LGF to 5-10^{o}F below its saturation temperature at atmospheric pressure, so as to prevent flashing of vapor in the spill pipe during spill tests.

LGF SPILL SYSTEM

The LGF spill system consists of the urethane-insulated, 1600-ft-long, 24-in.-diam main spill pipe, 18-in.-diam feeder pipes connecting to the LGF tanks, a nozzle and deflector plate at the spill point, the pipeline pig system, the dump tank system, and the LN_2 precooling system.

PIPE SIZE DETERMINATION

In order to properly size the spill pipe, it is important to predict the pressure drop that will occur at various flow rates. As the cryogenic LGF flows through the spill pipe, it will absorb heat from several sources: heat that leaks through the insulation from outside, heat from fluid frictional heating, and residual heat remaining in the pipe and insulation after precooling. The LGF in the tanks will initially be subcooled at atmospheric pressure.

However, if the heat abosorbed is great enough to raise it to boiling, some amount of LGF will be vaporized before it leaves the spill pipe, causing two-phase flow and a higher pressure drop than would occur with single-phase liquid flow for the same mass flow rate.

For conservatism, the spill pipe was sized and pressure drops predicted with two-phase-flow calculational methods, assuming no subcooling. The calculation method we used is based on the Martinelli and Nelson correlation for two-phase, single-component flow first published in 1948.[4] This correlation has been compared with experimental data for water, Freon-11, liquid nitrogen, liquid hydrogen, and other fluids. The comparison shows that the Martinelli and Nelson correlation fits the data well.

One calculation done with the Martinelli and Nelson correlation shows that liquid methane (LNG is 90-95% liquid methane), flowing at 200 m^3/min from inside the LGF tanks through 1600 ft of 24-in. pipe and out the valve and nozzle at the spill point, sustains a 100- to 120-psi pressure drop. Since a 150-psi drive-gas pressure is available, this leaves extra capacity in case there is additional two-phase flow due to transient or other effects. Some other results of this calculation are shown in Table 3.

This and similar calculations were used in determining that a 24-in. inside diameter would be adequate for the spill pipe.

SPILL PIPE SYSTEM

This system consists of the main spill pipe, expansion joints, and insulation. The primary part of the spill system is the main spill pipe, which will extend from the tankage area to the center of the spill pond 1500 ft away. In order to do a spill test, pressurized helium or nitrogen gas will be admitted to the storage tanks. The LGF will be driven out of the tanks through a spill valve attached to the exit nozzle of each tank, through a feeder pipe to the spill pipe, then through the spill pipe underground and underwater to the center of the pond, and finally out of the end of the spill pipe through a spill nozzle arrangement above the center of the spill pond.

Since a large portion of the pipe will be either buried or underwater in the pond, it will thereby be protected from damaging experimental effects such

TABLE 3. Calculated pressure drop through spill system for single-phase and two-phase flow. Includes pressure drop from inside LGF tank through nozzle, valve, feeder pipe, spill pipe, and exit check valve.

Flow rate (m^3/min)	Pipe diameter (in.)	Pipe length (ft)	Liquid methane pressure drop (psi)		Liquid hydrogen pressure drop (psi)	
			Single-phase	Two-phase	Single-phase	Two-phase
100	20	600	27	33	--	--
		1100	36	42	--	--
		1600	44	50	--	--
	22	600	21	25	4	5
		1100	26	31	5	6
		1600	31	36	5	7
	24	600	18	21	3	4
		1100	22	24	4	5
		1600	25	28	4	5
200	20	600	110	150	--	--
		1100	140	180	--	--
		1600	180	230	--	--
	22	600	90	110	15	18
		1100	110	130	18	21
		1600	120	150	21	25
	24	600	74	88	13	15
		1100	87	100	15	17
		1600	100	120	17	19

as pool fires, cloud explosions, fireballs, and rapid-phase-transformation explosions.

Pipe Material. The pipe material will be type 304L stainless steel, which is the generally accepted pipe material for cryogenic service. However, the material chemistry will be more tightly controlled than the standard ASTM A-312 chemistry specified for type 304L stainless steel. The allowable phosphorous

and sulfur levels will be lowered so that reliable welds can be more easily made in the material.

In order to use the material at liquid hydrogen temperature, the carbon, nickel, and nitrogen levels will be controlled to prevent the austenite-to-martensite transformation which tends to occur during temperature cycling to liquid hydrogen temperature and when the material is strained at liquid hydrogen temperature. This transformation is to be avoided because of the 2% volume change that occurs, which causes high stresses, and because the resulting martensite is more brittle than austenite. Avoiding the transformation, however, is not as simple as might appear. The nitrogen level necessary to prevent the transformation (0.04-0.08%) is too high for producing welds that will remain tough at cryogenic temperatures.

To prevent the austenite-to-martensite transformation and at the same time achieve tough welds, we will specify 0.04-0.08% nitrogen for the pipe material but use a welding procedure that adds a proper amount of filler metal to the weld for controlled dilution of the nitrogen content. Thus, by using a filler metal that is very low in nitrogen content we can produce a weld whose nitrogen content is only a little higher, well below that of the rest of the pipe material.

Insulation. The entire spill pipe will be well insulated to prevent excessive heat leaks and resulting boiloff of LGF during its transit of the spill pipe. A commercially available insulation system has been selected which consists of polyurethane foam applied to the fiberglass-wrapped pipe in two 2-in.-thick layers separated by a crack-barrier layer. A waterproof hull consisting of glass-reinforced epoxy or equivalent is applied over the outer layer of foam to serve as a water barrier and to protect the foam from damage when the pipe is buried. The inner layer of foam does not adhere to the pipe, so that the pipe and insulation can contract at different rates with temperature changes and thus avoid crushing the foam.

Each length of pipe will be insulated at the factory before shipment to Frenchman Flat. Field joints will be insulated using preformed foam sections fitted into place and covered with a fiberglass-epoxy moisture barrier.

Expansion Joints. Since the pipe temperature will range between ambient temperatures and liquid hydrogen temperature, provisions must be made for thermal contraction. The pipe will contract about 4.82 in. per 100 ft when it is cooled from 70°F to liquid hydrogen temperature. To permit the pig to travel straight through, bellows-type expansion joints will be used. The bellows assemblies will be installed at approximately 200-ft intervals along the pipe, depending on the amount of movement each bellows can take. The pipe will be anchored in such a way that there is one expansion joint between adjacent anchors, so that each expansion joint will take the same amount of movement.

The bellows expansion joints will be factory-insulated in the same manner as the pipe and will be welded to the pipe in the field. The field joints will be insulated using preformed foam sections fitted into place and covered with a moisture barrier.

SPILL NOZZLE SYSTEM

Provisions will be made on the end of the spill pipe for interchangeable spill nozzles to be added so that different spill configurations can be achieved. By changing the spill nozzle, LGF can be spilled sideways, upward, or down into the water. The exit velocity of LGF can also be varied independently of spill rate by using different nozzle diameters. Back-pressure and subcooling can be varied by placing orifices of different diameter in the exit nozzle.

PIG SYSTEM

The proposed spill pipe is 24 in. in diameter and 1600 ft long, with a volume of 140 m^3. In order to perform a spill without leaving a large amount of LGF in the spill pipe, a pipeline pig system will be used. The system will include a pig launcher at the tankage end of the spill pipe, a pig receiver at the spill-pond end of the pipe, and the pig itself.

The pig is a free piston that fits inside the pipe with a small clearance. Helium or nitrogen gas under pressure will be admitted behind the pig, which will force the pig through the length of the pipe, pushing out the liquid ahead of it. The pig will be loaded into the tankage end of the spill pipe

through a removable flange on the pig launcher before the spill pipe is cooled to LGF temperature. After the spill, the pig will be retrieved from a pig receiver at the pond end of the spill pipe or, alternatively, it may be allowed to leave the spill pipe through the spill nozzle. Results of our 1/8-scale LN_2 cryogenic tests indicate that the pipeline pig will function with a cryogenic fluid. Further development and testing at 1/4 scale is planned to measure pigging efficiency and control.

DUMP TANK SYSTEM

In order to approximate an instantaneous spill, a special dump tank will be placed at the end of the spill pipe. The dump tank will be hemispherical or similar in shape, and will be positioned in the spill pond underneath the spill nozzle. It will be filled with LGF through the spill pipe and then rapidly pulled underneath the water surface, forcing the LGF into contact with the water and forming a nearly instantaneous spill. Being underneath the water surface, the dump tank will be protected from damaging experimental effects such as fire and explosions, although it will still be exposed to the effects of rapid phase transition (RPT) explosions. The dump tank will be insulated to prevent excessive boiloff of LGF while awaiting dumping.

LIQUID NITROGEN PRECOOLING SYSTEM

Before a spill test is performed, the spill pipe must be cooled to LGF temperature. The pipe must be cooled in such a way that excessive differential thermal strains and resulting stresses do not develop. This means that cooling must be done uniformly around the circumference of the pipe from end to end, so that the pipe will not tend to bow due to thermal effects.

Precooling will be done by introducing nitrogen gas at -320°F (-196°C) into the tankage end of the spill pipe and venting it out the pipe at the spill point. When the pipe is cooled to within about 100°F (55°C) of the LGF (or liquid nitrogen) temperature, LGF (or liquid nitrogen) will be introduced into the pipe to complete the cooldown without excessive thermal strains. The exact amount of nitrogen and length of time required for precooling will be determined by further analysis, but it is expected that precooling using gaseous ni-

trogen could take about two to four hours and require up to 10,000 gallons of liquid nitrogen. During periods of test operations it may be necessary to maintain the spill pipe at LNG temperature continuously with LN_2 in order to be ready for a spill test on short notice.

HAZARDS CONTROL MEASURES

Hazards control measures for the spill test facility consist of hazards analysis, safe design, gas detection, fire detection, fire and explosion control, an emergency shutdown system, safe operating and testing procedures, and a quality assurance program.

A preliminary hazards analysis has been made for the 500-m^3 spill facility, and a hazards analysis for a 1000-m^3 Frenchman Flat spill facility was completed in 1978 (Ref. 2). On the basis of these analyses, the edge of the 500-m^3 spill facility's storage tank area was chosen to be 1500 ft (457 m) from the spill point. For test operations, a safety plan will be developed as part of the spill test operations project. The plan will prescribe test limitations, safety zones, and evacuation procedures for all spill tests.

GAS SENSOR SYSTEM

Flammable-gas detectors will be positioned at various points between the tankage area and the spill point. They will be used to monitor the portions of the facility where LGF leaks would be most likely to occur, and also to detect an approaching cloud of LGF vapor, such as might occur if the wind shifts during a spill test and blows the vapor back toward the facility. The sensors will be MSA or IST gages, with electronics that will transmit analog or digital signals to the control room. Panel meters and alarm indicators will display the calibrated signals as percent of flammability limit or absolute percent of gas in air.

FIRE SENSOR SYSTEM

The points in the facility where gas leaks are most likely to occur are candidate locations for ultraviolet detectors sensitive to fires. Fire sensor signals will be displayed at the control room and will be tied in to alarm systems and to the automatic shutdown system. This system, when activated, will reset all facility valves to their safest position, closed or open, and will activate alarms at the facility, the trailer park, and the NTS Fire Department.

FIRE AND EXPLOSION CONTROL

Fire and explosion control begins in the goal-setting phase of facility design. One of the critical goals of the project is to avoid serious injuries and equipment damage. A quality assurance program will be followed to ensure that this goal is attained. By using code-specified materials and designs for storage facilities, we can ensure a high probability of having leaktight equipment that is not subject to fires and explosions. Table 4 lists measures to be taken during design, construction, and operation of the facility to prevent leaks, fires, and explosions.

CONTROL AND MONITORING SYSTEMS

The basic goals of the control system are to control the spill volume to within $\pm$10% and to control the spill rate to within $\pm$10% for 70% or more of the spill time.

In conducting a spill experiment, the following sequence of actions will occur. First, the main spill pipe will be purged with nitrogen gas. Second, a predetermined amount of cold nitrogen will be driven into the spill pipe to precool it. Third, the LGF to be spilled will be driven out of the tank(s) and down the spill pipe by injecting nitrogen or helium drive gas into the vapor space of the LGF tank. The gas pressure will be controlled at some preset pressure ranging up to 150 psig, depending on the desired spill rate.

When the desired amount of LGF has flowed from the tank, the tank outlet valve will be closed. Gas will be admitted to the near end of the spill pipe, behind a pipeline pig inserted there, and will drive the pig to the far end of the pipe, forcing the remaining LGF out of the pipe at the spill point. Finally, the pipe will be purged with nitrogen gas.

SPILL SIZE CONTROL

In order to determine the amount of LNG spilled, a tank-level or weight gauge will be used. By monitoring and recording the tank-level and weight changes before, during, and after a spill, the quantity spilled as well as the spill rate can be determined to within 10% accuracy.

A short time after the spill pipe has been precooled, the spill test will be done. The smallest spill planned will be 10 m^3. For this case, 10 m^3 of LGF will be admitted into the spill pipe under low pressure (or hydrostatic head). The pig will then be launched, with the required drive-gas pressure applied behind it to drive the LGF out of the pipe. LGF remaining in the spill after a test will be pumped back into the tank. The final tank weight will then be recorded.

For larger spills, the pipe will first be filled with LGF as described above. Then, with the spill valve still open, drive gas will be admitted into the vapor space of the LGF tank to drive out LGF at the required spill rate. When the desired amount of LGF has flowed out of the tank (as determined by tank-level changes), the spill valve will be closed. Drive gas will then be admitted to the spill pipe behind the pig to drive the pig and the LGF in front of it as described above.

SPILL RATE CONTROL

In order to achieve different spill rates (i.e., different flow velocities through the spill pipe), different drive-gas pressures must be used. Calculations of frictional pressure drop through the spill pipe can be used to predict flow rate at various drive-gas pressures.

TABLE 4. Fire and explosion control measures to be used in the LGF spill test facility.

- Fracture-safe materials.
- Extended bonnets for leaktight cryogenic valves.
- Dikes around LGF tanks to contain spills.
- 100-ft spacing between LGF tanks.
- 1500-ft spacing between spill point and LGF tanks.
- Remotely actuated valves that automatically return to safe position in case of emergency.
- Recertification of surplus equipment for new operating conditions.
- Pressure relief and vent valves, exhausting to the vent stack, to prevent overpressuring the tanks and piping.
- Portable and fixed dry-chemical fire-extinguishing systems where appropriate.
- Explosion-proof electrical systems at appropriate code-required locations.
- Lightning grounding system.
- Grounding system for static buildup on spill pipe.
- Remote location of control point so that, in emergencies, valves can be safely actuated by operating personnel.
- Gas and fire detectors for early warning of leaks or fires.
- Quality assurance procedures for critical goals in design, procurement, construction, and operation.
- Qualified, trained supervisors and operators in control of the facility.
- Safety plan and safe operational procedures for LGF spill-test operations.
- NTS Fire Department stands ready to assist in emergencies.

The drive-gas pressure will be controlled by a manually preset pressure-control valve and an on/off valve. To change from one spill rate to another, one must change the set point on the pressure-control valve to the pressure required by the new spill rate. By observing the tank-level decrease and opening or closing the drive-gas valve, the operator can control LGF flow rate into the spill pipe.

At the beginning of the spill, it may take ten seconds or more to accelerate the flow to the planned flow rate. At the end of the spill, when the pig is being driven down the pipe, the flow will tend to accelerate beyond the planned rate if a constant drive-gas pressure is maintained behind the pig. To avoid this excess acceleration and to maintain the desired flow rate as long as possible, the drive-gas pressure in the pipe must be decreased as the pig progresses down the pipe. This will be done by shutting off the drive-gas supply to the spill pipe at an appropriate time and allowing the gas in the pipe to expand and drive the pig the remaining distance under steadily decreasing pressure. If shutting off the drive-gas supply does not decrease the pressure rapidly enough, it can be decreased further by venting the spill pipe. Thus the operator can control spill rate by observing the pig velocity, closing or opening the drive-gas valve as appropriate, and venting the spill pipe if necessary. This process could be computer-controlled if required.

The above paragraphs illustrate the general spill-control scheme, which involves the opening and closing of drive-gas and LGF valves. In addition, there are LGF unloading valves and vent valves which require actuator operation, and some other valves which require only manual operation. A total of about 30 electro-pneumatically actuated valves are required for the 200-m^3 Phase 1, plus about 20 more for the two 150-m^3 tanks to be added in Phase 2, for a grand total of about 50 such valves.

The LGF (and LN_2) valve actuators are pneumatically controlled spring-loaded pistons in cylinders; they are driven by the actuator gas supply system. Each actuator has a solenoid valve which can release pressurized gas into the cylinder to drive the piston (against spring pressure) to its "out" position, or exhaust the gas from the cylinder and allow the coil spring to drive the piston back into its fail-safe "in" position (valve open or closed depending on assembly direction).

The remote control panel for the facility will be located at the control point (CP), and a local control panel will be located at the tank loading area. The CP control panel will contain switches, interlocks, and possibly timing circuits for all of the actuated valves. A switch closure will send a low-voltage signal to the facility by hardwire or by telemetry. The receiving circuit at the facility will close a relay which will connect a higher voltage to the solenoid valve. This valve will then open, releasing N_2 gas at 40 to 80 psi into the pneumatic cylinder to actuate the LGF (or LN_2) valve.

The CP control system may contain electromechanical or microprocessor-preprogrammed valve actuation sequences and recorders, depending on the design selected. The criteria for the design are reliability, flexibility, cost, schedule constraints, and operational simplicity.

MONITORING

There will be 100-200 sensors in the spill facility to measure temperature, pressure, gas concentration, and liquid level. The output voltage from the sensors will be amplified and transmitted to the remote control point by wire or by telemetry, depending on cost and reliability trade-offs. For LGF velocity measurement, a series of magnetic flux detectors placed at 100-ft intervals along the spill pipe will sense the pig magnet as the pig travels through the spill pipe. In the control trailer the signals will be calibrated and displayed on analog or digital panel meters, and some of the signals will be recorded.

Some monitor signals (e.g., the liquid-level sensor) will be linked to alarms or automatic valve-actuator switches in case of emergencies. Also, gas-concentration and flame sensors may be linked to alarm and automatic actuation circuits.

CIVIL CONSTRUCTION

ROADS

There are several new roads required for the spill facility, including a secondary paved road, one or more gravel roads, and jeep roads for access to

instrumentation. The new paved road will extend 2500 ft from Road 5-01 to the tankage area and will be the main access road to the facility. It will be designed according to DOE NVO Standard Construction Specifications, Section 39.5.

SPILL BASINS

The spill basins will be used for spilling LGF on water and on land, as shown in Fig. 2. The spill-on-water berm will be 1000 ft (300 m) in diameter and about 2-1/2-ft high. Most of the pond it contains will be shallow (about a foot deep). The deep part of the pond, at the center, will be 25 ft deep and 25 ft in diameter. Outside this deep part, the bottom of the pond will slope upward to reach the shallow-water level at a diameter of 125 ft.

For spills on dry land, the shallow portion of the pond will be drained and a 2-ft-high by 400-ft-diam berm will be built to the east of the deep area. The spill pipe will be extended 100 ft to the new area.

An extended shallow-pond area will be constructed downwind from the spill pond for a distance of 2500 to 3000 ft, depending on water supply and evaporation rate. The berm will be about 1 ft high.

TANK FARM PAD

The tankage area will be built up to about 18 inches above the lake bed level with gravel. There will be a paved road area on the pad for LGF trucks and other traffic.

There are foundations required for LGF and nitrogen tanks, pipe supports, and power transformers. The foundations will be designed for appropriate loads and for the lake bed soil, which has a fairly low wet strength. Soil sampling and testing will be done in areas with unknown properties.

WATER LINE

There is an existing well (RNM2S) 1-1/2 miles NW from the spill pond. The well pumps water into a ditch which drains to the existing pond. We plan to install an irrigation pipeline from the well to the spill pond in order to avoid the seepage and evaporation losses from the ditch. A new pump will be

required to pump the water through the pipeline. There is power available at the well for the new pump. A portable gasoline-powered pump will be used to drain the pond when required.

DISPERSION LAKE SYSTEM

In order to approximate marine values of atmospheric parameters such as stability, the Richardson number, and humidity, a large area of watered surface will be required during warm weather. An area at least 1 km long by 300 m wide upwind of the spill pond must have some standing water in order to humidify the moving air and cool it somewhat. The area downwind from the spill pond also must be cooler than the air, but it need not humidify the air as much as the upwind area. The area downwind should extend for several kilometers.

A study made in 1980 indicates that a water supply of thousands of gallons per minute is necessary to wet down the area under consideration. A sprinkler system or ditch irrigation system will be designed and installed in the second phase of the spill facility project in 1984.

It may be necessary to install several miles of pipe from existing wells or to dig new wells and to build a temporary reservoir in order to store up the water needed for a series of tests in warm weather. During January and February, winter rains periodically cover Frenchman Flat with water many centimeters deep. This will provide marine conditions during cold weather for the 200-m^3 tests, if needed, at the end of the series, just before installation of the Phase 2 hardware.

ELECTRICAL SYSTEMS

The electrical systems consist of a power system for the tank farm area, one for the trailer park, and one for Well RNM2S (existing). In addition, at the tank farm area are a grounding and lightning-protection system, lights, and telephone. For the tankage-area power system a new pole line from Well 5B substation is required. The trailer park will be located next to an existing pole line near a substation if possible.

REFERENCES

1. An Approach to Liquefied Natural Gas Safety and Environmental Control Research, DOE/EV-0002 (February 1978).

2. J. L. Cramer and W. J. Hogan, Evaluation of Sites for LNG Spill Tests, Lawrence Livermore National Laboratory, Livermore, Calif., UCRL-52570 (September 15, 1978).

3. W. C. O'Neal and W. J. Hogan, Environmental Analysis for an LNG Spill Test Facility, Lawrence Livermore National Laboratory, Livermore, Calif., UCRL-52598 (June 1981).

4. R. C. Martinelli and D. B. Nelson, "Prediction of Pressure Drop During Forced Circulation Boiling of Water," Trans. ASME 70(8), 695 (1948).

REPORT K

Ecological Background Relevant to Proposed Liquefied Gaseous Fuels Test Site Development at Frenchman Flat, Nevada

D. R. McIntyre
J. H. Shinn

Prepared for the
Environmental and Safety Engineering
Division
U.S. Department of Energy
under Contract W-7405-ENG-48

Lawrence Livermore Laboratory
Livermore, California 94550

REPORT K

TABLE OF CONTENTS

SUMMARY

This report surveys ecological studies of the Nevada Test Site to determine what is known about ecosystems adjacent to Frenchman Flat where Liquified Gaseous Fuel (LGF) spill tests have been proposed. The background information is digested to determine what are the immediately obvious ecological needs to avoid any potential impact of LGF tests.

A considerable ecological baseline already exists in the vicinity of Frenchman Flats. The area has been subject to change in the past due to erosion, climate, and influences of man. Plant habitats and plant-animal nutritional dependencies are by now well documented. Of the several species of plants and animals which should be protected in the area, apparently none are found closer than 5 km from the playa. Several former study sites of Beatley and of Romney in Frenchman Flat provide excellent control sites and document the present status of important habitat. Two potential factors of concern are whether the proposed development and associated human activity will affect animal behavior, and whether the vegetation will propagate brush fires or suffer undesirable change as a result of a brush fire. Occasional brush fires may result from LGF tests, so recommendations are made primarily to address those ecological needs. These recommendations deal with methods of estimating fuel and biomass and other factors needed to estimate fire propagation rates, and with procedures to document any changes in animal populations and plant productivity.

INTRODUCTION

Historically, the ecology of the Frenchman Flat area in southern Nevada has changed much in the last 40,000 years (Wells and Jorgensen, 1964). The playa (flat lake basin) is at the lowest part of the closed valley. The bajadas (eroded slopes) are an undulating band of alluvial rock, gravel, sand, and clay that have eroded from the mountains surrounding the valley. This area contained species of plants (Juniperus) less than 40,000 years ago that now are only found at an elevation 2,000 ft higher in the near mountains. Packrat middens found near the playa contained juniper cones and leaves which are not found in the botanical inventory of the bajadas at the present time.

Rainfall, wind, and freezing of water cause erosion. The bajadas and playa are evidence of extensive rock, sand, and clay movement. What looks like an unchanging desert is really a dynamic movement of materials by water, wind, and animals. As rocks are broken from the mountains and washed or blown into the valley, animals burrow and rearrange the sediments and layers, thus causing new soils to be available for seedlings or to be blown or washed away and be utilized elsewhere by plants. These erosive forces are continually acting and do reform the desert floor pavement which influences the plant and animal habitats.

Typically, the elevation of the groundwater at Frenchman Flat is 2,380 ft above sea level while the surface of the lakebed is at 3,080 ft (Eckel, 1968). The construction of spill ponds for the LGF experiments can create an unusual amount of surface water available to plants and animals thus a new ecological habitat will develop with permanent waterbirds, plants, and animals. The relative abundance of species of animals and plants will change as the physical and chemical conditions change. The creosote bush (Larrea) is able to grow in

large areas of the desert as water availability and soil conditions become favorable (Beatley, 1974). Smaller, younger plants will be noticed along the edge of the playa and older and dying ones are in the mixed species of the bajadas where what was an advantage to the creosote bush has now become an area of biological advantage to other species.

Species of plants and animals either adapt to new conditions or are replaced by other plant and animal species that are more successful in existing in the new habitat. For example, the edge (ecotone) of a plant habitat-area shows a few scattered individuals and then none as soil or water conditions change. Another relevant example is that as fine sediments become available in the alluvial deposits, the kangaroo rat is able to have tunnels that do not collapse, and the rat is able to feed upon plants that grow on the new sediments (Olin and Cannon, 1970). Also minerals are now available for plant nutrition. Russian thistle (Salsola) is a pioneering type of vegetation and along with grasses will invade to utilize the decaying organics and protection provided (Wallace et al, 1972).

PLANT HABITAT

The flora of Frenchman Flat is a transition mix between the low Mojave Desert type plants and the high Great Basin type plants (Beatley, 1975). This mix produces several type-communities with the representative dominant forms. Shadscale (Atriplex confertifolia) is found at the north end of the playa. Boxthorn (Lycium pallidum) is southwest of the playa. Lycium shockleyi is south of the playa and only in a small area. Creosote bush (Larrea) is found in most of the areas of the bajadas of Frenchman Flat; it requires less than 7.2 inches of rainfall per year.

Dominant species of the desert alluvial bajadas area are creosote bush (Larrea) and Burro brush (Ambrosia) shrubs. Joshua trees in the upper bajadas provide nesting sites for birds and shelter in fallen branches. Around old trees are rings of younger joshua trees at a similar age level. Mice and kangaroo rats live under and within the fallen branches. The dominant animal forms are the deer, jackrabbit, coyote, and kit fox with their dependence upon the shrubs or animals living within the plant clumps (Seton, 1924). Larrea, Franseria, and Ambrosia shrubs are found on the bajadas at 3-4,000 ft elevations. Saltbush (Atriplex) grows around the playas (Munz, 1962). Winterfat (Eurotia lanata) and four-wing saltbush (Atriplex canescens) are also found adjacent to the playa.

Winter forbs (herbs other than grasses) and grasses are the dominant ground cover and produce most of the new-growth biomass each year. These plants can invade disturbed sites as is common by Russian thistle (Salsola) and grasses. Invasion by these plants into undisturbed sites is much more difficult as the surface of the soil is compacted. The desert floor has been disturbed in years past by nuclear blast, brush fires, heat, rainfall, and erosion. Roads, power

lines, installations, and off-road vehicles have sometimes damaged the bio-environment by crushing plants and powdering the soil. These changes of soil texture and soil cover may cause patterns of change resulting in a greater diversity of plants and animals. After such disturbance, an injured shrub is not able to keep other plants out and the more fertile soil beneath can then support grasses or shrubs of a different type. Revegetation of damaged areas has been by annual grasses and forbs which are able to move into damaged areas, require less water and do not have competition from dominant forms.

The stage of maturity of plants in desert habitats can be noticed from the size, complexity, and diversity of what is growing. At the Frenchman Flat bajada, the joshua trees are in a stage of young growth. These trees apparently had a few years of good seed germination in the years past. Therefore they are all of similar age. (When young, the joshua tree seedling produces very few leaves, about one new leaf for each of the first six years (Mazrimas, 1980). The creosote bushes at the north edge of the playa are at a maximum stage of development and very few young bushes are present.

PLANT-ANIMAL NUTRITIONAL DEPENDENCIES

The alluvial flat of Frenchman's dry lake has poor air drainage during cold winter nights which affects the success of plants around the playa. The soil is low in nutrients and with the salts from higher areas leaching down, an impermeable caliche layer is formed at 30-70 cm (12-28 inches) depth. Low organic content (<1%) and minimal micronutrients show the need for leaf recycling of nutrients. Larrea does not grow in high saline or high potassium soils. Larrea is found up and slightly away from the lake flat and extends back upslope on the bajadas toward the mountains. The playa soil contains up to 50% clay. The soil is low in sulfates and the amount of free lime is dependent upon the parent material in the alluvium. Micronutrients Mn, Fe, Cu, and Zn are low in concentration but no obvious deficiencies are visible. Recycling of leaves does provide some continued renewal of these nutrients (Mack, 1977). Soils have high cation exchange capacity and exchangeable potassium. The shrubs collect wind-blown soil, litter, and salts. Under the plants there is high carbon, organic nitrogen, and phosphorus present. Subsurface hardpans are continually being decomposed and penetrated by the roots of shrubs. The surface soils exhibit greater than 1% organic content where litter is present. Soil water is low and soil water potentials of -30 to -90 bars are known during dry times (Romney et al, 1973). (Permanent wilting occurs at potentials of -15 bars.) Summer dormancy of the plants is a response to the low water availability and a survival characteristic of these specialized plants in the desert soils.

Foods and feeding of both plants and animals depend upon foods present and new materials brought in (Hayward et al, 1963). Plants utilize minerals in the wind-blown dust, plant and animal remains, and minerals brought to the surface

by animals. Animals depend upon roots, leaves, twigs, seeds, and seedlings for food. A variety of plants offer a greater food source than only one dominant type of plant. A kangaroo rat can eat seeds of Salsola in the winter and spring vegetation in the Larrea-Ambrosia association-type (Soholt, 1977). Grass seeds provide food later in the year. Carnivores will eat what is available. A kit fox or coyote would eat kangaroo rats, birds, pocket mice, or large insects such as grasshoppers, depending upon availability.

All of these life forms in their relationships provide a food cycle and interdependence upon each other. Browsing of cattle, deer, and rabbits effectively prunes and stimulates the shrubs, keeping the growth compact and thus decreases evaporation (Nord et al, 1971). A more compact shrub provides more shelter and greater dust collection. Grasses will grow at the base of the shrubs and help protect soil from wind and water erosion.

An understanding of food webs and cycles emerges when one sees that a dynamic situation exists. North American eagles for example have been recorded as eating many different animals (Olendorff, 1976). The animals available at NTS that have been found in stomach analysis of eagles (throughout North America) are: badger, skunk, coyote, kit fox, bobcat, ground squirrel, mice, kangaroo rat, hares and rabbits, deer, calves, ducks, hawks, vultures, grouse, chukar, doves, roadrunners, owls, lark, raven, crow, and snakes. These animals do inhabit the desert environment and can be considered as potentially part of the food web. Each of the carnivorous animals have in turn eaten other animals and many depend upon the rats and mice which feed upon the desert plants, seeds, and insects. Owls catch and eat birds and mice and the owl pellets are eaten by mice in their need for trace minerals and salts. Uneaten pellets provide nourishment for the plants. Reproductive success of desert rodents is dependent

upon winter production of annuals which provide food and seeds (Beatley, 1969).

The turnover rate of living annuals of the desert is a span of several months from germinating seed to flower, death, and then reduction of remains. Joshua trees and creosote bushes are woody plants that live for many years in normal lifespan. Juniper trees have a very long lifespan and once lived in the Frenchman Flat area 40,000 years ago but are now found only at elevations 2,000 ft higher in the near mountains (Wells and Jorgensen, 1964).

Mineral turnover is rapid in that dropped leaves soon decay and are used as nutrient. Soils are brought to the surface by burrowing animals thus changing the soil texture and mineral nutrition.

Animal feces from rabbits, kangaroo rats, birds, and carnivores produce microhabitat areas which seeds use in germination. This can be seen especially in a "cow chip" which contains acid treated, scarified seeds in a moist fertile medium for new plant growth.

PLANT AND ANIMAL SPECIES CONSIDERATIONS

The desert environment is harsh and has produced some plants and animals that are now considered endangered or threatened because their habitat and range is very limited and their ability to reproduce elsewhere is difficult. In consideration of the U.S. List of Endangered Species, it has been found that in the bajadas of Frenchman Flat, the milkvetch plant (Astragalus nyensis) is present. However, it is also found in the Spotted Mountain Range nearby and has been found in 15 other locations all more than 16 km from the LGF test site (O'Farrell and Emery, 1976 and Rhoads, Cochrane, and Ackerman in O'Neal, 1979). The threatened plant (Arctomecon merriami) has been found elsewhere outside the Frenchman Flat area, and other plants of concern are not found closer than 5 km from the playa. Therefore, in respect to the LNG spill tests, none of the plants will be affected (O'Neal, 1979).

No animals of the Frenchman Flat area are on the endangered or threatened list as stipulated by the U.S. Department of Interior. The animals observed at the Frenchman Flat area are given in Table 1 (Moor et al, 1976).

The State of Nevada has a "protected" list which consists of predatory birds and two mammals. These animals are the kit fox, spotted bat, eagle, falcon, hawk, owl, osprey, turkey vulture, belted kingfisher, white pelican, white-faced ibis, common nighthawk, lesser nighthawk, roadrunner, and desert tortoise. If the proposed development site is kept free of brush, these animals will probably not be in the area during times of human activity and movement near the proposed ponds.

Beatley (1975) has established two study areas on the eastern slopes of Frenchman Flat, which serve as reference baseline plots. Also, studies by Romney et al (1973) were made on 32 sites around Frenchman Flat (ten in the

Table 1. Animals common to Frenchman Flat (Nevada Test Site EIS, Douthett et al, 1977).

Reptiles

Snakes

Chionactis occipitalis
(Western Shovel-nosed Snake)

Lizards

Callisaurus draconoides
(Zebra-tailed Lizard)

Cnemidophorus tigris
(Western Whiptail)

Phrynosoma platyrhinos
(Desert Horned Lizard)

Uta stansburiana
(Side-blotched Lizard)

Birds

Amphispiza belli
(Sage Sparrow)

A. bilineata
(Black-throated Sparrow)

Carpodacus mexicanus
(House Finch)

Erimophila alpestris
(Horned Lark)

Gymnorhinus cyanocephala
(Pinyon Jay)

Zenaidura macroura
(Mourning Dove)

Mammals

Rodents

Ammospermophilus leucurus
(White-tailed Antelope Squirrel)

Dipodomys merriami
(Merriam's Kangaroo Rat)

D. microps
(Great Basin Kangaroo Rat)

D. ordii
(Ord Kangaroo Rat)

Peromyscus maniculatus
(Deer Mouse)

Perognathus formosus
(Long-tailed Pocket Mouse)

P. longimembris
(Little Pocket Mouse)

Rabbits

Lepus californicus
(Black-tailed Jackrabbit)

Carnivores

Canis latrans
(Coyote)

Vulpes macrotis
(Kit Fox)

immediate downwind area) providing detailed baseline data on soil physics, soil and plant mineral composition, frequencies of plant species, and biomass distributions by species (Bradley and Moor, 1976). (See Fig. 1.) Plant populations documented by these studies may be monitored for signs of successional change due to possible disturbance (Beatley, 1975; Romney et al, 1973). Expected effects on plant and animal populations would be either due to disturbance from construction and operation of the facility or due to propagation of fire beyond the barren playa, perhaps carried by the vegetation. Thus the questions relevant to these effects are (1) will the development and associated human activity affect animal behavior in the area, and (2) what are the characteristics of the plant populations which might propagate fire or change as a result of fire.

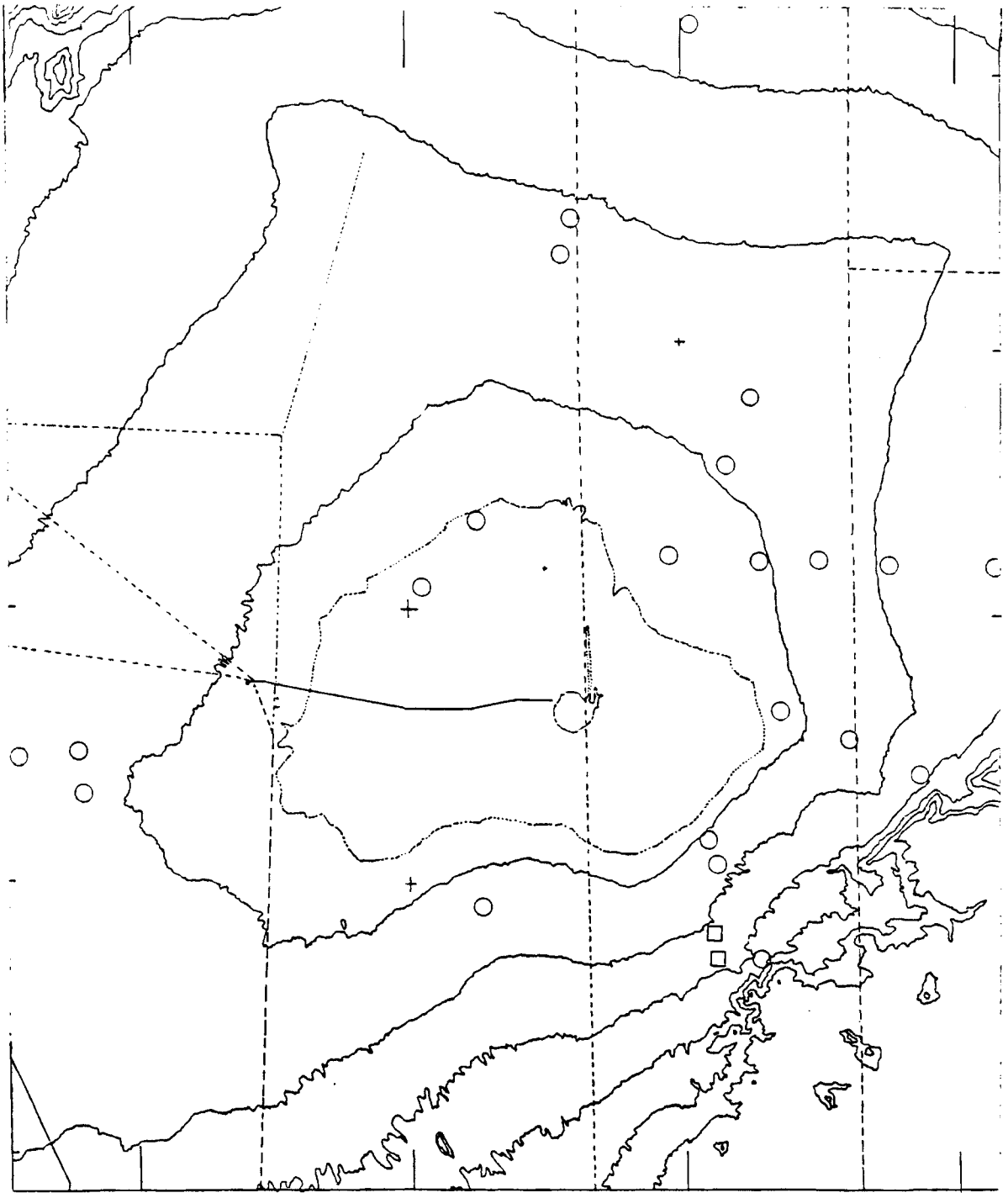

Fig. 1. Location of dominant vegetation types near Frenchman Flat playa showing two study plots (squares) of Beatley and 22 sites (circles) of Romney.

RECOMMENDATIONS

Although comprehensive food web studies have not been accomplished for the proposed experiment area, studies of similar areas can be used for comparison. Since proposed development includes potential brush-fire propagation, the nesting, cover, food availability, and the animals themselves should be understood to minimize potential damage. Analysis of plants and animals near the edge of the playa should include the interplay of foods, shelter, and reproduction of the species. Annuals, perennials, and woody shrubs can be considered in their relationship to insects, reptiles, birds, and mammals to understand what is going on in the plant and animal food web and life history cycles.

Analysis should be made of each vegetation type and its growth, age, reproduction, and competition to evaluate what irreversible or undesirable changes will occur as a result of disturbance. Are the plants in a climax state? Is there a succession of new seedlings present? The standing biomass, the spacing between plants, the amount of dead fuel (grass, brush, and litter), and the soil moisture, humidity, and other seasonal effects will be important to quantify, so that estimates of fire propagation rates and probabilities may be made (Nord and Countryman, 1971). For example, the burning of plants proceeds up to ten times faster if the standing biomass is a winter annual grass such as Bromus rubens. Following disturbance, the inevitable invasion by Russian thistle (Salsola) will delay the return to native vegetation because of competition for water. The question is whether the delay is serious or can it be mitigated by clever land management practices.

Control areas of desert life for comparison to the Frenchman Flat should be established on former study sites, away from the area of past nuclear blasts and yet in the same valley. The lack of Salsola and pioneering species will be

important. Without sudden changes of the moisture available, soil compaction or dust quantity the plant and animal species changes will be slow and minimal. Interdependence of plants and animals is more balanced in a stable area. (An example of imbalance is the throwout zone from Sedan crater where huge populations of Salsola, grasses, and kangaroo rats and mice find favorable habitat, yet soil moisture is low. Larrea, Lycium, and Atriplex have not been able to survive there yet nor will they be able to until the soil is more compact and nutrients and water are available in greater quantity.

In a study of the control areas for Frenchman Flat, plant densities and individual volumes under a plant canopy should be used as methods to indicate productivity and biomass of particular species. Leaf drop studies and fuel studies have been made (Nord et al, 1971 and Mack, 1977). Litter and mineral studies of Artemsia tridentata should be used to indicate recycling of trace elements. Size-biomass relationships should be calculated from basic plant measurements of Larrea, and are felt to be sufficiently accurate to permit productivity predictions over subsequent years (Ludwig et al, 1975). This is possible since the creosote bush has a characteristic growth form.

There is no strong indication that animal behavioral studies should be made. It is not expected that the gases (natural gas, propane, ammonia, and hydrogen) proposed for release at Frenchman Flat will be toxic at the concentrations expected much beyond the barren, dry lake. Baseline animal inventories are needed for key species which could be suspected to suffer from fire or explosion. For example, does the air-gas mixture penetrate burrows and could loss of that population of rodents have a long-term significant effect on the food chain? The suspected range of influence of thermal radiation produced from fire should be calculated so that estimates of injury to birds and furbearing animals may be made. Bird and mammal frequencies within that range should be estimated.

Finally, there are a significant number of studies which have already documented the important baselines of Frenchman Flat ecosystems. What remains to be done is to fill those particular gaps that have been made relevant by the nature of the proposed site development, especially the possibility of fire.

REFERENCES

Ackerman, T.L. 1979. Threatened and Endangered Plants at NTS. Personal communication to W.C. O'Neal.

Beatley, J.C. 1969. Dependence of Desert Rodents on Winter Annuals and Precipitation. Ecology 50:721-724.

Beatley, J.C. 1974. Effects of Rainfall and Temperature on the Distribution and Behavior of Larrea tridentata (creosote bush) in the Mojave Desert of Nevada. Ecology 55:245-261.

Beatley, J.C. 1975. Climates and Vegetation Pattern Across the Mojave/Great Basin Desert Transition of Southern Nevada. Am. Mid. Nat. 93:53-70.

Bradley, W.G. and K.S. Moor. 1976. Ecological Studies of Small Vertebrates in Pu-Contaminated Study Areas of Nevada Test Site and Tonopah Test Range. USERDA Nevada Operations Office, Las Vegas, Nevada. NVO-159. 53-65.

Cochrane, S. 1979. Threatened and Endangered Plants of NTS. Personal communication to W.C. O'Neal.

Eckel, E.B. 1968. Nevada Test Site (Geology). The Geological Society of America. Memoir 110. 290 p.

Environmental Impact Statement. 1977. Final Environmental Impact Statement for the Nevada Test Site. USERDA Nevada Operations Office, Las Vegas, Nevada. ERDA-1551.

Hayward, C.L., M.L. Killpack, and G.L. Richards. 1963. Birds of the Nevada Test Site. Brigham Young Univ. Sci. Bull., Biol. Ser. 3(1). 27 p.

Ludwig, J.A., J.F. Reynolds, and P.D. Whitson. 1975. Size-biomass Relationships of Several Chihuahuan Desert Shrubs. Am. Mid. Nat. 94:451-461.

Mack, R.N. 1977. Mineral Return via the Litter of Artemisia tridentata. Am. Mid. Nat. 97:189-197.

Mazrimas, J. 1980. Growth of Joshua Tree Seedlings. Personal communication.

Moor, K.S., W.G. Bradley, J.S. Miller, and S.R. Naegle. 1976. Standard Nevada Applied Ecology Group Procedures for Collection of Small Vertebrates from Intensive Study Areas. USERDA Nevada Operations Office, Las Vegas, Nevada. NVO-166. 139-148.

Munz, P.A. 1962. California Desert Wildflowers. Univ. of California Press. 122 p.

Nord, E.C. and C.M. Countryman. 1971. Fire Relations, Wildland Shrubs - Their Biology and Utilization. USDA Forest Service Gen. Tech. Report INT-1 Symposium. 88-97.

Nord, E.C., P.F. Hartless, and W.D. Nettleton. 1971. Effects of Several Factors on Saltbush Establishment in California. J. Range Management. 24:216-223.

O'Farrell, T.P., and L.A. Emery. 1976. Ecology of the Nevada Test Site: A Narrative Summary and Annotated Bibliography. USERDA Nevada Operations Office, Las Vegas, Nevada. NVO-167. 249.

Olendorff, R.R. 1976. The Food Habits of North American Golden Eagles. Am. Mid. Nat. 99:231-236.

Olin, G. and J. Cannon. 1970. Mammals of the Southwest Deserts. McGrew Co. 112 p.

O'Neal, W.C. and Collaborators. 1977-1980. Personal communications concerning Liquefied Gaseous Fuels (LGF) Project. Lawrence Livermore National Laboratory.

Rhoads, W.A. 1979. Threatened and Endangered Plants of NTS. Personal communication to W.C. O'Neal.

Romney, E.M., et al. 1973. Some Characteristics of Soil and Perennial Vegetation in Northern Mojave Desert Areas of the Nevada Test Site. University of California, Los Angeles, California. UCLA-12-916. 340 p.

Seton, E.T. 1924. Lives of Game Animals. Doubleday Company. Four volumes.

Soholt, L.F. 1977. Consumption of Herbaceous Vegetation and Water During Reproduction and Development of Merriam's Kangaroo Rat, Dipodomys merriami. Am. Mid. Nat. 98:445-457.

Wallace, A., E.M. Romney and Collaborators. 1972. Radioecology and Ecophysiology of Desert Plants at the Nevada Test Site. USAEC TID-25954. 439 p.

Wells, P.V. and C.D. Jorgensen. 1964. Pleistocene Woodrat Middens and Climatic Change in Mojave Desert: A Record of Juniper Woodland. Science 143:1171-1174.

REPORT L

Environmental Issues of the Proposed LNG Spill Tests at Frenchman Flat

J. H. Shinn

Prepared for the
Environmental and Safety Engineering
Division
U.S. Department of Energy
under Contract W-7405-ENG-48

Lawrence Livermore Laboratory
Livermore, California 94550

REPORT L

TABLE OF CONTENTS

PREFACE

The LNG Working Group has requested a report discussing the environmental issues of LNG spill-effects-tests proposed for Frenchman Flat, Area 5. (see Item 8, Minutes of LNG Working Group Meeting, February 18, 1981; Rhonda J. Folak, Recorder). The format of the report is to be in the form of answers to eleven questions, posed in a letter from Mahlon E. Gates, Manager, Nevada Test Site, to Dr. Richard L. Wagner, Lawrence Livermore National Laboratory.

This report attempts to address those questions with all the information now at hand, and where additional information is required, states the current research underway to obtain longer lead time data. Of course, this approach provides answers which are somewhat conditional. Nevertheless, they should suffice for review of the proposed first phase of LNG operations, and the LNG Working Group will have opportunity to review the environmental issues prior to each additional phase.

BRIEF OVERVIEW OF INTENDED LNG OPERATIONS

Some background information regarding proposed LNG operations at the NTS is necessary prior to environmental discussions. The current plan calls for the NTS Spill Facility to be built in two phases. The first phase, to be completed by April 1983 at the earliest, will have a 200 m^3 storage capacity with a maximum spill rate of 200 m^3/minute. When construction is completed, the facility will be used to conduct a series of progressively larger spill effects tests for a period of about six months. See Plot Plan, Fig. 1. (For comparison purposes 200 m^3 is about five LNG truckloads at 40 m^3 each; LNG ships typically hold 2000 to 5000 equivalent truckloads). The second phase calls for an additional 300 m^3 storage capacity to be completed by July 1984, subject to available funding. (W.C. O'Neal et al, 1981, Figure 3, pg 23, and other details, in Project Plan for Construction of the Liquefied Gaseous Fuels Test Facility, UCRL-53108-DRAFT.) At DOE's request, serious proposals have been made to conduct spills of as much as 1000 m^3 (Cramer and Hogan, 1978, Evaluation of Sites for LNG Spill Tests, UCRL-52570) but there are no current plans to increase the storage capacity of the facility beyond 500 m^3.

This phased development leads to two important facts:

- Significant effects from the smaller spills can be studied before scaling-up, hence providing time to review health and safety aspects,
- From our most conservative estimates (discussed later) it is unlikely that fire or significant detonation overpressures from the first phase tests (200 m^3) will extend beyond the dry lake playa, and is thus unlikely to have any environmental concern.

It is intended that operations of the spill-effects-tests will be carried out under full control by the CP-1, with the adequate weather support staff

(NOAA-WSNSO) and NV Test Controller's Advisory Panel review since this was one of the main reasons for conducting the LNG tests at NTS. Thus, even though details of the spill operations have yet to be worked out, it is clear that prior to each test execution the maximum credible effects will be developed and reviewed. Because of the need to refill the storage tanks by transporting LNG onsite and the limited availability and high cost of LNG, tests will be kept as small as possible and no more frequent than necessary. The design maximum spill rate is 200 m^3/min with 200 m^3 storage capacity in the first phase. We expect that a typical test plan will call for at most two tests per day, a small one followed by a larger one. One test per week is a more likely situation during a test series. The test durations will be typically less than 20 minutes. Weather holds before a test are common. A test series will consist of several clusters of tests, and would be unlikely to last more than six months. Only a few of the tests will be ignited. Most of the large tests will be vapor dispersion tests, unignited releases of vaporized natural gas, which from our experience will be so diluted by air that concentrations will be below levels of concern outside an exclusion area defined for each test.

Combustion tests will be either pool fires or more likely, vapor cloud fires. The pool fires are thermally very radiant and can entrain air leading to fireball formation. These "very showy" fireballs are however, only likely to cause damage in the vicinity of the spill pond. Vapor cloud fires on the other hand are unconfined releases which will burn after enough air (actually, oxygen) is entrained, and can extend long distances downwind. By controlling spills during the 200 m^3 first phase, vapor cloud fires will not reach beyond the dry lake playa. Thermal radiation levels are much lower than for pool fires, hence areas outside of the flammable cloud are unlikely to be effected. Experience has shown that unconfined vapor clouds do not detonate when ignited with low energy ignition sources such as will be used for the vapor burn tests.

Explosion tests either will be the flameless type due to rapid phase transitions of the LNG (RPTs are little understood phenomena of relatively small overpressure occurring near the spill release site) or will be due to detonations or deflagrations of the vapor cloud. Unconfined vapor cloud explosions do not occur as a point source, and cannot proceed as rapidly as high energy explosives (HE) because of their pancake shape and large area. Experience has shown that our empirical methods of estimating HE equivalence are very conservative, but exact analyses of this phenomena are part of the research program. The experimental program will begin with small vapor cloud explosions and proceed to larger ones only when it is proved safe to do so.

We can summarize this overview as follows:

- LNG releases will be operationally controlled by usual procedures of NTS operations from CP-1.
- Tests will be clustered in time and relatively infrequent with only a few of the large tests ignited in a given series.

- Most of the large LNG releases will be vapor dispersion tests, which are unignited and greatly diluted before exiting the controlled region.

- Combustion tests during the first phase (200 m^3) releases will be either pool fires or vapor cloud fires which by design will not reach beyond the dry lake playa.

- Many small, confined explosion tests and RPT's with only slight overpressures will occur.

- Detonated vapor cloud tests will be infrequent, and our HE equivalent estimates are very conservative because of turbulence.

Animals and plants beyond the barren dry lake playa would have infrequent exposure to small shock waves and no exposure to fire hazards, especially during the first phase tests.

COMMENTS ON THE ISSUES RAISED IN JANUARY 7, 1981 LETTER FROM M. GATES TO R. WAGNER

THE RESUSPENSION POTENTIAL OF RADIOACTIVE PARTICLES

The concern about resuspension of radioactive particles from aged deposits of ^{239}Pu, ^{238}Pu, and ^{241}Am arises from the possibility of inhalation exposure to respirable-size, long-lived, alpha emitters. This concern can be avoided simply by not disturbing the surface deposits on Frenchman Flats. The NVOO Plutonium Inventory Project has located the only significant deposits on Frenchman Flat, which are adjacent to and eastward of the NTS boundary with Nellis AFB. (See contours of pCi/g on Fig. 2). These deposits are about 1 mile (1.6 km) from the proposed spill pond, Fig. 1.

There is no intention or plan to use the contaminated area on Frenchman Flat for LGF experimentation. Vehicle traffic would be kept to a minimum. For two years (1979-1980) a weather station was operated there with service trips once a month. Hot alpha-contamination areas were well known and avoided simply by driving around. Exclusion areas are marked, but more highly visible barriers will be installed at key locations for additional protection for the duration of the proposed project. We will take measures to avoid combustion near the contaminated area.

Previous studies by us in another program (Anspaugh, et al, 1975; Homan, 1978) showed that the sites are not erodible or resuspendible by the wind, unless the surface is disturbed. Although calculations have been made of surface plutonium resuspension by LNG detonation at Frenchman Flat (Porch, in Appendix C. of Cramer and Hogan, 1978), the worst case assumptions that were made were used to illustrate a point and are not considered realistic. For example, a 6000-ton HE explosion from a point source on the ground at the site

of the highest soil contamination was assumed by Porch to simulate an LNG detonation. The actual detonations will be about a mile (1.6) km) away from plutonium contaminated soil and based on the historical studies of fuel explosions (Sutton, in Appendix B of Cramer and Hogan, 1978) would be less than 200-ton HE equivalent for 200 m^3 spill (less than 500-ton HE for 500 m^3, etc.). The resulting overpressures from a 200 m^3 fuel detonation (max capacity of the proposed first phase) would be less than 0.5 psi (0.03 atm, or 3 kPa) at one mile (1.6 km). This overpressure probably would break glass and cause slight structural damage but certainly would not shake loose any contaminated soil. At this range, temporary resuspension from combustion or detonation will not be greater than that occuring naturally by wind.

Two other uncertainties about resuspension problems are currently being investigated. (See workplan, Environmental and Meteorological Baseline Studies.) The first is to obtain a background of the month-by-month plutonium aerosol concentrations upwind and downwind of the test area. The second is to assure that dust created by the construction and by related vehicle traffic does not create an inhalation exposure. Along these lines, areas adjacent to construction and vehicle operations are being re-checked for possible missed contamination. Further, a special resuspension study is being conducted using personal dosimeters, a mobile resuspension laboratory, and a portable, bottomless wind-tunnel with the same techniques used in 1980 to investigate pulmonary deposition of plutonium aerosols at NTS, Little Fellar II site, and at a plutonium production facility at Savannah River Plant, Aiken, S.C. Results of Frenchman Flat studies will be available by September, 1981.

OPERATIONAL PROCEDURES PROTECTING ENDANGERED PLANTS

Concern about endangered plants originated with the first selection of LNG test sites when it was envisioned that fuel combustion could carry fire to distances up to 8.2 miles (13.1 km) for a 1000 m^3 spill. (See map, page 20, and Bowman's analysis Appendix A, in Cramer and Hogan, 1978). Because of the selection of test conditions and the dominant southwest winds the fire-zone will not be a circle (such as represented on the map, page 20, Cramer and Hogan, 1978) but will be a pie-shaped area extending to the northeast. In Bowman's worst-case estimate with low winds (2 m/s) and stable air (Pasquill-Gifford category F) the range to the lower flammability limit (LFL, 5% methane in air) will scale down to about 1.6 miles (2.6 km) for 200 m^3 spills and about 4.1 miles (6.6 km) for 500 m^3 spills. Selection of test conditions for slightly higher wind speeds and less stable conditions will reduce this range. Furthermore, experience has shown that flowing LNG combustion tests may be cut-off by a local range safety officer if the visible flame front proceeds past a pre-determined range point (for example 1.0 mile, discussed in Section D, later). The selection of test conditions has been proven feasible (Shinn and Cederwall, 1981) and with the degree of control such as above, the first phase 200 m^3 tests can be prevented from propagating beyond the barren, dry playa at Frenchman Flats. The distance between the proposed spill point and the northeast edge of the dry playa is about 1.2 miles (2 km). Better estimates of fire propagation can be made after this phase, which, after all, is the purpose of the LNG research.

Three species of endangered or candidate-threatened plants were pointed out by Douthett (Letter, NVOO to W.J. Hogan and W.C. O'Neal, LLNL, September 1978). These were Agave utahensis in the Ranger Mountains 5 miles (8 km) to the southwest of the presently proposed spill site, Penstamen thurberi in the Desert Game Range 5 miles (8 km) to the east-northeast, and Astragalus nyensis, suspected to occur 2.5 miles (4 km) to the southwest. Subsequent studies under our sponsorship were conducted by W.A. Rhoads (Letter, E.G.&G. to W.C. O'Neal, LLNL, September 1979) who considered an area 6.2 miles (10 km) from the spill site. He concluded that "no species will likely be affected by the tests if the experiments are controlled as currently proposed". He found that one population of Penstamen thurberi existed about 6.2 miles (10 km) to the northeast of the proposed spill site, in the quadrant of likely fire propagation. There is presently some dispute whether this plant is really a subspecies of a more common species, and it may not remain in threatened status. Rhoads also found a population of the endangered Astralgalus nyensis about 3.8 miles (6 km) south of the proposed spill site. This population, however, is not in a quadrant of likely fire propagation, and new populations recently found for this plant offsite may result in it being removed from endangered status. Agava utahensis and several other species of concern were found southeast of the site in the Ranger Mountains, but far removed and in a safe quadrant.

Additional studies of fire propagation potential into the Desert Game Range are in progress. These are discussed in Section J.

CALCULATIONS ON THE QUANTITY OF DUST GENERATED BY THE EVENTS

Discounting the potential for resuspension of radioactive particles which was discussed previously, we will address the concern about dust generation per se. Our best estimates using Sutton's method from historical fuel explosions to estimate explosive equivalents (discussed in Section A) are that a 200 m^3 LNG detonation is about equivalent to 200-ton HE and 500 m^3 is equivalent to 500-ton HE, etc. Porch (Appendix C in Cramer and Hogan, 1978) used the ratio 3000-ton HE/ton dust (after about an hour) based on HE explosions at Nevada Test Site. This reduces to .067 ton (134 pounds) dust for a 200 m^3 LNG detonation and .167 ton (335 pounds) dust for 500 m^3. Since the estimate is made an hour after the explosion, this represents dust not falling out locally, but drifting off the Nevada Test Site in a cloud.

Two additional factors act to make this estimate conservative. First, the spill site where the detonation is likely to occur is going to be usually covered with water which will moderate dust production. Second, intentional, unconfined-vapor explosions will not occur as a point source of HE but will be dispersed over a wide area with less surface-material entrainment; other, confined vapor explosion tests, such as bag tests will be much less than the maximum 200 m^3 capacity (since 200 m^3 of LNG when vaporized would need a hemispherical bag of 40 m radius, the size of a small coliseum).

In any case the amount of dust drifting offsite would be so dispersed and small in quantity as to be practically insignificant.

CALCULATIONS ON THE RATE OF HEAT RISE

Concern about the heat flux from pool fires, fireballs, and vapor cloud fires has been an important design criteria for the proposed LNG spill installation (pages 75-80, Project Plan for Construction of the Liquefied Gaseous Fuel Facility, O'Neal et al, January 1981). Details of the calculation are presented by O'Neal.

The important heat flux consideration is thermal radiant heat flux. The spill facility (located upwind) is designed to withstand heat at least one-half the wood ignition point. Pool fires on water with a maximum design capacity fuel-flow rate (200 m^3/min) will produce heat flux of the design criteria at a range of 400 m. Vapor cloud fires also fed by the max fuel rate will produce the criteria heat flux at 457 m in a typical 5 m/s wind. Fireballs created in calm wind will produce sufficiently high heat fluxes so that the amount of spilled LNG must be restricted to less than 60 m^3 and the range to the criteria heat flux will be less than 457 m. The design criteria of one-half the wood ignition point at 457 m also means that the range for sufficient heat flux to produce second-degree burns is less than 600 m and the range at which heat flux becomes equivalent to the solar constant (essentially background) is less than 1.3 km (0.8 mile).

In the preferred downwind spill direction during vapor cloud burns (northeast), where the distance from the proposed spill site to the boundary of the playa is about 2 km (1.2 mile) the critical range point for the range safety officer to avoid heat flux sufficient to ignite brush at the playa boundary is when the range to flammable gas is 1.6 km (1.0 mile) downwind. (Estimated using one-half the wood ignition heat flux as a criteria.)

CALCULATIONS OF OVERPRESSURES, UNDERPRESSURES, AND DUCTING PHENOMENA

Overpressures will result from detonations and flameless explosions due to rapid phase transitions (RPT). Significant underpressures (as compared to overpressures) are not expected to occur at all. Concern arises from both a safety viewpoint and the possible disturbance effect of acoustic waves which possibly would be enhanced by atmospheric ducting. The most realistic assessment of overpressures we have at this time is Sutton's analysis based upon historical fuel detonation (Appendix A in Cramer and Hogan, 1978). With a 200 m^3 LNG detonation (200-ton HE equivalent) the range to overpressure of 0.5 psi (0.03 atm or 3 kPa) is less than one mile (1.6 km). Similarly with a 500 m^3 detonation the range is less than 1.5 mile (2.4 km). Overpressure of that magnitude would be expected to break glass and cause minor structural damage. There remains doubt even if glass would be broken at that range because of the lack of knowledge about the length of time of the pressure impulse, and the poor analogy between HE point sources and the unconfined, area fuel source in a shallow, pancake form. Present estimates are therefore expected to be conservative.

The effects of atmospheric ducting will be negligible during the daytime from 8 a.m. to 6 p.m. because of the lack of low level temperature inversions in that period. (Larger detonations can be restricted to the daytime until these effects are better known through suitable smaller experiments.) Meteorological monitoring for inversions will be part of the operations.

The ranges predicted above are shorter than the distances from the proposed spill site to significant property. Road 5-01 which is 0.8 mi (1.2 km) to the west, and other facilities could be temporarily vacated. The proposed LGF storage tanks are designed to withstand 5 psi (0.3 atm or 30 kPa) which is the maximum estimated at that range from a 500 m^3 detonation, according to O'Neal et al in the Project Plan, 1981.

By extrapolating the above overpressure estimates 4.8 mi (7.7 km) from the spill site to the eastern border of Unit A-2, the area permitted by Nellis AFB for LNG testing, we estimate that overpressure at that border will be less than 0.06 psi (0.004 atm or 0.4 kPa) for a 200 m^3 detonation and 0.10 psi (0.0067 atm or 0.67 kPa) for a 500 m^3 detonation. These overpressures are 2 to 3 times the sonic boom overpressures (0.033 psi) occasionally generated by Air Combat Maneuvering missions over Nellis AF Range (Draft Environmental Statement, Renewal of Nellis Air Force Range, 1978). If we carry this extrapolation still further, a 200 m^3 detonation will produce equivalent sonic boom overpressures (0.033 psi, or 0.002 atm, or .2 kPa) at a range 7.8 miles (12.5 km) from the spill site, and a 500 m^3 detonation produces the same overpressure at a range 11.5 miles (18.5 km) from the spill site. The distance eastward from the spill site to the nearest known populations of desert bighorn sheep is about 10 miles (15 km). Thus the overpressures predicted by the above extrapolation would be about the same as a sonic boom in the vicinity of the sheep population. The extrapolation is crude because we have not considered that the Ranger Mountains, the Buried Hills, and their interconnecting ridge impose a 300 m vertical barrier which is likely to reflect and muffle sonic disturbances to the sheep.

According to the Draft Environmental Statement cited above, "sonic boom exposure to wildlife on the Range is a subject that has been evaluated by many authors". While admitting that "observed animal responses to previous sonic booms in this region have not been satisfactorily related to the likelihood of successful reproduction", the Environmental Statement goes on to say that the "data available does not show the behavior of big game animals has been altered by sonic booms in any appreciable way; although, they may show momentary concern". Further, "desert bighorn sheep have been observed to offer no reaction to single sonic booms". We can conclude safely that LNG detonations of smaller magnitude and at infrequent intervals will probably not change the present environment for the large desert mammals.

RPT explosions are of lesser concern but they are not well understood. They have been observed close to the spill when the liquid undergoes instantaneous vaporization like water droplets popping in a hot pan. Experience has shown that overpressures were less than 1 psi (0.06 atm or 6

kPa) at 25 m from the spill site for a spill 10% as large as proposed for NTS (unpublished measurements by C.D. Lind at China Lake Naval Weapons Center). We estimate that potential RPT overpressures are much less than for a detonation and should be only of concern in structural design near the underwater end of the spill pipe (pg 83, Project Plan, O'Neal et al, 1981).

DOCUMENTATION INDENTIFYING GASES RELEASED, QUANTITIES OF EACH GAS RELEASES, AND DOWNWIND CONCENTRATIONS WITH DISTANCE

In the present Project Plan (O'Neal et al, 1981 through 1984) only LNG will be released but potentially the Liquefied Gaseous Fuel Program could be capable of testing LPG, LNH_3, and LH_2 with some modifications. Since each of the latter fuels has different properties and possibly different environmental issues, they are beyond the scope of the present report. The LNG Working Group will have adequate opportunity to examine any new environmental issues should the opportunity arise to test fuels other than LNG.

The composition of LNG is approximately 92% methane, 5.5% ethane, 1% propane, and 1.5% nitrogen. For a 200 m^3 spill about 80 tons of methane and 6 tons of non-methane hydrocarbons (NMHC) are released. Federal air quality standards for NMHC are set as a guide for implementing oxidant air quality standards, for example, ozone. (See page 38, "A Handbook of Key Federal Regulations and Criteria for Multimedia Environmental Control", EPA-600/7-79-175, 1979.) Since methane, ethane, and propane do not participate in photooxidation reactions to a significant extent, the natural gas released will not contribute to ozone formation. (It is not ethane and propane which are the target hydrocarbons in the blanket NMHC air quality regulations.)

The emission level goals for ethane and propane as simple asphyxiant gases are 5000 ppm, each, which is higher than their concentrations expected at the LFL. (See pages A-4 to A-9, "Multimedia Environmental Goals for Environmental Assessment, Vol. III," EPA-600/7-79-176a, 1979.)

In Section B, we used Bowman's worst-case estimate (low wind speed, stable air) to obtain the range to the LFL for a 200 m^3 spill of 1.6 miles (2.6 km). The estimated concentrations of methane will be 5% and NMHC will be about 0.35% (3500 ppm) at the LFL ignoring the difference in their boil-off rate. The scaling-down of Bowman's estimate, the necessary assumptions, and the crudeness of the method will all be improved following the 200 m^3 tests at Frenchman Flat. Even so, EPA emission level goals for NMHC should be met at 1.6 miles (2.6 km).

Beyond the LFL, methane is of no significant threat to health and welfare since it is not flammable and relatively harmless with respect to toxicity and chemical effect. Natural gas at lower concentrations is classified as a simple asphyxiant and the threshold limit value (TLV-SA) for methane, ethane, or propane is 5000 ppm. Using Bowman's estimate, this concentration of methane (one-tenth the LFL) will be reached at about six times the range to

the LFL. For a 200 m^3 spill the range to simple asphyxiant TLV (5000 ppm) in the worst-case estimate is 9.6 miles (15 km). By definition, humans can be exposed 8 hours per day to the TLV without ill effect, and the brief exposures expected (a two minute spill in Bowman's estimate) at much higher concentrations will not effect either animals and plants. (Page A-4,"Multimedia Environmental Goals for Environmental Assessment, Vol. III," EPA-600/7-79-176a, 1979.) Brief exposures to methane of 100,000 ppm produce no effect (p 7-3, Air Quality Criteria for Hydrocarbons, U.S. Department of Health, Education, and Welfare, 1970). Methane has no appreciable physiological action except when it lowers the partial pressure of oxygen in air enough to cause oxygen deprivation. Ethane produces no systemic effects to humans breathing 50,000 ppm and brief propane exposures up to 10,000 ppm causes no symptoms in man (Chapter 28, Volume 2, Industrial Hygiene and Toxicology, 1967). Even at the LFL (5% natural gas in air) there is no asphyxiant danger for brief exposures, since oxygen concentration would be reduced (nominally) from 20% to 19%.

POTENTIAL FOR EXPLOSIVE CONCENTRATION OF GASES EXTENDING INTO STRUCTURES SINCE TESTING MIGHT TAKE PLACE WITH WINDS FROM A MULTITUDE OF DIRECTIONS

Actually, the experimental plan will call for spills of LNG to be limited to times when the wind is from the southwest. Since January 1979, we have learned a great deal about flow patterns and desirable periods to conduct the tests (Shinn and Cederwall, 1981). We found that between 11 a.m. and 6 p.m., almost any day of the year, the winds are from the southwest, intially at low speed then picking up speed regularly through the day. This means we can select any given hour to get a desired wind speed, while the persistent direction means we will only need to instrument a narrow sector to the northeast.

Another desired condition, that of selecting a given atmospheric stability, can be accomplished by choosing a certain month of the year, since stability will be determined by the water to air temperature difference. Paradoxically, over the spill pond the air will be stable during mid-day in summer and unstable during mid-day in winter. We also found that undesirable flow patterns for testing regularly occur from 8 a.m. to 11 a.m. (divergent upslope flow at the ground) and from 8 p.m. to 11 p.m. (convergent downslope flow at the ground).

The degree of selection for preferred test conditions at Frenchman Flat means that there is little chance of explosive concentrations of gas extending into structures. Especially since in the northeast quadrant any structures are very far removed.

THE EFFECTS OF WATER ON RADIOACTIVE PARTICLES IN FRENCHMAN FLAT

There will be ponded areas of water constructed at the northwestern end of the Frenchman Flat playa, adjacent to a pond which has existed there for many

years. See Plot Plan, Fig. 1. In addition, an irrigation system will be used to wet down an area 1 km long by 300 m wide to the southwest of the proposed pond. (See pg. 58, Project Plan, W.C. O'Neal et al, 1981). These ponded and irrigated areas are about 1 mile (1.6 km) to the west of the only significant radioactive contamination area at the east end of the playa. See Section A and Fig. 2. Because of the shortage of water for LGF test purposes, our water management practices, such as using dikes and irrigating mostly during the spring season, will intentionally prohibit "unnatural" water from escaping into the contamination area.

Natural precipitation on the playa is about 5.75 inches (146 mm) per year about half of which comes in the months of December through March. Since evaporation rates are only 30% of normal during those months, and since the playa collects runoff from the surrounding basin, there almost always is standing water on the playa for some time during the winter months. Thus the contamination area is sometimes naturally covered by standing water. The weathering of radioactive particle contamination in the soil, etc., is thus mostly controlled by natural conditions and will not be affected by the proposed LNG tests.

A POPULATION AND EFFECTS STUDY OF THE ANIMALS IN THE AREA

During the proposed first phase (200 m^3) as previously discussed, we do not expect unusual exposure of animal populations to fire, significant overpressures, or asphyxiating gases since those high exposures will be constrained to the dry playa which is nearly barren of animal life.

In the long term, however, it may be anticipated that necessary animal studies should be carried out before the LGF Program expands to larger tests or fuels other than LGF. A recent survey (McIntyre and Shinn, 1981) found that a considerable baseline already exists in the vicinity of Frenchman Flats. Twenty-four former study sites of Beatley (1969, 1975) and Romney (1973) in the eastern quadrants of Frenchman Flat basin provide excellent control sites and document the present status of important habitat. The plant-animal nutritional dependencies are now well understood.

Some animal population studies have been done nearby (O'Farrell and Emery, 1976). Expected effects on plant and animal populations would be either due to disturbance from construction and operation of the facility or due to propagation of fire beyond the barren playa, perhaps carried by the vegetation. Recommendations have been made (McIntyre and Shinn, 1981) for analysis of plants and animals near the edge of the playa including the interplay of foods, shelter, and reproduction of the species.

Current research under our sponsorship is being conducted by T.P. O'Farrell (See workplan, Environmental and Meteorological Baseline Studies, 1981), to conduct a population survey of important rodents and other mammals using trapping and release methods where possible and conducted along an east-west transect. The study areas are on the eroded hills southeast to

northeast of Frenchman Flat, extending from the NTS boundary eastward 3.5 miles (5.6 km), and including for reference purposes the vegetation study plots of Romney et al (1973) and Beatley (1969, 1975). A report will be available November, 1981. Effects studies, if necessary, will be developed following these surveys.

POTENTIAL OF RANGE FIRES

In Section B, we addressed the issue of fire and the range to the lower flammability limit (LFL) for natural gas in air. In the first phase (200 m^3) tests, the worst-case, maximum range to the LFL is estimated to be 1.6 miles (2.2 km). Selection of test conditions (wind speed, wind direction, and stability) and a cut-off control enable the local range safety officer to limit the flammable cloud to a pre-determined range point estimated at 1.0 miles (1.6 km) to avoid igniting brush at the playa boundary. The distance between the proposed spill site and the northeast edge of the dry playa is about 1.2 miles (2 km). Better estimates of fire propagation can be made after the first phase tests.

In the subsequent 500 m^3 test phase, the maximum range to the lower flammability limit is 4.1 miles (6.6 km) using our present worst-case estimate. This estimate, however revised, causes concern for fire propagation and destruction of vegetation from the playa (1.2 miles) up to 4.1 miles in the northeast quadrant. In Section B, a population of threatened plants was found at 6.2 miles (10 km). Recommendations were made (McIntyre and Shinn, 1981) to determine what are the characteristics of the plant populations which might propagate fire or change as a result of fire.

Current research has a subtask devoted to range fire assessment. (See Workplan, Environmental and Meteorological Baseline Studies, 1981). Fire zones and standing biomass will be mapped and evaluated for potential fire-carrying capacity. Coordination for fire management and firebreak effectiveness will be made with the Refuge Manager, Desert National Wildlife Range. Supplementary work under our sponsorship is being carried out by H.M. Borella and W.A. Rhoads, to map vegetation zones using aerial photographic methods where possible and estimating standing fuel per hectare such as dry annual plants and dry woody stems. The task will be conducted on the eroded hills southeast to northeast of Frenchman Flat, extending from the NTS boundary eastward 3.5 miles (5.6 km) and including for reference purposes the study plots of Romney et al (1973) and Beatley (1969). A report will be available, November 1981.

MAXIMUM ESTIMATED DAMAGE TO NELLIS PROPERTY AND THE DESERT NATIONAL WILDLIFE RANGE

Concern about damage to Nellis and the Desert National Wildlife Range (DNWR) has been maintained all along during the planning of the LGF Program. We discussed in Sections B and J the range to combustion effects, in Section E the detonation overpressures expected and extrapolations to the populations of

sheep on the DNWR, and in Sections F and G, the emissions of gases and range to the threshold limit concentration (TLC) for a simple asphyxiant gas. The shortest distance between the proposed spill site and the Desert National Wildlife Range is to the east 2.9 miles (4.6 km). In the preferred northeast direction the distance is 4.2 miles (6.7 km).

In the first phase experiments, the combustion effects will be contained on the playa less than 1.2 miles (2 km) from the proposed spill site. First phase detonation overpressures are estimated by conservative extrapolation to be less than typical sonic booms (.033 psi or 0.2 kPa) in the vicinity of bighorn sheep populations. Beyond the range to the Lower Flammability Limit (less than 1.6 miles from the spill site in the first phase) the brief exposures to methane concentrations above 5000 ppm will not produce effects on plants and animals.

There will be no damage to Nellis property and the Desert National Wildlife Range during the first phase of LNG tests, and the goal is to maintain range safety and to improve the hazards analysis so that there will be no significant damage in subsequent tests as well. Our current research is directed to fill gaps in our environmental assessment capability prior to the needed analysis of the effects of expanded LNG tests proposed for subsequent phases. At present, control of range fires ignited in larger, later tests appears to be the most significant potential effect. As mentioned previously and in our workplan, the assessment of this potential and our plans for control and mitigation will be coordinated with the appropriate Nellis AFR and DNWR officials through NVOO.

REFERENCES

1. Anspaugh, L.R., J.H. Shinn, P.L. Phelps, and N.C. Kennedy, Resuspension and redistribution of plutonium in soils, Health Physics 29 571-582, 1975.

2. Beatley, J.C., Dependence of desert rodents on winter annuals and precipitation, Ecology 50 721-724, 1969.

3. Beatley, J.C., Climates and vegetation pattern across the Mojave/Great Basin desert transition in Southern Nevada, American Midland Naturalist 93 53-70, 1975.

4. Cramer, J.L., and W.J. Hogan, Evaluation of Sites for LNG Spill Tests, Technical Report, Lawrence Livermore National Laboratory, UCRL-52570, 1978.

5. Environmental Protection Agency, A Handbook of Key Federal Regulations and Criteria for Multimedia Environmental Control, EPA-600/7-79-175, (NTIS #PB80-107998), 1979.

6. Environmental Protection Agency, Multimedia Environmental Goals for Environmental Assessment; Vol. III, EPA-600/7-79-176a, 1979.

7. Homan, D.N., Some Observations of Suspension of Dust by Wind from Dry Lakes, Technical Report Lawrence Livermore National Laboratory, UCID-17813, 1978.

8. McIntyre, D.R. and J.H. Shinn, Ecological Background Relevant to Proposed Liquefied Gaseous Fuel Test Site Development at Frenchman Flat, Nevada, Technical Report Lawrence Livermore National Laboratory, UCID-18921, 1981.

9. O'Farrell, T.P. and L.A. Emery, Ecology of the Nevada Test Site; A Narrative Summary and Annotated Bibliography, USAERDA Nevada Operations Office, NVOO-167, 1976.

10. O'Neal, W.C., D.L. Hipple, W.W. Wakeman, G.M. Bianchini, R.E. Blocker, and M. Ochoa, Project Plan for Construction of the Liquefied Gaseous Fuels Spill Test Facility, Technical Report Lawrence Livermore National Laboratory, UCRL-53108-Draft, 1981.

11. Patty, F.A. (ed.), Industrial Hygiene and Toxicology, Volume 2, Interscience Publishers, 1967.

12. Romney, E.M., V.Q. Hale, A. Wallace, O.R. Lunt, J.D. Childress, H. Kaaz, G.V. Alexander, J.E. Kinnear, and T.L. Ackerman, Some Characteristics of Soil and Perennial Vegetation in Northern Mojave Desert Areas of the Nevada Test Site, Technical Report, Laboratory of Nuclear Medicine and Radiation Biology, University of California (900 Veteran Avenue, Los Angeles), UCLA-12-916, 1973.

13. Shinn, J.H. and R.T. Cederwall, Selecting Optimum Periods for Atmospheric Dispersion Tests over Water Surfaces at Frenchman Flat, Nevada Test Site, Technical Report, Lawrence Livermore National Laboratory, UCID-18907, 1981.

14. U.S. Department of Health, Education, and Welfare, Air Quality Criteria for Hydrocarbons, 1970.

15. U.S. Department of Interior, Draft Environmental Statement, Renewal of the Nellis Air Force Range Withdrawal, Hdq. Tactical Air Command USAF for Bureau of Land Management, 1978.16.

16. (Workplan), Environmental and Meteorological Baseline Studies (FY-81) Frenchman Flat, Nevada Test Site, Liquefied Gaseous Fuels Program, Lawrence Livermore National Laboratory, 1981.

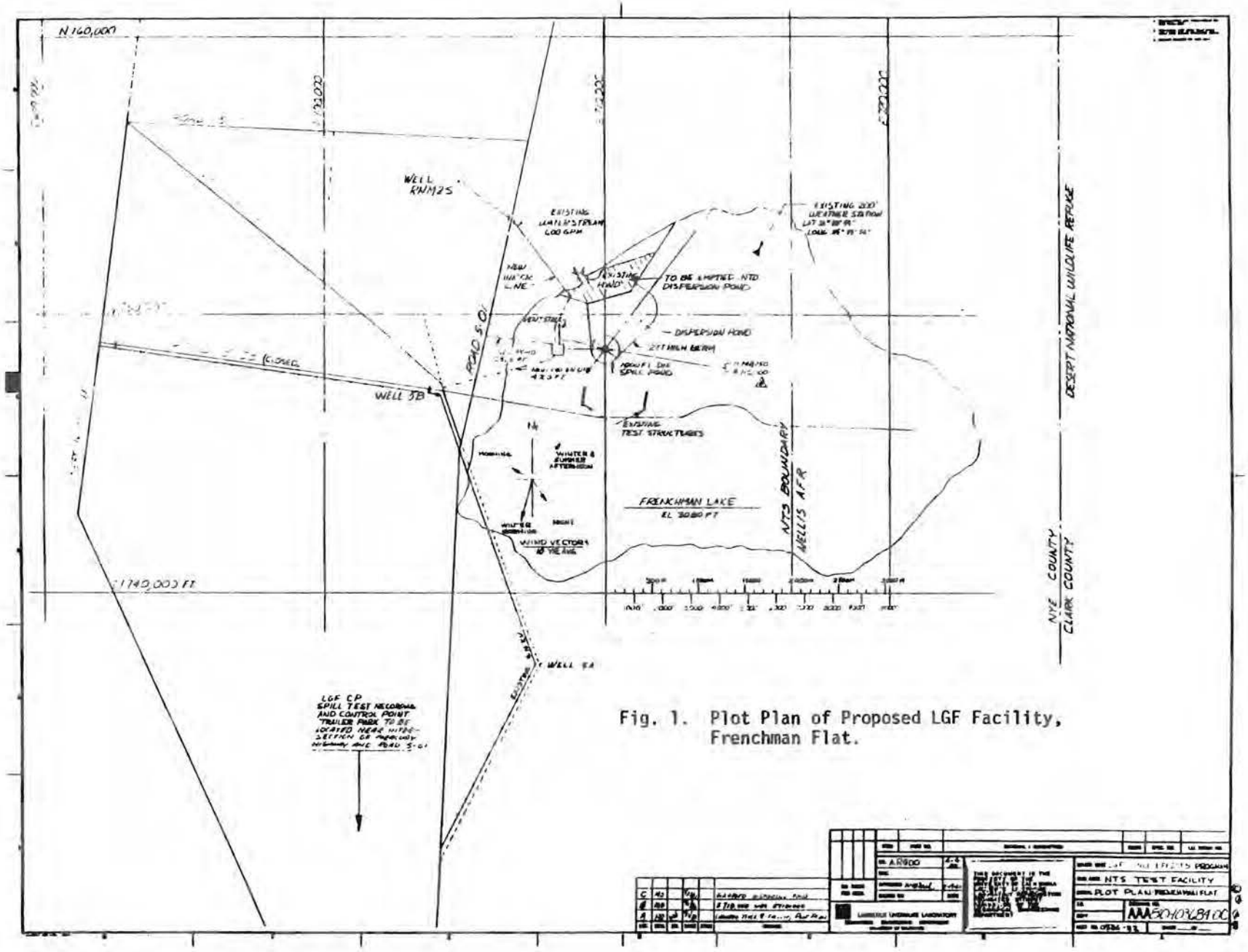

Fig. 1. Plot Plan of Proposed LGF Facility, Frenchman Flat.

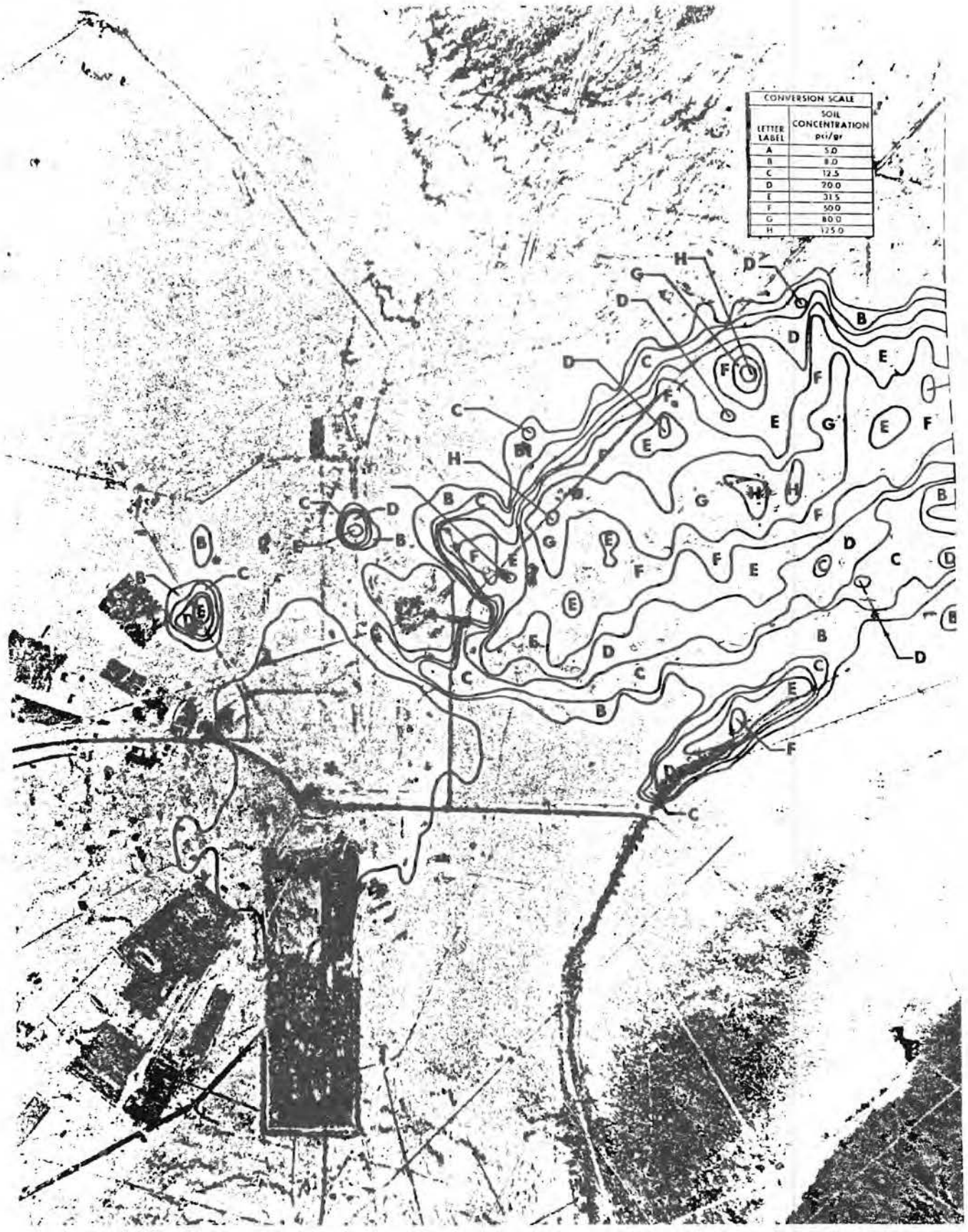

FIGURE 2. Soil Contamination of ^{241}Am Emitters, East End of Frenchman Playa

REPORT M

Selecting Optimum Periods for Atmospheric Dispersion Tests Over Water Surfaces at Frenchman Flat, Nevada Test Site

J. H. Shinn
R. T. Cederwall

Prepared for the
Environmental and Safety Engineering
Division
U.S. Department of Energy
under Contract W-7405-ENG-48

Lawrence Livermore Laboratory
Livermore, California 94550

REPORT M

TABLE OF CONTENTS

SUMMARY

This report utilizes meteorological data collected at Frenchman Flat, Nevada Test Site, as the basis of a strategy for conducting spill tests of liquefied gaseous fuels (LGF) over shallow water surfaces. Diurnal flow patterns show that the optimum period for atmospheric dispersion testing is between 11 A.M. and 8 P.M. in any season, while periods to be avoided are between 8 A.M. and 11 A.M. (radial flow divergence in the basin and upslope wind) and especially the period between 8 P.M. and 11 P.M. (radial flow convergence and air pooling in the basin). The temperature lapse rate over shallow water is most stable during the afternoons from May through December, most unstable during afternoons from December through March, and nearly neutral in April afternoons. The wind speed increases regularly every afternoon and is persistent from the south, south-west during March through November, which allows one to select for any desired speed and to fix an array of instruments along one direction. Because of the combined effects of lapse rate and wind speed the most-stable-atmosphere cases (large Richardson numbers) occur at 2 P.M. to 4 P.M., May through December. The most-unstable-cases (negative Richardson numbers) occur at 2 P.M. to 4 P.M., January to April, and the neutral-stability-cases (near zero Richardson numbers) occur between 4 P.M. and 6 P.M. in any season. Finally, including other factors such as maintaining a water surface with favorable precipitation/evaporation, avoiding freezing, and allowing for a range of stability conditions, in considering all factors together, we recommend that planned atmospheric dispersion tests be selected during afternoon periods from two seasons, March-April-May and October-November.

INTRODUCTION

When liquefied gaseous fuel (LGF) spill tests are conducted over water surfaces at Frenchman Flat, Nevada Test Site, it will be necessary to schedule tests so that meteorological conditions are optimized for experimental control and for operational safety.

Meteorological data collected at Frenchman Flat are utilized in this report as the basis of an operational strategy for conducting LGF spill tests over water. We have selected the time of year and time of day for atmospheric dispersion tests based on flow patterns, atmospheric stability, wind speed, wind persistence, temperature, and the precipitation and evaporation.

DIURNAL FACTORS (TIME OF DAY)

Flow patterns

Analysis of flow patterns on Frenchman Flat were conducted from hourly-averaged wind data collected by a six-station network that operated for nearly two years. (Details are presented in a separate data report.) These analyses show that there are two periods of the day, 8 A.M.-11 A.M. and 8 P.M.- 11 P.M., when spill tests are not desirable. During the morning period, 8 A.M.-11 A.M. in all seasons, a transition-flow pattern develops where surface winds diverge radially outward from the center of the dry lake playa to create a slow, upslope flow. This means that on the east side of the lake winds are usually light (2 m/s) from the west, while on the west side winds are light from the east, and so on for the north and south sides. During the morning divergence flow pattern (8 A.M.-11 A.M.)

it is dangerous to spill because the trajectory of combustible material would be unpredictable and clouds are likely to not disperse rapidly because of the low speeds. The second undesirable flow period occurs during the evening, 8 P.M.-11 P.M., and has the opposite flow pattern from the morning. The evening surface flow pattern has weak winds that converge radially inward toward the center of the lake. The evening convergence flow pattern (8 P.M.-11 P.M.) is most dangerous in the sense that combustible material would form a natural pool in the center of the lake and be sloshed around with no particular trajectory. The onset of the evening convergence flow pattern is not as distinct as the morning flow because the daily peak wind period occurs just before 8 P.M. and must decay before the convergence flow pattern is manifest.

Between the hours 11 A.M. and 8 P.M. in every season, the flow pattern is persistent and shows insignificant divergence or convergence for extended time which is most ideal for atmospheric dispersion testing. The winds are persistent from near south, south-west (by actual measure, 210^{o} from true north) every afternoon in each season, except occasionally more southerly winds during summer. (Traveling storms which change this pattern are very infrequent).

The late night flow regimes (12 P.M. to 8 A.M.) in all seasons, are generally too light (< 2 m/s) but also show a lack of consistent flow pattern, sometimes tending to retain the early evening convergence pattern toward the center of the dry lake. Whether these periods should be utilized for certain tests depends on how much effort can be placed into monitoring for the desired test conditions.

Temperature Structure

Analysis of water-to-air temperature differences revealed in the limited shallow pond and evaporation pan data show that the water temperature will be colder than air during all hours of the day and night from May through December, but difference is greatest during the mid-afternoon. Thus the lapse rate is most stable during the afternoons from May through December. Water temperatures are significantly greater than air only during mid-day from December to April. (This observation is modified by the condition that shallow water freezes often in the winter months and the ice serves as a thermal barrier between water and air). Both shallow-pond water temperature and air temperature go through similar diurnal cycles but by mid-afternoon during December to April, the water has absorbed more heat and is thus normally warmer than the air. By April this effect diminishes, so that the mid-day water-air temperature difference is then a minimum. The lapse rate is most unstable over open water during winter and early spring afternoons but is nearly neutral in April afternoons. These observations of lapse rate over shallow water are essential but insufficient to determine the atmospheric stability, because of the effects of wind speed.

Wind Speed Diurnal Variation

Wind speed is a minimum shortly after sunrise throughout the year (see Figure 1). From March to November, the wind speed increases nearly linearly from before noon until 4 to 6 P.M., followed by a rapid drop off of speed after 6 P.M. In winter, December to February, the wind remains relatively weak throughout the day. The regularity of slowly increasing wind speed nearly every afternoon from March to November provides an opportunity for selection of wind speeds to conduct atmospheric dispersion tests.

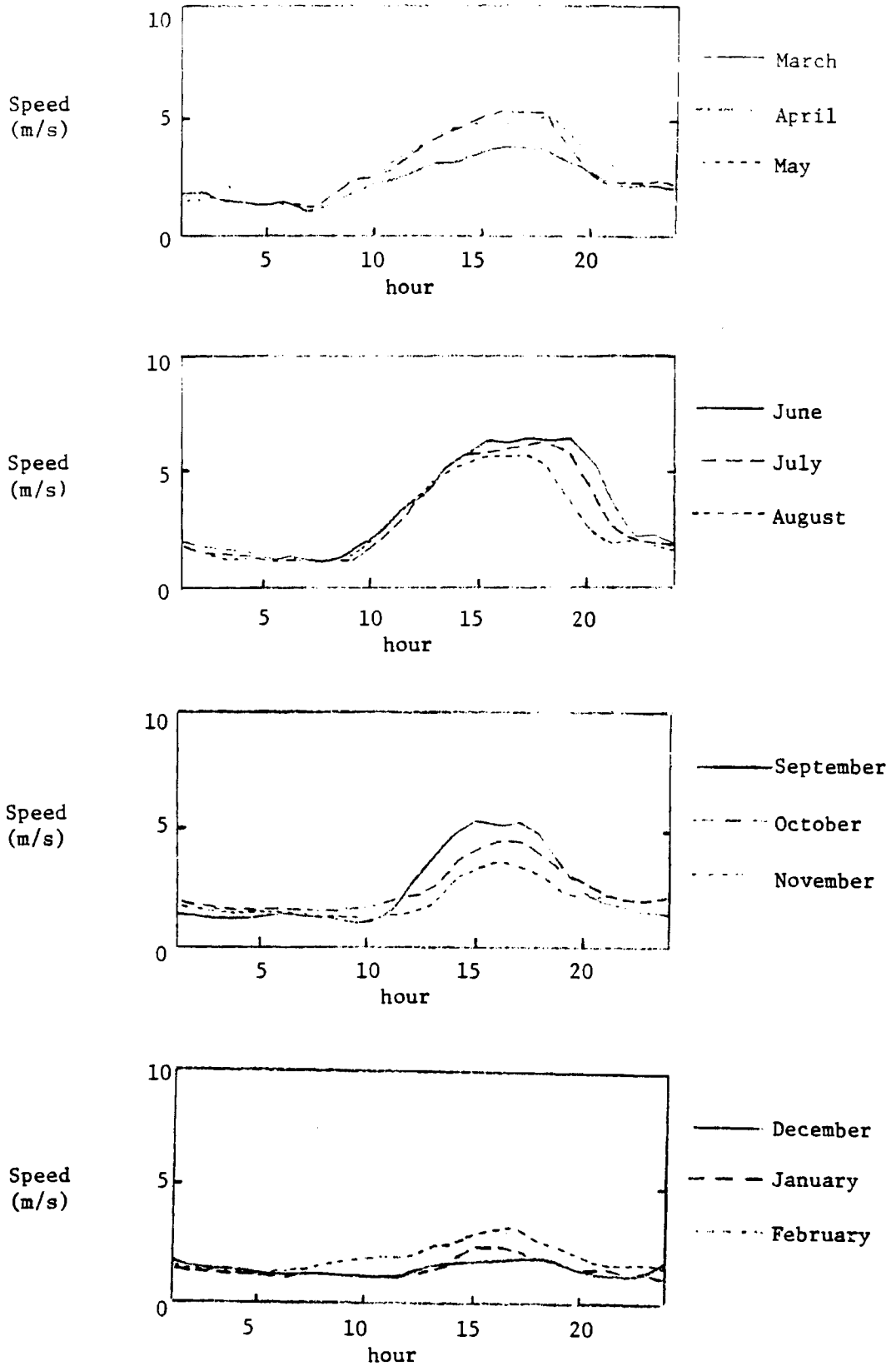

Figure 1. Diurnal variation of wind speed at 2 m height for Frenchman Flat (averaged over each month, 1979.)

The characteristic wind speed of the surface layer, the friction velocity, or u-star (u_*), is calculated from observed wind profiles and the surface roughness length, which is approximately 10^{-4} to 10^{-5} m over both the shallow pond and dry lake bed at Frenchman Flat. The diurnal pattern of u_* differs from the wind speed pattern in that the peak is sharper and occurs later in the day due to stability effects.

Diurnal Variation in Stability over Water Surfaces

Atmospheric stability can be characterized by the Richardson number, R, a collection of variables which includes the lapse rate in the numerator and the square of wind speed in the denominator. Because of the combined effect of lapse rate and wind speed, the most stable cases (largest positive Richardson numbers) will occur at 2 P.M.-4 P.M. of each day, May through December, before the winds have reached peak speed. The neutral stability cases (near zero Richardson numbers) will occur when the lapse rate is small and the winds are strongest--between 4 P.M. and 6 P.M. every day. The most unstable cases (largest negative Richardson numbers) will occur between 2 P.M.-4 P.M. of each day January to April.

SEASONAL FACTORS

Evaporation Rates

Maintenance of open water surfaces at Frenchman Flat will be difficult during summer months. Evaporation rates of open water surfaces average 19 mm/day (precipitation equivalent) from July to August. Precipitation is a maximum in February and a minimum in September, see Table 1. The winter months, December to February have the highest precipitation and lowest evaporation, but a shallow pond is frequently frozen then. The most favorable precipitation and evaporation with low frequency of freezing occur in two periods: March-April-May and October-November.

Table 1. Precipitation and evaporation at Frenchman Flat.

Month	J	F	M	A	M	J	J	A	S	O	N	D
Evaporation (mm/day)	1.0	2.2	5.6	7.9	11.9	18.5	21.6	18.0	11.9	4.8	1.7	2.0
Precipitation (mm/day)	.67	.78	.63	.32	.29	.36	.31	.26	.13	.26	.31	.44

Wind and Stability Over a Water Surface

As previously discussed, the maximum air-water temperature difference occurs in the afternoons. Also the desirable flow patterns occur when the winds over the region are unidirectional, prevalent from 210°, every afternoon. Since the wind speed increases regularly and persistently with time during afternoons, except in December-February, the opportunity for wind selection exists also. The 3:00 P.M. wind speed and stability (Richardson number) over a shallow water surface at Frenchman Flat are taken as characteristic of the afternoon period, see Table 2. The highest winds are in July, the lowest in November-December. The most

unstable days (largest negative Richardson number) are those in February, March and April. Near neutral conditions occur on days in May and the most stable conditions occur in October and November. The best selection of moderate winds over a range of stability conditions is the two periods: March-April-May and October-November.

Table 2. Afternoon (3:00 P.M.) wind speeds and Richardson number (R) over shallow water at Frenchman Flat.

Month	J	F	M	A	M	J	J	A	S	O	N	D
Wind Speed (m/s)	2.2	2.9	3.8	3.8	4.0	4.1	4.4	3.6	3.5	2.6	2.1	2.1
R at 2 m Height	-.07	-.33	-.24	-.15	.03	.07	.08	.12	.11	.15	.16	.07

(Wind speed is that measured at Well 5-B, averaged over an 8-year period)

Seasonal Temperature Effects

The minimum air temperatures are usually below freezing from late November through mid-February, see Table 3. As a result, water surfaces will be frozen frequently. Evaporation pans are frozen with a solid ice cover about 20% of the time during this period at Frenchman Flat. In January-February 1979, the shallow pond remained frozen for 3 weeks. The winter period is undesirable if ice forms because the heat exchange and atmospheric mixing would be so affected as to appear as if the pond were not present, futhermore equipment malfunction and personal discomfort would be factors to consider. The maximum air temperatures will equal or exceed 35 C (95 F) in June, July, and August, again of concern because of equipment malfunction and personal discomfort.

Table 3. Max and min air temperatures at Frenchman Flat.

Month	J	F	M	A	M	J	J	A	S	O	N	D
Max C	13.9	15.0	17.8	21.7	27.8	35.0	37.2	36.1	31.1	22.8	17.2	13.9
Min C	-6.7	-.6	0	2.8	8.9	15.6	15.6	11.7	6.7	3.9	-5.0	-7.2

CONCLUSIONS AND RECOMMENDATIONS

The diurnal and seasonal trends of flow patterns, atmospheric stability, wind speed, precipitation/evaporation, and temperature have been reviewed. The general conclusions are that for atmospheric dispersion testing over water surfaces at Frenchman Flat; (1) the optimum daytime period is between 11 A.M. to 6 P.M. from March through November, because of a persistent flow pattern and unidirectional flow as well as moderate, regularly increasing (selectable) wind speeds, (2) using this time period as optimum, the atmospheric stability over water surfaces will be unstable in March-April, neutral in May, mildly stable through summer, and strongly stable October - November, (3) the most favorable periods to maintain open water surfaces considering both freezing and favorable precipitation/evaporation ratios are the two periods March-May and October-November, and these also are the periods of minimum thermal stress on equipment and personnel.

ACKNOWLEDGMENTS

We would like to express our thanks to Cleo Fry for coordination of meteorological instrumentation, to Donald Homan and Muffet Wilkerson for data base management, and to Ralph Quiring of the Nuclear Weather Support Office, NOAA, Las Vegas for providing climatological records. "Work performed under the auspices of the U.S. Department of Energy by the Lawrence Livermore National Laboratory under contract number W-7405-ENG-48."

REPORT N

LNG Annotated Bibliography

H. J. Bomelburg
C. A. Counts
W. E. Davis
J. G. DeSteese
P. J. Pelto

Prepared for the
Environmental and Safety Engineering
Division
U.S. Department of Energy
under Contract DE-AC06-76RLO 1830

Pacific Northwest Laboratory
Richland, Washington 99352

SUMMARY

This bibliography provides brief summaries of literature related to LNG safety and environmental control, organized alphabetically by author.

Adkins, R. E. "LNG: New Driving Force." Pipeline & Gas J. 209(13):45-52, 1981.

The history of using liquefied methane as motor fuel is briefly outlined. The advantages as well as safety problems of LNG in automobile propulsion are discussed. The "Methane Transportation Use and Demonstration Act of 1980" indicates the intent of the U.S. Congress to encourage the use of LNG in automobile, aircraft and ship propulsion.

Affleck, W. S., Harrow, G. A. and Mills, W. D., "Converting a Small Car to LNG: What Are the Problems and What Can It Do for Economy and Emissions," Shell Research Ltd., United Kingdom, SAE Preprint #760376, February 1976.

The results of a comparison between a two-liter compact car run on gasoline and one converted to LNG are discussed. Fuel economy improvements for both normal road use and taxi service on the LNG-powered car are described.

Alger, A. S., Corlett, R. C., Gordon, A. S. and Williams, F. A., Some Aspects of Structures of Turbulent Pool Fires. WSS/C1 76-46, October 1976.

Results are reported on the burning of JP-5 and methanol pools 305 cm in dia. Measurements made include radiant energy fluxes outside and within the fire, temperatures and chemical compositions within the fire and rates of weight loss of the pool. Results emphasize structural differences between JP-5 and methanol fires and importance of radiant feedback of energy to the pool surface in controlling rates of burning.

Allan, D., Atallah, S., Drake, E., Hinckley, R. and Mathias, S., Technology and Current Practices for Processing, Transferring and Storing Liquefied Natural Gas. Department of Transportation/OST, Office of Pipeline Safety, Washington, DC, (prepared by Arthur D. Little, Inc., Report No. C-76971) December 1974.

Current state-of-the-art safety information related to the design, location, construction, operation and maintenance of facilities required for liquefaction, transfer, storage, and revaporization of natural gas is assembled and summarized. A detailed review of codes, standards and practices pertaining to LNG installations is presented along with an evaluation of present trends in LNG safety requirements. LNG safety research programs completed or in progress are described and key research results summarized. Finally a methodology for quantitative assessment of risks associated with LNG facilities is outlined.

Allen, D. S., R. L. Phani Raj, P. Athens, E. G. Pollack, N. M. Laurendeau, R. N. Caron, and A. A. Fowle. The Feasibility of Methods and Systems for Reducing LNG Tanker Fire Hazards. DOE/EV/04734-T1, Department of Energy, Washington, D.C., 1980.

Various methods have been analyzed for their suitability of reducing LNG tanker fire hazards. None of them appear to be promising, nevertheless, the feasibility studies should be continued to include some test work.

Almgren, D. W. and Smith, J. L., Jr., "The Inception of Nucleate Boiling With Liquid Nitrogen." Journal of Engineering for Industry. pp. 1211-1216, November 1969.

The phenomena of patchwise boiling are discussed, and the significant parameters restricting the growth of a boiling patch are analytically determined to be: a high nucleate boiling heat-transfer coefficient; a low total heat flux; the absence of cavities with a trapped liquid vapor interface outside the boiling patch; an appropriate value of wall thermal conductivity; a high vapor enthalpy per bubble.

American Gas Association, LNG Fact Book. Planning and Analysis Group, AGA Arlington, VA 22209, 1977.

This report summarizes the American Gas Association view of LNG importation and its advantages. Issues and project status at the time of publication are also reviewed.

An Economic Analysis of Imported LNG in Selected End Use Markets. Prepared for the American Gas Association by Booz Allen and Hamilton, Inc., May 1978.

Economics of LNG usage in space heating, with and without advanced equipment, and in industrial applications is reviewed.

An Experimental Study of the Mitigation of Flammable Vapor Dispersion and Fire Hazards Immediately Following LNG Spills on Land. A report by University Engineers, Inc., to the American Gas Association, February 1974.

A series of fire control, fire extinguishment and vapor dispersion tests were conducted under the high boil-off rates which occur immediately following an LNG spill on land. Correlations of the results provide fire control and extinguishment times with dry chemical agents and high expansion foams. The magnitude of the reduction in downwind concentrations of methane vapors by the application of high expansion foam on the spill was also determined.

Analysis of Risk in the Water Transportation of Hazardous Materials. U.S. Coast Guard Report, CG-D-39-76. NTIS No. AD/A025298, January 1976.

This report assesses the utility and feasibility of using risk analysis to assist in management decisions regarding the regulation of water transportation of bulk hazardous materials. A number of risk analysis studies were surveyed. Barge transportation on inland waterways was chosen for special study, and a probabilistic model of risk was selected. It was concluded that the greatest utility of the methodology lies in answering specific questions with output of a specific predetermined nature.

Andersen, W. H., Garfinkle, D. R., Carpenter, G. E. and Brown, R. E., "Energy Absorption Near and Below the Burning Surface of Hydrocarbon Pools." Paper presented at the 1969 Meeting, Central States Section, The Combustion Institute, March 18-19, 1969.

The burning behavior of a liquid fuel pool is discussed in terms of the heat feedback from the flame that is transported into and through the fuel via conduction and radiation. It is shown that the radiant flux contribution to the total heat flux input is greatest for benzene, and decreases consecutively for gasoline, kerosene, and alcohol.

Anderson, A. D., "Analytical Modeling of Practical Combustion Systems." DOE/Final Report FE-2589-TI, Department of Energy, Washington, D.C., 1978.

The author applies Spaulding's approach to model a two-dimensional, steady-state, recirculating and reacting flow. An attempt is made to incorporate the effect of turbulence on the reaction rate through a two-equation turbulence model (K-E). Analytical and experimental results are compared with fair to good agreement.

Anderson, J. and Smith, M., "Safety-Guided Design of LNG Terminal." Oil and Gas Journal, 77(25):93-97, 1979.

Safety was the basic consideration in the design of Southern Energy's LNG import terminal at Elba Island, Alabama. The terminal sits on an island in the Savannah River. Its three storage tanks can each store 400,000 bbl of LNG. Nine 125,000 m^3 tankers supply the terminal from Algeria.

Anderson, P. J., "Recent Developments in Regulations for LNG Storage in the United States." CONF-790985-1, 1979.

The paper reports on the ongoing debate for a new version of the principal standard for LNG facilities: NFPA-59A. A target date for final approval was set for November 1979.

Anderson, P. J., "Steady Growth Seen in Next Decade for World Trade in LNG." Pipeline and Gas Journal, 121(3):39-45, 1980.

It is expected that until the mid-1980's, the size of world trade in LNG will more than double, with an annual growth rate of about 16%. However, this must be compared with an annual growth rate of an average 23.5% for the last 15 years.

Anderson, P. J. "The Potential for LNG World Trade." Chem. Eng. Progr. 77(1):73-79, 1981.

Statistical data on production and trade of natural gas are presented. The LNG industry registered an average 23% annual growth during the last 20 years. Future growth is expected to continue at a measured pace, at least for this decade.

Anderson, R. P. and Armstrong, D. R., "Experimental Studies of Vapor Explosions." 3rd International Conference on Liquefied Natural Gas, paper 3 of Session VI, Chicago, 1972.

Small scale experiments with molten salts and molten metals, injected into water, are described. In some cases ensuing reactions can turn into vapor explosions.

Anderson, R. P. and Armstrong, D. R., "Experimental Study of Vapor Explosions." Paper presented at the Third International Conference and Exhibition on Liquefied Natural Gas, September 24-28, 1972, Washington, DC.

Present knowledge about various aspects of vapor explosions is summarized. Particular emphasis is placed on methods of evaluating the destructive kinetic energy release from a specified accident. A theoretical method of calculating the maximum destructive energy is outlined.

Andrews, G. E. and Bradley, D., "The Burning Velocity of Methane-Air Mixtures." Combustion and Flame. 19:275-288, 1972.

Results are presented for the variation of burning velocity with equivalence ratio for methane-air mixtures at one atmosphere pressure. Values were determined by the bomb-hot wire and corrected density ratio techniques, for combustion during the pre-pressure period. The former of these methods gives a maximum burning velocity of 45 $\pm$ 2 cm/sec, at an equivalence ratio of 1.07.

Androulakis, J. G., "Thermal Barrier System for a Liquefied Gas Tank." U.S. patent 4,140,073 (to Frigitemp, New York), 1979.

It is claimed that radiation is the main contributor for heat transfer to an LNG cargo tank. Therefore, it is proposed to surround the tank with a high reflectance material acting as a thermal shield for radiation.

Anselmann, H. H. and R. Bellemann. "Test Run of Safety Valves for LNG." Oil and Gas J., pp. 68-69, October 6, 1980.

The temperature gradients in an LNG safety relief valve were experimentally determined by tests with liquid nitrogen under simulated operating conditions. These measurements provide criteria for selecting the proper materials for the valve components.

Anspach, G., Baseler, R. and Glasfeld, R., "A Floating LNG Receiving Terminal." Chem. Eng. Progr. 75(10):86-91, 1979.

The paper presents the floating LNG terminal as a practical alternative to land-based storage and regasification facilities. Lower cost and independence of seismic restraints are its prime advantages. However, so far no such terminal has been designed or ordered.

Anthony, E. J., "Some Aspects of Unconfined Gas and Vapor Cloud Explosions," Journal of Hazardous Materials. 1:284-301, 1975-77.

A critical review is presented of experimental and theoretical work on unconfined vapor explosions with emphasis on modeling studies.

Arkharov, A. M., Yu. A. Berestyanskiy, "Natural Gas Liquefaction Plants with Expanders in the Return Flow." In: Problems of Modern Cryogenics. NASA TT F-16, 841, 1976.

A theoretical study shows the possibility of using a Le Rouge cycle with a turbo-expander in the return flow for liquefying natural gas. The pressure differential between the main supply line and the distribution network is sufficient for 6-15% liquefaction.

Arnoni, Y. G., "The Marriage of LNG and Offshore Facilities." Chem. Eng. Progr. 75(10):60-65, 1979.

The article deals with the advantages and problems of an LNG offshore facility on technical, economic and sociological grounds. Even though no such facilities have been built, several are in the planning and engineering phase.

Arthur D. Little, Inc., A Report on LNG Safety Research, Vol. I. to A.G.A., A.G.A. Project I U-2-1, A.G.A. Catalog No. M19711, January 31, 1971.

It is concluded that smaller releases are rather rare and usually not damaging; probability is low that a large spill will occur from currently constructed facilities; spills from containers may have acceptable probability but some additional protection should be provided; risk of transfer line failure requires higher level of protection; further consideration should be given to hazards involved with LNG transport.

Asselineau, P. R., "Experience With LNG as a Vehicle Fuel for the Public Transport System of Paris." Paper No. A3.11 presented at the 14th International Congress of Refrigeration, Moscow, (in French), September 20-29, 1975.

This paper discusses the results and recommendations of field tests conducted by Gas de France to assess the economic and practical aspects of operating LNG-powered vehicles. Three buses from the Paris public transport network were used in the testing.

Atallah, S. and Allen, D. S., "Safe Separation Distances From Liquid Fuel Spill Fires." Paper presented at Central States Section, Combustion Institute Meeting on Disaster Hazards, Houston, TX, April 1970.

This paper critically reviews the methods generally used to calculate safe separation distances from liquid fuel spill fires. Correlations for predicting flame height and other radiative properties are reviewed. Distances at which the thermal radiation flux falls below the minimum level needed to ignite cellulosic materials are calculated and the results are presented in convenient graphical form.

Atallah, S. and Raj, P., "Thermal Radiation From LNG Spill Fires." Paper P-3 presented at the Cryogenic Engineering Conference, Atlanta, GA, August 10, 1973.

This paper reviews the present state of knowledge relating to thermal radiation from LNG fires. Utilizing data from recent AGA-sponsored LNG fires in seven 6-ft, six 20-ft, and one 80-ft diameter pools, equations were derived for predicting LNG flame height and the angle of tilt of LNG flames in the presence of wind. A model for predicting the thermal radiative flux at various locations away from an LNG fire is presented.

Atallah, S., E. Drake and R. Reid. Summary of LNG Safety Research. PB273378, 1974.

A critical comprehensive overview of LNG safety. The document goes into considerable technical details with an extensive bibliography.

Auton, T. R. and J. H. Pickles. The Calculation of Blast Waves from the Explosion of Pancake-Shaped Vapor Clouds. Central Electricity Research Laboratories, Laboratory Note No. RD/L/N 210/78.

A theoretical model for the explosion of a circular pancake-shaped cloud of inflammable vapor is proposed. The model is an extension of the piston model familiar in the treatment of spherical or hemispherical clouds.

Backhaus, H., "LNG - A Fuel for Motor Vehicles." Gas Warme Int. 21:257-64, (in German), June 1972.

The merits and advantages of converting motor vehicles to compressed or liquefied natural gas to reduce pollution are discussed. Present and future costs of LNG in West Germany and an incentive to encourage private conversion of fleet vehicles to LNG are also discussed.

Bailey, F. B., "Status of United States Codes and Regulations Affecting Land Based LNG Facilities." 1978 Operating Section Proceedings, American Gas Association, Montreal, Quebec, May 1978.

This report summarizes current safety and non-safety regulations, and activities concerning regulations. NEPA59A versions and applications are listed.

Baitis, A. E., Bales, S. L. and Meyers, W. G., Prediction of Lifetime Extreme Accelerations for Design of LNG Cargo Tanks. U.S. Coast Guard Report CG-D-89-74. NTIS No. AD/779635, March 1974.

A procedure is developed to predict the extreme accelerations needed for design of the cargo tanks in LNG vessels. The validity of the prediction tool is discussed. Comparisons are made with accelerations measured in model and full scale experiments.

The results of a pilot study on a single, large typical LNG ship are presented. Acceleration response variations due to changes in ship load conditions and changes due to longitudinal, lateral and vertical locations are examined.

Baker, C. R., H. Cheung. Ethylene Production with Utilization of LNG Refrigeration. U.S. Patent 4,121,917; to Union Carbide Corporation, 1978.

Union Carbide Corporation suggests using the cold energy available in LNG as a source of refrigeration in an ethylene plant. By closely matching the cooling curve of the ethylene plant with the LNG warming curve, a highly efficient utilization of the LNG refrigeration is obtained.

Baker, C. R., and H. Cheung. Ethylene Production with Utilization of LNG Refrigeration. U.S. Patent 4,121,917, 1978.

By closely matching the cooling curve of the ethylene plant with the LNG warming curve, highly efficient utilization of the LNG refrigeration is achieved.

Baker, J. Microcomputer Firmware Description, LGF Data Acquistion System. UCID 18745, 1980.

Two firmware systems (a weather system and a gas and turbulence system) for data acquisition in the LNG dispersion test at China Lake are described.

Bartknecht, T. W. "The Course of Gas and Dust Explosions and their Control." First International Loss Prevention Symposium, 1974, 159-174.

The paper describes the course of explosions in vessels and in pipelines. The author discusses the different probabilities of applied explosion protection.

Basevich, Y. Ya., Volodin, V. P., Kogarko, S. M. and Peregadov, N. I., "Calculation of Turbulent Flame in the One-Dimensional Approach." Combustion and Flame, 36(1):September 1979.

The authors model the effect of turbulence on flame structure (e.g., flame thickness and propagation velocity) in imperfectly mixed deflagrations. Good agreement between their experimental and analytical results were presented. The approach outlined is somewhat obscure but deserves careful scrutiny because of the importance of deflagrations in large, partially mixed LNG vapor clouds for safety considerations.

Baysinger, F. R. Liquefied Natural Gas Tank Construction, U.S. Patent 4,181,235, assigned to Kaiser Aluminum, 1980.

An improved method for fabricating a spherical storage tank for liquefied or compressed natural gas is described. This method results in a reduction of scrap losses and in a reduced number of weldments.

Becker, H. and Liang, D., "Viable Length of Vertical Tree Turbulent Diffusion Flames." Combustion and Flame. 32:11-137, 1978.

The authors of this paper propose and review correlations for the visible length of turbulent diffusion flames. This paper may be useful for determining the magnitude of thermal radiation from LNG pool fires.

Beer, J. M., "Methods for Calculating Radiative Heat Transfer from Flames in Combustors and Furnaces." Heat Transfer in Flames. Chapter 2, John Wiley and Sons, 1974.

Recent advances in methods for predicting radiative heat flux distribution in furnaces and combustors are reviewed with special reference to the zone method of analysis and the flux methods. Recent experimental studies specially designed to test these prediction procedures under sufficiently severe conditions are discussed.

Bellus, F., Cochard, H., Vincent, R. and Mauger, J., Controlling the Hazards from LNG Spills on the Ground LNG Firefighting Methods and Their Effects Application to Gaz de France Terminals. Gaz de France, DOE-Tr-18.

Three basic areas are examined in this paper. A mathematical model to calculate vapor dispersion from accidental LNG spills on land is described. This model is used to investigate various types of impounding areas and their minimization of methane cloud travel. A method to calculate water spray rates for the protection of LNG tank walls from the energy radiated by an adjacent fire is described and a numerical example is given. The authors describe the details of design and construction of the new 80,000 m^3 LNG tank at the Fos Terminal.

Bellus, F., Vincent, R., Cochard, H. and Mauger, J., "Controlling the Hazards from LNG Spills on Land." Fifth International Conference on LNG, Session III, paper 5, Institute of Gas Technology (in French), 1977.

A new mathematical model is described which allows the calculation of vapor dispersion from accidental spills of LNG on land.

Bellus, F. and Humbert--Basset, R., "LNG as Motor Fuel: French Studies and Results." Paper presented at The Fourth International Conference on Liquefied Natural Gas, Algiers, Algeria, (in French), June 24-27, 1974.

Gas de France's comparison studies and test results with gas-fueled engines over motors using gasoline or diesel-oil, and their arrangements for cryogenic equipment that is necessary for storing and vaporizing the LNG on the vehicle, are described.

Benedick, W. B., "High-Exposure Initiation of Methane-Air Detonations." Combustion and Flame." 35:89-93, 1979.

The detonation limits of a stoichimetric methane-air mixture have been determined under "free-field" and "confined" conditions. Such a mixture is generally more difficult to detonate than an LNG vapor cloud.

Bennett, C. P., "Marine Transportation of LNG at Intermediate Temperature." Chartered Mechanical Engineer. 26(3):63-66, 1979.

The paper details advantages of transporting LNG at intermediate temperatures in pressure vessels.

Bensesh, M. E., "The Use of Gas Hydrates in Improving the Load Factor of Gas Supply Systems." U.S. Patent 2,090,163 (to Chicago By-Products Corp), 1942.

This method recommended using excess natural gas, during low demand periods, for hydrate formation and storage. The natural gas would be regenerated for peak demand.

Berger, E., "LNG Plants on Floating Structures - Intermediate Reports on an Extensive Test Program." Chemical Economy and Engineering Review. 10(10):22-29, 1978.

The paper reports on progress in designing floating LNG liquefaction plants which could be used for marginal offshore gas fields where subsurface pipelines are not economical.

Bernert, R. E., "Technical Aspects of Ambient Vaporizers and Superheaters." Applications of Cryogenic Technology. Vol. 6. Proc. Cryo 173 Conf. 6th Los Angeles, CA, October 2-4, 1973, pp. 85-93, 1974.

This paper discusses aspects governing the performance of ambient water and air cryogenic vaporizers and superheaters. This paper also includes some design limits due to ice and frost formation.

Beychok, M. R., "How Accurate are Dispersion Predictions?" Hydrocarbon Processing. pp. 113-116, October, 1979.

This paper cautions the reader against assuming that generalized dispersion models have a fixed accuracy in all applications. Examples of the variability are shown.

Bijl, P., Vet, P. N., "Novel Approach Required for LNG Peakshaving Plant in the Netherlands." Oil and Gas Journal. pp. 81-85, November 28, 1977.

This article describes a unique peakshaving facility which produces both LNG and liquid nitrogen, LN_2. Because of the high N_2 content of the gas in the Netherlands, a slightly modified expander liquefaction cycle was designed which allowed separation of LN_2 from the LNG.

Bingham, G. E., Gillespie, J. H. and McQuaid, J. H., Small Battery-Powered Infrared Absorption Sensor for Methane, Ethane, and Other Hydrocarbons. UCID-17968-79-1, pp. 23-42 Lawrence Livermore Laboratory 1979.

The concept for a portable gas sensor capable of measuring LNG vapor concentrations is described. It is based on infrared absorption by hydrocarbons between 3 and 4 pm.

Biro, P., "Fire Protection for LNG Storage, Transportation and Distribution Facilities." gwf-gas/erdgas. 118(8):344-346, 1977 (in German).

The requirements for fire protection of LNG facilities are described. Specifically, liquefaction plants, storage facilities, LNG terminals and LNG tankers are addressed.

Blackshear, P. L., ed., Heat Transfer in Fire: Thermophysics, Social Aspects, Economic Impact. John Wiley & Sons, 1974.

The book, in five parts, considers social and economic aspects of fires; geometric parameters for classifying full-scale fires; heat and mass transfer in gaseous and condensed phases; radiative heat transfer associated with fire problems, and radiative transfer parameters.

Blanchard, R. L., A. E. Sherburn, J. L. Middleton. "An LNG Cargo System Simulator for Crew Training." Presented at Gastech 78 LNG/LPG Conference, Monte-Carlo, Monaco, November 7-10, 1978.

This paper describes an LNG Cargo System Simulator that has been built and is used for training crews for large LNG tankers.

Blinov, V. I. and Khudyakov, G. N., "Certain Laws Governing Diffusion Burning of Liquids." Doklady Akademii Nauk U.S.S.R. 113:1094-1098, 1957.

An investigation of the burning of gasoline, diesel oil, solar oil and a number of other petroleum products in containers having different diameters enabled the authors to determine some important relationships for diffusion of burning liquids.

Board, S. J., Farmer, C. L. and Poole, D. H., "Fragmentation in Thermal Explosions." International Journal of Heat and Mass Transfer. 17:331-339, 1974.

Experiments involving explosions between molten tin and water are described. Results indicate that thermal explosions usually involve several distinct interactions; a small disturbance can escalate by successive growth and collapse cycles; vapor collapse is the main cause of dispersion in many thermal explosions, and the jet penetration hypothesis can account for both the time scales and energy transfer rates.

Bongers, A., TenBrink, G. Rulkans, P. "Release of a Pressurized Hydrocarbon from a Pilot-Plant-Scale Pressure Vessel; Experiments and Theory." Third International Loss Prevention Symposium, 1980, 16/1198-16/1209.

This paper describes experiments concerning the unsteady release of pure propylene from a 20-ℓ pressure vessel through an 8 mm opening in the top of the vessel.

Boni, A. A., Wilson, C. W., Chapman, M. and Cook, J. L., "A Study of Detonation in Methane/Air Clouds." Acta Astron. 5:1153-1169, 1978.

A numerical simulation of the detonation in unconfined, gaseous mixtures of methane/oxygen/nitrogen is attempted. Results show that initiation of such detonations requires very large trigger charges (10 to 1000 t of tetryl).

Booth, S. H. and Vance, R. W. (ed.), Applications of Cryogenic Technology, Vol. 8. Scholium International, Inc., New York, 1976.

This text presents papers comparing Cryogenic Applications Symposia on Liquefied National Gas (LNG) presented at CRYO '75 and CRYO '76, conferences of the Cryogenic Society of America.

Boulanger, A., "Method of Storing Liquefied Gases at Low Temperature in a Subterranean Cavity." U.S. patent 4,140,423 (to Geostock, Paris, France), 1979.

It is claimed that leak tightness of the underground cavity can be obtained by freezing the surrounding ground. Fissures that might be generated during the cooling process can be plugged by spraying water into them. For this purpose, the cavity must be under visual observation during the initial cooling program.

Bourguet, J. M. "LNG Cold: Still a Problem." Hydrocarb. Proc. 60(1):167-172, 1981.

A wide variety of possibilities is discussed on how to use the "cold" energy of LNG in energy-saving applications. Many of these possibilities are still beset with technical problems.

Bowman, B. R., "Dispersion Model Comparisons." Report B, Liquefied Gaseous Fuels Safety and Environmental Control Assessment Program: A Status Report. DOE/EV-0036, Department of Energy, Washington DC, 1979.

Various mathematical models for the dispersion process following an LNG spill are evaluated. Deficiencies are pointed out and needs for further work are outlined.

Bowman, B. R., Sutton, S. B. and Comfort, W. J., "The Impact of LNG Spills on the Environment: A Comparison of Dispersion Models and Experimental Models." Proceedings of the 25th annual technical meeting of the Institute of Environmental Sciences, Seattle, WA, April 1979.

A Gaussian and Three-Dimensional Navier-Stokes model for LNG spills and subsequent dispersion are compared. Data including hydrocarbon concentrations from three 5-m LNG spill tests are used to evaluate the models.

Boyle, G. J., "Vapor Production From LNG Spills on Water." American Gas Association Distribution Conference, May 1973.

The results indicate that LNG spilled onto water will spread outward with a rate that decreases with time; vapor production will equal the discharge rate as long as the discharge is occurring; with a batch spill it is necessary to take into account the LNG which evaporates to calculate the maximum pool and the peak vapor production rate; the dispersion plume from a large LNG spill on water will be wide and shallow.

Boyle, G. J. and Kneebone, A., Laboratory Investigation into the Characteristics of LNG Spills on Water, Evaporation, Spreading and Vapor Dispersion. Re 6Z32, Shell Research Limited, Released by the American Petroleum Institute, March 1973.

This is a laboratory and small-scale wind tunnel investigation of the characteristics of LNG spills on water. One characteristic investigated, that has not been studied by others, is the appreciable incorporation of water in the vapor cloud.

Bradford, R. H. Supporting Structure for Containers Used in Storing Liquefied Gas. U.S. Patent 4,136,493, assigned to: NRG Inc., 1979.

Land-based storage vessels for LNG are thermally insulated all around with a solid insulating material which must carry the total weight of the tank. The patented structure design minimizes the squeezing of the insulating material from the space below the tank bottom.

Bradley, D. and Mitcheson, A., "The Venting of Gaseous Explosions in Spherical Vessels I, II." Combustion and Flame. 32:221-237, 1978.

The authors present various theoretical analyses of the pressure rise in partially confined reactive systems. The results of these investigations are then compared with experimental data and recommendations are made for proper venting procedures.

Brecht, C. "Gas - Energy of the Future." Hydrocarbon Process. 59:76-0-76-UU, November 1980.

Since proven reserves of natural gas are more plentiful than those for oil, natural gas will play an increasingly important role in the future energy supply, particularly in Europe. LNG will be restricted primarily to world areas which are not close enough to be reached by pipeline.

Briscoe, F. and Vaughn, G. J., "LNG/Water Vapor Explosions--Estimates of Pressures and Yields." Paper presented at the Gastech 78 LNG/LPG Conference, Monte Carlo, November 1978.

The essentials for the occurrence of LNG vapor explosions are discussed. The maximum possible yields and pressures in such explosions are determined by various theoretical approaches.

Briscoe, F. and Fog, G. F., A Guide to the Use of BKWAVE - A Computer Program for the Calculation of One-Dimensional Shock Wave Propagation from Explosions. United Kingdom Energy Authority, SRO-R-104, Calceth Warrington, U.K., May 1978.

This report is a description of a computer code, BKWAVE, which can calculate the shock wave resulting from an explosion of known strength. The reaction is assumed to be over instantaneously.

Britter, R. E., "The Spread of a Negatively Buoyant Plume in a Calm Environment." Atm. Envir. 13:1241-1247, 1979.

The paper presents the results of a laboratory experiment to study the spread of a negatively buoyant plume in a calm environment including semi-empirical relation for the cloud leading edge. Under conditions where the effects of wall frictions and ambient wind can be neglected, most or all mixing occurs at the cloud leading edge.

Bröty, W., Schössbucher, A., Scheller, V. and Kettler, A., "Electronically Produced Equidensities From Time Exposures and Instantaneous Photographs in the Investigation of Pool Flames." Combustion and Flame, 37(1):January 1980.

This paper essentially describes an experimental method by which information on the temperature, soot formation, turbulence and other fire phenomenon may be obtained photographically. Some experimental data are also presented.

Brown, G. H. "Wisconsin National Gas Makes Successful LNG Turnaround." Pipeline & Gas J. 209(13):41-43, 1981.

The modification of an LNG peakshaving plant built in 1965 required taking the storage tank out of service, inspecting it, increasing LNG pumping capacity, adding regasification capacity, adding instrumentation and building a new containment dike.

Brown, L. E. and Romine, L. M., "Liquefied Gas Fires: Which Foam?" Hydrocarbon Proc. 58(9):321-332, 1979.

Six different types of foam were evaluated for their effectiveness in controlling liquefied gas fires. Medium and high expansion foams proved to be most efficient.

Brown, L. E., Martinsen, W. E., Muhlenkamp, S. P. and Puckett, G. L., Small Scale Tests on Control Methods for Some Liquefied Natural Gas Hazards. Final Report, prepared by University Engineers, Inc., Norman, Oklahoma, for the U.S. Coast Guard, Report No. CG-D-95-86. NTIS No. AD/A033522, May 1976.

A report of results of small scale (100 ft^2) tests of some liquefied natural gas (LNG) hazard control methods and concepts. Tests of water spray screens showed that the concept is practical and effective for small LNG spills. Tests of water spray screens to reduce radiant heating of exposures demonstrated no practical value.

Brown, T. T. and Hubbard, J. K., Application of Gas Turbine/Compressors in LNG Plants. 1979.

This paper discusses key considerations associated with selection of Gas Turbine Driven LNG Turbo Compressors. Use of gas driven versus steam driven compressors is compared.

Browning, R. L., "Estimating Loss Probabilities." Chemical Engineering. pp. 135-140. December 15, 1969.

This article presents a technique for analyzing industrial risks. Methods for obtaining the loss incident frequencies are described and the relative probabilities of loss incidents are included.

Brzustowski, T. A., "A New Criterion for the Length of a Gaseous Turbulent Diffusion Flame." Combustion Science and Technology. 6:313-319, 1973.

The flame tip is identified with the point on the axis of maximum fuel concentrations where the fuel has been diluted to the lean flammability limit. Flame-length equations are derived using the new criterion, together with data from the literature on entrainment of air into flames, transverse concentration profiles in turbulent jets, and flammability limits.

Brzustowski, T. A., "The Hydrocarbon Turbulent Diffusion Flame in Subsonic Cross-Flow." AIAA Paper 77-222, January 1977.

The flame is modeled as a bent-over initially vertical circular jet with top-hat profiles of composition, temperature, and velocity. The hydrocarbon pyrolyzes in a zero-order reaction and the pyrolysis products are oxidized at a rate proportional to the rate of entrainment of air into the flame.

Buch, E., "Utilizing the Cold of LNG for Power Generation." Energie. 29:182-183, 1977 (in German).

When vaporizing LNG, it would be economical to take advantage of the low temperature of the LNG as a heat sink in a closed gas turbine cycle. Such a scheme could recover 14% of the total LNG energy, which otherwise could be lost in the vaporization process.

Buchholz, C. D. and Senkowski, E., "Unique Design and Operating Features of Philadelphia Electric Company's LNG Plant." Paper presented to Seminar and Study Tour on LNG Peakshaving, Washington DC, March 5-9, 1979.

The design and operating experience of the West Conshohocken LNG Plant is reviewed. The plant utilized a nitrogen expansion cycle for liquefaction, a double-walled, double-roofed above ground storage tank, and submerged combustion vaporizers.

Bukacek, R. F., "Operating Characteristics of LNG Storage Tanks." CONF 780457-1, 1978.

The interactions which exist among the various operating parameters of an LNG storage tank are elucidated in a quantitative way. The origination of a "rollover" incident is explained.

Bull, D. C., Ellsworth, J. E., Hooper, G. and Quinn, C. P., "A Study of Spherical Detonation in Mixtures of Methane and Oxygen Diluted by Nitrogen." J. Phys. D: Apply. Phys. 9:1991-2000, 1976.

Experiments are described which examine the behavior of spherically propagating detonation waves in methane/oxygen/nitrogen mixtures. Such tests have a bearing on the safety question of LNG.

Bull, D. C., Ellsworth, J. E. and Hooper, G., "Susceptibility of Methane-Ethane Mixtures to Gaseous Detonation in Air." Combustion and Flame. 34:327-330, 1979.

Experiments are described which determine the detonation limits of methane-ethane-air mixtures. The presence of even small amounts of the heavier hydrocarbons has a significant effect on these limits.

Bureau Veritas. "Liquefied Gas Carriers-Damage, Stability, Investigation." Guidance Note NI 162 A BM.1, März 1977.

The paper describes the proceeding at the classification of liquefied gas carriers.

Burgess, D., Biordi, J. and Murphy, J., Hazards of Spillage of LNG into Water. PMSRC Report No. 4177, U.S. Department of the Interior, Bureau of Mines, Pittsburgh, PA, 1972.

These are reports of experimental investigations of LNG spills on water. The pool spread, evaporation rate, vapor gravity spread, downwind drift and dispersion were studied in spill sizes up to 0.5 m^3. In unconfined spills coherent ice flow formation was not observed. In several cases small scale physical explosions were observed but no attempt was made to study the initiation or burning of the cloud.

Burgess, D. S. and Hertzberg, M., "Radiation From Pool Flames." Heat Transfer in Flames. Chapter 27, John Wiley & Sons, 1974.

Some radiation data from pool flames is summarized and our understanding of the problem is reviewed. Spectral data yield a 1500¾ K temperature for hydrocarbon pool fires, which is consistent with the 40 percent maximum in the fraction of combustion energy radiated, and with limited flame temperatures for the mixing limited systems. A revised correlation of mass burning rate with $\Delta H_c/\Delta H_v$ is presented, and derived fundamentally.

Burgess, D. S., Murphy, J. N. and Zabetakis, M. G., Hazards Associated with the Spillage of Liquefied Natural Gas on Water. Report RI 7448, U.S. Department of the Interior, Bureau of Mines, November 1970.

The hazard of spilling LNG onto water is discussed. After spillage, the initial vaporization rate of LNG was determined to be 0.037 lb/ ft^2 sec. If the LNG was confined, this rate was modified by the formation of ice on the water surface. Using a 2000-gallon LNG sample, the maximum diameter (in feet) of the spreading pool was calculated at 6.3 $w_o^{1/3}$ where w_o is the weight of LNG in pounds.

Burgess, D. S., Murphy, J. N. and Zabetakis, M. G., Hazards of LNG Spillage in Marine Transportation Final Report. NTIS No. AO/70578, for USCG, Office of Research Development, February 1970.

The hazard of spilling LNG onto water is discussed. After spillage onto water, the initial vaporization rate of LNG was determined to be 0.037 lb/ft^2 sec. If the LNG was confined, this rate was modified by the formation of ice on the water surface. Using a 2000-gal LNG sample, the maximum diameter (in feet) of the spreading pool was calculated at 6.3 $W_o^{1/3}$ where W_o is the weight of LNG in pounds.

Burgess, D. S., Murphy, J. N., Zabetakis, M. G. and Perlee, H. E., "Volume of Flammable Mixture Resulting from the Atmospheric Dispersion of a Leak or Spill." Application of Cryogenic Technology, Vol. 8. Combustion Institute 15th Symposium on Combustion, 1976.

The paper discusses atmospheric dispersion of flammable vapors, the struture of gas clouds and the explosion potential of flammable mixtures.

Burgess, D. S., Strasser, A. and Gumer, J., "Diffusive Burning of Liquid Fuels in Open Trays." Fire Research Abstracts and Reviews. 3(3):177-192, 1961.

The paper describes the effects of fuel temperature and wind on burning rate, discusses the problem of cryogenic fuels, and suggests that burning rate may be predicted from heats of vaporization and combustion of the fuel. Data on methanol, LNG, liquid hydrogen, amine fuels, and typical hydrocarbons are included.

Burgess, D. S. and Zabetakis, M. G., Detonation of a Flammable Cloud Following Propane Pipeline Break: The December 9, 1970 Explosion in Port Hudson, Missouri. Report RI 7752, U.S. Department of the Interior, Bureau of Mines, 1973.

This report summarizes the incidents that preceded the December 9, 1970, propane-air explosion in Port Hudson, MO. Both near- and far-field damage indicated that this explosion may be attributed to the detonation of propane in air with an energy release equivalent to that from about 50 tons of detonating TNT.

Burgess, D. and Zabetakis, M. G., Fire and Explosion Hazards Associated With Liquefied Natural Gas. Report RI 6099, U.S. Department of the Interior, Bureau of Mines, 1962.

Factors that should be considered in evaluating the fire and explosion hazards relating to any fuel are discussed. These factors are utilized in the design of experiments to evaluate the hazards associated with LNG as compared to those hazards associated with other fuels.

Buschmann, C. H., "Experiments on the Dispersion of Heavy Gases and Abatement of Chlorine Clouds." Proceedings of the Fourth International Symposium on Transport of Hazardous Cargoes by Sea and Inland Waterway, Jacksonville, FL, October 26-30, 1975, Report No. AD/A023505, pp. 475-488, October 1975.

The experiments comprised four different parts: dispersion of heavy gases offer an instantaneous release; penetration of heavy gases in buildings during the passage of a gas-cloud; influence of a chlorine-cloud on motorized traffic, and suppression and abatement of chlorine-clouds.

Bush, S. H., "Pressure Vessel Reliability." Journal of Pressure Vessel Technology. 97(J):54-70, February 1975.

An informative review pertaining to United States pressure vessels is made and compared to data available from Germany. An attempt to understand the apparent differences in reliability of these two countries on the bases of the ASME codes covering materials, design, and construction, on operating procedures, and on differences in reporting techniques. Some attention is given to failure modes to possibly understand the low incidence of operational failures in the United States.

Byram, G. M., "Scaling Laws for Modeling Mass Fires." Pyrodynamics. 4:271-284, 1966.

The paper is concerned with the development of scaling laws necessary for modeling and is restricted to the stationary mass fire.

Byram, G. M. and Nelson, R. M., Jr., "Buoyancy Characteristics of a Fire Heat Source." Fire Technology. 10(1):68-79, 1974.

Buoyancy production rates for a pure heat source and for a fire heat source of burning woody fuels show that fire may be regarded as a pure source yielding heated air rather than heated combustion products.

Byram, G. M. and Nelson, R.M., Jr., "The Modeling of Pulsating Fires." Fire Technology. 6(2):102-110, 1970.

The authors present scaling relationships for modeling pulsating fires. Data gathered from various sizes of pulsating fires compared favorably with the predicted relationships between fire diameter and pulsation frequency.

Cahn, R. P., Johnston, P. H. and Plumstead, J. A., Transportation of Natural Gas Hydrate. U.S. Patent 3,514,274 (to Esso Research and Engineering Co.), 1970.

Natural gas was combined at 25 to 40°F and >80 psia with a slurry of propane hydrate in propane. This mixture was cooled to -40°F to give methane hydrate slurry in propane. Treating this product with propane gas at 25-40°F and <80 psia regenerated methane and propane hydrate.

Carne, M., Thomas, J. R. and Hutchinson, E. A., Buxton Bund-Fire Tests. The Gas Council, December, 1971.

Ignition and burnout tests were conducted on LNG contained within walls of clay or pulverized fuel ash. The test objective was to establish whether walls of this construction would be damaged by a combination of cold LNG and flame radiation. Results showed no damage to the walls apart from a superficial calcining of the turf and slight spalling of the concrete covering. Flame radiation agreed reasonably well with predicted values.

Cermak, J. E., "Applications of Fluid Mechanics to Wind Engineering - A Freeman Scholar Lecture." Journal of Fluids Engineering. 97:9-38, March 1975.

The objectives of this review are to establish an initial subject-matter base for wind engineering, to demonstrate current capabilities and deficiencies of this base for an engineering treatment of wind-effect problems, and to indicate areas of research needed to broaden and strengthen the subject-matter base.

Chan, S. T. and Gresho, P. M., A Comparison of Hydrostatic and Nonhydrostatic Models as Applied to the Prediction of LNG Vapor Spread and Dispersion. UCID-18097, Lawrence Livermore Laboratory, March 1979.

Two mathematical models are described and after numerical implementation, results of a series of computations for LNG vapor dispersion are compared. Conclusions are drawn on how to further develop the less elaborate model into a more cost-effective code.

Chan, S. T., Gresho, P. M. and Lee, R. L., Simulation of LNG Vapor Spread and Dispersion by Finite Element Methods. UCRL-82441, Lawrence Livermore Laboratory, July 1979.

Two finite element models are described: one based on solving the time-dependent, two-dimensional conservation equations of mass, momentum, and energy, with buoyancy effects included via the Boussinesq approximation; the other based on solving the otherwise identical set of equations except using the hydrostatic assumption, and applied these models to predict some aspects of the vapor dispersion phenomena associated with LNG spills.

Chan, S. T., P. M. Gresho, and R. L. Lee. "Simulation of LNG Vapour Spread and Dispersion by Finite Element Methods." Appl. Math. Model. 4:335-344, 1980.

Two analytical models are described which predict the dispersion of vapour clouds after an LNG spill. These models appear to be slightly superior when compared with existing models.

Chang, H. R. and R. C. Reid. Simultaneous Boiling and Spreading of LPG on Water. DOE/EV/04548-1, Department of Energy, Washington, D.C., 1981.

Theoretical and experimental studies on the boiling and spreading of certain cryogenic fluids were conducted. A mathematical model was developed to describe the phenomena in the test apparatus. Its results agreed fairly well with actual observations.

Chatterjee, N., Gaumer, L. S. and Geist, J. M., "Operational Flexibility of LNG Plants Using the Propane Precooled Multicomponent Refrigerant MCR Process." LNGS - International Conference on LNG, Duesseldorf, Germany, August 29-September 1, 1977.

This paper discusses the operation of the MCR liquefaction process over a wide range of conditions. A computer program which models the porcess is described.

Chatterjee, N. and Geist, J. M., Spontaneous Stratification in LNG Tanks Containing Nitrogen. ASME Publication 76-WA/PID-6, December 5, 1976.

LNG containing significant concentrations of nitrogen can stratify spontaneously during weathering in storage tanks. Mixing of stratified layers leads to an increase in boil-off rates, commonly referred to as "rollover". LNG storage tanks can be designed and operated safely if stratification and associated problems are taken into account.

Chatterjee, N. and Geist, J. M., "The Effects of Stratification on Boil-off Rates in LNG Tanks." Paper presented at the A.G.A. Distribution Conference, Atlanta, GA, May 8-10, 1972.

The addition of LNG to a partially filled tank containing liquid of a different density may lead to the temporary formation of stratified layers. The physical phenomena associated with the mixing of stratified layers of LNG have been simulated on the computer. One method for mitigating potential hazards associated with stratification is by limiting the density and the temperature difference between fresh liquid and LNG in the tanks.

Chippet, S. and Gray, W. A., "The Size and Optical Property of Soot Particles." Combustion and Flame. 31:149-159, 1978.

This paper presents the results of an experimental inventigation to determine the spectral transmissivity and size distribution of soot aggregates. Measured attenuation and light scattering were found to be in best agreement with theoretical results when the complex refractive index, $\bar{u}$, was taken to be 1.9-0.35i.

Chiu, Chen-Hwa, "Evaluate Separation for LNG Plants." Hydrocarbon Processing. pp. 266-272, September 1978.

Energy losses from various processes involved in separation of LNG components during liquefaction are discussed. Losses due to compression and liquefication were cited to show areas for improvement in energy use.

Chiu, C. H. and C. L. Newton. "Second Law Analysis in Cryogenic Processes." Energy. 5:899-904, 1980.

Two different processes for liquefying natural gas are compared on the basis of conserving energy. It is shown that one of the processes (the propane-precooled mixed refrigerant process) is clearly more efficient for producing LNG than the other.

Clancey, V. J. "The Development of Hazardous Clouds." Second International Loss Prevention Symposium, 1977, 323-331.

Equations are presented to estimate the quantity of vapor generated and the growth and dispersion of a large cloud of inflammable vapor. The mechanism of flame acceleration and the generation of pressure pulses into the environment is discussed. The phenomenon of pressure propagation to yield shock waves at a distance is indicated.

Clapp, M. B. and Litziner, L. F., "Marine Terminals for LNG, Ethylene, and LPG." A paper presented at the 68th National AICHE Meeting, Houston, Texas, February 28 - March 4, 1971.

The design and economics of marine terminals for LNG, Ethylene, and LPG are discussed. Some discussion of safety features is included.

Closner, J. J. and Parker, R.O., "A Careful Accident Assessment Key to LNG Storage Safety." Oil and Gas Journal. pp. 47-51, February 6, 1978.

This article discusses potential accidents and related hazards associated with LNG storage facilities. A list of mitigating measures which would prevent an accident or reduce its consequences is included.

Closner, J. J. and Parker, R. O., "Safety of Storage Designs Compared." Oil and Gas Journal. pp. 121-125, February 13, 1978.

Eight different types of LNG storage designs are compared with respect to the likelihood and potential consequences of a spill or accident.

Coevert, K., Groethuizen, Th. M., Pasman, H. S., Trense, R. W. "Explosions of Unconfined Vapor Clouds." First International Loss Prevention Symposium, 1974, 145-157.

Accidental releases of combustible liquids or gases into the open air are associated with the hazard of subsequent ignition which initiates a large fire or an explosion. The paper presents a tentative evaluation of the problem. The basic concepts of deflagrative and detonative combustion are reviewed and current research studies are discussed, with particular regard to the blast wave generation by unconfined vapor-cloud explosions.

Cole, R. S. and Moulsley, T. J., "The Use of the Atmospheric Acoustic Sounder to Track Methane Gas Plumes." Atm. Envir. 13:1437-1441, 1979.

The usefulness of the acoustic sounder as a method of tracking elevated methane plumes is explored.

Colenbrander, G. W. "A Mathematical Model for the Transient Behaviour of Dense Vapor Clouds." Third International Loss Prevention Symposium, 1980, 15/1104-15/1132.

On the basis of an existing steady-state model, a quasi-steady-state description has been developed for the atmospheric dispersion of heavy gases.

Colgate, S. A. and Sigurgeirsson, T., "Dynamic Mixing of Water and Lava." Nature. 244:552-555, August 31, 1973.

It is suggested that lava eruptions under the ocean might result in vapor explosions, similar to those which have been observed when liquid metals or LNG come into contact with water. Violent mixing of water and lava are believed to be the cause of such explosions.

Collins, M. H., et al. Method of Producing a Barrier in a Thermally Insulated Container. To Shell Internationale Research Maatschappij B.V. (U.S. Patent 4,120,418) 1978.

The Netherlands' Shell Internationale Research Maatschappij B.V. has developed an essentially pinhole-free barrier for LNG storage/transport tanks. The barrier consists of layers of an epoxy-resin formulation and glass-fiber material, applied in a special sequence to produce a barrier of superior quality.

Colton, J. W., Pretreatment of Raw Natural Gas Prior to Liquefaction. U.S. Patent 4,150,962, 1979.

A process for pre-treating raw wellhead gas is described that reduces the liquefaction refrigeration power requirements by expanding the gas through an expansion turbine, which in turn drives the liquefaction compressor.

Conners, T. G., "LNG Primer." Hazardous Chemicals--Spills and Waterborne Transportation. AICHE Symp. Ser. 194, 76, pp. 62-69 1980.

The paper gives a brief description of the cargo operations of an LNG tanker and outlines the basic types of LNG containment and insulation systems.

Corlett, R. C., "Gas Fires With Pool-Like Boundary Conditions: Further Results of Interpretation." Combustion and Flame. 14:351-360, 1970.

A circular, upward-facing burner, supplying uniform flux of fuel gas from a water-cooled surface, preserves the essential features of a pool fire. Addition of up to 2% methyl bromide to several fuels had no effect on heat transfer. At high fuel supply rates, the data tend to correlate independently of the air requirement of the fuel; at low supply rates, the data tend to correlate independently of volumetric supply rate.

Corlett, R. C. and Fu, T. M., "Some Recent Experiments With Pool Fires." Pyrodynamics. 4:253-269, 1966.

Steady burning rates of methanol, ethanol and acetone in thin-walled stainless steel burners of 0.6 to 30 cm diameter have been studied. Radiation levels were estimated and are found consistent with results of earlier experiments with water-cooled gas burners. Measured water absorption rates are in reasonable agreement with those inferred from burning rate data on the basis of heat and mass transfer similarity.

Cox, R. A., Roe, D. R. "A Model of the Dispersion of Dense Vapor Clouds." Second International Loss Prevention Symposium, 1977, 359-366.

This paper presents a model for the dispersion of dense vapor clouds and describes its particular application to LNG-Spills.

Crawford, D. B. and Eschenbrenner, G. P., "Heat Transfer Equipment for LNG." Chemical Engineering Progress. September 1972.

This article describes liquefaction heat exchangers and vaporizers for LNG facilities. Advantages, disadvantages, and relative costs for each type are included.

Creighton, J. R., A Two Reaction Model of Methane Combustion for Rapid Numerical Calculations. UCRL-79669, Rev 1, Lawrence Livermore Laboratory, September 28, 1977.

Inclusion of chemical kinetics in the computational schemes for multi-dimensional thermo-hydrodynamic codes (involving flame propagation) results in prohibitively expensive computational time. The author of this report attempts to develop a simplified flame propagation model (of possible use in Langrangian-Eulerian hybrid codes)which yields acceptable values of flame velocity, temperature and pressure.

Crescittelli, S., Russo, G., Tufano, V. "Mathematical Modeling of Relief Venting of Gas Explosions: Theory and Experiment." Third International Loss Prevention Symposium, 1980, 16/1187-16/1197.

Two different dimensionless models for the venting of gas explosions are presented which are based on the hypotheses that there is unburnt gas. The results are compared with experimental data.

Crouch, W. W. and Hillver, J. C., "What Happens When LNG Spills?" Chem. Tech. 2(4):210-215, 1972.

Authors try to assuage certain exaggerated fears about the safety hazards of LNG spills. They stress, however, the need for more information on the behavior of large spills.

Culbertson, L. and Emery, W. B., "Liquefaction Plant Experience at Lenai." Presented at the 3rd International LNG Conference and Exhibition, Washington, DC, September 24-28, 1972.

This paper reviews the more significant problems encountered and solutions employed in the operation of the Alaska to Japan LNG project. This is a follow-up to earlier papers describing design and startup at the Kenai plant.

Dailey, W. V. and Long, E. V., "Remote Sensing of Combustible and Toxic Gases." Analysis Instrumentation, Vol. 17. pp. 89-96, Pro. 1979 Symposium Measurement Technology for the 80's. Instru. Soc. Am., 1979.

Remote sensing systems with central control readout for detecting and monitoring levels of combustible gas (as, e.g., contained in LNG) are described. Detailed specifications are listed. The systems can be obtained from the Mine Safety Appliance Company.

Daniels, E. J., K. G. Darrow, and H. R. Linden. "Energy Alternatives to LNG." Session I, Paper 4, Sixth International Conference on Liquefied Natural Gas, 1980.

In addition to the economic competitiveness of LNG relative to the other energy-supply alternatives, this paper considers the relative impact on the balance of trade. It is debated how to price LNG in a manner that adequately compensates the producer, but still makes it available to the ultimate consumer at a marginal price which is competitive with alternative energy sources.

Davenport, J. A., "A Survey of Vapor Cloud Incidents." Loss Prevention. 11:39-49, A CEP Technical Manual, 1977.

The paper gives a survey of open-air, unconfined vapor cloud explosions which have occurred during the last 25 years. The survey is taken from the viewpoint of a major insurance company and is primarily concerned with the property loss (in $) in the various types of accidents. LNG accidents represent only a minor fraction of all reported cases.

Deaton, W. M. and Frost, E. M., "Gas Hydrate Composition and Equilibrium Data." Proc. Natural Gas Department, American Gas Association. pp. 49-56, 1946.

Phase diagrams as well as equilibrium data were presented.

DeFrondeville, B., "Reliability and Safety of LNG Shipping: Lessons from Experience." Paper presented to the Annual Meeting of the Socity of Naval Architects and Marine Engineers, New York, New York, November 10-12, 1977.

This paper reviews LNG shipping experience in Europe, Japan, and the United States. The review concentrates on reliability and safety aspects. The safety/reliability record for liquefaction/ loading ports and receiving are also summarized.

DeLeon, C. "An Overview of the Development of LNG Facility Regulations by MTB." LNG Terminals and Safety Symposium, pp. 287-292, in Applications of Cryogenic Technology 9. Scholium International, Flushing, New York, 1979.

A brief overview is given of the development of LNG facility safety regulations by the Materials Transportation Bureau of DOT. The need for comprehensive new federal LNG safety standards is stressed.

Del Tatto, D. L., "LNG Satellite Peakshaving." Presented at the AGA Distribution Conference, Houston, Texas, May 6-9, 1968.

This paper presented by an engineer from Chicago Bridge and Iron describes one of the first LNG satellite operations in the U.S. Both primary liquefaction and peakshaving plant and the satellite peakshaving facility are discussed.

Department of Transportation, "Liquefied Natural Gas Facilities; Federal Safety Standards: Development of New Standards." Federal Register. pp. 8142-8182, Thursday, February 8, 1979.

The notice proposed establishment of a set of comprehensive safety standards governing design, site selection and construction of LNG facilities used in pipeline gas transportation or interstate or foreign commerece. Implications of the regulations and comments are also discussed.

Department of Transportation, "Liquefied Natural Gas Facilities; Federal Safety Standards; Final Rule and Proposed Rule Making." Federal Register. pp. 9184-9237, February 1980.

The final rule establishing a set of comprehensive safety standards governing the design and construction of liquefied natural gas facilities is given. A proposed rule establishing safety standards governing operation and maintenance is also described.

Department of Transportation, "Liquefied Natural Gas Facilities, (LNG); Federal Safety Standards: Development of New Standards," Federal Register, pp. 70776-70800, Thursday, April 21, 1977.

The article sets forth proposed safety standards for LNG facilities. The proposed rules are based largely on National Fire Protection Association Rules (NFPA 59A 1975) and an Arthur D. Little Report summarizing LNG Technology.

Desgroseilliers, G. J. Radiation from Burning Hydrocarbon Clouds. M.S. Thesis, MIT Department of Mechanical Engineers, p. 88, 1978.

Radiation test data from the combustion of methane, ethane and propane are reported. Tests are of small scale with the vapors initially contained in soap bubbles. A newly-developed mathematical model agrees fairly well with the experimental results.

Det Norske Veritas. Guidelines for the Classification of Floating Facilities for Gas Processing, Liquefaction and Storage. Classification Notes No. 8, Hovik, Norway, 1976.

The purpose of this note is to provide a uniforn guidance for those who intend to build or operate floating facilities for gas processing, liquefaction, and storage with classification by Det Norske Veritas. The note contains principles and criteria which will form the basis for classification of such facilities.

Det Norske Veritas. Programme for Gas Explosion Research. Exhibit A-Project Description, Hovik, Norway, 1980.

Det Norske Veritas proposes research to further understand: 1) Vented Gas Explosions, including flame accelerations, methods for practical scaling, and variation of geometry and 2) Coupled Explosions, including jet ignition of gas clouds and explosion propagation in interconnected rooms.

Devanna, L. and Doulames, G., "Planning is the Key to LNG Tank Purging, Entry and Inspection." Oil and Gas Journal. pp. 74-82, September 8, 1975.

Procedures used by the Lowell Gas Co. to purge a one billion cu-ft tank out of service are described in detail. The article includes a drawing showing the piping, valves, and fittings on the tank which are used for purging.

Diller, D. E., "LNG Thermophysical Properties Data and Custody Transfer Measurements." American Gas Association Monthly. March 1979.

Measurement research for custody transfer discussed along with the economic reason for pursuing these studies. Publications in Thermophysical properties of LNG are referenced.

DiNapoli, R. N., "Design Needs for Base-load LNG Storage, Regasification." Oil and Gas Journal. pp. 67-70, October 22, 1970.

Design of base-load storage and vaporization equipment and facilities is described. The article contains particularly good information on the operation and control of sendout pumps and seawater vaporizers.

DiNapoli, R. N., "LNG Peakshaving Plants Require Careful Cost Estimating." Pipeline and Gas Journal. pp. 28-36, May 1978.

The paper reports a dearth of data on the costs of LNG peakshaving plant construction probably due to the competitive nature of the LNG construction industry. Generalized costs of peakshaving and satellite facilities are presented.

DiNapoli, R. N., "Gas Turbines Prove Effective as Drivers for LNG Plants." Oil & Gas J., 78(31):47-52, August 4, 1980.

Since fuel costs have risen dramatically, even small differences in the mechanical efficiencies of equipment drivers in LNG plants become important. Therefore, the substitution of gas turbines for steam turbines might be economically attractive now and in the foreseeable future.

Dincer, A. K., Drake, E. M. and Reid, R. C., "Boiling of Liquid Nitrogen and Methane on Water. The Effect of Initial Water Temperature." Int J. Heat Mass Transfer. pp. 176-177, 1977.

This note reports on the results of studies carried out in a vessel equipped to measure the temperature-time history at a number of locations in the bulk water phase as different cryogens were spilled on the surface. It is concluded that if the initial water temperature is low, heat transfer to the cryogen occurs through a growing ice shield, with little effect on the underlying water. If the water is initially warm, ice forms more slowly and cool surface water is mixed through the bulk.

Drake, E. M., "LNG Rollover--Update." Hydrocarbon Processing. 55:119-122, January, 1976.

The article considers LNG density, effects preceding rollover, rollover time prediction, heat storage, and discusses three documented cases of rollover.

Drake, E. M., Geist, J. M. and Smith, K. A., "Prevent LNG Rollover." Hydrocarbon Processing. 52:87-90, March 1973.

Studies were undertaken of basic mechanisms involved in LNG "rollover", to predict when they may occur and to evaluate effectiveness of possible preventive measures. Such measures include mixing during filling, limiting variations in LNG composition and lowering tank set point pressure.

Drake, E. M., Jeje, A. A. and Reid, R. C., "Transient Boiling of Liquefied Cryogens on a Water Surface. I - Nitrogen, Methane, and Ethane." International Journal of Heat Mass Transfer. 18:1361-1368, 1975.

The results of an experimental study of the transient boiling rates of pure liquefied nitrogen, methane, and ethane in water are discussed. Nitrogen boiled with the lowest heat flux rate and the highest vapor superheat. For nitrogen, the heat flux rate was found to be proportional to the square root of the liquid head. The heat flux rate for ethane was the lowest and that for methane was intermediate.

Drake, E. M., Jeje, A. A. and Reid, R. C., "Transient Boiling of Liquefied Cryogens on a Water Surface. II - Light Hydrocarbon Mixtures." International Journal of Heat Mass Transfer. 18:1369-1375, 1975.

Light hydrocarbon mixtures similar to liquefied natural gas were boiled on a water surface. The rate of vaporization was measured and the heat fluxes were found to be much higher than that measured for pure liquid methane. Like methane, the rate of vaporization increased during the course of the experiment unless a continuous thick ice layer formed. No significant vapor superheat was noted.

Drake, E. M. and Reid, R. C., "How LNG Boils on Soils." Hydrocarbon Processing. 54(5):191-194, May 1975.

Implications of the paper are that: boil rates of LNG on compacted soils are influenced by soil type, moisture content and LNG composition; reduction in boiling rates can be obtained by sealing the dike surface; dikes of crushed rock or stone will have higher evaporization rates than compacted soil dikes; more studies are needed to assess insulating or sealing materials under LNG spill conditions and on LNG foaming behavior.

Drake, E. M. and Reid, R. C., "The Importation of Liquefied Natural Gas." Sci. Am. 236(4):22-29, 1977.

Arguments in favor and against large-scale importation of LNG are discussed, with the safety question receiving primary attention. On balance, LNG appears to be a relatively safe and promising alternative energy source.

Drake, E. M. and Wesson, H. R., "Review of LNG Spill Vapor Dispersion and Fire Hazard Estimation and Control Methods." Proceedings of A.G.A. Transmission Conference, Las Vegas, NV, May 1976.

This paper reviews techniques presently being used by the LNG industry for evaluating potential LNG vapor dispersion and fire hazards and will describe practical methods for reducing the severity of LNG spill accidents.

Duckham, H. E., "LNG Import Terminal Design Considerations." Cryogenics and Industrial Gases. pp. 41-48, September/October 1972.

This article describes the many processes and mechanical parameters involved in the design of an LNG import terminal. Included are discussions on facilities location, transfer lines, insulation, storage tanks, vapor handling systems, and LNG vaporizers.

Duffy, A. R., Gideon, D. N. and Putnam, A. A., Comparison of Dispersion From LNG Spills over Land and Water. Prepared by Battelle Columbus Laboratories for the American Gas Association, Project SI-3-7, September 4, 1974.

This study examines and compares the available data on dispersion from land and water spills, and explains similarities and differences in results on the basis of differences in experimental techniques and test conditions, and possible differences in pertinent phenomena.

Duffy, A. R., Gideon, D. N., Putnam, A. A. and Bearint, D. E., LNG Safety Program - Phase I - Potential LNG Spills. Report by Battelle Columbus Laboratories and University Engineers, Inc., to the American Gas Association, February 25, 1971.

The report presents data on known spills of LNG or other cryogens, a discussion and analysis of problem areas, and a discussion of consequences of spills including downwind dispersion, radiation from fires, and reactions with water. Conclusions are summarized and recommendations made for future research.

Dunn, W. A. and Tullier, P. M., Spill Risk Analysis Program Phase II Methodology Development and Demonstration. NTIS No. AD/785026, August 1974.

This report describes research and results in the development and demonstration of systematic methods of assessing the effectiveness of either proposed or recently implemented merchant marine safety regulations. The methods have been designed primarily to assist Coast Guard regulatory decision-makers in their selection of alternative means of reducing marine transportation casualties and spills of hazardous or polluting materials.

Durr, C. A. and Crawford, D. B., "LNG Terminal Design." Hydrocarbon Processing. November 1973.

This article discusses the special problems associated with design of an LNG terminal. Particular attention is given to the transfer line and the vapor handling and pressure control system.

Durr, C. A., "Process Techniques and Hardware Uses Outlined for LNG Regasification." Oil and Gas Journal. May 13, 1974.

The following components of an LNG terminal are discussed by a process engineer from M. W. Kellog: LNG unloading, storage, vapor handling, sendout pumps, vaporizers, power generation, nitrogen system, and heat recovery.

Eckhoff, R. K. "Large-Scale Gas Explosion Experiments in Norway." From Discussion on Explosion Hazards at the 7th International Colloquium on Gas Dynamics of Explosions and Reactive Systems, ed. H. Wagner, pp. 82-87, Max-Planck-Institute Für Strömungsforschung, Göttingen, 1979.

As a consequence of discovery of oil and natural gas on the Norwegian continental shelf, the question of fire and explosion hazards associated with oil and gas activities on- and offshore has become an important issue in Norway. A research project is underway which is concerned with flame propagation and pressure development resulting from explosions in confined and semi-confined geometries, as encountered on offshore oil and gas platforms. Preliminary results indicate that for large vessels containing propane/air mixtures, the classical explosion venting type of volume scaling is invalid. A non-steady gas dynamic analysis accounting for shock waves and various complex mechanisms of flame acceleration must be used to achieve a realistic description of the pressure transients inside and outside the vessels.

Eckhoff, R. K., K. Fuhre, O. Krest, C. M. Guirao, and J. H. S. Lee. Gas Explosions on Offshore Platforms - Flame Propagation and Pressure Development. Report CMI No. 790750-1, 1980.

Flame propagation and pressure development during semi-confined combustion of turbulent propane-air has been studied experimentally in a 50-m^3 cylindrical test vessel with a 5-m^2 open vent to the atmosphere. Blast-wave decay characteristics have been determined for various modes of combustion, up to detonation. Experimental results are compared with theoretical predictions by alternative models.

Ecosystems, Inc., Expected Behavior of an LNG Release Under Specified Conditions. Report to Federal Power Commission, August 17, 1973.

The report comprised an assessment of hypothetical LNG spill situations in the Staten Island area. Results were calculated using methods of the Esso Research and Engineering Company. Three tasks described are analyses of a 100,000 m^3 spill over water, analyses of evaporation and dispersion following an LNG tank roof failure, and a description of the New York Harbor climate.

Edeskuty, F. J., Critical Review and Assessment of Problems in Hydrogen Energy Delivery Systems. Initial Report, Los Alamos Scientific Laboratory LA-74-PR Progress Report UC-41, August, 1978.

A preliminary risk assessment for the transport of gaseous hydrogen by pipeline and liquid by tank trucks is presented. Metal imbrittlement by liquid hydrogen is discussed and regulations are reviewed.

Edwards, J. G., "A Combustible Gas Detection System for an LNG Terminal." Analysis Instrumentation, Vol. 17. Proc. 1979 Symposium on Measurement Technology for the 80's. Instr. Soc. Am., pp. 84-88, 1979.

For reasons of personnel safety and plant integrity, combustible gas detection systems are required in all LNG facilities. Practical guidelines are given for the reliable operation of such systems.

Edwards, R. M., "The Application of Sub-X Heat Exchanger for Vaporization of Liquid Natural Gas." American Society of Mechanical Engineers publication, 8 pp., September 1967.

The basic design and development of the Sub-X heat exchanger for vaporization of liquefied natural gas is presented in this paper. Detailed drawings and discussions are included.

Eichhoff, H. E. and Grethe, K., "A Flame Zone Model for Turbulent Hydrocarbon Diffusion Flames." Combustion and Flame. 35(2):267-275, August 1979.

The authors present a flame zone model which corrects the deficiency of two previous models (called the flame sheet and equilibrium models) by more correctly accounting for the intermediate reaction species. Comparison with experiment supported their model.

Eichler, T. V. and Napadensky, H. S. Accidental Vapor Phase Explosions on Transportation Routes Near Nuclear Power Plants. U.S. Nuclear Regulatory Commission, NUREG/CR-0075, 1977.

A review of vapor cloud explosion literature is used to develop a method to estimate TNT equivalency for accidental blasts as a tool for calculating exclusion distances for hazardous materials near nuclear plants.

Eidsvik, K. J. A Model for Heavy Gas Dispersion in the Atmosphere. Norsk Institutt for Luftforskning, ISBN 82-7247-113-2, 1979.

A simple model is developed for the dispersion of heavy and cold gas cloud. The theoretical solutions are justified with experimental data. The hazard of heavy gas clouds is predicted.

Enger, T., "Explosive Boiling of Liquefied Gases on Water." Conference Proceedings on LNG Importation and Terminal Safety, Boston, MA, June 13-14, 1972.

Explosive boiling of a liquefied gas mixture such as LNG on ambient water can only be produced when the methane content is less than 40 mole percent. The potential hazard of having explosive boiling from an LNG spill is negligible during commercial transportation of LNG. In addition, energy estimates show that the potential damage from explosive boiling of a liquefied gas is minimal.

Enger, T. and Hartman, D. E., "Mechanics of the LNG-Water Interaction." Paper presented at the American Gas Association Distribution Conference, Atlanta, GA, May 8, 1972.

Shell Pipe Line Labs has conducted research since 1970 on rapid phase transformation which can occur when LNG is spilled onto water. "Explosive" LNG-water interaction results because of rapid phase transformation and violent expansion of a thin layer of superheated LNG at the interface between the LNG and water. It is stated that "explosions occur only when LNG is in a weathered state, i.e., when the methane content of LNG is less than 40 mole percent."

Enger, T. and Hartman, D. E., "Rapid Phase Transformation During LNG Spillage on Water." Paper presented at the Third International Conference and Exhibition on LNG, Washington, DC, September 24-28, 1972.

It is shown that "explosions" can only occur with "aged" LNG which contains less than 40 mole percent methane. The "explosive" interaction between a liquefied gas and water is caused by the rapid phase transformation and violent expansion of a thin layer of superheated liquefied gas at the liquefied gas-water interface.

Enger, T., Hartman, D. E. and Seymour, E. V., "Explosive Boiling of Liquefied Hydrocarbon/Water Systems." Paper presented at the Cryogenic Engineering Conference, National Bureau of Standards, Boulder, CO, August 9-11, 1972.

The conditions which produce "explosions" when LNG is spilled on water at ambient temperature have been isolated and verified experimentally. It has been shown that "explosions" can only occur with "aged" LNG which less than 40 mole percent methane. Contact between water and LNG with more than 40 mole percent methane produces normal vaporization.

Enger, T., Hartman, D. E. and Seymour, E. V., "Explosive Boiling of Liquefied Hydrocarbon/Water Systems." Adv. Cryo. Eng. 18:32-41, 1973.

The mechanism of LNG/water interactions, and the conditions under which they can occur, are described. The explosive boiling, which has been observed, is explained as a result of superheating of the liquefied gas.

England, W. G., Teuscher, L. H., Hauser, L. E. and Freeman, B. E., "Atmospheric Dispersion of Liquefied Natural Gas Vapor Clouds Using Sigmet, a Three Dimensional Hydrodynamic Computer Model." Proceedings of the 1978 Heat Transfer and Fluid Mechanics Institute, Washington State University, Pullman, Washington, June 26-28, 1978.

The SIGMET dispersion model is presented in the form that it is applied to LNG vapor dispersion problems. Model results are presented for examples of plume behavior and to verify model predictions. Model numerical methods are also described.

Ermak, D. L. and Bowman, B. R., "Average Dispersion of a Liquefied Natural Gas Vapor Plume." UCID-17968-79-1, pp. 1-10, Lawrence Livermore Laboratory, 1979.

The theoretical predictions for the vapor spread from an LNG spill are compared with experimental data obtained in a China Lake test. Agreement is fair. Prevailing winds are shown to have a significant influence but are hard to model.

Escudier, M. P., "Aerodynamics of a Burning Turbulent Gas Jet in a Crossflow." Combustion Science and Technology. 4:293-301, 1972.

The study extends the entrainment theory for weak plumes by including into its framework the influences of radiative thermal-energy transfer, large density variations, and thermal-energy generation through chemical reaction. Thermal radiation is found to be of secondary importance to plume dynamics. Calculations show that a plume's motion is not significantly influenced by buoyancy forces until well downstream of the reaction zone.

Etzbach, V. et al. Cascading Refrigeration Cycles for Liquefying Low-Boiling Gaseous Mixtures. U.S. Patent 3,970,441, assigned to: Linde A.G., 1976.

The invention involves some minor modification in the standard procedures for liquefying natural gas. Thereby, the overall complexity of the process is somewhat simplified.

Evaluatie van de Gevaren Verbonden aan Aanover, Overslag en Opslag van Vloeibaar Aardgas. TNO-Report, 1976.

A hazard assessment study of the supply and storage of LNG for the conditions applicable to the situation at the Dutch coast near the entrance of the river Maas has been carried out.

Evaluation of LNG Vapor Control Methods. Report to the American Gas Association by Arthur D. Little, Inc., Cambridge, Massachusetts, October 1974.

It is shown that, for the high spill rates, the maximum downwind hazard zone is not significantly affected by shutdown of the leak in the 10-minute period specified in the NFPA Code. To be effective in reducing downwind hazards shutdown of the leak should be accomplished as soon as possible, preferably under 2 minutes.

Fannelop, T. K. and Waldman, G. D., "The Dynamics of Oil Slicks - Or 'Creeping Crude'." AIAA Paper No. 71-14 presented at the AIAA 9th Aerospace Sciences Meeting, New York, New York, January 25-27, 1971.

The spread of an oil slick into calm water is considered from a theoretical viewpoint. The equations of motion are derived for the gravity-inertial and gravity-viscous flow regimes. For both two-dimensional and radial slicks, similarity solutions are obtained for the two flow regimes which give adequate agreement with available experimental data.

Farley, M., "The LNG Plant Design Engineer." LNG/Cryogenics. pp. 25-27, February/March 1973.

This article, through interviews with six individuals involved in LNG plant design activities, provides a brief overview of some of the problems they have had to cope with on various projects.

"Fast LNG-leak Detector Developed." Oil and Gas Journal. pp. 52, December 19, 1977.

A new device developed and patented by the Direction of Studies and New Techniques of Gaz de France is claimed to provide fast detection and location of leaks in large storage tanks. The location for the detector, at the bottom of the annular space between the walls and next to the internal tank, was determined following tests made on a reduced model tank.

Fauske, H., "The Role of Nucleation in Vapor Explosions." Transactions of the American Nuclear Society. 15:813-815, 1972.

The paper suggests a possible mechanism for vapor explosion and examines the validity of the mechanism in light of available experimental facts.

Fay, C., Desgroseillier, G., and Lewis, D., "Radiation from Burning Hydrocarbon Clouds." Combustion Science and Technology. 20, 1979.

This paper is a report of a series of experiments performed at M.I.T. Small scale fireballs were created in the laboratory and the time-dependent thermal emission was measured by a radiometer. Various correlations concerning fireball parameters (diameter, temperature, etc.) are presented.

Fay, J. A., Scale Effects in LNG Hazard Analysis and Testing. Progress Report for period 12/1/76 to 8/21/77. ERDA Contract No. EE 77-S-02-4204.

The effect of LNG spill size on the physical parameters in hazard analysis has been investigated. Measurements of radiant heat envisions have been made.

Fay, J. A., "Unusual Fire Hazard of LNG Tanker Spills." Combustion Science and Technology. 7:47-49, 1973.

This report gives theoretical expressions for the pool spread and evaporation rate of liquefied natural gas spilled on water, the gravitational spread, and the heating and downwind spread of the vapor cloud. It does not treat the diffusion or mixing of the vapor with air.

Fay, J. A. "Risks of LNG and LPG." Ann. Rev. Energy 5:89-105, 1980.

This paper reviews some of the more pertinant recent papers and studies on LNG and LPG safety and risk analysis.

Fay, J. A. and Lewis, D. H., Jr., "The Inflammability and Dispersion of LNG Vapor Clouds." Proceedings of the Fourth International Symposium on Transport of Hazardous Cargoes by Sea and Inland Waterway, Jacksonville, FL, October 26-30, 1975, NTIS No. AD/A023505, pp. 489-498, October 1975.

The paper considers the statistical properties of LNG vapor concentration, the mean vapor concentration in dispersing cloud and downwind distances for two flammability conditions.

Fay, J. A. and Lewis, D. H., "Unsteady Burning of Unconfined Fuel Vapor Clouds." 16th International Symposium on Combustion, 1976.

The problem of fireball hazards associated with LNG and LPG spills is investigated. A derivation of fireball maximum radius, height above surface and time required, are obtained by phenomenological, empirical and dimensional (with some physical and mathematical) analysis. Experimental corroboration is included.

Federal Power Commission (Bureau of Natural Gas). Construction and Operation of an LNG Import Terminal in Calcasieu Parish, PB 278071, September 1976.

An environmental impact statement for an LNG terminal in the Calcasieu Ship Channel in Louisiana.

Feirabend, C. E., "Design Considerations for LNG Production Facilities in Arctic Regions." 1978 Operating Section Preceedings, American Gas Association, Montreal, Quebec, May 1978.

Operational and engineering design responses to extremes of temperature and windspeed in arctic regions are considered.

Feldbauer, G. F., Heigl, J. J. and McQueen, W. et al., Spills of LNG on Water - Vaporization and Downwind Drift of Combustible Mixtures. Report No. EE61E-72, Esso Research and Engineering Company, May 24, 1972.

A total of seventeen LNG spill tests, ranging in size from about 250 to 2500 gallons, were carried out under a variety of weather conditions. The main thrust of the experimental work was aimed at measuring the

parameters required to predict downwind concentrations. The aim of the experimental work was to measure the plume shape and other information which would permit the data on these variables to be extrapolated.

Felske, J. D. and Tien, C. L., "Calculation of the Emissivity of Luminous Flames." Combustion Science and Technology. 7:25-31, 1973.

A simple analytical basis for determining the total emissivity of luminous flames is developed. The analysis considers flames whose dominant emitting species are water vapor, carbon dioxide and soot particles. Calculations are made to illustrate the relative importance of gas and soot emission under typical flame conditions.

Filstead, C. G., "The Design and Operation of LNG Ships with Regard to Safety." Shipping World and Shipbuilder. pp. 259-262, February 1972.

This article summarizes the safety features and operating procedures of LNG ships particularly the Methane Princess and Methane Progress.

Findlater, A. E. and Prew, L. R., "Operational Experience with LNG Ships." LNG 5 - International Conference on Liquefied Natural Gas, 5th Proceedings, Session IV Paper 5, 16 pp., Duesseldorf, Germany, August 29-September 1, 1977.

Some of the experience gained during the initial years of operation of the shipping phase of the Shell Bruenei/Japan LNG scheme are presented in this paper. The operational planning required for the successful commissioning and operation of a fleet of gas carriers and the wide range of disciplines and expertise involved is also included in this paper.

Fortson, R. M., Holmboe, E. L., Brown, F. B., Kirkland, J. T., Tullier, P. M. and Dayton, R. B., Maritime Accidental Spill Risk Analysis Phase I: Methodology Development and Planning. NTIS No. AD/761362, January 1973.

This report develops a methodological approach and task plan for assessing alternative methods of reducing the potential risk caused by the spill of hazardous cargo as the result of vessel collisions and groundings. In addition to developing the overall study approach, a very preliminary analysis of ship/barge accidents in U.S. territorial waters and port traffic was done to identify types of accidents to be examined in the next phase of the study effort.

Fourth International Conference on Liquefied Natural Gas. Papers, Place of Nations, Algiers, Algeria, June 24-27, 1974.

This book is a collection of papers presented at the conference. The papers have been divided into 8 sessions according to their subject matter.

Fowles, G. R., "Vapor Phase Explosions: Elementary Detonations?" Science. 204:168-169, 1979.

A new theory is outlined which would explain a vapor explosion as an elementary detonation. It predicts the energy resulting from a superheated liquefied methane vapor explosion as 95 J/g.

Freeman, G. H., K. Potter and W. J. Walters. "Relative Roles of LNG and LPG in Today's and Tomorrow's Energy Market." Session I, Paper 7, Sixth International Conference on Liquefied Natural Gas, 1980.

Past, present, and predicted future world trade in LNG and LPG is compared and changes in the relative supply levels of both gases are considered. A significant increase in LPG supplies is forecast for the mid-1980s. Relative prices of LNG and LPG to consumers will be influenced mainly by the supply and demand balance of those products.

Fuller, M. E. Site Considerations for LNG Facilities. LNG Terminals and Safety Symposium, pp. 324-339, in Applications of Cryogenic Technology 9. Flushing, New York, 1979.

The paper gives an overview of the multitude of federal and state regulations which must be met before an LNG terminal can be sited. More likely than not, a major siting process will become politicized, as shown in the example of the Point Conception terminal.

Fumarola, G., et al. "Vapor Clouds Release and Explosion in Naphta Cracking Units." Third International Loss Prevention Symposium, 1980, 1/148-1/160.

Several disasters in naphta cracking units are considered and compared with particular reference to the dynamic vapor cloud release, diffusion, and explosion.

Garforth, A. and Pallis, C., "Luminar Burning Velocity of Stoichiometric Methane-Air; Pressure and Temperature Dependence." Combustion and Flame. 31:69-83, 1978.

The authors of this paper determine the flame velocity in a stoichiometric methane-air mixture (for initial various temperatures and pressure) experimentally and analytically, with resulting good agreement between the two.

Garland, F. and Atkinson, G., The Interaction of Liquid Hydrocarbon With Water. U.S. Coast Guard, Office of Research and Development, NTIS No. AD/753561, October 1971.

This is an investigation of the phenomena reported in a Bureau of Mines report which studied the hazards of LNG. During the investigation, LNG was dropped onto a variety of liquid samples. Explosions did not occur when pure water was used as the sample, but water

contaminated with n-hexane or toluene gave an explosion every time. Peak explosion pressures are given for a variety of experimental conditions.

Gaydon, A. G. and Wolfhard, H. G., Flames - Their Structure, Radiation and Temperature. Chapman & Hall Ltd., London, 1960.

The book includes information concerning premixed flames, flow patterns and shapes, burning velocity; propagation, diffusion, stability, carbon in flames, radiation, temperature, ionization, combustion processes of rocket fuels, and recent progress on some flame problems.

Geiger, W. "Explosion Hazards of Transport Gases - Research Within the Reactor Safety Program of the Federal Republic of Germany." From Discussion on Explosion Hazards at the 7th International Colloquium on Gas Dynamics of Explosions and Reactive Systems, ed. H. Wagner, pp. 46-59, Max-Planck-Institute Für Strömungforschung, Göttingen, 1979.

In West Germany every nuclear power plant has to be protected against external events such as aircraft crashes, earthquakes, and explosions. Explosions are considered to arise as unconfined vapor cloud events from accidental release of transported hydrocarbon gases. This paper describes a research program to be undertaken to develop information for use in refining Reactor Safety Guidelines. The research program is expected to cover three areas: 1) the mechanisms by which a quasi-detonation unconfined vapor cloud can take place, 2) the interactions between characteristic parameters of an incident pressure wave and structural response of nuclear power plant complex structures, and 3) pressure wave characteristics of a real gas cloud which detonated.

Geiger, W., Synofzik, R. "A Simple Model for the Explosion of Pancake-Shaped Vapor Clouds." Third International Loss Prevention Symposium, 1980, 7/505-7/514.

A simple explosion model for pancake-shaped vapor clouds has been developed. It describes the blast wave over pressures for the case of detonation as well as for the case of deflagration.

General Accounting Office. "Need to Improve Regulatory Review Process for Liquefied Natural Gas Imports." ID-78-17, PB 283293, 1978.

It is shown how inadequacies and shortcomings in federal energy policy adversely affect the import of LNG. Recommendations are given for improving present U.S. conditions. The appendices describe relevant conditions in certain other countries (e.g., Japan) to be more favorable.

Georgakis, C., Congalidis, J. and Williams, G. C., "Model for non-instantaneous LNG and Gasoline Spills." Fuel. 58:113-120, February 1979.

A predictive model for non-instantaneous spills is presented which is applied to holes in storage vessels for gasoline and LNG. Effects of spill size and shape and combustion are discussed and results are compared to those for instantaneous spills.

Germeles, A. E., "A New Model for LNG Tank Rollover." Paper presented at the Cryogenics Engineering Conference, Kingston, Ontario, July 1975.

A dynamic model is presented which can give very accurate rollover predictions and is a potentially powerful tool in rollover prevention strategies. The excellent agreement between the predictions of the model and observations for the La Spezia rollover indicate that the model is valid. Uncertainties in the model transport coefficients indicate that further validation of the model would be desirable. The model has been computerized.

Germeles, A. E., "Forced Plumes and Mixing of Liquids in Tanks." Journal of Fluid Mechanics. 71:601-623, 1975.

A mathematical model for the mixing of two miscible liquids of different density is presented, from which the tank stratification can be computed.

Germeles, A. E. and Drake, E. M., "Gravity Spreading and Atmospheric Dispersion of LNG Vapor Clouds." Proceedings of the Fourth International Symposium on Transport of Hazardous Cargoes by Sea and Inland Waterway. Jacksonville, FL, October 26-30, 1975, NTIS No. AD/A023505, pp. 519-539, October 1975.

The paper presents methods for estimating the extent and location of flammable vapors as a function of spill and weather conditions, assuming that ignition does not occur. Models allow the width of the vapor cloud to be computed at the point of ignition for consequence analysis.

Geschwindt, S. "Dutch Drive for LNG Substitute." Chem. Age, p. 8, 1980.

Because of the Algerian postponement of an increased LNG production, the Netherlands plans to rely more on coal gasification. They consider the Shell-Koppers process as the most economical way for gasification.

Gibson, G. H., "Consider Safety, Reliability, Cost in Selecting Type of LNG Storage." Oil and Gas Journal. pp. 65-69, February 8, 1971.

Several types of LNG storage are compared with respect to safety and cost.

Gideon, D. N. and Putnam, A. A., "Dispersion Hazard from Spills of LNG on Land and on Water." Cryogenics. 17, January 1977.

This report analyzes the pertinent published data on dispersion of vapors from LNG spills on land and water. Correlation of these data is based on the commonly used relationships from dispersion theory. The report has emphasized peak concentration rather than average or 'maximum average' concentrations and for instantaneous spills. The peak concentrations of major interest to safety, are related to the peak vaporization rates.

Gideon, D. N., Putnam, A. A. and Duffy, A. R., Comparison of Dispersion from LNG Spills Over Land and Water. Report to the American Gas Association by Battelle Columbus Laboratories, Project IS-3-7, A.G.A. Catalog No. M19877, September 4, 1974.

The report discusses dispersion variables, spill characteristics on water, a description of LNG programs, and provides comparisons of dispersion data.

Gideon, D. N., Putnam, A. A. and Duffy, A. R., "Safety Aspects of LNG Spills on Land." Advances in Cryogenic Engineering. 21:377-386. Paper presented at 1975 Cryogenic Engineering Conference held at Queen's University, Kingston, Ontario, July 22-25, 1975.

The paper provides information concerning experimental spills of LNG. Instrumentation and procedures, the dispersion hazard, the radiation hazard, and fire control and vapor suppression are discussed.

Gifford, F. A., Jr., "Use of Routine Meteorological Observations for Estimating Atmospheric Dispersion." Nuclear Safety. 2(4):47-51, June 1961.

The article considers vertical dispersion of a cloud or plume and gives estimates of the lateral spread as well as wind speed and direction.

Goldfeder, L. B., "Control Valves for LNG Facilities." Pipeline and Gas Journal. pp. 58-74, January 1972.

The types, applications and materials of construction of control valves for LNG are reviewed.

Goodwin, R. D., The Thermophysical Properties of Methane, from 90 to 500 K at Pressures to 700 Bar. NBS Tech. Note 653, 1974.

An extensive tabulation of the thermophysical property data for methane is presented. The temperatures covered range from 90 to 500 K and the pressure up to 700 bars.

Gotaas, Y. "Aircraft Measurements in the Gas Cloud from the Blowout at an Oil Platform in the North Sea." Journal of Air Poll. Cont. Association. 30(7), 1980.

A report is made on methane measurements for air concentrations and diffusion from a blowout at an oil platform. Estimates were made of the lower flammability point for the plume.

Green, K. A., Tiffin, D. L., Luks, K. D., and Kohn J. P., "Solubility of Hydrocarbons in LNG, NGL." Hydrocar. Process. 58(5):251-253, 1979.

Experiments are described to verify correlations for multicomponent solid-liquid-vapor behavior of realistic natural gas systems. The resulting test data are in essential agreement with correlations derived earlier.

Greunert, H. P. and M. Bookenhauer. "Studies of the Resistance of LNG Carriers to Collisions." Paper presented at the 6th International Conference on LNG, Session III, paper 6, 1980.

The study gives estimates for the limit of collision speeds beyond which the LNG containers aboard ship would incur rupture. Double-wall tankers are declared safe in collisions.

Griffis, K. A. and Smith, K. A., "Convection Patterns in Stratified LNG Tanks - Cells Due to Lateral Heating." Paper presented at the 3rd Conference on Natural Gas Research and Technology, Dallas, TX, March 6-8, 1974.

The paper treats the subject of layer formation due to a uniform lateral heat flux, such as exists at an LNG tank wall. Experimentally, a water sugar system has been used to model the methane-higher hydrocarbon system. Preliminary results indicate that convective layers will be relatively thin for cases which are germane to LNG storage.

Guise, A. B., "How to Fight Natural Gas Fires." Hydrocarbon Processing. 54:76-79, August 1975.

The following recommendations are made for coping with natural gas fires: 1) assume all fires to be impinging, 2) use potassium bicarbonate-base dry chemical, 3) use multipurpose dry chemical where water is not available, 4) use high velocity concentrated streams, and 5) use protective clothing and face shields.

Gullberg, R. W., "NWNG's Newport LNG Facility First User of CRYEX Purification." Pipeline and Gas J. 206(13):40-48, 1979.

A new concept for removing carbon dioxide from a gas stream is incorporated into Northwest Natural Gas Co.'s LNG peakshaving facility on Yaquina Bay, 114 miles southwest of Portland, Oregon.

Guthrie, J. K. and Gregory, E. J., "Design of Baseload Evaporators for LNG."

The design and operation of an open rack vaporizer and an indirect fired vaporizer are discussed.

Hadenhorst, H. G., Lorenzen, H. "Studies of the Storage of LNG in Salt Cavities." Fifth International Conference on LNG, 1977, Session II, paper 8.

The authors studied the thermodynamic behavior of the LNG/rock system as a function of time and the change in the rock mechanics resulting from the thermal influence of the LNG. Tests with liquid nitrogen were made to justify the theoretical studies.

Haines, G. H. and Thompson, J., "Offshore Gas Liquefaction Without Offshore LNG Plants. Oil & Gas J. 78:87-91 February 18, 1980.

It is proposed to liquefy natural gas with liquid nitrogen stored aboard a tanker moored to an offshore drilling platform. At the shore-based terminal, the liquid nitrogen in turn is produced with some of the "cold" derived from vaporizing the LNG. It is claimed that such an operation is well within existing technology and is also economical.

Hale, D., "LNG Projects Develop Overseas, Only Regulations Develop in U.S." Pipeline and Gas Journal. pp. 17-21, June 1979.

The article provides an industry summary of LNG activities in 1978 and includes a list of foreign and U.S. LNG facilities.

Hale, D., "Peakshaving Capabilities Ready for 1979 - 1980 Winter Season." Pipeline and Gas J. 206(13):22-25, 1979.

U.S. peakshaving capabilities will be at a record high for the 1979-1980 winter seasons as underground gas storage capacity and withdrawal/send-out capacity reach new peaks and LNG peakshaving capacity reaches an all-time high; new peakshaving capacity is about 70 billion ft^3/day.

Hale, D., "Developments Proceed Slowly in World LNG Industry." Pipeline and Gas Journal, 121(3):17-19, 1980.

New regulations of the LNG industry are listed. New projects and potential supply sources, both in the U.S. and abroad, are described. LNG prices are shown to escalate. LNG accidents that occurred in 1979 are briefly discussed. The major LNG activity now appears to be in Europe, Japan, Southeast Asia, and Africa.

Hale, D. "Industry Peakshaving Capacity Greatest Ever for 1980-1981 Winter." Pipeline & Gas J. 207(13):17-25, 1980.

An overview is given on the present storage capacity for various forms of gas storage, which includes storage in the form of LNG. The article contains also a brief discussion of significant new LNG developments, new LNG regulations for the past year.

Hall, A. R., "Pool Burning." Oxidation and Combustion Reviews. 6:169-225, Elsevier Scientific Publishing Company, 1973.

This review of literature includes: influence on the burning characteristics; temperature distribution in the liquid and the phenomena of hot zone formation and boilover; prevailing concepts of heat transfer from the flame to the liquid; effect of water as a dispersed phase, and as a substrate, on burning.

Hall, D. J., Barrett, C. F. and Ralph, M. O., Experiments on a Model of an Escape of Heavy Gas. LR 217 (AP), Warren Spring Laboratory. Department of Industry, Hertfordshire, United Kingdom, 1976.

The report describes model experiments on a release of a heavy explosive gas, propane or butane, into the atmosphere at ground level. Both long and short term released are considered and the validity of the model is discussed. A method of extrapolating the experimental results to full scale is provided.

Hall, R. J., "CARS Spectra of Combustion Gases." Combustion and Flame. 35(1):47-60, May 1979.

The author presents a theoretical basis for obtaining species concentration and temperatures in turbulent, sooty flames using Coherent-Anti-Stokes Ramen Spectroscopy (CARS). Comparisons of theory and experiment are presented.

Hall, S. F., A Simple Homogeneous Equilibrium Critical Discharge Model Applied to Multi-Component, Two Phase Systems. Safety and Reliability Directorate (U.K.), Report SRO R 127, May 4, 1978.

Two models of two phase critical discharge from reservoirs are presented which are applicable for spill calculations from breaches in storage tanks or piping.

Halverson, G., "Automatic Continuous LNG Level-Gauging and Temperature Measuring System." Proceedings of the 1st Biennial Symposium on Cryogenic Instrumentation, Vol. 1, 1976.

This paper describes a system which is being used to make accurate measurements of the liquid level and temperature profile in LNG storage tanks.

Handman, S. E., "Pros and Cons of LNG Safety." Pipeline Industry. pp. 39-42, September, 1979.

This paper reviews types of existing LNG facilities, agencies which have jurisdiction over the facilities, and risks associated with LNG facilities versus risks associated with other human activities.

Hankel, C. C., LaFare, I. V. and Litzinger, L. F., "Purging LNG Tanks Into and Out of Service Considerations and Experience." Paper presented to the AGA Transmission Conference, Minneapolis, Minnesota, May 6-8, 1974.

This paper discusses detailed procedures used by Chicago Bridge & Iron for purging LNG tanks into and out of service.

Hankinson, R. W. and Thomson, G. W., "Calculate Liquid Densities Accurately." Hydrocarbon Processing. pp. 277-282, September, 1979.

Liquid density calculation methods are compared on 3000 compounds; results on 190 of these are presented. The Costald - Corresponding States Liquid Density method was found to be more accurate than the Yen-Woods or modified Rackett Equation (SDR) methods.

Hardee, H. C., Lee, D. O. and Benedick, W. B., "Thermal Hazards from LNG Fireballs." Combustion Sci. and Techn. 17:189-197, 1978.

LNG fireballs can pose serious burn hazards in their vicinity. Third degree burns from a very large LNG fireball (several 10^7 kg) could occur out to several kilometers from its center.

Harris, N. C. "The Control of Vapor Emission from Liquefied Gas Spillages." Third International Loss Prevention Symposium, 1980, 15/1058-15/1067.

The paper discusses the physical mechanism which determines the extent of cloud formations and dispersion.

Harsha, P. T., LNG Safety Program Topical Report: Dispersion Modeling. Report RDA-TR-1100-003, by R&D Associates for the American Gas Association, July 1976.

A variety of techniques exist for near-field LNG dispersion phenomena; Gaussian plume models are inappropriate; hydrostatic models are appropriate; three-dimensional numerical models have been demonstrated; a general LNG vapor dispersion model should incorporate sophisticated state-of-the-art turbulence models.

Hasegawa, K. and K. Sato. "The Experimental Study on the Thermal Radiation and the Blast Effect from Unconfined Vapor-Cloud Explosions." From Discussion on Explosion Hazards at the 7th International Colloquium on Gas Dynamics of Explosions and Reactive Systems, ed. H. Wagner, p. 70, Max-Planck-Institute Für Strömungsforschung, Göttingen, 1979.

The hazardous fratures of unconfined vapor-cloud explosions, its size, duration, thermal radiation, and blast effect have been studied on the basis of results obtained from semi-real scale experiments. The experiments were performed in the open air using samples of propane, pentane and octane. The maximum size of fireballs formed was empirically related to the mass of the samples. Fireball duration was found to depend on type

of combustion and flame propagation velocity. The over-pressure due to the blast wave was related to flame propagation velocity. Conclusions could be applied to risk evaluation of accidents in chemical industries.

Haselden, G. G., "Developments in Gas Liquefaction and Separation. " Int. J. Refrig. 2(6):207-210, November, 1978.

Some of the most interesting papers presented to the Gas Liquefaction and Separation Commission of the IIR are reviewed. A novel LNG peak-load storage plant was described in which the excess cooling capacity available during most of the year is used to produce low cost liquid oxygen and nitrogen. On a larger scale, design studies were reported showing the advantages to be gained by cooling natural gas before admitting it to very long transmission pipelines. For duties above 100 x 10^9 m^3/year, piping LNG is recommended.

Haselden, G. G., "The Achievements and Potential of LNG for Energy Storage and Transport." Inst. Chem. Eng. Sym. 44:7-13, 1976.

The paper presents a brief general overview on present LNG technology, highlighting those features that make LNG transport economically attractive.

Haselden, G. G. "The Challenge of LNG in the 1980s." Mech. Eng. 103(3):46-52, 1981.

An overall review is given on current developments in the field of LNG technology. The paper is based on presentations given at the 6th Conference on LNG held in Kyoto, Japan, April 1980. It is expected that LNG trade will keep growing, since presently at least four times as much gas is still vented or flared as is liquefied and traded.

Hashemi, H. T., Lott, J. L., Wesson, W.,D. and Wesson, H. R., "Effect of Barometric Pressure Changes on Rate of Boiloff in a Storage Tank of Saturated Liquids." 1978 Operating Section Proceedings, American Gas Association, Montreal, Quebec, May 1978.

An analytical model for prediction of boiloff variations due to atmospheric pressure changes in atmospheric storage tanks is presented. LNG examples are shown although the model can be applied to various other cryogenic gases.

Hashemi, H. T. and Wesson, H. R., "Cut LNG Storage Costs." Hydrocarbon Processing. pp. 117-120, August 1971.

Better, more precise designs can be made using a new mathematical model which more closely predicts actual boil-off rates. LNG losses and storage costs are reduced.

Hasselbacher, H. "Nitrogen Gas Turbines for LNG Regasification." Fifth International Conference on LNG, 1977, Session II, paper 12.

The paper describes the design of a standard nitrogen gas turbine for a plant with a LNG regasification rate of 210 t/h. Two alternatives, a closed-cycle gas turbine and an open-cycle gas turbine, are also discussed.

Havens, J. A., A Description and Assessment of the SIGMET LNG Vapor Dispersion Model, U.S. Coast Guard Report, CG-M-3-79, 1979.

The mathematical model SIGMET, which has been developed to predict dispersion of LNG vapor clouds from large spills on water, is described in great detail. The particular features of the model are discussed and evaluated. Conclusions and recommendations for further improvement of the model are given.

Havens, J. A., Predictability of LNG Vapor Dispersion From Catastrophic Spills Onto Water: An Assessment. Report prepared by the University of Arkansas for the Cargo and Hazardous Materials Division, Office of Merchant Marine Safety, U.S. Coast Guard, April 1977.

The author has reviewed various mathematical models and the methodology described by SAI and believes that such techniques hold the most promise for accurate prediction of vapor dispersion from catastrophic spills on water. A program designed to evaluate the accuracy of the SAI model or other models should now be considered high priority.

Havens, J. A. "An Assessment of Predictability of LNG Vapor Dispersion from Catastrophic Spills on Water." J. Hazard. Mat. 3:267-278, 1980.

Seven different models for the dispersion of LNG vapors are evaluated. They give drastically different results. None of them can be considered satisfactory.

Health and Safety Executive. Canvey, an Investigation of Potential Hazards from Operations in the Canvey Island/Thurrock Area. London: Her Majesty's Stationary Office.

A two-part report: part 1 contains a summary by the Health and Safety Executive and part 2 contains the report of the investigating team. In the appendix, detailed information is given about the applied models.

Heat Transfer at the Air-Ground Interface With Special Reference to Airfield Pavements. Report Prepared by the Massachusetts Institute of Technology, Department of Civil and Sanitary Engineering, Soil Engineering Division, Technical Report No. 63, January 1961.

The variables which affect the transfer of heat at the air-earth interface were studied as a part of an investigation to improve techniques for predicting subsurface temperatures. The investigation demonstrates that certain readily obtainable measurements may be utilized to predict the amounts of heat flow at the ground surface due to various atmospheric phenomena.

Hefflington, W. M., "Use the Right Heating Value." Hydrocarb. Process, 58(6):141-142, 1979.

When based on the heating value of methane, the heating value of natural gas is around 1,000 Btu/SCF. However, regasified LNG can have heating values up to 1,150 Btu/SCF. The article explains how to calculate the right heating value.

Henry, R. E., Gabor, J. D., Winsch, I. O. and Spleha, E. A. et al., "Large Scale Vapor Explosions." Argonne National Laboratory, Argonne, IL. Paper presented at the Fast Reactor Safety Meeting, Beverly Hills, CA, April 2-4, 1974.

Experimental results with Freon-22 and water show that the interface temperature homogeneous nucleation model accurately predicts the necessary temperature conditions for the onset of large scale vapor explosions. Test results for many different contact modes revealed that the magnitudes of explosions were highly dependent upon contact mode.

Hertzberg, M., "The Theory of Free Ambient Fire. The Convectively Mixed Combustion of Fuel Reservoirs." Combustion and Flame. 21:195-209, 1973.

The theory of fuel-reservoir fires is extended and amplified into a quantitative formulation that includes all the significant physical processes: mass diffusion, heat conduction, convective mixing, convective heat transport, and radiative heat transport. The predictions are compared with the data for 3 fuels (gasoline, liquid hydrogen, and methanol), and the comparison gives reasonable agreement.

Hertzberg, M., Cashdollar, K., Litton, C. and Kansa, E., "The Diffusion Flame in Free Convection. Buoyancy-Induced Flows, Oscillations, Radiative Balance and Large-Scale Limiting Rates." Paper presented at the Central States Section, Combustion Institute Meeting on Fluid Mechanics of Combustion Processes, Cleveland, OH, March 29-30, 1977.

Early studies of flame oscillations are reviewed and new data are presented for the fundamental infrared flicker frequencies of methanol pool flames and other diffusion flames. Measured frequencies decrease monotonically with increasing size, in good agreement with independent data obtained photographically and acoustically.

Heskestad, G., Kung, H. C. and Todtenkopf, N. F., "Air Entrainment into Water Sprays and Spray Curtains." ASME Winter Annual Meeting, New York, New York, 1976.

Theoretically derived volumes of entrained air were found to agree with experimental values to within 17%. While no explicit reference is made to LNG, the results are sufficiently general to apply to the vapor stage of an LNG spill.

Hess, K., Hoffmann, W., Stoecke, A. "Propagation Processes after the Bursting of Tanks Filled with Liquid Propane - Experiments and Mathematical Model." First International Loss Prevention Symposium, 1974, 227-234.

With geometrically similar tanks filled with liquid propane, tests were made to explain the bursting of the tanks under the pressure of the liquid and the development of explosive unconfined vapor-clouds. Ignition experiments show that the propagation processes after the bursting of the tanks can be described with a mathematical model for the nonsteady turbulent transfer of material. This mathematical model gives the reactive gas volume, the explosive energy, and the effect of the pressure upon the environment.

Hess, K., Leuckel, W., Stoecke, A. "Ausbildung Von Explosiblen Gaswolken Bei Überdachentspannung Und Maßnahmen Zu Deren Vermeidung." (The Formation of Explosive Gas Clouds from Jet Releases and Measures to Avoid Them.) Chemie-Ing. Techn. 45:323-329, 1973.

The paper describes a mathematical model for the jet dispersion considering the difference of density between the gas and the environmental air. The solutions show that for a gas heavier than air, a larger amount of an inflammable mixture accumulates within the cloud at the top of the jet because of the gravity spreading. The different concentration profiles for such a cloud and the jet, as well as their influence on the course of a possible explosion, are discussed.

Higgins, K. and Baum, M., "Assessing LNG Tank Volume Calibrations." Dimensions/NBS 63(9):19, 1979.

Photogrammetric survey techniques are now used to determine the volume of LNG tanks. An NBS evaluation of such methods reveals that more accurate procedures for checking the photogrammetric methods are difficult to find.

Hikita, T. "A Film of Large Scale Field Experiments on Ethylene Hazards." From Discussion on Explosion Hazards at the 7th International Colloquium on Gas Dynamics of Explosions and Reactive Systems, ed. H. Wagner, pp. 72-74, Max-Planck-Institute Für Strömungsforschung, Göttingen, 1979.

Two large scale field experiments on ethylene hazards were conducted in 1969 and 1974 under sponsorship of Japanese Government with cooperation of industries, universities and national laboratories. An English-language motion picture was produced which demonstrated special test features such as dispersion of a liquid ethylene spill, fire control using a dry chemical foam, burning showing fire ball foundation, and explosion. The number of tests carried out were small because of difficulties involved in large scale tests.

Hindle, W., Artic Islands LNG. Presented to the American Gas Association Transmission Conference, Montreal, Quebec, May 8-10, 1978.

Trans Canada has begun the study and design of an LNG project which would transport LNG from the high Arctic Islands to Quebec. The type of ship that would be used, an icebreaking LNG carier, is described.

Hoehne, V. O. and Luce, R. G., "The Effect of Velocity, Temperature, and Molecular Weight on Flammability Limits in Wind-Blown Jets of Hydrocarbon Gases." Proceedings, Division of Refining. API, 50:1057-1081, 1970.

Various diameter jets of methane, ethane, butane, and heptane gas were directed perpendicular to the wind stream in a wind tunnel. Measurements were made to define the flammable zone caused by the jet-wind interaction. The application of the test results to practical process plant vent spacing to minimize hazards during windy atmospheric conditions is illustrated.

Hogan, W. J., "LLL Participation on LEF Safety Research." DOE/EV-0046, Department of Energy, Washington, D.C., Vol. 2, pp. 481-492, 1979.

Lawrence Livermore Laboratory (LLL) has the responsibility to develop analytical models to describe the effects of large LNG releases to the environment and to verify such models by performing spill tests. The paper gives a qualitative overview of the results that so far have been derived from the program.

Hogan, W. J., Bowman, B. R. and Haselman, L. C., Numerical Modeling of LNG Spill Phenomena. UCRL 82031, 1978.

The various existing models for LNG spills, vapor dispersion, and combustion effects are reviewed. The limitations of the models are discussed. The need for further improvements is emphasized.

Holman, O. B., "LNG Peakshaving Plant Design Features and Operating Experiences." Paper presented to Seminar and Study Tour on LNG Peakshaving, Washington DC, March 5-9, 1979.

This paper reviews the design features and operating experiences of the Philadelphia Gas Works Richmond Peakshaving Plant. The plant uses a cascade liquefaction process, a prestressed concrete type design for storage and running film vaporizers.

Hottel, H. C. and Sarofim, A. F., Radiative Transfer. Chapter 6, McGraw-Hill Book Company, 1967.

Chapter 6 deals with gas emissivities and absorptivities.

Hoult, D. P., "The Fire Hazard of LNG Spilled on Waters." Proceedings on LNG Importation and Terminal Safety. NTIS No. AD/754326, Boston, MA, June 13-14, 1972.

The paper considers the rate of evaporation of LNG spilled on water, the negatively buoyant plume, heat transfer to the plume, the buoyant puff, and concludes that there is no single rule whereby the fire hazard of an LNG spill may be estimated.

Howard, J. L., and Andersen, P. G., "Barge-Mounted Gas Liquefaction and Storage Plant." Chem. Eng. Progr. 75(10):76-81, 1979.

The design and operation of a floating LNG facility for liquefaction, storage and export of natural gas are described. This new plant was to be built in modules by shipyards in highly industrialized areas and to be towed to Iran for installation near Kangan.

Howard, M. A., "Second Generating Peakshaving Plant Benefits from Experience." Pipeline and Gas Journal. November 1978.

Northern Natural Gas has two peakshaving plants, one built in 1975 and other in 1978. This article discusses the lessons learned at the first facility and the various design changes in the second facility that resulted.

Humbert-Basset, R. and Montet, A., "Dispersion dans l'Atmosphere d'un Nuage Gazeux Forme par Epondage de G.N.L. sur le Sol." Paper presented at the Third International Conference on LNG, September 1972.

An experimental study conducted by GAZ de FRANCE at the test station of NANTES is described. To investigate the hazards occurring from spillage, measurements of evaporation rates of LNG on various soils were made. In addition, measurements were made of the extent that clouds generated from spillage in diked areas up to 200 m^2. A mathematical model was utilized in the extensive study of the hazards problem.

Hunt, L. "Computer Analysis Reveals Cold Facts of LNG Storage." Process Engineering, p. 137, November 1979.

A computer program is briefly described which determines the thermal stresses existing in LNG storage vessels and their supporting structure.

Hynes, J. P., J. Dahlgren, M. A. Aguilar, Oceanborne Transportation of Liquefied Natural Gas, Petroleum, and Methanol Fuels. EPRI-EA-1256, 1979.

The report presents an overview of the economic, technical, and environmental aspects of oceanborne transportation of LNG and petroleum liquids. Methanol has been considered as an alternative to LNG.

Ing., Dr., H. R. Hansen. "Safety and Reliability of Marine Gas Liquefaction and Storage Units." Presented at Gastech 78 LNG/LPG Conference, Monte-Carlo, Monaco, November 7-10, 1978.

This paper discusses very generally some safety related aspects of Marine LNG facilities. Much of the discussion is related to segregation of process equipment and storage areas on a floatable marine facility.

Ishchenko, A. Ya, N. V. Novikov, "Mechanical Properties of Soviet and American Al-Mg Alloy Plates and Welds for LNG Systems." Adv. Cryo. Eng., 24:491-509, 1978.

Two Al-Mg alloys (one of U.S., one of USSR manufacture), widely used for LNG applications, have been tested in a Russian laboratory. Results showed them to be very similar and to be well-suited for cryogenic use.

Jackson, R. H. F., "Custody Transfer Systems for LNG Ships: Tank Survey Techniques and Sounding Tables." NBSIR 79-1751, 1979.

A precise photogrammetric method is described which allows determining the exact volume of large LNG storage containers. Sounding tables are generated from the photogrammetric survey so that the LNG volume in a vessel can be determined from simple height measurements.

Jamison, L. R., "United States Codes and Regulations Affecting the Marine Aspects of LNG Movements." 1978 Operating Section Proceedings, American Gas Association, Montreal, Quebec, May 1978.

This paper presents a collection of regulations which influence marine movement of LNG. Agencies regulating this transport are the U.S. Coast Guard, Intergovernmental Marine Consultative Organization, and the Republic of Liberia Bureau of Marine Affairs.

"Japanese Market to Keep Top LNG Role." Oil & Gas J. 78:22-23, July 21, 1980.

A forecast is made for the development of world LNG trade during the 1980s and 1990s. A growth rate of 12% per year is predicted. The main consumers for LNG will be Japan, followed by the USA and Western Europe.

The Japan Gas Association, A Study of Dispersion of Evaporated Gas and Ignition of LNG Pool Resulted From Continuous Spillage of LNG Conducted During 1975. April 1976.

LNG spill tests were conducted for continuous releases to determine the characteristics of evaporation, dispersion, and ignition of pool fires. Tests were concerned mainly with the vapor cloud dispersion and the resultant cloud dimensions and character.

Jaquette, D. L., Possibilities and Probabilities in Assessment of the Hazards of the Importation of Liquefied Natural Gas. Rand Corporation. Study P-5411, AD/A019353, 1975.

Currently prevailing assessment of the safety hazards of LNG spills is criticized. The unknowns of such spills are listed and the need for more definitive information is stressed.

Javelle, B. and Raynaud, J., "Structural Problems in Methane Carriers." Shipping World and Shipbuilder. pp. 831-833, September 1975.

The authors briefly discuss stress calculations for LNG ships. They include fatigue, lamellar teaming, crack propagation, and liquid motions.

Jeje, A. A. and Reid, R. C., "Boiling of Liquefied Hydrocarbons on Water." Paper presented at the Third Conference on Natural Gas Research and Technology, Dallas, TX, sponsored by the American Gas Association, March 1974.

The cryogens studied were liquid nitrogen, methane, ethane, and several typical LNG compositions. In general, boiling fluxes increased slightly as the initial water temperature was lowered and as more cryogen was spilled. For LNG mixtures, significant foaming resulted and it is also suspected that ice is rapidly formed and remelted by eddy circulation in the upper layer of water.

Jeje, A. A. and Reid, R. C., Transient Pool Boiling of Cryogenic Liquids on Water.

Boiling rates of LNG and LPG on water are determined as a function of water temperature and liquefied gas composition.

Jenrich, J. "Price, Policy Cast Cloud on U.S. Imports of LNG." Oil & Gas J. 78:17-21, July 21, 1980.

The present uncertainty about future LNG imports is discussed from various viewpoints. The outlook lies somewhere between the extremes of vigorous growth and complete phaseout. The U.S. government presently does not favor LNG imports, primarily because of recent large price hikes by the main exporters.

Jensen, D. E. and Jones, G. A., "Reaction Rate Coefficients for Flame Calculations." Combustion and Flame. 34:1-34, 1978.

Current functional forms for chemical reaction notes and corresponding uncertainty factors are presented.

Jensen, D. E., Spalding, D. B., Tatchell, D. G. and Wilson, A. S., "Computation of Structures of Flames with Recirculating Flow and Radial Pressure Gradients." Combustion and Flame. 34(3):300-326, April 1979.

The authors present a technique for modeling steady-state, axis symmetric, highly-turbulent chemically reacting flow from a rocket engine. This technique has many features relevent to LNG pool fire modeling.

Kamal, M. M. and A. Khalil. "Explosion Hazards of LNG and LPG Carriers During Transport." Adv. Cryo. Eng. 25:757-762, 1979.

An analytical method is briefly described for computing the pressure rise resulting from an LNG vapor cloud deflagration. The detonation limits are included in the treatise.

Kamel, M. M. "Explosion Hazards in the Suez Canal-An Overview." From Discussion on Explosion Hazards at the 7th International Colloquim on Gas Dynamics of Explosions and Reactive Systems, ed. H. Wagner, pp. 34-39, Max-Planck-Institute Für Strömungsforschung, Göttingen, 1979.

This paper is a concise exposition of the explosion danger that the densely populated Suez Canal Zone is subjected to due to the passage of supertankers and liquefied natural and petroleum gas (LNG and LPG) carriers. Accidental causes of explosions are enumerated, different scenarios leading to the detonation of explosive fuel-air clouds resulting from liquefied gaseous fuel spills are discussed and, finally, possible avenues of research in this field are outlined.

Kardaun, G. "How LNG Fits in Dutch Gas Planning." Session I, Paper 1, Sixth International Conference on LNG, 1980.

The need for international cooperation in the whole LNG delivery system from well-head to user is discussed. The technical aspects of this program are stressed from plant start-up to personnel training.

Kato, D., "Ultra Low-Temperature LNG Compressors." Fifth International Conference on LNG, Session II, paper 10, Institute of Gas Technology, 1977.

Special compressors for recompression of LNG boil-offs in storage facilities are described.

Katz, D. L., "LNG-Water Explosions." NTIS No. AD/775005, 1973.

The "limit of superheat" is identified as the cause of LNG-water explosions. However, theoretical support for this argumentation is mainly speculative.

Katz, D. L., "Superheat-Limit Explosions." Chemical Engineering Progress. 68:68-69, May 1972.

The rapidity of this superheat-limit event as compared to nucleated bubble growth in a partially superheated liquid provides an explanation for vapor explosions discussed in the literature.

Katz, D. L. and Sliepcevich, C. M., "LNG/Water Explosions: Cause and Effect." Hydrocarbon Processing. 50:240-244, November 1971; also NTIS No. AD/775005.

The paper discusses the limit of superheat, the methane-water system, LNG mixtures, massive LNG spills, and considers other systems such as liquid methane poured into pure pentane in the absence of water.

Katz, D. L. and West, H. H., "LNG Shipping and Storage." Paper Presented to the Engineering Foundation Conference on Risk/Benefit Methodology and Application, Asilomar, California, September 21-26, 1975.

This article gives an overview of the history and development of the LNG industry with emphasis on storage and shipping. Potential hazards associated with LNG are discussed briefly.

Kaustinen, O. M., "Polar Gas Project." Presented to the American Gas Association Transmission Conference, Montreal, Quebec, May 8-10, 1978.

Some of the alternative methods of moving natural gas from Canada's Arctic Islands are discussed.

Kee, R. J. and Miller, J. A., "A Split-Operator, Finite Difference Solution for Axisymmetric, Laminar-Jet Diffusion Flames." AIAA Journal. 16(2), February, 1978.

An economical numerical solution of a vertical diffusion flame is presented. The complete chemical kinetics of the problem are included. Discussions of possible numerical treatment of the thermo-hydrodynamics and the "stiff" chemical kinetics are presented. "Majorant" splitting (as opposed to ADI methods) and the Gear-Hindmarsh "stiff" equation methods are utilized in the paper.

Kee, R. J., The Computational Nature of Combustion Modeling, Sandia Laboratories, SAND78-8245, Albuquerque, New Mexico, July 1978.

The report presents a fundamental approach to computations for combustion systems. Specific problems and numerical algorithms are presented.

Keeny, R. L., Kulkarni, R. B. and Nair, K., "Assessing the Risk of an LNG Terminal." Technology Review. pp. 65-71, October 1978.

The report presents a description of LNG risk analysis methods for an import terminal using as its example the risk study prepared for the proposed Elaspsed Natural Gas Co. Matagordo Bay Terminal.

Keens, D., "Technology of LNG Plants Still Undergoing a Steady Evolution." Oil and Gas Journal 78:84-89, April 7, 1980.

In order to improve the profitability of LNG operations, various new engineering development schemes are discussed. These include areas in gas pre-treatment, cryogenic heat exchangers, refrigerant compression, compressor drives, offshore loading, and energy recovery in revaporization. Some of the schemes are already being applied to new LNG projects.

Kelley, C. S., Radiative Transfer Between Flame Burning Zone and Unburned Fuel. EATR-4555, Edgewood Arsenal, Maryland, NTIS No. AD/732405, October, 1971.

An assessment of the complex role of radiative heat transfer in the interaction of fuel and flame is presented. The thermo-physical properties of the fuel are included in the analysis.

Kelsey, R. A., F. G. Nelson, "Mechanical Properties of US/USSR Al-Mg Plate and Welds for LNG Applications." Adv. Cryo. Eng., 24:505-518, 1978.

The two Al-Mg alloys tested were found to be quite similar and showed favorable properties for low temperature (LNG) applications.

Kempen, H. W. J., "Natural Gas as Vehicle Fuel." Gas 93:8-13 Netherlands, (in Dutch), January 1973.

Topics include comparison with other fuels, storage tank requirements, tank filling, and safety. Also described is the plan by four companies, along with government assistance, to install a small test installation to liquefy natural gas and to convert some 400 vehicles to LNG operation.

King, W. S., On the Fluid Mechanics and Heat Transfer of Liquefied Natural Gas Spills. RAND Corp., P5396, 1975.

A new mathematical model for the interaction between LNG and water is proposed. However, no details are supplied on the analytical and numerical details for practical use of the model.

Kiveylo, J. "Evaluation of the Effects of Detonation in a Spherical Bomb." From Discussion on Explosion Hazards at the 7th International Colloquium on Gas Dynamics of Explosions and Reactive Systems, ed. H. Wagner, pp. 100-110, Max-Planck-Institute Für Strömungsforschung, Göttingen, 1979.

Presented here is an analysis of the time-dependent pressures and impulse loadings on the walls of the hemispherical dome of a nuclear reactor pressure vessel arising from a centrally ignited hydrogen-oxygen detonation. Investigated in this context are the effects of richness of the detonable gas mixture as well as those due to the inclusion of water vapor. In the analysis the gas mixture was treated as a perfect gas, and the partial differential equations governing the gasdynamic flow were integrated using a finite-difference technique set in Lagrangian coordinates and incorporating the smoothing action of artificial viscosity. The most interesting results pertain to the ringing of pressure pulses at the walls. Their frequency is quite uniform, and their pressure peaks, at levels significantly higher than that of combustion at constant volume, decay at a negligible rate.

Kletz, T. A., "Consider Vapor Cloud Dangers When You Build a Plant." Hydro-Carb. Proc. 10:205-212, 1979.

A catalog of 15 items is presented which should be considered when building a facility in which vapor cloud explosions could occur (such as in an LNG plant).

Kneebone, A. and Prew, L. R., "Shipboard Jettison Tests of LNG Onto the Sea." Paper presented at the Fourth International Conference on LNG, Session 5, Paper 5, 1974.

The first part of the paper describes the procedures and results of a series of jettison tests carried out on board ship and discusses the operational safety aspects of such discharges. The second part is concerned with the environmental hazards associated with the release of large quantities of LNG to the sea in terms of the extent of vapor cloud formed; its characteristics and rate of dispersal.

Kodaira, N. "Energy Problems and Measures Taken to Promote Wider Use of LNG in Japan." Session I, Paper 3, Sixth International Conference on Liquefied Natural Gas, 1980.

This report takes up the current problems of LNG - one of Japan's major primary energy sources - and the measures being considered in order to deal with them. State subsidies are under consideration to encourage wider LNG use by industry.

Kogarko, S. M., "Detonation of Methane-Air Mixtures and the Detonation Limits of Hydrocarbon-Air Mixtures in a Large Diameter Pipe." Soviet Physics. 3, 1958.

A review is made of the Russian literature on methane-air detonation. The author describes his work using tubes with diameters up to 0.305 meter and lengths to 12.2 meters. Gas mixtures were initiated with 50/50 amatol explosive charges. The author concludes that the limits and the possibility of a detonation vary with the diameter.

Kolodner, H. J. "A Practical Approach to Vapor Cloud Protection." Second International Loss Prevention Symposium, 1977, 333-337.

Some researchers have dwelt on early detection, isolation of leaks, remotely activated valves and other means of cloud prevention. Others have concentrated on cloud dispersion, better constructions of buildings or other means of secondary protection. This paper details these two approaches to the vapor cloud problem and gives suggestions as to the advantages and disadvantages of each. Recent study results and risk and system analysis techniques will be discussed.

Knystentos, R., Lee, J. H., Moen, I. and Wagner, H. G. G., "Direct Initiation of Spherical Detonation by a Hot Turbulent Gas Jet," Proc. 17th Symp. on Combustion, The Combustion Institute, pp. 1235-1245, 1979.

It has been shown experimentally that transition from deflagration to spherical detonation is possible if large-scale eddies, superimposed by fine-scale turbulence, are present in burning vapor clouds. Since tests were conducted only with $C_2H_2/02_2$ mixtures, the question of detonations in LNG vapor clouds remains unresolved.

Kraus, H. Techniques of an LNG Chain. AED-CONF 78-155-038 (in German) 1978.

The paper describes briefly LNG production (liquefaction), transportation, storage, re-evaporation, and distribution to the end-user.

Krey, G. and D. Weber. "How to Improve the Economy of LNG Terminals." Session II, Paper 7, Sixth International Conference on Liquefied Natural Gas, 1980.

Using the cold energy in an LNG terminal with a closed-cycle gas turbine for electricity generation and LNG vaporization means a potential worldwide saving of 4.2×10^6 kg of LNG/day, referred to 1985.

Kuhl, A. L., H. J. Carpenter, and F. R. Gilmore. "Perspectives on Research on LNG Vapor Cloud Dispersion." From Discussion on Explosion Hazards at the 7th International Colloquium on Gas Dynamics of Explosions and Reactive Systems, ed. H. Wagner, pp. 90-99, Max-Planck-Institute Für Strömungsforschung, Göttingen, 1979.

In this paper, key physical mechanisms affecting cloud dispersion are discussed and a research approach for predicting dispersion of vapor clouds from large LNG spills is suggested.

Lancaster, John F., "What Causes Equipment to Fail?" Hydrocarbon Processing. pp. 74-76, January 1975.

This article deals with four main causes of service failure in process equipment. They are: fatigue, general corrosion, stress corrosion cracking and manufacturing defects. Comments and suggestions for reducing each type of failure are included.

Laoussine, N. A., "LNG Grows as World Energy Source." Hydrocarb. Process, 59(4):130-133, 1980.

It is claimed that proven natural gas reserves are about 2.2 x 10^{12} ft^3 and constitute (next to coal) the world's most abundant energy source. Estimated reserves are in the order of 10^{13} ft^3, which is equivalent to 2,000 billion barrels of oil. Algeria is the biggest exporter of LNG. Presently, about 11% of the natural gas production in the world is still flared or vented.

Lautkaski, R., Fieandt, J. "Risk Assessment of the Transportation of Hazardous Liquefied Gases in Bulk." Third International Loss Prevention Symposium, 1980, 14/1052-14/1057.

Risk assessment of the transportation of hazardous liquefied gases in Finland has been performed. The gases are: chlorine, sulphur dioxide, ammonia and liquefied petroleum gas. The actual transportation modes (rail, road, and ship transport) have been covered.

Lawrence, G. H., "Comments of the American Gas Association on Delegation of Functions by the Secretary of Energy to the Administrator of the ERA and FERC." American Gas Association, November 15, 1978.

The American Gas Association requests revision of the delegation due to confusing and inconsistent language, a failure to correct jurisdictional overlaps, and the increasing cost of regulations.

Lawrence, G. H. "Role of Liquefied Natural Gas in a Worldwide Gas Energy Option." Session I, Paper 6, Sixth International Conference on Liquefied Natural Gas, 1980.

A concentrated effort is expended to utilize natural and supplemental gas energy in a variety of ways to offset the precipitiously high use of oil. World supply/demand imbalances for gas energy can be alleviated only through accelerated development of LNG as a dependable and effective worldwide natural gas energy transportation system.

Ledbetter, H. M. "Anomalous Low-Temperature Elastic Constant Behavior in Fe-13 Cr-19 Mn." Metall. Trans. 11A:543-544, 1980.

A new Soviet steel has been investigated for its behavior at low temperatures so that its fracture mechanics parameters could be established. It was found to be well-suited for LNG applications.

Lee, J. H. S. and I. O. Moen. "The Mechanism of Transition from Deflagration to Detonation in Vapor Cloud Explosions." Progr. Energy Combust. Sci. 6:359-389, 1980.

An extensive review is given on the role of turbulence in the transition from deflagration to detonation. It is shown to be possible that the transition proceeds only part of the way, resulting in blast waves which are not as strong as detonation waves but which are still substantially above the pressure level of simple deflagration waves.

Lee, R. H. C. and Happel, J., "Thermal Radiation and Methane Gas," I&EC Fundamentals. 3:167-176, May 1964.

The infrared absorption of methane in three wavelength regions (2.37, 3.31, and 7.65 microns) has been determined at various temperatures and optical depths. The semi-empirical expressions for the bank absorption so obtained are used to calculate the total and band emissivities of methane from 0.01 to 2.0 ft-atm. and from 500° to 3750°R.

Lee, W. A. and M. Weinstein. "Computer Modeling of Massive LNG Spills from Storage Tanks at Point Conception, Oxnard and Los Angeles Harbor, California." ASME Century Two Engineering Technology Conference, Cryogenic Processing Equipment Section, pp. 83-99, 1980.

The distance for an LNG vapor cloud to reach the lower flammability limit has been computed for a massive spill of two million barrels of LNG. Two different computational methods were utilized and applied to the three candidate sites for LNG terminals on the California coast.

Leeper, J. E. "Mercury - LNG's Problem." Hydrocarbon Process. 59:237-240, November 1980.

Mercury is present in trace amounts in certain natural gas wells. Upon gas liquefaction this mercury can cause corrosion in the heat exchangers of mixed refrigerant LNG plants. A method is proposed for removing the mercury from the raw gas.

Lees, F. P., "Some Data on the Failure Modes of Instruments in the Chemical Plant Environment." Chem. Engineer. 277:418-421, September 1973.

Failure mode data are given based on a previously presented survey of failure rate data for 9500 instruments in chemical works.

Lehrer, P. "Brandversuche Mit Flüssigem Erdgas an Modell-Behältern." (Experimental Investigation of LNG Fires on Storage-Tank Models) Gas Wasserfach, Gas Erdgas, 114:340-344, July 1973.

Leakage of LNG storage tank can cause fire and explosion hazards. With the purpose of getting insight into the mechanics of such hazards an experimental study on LNG tank of 4.5 m dia. has been carried out by the Technical works of the city of Stuttgart, W. Germany. It has been ascertained that LNG tanks do not present greater fire hazards than other fuel tanks of similar dimensions. Indeed poor ignition behavior and the short

distance from the tank up to which an ignition can occur have to be considered as an advantage. Inert powder was found to be the most efficient LNG fire extinguisher.

Lehto, D. L. and Larson, R. A., Long Range Propagation of Spherical Shock-waves From Explosions in Air. NOLTR 69-88, NTIS No. AD/698121, U.S. Naval Ordinance Laboratory, White Oak, Maryland, July 22, 1969.

Hydrocode calculations for spherical shock propagation using the artificial-viscosity method are carried out to 0.2 psi overpressure for a nuclear explosion and for a TNT explosion. An ideal-gas integration from the literature is used to extend the results to 1.6×10^{-4} psi. Below 1.0 psi, 1 kiloton nuclear is equivalent to 0.7 kilotons of TNT.

Leonard, D. A., and Caputo, E., Technical Report: Remote Sensing of LNG Spill Vapor Dispersion Using Raman LIDAR. UCRL-13984, Computer Genetics Corp., Wakefield, MA, 1979.

The feasibility of using a Raman LIDAR scheme for the measurement of LNG vapor concentration has been demonstrated. The report describes the test apparatus and discusses the quality of the obtained results.

Lester, T. W. and Wittig, S. S. K., "Soot Nucleation Kinetics in Pre-mixed Methane Combustion." Presented at the 16th International Symposium on Combustion, 1976.

This paper is an investigation of the early chemical kinetics of soot formation in fuel rich methane flames.

Levine, A. D., Theoretical Models of LNG Dispersion Studies (Phase III - LNG Safety Program), Part I: Modeling of LNG Spills. AGA Project IS-129-1, Technical Report TLN-1, October 17, 1975.

A series of theoretical models relating to the growth and evaporation of cryogenic pools is reviewed, and new ones added in order to allow for complete empirical correlation. Agreement with all experimental results is quite good although the scaling law is somewhat questionable. Continuous spills are modeled using harmonic function analysis with adequate results.

Levine, A. D., Theoretical Models for LNG Dispersion Studies. Report on A.G.A Project IS-129-1, 1975.

Progress reports survey basic relations of detonation phenomena used to emphasize the importance of kinetics and induction time for the initiation process. Current knowledge of explosives in open air gas mixtures suggest that induction time may be very important in correlating experiments with theory.

Levy, M.M., "The Cove Point LNG Terminal: Its First Year of Operation." Paper presented to Seminar and Study Tour on LNG Peakshaving, Washington DC, March 5-9, 1979.

The design and operating experience of the Cove Point LNG terminal is reviewed.

Lewis, D. H., The Dispersion and Ignitability of LNG Vapor Clouds. M.S. Thesis, Massachusetts Institute of Technology, Cambridge, Massachusetts, June 1974.

The flammability of vapor clouds resulting from instantaneous spills of LNG is determined quantitatively using statistical methods. A new physical theory on the vapor dispersion process is presented and compared to available experimental data. Numerical predictions of distance to various flammability limits are presented graphically.

Leyer, J. C. "Unconfined Hydrocarbon Air Mixture Explosion Studies Performed in France by CEA-EDF-GDF and the University." From Discussion on Explosion Hazards at the 7th International Colloquium on Gas Dynamics of Explosions and Reactive Systems, et. H. Wagner, pp. 40-45, Max-Planck-Institute Für Strömungforschung, Göttingen, 1979.

This paper summarizes vapor cloud theoretical and experimental studies initiated in France in 1976 aimed at protection of nuclear power plants located in regions where large quantities of hydrocarbons are transported or stored. Research on two different topics had been undertaken at the time of this presentation: 1) blast effects produced by detonation of ethylene, acetylene, and propane-air mixtures and 2) acceleration of various fuel and air mixtures in the deflagration made. Future work includes investigation of maximum flame velocity to be expected by interaction with obstacles and partical confinements displayed on the flame path.

Lind, C. D., Explosion Hazards Associated With Spills of Large Quantities of Hazardous Materials - Phase I. U.S. Coast Guard Report CG-D-30-75. NTIS No. AD/A001242. October 1974.

This report documents the results of a program to quantify the explosion hazards associated with spills of material such as LNG, LPG, or ethylene. The results are: a phenomenological description of a spill; an examination of the detonation properties of methane; a qualitative theory of non-ideal explosions; a plan for Phase II of the study.

Lind, C. D. and Whitson, J. C., Explosive Hazards Associated with Spills of Large Quantities of Hazardous Materials. Phase II. U.S. Coast Guard Report CG-D-85-77. NTIS No. AD/A047585, 1977.

Tests have been conducted to investigate the burning behavior of LNG type materials. No detonations have been observed in any of these tests.

Lind, C. D. and Strehlow, R. A., "Unconfined Vapor Cloud Explosion Study." NTIS No. AD/A023505, presented at the Fourth International Symposium on Transport of Hazardous Cargoes by Sea and Inland Waterways, Jacksonville, FL, October 26-30, 1975.

Five-meter radius hemispherical bag tests of ignition of 10% methane/propane-air mixture were conducted. Results indicated that ignition of fuels in this amount does not produce a detonation or damaging pressure waves.

Lind, C. D. and Whitson, J. C., "China Lake Spill Tests." Report L, Liquefied Gaseous Fuels Safety and Environmental Control Assessment Program: A Status Report. DOE/EV-0036, Department of Energy, Washington, DC, 1979.

The 1978 LNG spill tests at China Lake are briefly described. No data analysis is included.

Lind, C. D. and J. C. Whitson. "Update of Dispersion, Fire, and Explosion Testing at China Lake." LNG Terminals and Safety Symposium, pp. 340-345, in Applications of Cryogenic Technology 9. Scholium International, Flushing, New York, 1979.

Overall results from combustion/detonation tests of various cryogenic fuels are given which were contained as vapors in plastic hemispheres. LNG spill tests on water ponds are also described briefly.

Lindblom, U. LNG in Rock: A New Storage Option. STU Report 75-4514, 1978.

It is argued that storage of natural gas in underground caverns is safer and more economical than storage in conventional LNG surface tanks. This claim is backed up by computer analysis and various types of tests and laboratory experiments.

Liquid Natural Gas, Characteristics and Burning Behavior. Conch Methane Services, Ltd., Villers House, Strand/London, W.C. 2, England.

A synopsis of a comprehensive engineering report prepared for Conch Methane Services Ltd., based on large-scale field tests conducted near Lake Charles, Louisiana, plus laboratory data from the Bureau of Mines and available information in the literature. Field tests measured the levels of radiation by use of thermopiles; and extinguishment trials, using various extinguishment media, were conducted in conjunction with burning tests.

Litchfield, A. B. "LNG Terminal for Storage and Regasification." Chem. Eng. Progr. 77(1):83-88, 1981.

The design and operation of the new LNG terminal at Cove Point, MD is described. Safety considerations are included. When in full operation, the facility is capable of regasifying LNG at the rate of 28,000,000 m^3/d.

LNG Safety Program - Interim Final Report. (Draft) R&D Associates Report RDA-TR-1100-006 to the American Gas Association, September 30, 1976.

This program represents a comprehensive LNG safety study and includes the following tasks: LNG spread and boiloff rates, subscale land experiments performed in a wind tunnel, dispersion modeling, radiation and detonation studies, and a field test program definition which represents a major focal point of all other tasks. Emphasis is placed on scaling, instrumentation, and data analysis methodologies.

LNG Safety Program - Interim Report on Phase II Work. A.G.A. Project IS-3-1, Report to the American Gas Association by Battelle Columbus Laboratories, July 1, 1974.

Models for dispersion and radiation were developed, which fit data for 80-ft spills and will predict the hazard for spills into dikes up to 400 to 500 ft dia. Experiments verified reduction of dispersion hazards by insulated dike floors and high dikes. Predictions are given of downwind distances of travel of flammable vapors and radiation intensities on targets near fires on soil, and in low dikes up to 500 ft in dia.

LNG Terminal Risk Assessment Study for Los Angeles. Report by Science Applications, Inc., for Western LNG Terminal Company, December 22, 1975.

Science Applications, Inc., concludes on the basis of this study that LNG risks to populated areas near the Los Angeles Harbor site are extremely low. The physical characteristics of LNG, the design of the facility and tankship and the planned operating rules account for the low risk values.

LNG Wind Tunnel Simulation and Instrumentation Assessments. Report RDA-TR-105700-003, Draft by R&D Associates for the U.S. Energy Research and Development Administration, April 1977.

Information is presented on LNG flame radiation, test site criteria, wind tunnel modeling, and test instrumentation.

Lootvect, R. and P. Jean. Fastening Arrangement for Sealing Barrier in Insulating Wall of Insulated Compartment Built into a Ship's Hull. U.S. Patent 3,990,382, assigned to: Gaz Transport, 1976.

A detailed design is described on how two fluid-tight layers and two heat-insulating layers are arranged around LNG storage vessels aboard LNG tankers.

Love, T. J., Hood, J. D., Shahrokhi, F. and Tsai, Y. W., "A Method for the Prediction of Radiative Heat Transfer From Flames." ASME Publication 67-HT-47 presented at the ASME-AIChE Heat Transfer Conference and Exhibit, Seattle, WA, August 6-9, 1967.

This paper presents a method, based on the transport equation, to predict the radiative heat flux from methanol and acetone flames of arbitrary size and geometry. Predicted and measured values of the radiative flux were compared for several larger flames and found to be in good agreement for free-burning flames of acetone and methanol.

Lützke, K. "Untersuchungen über das Verhalten von Flüssiggas beim Ausströmen ins Freie." (Investigation on the Behavior of LPG Escaping into Open Air.) Erdöl Kohle-Erdgas-Petrochem.ver mit Brennst.-Chem. 24:165-172, März, 1971, 231-238, April 1971, (2 papers).

The two-part paper presents results of an experimental investigation on the behavior of releases from gaseous and liquefied propane and butane. Escaping volume and the velocity and the direction of the wind were taken into account. The measured ignition distances on the releases from liquefied propane and butane as function of escaping volume and wind velocity were used to devlop an empirical formula for estimating the maximum ignition distance.

Mackay, D. and Matsugu, R. S., "Evaporation Rates of Liquid Hydrocarbon Spills on Land and Water." The Canadian Journal of Chemical Engineering. 51:434-439, August 1973.

Experiments on the evaporation of cumene, water and gasoline are described and the evaporation mass transfer coefficient correlated with the windspeed, liquid pool size and the vapor phase Schmidt Number. Comparison of the correlation with flat plate mass transfer correlations shows satisfactory agreement and suggests that turbulent transfer occurs, the rate being enhanced by liquid surface roughness.

Maezawa, M., Experiments on Fire Hazards of Liquefied Flammable Gases. Osaka Gas Company, Ltd., May 1973.

Part I discusses the fire properties of liquefied flammable gases. Part II presents the results of an experiment in fire extinguishing. Part III is concerned with a dispersion experiment. Briefly, the flame temperature of each liquefied gas is 700 to 800°C compared to gasoline at 1100°C. LNG burning rates are much larger than gasoline. Radiation energy is also larger than gasoline.

Magnussen, B. F. and Huertager, "Mathematical Modeling of Turbulent Combustion with Special Emphasis on Soot Formation and Combustion." Presented at the 16th International Symposium on Combustion, pp. 719-729, 1976.

This paper presents a mathematical model of turbulent diffusion and/or premixed flames. Methods for thermal radiation and soot formation predictions are also presented. Soot formation is analyzed as a two-step process (nucleation site formation and soot particle formation). Thermal radiation is evaluated using a two-flux equation.

Maher, J. B. and Van Gelder, L. R. "Rollover and Thermal Overfill in Flat Bottom LNG Tanks." Pipeline and Gas Journal. 199:46-48, September 1972.

Conclusions are that high venting incidents involve thermal overfill; surface layer phenomena occurs in flat bottom LNG tanks filled through bottom with a liquid of saturation pressure greater than pressure capability of the tank; bottom filled tanks should provide venting over entire fill time consistent with degree of thermal overfill; if top layer is continually agitated during filling, thermal overfill will not occur.

Marchaj, T. J. System for Storing Liquefied Gas. U.S. Patent 4,110,995, assigned to: Preload Technology, Inc., 1978.

A design for LNG storage tanks is proposed which minimizes the contact of the relatively warm gases below the dome of the storage tank with the LNG surface. This helps to reduce undesirable gas vaporization.

Markstein, G. H., "Scaling of Radiative Characteristics of Turbulent Diffusion Flames." Paper presented at the 16th International Symposium on Combustion, 1977.

It is shown that radiative properties of gaseous-fuel turbulent diffusion flames can be scaled successfully over a fairly wide range of fuel flow rates. In addition, radiometric scans were found to provide quantitative information on flame length and diameters and their scaling properties. The work was part of a program to develop a generally applicable model of fire radiation.

Marshall, M. R. "Gaseous and Dust Explosion Venting: Determination of Explosion Relief Requirements." Third International Loss Prevention Symposium, 1980, 16/1210-16/1229.

The paper gives a brief description of the processes which take place during a vented explosion. From this description the required characteristics of an explosion relief vent are derived. The influence on the explosion pressure generated of parameters other than those pertaining to the explosion vent is also discussed, e.g., properties of the fuel-air mixture ignited.

Martin, K., "Utilization of Cold of Liquefied Natural Gas." Erdoel-Erdgas Z, 95:(6):200-206, June 1979.

Various possible processes for utilizing the cold from LNG are described. In addition to supplying the power for the LNG terminal itself, some processes can export and sell surplus energy.

Martinsen, W. E., S. P. Muhlenkamp, J. Olson, "Disperse LNG Vapors With Water." Hydrocarbon Processing. 56(7):261-266, July 1977.

This paper discusses the potential for enhancing LNG vapor cloud dispersion by water sprays into the cloud. Experiments showed increased mixing due mainly to mechanical turbulence induced by the watery sprays and a resultant decrease in the distance a vapor cloud spreads before reaching the lower flammability limit.

Masliyah, J. H. and Steward, F. R., "Radiative Heat Transfer From a Turbulent Diffusion Buoyant Flame With Mixing Controlled Combustion." Combustion and Flame. 13:613-625, 1969.

A mathematical model of a turbulent buoyant diffusion flame is postulated. The radiative interchange between the flame and a plane surrounding its base is determined. From this radiative distribution, it is possible to determine the radiative heat flux to the liquid fuel which is vaporizing to feed the flame. A graphical solution is presented which yields the rate of burning of a liquid fuel of given physical properties in a fixed diameter fuel source.

Mathiesen, T. C., Flatseth, H. H., Solberg, D. M. and Tueit, O. J., "Risk Management in Marine Transportation of LNG," 1979.

Measures are being described for dealing systematically with LNG hazards as they might occur in marine transportation. The measures are largely based on reliability engineering results.

Matsui, H. and Lee, H., "On the Measure of the Relative Detonation Hazards of Gaseous Fuel-Oxygen and Air Mixtures," Proc. 17th Symp. on Combustion, The Combustion Institute, pp. 1269-1280, 1979.

The critical energies for direct initiation of spherical detononations for eight gaseous fuels have been measured. These fuels include pure methane and pure higher alkenes, which are the main constituents of LNG. The measured values extend over about six orders of magnitude.

Maurer, B., Hess, K., Giesbrecht, H., Leuckel, W. "Modeling of Vapor Cloud Dispersion and Deflagration after Bursting of Tanks Filled with Liquefied Gas." Second International Loss Prevention Symposium, 1977, 305-319.

The processes of flash evaporation, atmospheric vapor cloud formation, ignition, and explosion after the bursting of liquefied gas vessels have been studied by model experiments with propylene.

May, W. G. and McQueen, W., "Radiation From Large LNG Fires." Combustion Science and Technology. 7(2):51-56, 1973.

Radiation from flames of burning LNG were measured in a burning pool contained in a trench. Burning rates over the range of 13,500 to 40,000 BBL/D of LNG were studied. Measured flux varied from 60 to 480 Btu/hr/ft^2 at ground level and 300 to 600 feet from the flame center and from elevated points. An inverse square law of radiation versus distance held fairly well.

May, W. G., McQueen, W. and Whipp, R. H., "Dispersion of LNG Spills." Hydrocarbon Processing. 52:105-109, May 1973.

The paper discusses data analysis of plume shape and plume dispersion characteristics. Correlations show that dispersion of LNG vapors can be predicted from observed facts and controlled conditions.

May, W. G., McQueen, W. and Whipp, R. H., "Spills of LNG on Water." Paper presented at the American Gas Association Distribution Conference, Washington, DC, May 14, 1973.

The conclusions reached cover: effect of variables on flow rate; inequality of downwind flow rate and evaporation rate; effect of density on plume shape; dependence of plume density on air humidity; effect of plume heating; weather effects; predictions of downwind plume travel.

May, W. G., McQueen, W. and Whipp, R. H., "Spills of LNG on Water." Proc. Div. of Refining, API, pp. 626-653, 1973.

The vapor dispersion from large LNG spills on water was experimentally determined. The tests, carried out by Exxon, were intended to verify and extend results obtained earlier in the Bureau of Mines and Gaz de France tests.

May, W. G., and Perumal, P. V. K., The Spreading and Evaporation of LNG on Water. ASME paper 74 - WA/PID-15, 1974.

The paper proposes a semi-empirical relationship for estimating the total evaporation from a LNG spill on water. Correlations are based on LNG spread rate, maximum pool diameter and evaporation rate per unit area.

McCarthy, D., A Comparison of Mathematical Models for the Prediction of LNG Densities. NBSIR 77-867, National Bureau of Standards, October 1977.

Four mathematical models of the equation of state for LNG like mixtures are compared using experimental data optimized for each model. The objective of predicting LNG densities to within ±0.1% could not be assessed due to discrepacies in the input data. Model listings are included.

McHenry, H. I., et al., "Low-Temperature Fracture Properties of USSR Aluminum--6% Magnesium Alloy." Adv. Cryo. Eng., 24:519-528, 1978.

The fatigue crack growth rates and the fracture toughness of the Russian alloy AMg6 were determined at cryogenic temperatures. The results indicate that the alloy should be very useful in LNG applications.

McNaughton, D. J. and Berkowitz, C. M., "Overview of U.S. Research Activities in the Dispersion of Dense Gases." Symposium Schwere Gase (Heavy Gas), Battelle-Institute, Frankfurt, F6 R, September 3-4, 1979.

This paper presents an overview of U.S. research in heavy gases particularly LNG. Topics include mathematical modeling, experiments, and facility controls available to decrease gas release or increase gas cloud dilution. Recommendations on further research are included.

McQuaid, J. Dispersion of Heavier-than-Air Gases in the Atmosphere: Review of Research and Progress Report on HSE Activities. Health and Safety Laboratories, Technical Paper 8, ISBN 07176 00297, 1979.

The Chemical Defence Establishment (Porton Down) has executed a program of trials on sudden releases of heavier-than-air gases. The recent report presents the justification for the form of the trials chosen and describes the way in which account was taken of existing information on the behavior of dense gas clouds. The program of trials and the conclusions that can immediately be drawn from them are summarized and the need for further work is reviewed.

Meinen, E., "LNG Storage in Prestressed Concrete Safety Walls - 1." Oil and Gas Journal. May 14, 1979.

The concrete safety wall incorporated in the design of the Maasvlakte LNG plant in the Netherlands is described. The properties of steel and concrete at cryogenic temperatures are reviewed.

Meinen, E., "LNG Enclosure Design - 2." Oil and Gas Journal. May 21, 1979.

The design, testing and construction steps for the retaining wall and the tank foundation of the Maasvlakte LNG plant are outlined. Analytical procedures and test results are described.

Mellor, G. L. and Yamada, T., "A Hierarchy of Turbulence Closure Models for Planetary Boundary Layers." Journal of the Atmospheric Sciences. pp. 1791-1806, October 1974.

Turbulence models centered on hypotheses by Rotta and Kolmogoroff are complex. In the present paper, we consider systematic simplifications based on the observation that parameters governing the degree of anisotropy are small. Discussion is focused on density stratified flow due to temperature.

Meroney, R. N., Neff, D. E. and Cermak, J. E., "Wind Tunnel Modeling of LNG Spills." 1978 Operating Section Proceedings, American Gas Association, Montreal, Quebec, May 1978.

The author's report scales of spill conditions that may be successfully simulated in Colorado State University wind tunnels. Simulations of 1974 AGA LNG land spill experiments and uses of wind tunnels in experimental design are also discussed.

Miller, B., "Possibilities in Hydrate Storage of Natural Gas." Gas Age. 97:37-40, May 1942.

The formation of methane and LNG hydrates was reviewed. Data concerning hydrate storage, properties and decomposition pressures were discussed. Refrigeration and heat requirements for hydrate storage and regeneration were also presented.

Miller, R. C. and Hiza, M. J., "Experimental Molar Volumes for Some LNG-Related Saturated Liquid Mixtures." Fluid Phase Equilibria. 2:49-57, 1978.

Saturated (orthobaric) liquid molar volumes are reported for some methane-rich mixtures containing ethane, propane, isobutane, normal butane and nitrogen at temperatures between 100 and 115 K. These data were obtained with a gas-expansion system calibrated against pure methane orthobaric liquid molar volumes. Comparisons are shown between the experimental molar volumes and the results of some recent calculational methods.

MITRE Corp., A Summary of Accidents Related to Non-Nuclear Energy. EPA 600/9-77-012, PB-271506, 1977.

This report is an executive summary of a more extensive EPA study on accidents, in non-nuclear energy. LNG accidents are covered rather briefly, since only a few accidents have occurred in this category.

Miyahara, S. "Power Generation from Cryogenic Energy." Section II, Paper 8, Sixth International Conference on Liquefied Natural Gas, 1980.

The effective utilization of LNG cold becomes important in Japan because of the large amounts of LNG to be imported in the future. The technical problems to commercialize the various porjects in the use of LNG cold are reviewed.

Modak, A. T., "Thermal Radiation From Pool Fires." Paper presented at Western States Section, The Combustion Institute Meeting, La Jolla, CA, October 18-20, 1976.

This analysis computes: radiative energy fluxes to surfaces located external to the fire in any arbitrary orientation; variations of radiative heat flux along the fuel surface; total radiative heat

transfer from flames to fuel surface; forward radiative heat transfer from fire to virgin fuel bed external to the fire; angular distribution of radiative flux emitted by the pool fire; total radiative power output of the fire.

Moen, I. O. and J. H. S. Lee. "Research on Vapor Cloud Explosions and Related Phenomena in Canada." From Discussion on Explosion Hazards at the 7th International Colloquium on Gas Dynamics of Explosions and Reactive Systems, ed. H. Wagner, pp. 25-33, Max-Planck-Institute Für Strömungsforschung, Göttingen, 1979.

In Canada, there is increasing interest in the field of vapor cloud explosions and related phenomena, and various government and industrial bodies are engaged in conducting studies for safety aspects of regulations. Atomic Energy of Canada, Ltd. is involved in a 5-year investigation into the combustion properties of hydrogen-air-steam under confinement conditions particularly regarding pressure transient. At McGill University, research is focused on the influence of turbulence, obstacles, mixture inhomogeneities and confinement on combustion processes in vapor clouds. At the University of Calgary, the fire-spread characteristics through nonhomogeneities formed under the combined effect of diffusion and buoyancy are being studied.

Mori, H., Y. Miyata, N. Akagawa, Y. Sato, "Technical Improvements in LNG Vaporizers for Receiving Terminals in Japan." Presented at LNG 6 - International Conference on LNG, Kyoto, Japan, April 7-10, 1980.

This paper considers the following areas related to Open Rack Vaporizers (ORV) and Submerged Combustion Vaporizers (SCV):

- *Fundamental Heat Transfer Phenomena*
- *Improvements (ORV) or Developments (SCV)*
- *Operation and Maintenance*
- *Corrosion Protection and Durability*

This paper provides background information on these two types of vaporizers and points out areas relating to release prevention.

Montoya-Lirola, C., "Manufacture of Gels, Especially Liquid Fuels, and Their Subsequent Reversible Liquefaction." Chem. Abstrac. 76:27001g, Span. 362, 146 (to Gelsa S. A.), 1970.

LNG could be gelled by generating a mixture of 20 percent water containing 2.5% of a vegetable albuminoid, saponin or viscous resinous gum with 80% LNG.

Morton, B. R., "Modeling Fire Plumes." Paper presented at the Tenth International Symposium on Combustion, Cambridge, UK, August 17-21, 1964.

Theoretical treatments for turbulent diffusion flames and for the strongly heated regions of fire plumes in a still environment may be based on those developed for weakly buoyant plumes. A discussion

is given of some of the modifications that are needed, and the effects of large variations in density on the plume dynamics are aspects of heat transfer by radiation are presented separately.

Mullen, F. et al., Thermal Radiation and Overpressures from Instantaneous LNG Release into the Atmosphere - Phase II. TRW Systems Group Report No. 08072-9, to A.G.A., A.G.A. Catalog No. M60015, May 1969.

This report considers the fluid mechanics and thermochemistry of thermal radiation; boil-off, LNG vapor/air mixture dispersion experiments, and blast of overpressure; dike design; and a discussion of the flame program and vapor cloud studies.

Multhauf, L. G., Frank, A. M. and Koopman, R. P., Remote Measurement of LNG Vapor Dispersion Using LIDAR. UCID-17968-79-1, pp. 15-22 Lawrence Livermore Laboratory, 1979.

This is essentially an abbreviated version of Lawrence Livermore Laboratory report UCID-18237.

Multhauf, L. G., Frank, A. M. and Koopman, R. P., Remote Sensing for Diagnosing Vapor Dispersion in Spills of Liquid Energy Fuels. UCID-18237, Lawrence Livermore Laboratory, 1979.

A laser ranging (LIDAR) technique is described for measurement of gas concentrations in vapor clouds emanating from LNG spills. Results of a feasibility test at China Lake are discussed.

Munson, R. and Clifton, R. A., "Natural Gas Storage with Zeolites." PB Report No. 203892. U.S. National Technical Information Service, 1971.

Zeolites were used as an adsorbent for methane. For instance, Calcium A zeolite would retain up to 5 weight percent methane at 72°F and 200 psia. The potential of zeolites for vehicular natural gas storage was discussed.

Murata, T. and Nakanishi, E., "How Osaka Gas Uses the Cold from LNG." Pipeline and Gas Journal 121(3):23-38, 1980.

Osaka gas will effectively use the cold available in LNG for power recovery, ammonia synthesis, desalination, air separation, food freezing and storage, cryogenic crushing and related operations. Regasification at Osaka will amount to about 6.3 million tons LNG annually.

Murgai, M. P., "Radiative Transfer Effects in Natural Convection Above Fires." Journal of Fluid Mechanics. 12(3):441-448, March 1962.

This paper describes the results of examining the influence of radiative heat transfer on turbulent natural convection above fires in an atmosphere of constant potential temperature, under both the

'opaque' and 'transparent' approximations. It turns out that on the basis of the overall approximations introduced in this investigation, the former case reduces to that of no radiative transfer.

Murgai, M. P. and Emmons, H. W., "Natural Convection Above Fires." Journal of Fluid Mechanics. 8:611-624, 1960.

The turbulent natural convection above fires in a dry calm atmosphere with a constant lapse rate has been the subject of several recent investigations. The present paper presents solution curves from which the natural convection may be computed over a fire of arbitrary size in an atmosphere with arbitrary lapse-rate variation.

Murray, F. W., Atmospheric Dispersion of Vaporized Liquefied Natural Gas. Rand Corp. Rpt. P5360, AD/A010940, 1975.

A sophisticated mathematical model for the dispersion of LNG clouds is proposed. However, no details on the equations and on their numerical treatment are given.

Murray, F. W., Jaquette, D. L. and King, W. S. Hazards Associated with the Importation of Liquefied Natural Gas. Rand Corp., NTIS No. AD/A037928, June 1976.

Four previous reports by Rand Corporation are summarized and updated in this most recent publication, which discloses probable cause of accidental spills of LNG, the hazards surrounding these spills, and methods of estimating the probabilities of major accidents. In assessing the risks associated with LNG transport and processing, it is concluded that not enough evidence has been collected to comment on the safety of LNG or the ability to extrapolate from past experience.

Muscari, C. C., The Evolution of Liquid Natural Gas on Water. M. S. Thesis, MIT, 1974.

Governing equations are given for the simultaneous spread and evaporation (burning) of an LNG spill on water. Equation solutions determine the 1) maximum radial extent of the spill, 2) time duration of complete dissipation of spill volume, 3) graphics of spill volume versus time, evaporation rate versus time and spill thickness versus distance (from origin of spill).

Muska, V. A. Liquefaction of a Vapor Utilizing Refrigeration of LNG. U.S. Patent 3,962,881, assigned to: Airco, Inc., 1976.

The cold contained in LNG is utilized to condense another gas, such as CO_2. The methods and equipment used for this purpose are the object of the patent claim.

Nakagawa, A., "Japanese LNG Receiving Terminal is Reliable." Oil and Gas Journal. pp. 174-182, January 28, 1980.

The design, operation, and maintenance characteristics of the Sodegaura Terminal are described. The computer control system and the preventive maintenance operations are outlined.

Nakanishi, E. and Reid, R. C., "Liquid Natural Gas-Water Reactions." Chemical Engineering Progress. 67:36-41, December 1971.

This paper cites previous studies and discusses both quantitative and qualitative experimental results. Consideration is given to water on cryogens, underwater release of cryogens, cryogens on ice, cryogen spills on water and on coated liquids. Finally, a tentative hypothesis is presented for the explosion phenomena.

National Fire Protection Association. Standard for the Production, Storage, and Handling of Liquefied Natural Gas. NFPA No. 59A - 1979. National Fire Codes, Vol. 5, 1980.

An especially established committee on LNG has formulated a standard for the production, storage, and handling of LNG. This code is primarily intended for the day-to-day operation of LNG facilities. Only general rules for fighting LNG fires are given.

Neary, R. M., "Safety in LNG Semi-Trailer Design." Paper presented to the AGA Transmission Conference, Las Vegas, Nevada, May 3, 1976.

Included in this paper is a description of LNG semi-trailers and the various DOT regulations regarding them. Also included is a discussion of and a picture of an LNG trailer that was exposed to a fire as a result of an accident.

Nelson, W., "A New Theory to Explain Physical Explosions." Combustion. 44, May 1973.

This paper summarizes some known facts about explosions, with emphasis on physical explosions, describes a new explosion mechanism, and suggests current and future applications of the new theory to prevent smelt-water explosions in kraft chemical recovery furnaces.

Nelson, W. L., "What is Cost of Cryogenic Gas Processing Plants?" Oil and Gas Journal 77:96-97, June 18, 1979.

The costs of various cryogenic gas processing plants are compared. It is found that LNG baseload and LNG peak-sharing plants are the most expensive when based on equal capacity.

Newell, R. G., "Station Coordination Critical in LNG Pipeline Efficiency." Oil and Gas J. 77(18):239-244, 1979.

Pumping and cooling stations along an LNG pipeline must be designed for unattended operation and must use only LNG as the source of energy. Technology for such pipeline operation is proven. The paper presents guidelines for the overall design of an LNG pipeline.

Nicholls, J. A., Sichel, M., Gabrijel, Z., Oza, R. D. and Vandermolen, R., "Detonability of Unconfined Natural Gas-Air Clouds," Proc. 17th Symp. on Combustion, The Combustion Institute, pp. 1223-1234, 1978.

It is experimentally and analytically investigated under what conditions a methane/oxygen mixture with various amounts of nitrogen diluent can be detonated. The results confirm the presently held opinion that natural gas clouds mixed with air will almost never detonate. However, there is not yet absolute certainty about this conclusion.

Nielson, H. J. and Tao, L. N., "The Fire Plume Above a Large Free-Burning Fire." Paper presented at the Tenth International Symposium on Combustion, Cambridge, U.K., August 17-21, 1964.

A model which describes the variation with altitude of the composition, temperature, and velocity of the gases within a plume above a large free-burning fire is presented. This model is an extension of previous analysis of buoyant plumes which includes the effects of combustion, composition variation, and radiation losses from the hot gases.

Nierman, A. J., "Transportation of Natural Gas as a Hydrate." U.S. Patent 3,975,167 (to Chevron Research Co.), U.S. Patent Office, 1976.

Transportation of LNG hydrate by submarine was described. This procedure required supplementary refrigeration, a hold or void in which natural gas can be hydrated, and a membrane pervious to gas and water within the hold. Provisions were suggested for in situ removal of hydrate heat of formation.

Nikodem, H. J., D. Flothmann, W. Geiger, B. Oberbacher, G. Schnatz, and W. Schneider. Risk Assessment Study for the Harbor of Gothenburg. Prepared for the Swedish Energy Commission by the Battelle-Institute e.v. Frankfurt BF-R-63.371-1, 1978.

An assessment was made of the risk to the general public which arises from transport, storage and refining of crude oil and petroleum products. A large contribution to the overall risk, in particular cases with large numbers of fatalities per event, results from LPG operations.

Nikodem, H. J., Flothmann, D., Geiger, W., Schnatz, G. and Schneider, W., "Risk Assessment Study for an Assumed LNG Terminal in the Lysekil Area." prepared for the Swedish Energy Commission by the Battelle-Institute E.V. Frankfurt BR-R-31.109-1, 1978.

This report presents a risk assessment for a proposed LNG terminal and distribution system in Sweden using state-of-the-art dispersion and gravity/spread models. Risks included direct contact with LNG, suffocation, radiation and pressure wave destruction.

Nuclear Regulatory Commission, "Safety Evaluation by the Office of Nuclear Reactor Regulation Regarding the Proximity of Cove Point LNG Facility: Baltimore Gas and Electric Company Calvery Cliffs Nuclear Power Plant Units Nos. 1 and 2." Docket Nos. 50-317 and 50-318, March 13, 1978.

An analysis is described which shows the effects of various hypothetical LNG accidents at Cove Point on the Calvert Cliffs Power Plant. Results indicated that no new operating restrictions or other limitations needed to be placed on the plant to assure normal operations.

Odishariya, G. E., et al., "Technical and Economic Aspects of Integrating LNG Pipelines and Cryogenic Electric Power Transmission Lines." In: Problems of Modern Cryogenics. NASA TT-F-16, 841, 1976.

It is proposed to use coaxial pipelines for the simultaneous transmission of electric power and of LNG over long distances (Siberia to European USSR). The electric power would be carried by superconducting metals (along the inner channels), cooled by liquid helium, which is derived from the LNG. The latter is carried through an outer channel of the concentric piping.

Office of Technology Assessment, Transportation of Liquefied Natural Gas. Congress of United States, Washington, DC.

A review of LNG transportation technology provided as support for Congress on Future Energy Legislation. The LNG import system is criticized; public concerns are summarized; and laws, permit requirements and pending legislation are examined.

Office of Technology Assessment. Alternative Energy Futures, Part I. LNG Imports. OTA-E-110, 1980.

The economic and energy implications of future LNG imports into the U.S. are evaluated for the next two decades. It is expected that these imports will have doubled by 1995.

"Offshore LNG Terminal Deemed Feasible." Marine Equipment News. pp. 6-7, Spring 1977.

This article discusses the potential of offshore receiving terminals and describes several generic types that could be used. There are currently no offshore terminals in operation or construction, however, due to onshore siting difficulties they are being given serious attention.

Ohsaka, K. et al., Membrane Structure in a Liquefied Gas Storage Tank. U.S. Patent 4,149,652, 1979.

An improved structural design for LNG storage tanks is described. It minimizes thermal strains and practically eliminates potential sources of leaks that were present in earlier designs. Required labor for installing the new tanks is also greatly reduced.

Oiern, P. J. and K. H. Osmundsvaag. Vessel Comprising a Hull for Transporting Cooled Liquefied Gas. U.S. Patent 4,004,535, assigned to: A/S Akers Mek., 1977.

New design features for LNG tankers are proposed which allow better utilization of the maximum permissible dead weight of the ship. It is implied that oil and LNG are transported by the same vessel.

Okamoto, T. et al. Tank Supporting Structure for Ships. U.S. Patent 4,000,711, assigned to: Hitachi Ltd., 1977.

Repetitive loading and unloading LNG causes temperature cycles in the storage vessel, which then causes fatigue to the tank and its support members. The invention proposes ways to minimize the stresses in the support structure by providing chocks around the tanks which engage corresponding chocks tied to the ship's hull.

Okumura, T. "Recommended Practice for LNG Inground Storage." Session II, Paper 10, Sixth International Conference on Liquefied Natural Gas, 1980.

This is the first technical and safety standard manual for LNG concrete and membrane type inground storage tanks. It contains results from freezing and seismic tests, as well as field safety surveys of LNG terminals throughout the world.

Ong, H. L. "Current Status of California LNG Regulations." LNG Terminals and Safety Symposium, pp. 281-286, in Applications of Cryogenic Technology 9, Scholium International, Flushing, New York, 1979.

The main aspects of the proposed safety standards for LNG facilities in California are briefly discussed. According to the Liquefied Natural Gas Terminal Act of 1977, the California Public Utilities Commission has the exclusive power to issue building permits for LNG terminals.

Ooms, G., Mathieu, A. D., Zelis, F. "The Plume Path of Vent Gases Heavier than Air." First International Loss Prevention Symposium, 1974, 211-219.

The plume path theory developed at Koninlijke/Shell-Laboratorium, Amsterdam (KSLA) for predicting the dispersion of stack gases having a density equal to or lower than that of the surrounding air was checked on its validity for gases heavier than air.

Opschoor, G., "Investigations into the Spreading and Evaporation of LNG Spilled on Water." Cryogenics. 17:629-633, 1977.

Analytical expressions for the spreading of LNG spills on open and confined areas of water have been derived. They agree with known available experimental data.

Opschoor, G. "The Spreading and Evaporation of LNG- and Burning LNG-Spills on Water." J. of Hazardous Materials, 3:249-266, 1980.

This paper contains the results of a theoretical investigation into the evaporation and spilling of LNG and the burning of LNG on open water and on a confined water surface.

Opschoor, G. "Investigations into the Evaporation of Liquefied Gases Spreading on Land." Cryogenics. 21:281-286, 1981.

Based on a semiempirical model, the evaporation of spilled liquefied gases from dry and wet land is predicted. Also, described analytically is the spreading of a spill on a flat surface.

Ordin, Paul M., Bibliography on Liquefied Natural Gas (LNG) Safety. NASA Technical Memorandum, NASA TM X-73408, April 1976.

This bibliography contains citations concerned with the safety of LNG and liquid methane. The raw data for this report was a computer printout based on a keyword search strategy of descriptions in the cryogenic safety data bank dealing with LNG.

O'Rourke, P.J. and F. Bracco, "Two Scaling Transformations for the Numerical Computation of Multidimensional Unsteady Laminar Flames." Journal of Computational Physics. 3(2), November 1979.

The authors of this paper address the problem of flame propagation in a multi-dimensional system. Problems involving sonic propagation and small flame thickness are solved by means of a transformation. An actual simulation of combustion of methane in a chemical bomb are presented.

Otterman, B., "Analysis of Large LNG Spills on Water - Part 1: Liquid Spread and Evaporation." Cryogenics. 15(8):445-460, August 1975.

The first part of this two-part review considers the theoretical and experimental results obtained on liquid spread and evaporation of

large LNG spills on water. Both instantaneous spills, in which the spill time is much smaller than the time for complete vaporization, and continuous spills are considered. Also, applications of the correlations are discussed.

Overly, J. R. and Overholsen, K. A., "Calculation of Minimum Ignition Energy and Time Dependent Luminar Flame Profiles." Combustion and Flame. 31:60-83, 1978.

The authors simplify the calculational method of Spalding by use of a transformation of variable. The authors employ this technique to calculate ignition energy and flame propagation.

Oyez Intelligence Report. An Analysis of the Canvey Report. ISBN 085120 4651, 1980.

An independent study was carried out on the Canvey Report (1.5.38). Several criticisms of their conclusions were made in the report. Including the use of a Gaussian model for dispersion of LNG.

Oyez Intelligence Report. The Bulk Storage and Handling of Flammable Gases and Liquids. ISBN 085120 4597, 1980.

This report includes papers presented at a recent Oyez conference dealing with bulk storage and handling of flammable gases and liquids.

Oyez Intelligence Report. The Carriage of Hazardous Goods Overland. ISBN 085120 399X, 1980.

The conference was concerned with increased hazards due to increased shipment of hazardous goods. Discussions were presented on the economic factors as well as the technological aspects of designing equipment for use in shipping these goods.

Panofsky, H. A., "The Atmospheric Boundary Layer Below 150 Meters." Annual Review of Fluid Mechanics. 6:147-177, 1974.

The article considers profiles and fluxes over homogeneous terrain (surface layers, extension to the tower layer) and profiles over changing terrain (wind profiles, temperature characteristics, energy budgets, horizontal velocity components, temperature and humidity spectra, cospectra, and boundary layer models).

Pappas, J. A. and D. M. Solberg. Unconfined Vapor Cloud Explosions: A Prestudy. Veritas Report No. 79-0615, 1979.

A thorough review of the current knowledge on vapor cloud explosions is given. Special emphasis is placed on problems of understanding phenomena caused by non-ideal features of vapor clouds. Suggestions for further research are presented.

Parent, J. D., "The Storage of Natural Gas as Hydrate." Institute of Gas Technology Bulletin No. 1. 1948.

A very thorough review of the technical literature was presented. This included phase diagrams, heats of reaction, equilibrium ratios, cooling requirements, and operating pressures.

Parker, R. O., "Calculating Thermal Radiation Hazards in Large Fires." Fire Technology. 10(2):147-152, 1974.

The author has developed, and discusses here, a method for assessing the thermal radiation hazards to objects from fires. A comparison of the calculations to an actual fire experience seems to indicate that the method is reasonably accurate, though somewhat conservative.

Parker, R. O., "Study of Downwind Vapor Travel From LNG Spills." Paper presented at the American Gas Association Distribution Conference, May 1970.

The problem can be treated as a heat transfer calculation at the earth-liquid interface yielding the input; a second heat transfer problem if there is no wind, or if there is wind, an atmospheric dispersion problem. The conclusion is that it is very unlikely that vapor concentrations of more than 1/2 the lower flammable limit will exist 600 or more feet downwind of the lee dike.

Parker, R. O. and Spata, J. K., "Downwind Travel of Vapor From Large Pools of Cryogenic Liquids." Paper presented at LNG-1 Conference, Chicago, IL, 1968.

A method is developed for calculating vapor concentrations downwind of large pools of cryogenic liquids. Vapor concentrations at any downwind position is found as a function of time, wind speed, and wind structure. Lateral and vertical dispersion coefficients are determined using meteorological observations. Practical applications include hazard studies and air pollution estimates.

Parnarouskis, M. C., C. D. Lind, P.K. Raj and J. M. Cece. Vapor Cloud Explosion Study, Paper 12, Session III, 6th International Conference on LNG, 1980.

A major multifaceted test program has been conducted in an attempt to quantify the potential hazards resulting from the accidental spill of liquefied, flammable gases. Data has been collected on pool formation, vapor concentration, flame radiation, and detonability of LNG, LPG, and gasoline.

Parrish, W. R., Arvidson, J. M. and LaBrecque, J. F., "Evaluation of LNG Sampling Measurement Systems for Custody Transfer." 1978 Operating Section Proceedings, American Gas Association, Montreal, Quebec, May 1978.

A method for sampling moving LNG streams for composition and heating value is described. The main component of the technique and the main source of error is a gas chromatograph.

Parrish, W. R., Arvidson, J. M. and LaBrecque, J. F., "System is Accurate, Precise for LNG Sampling." Hydrocarbon Processing. April 1978.

A three component system including a sampling probe, vaporizer, and gas analyzer is described which can be used to monitor heating value from moving streams of LNG. Detection error is derived mainly from error in the gas analyzer.

Parrish, W. R., Brennen, J. A. and Siegwarth, J. D., "LNG Custody Transfer Research at the National Bureau of Standards." 1978 Operating Section Proceedings, American Gas Association, Montreal, Quebec, May 1978.

This paper presents a summary of research on determining the thermophysical properties of LNG components, on flowmeters, and on LNG sampling and composition measurements.

Pasman, H. S., Groethuizen, Th. M., DeGooijer, H. "Design of Pressure Relief Vents." First International Loss Prevention Symposium, 1974, 185-189.

A numerical method for the calculation of the vent opening area required to relieve explosive pressure is given.

Patankar, S. V. and Spalding, D. B., Heat and Mass Transfer in Boundary Layers. International Textbook Company, Ltd., 2nd edition, London, U.K., 1970.

The authors of this text describe a computational technique for solving the time dependent conservation equations (mass, momentum, energy and species) needed to describe flame propagation in one-dimensional planar, cylindrical or spherical geometry.

Peebles, M. W. H. "World LNG Trade: Current Status and Prospects for Growth." Session I, Paper 8, Sixth International Conference on Liquefied Natural Gas, 1980.

This paper reviews the progress that the international LNG industry has achieved to date. Discussion is concentrated on the prospects for growth in LNG supplies in the United States, Western Europe, and Japan through to 1990.

Pelloux-Gervais, P. and Sermanet, G., "Liquid Natural Gas Service Station for Vehicles." Paper No. A3.13 presented at the 14th International Congress of Refrigeration, Moscow, (in French), September 20-29, 1975.

L'Air Liquide's completely automated LNG service station for fueling vehicles quickly and safely is described.

Pelto, P. J., Baker, E. G. and Hall, R. J., "Assessment of LNG Release Prevention and Control." DOE-EV 0046, Department of Energy, Washington, D.C., Vol. 2, pp. 471-480, 1979.

The early results of a program of finding ways to minimize the frequency of occurrence and the size of a potential LNG release are described. Three systems are discussed: release prevention, release detection, and release control.

Pergament, H. S. and Fishburne, E. S., "Influence of Buoyancy on Turbulent Hydrogen/Air Diffusion Flames." Paper presented at the Central States Section Combustion Institute Meeting on Fluid Mechanics of Combustion Processes, Cleveland, OH, March 29-30, 1977.

The results show that: flame properties scale with nondimensional distance for Froude numbers (Fr) greater than about 10^6; buoyancy affects temperature decay rates downstream of the location of maximum temperature (after all the H_2 has burned); the predicted influence of Fr on buoyant flame lengths is consistent with the available data.

Petsinger, R. E. and Vance, R. W., LNG Terminals and Safety Symposium - Applications of Cryogenic Technology Volume 9, 1979.

The proceedings of the LNG Terminals and Safety Symposium held October 12-13, 1978, in San Diego, CA, are provided. Session topics include: LNG Export Terminals, LNG Import Terminals, and LNG Research and Safety.

Petrash, D. A., Barber, J. R., Chambellan, R., and Englund, D. R., "Gelled Liquid Methane." NASA Spec. Publ. NASA SP-5103, Sel. Technol. Gas Ind. pp. 86-88, 1975.

Results of work toward use of LNG as fuel for supersonic aircraft was reported. The problem of "boiloff" due to decrease of pressure with altitude was eliminated by preparing LNG gels with water or methanol. LNG-methanol gel was recommended due to the total heat of combustion.

Pfoertner, H., "Ignition Behavior of Natural-Gas/Air Mixtures in Free Clouds." Gas-Wasserfach, Gas/Erdas. 120(1):19-24, 1979 (in German). (For translation see Lawrence Livermore Laboratory UCRL-TRANS-11478.)

Based on combustion analysis it is concluded that only deflagrations and no detonations would occur when a natural-gas/air cloud is ignited. This conclusion is backed up by a series of tests.

Phillips, H. "Research on Vapor Cloud Explosions in the U.K." From Discussion on Explosion Hazards at the 7th International Colloquium on Gas Dynamics of Explosions and Reactive Systems, ed. H. Wagner. pp. 69-70, Max-Planck-Institute Für Strömungsforschung, Göttingen, 1979.

The UK attitude to research into vapor cloud explosions is inspired by their experience at Flixborough and the desire to prevent further disastrous explosions. To this end the Health and Safety Executive continuously reviews current knowledge and engage in developing procedures that will identify plants that are subject to risk and to advise legislators how to avoid the risk. The data they draw on is derived largely from the accumulated experience of accidents in chemical plant in UK and elsewhere.

Philipson, L. L. "The Reliability of LNG Systems." Energy Sources 5:13-29, 1980.

A qualitative evaluation of the reliability of the entire LNG supply chain has been provided. Even though the reliability has been high so far, a certain degree of redundancy in the LNG systems is recommended.

Picciotti, M., "Why an LPG Olefins Plant?" Hydrocarb. Process, 59(4):223-228, 1980.

In order to ensure a steady supply of olefins, the possibility of cracking LPGs and/or naphtha in existing ethylene plants has been considered. Some modifications in the chemical plans would be required, however, to make such processes economical.

Picknett, R. G. "Field Experiments on the Behaviour of Dense Clouds." Report PTN/TL 1154/78/1, Chemical Defense Establishment, Porton Down, Wilts., Contract report to the Health and Safety Executive, Sheffield, 1978.

This report gives information about the field experiments on the behavior of dense clouds, which were performed on request from the Health and Safety Executive. The report contains a review of the results, a discussion of the observed behavior of the dense clouds, and a theoretical model of dispersion. The distinctive features of dense gas dispersion are presented and predictions are made concerning larger scale releases of dense gas.

Pipkin, O. A. and Sliepcevich, C. M., "Effect of Wind on Buoyant Diffusion Flames." Industrial and Engineering Chemistry Fundamentals. 3:147-154, 1964.

Buoyant diffusion flames of natural gas were observed in wind tunnel experiments to determine the extent of bending by wind. A flame drag coefficient, C_f, is introduced in the flame momentum balance. A single straight-line correlation of In C_f(Re) versus In Re is obtained after extracting the influence of flame angle of tilt and applying an empirical correction to account for increasing flame roughness at larger diameters.

Ploum and Arnold, J. W., "The Brunei Liquefied Natural Gas Plant." LNG 5 - International Conference on Liquefied Natural Gas, Duesseldorf, Germany, August 29-September 1, 1977.

This paper reviews and highlights some of the design concepts and operating experiences gained particularly from the liquefaction plant at Brunei.

Pluta, P. J. and R. G. Williams. "U.S. Coast Guard LNG Regulations." pp. 243-323, in Applications of Cryogenic Technology 9, Scholium International, Flushing, New York, 1979.

U.S. Coast Guard's efforts consist mainly in implementing codes developed by the Intergovernmental Maritime Consultive Organization (IMCO). These codes relate primarily to cargo containment and safety systems of LNG tankers. LNG terminals are regulated in the U.S. by the Coast Guard and also by DOE and the Materials Transportation Board of DOT.

Poll, J. "Versuche zur Verdampfung von ausgelaufenem Flüssiggas." (Experiments on LNG Vaporization from Pools.) Gas- und Wasserfach 116, 263-265, 1975.

Practical devices and experimental procedures are described. The results are discussed and presented in graphical and tabular form. The tests showed that the spontaneous evaporation of LNG is by orders of magnitude smaller than mentioned previously.

Porricelli, J. D., Keith, V. E. and Paramore, B., Recommended Qualifications of Liquefied Natural Gas Cargo Personnel, Volumes I, II and III. NTIS No. AD/A026109, AD/A026110, April 1976.

The report presents recommendations, based on task analysis, concerning training and other qualification requirements appropriate for personnel of liquefied natural gas (LNG) ships and barges.

The study was a pilot effort to demonstrate a method of determining qualifications for new technology ship occupations when there are few or no operating examples to study.

Porter, G. and Higgins, K., "Liquefied Natural Gas: An Energy Alternative." Dimensions/NBS 63(9):14-18, 1979.

Presently, there are no internationally agreed-upon standards for measuring the quantity and quality of LNG contained in a tanker. The ultimate goal of the NBS LNG thermophysical properties program is, therefore, to reduce the total uncertainty in LNG measurements from the current estimates of from 5% to 7% to a much more tolerable 1% potential error per shipment.

Porteous, W. M. and Blander, M., "Limits of Superheat and Explosive Boiling of Light Hydrocarbons, Halocarbons, and Hydrocarbon Mixtures." AIChE Journal. 21:560-566, May 1975.

Thirteen light hydrocarbons and 4 light halocarbons were tested to determine their limits of superheat at one atmosphere pressure using a superheating column. Even with some variation in temperature to which a compound could be superheated before boiling explosively, the reduced limits T_L/T_C were always close to 0.88. Super heat limits of binary hydrocarbon systems and tertiary mixtures were close to mole fraction averages of the limits of the pure compounds.

Porteous, W. M. and Reid, R. C., "Light Hydrocarbon Vapor Explosions." Chemical Engineering Progress. 73:83-89, May 1976.

This article includes information relating to spills on water of propane, propylene, isobutane, binary mixtures containing ethane, pure alkanes and pure alkenes. Some explosive compositions and ranges for hydrocarbon spills are also given. Previous studies are cited and factors affecting violence of explosions are discussed.

Poten & Partners, Inc. Liquefied Gas Ship Safety, Analysis of the Record. 1964-1979, Poten & Partners, Inc., New York, 1980.

The analysis reveals that the safety record for LNG tankers has been superior. Of the total of 7 incidents only one resulted in a minor LNG spill. No fire ensued.

Price, J. P. et al. Environmental Impacts of Energy Transportation: Liquefied Natural Gas. EPRI-EA-2039, Section 4, Electric Power Research Institute, 1981.

A wide ranging summary has been given on potential environmental problems of LNG transport and storage. Since the paper is concise and rather brief, it can serve as an introduction to the subject matter.

Priestley, C. H. B. and Taylor, R. J., "On the Assessment of Surface Heat Flux and Evaporation Using Large-Scale Parameters." Monthly Weather Review. 100(2):81-92, February 1972.

Data from a number of saturated land sites and open water sites in the absence of advection suggest a widely applicable formula for the relationship between sensible and latent heat fluxes.

Putnam, A. A., "A Model Study of Wind-Blown Free-Burning Fires." Paper presented at the 10th Symposium on Combustion, The Combustion Institute, 1965.

Specifically, the dimensionless flame height varied with the negative 1/4-power of the Froude number based on cross-wind velocity and undisturbed flame height, above a Froude number

of 0.2. The horizontal extension of the flame, on the other hand, increased rapidly with increasing cross wind at first, and then less rapidly with the 1/6-power of the Froude number.

Putnam, A. A., "Area Fire Considered as a Perimeter-Line Fire." Combustion and Flame. 7:306-307, 1963.

The hypothesis that line fires and area fires are basically related was tested by examining available data on sources in a line and in a hexagonal pattern. A mathematical analysis is given to justify the hypothesis.

Putnam, A. A. and Grinberg, I. M., "Axial Temperature Variation in a Turbulent, Buoyancy-Controlled, Diffusion Flame." Combustion and Flame. 9(4):419-420, 1965.

An analytical expression was formulated which correlated the temperature profile of a turbulent diffusion, buoyancy-controlled flame to fuel properties and flow conditions. The expression is valid in the region after combustion is completed, and is valid at higher temperature levels than previously used correlations which are accommodated as a limiting case.

Putnam, A. A. and Speich, C. F., "A Model Study of the Interaction of Multiple Turbulent Diffusion Flames." Paper presented at the 9th International Symposium on Combustion, 1963.

This research program has shown that a valid model for studies of mass fires can be produced using multiple jets of gaseous fuels. The basic requirement is that the fuel jets produce turbulent diffusion flames which are buoyancy controlled. A specific operating range where this requirement is met was found for this model.

Radiative Transfer in Multidimensional Systems of Non-Gray Molecular Gases - Effects on Combustion. Columbia University. A.G.A. Project on LNG Fire Study. (See LNG 1976 Annual Report).

An analytical technique has been developed to treat band radiation from non-gray molecular gases. The technique has been simplified so that the frequency integrations can be performed with simple quadrature formulae. The simplified technique is being applied to multidimensional radiative transfer problems as well as problems involving combustion.

Raj, P. K., "A Criterion for Classifying Accidental Liquid Spills into Instantaneous and Continuous Types." Comb. Sci. & Techn. 19:251-254, 1979.

A dimensionless critical time is suggested, which could serve to divide LNG spills into "instantaneous" and "continuous" types.

Raj, P. and Atallah, S., "Thermal Radiation from LNG Spill Fires." Advances in Cryogenic Engineering.

The authors of this paper present results of experimental measurements made in LNG fires which were 6, 20 and 80 ft in diameter. Correlations are given for the wind induced plane tilt angle and length to diameter ratio of the flame. Also measured are the radiative absorption coefficient, radiative flux at a distance from the plume and the fraction of energy which leaves the fire as thermal radiation.

Raj, P. and Emmons, H. W., "Burning of a Large Flammable Vapor Cloud." Paper presented at the Central States Section, Combustion Institute Meeting, San Antonio, Texas, April 21-22, 1975.

A theoretical analysis is presented to estimate the ground level width of a two-dimensional turbulent flame as a function of time for the burning of a large combustible vapor cloud in the atmosphere for a given turbulent flame speed. The base width of the flame is assumed to be controlled by the rate at which the vapor is fed into the combustion zone and the air entrainment rate.

Raj, P. and Kalelkar, A. S., Assessment Models in Support of the Hazard Assessment Handbook. A report by Arthur D. Little, Inc., to the Department of Transportation, U.S. Coast Guard, Report Numbers CG-D-65-74. NTIS No. AD/776617, January 1974.

Analytical models are derived to describe the hazards caused by the accidental release of chemicals into the atmosphere or spills onto water. The models encompass a variety of physical phenomena that can occur such as dispersion of vapor in the atmosphere, dispersion of liquid in water, spreading on water, burning of a liquid pool, etc. Analyses include the modeling of the phenomenon and solution to equations.

Raj, P. and Kalelkar, A. S., "Fire Hazard Presented by a Spreading, Burning Pool of Liquefied Natural Gas on Water." Paper presented at the Western States Section, Combustion Institute Meeting, 1973.

A time-growth rate for an LNG spill on water is obtained and the fire duration, determined by complete evaporation time, is established. An effective flame height is established and the radiation field about the flame calculated. Based on thermal radiation flux and fire duration, safe separation distances from the LNG pool fire for people and combustible materials (wood) are determined.

Ramsdell, J. V., Jr. and Hinds, W. T., "Concentration Fluctuations and Peak-to-Mean Concentration Ratios in Plumes From a Ground-Level Continuous Point Source." Atmospheric Environment. 5:483-495, 1971.

Diffusion data were collected by 63 incremental samplers during four short duration, continuous releases of ^{85}Kr. Cumulative frequency distributions and the intensity of short-term concentrations are shown to be a function of the relative crosswind position within the mean plume. Peak-to-mean concentration ratios are shown as a function of relative crosswind position within the plume and the ratio of the durations of the mean and peak.

Rasbach, D. J., Rogowski, A. W. and Stark, G. W. V., "Properties of Fires of Liquids." Fuel. 35:94-107, 1956.

Alcohol, petrol, benzole and kerosene fires, burning freely in a vessel of 30 cm dia, have been studied. Measurements were made on the temperature, rate of burning and change in composition of the liquid, and on the dimensions, upward velocity, temperature and emissivity of the flames. It was estimated that with hydrocarbon liquid fires, heat transfer to the surface was mainly by radiation, but for the alcohol fire mainly by conduction.

Rausch, A. A. and Levine, A. D., "Rapid Phase Transformations Caused by Thermodynamic Instability in Cryogens." Cryogenics. 13:224-229, April 1973.

Thermodynamic metastability and incipient stability are used to explain the cause of rapid phase transformations. When liquid cryogen comes into sudden contact with a warmer host liquid, it is heated and forms a thin layer of metastable, superheated liquid at the interface. A heat transfer and thermodynamic model is used to predict the host liquid temperature that will cause a shockwave for a given cryogen.

Raynor, G. S., Michael, P., Brown, R. M. and SethuRaman, S., "A Research Program on Atmospheric Diffusion from an Oceanic Site." BNL 18924 presented at the Symposium on Atmospheric Diffusion and Air Pollution, Santa Barbara, CA, September 9-13, 1974.

Analyses of meteorological data collected in this program show that wind profiles measured on the beach are representative of those over the ocean during onshore flows. Data obtained from tracer releases show that diffusion over the sea differs appreciably from that over land at the same time and is largely determined by the air-water temperature difference.

Raynor, G. S., Michael, P., Brown, R. M. and SethuRaman, S., Studies of Atmospheric Diffusion From a Near-Shore Oceanic Site. BNL 18997, Brookhaven National Laboratory, June 1974.

Preliminary results show that diffusion is governed primarily by water and air temperature differences. With colder water, low-level air is very stable and diffusion minimal but water warmer than the air induces vigorous diffusion.

Raynor, G. S., R. M. Brown and S. SethuRaman. 1978. "A Comparison of Diffusion from a Small Island and an Undisturbed Ocean Site." Journal of Applied Meteorology. 17(2).

Comparison of oil fog plumes from a small island (∿800 m x ∿175 m) with a plume from a ship showed increased widths (1.5 to 4 times) and decreased centerline concentrations (1/2) with those from the boat's plume.

Reid, R. C., "Possible Mechanism for Pressurized-Liquid Tank Explosions or BLEVE's." Science. 203:1263-1265, 1979.

The hypothesis is made that rapid depressurization of hot saturated liquids may result in an explosion. Such a situation could arise, e.g., if a tank filled with liquefied propane would be engulfed in a fire due to some accident.

Reid, R. C., "Superheated Liquids." American Scientist. 64(2):146-156, March - April 1976.

The article cites numerous studies concerning superheated liquids and indicates that significant evidence suggests that superheated liquids are a trigger leading to the extensive arrangementation that may well set off large vapor explosions.

Reid, R. C. et al., Flameless Vapor Explosions. American Gas Association, Catalog No. M20177, 1977.

Flameless vapor explosions are discussed for a wide variety of substances, including LNG. Theoretical explanations are based on the superheat limit temperature.

Reid, R. C. and Smith, K. A., "Behavior of LPG on Water." Hydrocarbon Processing. pp. 117-121, April 1978.

Boiling of LPG is described as initially but very briefly violent followed by quilt evaporation. Boiling rates are not sensitive to changes in composition.

Reid, R. C. and Smith, K. A., Boil-Off Rate of Liquid Nitrogen and Liquid Methane on Insulated Concrete. Interim Report from MIT LNG Research Center to A.G.A., December 1975.

Experiments were conducted to measure the boil-off rate of both liquid nitrogen and liquid methane on insulation concrete. Results are fragmentary but do allow approximations of the rate of vapor generation that could result from spills of cryogens on typical insulating concretes.

Reid, R. C. and Wang, R., "The Boiling Rates of LNG on Typical Dike Floor Materials. Cryogenics. 18(3):401-404, 1978.

The insulating qualities for various types of floor materials for LNG dike storage compounds have been determined in LNG boiling tests. Their numerical values are tabulated.

Reid, R. C., L. M. Shanes and P. S. Virk. LNG Gels: Structure, Rheology, and Production Energy Requirements. GRI-77/0012, Gas Research Institute, 1979.

Twice as much energy was required for the production of gelled LNG over normal LNG. Additional tests are suggested to reduce the high energy costs.

Reid, R. C., L. S. Wilkens and P. S. Virk. "Liquefied Natural Gas Gels," Cryogenics 20:567-570, 1980.

Laboratory methods are described to gell LNG with water or methanol. Even though static yield stress of the LNG can be increased easily, the flow viscosity is much less affected. Safety benefits are not yet discernible, especially if the cost of gelling is taken into account.

Reid, R. C. Boiling of LNG on Typical LNG Dike Floor Materials. GRI-79/0026. Prepared for Gas Research Institute by LNG Research Center, Massachusetts Institute of Technology, Cambridge, Massachusetts, 1980.

Boiling rates of LNG and liquid methane were measured for various substrates which are or could be used as dike floor materials. These rates were correlated with theoretical heat transfer models to allow interpolation and extrapolation. Two very effective insulations were identified: Grace Zonolite insulating concrete and corrugated metal plates. The former has very low density, is quite strong, and has a low thermal conductivity. The latter is inexpensive, easily placed into position and leads to quite low boiling rates. Also shown was the fact that LNG vaporizing on a solid surface is in vapor-liquid equilibrium and, therefore, standard thermodynamic correlations may be used to estimate the composition of the evolved cloud.

Reisler, R. E., Ethridge, N. H., LeFevre, D. P. and Giglio-Tos, L., Air Blast Measurements From the Detonation of an Explosive Gas Contained in a Hemispherical Balloon (Operation Distant Plain, Event 2a). Ballistic Research Laboratories, BRL MR 2108, AD/73216, U.S. Army Aberdeen Research and Development Center, Aberdeen Proving Ground, Maryland, July 1971.

Air blast was measured from the detonation of a mixture of oxygen and propane equivalent to 20 tons of TNT in a hemispherical balloon anchored to the ground surface. Comparisons made of overpressure waveshape and impulse as a function of shock overpressure show an equivalent yield of 20 tons or larger and a dynamic pressure impulse about 60 percent larger than for a corresponding 20 ton TNT charge.

Rhoads, R. E. and Johnson, J. F., "Risk in Transporting Materials for Various Energy Industries." Nuclear Safety. 19(2):135-149, March-April 1978.

A risk assessment model is presented to assess the comparative safety of various energy systems in relation to other natural or man-related risks. Examples from assessments using the analysis technique are also presented along with future assessment plans. This paper encourages risk sensitivity studies and risk comparisons to provide a basis for decisions.

Ricou, F. P. and Spalding, D. B., "Measurements of Entrainment by Axisymmetrical Turbulent Jets." Journal of Fluid Mechanics. 11:21-32, 1961.

Measurements have allowed the deduction of an entrainment law relating mass flow rate, jet momentum, axial distance, and air density. When the injected gas burns in the jet the entrainment rate is up to 30% lower than when it does not.

Riedl, R. G., "Consumers' Gas LNG Satellite Firms Ottawa Valley Gas Supply." Pipeline & Gas J. 206(13):30-36, 1979.

New LNG peakshaving satellite plant, supplied from Montreal LNG peakshaving/ liguefaction plant, is ideally located in middle of service area and has proven itself in both emergenices and for peakshaving service.

Rigard, J. and Vadot, L., "Evaluate LNG's Storage Hazards." Hydrocarb. Process. pp. 267-268, July 1979.

It is shown that experimental water modeling, based on Neyrtrec's water analog technique, can be a useful aid to planning protection of LNG tankage.

Rivard, W. C., Farmer, O. A. and Butler, T. D., RICE: A Computer Program for Multicomponent Chemically Reactive Flows at All Speeds. LA-5812, March 1975.

A computer code capable of solving the thermal-hydrodynamics of chemically reactive flows is presented. A strong point of the code is that it is not limited by sonic propagation constraints.

Rosak, J., Skarka, J. "Methods for Estimation of the Effects of Accidental Releases of Liquefied Gases." Third International Loss Prevention Symposium, 1980, 15/1173-15/1182.

The paper deals with the method for estimating the effects of accidental release of inflammable substances. The estimation is based on two models. The first one is the statistical model for the dispersion of exhalations, the second one is for an abrupt release of large amounts of the substance kept under pressure in an equipment.

Rosenberg, S. D. and Vander Wall, E. M., "Gelled Cryogenic Liquids and Method of Making Same." U.S. Patent 4,011,730 (to Aerojet-General Corp.), 1977.

LNG or methane hydrates were prepared by introducing finely divided solid water or methanol into the cryogenic liquid. Less than 2 weight percent decreased the solubility of nitrogen in LNG to nearly zero at -280°F.

Rudnicki, M. I. et al. Study of Gelled LNG. DOE/EV/02057-T2, 1980, Department of Energy, Washington, D.C.

Characteristics of gelled LNG have been determined in an experimental program. Static yield stress is increased significantly, but apparent viscosity only slightly. Boil-off rates are reduced. It is still not entirely clear what significance this will have on the overall LNG safety problems.

Russ, R. M., Detection of Atmospheric Methane Using a 2-Wavelength H_eN_e Laser System. Masters Thesis, Mass. Institute of Tech., June 1978.

The report describes the design of a system to reliably measure concentrations of methane in air of 0.1 to 100% which may arise in LNG spill tests. Discussions of design requirements, alternatives, and model and laboratory test results are presented.

Santman, L. D., "The Department of Transportation's Role in LNG Safety Regulations." 1978 Operating Section Proceedings, American Gas Association, Montreal, Quebec, May 1978.

DOT authority over LNG safety is derived from the ports and waterways safety Act of 1972 and the natural gas pipeline safety Act of 1968. Proposed regulatory action on HR. 11622 is discussed.

Sarkes, L. A., Iribe, P. C. and Smith, R. B., "LNG: Current Status Confirms Its Technical Maturity." Pipeline and Gas Journal. November 1978.

The history and current developments in the LNG industry are summarized. Some of the safety concerns and safety related research are discussed.

Sarsten, J. A., "LNG Stratification and Rollover." Paper presented at the API Division of Refining, Philadelphia, PA, May 17, 1973.

This report covers an incident where LNG was stratified in an LNG storage tank during filling and how that stratification subsequently resulted in a rollover of the tank contents and the release of a large quantity of gas. A repetition will be positively prevented by the installation of a jet mixing nozzle that will thoroughly mix off-loaded cargo with different composition initial tank heels.

Schneider, A. L., "Liquified Natural Gas Safety Research." American Gas Association - Cryogenic Society of America, LNG Terminal and Safety Symposium, San Diego, 1978.

The paper summarizes experimental research programs for safety issues related to LNG transportation and storage.

Schneider, A. L. "Liquefied Natural Gas Safety Research Overview." LNG Terminals and Safety Symposium, pp. 195-271, in Applications of Cryogenic Technology 9, Scholium International, Flushing, New York, 1979.

A very thorough and comprehensive review is given on LNG research, conducted over the last two decades. For this purpose the research projects are divided into three sections, those dealing with shore-side facilities, those with water transportation, and those independent of land and water.

Schneider, A. L., "LNG Research Overview." Proceedings of the Marine Safety Council, 36(3):52-54, 1979.

A condensed overview is given on U.S. Coast Guard sponsored safety projects connected with the marine transportation of LNG. The projects and their main results are listed briefly.

Schneider, A. L., Lind, C. D. and Parnarouskis, M. C., "U.S. Coast Guard Liquefied Natural Gas Research at China Lake," CG-M-03-80, 1980.

The paper presents an overview of the LNG safety research projects that have been sponsored by the U.S. Coast Guard over the last decade. Results of the various projects are briefly outlined.

Schuller, M. R., Murphy, J. C. and Glasser, K. F., "LNG Storage Tanks for Metropolitan Areas." Paper presented at the 4th International LNG Conference, Algiers, Algeria, June 24-27, 1974.

This article describes in some detail the special design features of the 290,000 BBL storage tank built for Consolidated Edison of New York by the Pittsburg Des Moines Steel Company. The special design features, including a 9% Ni outer tank shell and a concrete berm wall around the outside of the tank, were used because of the heavily populated surrounding area and the proximity of the facility to LaGuardia Airport.

Schulte, K. "The Gas Cloud Explosion Program on the PNL-Project." From Discussion on Explosion Hazards at the 7th International Colloquium on Gas Dynamics of Explosions and Reactive Systems, ed. H. Wagner, pp. 60-68. Max-Planck-Institute Für Strömungsforschung, Göttingen, 1979.

The situation under study involved the use of waste heat from a nuclear power plant in a coal gasification process. The close proximity of the two facilities and West Germany's Reactor Safety Guidelines dictate

consideration of damage potential to the nuclear power plant from explosion of a gas cloud released from the gasification process. The main areas under study involve: 1) finding the pressure and pressure front shape of realistic gas explosions and 2) determining the behavior of typical structure's expected pressure loadings. The ultimate goal is to develop a representative pressure-time-function or a set of such functions that could be used as the basis for safe design criteria for coal gasification plants utilizing nuclear power plant waste heat.

Science Applications, Inc., LNG Terminal Risk Assessment Study for Los Angeles, California. SAI-75-614-LJ, for Western LNG Terminal Company, Los Angeles, CA, 1975.

SAI analyzed the potential risk of a proposed LNG import terminal in Los Angeles Harbor.

Sergeant, R. J. and Robinett, F. E., An Experimental Investigation of the Atmospheric Diffusion and Ignition of Boil Off Vapors Associated With a Spillage of Liquefied Natural Gas. TRW Systems Group Report No. 08072-7, to A.G.A., A.G.A. Catalog No. M19715, November 14, 1968.

Results of experimental spills of LNG into scaled earthen dikes are described. Emphasis of this phase of the program was directed toward qualitatively determining the path of the boil-off vapors, quantitatively measuring the gas/air mixture in the surrounding environment, and demonstrating the extent of the flammability with an ignition source. Correlation of the experimental data into empirical form is presented; radiation data were also obtained.

Seroka, S. and Bolan, R. J., "Safety Considerations in the Installation of an LNG Tank." Cryogenics and Industrial Gases. pp 22-27, September/October, 1970.

Design codes and standards for LNG storage tanks are detailed. Diagrams showing instrumentation for a typical tank are included.

Shaheen, E. I. and Vora, M. K., "Worldwide LNG Survey Cites Existing, Planned Projects." Oil and Gas Journal. pp 59-71, June 20, 1977.

This article discusses the various types of LNG facilities and briefly describes several existing facilities. A list of all the LNG facilities worldwide is included.

Shaw, P. and Briscoe, F., Evaporation from Spills of Hazardous Liquids on Land and Water. SRD R-100, 1978.

Mathematical models for an analytical description of cryogenic liquid spills both on water and on land are being developed and evaluated. Numerical results are given.

Shell International Research, "Transportation of Liquefied Natural Gas." Chem. Abstr. 66:97298b, Neth. Appl. 6,506,843, 1966.

An aqueous isopentane emulsion was used as a recyclable thermal carrier for heating or cooling LNG. A solid phase, such as silica-gel, was also suggested.

Shultz, F. D., "Safety at an LNG Peakshaving Facility." Presented at the ASME Winter Meeting, New York, NY, November 17-22, 1974.

Design and operation of the many safety related aspects of Long Island Lighting Company's Holbrook LNG plant is described. Such features include gas detectors, fire protection and vapor dispersion systems, and the emergency shutdown systems.

Sidjak, W., Arctic Pilot Project. Presented to the American Gas Association Transmission Conference, Montreal, Quebec, May 8-10, 1978.

This paper describes a pilot study involving a barge-mounted liquefaction and storage facility in the Arctic. The pilot study is in support of the Arctic Islands LNG project (see above).

Siegwarth, J. D., Radio Frequency Liquid Level Gauging In Propane Tank Car Safety Tests - A Feasibility Study. NBSIR 79-1660, National Bureau of Standards, 1979.

The report presents details of experiments to gauge liquid levels in tank cars using the change in resonant radio frequencies. Precision was tested and the method was recommended for routine tank car gauging.

Simanek, J. and Pick, P., "Hydrates of Natural Gas." Plyn. 53:167-9, June 1973.

Crystallographic data was presented concerning the unit cell and crystal dimensions. In natural gas, up to seven components can participate in mixed hydrate formation. Phase diagrams for several of the mixtures were shown.

Simmons, John A., Risk Assessment of Storage and Transport of Liquefied Natural Gas and LP-Gas. Science Applications, Inc., November 25, 1974.

A method for assessing the societal risk of transporting LPG and LNG is described. From an estimated 52 significant accidents per year with LPG tank trucks at the present truck-associated transportation rate of 20 billion gallons of LPG per year, a fatality rate of 1.2 per year is calculated. For the projected 1980 importation of 33 billion gallons by tanker ship, a fatality rate of 0.4 per year is calculated.

Simplified Methods for Estimating Vapor Concentration and Dispersion Distances for Continuous LNG Spills into Dikes with Flat or Sloping Floors. A. D. Little, Inc. for American Gas Association, AGA No. X50978, April 1978.

The report describes a set of techniques which allow calculation of dispersion of LNG spilled on a flat or sloped dike floor. Calculations include leakage flow rate, LNG flash vaporization, LNG boiling and vapor overflow, and vapor dispersion.

Sindt, C. F. and Ludtke, P. R., "Characteristics of Slush and Boiling Methane and Methane Mixtures." Proceedings of 13th Int. Congr. of the Int. Institute of Refrigeration. pp. 315-320, 1971.

Experiments were performed to determine the boiling behavior of methane and methane mixtures and also of the slush which is formed when vacuum pumping the ullage over the mixture.

Singer, I. A., "The Relationship Between Peak and Mean Concentrations." Journal of the Air Pollution Control Association. 11:336-341, July 1961.

A method of predicting average concentrations has been presented. It has been shown that the simplified normal bivariate distribution describing the average concentration pattern is composed of various short-term periodic distributions which may differ from it significantly. A descriptive, empirical method has been described.

Singer, I. A. and Smith, M. E., "Atmospheric Dispersion of Brookhaven National Laboratory." Air and Water Pollution - An International Journal. 10:125-135. 1966.

A variety of data relating to atmospheric dispersion has been obtained at the Brookhaven Laboratory site and its environs. Concentration measurements were made at distances ranging from 10 m to 60 km. Dispersion patterns developed are discussed in detail and values of the parameters appropriate for various theoretical treatments are summarized.

Slade, D. H., "Atmospheric Dispersion Over Chesapeake Bay." Monthly Weather Review. pp 217-224, June 1962.

It was found that, after the air had traveled for about 7 miles over the water, its direction fluctuations were always less than they had been before reaching the water. The wind speed usually increased as the air crossed the water. The ratio of overland to overwater dispersive capacity varied from less than 5:1, for heating from below, to greater than 35:1 for cooling from below.

Slagg, N. "Vapor Cloud Explosion Studies in the United States." From Discussion on Explosion Hazards at the 7th International Colloquium on Gas Dynamics of Explosion and Reactive Systems, ed. H. Wagner, pp. 111-113, Max-Planck-Institute Für Strömungsforschung, Göttinger, 1979.

In the United States, several government agencies and other institutions are involved in programs that contibute to a basic understanding of unconfined explosions. Practical considerations associated with the accidental dispersion of energetic materials dictate the need for including the role of confinement in studies. Buildings, warehouses, ship's hulls, and associated pathways all present an opportunity for confinement to aid in acceleration of a deflagration that may eventually develop into a detonation. Major technical areas under study in the U.S.A include mechanisms that cause flame acceleration, initiation requirements, affect variations in fuel/air ratio, blast effects estimating, and blast scaling.

Slawson, P. R. and Csanady, G. T., "The Effect of Atmospheric Condition on Plume Rise." Journal of Fluid Mechanics. 47:33-49, 1971.

The buoyant rise of chimney plumes is discussed for relatively large distances from the source, where atmospheric turbulence is the dominant cause of mixing (rather than turbulence due to the plume's own upward motion). A simple theory is developed which shows a number of different shapes plumes can have under different atmospheric conditions (particularly in an unstable environment).

Sloan, E., Dendy, Khoury, F. M., and Kobayashi, R., "Water Content of Methane Gas in Equilibrium with Hydrates." Ind. Eng. Chem. Fundam. 15:318-23, April 1976.

Experimental measurements of water content of methane gas in equilibrium with hydrate were presented at 1000 and 1500 psia for temperatures greater than -10°F. The differences between methane and natural gas hydrates were stressed.

Smith, J. M. S., Mathew, R. C. and Cool, J. A. F., "The Safety of Gas Carriers with Particular Reference to the ICS Tanker Safety Guideline (Liquefied Gas)." Presented at Gastech 75, Paris, September 30-October 3, 1975.

This paper provides an overview of the hazards of operating an LNG carrier with particular emphasis on personnel training.

Smith, K. A., Lewis, J. P., Randall, G. A. and Meldon, J. H., "Mixing and Rollover in LNG Tanks." Paper presented at the Cryogenic Engineering Conference, Atlanta, GA, August 8, 1973.

Criteria and data are presented for deciding whether a specific LNG installation need have both top and bottom fill capacity. In general, a large facility will benefit from such capability if it is to receive a variety of LNG compositions from a variety of ships. It is further shown that the top fill device requires surprisingly careful design in order to assure good mixing at the free surface.

Smith, K. A. and Reid, R. C., The Effect of Composition on the Boiling of LNG on Water. M.I.T. LNG Research Center, 1976 Annual Report, Task IV, to the American Gas Association BR 87-6, January 1977.

The results obtained thus far with binary and ternary mixtures indicate that a preferential evaporation of methane does indeed take place, followed by the preferential evaporation of the next more volatile component ethane. Propane is the last component to evaporate. Although a preferential evaporation takes place, the vapors are a mixture very rich in the volatile component but a mixture after all.

Smith, K. A. and Reid, R. C., Electrostatics and its Hazards in Petroleum Industry and LNG Systems. M.I.T. LNG Research Center, 1976 Annual Report, Task V, to the American Gas Association BR 87-6, January 1977.

The paper discusses streaming potentials and sedimentation potentials in relation to static charge generation as a consequence of hydrocarbon flow through pipes.

Smith, K. A. and Reid, R. C., Boiling of LNG on Dike Floor Materials. M.I.T. LNG Research Center, 1976 Annual Report, Task VI, to the American Gas Association BR 87-6, January 1977.

The rate of vaporization of LNG spilled on a number of substrates was measured experimentally. Included in the materials tested: insulated concrete of two densities, soil, sand, pebbles, wet and dry polyurethane. In all cases, the early rate of vaporization could be well correlated with simple, one-dimensional conduction heat transfer.

Smith, M., ed., Recommended Guide for the Prediction of the Dispersion of Airborne Effluents. Published by the American Society of Mechanical Engineers, May 1968.

The guide discusses meteorological fundamentals, airborne effluents, stack height, dispersion and deposition, data sources and experimental methods, and gives calculation methods and examples.

Smith, R. V., "The Influence of Surface Characteristics on the Boiling of Cryogenic Fluids." J. of Eng. for Industry. 91:1217-1221, 1969.

The influence of a solid heating surface on the boiling behavior of liquid helium, hydrogen and nitrogen is being discussed. This is a review article and contains essentially no new information.

Snellink, I. G., "Hazard Assessment of LNG Supply and Storage." Communication of the Netherlands Delegation, January 1978.

The author describes a risk analysis of the supply and storage of LNG at a facility near the river Maas on the Dutch coast.

Solberg, D. M., Nylund, J. and Hansen, H. R., "Safety and Reliability of Floating LNG Protection Facilities." Fifth International Conference on LNG, Session III, paper 6, Institute of Gas Technology, 1977.

Safety guidelines for the construction and classification of floating facilities for gas processing, liquefaction, and storage are being reviewed.

Solberg, D. M., J. A. Pappas and E. Skramstad. "Observations of Flame Instabilities in Large Scale Vented Gas Explosions." Paper presented at the 18th International Symposium on Combustion, August 17-22, University of Waterloo, Canada, 1980.

Experiments on vented gas deflagrations performed in a 35-m^3 prismatic steel module showed that Taylor instabilities may be the dominating mechanism governing the pressure load from even freely vented explosions depending on the point of ignition and venting layout. The pressures obtained were higher than expected based on simple volume scaling of previous explosion tests on laboratory scale. The simple volume scaling of vented gas deflagration based on constant burning speed thus seems to be invalid for vessel volumes at least up to 35 m^3 and is furthermore non-conservative.

Solberg, D. M., J. A. Pappas and E. Skramstad. "Experimental Investigations of Flame Acceleration and Pressure Rise Phenomena in Large Scale Vented Gas Explosions." Paper presented at the 3rd International Symposium on Loss Prevention and Safety Promotion in the Process Industries, Basle, 1980.

Existing equations and formulas used to relate maximum pressure-to-vent area are mainly based on small scale laboratory tests and show very large discrepancies. Experiments performed in a 35-m^3 prismatic steel module show that deflagrations in larger rooms are of much more complex nature and may give higher pressures than expected from small scale tests. Explosions with uncovered vents show several pressure peaks and the maximum pressure rise occurs at a higher gas concentration than the one giving maximum laminar burning velocity.

Several phenomena which explain the pressure-time history from gas explosions in larger enclosures have been observed. This includes distortion of the flame front by the flow field set up by the venting, confinement and vent area geometry and combustion instabilities. An improved calculation model is presented and estimated values compared to observed ones.

The results of this investigation are useful for the understanding of deflagration processes and for prediction of the loads from deflagrations.

Solberg, D. M. Unconfined Vapor Cloud Explosions-A Prestudy. Report No. 79-0615. Det Norske Veritas, Hovik, Norway, 1979.

This study reviews the hazard potential to offshore facilities from unconfined vapor cloud explosions and examines ways that this hazard can be predicted and reduced by preventive and protective design. Damage potential from an unconfined vapor cloud is determined by the rate of energy release (or flame speed) during explosion. Factors that accelerate the flame increase the damage potential. Additional research to quantitatively define the mechanism of flame acceleration is recommended. Vapor cloud explosions on offshore platforms may be coupled to confined vented explosions. Additional research is needed on situations where a confined explosion propagates to an external vapor cloud with subsequent explosion.

Solomon, B., "Cove Pt. LNG Terminal to Resume Operation After Accident." The Energy Daily. pp. 1-2, October 19, 1979.

A recent accident at the Cove Point, Maryland liquefied natural gas facility is described. Seepage of LNG from a high pressure pump resulted in a gas explosion which killed one employee and critically injured another.

Spangler, C. V., "Storing Gases." U.S. Patent 2,663,626 (to J. F. Pritchard and Co.), 1953.

Natural gas was cooled to slightly above its boiling point and adsorbed on activated carbon or silica gel. Release of adsorbed gas was achieved by contacting heated natural gas with the solid support.

Speir, G. A., "Indonesia's Badak LNG Project Sets New Records." Pipeline and Gas Journal. June 1978.

This article discusses design, construction, startup and operation of the Badak export terminal. The facility liquefies gas for shipment to Japan.

Srinivason, K., et al., "Effect of Floating Insulation on Free Surface of Cryogenic Liquids in Open Containers." 6th Internat. Cryog. Eng. Conf., pp. 258-262, IPC Science and Technology Press Ltd., Guilford, England, 1976.

The effect of floating insulation materials on the evaporation rate of cryogenic liquids is investigated. Normally, this rate can be reduced by up to 25%.

Staff Writer. "Thyssengas Uses LNG as Reserve Supply." Pipeline & Gas J. 207(13):28-30, 1980.

A mobile LNG trailer is described that can be used to provide continued gas supply for both scheduled and unscheduled emergency interruptions. The full unit consists of the LNG tractor-trailer, a mobile vaporizer, and a portable power supply.

Staff Writer. "LNG Scorecard." Pipeline & Gas J. 209(13):26-36, 1981.

The latest listing of U.S., Canadian and International peakshaving facilities is presented, including both small and large satellite plants as well as baseload LNG facilities and import/receiving terminals around the world.

Staff Writer. "Worldwide LNG Projects Hit by Price, Contracts." Pipeline & Gas J. 209(13):23-24, 1981.

Three-fourths of the world's LNG trade was going to Japan in 1980. Controversy over LNG pricing has affected exports from Algeria to the U.S. A new contract is still under negotiation.

Stanfill, I.C., "Startup Experiences and Special Features at Memphis LNG Plant." Presented at the First LNG International Conference, Chicago, IL, April 7-12, 1968.

This paper describes four major and several minor equipment malfunctions which occurred during startup and the first six months of operation at the Memphis LNG plant. Several process flow diagrams for the Memphis plant are included.

Stein, W., LNG Fireball Thermal Radiation. UCID-18190, Lawrence Livermore Laboratory, 1977.

The highly simplified computational method is presented for the determination of thermal radiation, emanating from a LNG fireball. Quantitative results are given in a series of diagrams.

Stein, W., Vapor Generation from a 40 m^3 Instantaneous LNG Spill into a 100 m^2 Diked Soil Area. UCID-18188, Lawrence Livermore Laboratory, 1978.

A simple heat transfer model is presented in the evaporation of LNG spilled into a diked area. Some numerical results are given.

Stein, W., "The Spreading of Differential Boil-Off for a Spill of LNG on a Water Surface." Report A, Liquefied Gaseous Fuels Safety and Environmental Control Assessment Program; A Status Report. DOE/EV-0036, Department of Energy, Washington, DC, 1979.

A computer program is described which calculates pool size, differential boil-off and spreading rate for LNG spills on water. Results compare favorably with experimental data.

Stein, W. and D. L. Ermak. One-Dimensional Numerical Fluid Dynamics Model of the Spreading of Liquefied Gaseous Fuel (LGF) on Water. Report No. UCRL-530378, Lawrence Livermore Laboratories, Livermore, California, 1980.

A computer model is described which calculates the height and the diameter of a continuous and instantaneous spill of LGF on water. Typical results of the calculations are presented in both tabular and graphical form. However, there are no comparisons with actual test data.

Steinmetz, G. F., "Special Combustion Characteristics and Blending Problems of LNG, SNG, and LPG Gases." Symp., New Fuels and Advances in Combustion Technologies, pp. 1-14, 1979.

Imported LNG is interchangeable with domestic natural gas if minor changes in the supply facilities and their operation are tolerable and if burners are derated or physically changed. Otherwise, minor problems might arise, which would reduce efficiency and would require more frequent service of the burners.

Stephan, K., "Evaporation Rate of Liquid Natural Gas in Large Containers." Thermo and Fluid Dynamics. 11:53-61, 1973.

Natural gas is often stored in large isolated metal containers. Heat flow through the bottom, the side wall and the cover to the stored liquid are practically independent from each other due to the large dimensions of such containers. Based on this simplification the evaporation rate of the liquid is calculated by means of the Laplace Transformation and a specific difference equation. With the results it is possible to determine the time after which freezing in the surrounding soil commences. The rate of heat flow to the condensed gas proved to be practically unaffected by the ice-formation in the soil. (in German)

Steward, F. R., "Linear Flame Heights for Various Fuels." Combustion and Flame. 8(3):171-178, September 1964.

The flame heights of linear diffusion flames for several different fuels have been correlated with a single parameter derived from a model assuming mixing controlled combustion. The assumptions involved are stated clearly.

Steward, F. R., "Prediction of the Height of Turbulent Diffusion Buoyant Flames." Combustion Science and Technology. 2:203-212, 1970.

A mathematical model of a turbulent diffusion buoyant flame based on a number of simplifying assumptions is presented. It was found that the height at which 400% excess air has been entrained corresponds to the visible flame height according to data taken in our laboratory as well as that presented by a number of other workers.

Stewart, A. "San Diego Gas & Electric Company LNG Plants." LNG Terminals and Safety Symposium, pp. 364-369, in Applications of Cryogenic Technology 9, Scholium International, Flushing, New York, 1979.

The operation of LNG peakshaving plants is described. This includes: cleaning the feed gas, chilling the gas, liquefying the gas, storage, and revaporization.

Stewart, A. N. "LNG Research Programs." LNG Terminals and Safety Symposium, pp. 190-194, in Applications of Cryogenic Technology 9, Scholium International, Flushing, New York, 1979.

The objectives for LNG research, sponsored by the Gas Research Institute, are outlined. They are primarily concerned with LNG properties, LNG vapor dispersion, LNG fire control, and basic LNG research being conducted by MIT LNG Research Center.

Strehlow, R. A., "Unconfined Vapor Cloud Explosions - An Overview." Paper presented at the 14th Symposium on Combustion, The Combustion Institute, Pittsburgh, PA, 1973.

The author summarizes the history of accidental vapor cloud explosions, reviews the work that has been done to understand the dispersion, ignition, propagation and blast effects produced, then points out areas for future investigation.

Strehlow, R. A. et al., "On the Measurement of Energy Release Rates in Vapor Cloud Explosions." Combustion Science and Technology. 6:307-312, 1973.

The method is based on the finite amplitude isentropic acoustics of a centered spherical wave and involves the reduction of data from 3 pressure gauges which are measuring the explosion. The method of characteristics is used to back calculate to an effective spherical piston which replaces the explosion so energy release rates of the explosion can be calculated.

Strehlow, R. A. and Baker, W. E., "The Characterization of Accidental Explosions." Prog. Energy Combustion Science. Pergammon Press, 1976.

The authors review actual explosion incidents and classify them into several categories. Basic theory in blast wave damage is also discussed along with the effects of "non-ideal" blast waves. Future areas of research are recommended.

Strehlow, R. A., Luckiatz, R. T., Adamczyk, A. A. and Shimpi, S. A., "The Blast Wave Generated by Spherical Flame." Combustion and Flame. 35(3):297-310, August 1979.

The authors report on their work for determining the overpressures and impulses resulting from reactive fronts. Some results are presented for hydrocarbon mixtures. This paper may have application to blast wave effects estimation.

"Strong Global LNG Trade Growth Seen." Oil and Gas J. 77:36-37, December 1979.

It is expected that world LNG trade will double in the next 5 years, reaching about 3 trillion cu ft/yr by 1985. However, U.S. import policy will remain uncertain because of safety, siting, liability, and insurance issues.

Stuckly, J. M. and Walker, G., "Hydraulics a Key to Optimizing LNG Pipelines." Oil and Gas J. 77(17):68-70, 1979.

By carrying out detailed numerical calculations for the considered LNG pipeline, it is shown that under optimized conditions a liquid carrying pipeline offers improved fuel efficiency when compared with a conventional vapor-phase line.

Stuckly, J. M. and Walker, G., "LNG Long-Distance Pipelines--A Technology Assessment." Oil and Gas J. 77(16):59-63, 1979.

An outline design study for a 1,430-mile LNG pipeline in Northern Canada is described. The tradeoffs between operating temperatures, pressures, pipe diameter, insulation, and material requirements are discussed in some detail. So far no large-diameter, long-distance LNG pipelines have actually been built, but they have received a lot of attention recently.

Study of LNG Safety - Parts I and II. Tokyo Gas Company Ltd., Central Laboratory, February 1971.

This two-part study presents experimental results on LNG evaporation, combustion and dispersion characteristics in a dike, and on LNG evaporation, ice formation, and LNG dispersion on water.

Stuhmiller, J. H. and Ferguson, R. E., Comparison of Numerical Methods for Fluid Flows, EPRI Report NP-1236, RP 888-1, November 1979.

The numerical dispersion (velocity) and dissipation (amplitude) of initial value data for the transient convection equation (1-D) for fourteen numerical methods are studied. Three initial data profiles are used and results are compared to the analytic answer.

Sunvala, P. D., "Dynamics of the Buoyant Diffusion Flame." Journal of the Institute of Fuel. 40:492-497, 1967.

A new theoretical treatment of the axial velocity growth and mass concentration decay in a buoyant diffusion flame is presented. It has been found that for the flame lengths of burning of various fuel gases, organic liquids as well as fuel oils, the one-fifth power index for the Froude Number holds good. However, for the flame lengths of burning firewood in cribs, the two-fifths power index for the Froude Number is suggested.

Sutherland, V. and J. E. Hughes, "Subterranean LNG Storage." Energy Digest. 3:15-17, October 1978.

The construction of six storage cavities in underground salt formations is described. Each cavity can hold about 60 x 10^6 m^3 LNG at pressures between 120 and 270 bar.

Sutton, S. B., Overpressure Prediction. UCID-18189, Lawrence Livermore Laboratory, 1977.

A simple calculation is performed to determine the energy within a burning cloud of LNG. This energy is assumed to have the same pressure effect as an energy-equivalent quantity of TNT.

Taki, S. and Fujiwara, T., "Numerical Analysis of Two-Dimensional Nonsteady Detonators." AINA Journal. 16, January 1978.

This paper is a report about the numerical calculation of two-dimensional detonation propagation in a confined channel. A simplified chemical kinetics was employed. The method may have application to the study of detonation probabilities for methane-air mixtures.

Tanker Structural Analysis for Minor Collisions. U.S. Coast Guard Report CG-D-72-76. NTIS No. AD/A031031, December 1975.

This report describes the work accomplished during the course of the project of the Evaluation of Tanker Structure in Collision. The intent of the report is to present the investigations performed in evaluating the phenomena that contribute to the ability of a longitudinally framed ship, particularly a tanker, to withstand a minor collision. A minor collision is one in which the cargo tanks remain intact. The ability to withstand a minor collision is quantized by the total energy that can be absorbed during the collision.

Tarifa, C. S., Del Notario, P. P. and Valdes, C. F., Open Fires. Final Report, U.S. Department of Agriculture, Forest Service, Grant FG-SP-114 and 146, May 1967.

An experimental study was made of some basic laws of open fires by utilizing the pool fire techniques. Data were obtained for burning rates, energy balances and flame characteristics, including the influence of fuel type, vessel size and vessel configuration.

Taylor, P. B. and Foster, P. J., "Some Gray Gas Weighting Coefficients for CO_2-H_2O Soot Mixtures." International Journal of Heat Mass Transfer. 19:1331-1332, 1975.

Two tables are provided which give 1) the values of constants which specify weighting factors for various soot concentrations applicable in the temperature range 1400 to 2400°K and 2) values of constants which specify the gray gas absorption coefficient applicable in the 1200 to 2400°K temperature range.

te Riele, P. H. M. "Atmospheric Dispersion of Heavy Gases Emitted at or Near Ground Level." Second International Loss Prevention Symposium, 1977: 347-357.

This paper presents a theory developed at Koninklijke/Shell-Laboratorium, Amsterdam (KSLA) for predicting the atmospheric dispersion of heavy gases emitted at or near ground level. The paper showns the validity of the theory by comparing it with available experimental data, and discusses its applicability.

Terry, M. C., "Floating LNG Facilities May Solve Many Problems." Pipeline and Gas Journal. pp. 25-28, June 1977.

This article discusses the history of development of offshore liquefaction facilities. Various generic types of floating facilities are discussed and their potential evaluated.

Thermal Radiation and Overpressure from Instantaneous LNG Release into the Atmosphere. TRW Systems Group Report No. 08072-4, to A.G.A., April 26, 1968.

The report conclusions express belief that 1) a stoichiometric mixture of natural gas and air at atmospheric pressure will not detonate with a charge of high energy explosive equivalent to 625 grams of TNT; 2) the parameters of charge energy, mixture composition and confining wall geometry should be further investigated.

Thomas, P. H., "The Size of Flames From Natural Fires." Paper presented at the 9th International Symposium on Combustion, 1963.

Uncontrolled fires produce flames where the initial momentum of the fuel is low compared with the momentum by buoyancy. The heights of such flames with wood as the fuel are examined and discussed in terms of both a dimensional analysis and the entrainment of air into the turbulent flame. Some recent experiments on the effects of wind on such flames are also reported.

Thomas, P. H., Baldwin, R. and Heselden, A. J. M., "Buoyant Diffusion Flames: Some Measurements of Air Entrainment, Heat Transfer, and Flame Merging." Paper presented at the 10th International Symposium on Combustion, the Combustion Institute, 1965.

Thistledown has been used as a tracer to measure the flow of air toward ethyl alcohol and wood fires 91 cm in diameter, and a smaller town gas fire. The measured mean axial temperature rise at the mean flame height was about 300° to 350°C for wood and alcohol and 500°C for town gas.

Thurley, J., Drouineau, M. and Santoleri, J. J., "Economic Considerations in the Selection Between Fired and Seawater Vaporizers." GasTech Workshop, Houston, 1979.

Submerged combustion vaporizers for LNG are usually preferred over seawater vaporizer for ecological reasons, even though the latter are more economical. A combination of the two versions appears to be the best overall choice.

Timmerhaus, K. D. and Flynn, T. M., "Safety with Cryogenic Systems." Advances in Cryog. Eng. 23:721-729, 1978.

Safety aspects of cryogenic fluids are discussed from a practical point of view. Rules and suggestions for the safe handling of such fluids are given.

TNO. Methods for the Estimation of the Consequences of the Releases of Dangerous Material (Liquid and Gases). TNO-Report 3386, 1979.

A report was made to Directorate-General of Labor of the ministry of Social Affairs dealing with the releases of dangerous liquids and gases. These include outflow, spray releases, evaporation heat radiation from burning pools, and dispersion of natural gas cloud.

Tomkins, B. G., "LNG Plant Computer System: A Conceptual Philosophy." Oil and Gas J. 77(48):56-60, 1979.

A computer in an LNG plant must be designed around the plant operating plan. Consideration must also be given to maintenance and safety plants. Suggestions for useful hard and software selections are provided.

Tonnessen, A., Insulated Tanks for Liquefied Gas. U.S. Patent 4,141,465, 1979.

To reduce boil-off in spherical LNG tanks, the tank skirt is supplied with a special low conductivity ring insert, made of 18-8 SS. Such a heat flow resistance can reduce the heat leak through the skirt by about 50 percent.

Tsai, S. S. and Chan, S. H., A General Formulation and Analytical Solution for Multi-Dimensional Radiative Transfer in Non-Gray Gases. A.I.Ch.E., A.S.M.E. Heat Transfer Conference, Salt Late City, Utah, (77-HT-51), August 1977.

The equations of radiative transfer (spectral) are cast into band absorptance from the multidimensional geometries. Optically thick and thin limiting expressions are thus deduced and discussed.

Tsatsaronis, G., "Prediction of Propagating Laminar Flames in Methane, Oxygen, Nitrogen Mixtures." Combustion and Flame. 33:217-239, 1978.

A fundamental analysis of one dimensional flame propagation (including chemical kinetics and transport [processes] of methane flames) is performed. Flame speed, flame structure and pressure effects are enumerated.

"Turbine/Compressor Serves First 50/50 Methane-Nitrogen Cycle Gas System." Diesel and Gas Turbine Progress.

A unique liquefaction plant at a peakshaving facility is described. Considerable detail, including several photographs, on the refrigerant compressor is provided.

Turner, D. B., Workbook of Atmospheric Dispersion Estimates. Publication No. 99-AP-26, Public Health Service, 1969.

This workbook presents methods of practical application of the continuous plume dispersion model with a Gaussian distribution to estimate concentrations of air pollutants. Estimates of dispersion are those of Pasquill as restated by Gifford. Emphasis is on the estimation of concentrations from continuous sources for sampling times up to 1 hour.

Tutko, T. J., "How to Design an Integrated Security System for an LNG Facility." Pipeline and Gas Journal. 121:50-62, July 1979.

The need for a integrated security system at all major LNG facilities is demonstrated. Various suggestions are given as how to best implement such a system.

Uhl, A. E., Amoroso, L. A. and Seitir, R. H., "Safety and Reliability of LNG Facilities." Presented at the ASME Petroleum Mechanical Engineering and Pressure Vessels and Piping Conference, New Orleans, LA, September 17-21, 1972.

The prime factors behind the fine operational safety and reliability record of LNG facilities are the early definition and understanding of the nature of LNG, the establishment and utilization of relevant codes, the casting and observation of pertinent quality assurance programs, and thorough training of plant operators. This paper discusses each of these factors in detail.

Uldenvan, A. P., "The Unsteady Gravity Spread of a Dense Cloud in a Calm Environment," paper presented at the International Technical meeting on Air Pollution Modeling and its Application, NATO-CCMS, Rome, October 26, 1979.

Simplified bulk momentum equations for one dimensional and axisymmetric gravity spreading of dense clouds are presented. Analytical solutions indicate that a steady state is not reached during cloud spreading.

U.S. Coast Guard. Experiments Involving Pool and Vapor Fires from Spills of Liquefied National Gas on Water. Report No. CG-D-55-79. National Technical Information Service, Springfield, Virginia, 1979.

A series of 16 tests were conducted at the Naval Weapons Center involving the spill and ignition of liquefied natural gas (LNG) on water. Two kinds of fires were studied; namely, pool fires and vapor cloud fires. The principal objective of the tests was to measure the thermal characteristics. The quantities of spilled LNG varied between 3 and 5.5 m^3 with spill durations from 30 to 250 s. Thermal radiation from the fires was measured using wide-angle and narrow-angle radiometers and a spectrometer. The data from the tests have been analyzed for pool spread, liquid regression rate, flame heights, thermal radiative output and LNG fire spectra. Models useful for evaluating LNG fire hazards are indicated in the report. Mean flame emissive power measured was about 210 kW/m^2 and estimated flame temperature was 1500 K. Co_2, H_2O, and soot appear to be the principal radiating species. Vapor cloud burning was close to the ground with a propagating plume fire. The velocity of propagation was function of the wind speed. A peculiar fire halting behavior noticed was observed and possible reasons for the behavior are discussed in the report.

U.S. Comptroller General, Need to Improve Regulatory Review Process for Natural Gas Imports. ID-78-17, General Accounting Office, July 14, 1978.

The article highlights difficulties in the review process for LNG importation facilities and makes recommendations to Congress and federal agencies to mitigate the impacts.

U.S. General Accounting Office, Information on the U.S. Importation of Liquefied Natural Gas. EMD-79-48, March 22, 1979.

The report deals with questions on LNG consumption in the U.S., the sources and prices for the imported LNG and with its end use by the utility companies. It also addresses size and ownership of the LNG tanker fleet.

"Using LNG Cold Energy More Efficiently." Oil and Gas Journal 78:174-182, March 17, 1980.

Several advanced methods are described that allow a more efficient vaporization of LNG. These include: submerged combustion, seawater vaporization, ethylene plants using LNG for refrigeration, power generation with closed and open gas turbine cycles, and use of multicomponent working fluids.

Valencia-Chavez, J. A. and Reid, R. C., "The Effect of Composition on the Boiling Rates of Liquefied Natural Gas for Confined Spills on Water." Int. J. Heat Mass Transfer. 22:831-838, 1979.

Boiling rates for spills of LNG on a confined area of water (calorimeter) were measured for various LNG compositions. A simplified model was developed which compared well with experimental results.

Van Buijtenen, C. J. P., et al., Dispersion and Analysis of Methane in the Atmosphere. N78-26644, 1976.

An analytical model, based on atmospheric diffusion, has been developed for the dispersion of methane from a large LNG spill. No experimental verification is supplied.

Van Buijtenen, C. J. P. Calculation of the Amount of Methane in the Explosive Region of a Time-Dependent Source. Chemisch Laboratorium TNO Report 1975-10.

As an extension of the work on instantaneous and continuous sources, a model was developed to calculate the downwind concentrations as functions of time for a time-dependent source. The calculated concentrations are compared with published experimental data.

Vanderwall, E. M., "Investigation of the Suitability of Gelled Methane for Use in a Jet Engine." NAS 3-14305, NASA CR-72876, 1971.

Methanol gelled cryogenic methane was storable at -263°F for periods exceeding 100 hours with no significant gel structure degradation. The gel could be transferred through properly designed heat exchangers at comparatively high flow rates (10 lb/hr) without clogging. Fuel consumption by jet engines was not excessive due to the gelant.

Van Horn, A. J. and Wilson, R., Liquefied Natural Gas: Safety Issues, Public Concerns, and Decision Making. BNL 22284, Energy and Environmental Policy Center, Jefferson Physical Laboratory, Harvard University, November 1976.

The report provides background information on LNG and discusses safety issues, LNG facilities siting disputes, public concern for LNG facilities siting, LNG decision making, and gives recommendations concerning LNG terminal siting facilities.

Vanta, E. B. et al., Detonability of Some Natural Gas-Air Mixtures. Technical Report AFATL-TR-74-80, Air Force Armament Laboratory, Elgin Air Force Base, April 1974.

A bag test method to screen natural gas-air mixtures (5.2 to 12.5% by vol. natural gas) to determine detonability. At the 8.6 to 8.8% concentration level, erratic, uneven detonations were initiated and explosive charges ranged from 1001 to 1020 grams. Deflagration occurred at all other fuel concentrations. The detonations propagated the length of the bag, but a steady Chapman-Jouguet type wave front was not observed.

Van Ulden, A. P., "On the Spreading of a Heavy Gas Released Near the Ground." Loss Prevention and Safety Promotion in the Process Industries. Bushman, C. H., ed. Proceedings of the First International Loss Prevention Symposium. The Hague/ Delft, The Netherlands, May 28-30, 1974, Elsevier Scientific Publishing Company, 1974.

It is shown that the spreading of a heavy gas differs essentially from the spreading of a neutral gas. Horizontal spread is increased considerably by gravity effects, whereas vertical spread is limited. Calculations are compared with experimental results.

Varma, R. K., Murgai, M. P. and Ghildyal, C. D., "Radiative Transfer Effects in Natural Convection Above Fires - General Case." Proc. Roy. Soc., London, A314, 1970.

The effect of radiation, on the overall dynamics of a hot plume above fires, has been considered. An approximate multidimensional transfer equation for heat radiation is derived from the Schwarzschild's equation. The plume material is assumed to be grey and the outside atmosphere is considered calm and is, otherwise, in a state of arbitrary lapse rate variation.

Verma, S. B. and Cermak, J. E., "Mass Transfer From Aerodynamically Rough Surface." International Journal of Heat and Mass Transfer. 17:567-579, 1974.

Mass transfer rates were determined by directly measuring the actual volume of water evaporated from saturated wavy (sinusoidal) surfaces in micrometeorological wind tunnel. Simultaneous measurements of mean velocity, humidity and temperature distributions were made over these saturated waves.

Vielvoye, R., "Abu Dhabi Activity Soars, but Government Keeps Lid on Production." Oil and Gas Journal. p. 74, July 9, 1978.

Included in this article is a discussion of some of the problems which have plagued the Das Island export terminal. These include cracked cryogenic pipelines, corrosion from high-sulfur gas, and a leak in the inner shell of a storage tank which eventually caused a crack in the outer shell.

Vora, M. K., Shaheen, E. I. and Knieves, D. V., "U.S. Energy Future: Higher LNG Imports Will be Needed." World Oil. pp. 134-148, June 1978.

The future U.S. energy needs and the potential of LNG imports are discussed. It is predicted that LNG could supply 4.7% of total U.S. energy requirements by 1985. This would require an import of 4.86 tcf including 1.17 tcf from Alaska.

Vreedenburger, H., "Steel or Prefab Concrete for Inshore Plants." Chemical Engineering Progress. pp. 82-85, 1979.

The use of steel and concrete in the construction of a floating LNG receiving terminal is discussed. Concrete can offer some advantages in the storage tank design and construction.

Wakeshima, H. and Takata, K., "On the Limit of Superheat." Journal of the Physical Society of Japan. 13(11):13-1403, November 1958.

A new method was devised in which small drops of a sample liquid are heated as they rise up in the nonsoluble heating liquid with a suitable temperature gradient upward. The limit of superheat was determined for saturated hydrocarbons and polymethylenes. The agreement between (Doring's) theory and experiment was satisfactory.

Weber, D., "Electric Power Generation and LNG Evaporation with the Aid of Gas Turbines Within a Closed Cycle Process." CONF 78-155-010, (in German), 1978.

By taking advantage of the low temperature of evaporating LNG, the efficiency of a closed-cycle gas turbine could be substantially increased. This would represent a valuable contribution to energy conservation in LNG evaporating plants.

Weber, D., "Recovery of Energy from LNG Vaporization." Presented at the Meeting on Industrial Processes: Energy Conservation R and D. pp. 173-189. H. Ehringer, G. Hoyaux (eds.). Washington, DC; European Community Information Service, 1979.

With the proposed cold utilization process of a closed-cycle gas turbine plant, an electrical output of 182 MW is produced with an efficiency of 53%. The specific power generation costs are 0.043 DM/kWh in baseload operation. With the combination of a closed-cycle gas turbine and a diesel engine, an efficiency of 60% can be achieved.

Welker, J. R., Brown, L. E., Ice, J. N., Martinsen, W. E. and West, H. H., Fire Safety Aboard LNG Vessels. U.S. Coast Guard Report No. CG-D-94-76. NTIC No. AD/A030619, January 1976.

This report presents results of an analytical examination of cargo spill and fire hazard potential associated with the marine handling of liquefied natural gas cargo. Principal emphasis was on cargo transfer operations at receiving terminals, and more specifically on the LNG tanker's cargo handling and hazard sensing and control equipment and operations.

Welker, J. R., Wesson, H. R. and Brown, L. E., "Use of Foam to Disperse LNG Vapors?" Hydrocarb. Process. pp. 119-120, 1974.

Tests have shown that a blanket of high-expansion foam effectively reduces ground-level methane concentrations downwind of an LNG spill.

Welker, J. R. et al., "LNG Spills: To Burn or Not to Burn." Paper presented at the A.G.A. Operating Section Distribution Conference, 1969.

This paper concludes that: flammable mixtures from large spills will penetrate a long distance downwind; a major spill should be ignited as soon as possible; a high-expansion foam system offers the best protection by suppressing either LNG evaporation or the burning rate and present standards that specify separation distance irrespective of pool size are meaningless.

Welker, J. R., Pipkin, O. A. and Sliepcevich, C. M., "The Effect of Wind on Flames." Fire Technology. 1(2):122-219, 1965.

A simplified and improved correlation for the drag coefficient of windblown natural gas flames is given. Experimental results leading to the correlation were obtained in a low-speed wind tunnel specifically designed for such studies at the University of Oklahoma North Campus.

Welker, J. R. and Sliepcevich, C. M., "Bending of Wind-Blown Flames From Liquid Pools." Fire Technology. 2, 1966.

The bending of a flame by wind influences the amount of heat transferred by radiation and convection, the fuel burning rate, and the flame spread rate. To what extent will a flame be bent by wind? The author presents correlations of data taken from liquid pool fires, which enable us to predict flame bending and trailing for large fires.

Welker, J. R., West, H. H., Mento, M. A. and Ice, J. N., A Survey of the Effectiveness of Control Methods for Fires in Some Hazardous Chemical Cargoes. U.S. Coast Guard Report CG-D-64-76. NTIS No. AD/A026300, March 1976.

Assessment of fire safety of marine bulk chemical carriers was attempted. It is recommended that standard fire control test methods be developed together with standardized test data collecting and reporting methods and that large-scale fire tests be made on chemicals from different families to attempt to develop methods of correlation with small-scale test results. If a reliable correlation can be developed, small-scale tests could be used in the future with more confidence to both predict behavior of chemical cargoes under fire conditions and to assess large fire extinguishing effectiveness.

Wesson, H. R. "LNG Fire Training Schools." LNG Terminals and Safety Symposium, pp.340-345, in Applications of Cryogenic Technology 9. Scholium International, Flushing, New York, 1979.

The paper presents a summary of the training materials presented and the type of fire training problems used at two nationally known fire training schools that specialize in LNG fire fighting.

Wesson, H. R., Lott, J. L., Feldman, R. and Closner, J. J., "Thermal Performance of a Fire Resistant Coating Applied to Prestressed Concrete." 1978 Operating Section Proceedings, American Gas Association, Montreal, Quebec, May 1978.

The fire resistance of coatings designed to protect weakening of prestressing wire in cryogenic tanks is tested. Degree of protection with coating thickness is discussed.

Wesson, H. R., Welker, J. R. and Brown, L. E., "Control LNG-Spill Fires." Hydrocarb. Process. 51:61-64, December 1972.

Control of LNG-spill fires is obtained by application of high expansion foam. Follow-up with dry chemical fire extinguishers will quickly extinguish the fire.

Wesson, H. R., J. R. Welker, L. E. Brown, "Control of LNG Spill Fires on Land." Advances in Cryog. Engg., 20:151-163, 1974.

The effects of high expansion foam and of commercially available dry chemical agents on LNG fires have been evaluated in a quantitative way. Both fire control and vapor dispersion were investigated at various application rates of the agents.

West, H. H., Brown, L. E. and Welker, J. R., "Vapor Dispersion, Fire Control, and Fire Extinguishment for LNG Spills." NTIS No. AD/A023505, pp. 509-518, Proceedings of the Fourth International Symposium on Transport of Hazardous Cargoes by Sea and Inland Waterway. Jacksonville, FL, October 26-30, 1975.

Dry chemical fire extinguishment systems can provide rapid extinguishment of LNG fires. High expansion foam can reduce the radiant flux from LNG fires, provide protection for the surroundings until the fire burns out, and reduce the concentration of methane in the vapor cloud downwind from an LNG fire.

West, H. H., Brown, L. E. and Welker, J. R., "Vapor Dispersion Fire Control and Fire Extinguishment for LNG Spills." The Combustion Institute, 1975 Spring Technical Meeting. San Antonio, Texas, 1975.

The paper reports results on AGA tests of LNG evaporation and pool fire radiation reductions by foam application. Tests also demonstrated flame extinguishment by dry chemicals if applied a short time after pool fire ignition.

Westbrook, C. K., A Generalized ICE Method for Chemically Reactive Flows in Combustion Systems. UCRL-78915, Rev. 1, Lawrence Livermore Lab., August 1977.

The ICE method is modified to allow the pressure calculated at a new time step to include the effects of changes in internal energy and species over that time step. This is important for reactive flows in which the change in temperature and/or species contributes significantly to changes in pressure.

Westbrook, C. K., "An Analytical Study of the Shock-Tube Ignition of Mixtures of Methane and Ethane." Comb. Sci. & Techn. 20:5-17, 1979.

The results of a detailed analytical study of the ignition of methane/ethane mixtures show good agreement with previous shock tube experiments. Even small amounts of ethane, as found in LNG, will drastically reduce the ignition delay times of pure methane.

Westbrook, C. and Haselman, L., Chemical Kinetics of LNG Detonations. UCRL-82293, Lawrence Livermore Laboratory, February 1979.

The authors of this paper theoretically investigate the effect of ethane on the detonability of methane. Small amounts of ethane were found to significantly increase the possibility of a detonation occurring. The chemical kinetics of the reaction mechanism are also presented.

Westbrook, C. K., Modeling of Laminar Flames in Mixtures of Vaporized Liquefied Natural Gas (LNG) and Air." UCID-18540, 1980.

A simplified chemical kinetics submodel is described which analytically represents the fuel/air burning in a large LNG spill.

Weston, H. and Brown, L.E., "Analyze Fire Protection System." Hydrocarbon Processing. pp. 89-92, August 1977.

This paper outlines a systems approach to fire safety and gives an example application to LNG Fire Control.

Wethenbach, H. G. "Ausbreitung von Flammen an zylindrischen Behältern (Tanks) für flüssige Kohlenwasserstoffe." (Spreading of Flames on Cylindrical, Liquid Hydrocarbons Tanks.) Gas-Wasserfach, Gas Erdgas. 112:383-386, August 1971.

Storage of LNG can take place either in surface - or underground tanks. Either solution requires adequate safety and fire prevention measures. For storage of LNG, the same criteria concerning fires apply as for liquid petroleum products.

Wilcox, D. C., "Model for Fires With Low Initial Momentum and Nongray Thermal Radiation." AIAA Journal. 13(3):381-386, March 1975.

A new ambient-air entrainment law accounts for rapid fluid acceleration from initially low velocity at a liquid pool, to higher velocities established under buoyant rise of the combustion products. Radial-radiation heat transfer is computed with the exact radiation transport equation. Fire-model predictions fall within scatter of experimental flame-height and spectral-radiation data for LNG fires.

Wilcox, D. C., Non-Gray Thermal Radiation From a Flame Above a Pool of Liquid Natural Gas. Report by TRW Systems to A.G.A., A.G.A. Catalog No. M19714, February 1971.

This report indicates that a) spectral distribution of the radiation heat flux vector can be calculated, b) minimal data are required to extrapolate from small to large fires, c) an important scaling relationship may have been uncovered, and d) the flame model and associated computer program represent a solid foundation for investigation of radiation properties of a large LNG fire.

Williams, F. A., Combustion Theory - The Fundamental Theory of Chemically Reacting Flow Systems. Addision-Wesley Publishing Company, Inc., 1965.

Chapter 2 discusses Rankine-Hugoniot relations and pages 25-27 the properties of the Hugoniot curve.

Wissmiller, I. L. and Mattocks, E. O., "How to Use LNG Safely." Pipeline and Gas Journal. March 1972.

This article provides a general description of LNG equipment and facilities and how they are designed and operated for safety.

Withrington., J. K., "Analytical Methods for Verifying the Structural Integrity of LNG Carriers." LNG 3 - International Conference on Liquefied Natural Gas, Washington DC, September 24-28, 1972.

This paper identifies some of the structural problems that might occur with a very rapid increase in the size of LNG carriers and advocates the adoption of additional analytical methods to be used in conjunction with the normal procedures of the Classification Societies.

Witte, L. C. and Cox, J. E., Nonchemical Explosive Interaction of LNG and Water. ASME Preprint 71-WA/HT-31, 1972.

When LNG contacts water, an explosive incident may occur due to extremely rapid production of LNG vapor as heat is transferred from the surrounding water. Pertinent literature is summarized on similar reported explosions when hot molten materials contact cool liquids. Fragmentation of the LNG is believed to be the triggering mechanism for explosive vapor formation. Recent results of fragmentation research are presented.

Witte, L. C., Cox, J. E. and Bouvier, J. E., "The Vapor Explosion." Journal of Metals. 22:39-44, February 1970.

The article reviews the four theories of entrapment, violent boiling, shell theory, and Weber Number Effects. A common factor exists in that when molten material is fragmented prior to liquid contact, explosion danger is lessened.

Witte, L. C., Vyas, T. J. and Gelabert, A. A., "Heat Transfer and Fragmentation During Molten-Metal/Water Interactions." Journal of Heat Transfer. 95:521-527, November 1973.

This study indicates strongly that fragmentation occurs when a sample is molten and fragmentation is a response to an external stimulus. Alternate causes of fragmentation are proposed and are predicated upon the initial collapse of a vapor film around the molten metal.

Wolf, Sidney M., "Liquefied Natural Gas." The Bulletin of the Atomic Scientists. 25, Chicago, December 1978.

Wolf presents a review of LNG import questions including safety, security, and price applicable at the time of publication.

Wood, B. D., Blackshear, P. L., Jr, and Eckert, E. R. G., "Mass Fire Model: An Experimental Study of the Heat Transfer to Liquid Fuel Burning From a Sand-filled Pan Burner." Combustion Science and Technology. 4:113-129, 1971.

Heat flux data and the radiation heat flux data indicate that radiation contributes between 20 and 40 percent of the thermal load to the fuel surface for the methanol flame. For the acetone flame, approximately 40 to 60 percent of the total heat flux is radiation during the two steady burning rate periods.

Woolers, R. G., Marine Transportation of LNG and Related Products. Cornell Maritime Press, Cambridge, MD, 1975.

This book describes aspects of marine transport of LNG including ship design, container design, control systems, and a description of hazards and LNG importation. The hazards section describes experiments performed by the Bureau of Mines to determine the effects of LNG spillage on water.

Yamanouchi, N., and Nagasawa, H., "Using LNG Cold for Air Separation." Chem. Eng. Progr. 75(7):78-82, 1979.

By using the cryogenic energy contained in LNG, liquid oxygen, liquid nitrogen and liquid argon can be produced at a 40% saving in power consumption. In the same process LNG is evaporated. Three plants based on this principle are already operating in Japan, and a fourth one is under construction.

Yamazaki, D., Yokoyama, N, and Hino, M., "Storing and Transportation of Hydrocarbon Gases." Chem. Abstr. 80:85488q. Japan Kokai 73-92, 401 (to Mitsubishi Heavy Industries, Ltd.), 1973.

Natural gas was contacted with aqueous aliphatic amine solutions to obtain the hydrate. The hydrate product had a vapor pressure of 35 kg/cm^2 at 40°F.

Yang, K., "Explosive Interaction of Liquefied Natural Gas and Organic Liquids." Nature. 243:221-222, 1973.

Small scale experiments are described in which LNG is poured into organic liquids. In some cases resulting reactions were rather violent, indicating the possibility of vapor explosions.

Yilmaz, B. S., Clarke, S. F. and Westwater, J. M., Heat Transfer From Water in Film Boiling to an Upper Layer of Paraffinic Hydrocarbon. ASME paper 76-HT-24, 1976.

Laboratory experiments have been performed to measure the flux from a layer of water in the state of film boiling to a superimposed layer of various types of hydrocarbons.

Yumoto, T., "Heat Transfer From Flame to Fuel Surface in Large Pool Fires." Combustion and Flame. 17:108-110, 1971.

The study was made to obtain experimentally the ratio of radiation and convection transfers to total heat transfer from the flame to the fuel surface in the range where the burning rate has a constant value regardless of pan diameter.

Zahn, C. W. and Clayton, H. A., Recovery of Natural Gas Liquids by Partial Condensation. U.S. Patent 4,142,876, 1979.

A complex control scheme is proposed which sets the minimum temperature of the natural gas stream to the separator, allowing for the recovery of natural gas liquid by partial condensation of the inlet feed stream.

Zeeuwen, J. P., Schippers, J. "Unconfined Vapor Cloud Explosion Modeling and Estimation of Structural Damage as the Consequences of Explosions in Hazard Analysis and Risk Evaluation." Third International Loss Prevention Symposium, 1980, 7/515-7/541.

A model is presented that estimates peak overpressure and positive phase duration of the pressure wave caused by an unconfined vapor cloud explosion. The kind of loading and the structural elements of the exposed structure are taken into account in the estimation of the expected degree of damage and the probability that this damage will occur.

Zeeuwen, J. P. "Description of Research Related to Vapor Cloud Explosions in the Netherlands." From Discussion on Explosion Hazards at the 7th International Colloquium on Gas Dynamics of Explosions and Reactive Systems, ed. H. Wagner, pp. 79-80, Max-Planck-Institute Für Strömungsforschung, Göttingen, 1979.

Research is underway to improve a previously developed model which can be used to predict blast overpressure characteristics from the amount and kind of fuel present in a vapor cloud and structures in the vicinity of the vapor cloud. Studies are concerned with flame acceleration and transition to detonation and the influence of obstacles on flame fronts.

Zeman, O. The Dynamics and Modeling for Heavier-than-Air, Cold Gas Releases. UCRL 15224, 1980.

A new analytical model for the spreading of heavier-than-air LNG vapors is presented. dispersion by mixing with air is included. No test data are available that would quantitatively verify the model.

Zuber, K., "LNG Facilities - Engineered Fire Protection Systems." Fire Technology. 12:41-48, 1976.

Dry chemical fire extinguishers used in conjunction with high expansion foam have been used successfully in tests to extinguish LNG spill fires.

Zubiate, R., Pomonik, G. and Mostarda, S., "Single Point Mooring System for Floating LNG Plant." Ocean Industry. pp. 75-78, November 1978.

The advantages of portable floating offshore LNG terminals are discussed as a preface to a description of a mooring system for such a facility.

DISTRIBUTION

No. of Copies

A. A. Churm
DOE Patent Division
9800 South Cass Avenue
Argonne, IL 60439

10 J. M. Cece (EP-32)
Office of Environmental Protection, Safety and Preparedness
U.S. Department of Energy
Washington, D.C. 20545

10 H. F. Walter (EP-32)
Office of Environmental Protection, Safety and Preparedness
U.S. Department of Energy
Washington, D.C. 20545

27 DOE Technical Information Center

A. A. Allen
Alaskan Beaufort Sea Oilspill Response Body
6700 Arctic Spur Road
Anchorage, AK 99502

J. A. Anderson
South Georgia Natural Gas Company
P. O. Box 1279
Thomasville, GA 31792

P. J. Anderson
Institute of Gas Technology
3424 South State Street
Chicago, IL 60616

S. Atallah
Gas Research Institute
8600 West Bryn Mawr Avenue
Chicago, IL 60631

No. of Copies

S. M. Barkin
Committee on Hazardous Materials
National Research Council
2101 Constitution Avenue
Washington, D.C. 20418

A. C. Barrell
Major Hazards Assessment Unit
Health and Safety Executive
25 Chapel Street
London, NW1 5DT, UK

C. Batty
British Petroleum North American, Inc.
620 Fifth Avenue
New York, NY 10020

L. E. Bell
Western LNG Terminal Associates
700 South Flower Street
Suite 3300
Los Angeles, CA 90017

W. M. Benkert
American Institute of Merchant Shipping
1625 K Street, N.W.
Washington, D.C. 20006

G. F. Bennett
Professor of Biochemical Engineering
University of Toledo
2801 Bancroft Street
Toledo, OH 43606

E. Bialik
New York State Attorney General Office
2 World Trade Center
New York, NY 10047

No. of
Copies

K. Blower
Standard Oil of Ohio
1748 Guildhall Building
Cleveland, OH 44115

F. Bodurtha
DuPont Company
Louviers Building 1351
Wilmington, DE 19898

A. Boni
Science Applications
Inc.
1200 Prospect Street
La Jolla, CA 92037

W. J. Bradford
Olin Corporation
120 Long Ridge Road
Stamford, CT 06904

W. C. Brasie
Dow Chemical USA
633 Building
Midland, MI 48640

F. E. Brinker
Trunkline LNG Company
P. O. Box 1642
Houston, TX 77001

W. Brobst
The Transport Environment
285 Old Squaw Drive
Kitty Hawk, NC 27949

S. J. Broussard, P.E.
Manager, Occidental Chemical
Company
P. O. Box 1185
Houston, TX 77001

C. P. Buckley
Boston Gas Company
One Beacon Street
Boston, MA 02108

No. of
Copies

D. J. Campbell
Trunkline LNG Company
P. O. Box 1642
Houston, TX 77001

T. Carlisle
Senior Mechanical Safety
Engineer
Santa Fe Pipeline Company
1200 Thompson Building
Tulsa, OK 74103

A. M. Clarke
Algonquin Gas Transmission Company
1284 Soldiers Field Road
Boston, MA 02135

John J. Closner
Preload Technology
839 Stewart Street
Garden City, NY 11530

R. I. Cole
American Gas Association
1515 Wilson Boulevard
Arlington, Va 22209

S. Colgate
Los Alamos National Laboratory
Los Alamos, NM 87545

G. Colonna
U.S. Coast Guard (G-DMT-1)
2100 Second Street, S.W.
Washington, D.C. 20593

Committee on Commerce,
Science and Transportation
U.S. Senate
Washington, D.C. 20510

C. Corbett
Commandant (G-WEP)
U.S. Coast Guard
2100 Second Street, S.W.
Washington, D.C. 20593

No. of
Copies

P. Cubbage
British Gas Corporation
Research & Development Station
Midlands Research Station
Whaft Lane, Solihull,
West Midlands B9K 2JW
ENGLAND

R. Danielson
Bay State Gas Company
120 Royall Street
Canton, MA 02021

R. E. DeHart, II
Union Carbide Corporation
P. O. Box 8361
South Charleston, WV 25303

W. Dennis
Office of Pipeline Safety
Regulations
400 7th Street, S.W.
Washington, D.C. 20590

L. C. Doelp
Corporate Engineering
Air Products and Chemicals
Allentown, PA 18105

E. Drake
Arthur D. Little, Inc.
Acorn Park
Cambridge, MA 02140

F. Edeskuty
Los Alamos Scientific
Laboratory
P. O. Box 1663
Los Alamos, NM 87545

J. Edgell
Bulk Plant Operations
Columbia Hydrocarbon
Corporation
1600 Dublin Road
Columbus, OH 43215

No. of
Copies

R. J. Eiber
Battelle Columbus Laboratories
505 King Avenue
Columbus, OH 43201

T. Eichler
IIT Research Institute
10 West 35th Street
Chicago, IL 60616

N. Eisenberg
U.S. Nuclear Regulatory
Commission
5650 Nicholson Lane
Rockville, MD 20852

W. G. England
Energy Resources Company, Inc.
3344 North Torrey Pines Court
La Jolla, CA 92037

H. K. Fauske
Fauske & Associates, Inc.
16070 West 83rd Street
Burridge, IL 60521

J. A. Fay
Department of Mechanical
Engineering
Massachusetts Institute of
Technology
Cambridge, MA 02139

J. P. Frazier
Natural Gas Pipeline Company
of America
122 South Michigan Avenue
Chicago, IL 60603

S. Fujinami
Tankage Designing Section
Kawasaki Heavy Industries, LTD
118, Futatsuzuka, Noda-shi,
Chiba 278, JAPAN

No. of Copies

M. Futana
No. 3 Group Chemical Plant
and Machinery Department B
Mitsubishi Heavy Industries, LTD
118, Ichigaya Tomihisa-Cho,
Shinjuku-ku
Tokyo 162, JAPAN

W. Geiger
Battelle-Institut e.V.
Am Roemerhof 35
6000 Frankfurt am Main 90
FEDERAL REPUBLIC OF GERMANY

R. D. Gerges
Manager, Process Hazard
Analysis
Rohm & Haas Company
Engineering Division
Box 584
Bristol, PA 19007

D. Gideon
Battelle Columbus Laboratories
505 King Avenue
Columbus, OH 43201

E. B. Graham
British Gas Corporation
326 High Holborn
London WC17PT, ENGLAND

K. Hagiwara
No. 1 Sales Department
J.G.C. Corporation
2-1, Otemachi 2-chome, Chiyoda-ku
Tokyo 100, JAPAN

E. Halevy
Scientific Counselor
Embassy of Israel
1621 22nd Street, N.W.
Washington, D.C. 20008

W. T. Hanna
Battelle Columbus Laboratories
505 King Avenue
Columbus, OH 43201

No. of Copies

H. C. Hardee
Supervisor, Fluid Mechanics
and Heat Transfer
Sandia Laboratories
Albuquerque, NM 87115

J. Havens
College of Engineering
University of Arkansas
227 Engineering Building
Fayetteville, AR 72701

R. W. Headrick
Pacific Gas and Electric
Company
77 Beale Street
San Francisco, CA 94106

T. Hellman
Director, ENRL Services
Allied Corporation
P. O. Box 2120
Houston, TX 77001

E. W. Hofer
Process Engineering Manager
Allied Corporation
P. O. Box 2105R
Morristown, NJ 07960

10 W. J. Hogan
Lawrence Livermore Laboratory
P. O. Box 808
Livermore, CA 94550

C. C. Hong
Columbia Gas System Service
Corporation
1600 Dublin Road
Columbus, OH 43215

W. B. Howard
Manager, Process Safety
Monsanto
800 North Lindbergh Boulevard
St. Louis, MO 63166

No. of
Copies

P. E. Hyam
Directorate Staff
Imperial Chemical Industries
Box 1
Billingham Cleveland
TS23 1LB ENGLAND

D. Igo
Transportation Research
Department of Transportation
400 7th Street, S.W.
Washington, D.C. 20590

K. Ishida
Technical Department
Measuring Instrumentation
Division
Fuji Electric Company, LTD
No. 1, Fuji-machi, Hino-shi,
Tokyo 191, JAPAN

F. Jeglic
National Energy Board
473 Albert Street
Ottawa, Ontario K1A 0E5
CANADA

W. H. Johnson
National L. P. Gas
Association
1301 West 22nd Street
Oak Brook, IL 60521

C. L. Jones
Energy Counselor
British Embassy
3100 Massachusetts Avenue,
N.W.
Washington, D.C. 20008

L. J. S. Kaplan
Dangerous Commodities Review
Committee Officer
Railway Transport Committee
Ottawa, K1A 0N9, CANADA

No. of
Copies

J. W. Kime
U.S. Coast Guard (G-W)
2100 Second Street
Washington, D.C. 20593

W. C. Kohfeldt
Exxon Chemical Company
P. O. Box 271
Florham Park, NJ 07932

H. J. Kolodner
Director, Corporate Safety
Celanese Corporation
P. O. Box 32414
Charlotte, NC 28232

L. M. Krasner
Factory Mutual Research
Corporation
1151 Boston - Providence
Turnpike
Norwood, MA 02062

J. K. Lathrop
National Fire Protection
Association
470 Atlantic Avenue
Boston, MA 02210

P. E. Laurie
Acres Consulting Services Limited
5259 Dorchester Road
P. O. Box 1001
Niagara Falls, CANADA L2E 6W1

J. A. Lawrence
Vice President and Manager of
Nitrogen Operations
CF Industries, Inc.
Salem Lake Drive
Long Grove, IL 60047

L. Lemon
Energy and Minerals Research
Company
P. O. Box 389
Exton, PA 19341

No. of
Copies

M. Levy
Columbia LNG Corporation
20 Montchanin Road
Wilmington, DE 19807

D. J. Lewis
Imperial Chemical Industries, LTD
Mond Division, Research and
Development Department
P. O. Box 7 Winnington
Northwich Cheshire, CW8 4DJ, UK

J. P. Lewis
Project Technical Liaison
Associates, Inc.
505 North Belt, Suite 260
Houston, TX 77060

C. D. Lind
Code 3262
U.S. Naval Weapons Center
China Lake, CA 93555

G. Logan
Phillips Chemical Company
Seneca Building
Bartlesville, OK 74004

P. Lunnie
Asst. VP, Industrial Relations
Director, OSH
National Association of
Manufacturers
1776 F Street, N.W.
Washington, D.C. 20006

L. Mallon
Committee on Merchant Marine
and Navy
House of Representatives
Washington, D.C. 20515

J. Manney
American Petroleum Institute
2101 L Street, N.W.
Washington, D.C. 20037

No. of
Copies

Commanding Officer
Marine Safety Office
U.S. Coast Guard
Baltimore, MD 21202

D. H. Markstein
Factory Mutual Research
Corporation
1151 Boston - Providence
Turnpike
Norwood, MA 02062

J. Martin
Shell International Gas
Shell Centre
London, SE1 7NA, UK

W. E. Martinsen
Energy Analysts Inc.
2001 Priestley Avenue
P. O. Box 1508
Norman, OK 73070

J. D. Massie
The Fertilizer Institute
1015 18th Street N.W.
Washington, D.C. 20036

M. Matallana
Spanish Embassy (Room 1020)
1875 Connecticut Avenue, N.W.
Washington, D.C. 20009

Y. Matsui
Systems Department
Toyo Engineering Corporation
12-10, Higashi-funabashi 6-chome
Funabashi-shi, Chiba 273, JAPAN

H. Mayo
COOP Farm Chemical Association
P. O. Box 308
Lawrence, KS 66044

No. of
Copies

R. N. Meroney
Fluid Mechanics and Wind
Engineering Program
Department of Civil
Engineering
Colorado State University
Fort Collins, CO 80523

R. C. Mill
Exxon Chemical Company
200 Park Avenue
P. O. Box 271
Florham Park, NJ 07932

R. Morrison
Boston Gas Company
One Beacon Street
Boston, MA 02108

N. Neafus
EDECO Engineering Company
1601 South Main Street
P. O. Box 589
Tulsa, OK 74101

J. A. Nicholls
Department of Aerospace
Engineering
University of Michigan
Ann Arbor, MI 48109

R. Norton
Distrigas, Inc.
125 High Street
Boston, MA 02110

O. Okawa
Chiyoda Chemical Engineering
Company
P. O. Box 10
Tsurumi, Yokohama 230, JAPAN

A. K. Oppenheim
Department of Mechanical
Engineering
University of California
Berkeley, CA 94720

No. of
Copies

P. M. Ordin, P.E.
16705 Van Aken Boulevard
Shaker Heights, OH 44120

J. C. Pace, Jr.
Long Island Lighting Company
175 East Old Country Road
Hicksville, NY 11801

M. C. Parnarouskis
U.S. Coast Guard (G-DMT-1)
2100 2nd Street, S.W.
Washington, D.C. 20593

H. Pasman
Prins Maurits Laboratory TNO
Technological Research
P. O. Box 45
2280 AA Rijswikj, NETHERLANDS

E. Pearlman
JRB Associates
8400 Westpark Drive
McLean, VA 22102

J. Peebles
Commandant (G-WPE)
U.S. Coast Guard
2100 Second Street, S.W.
Washington, D.C. 20593

W. H. Penn
Tennessee Gas Pipeline Company
P. O. Box 2511
Houston, TX 77001

H. W. Peter
Brooklyn Union Gas Company
195 Montague Street
Brooklyn, NY 11201

C. Peterson
SRI Washington
1611 North Kent Street
Rosslyn Plaza
Arlington, VA 22209

No. of
Copies

R. E. Petsinger
LNG Services, Inc.
1815 Washington Road
Pittsburgh, PA 15241

C. N. Petterson
Northwest Natural Gas Company
123 Northwest Flanders Street
Portland, OR 97209

A. Pfeiffer
Institute for Reactor Safety
Glodkengrasse 2
5000 Cologne 1
FEDERAL REPUBLIC OF GERMANY

W. B. Porter
Process Engineer
W. R. Grace Company
100 North Main Street
Memphis, TN 38101

A. A. Putnam
Battelle Columbus Laboratories
505 King Avenue
Columbus, OH 43201

P. Raj
Technology and Management
Systems, Inc.
102 Drake Road
Burlington, MA 01803

R. C. Reid
Department of Chemical
Engineering
Masschusetts Institute
of Technology
Cambridge, MA 02139

A. Roberts
Office of Hazardous Materials
Regulations
Department of Transportation
Transpoint Building
2100 Second Street, S.W.
Washington, D.C. 20590

No. of
Copies

A. Rosenbaum
National Tank Truck
Carriers, Inc.
1616 P Street, N.W.
Washington, D.C. 20036

P. Rothberg
CRS/SPR
Library of Congress
Washington, D.C. 20450

M. I. Rudnicki
Aerojet Energy Conversion Company
P.O. Box 13222
Sacramento, CA 95813

Monsieur A. Salvadori
Gaz de France
Direction des Etudes et Techniques
Nouvelles
Department des Etudes Cryogenics,
Industrielles et Metallurgiques
23, rue Philibert-Delorme
Paris-17, FRANCE

L. Santman
Materials Transportation
Bureau
U.S. Department of
Transportation
400 7th Street, S.W.
Washington, D.C. 20590

L. Sarkes
American Gas Association
1515 Wilson Boulevard
Arlington, VA 22209

L. C. Schaller
E. I. du Pont de Nemours & Co.
12430 Nemours Building
Wilmington, DE 19898

M. Scherb
P. O. Box AG
Beverly Hills, CA 90213

No. of
Copies

B. Schnurman, CPCU
Reed Stenhouse
1010 Collingwood Drive
St. Louis, MO 63132

H. P. Schorr
Brooklyn Union Gas Company
195 Montague Street
Brooklyn, NY 11201

S. Schreiber
Allied Corporation
P. O. Box 2332R
Morristown, NH 07960

P. Schreurs
Katholieke Universiteit Leuven
CIT
De Croylaan 2
B.3030 Leuven
THE NETHERLANDS

R. J. Schuttler
Manager
Hooker Chemicals
P. O. Box 728
Niagara Falls, NY 14302

R. F. Schwab
Manager, Process Safety & Loss
Prevention
Allied Corporation
P. O. Box 2332R
Morristown, NJ 07960

J. G. Seay
Institute of Gas Technology
3424 South State Street
Chicago, IL 60616

P. Seay
Technical Division
Office of Hazardous Materials
Regulations
Materials Transportation Bureau
400 Seventh Street, S.W.
Washington, D.C. 20590

No. of
Copies

J. Seelinger
Office of Commercial Development
U.S. Maritime Administration
U.S. Department of Commerce
Washington, D.C. 20230

S. M. Settle
Associate Director, OSH
NAM
1776 F Street, N.W.
Washington, D.C. 20006

J. D. Shefford
British Gas Corporation
59 Bryanston Street
Marble Arch
London W1A2AZ, ENGLAND

R. B. Smith
Battelle Columbus Laboratories
505 King Avenue
Columbus, OH 43201

J. Sorel
French Atomic Energy
Commission
29 Rue de la Federation
Paris 15, FRANCE

J. K. Speckhals
Columbia LNG Corporation
20 Montchanin Road
Wilmington, DE 19807

Spill Technology Newletter
Environmental Protection Service
Ottawa, Ontario KIA 1C8 CANADA

A. N. Stewart
San Diego Gas & Electric Company
P. O. Box 1831
San Diego, CA 92112

R. A. Strehlow
105 Transportation Building
University of Illinois
Urbana, IL 61801

No. of
Copies

J. D. Swanburg
Supt. of Process Engineering
Union Chemical Division
Union Oil Company of California
P. O. Box 1280
Brea, CA 92621

B. Sweedler
National Transportation
Safety Board
800 Independence Avenue
Washington, D.C. 20591

T. Tanaka
System Engineering Department
J. G. C. Corporation
14-1, Bessho-cho 1-chome, Minami-ku
Yokohama-shi, Kanagawa 232 JAPAN

J. Tatematsu
Technology Transfer Institute
Kyodo Building
3-1, Akasaka 4-chome, Minato-ku
Tokyo 105, JAPAN

R. Tatge
CV International, Incorporated
2741 Toledo Street, Suite 208
Torrance, CA 90503

M. J. Turner
Health and Safety Executive
25 Chapel Street
London NW1 5DT, ENGLAND

T. Uozumi
Assistant to the Manager
EDP Education Department
Fujitsu LTD
17-25, Shinkamata 1-chome, Ohta-ku
Tokyo 144, JAPAN

W. Walls
National Fire Protection
Association
470 Atlantic Avenue
Boston, MA 02210

No. of
Copies

S. K. Wakamiya
Product Engineering Division
National Bureau of Standards
Department of Commerce
Washington, D.C. 20234

D. J. Watters
Union Carbide Corporation
P. O. Box 8361
South Charleston, WV 25303

S. J. Wiersma
Gas Research Institute
8600 West Bryn Mawr Avenue
Chicago, IL 60631

J. R. Welker
Applied Technology Corporation
P. O. Box FF
Norman, OK 73070

M. M. Williams
U.S. Coast Guard
Technical Advisor (G-MHM/83)
400 Seventh Street, S.W.
Washington, D.C. 20590

W. Wilson
San Diego Gas & Electric Company
P. O. Box 1831
San Diego, CA 92112

RADM K. E. Wiman
U.S. Coast Guard (G-D)
2100 Second Street, S.W.
Washington, D.C. 20593

B. Witcofski
NASA-Langley
Hampton, VA 23665

R. E. Witter
Monsanto Company
800 North Lindbergh Boulevard
St. Louis, MO 63166

No. of
Copies

J. L. Woodward
Exxon Research & Engineering
P. O. Box 101
Florham Park, NJ 07932

R. Zalosh
Factory Mutual Research
1151 Boston-Providence Turnpike
Norwood, MA 02062

ONSITE

DOE Richland Operations

H. E. Ransom

57 Pacific Northwest Laboratory

W. J. Bair
H. J. Bomelburg
D. L. Brenchley
C. A. Counts
W. E. Davis
J. G. DeSteese (40)
C. A. Geffen
P. J. Pelto
W. L. Rankin (HARC)
R. E. Rhoads
R. Shikiar (HARC)
L. D. Williams
Library (5)
Publishing Coordination Ha (2)

Technical Report Documentation Page

1. Report No.	2. Government Accession No.	3. Recipient's Catalog No.
PNL-4172		

4. Title and Subtitle	5. Report Date
LIQUEFIED GASEOUS FUELS SAFETY AND ENVIRONMENTAL CONTROL ASSESSMENT PROGRAM: THIRD STATUS REPORT	January 1982
	6. Performing Organization Code
7. Author(s)	8. Performing Organization Report No.
9. Performing Organization Name and Address Pacific Northwest Laboratory Post Office Box 999 Richland, WA 99352	10. Work Unit No. 11. Contract or Grant No. 13. Type of Report and Period Covered
12. Sponsoring Agency Name and Address U.S. Department of Energy Environmental and Safety Engineering Division Mail Room (EP-32) Washington, DC 20545	14. Sponsoring Agency Code

15. Supplementary Notes

This report was prepared by John G. DeSteese, Cary A. Counts and Nancy M. Burleigh of PNL and staff under the cognizance of Dr. John M. Cece and Dr. Henry F. Walter. Comments about this document may be directed to the latter at the address in Box 12.

16. Abstract

The U.S. Department of Energy, Office of the Assistant Secretary for Environmental Protection, Safety and Emergency Preparedness (DOE/EP) has a responsibility for identifying, characterizing and mitigating environmental, safety and health issues associated with the commercial use of specific energy materials. Consequently, the Environmental and Safety Engineering Division (ESED), in the DOE/EP Office of Operational Safety, is conducting a program to assess the safety and environmental control of some of these materials, including LNG, LPG, ammonia and hydrogen. The overall objective is to gather, analyze and disseminate technical information that will aid future decisions made by industry, regulatory agencies and the general public on facility siting, system operations and accident prevention and mitigation. This effort is supported by a number of contributors including national laboratories, universities, technical institutions and industrial research contractors. This report (like previous Status Reports) contains a collection of reports supplied by contributors to the LGF Assessment Program. This status report emphasizes LNG research conducted by Lawrence Livermore National Laboratory (LLNL). Section II contains 13 reports (A through M) on LLNL efforts in the following categories: (1) 40-m^3 LNG spill experiments; (2) LNG dispersion; (3) LNG combustion and (4) planning assessments for a 500-m^3 spill test facility. The LNG Bibliography (Report N) was prepared by Pacific Northwest Laboratory. Preceding documents reporting earlier information are DOE/EV-0002 (February 1978), DOE/EV-0036 (May 1979) and DOE/EV-0085 (October 1980).

17. Key Words	18. Distribution Statement
• Liquefied Gaseous Fuels (LGF) • LNG Spills • Gas/Vapor Cloud Dispersion • Rapid Phase Transition (RPT) Explosions • Vapor Dispersion Simulation Models • Flame Propagation • Gaseous Detonation	Release unlimited

19. Security Classif. (of this report)	20. Security Classif. (of this page)	21. No. of Pages	22. Price
Unclassified	Unclassified		